

Dissertation zur Erlangung des Doktorgrades  
der Fakultät für Chemie und Pharmazie  
der Ludwig-Maximilians-Universität München

**Total Synthesis and Racemization of  
(–)-Sinoracutine**

**and**

**Studies Towards the Total Synthesis of  
Herqulines A and B**

von

Giulio Volpin

aus

Bruneck, Italien

2017

## **Erklärung**

Diese Dissertation wurde im Sinne von § 7 der Promotionsordnung vom 28. November 2011 von Herrn Prof. Dr. Dirk Trauner betreut.

## **Eidesstattliche Versicherung**

Diese Dissertation wurde eigenständig und ohne unerlaubte Hilfsmittel erarbeitet.

München, den 16.01.2017

.....

Giulio Volpin

Dissertation eingereicht am:	17.01.2017
1. Gutachter:	Prof. Dr. Dirk Trauner
2. Gutachter:	Prof. Dr. Franz Bracher
Mündliche Prüfung am:	27.02.2017

*To mom and dad*



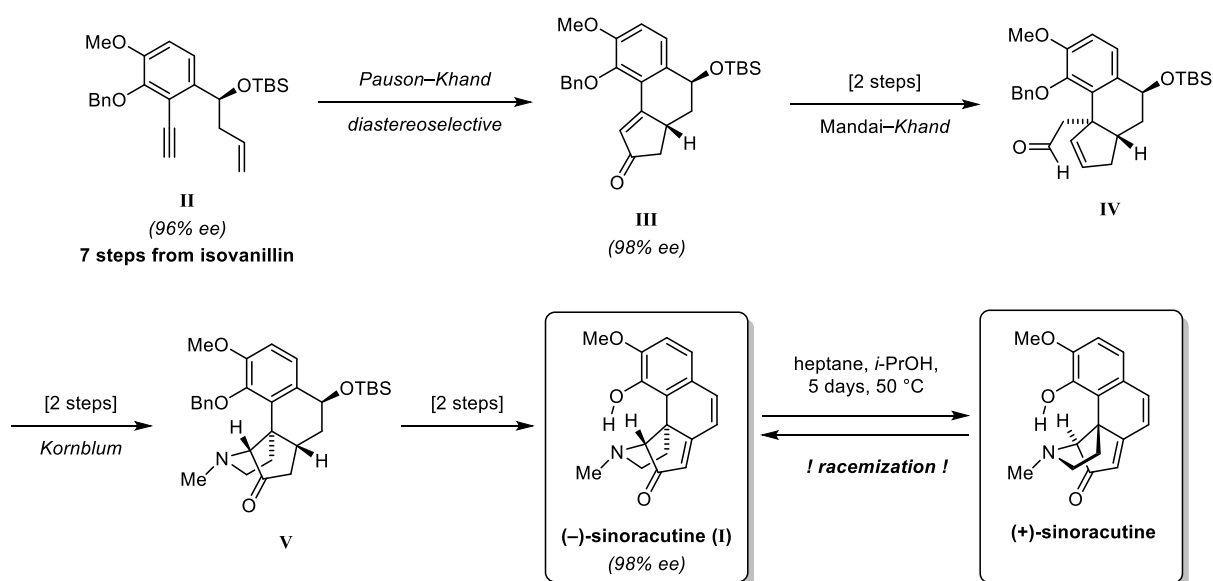
**Parts of this work have been published in peer-reviewed journals:**

“*Enantioselective Synthesis and Racemization of (-)-Sinoracutine*”, Giulio Volpin, Nynke A. Vepřek, Andreas B. Bellan, Dirk Trauner, *Angew. Chem. Int. Ed.* **2017**, 56, 897–901.



## Abstract

**PART I:** Benzyloisoquinoline alkaloids derived from either enantiomer of reticuline represent a large class of secondary metabolites that occur across many families of herbaceous plants. Oxidative enzymatic transformations give rise to a variety of skeletal subtypes and complex polycyclic frameworks that have been used as therapeutic agents for centuries, often serving as lead compounds for the development of new drugs. While different enantiomers of the same molecule are known to be produced across plants of different species, the occurrence of the same compound in scalemic fashion in the same host is highly unusual, given that the enzymes involved in their biosynthesis normally operate with very high enantioselectivity. **Sinoracutine** however (**I**, Scheme A), which was isolated from *Stephania cepharantha* and *Sinomenium acutum*, was found to occur in different optical purities across the different source plants. With the ultimate goal to determine the origin of discrepancy, we devised an enantioselective approach to sinoracutine, in which the stereochemistry could be controlled by a benzylic alcohol introduced early in the synthesis. Starting from inexpensive isovanillin, an enantioselective reduction delivered enantiopure **II** which was transformed into tricycle **III** by Pauson–Khand reaction. Stereoselective reduction and Claisen rearrangement gave aldehyde **IV**. After reductive amination, a iodoamination–Kornblum oxidation sequence delivered tetracycle **V**, which could provide sinoracutine in excellent optical purity. We determined that upon mild heating in protic solvent, this material underwent complete racemization within five days. Our results suggest that the pyrrolidine ring of sinoracutine could undergo ring-opening and closure to factually destroy the stereochemical configuration of the all-carbon quaternary stereocenter and allow for the formation of (+)-sinoracutine, explaining the optical variability observed in plant-derived samples of sinoracutine.

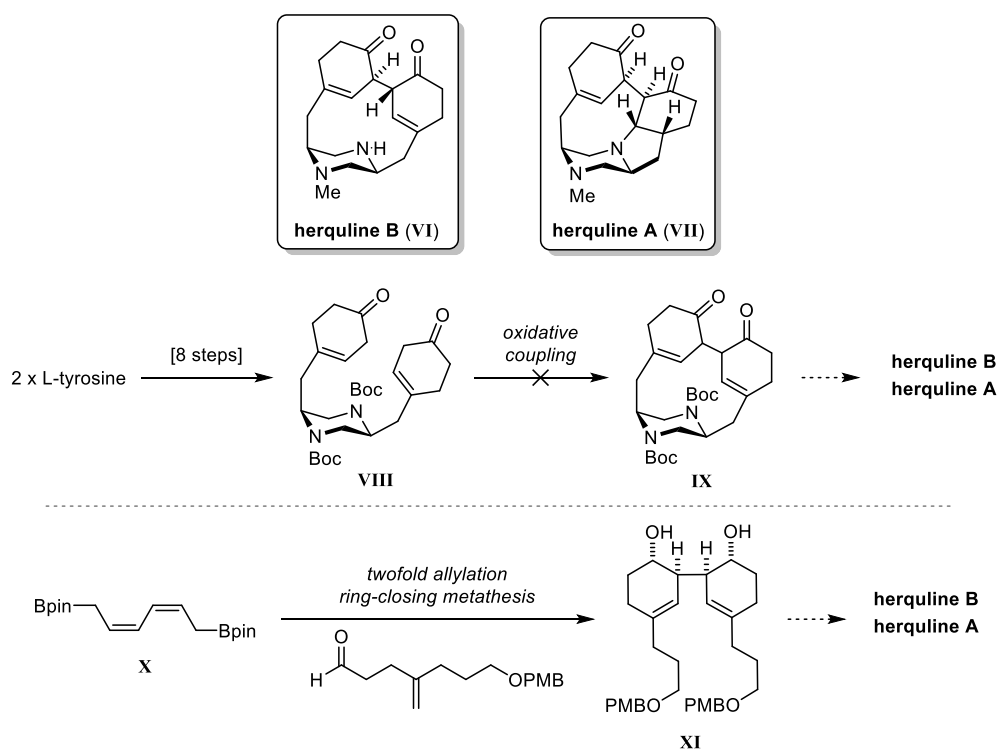


**Scheme A. Enantioselective synthesis of (–)-sinoracutine using a series of diastereoselective synthetic transformation and its facile racemization**

**PART II:** The second part of this thesis describes investigations towards the strained piperazine alkaloids **herquline A (VI)** and **B (VII, Scheme B)**. Isolated from the fungus *Penicillium herquei*, they have shown interesting blood-platelet aggregation activity, as well as anti-influenza properties. In our synthetic approaches, we wanted to take advantage of the pseudosymmetrical nature of herquline B and devise a two-directional strategy aimed at the first total syntheses of these unique natural products.

An oxidative enolate coupling strategy was pursued for the formation of the 12-membered ring. The required precursor (**VIII**) could be prepared from two L-tyrosine units by a short reaction sequence. Several conditions for the formation of **IX** were investigated, either from **VIII** itself, its derived bis-enolate, or the bis-silyl enol ether. Unfortunately, **IX** was not formed, and studies on different model systems suggest that  $\beta,\gamma$ -unsaturated ketones are not able to undergo radical dimerization at the  $\alpha$ -position under the conditions examined.

A second approach based on the early introduction of the 1,4-dicarbonyl moiety was next investigated. For the synthesis of the bis-cyclohexenone rings of herquline B, a twofold allylation strategy was investigated. After extensive optimization, we determined that bifunctional allylboron reagent **X** was uniquely suited for the formation of the required products. The reactivity of **X** is explored, and its use in the double allylation / double ring-closing metathesis sequence has been demonstrated on model substrates (e.g. giving **XI**) to successfully form the northern bis-cyclohexene segment featured in herquline B (**VI**).



**Scheme B. Synthetic approaches towards herquline B outlined in this thesis: oxidative coupling strategy (top) and two-fold allylation – metathesis sequence (bottom)**

## **Acknowledgements**

First and foremost, I want to thank Prof. Dr. Dirk Trauner for the extraordinary possibility I was given to conduct my PhD work under his guidance. I cannot thank him enough the intellectually challenging projects, the freedom to test my ideas in the field of total synthesis, and the trust he put in my capacities. His confidence, enthusiasm and generosity were truly inspiring and constant motivation to pursue new ideas in the exceptional working environment he created.

I am very thankful to Prof. Dr. Franz Bracher for agreeing to be the second reviewer of this thesis. I thank Prof. Dr. K. Karaghiosoff, Prof. Lena Daumann, Prof. Paul Knochel and Prof. Rasmus Linser for their comments and for agreeing to serve as examination committee members.

I am especially grateful to the co-workers who shared responsibility for the projects I have been working on: Andreas Bellan, Nynke Vepřek, Belinda Hetzler, Elisa Vignoni, Aylin Hirschvogel, Till Reinhardt, Marius Schmicker, Andrea Stegner, Stephan Blum, Alexander Pütz, Bichu Cheng.

My gratitude goes to Bryan Matsuura, Shu-An Liu, Julius Reyes, Benjamin Williams, Sebastian Strych, and Desiree Stichnoth for proofreading this thesis.

The generous support of this work by the Chemical Industry Fund of the German Chemical Industry Association in form of a Chemiefonds Fellowship is gratefully acknowledged.

Furthermore, I want to thank the one and only Heike Traub, Aleksandra Sarman Grilc, Dr. Martin Sumser, Carrie Louis and Luis De La Osa de la Rosa for their precious assistance and for keeping the group running. Dr. Peter Mayer and Prof. Dr. Konstantin Karaghiosoff have been very helpful with X-ray structure determination and low temperature NMR experiments. I am indebted to Dr. David Stephenson, Dr. Werner Spahl, Claudia Dubler and Sonja Kosak for outstanding analytical support. I also thank Dr. Anja Haniel, Birgit Carell, Felix Kalfa, Dr. Bernhard Kempf, Heidi Buchholz, Ronald Schürer, Michael Gayer, Alessandra Wührer, the team in the machine and glassblowing shops, who have also been very forthcoming and helpful during my time at LMU.

I want to thank all past and present Trauner group members which I had the pleasure to meet and spend time throughout these years, especially members of the Blue Lab. I would also like to thank Dr. Thomas Magauer and his group for advice and assistance.

Thanks to my mom and dad, as well as my uncle and aunt, for their never-ending love and support throughout all these years.

## List of Abbreviations

Å	Angstrom
acac	acetylacetone
Ar	undefined aryl substituent
ATR	attenuated total reflection
BC	before Christ
Bn	benzyl
Boc	<i>tert</i> -Butyloxycarbonyl
bpy	2,2'-bipyridine
br	broad (NMR spectroscopy, IR spectroscopy)
Bu	butyl
°C	degree Celsius
CAN	ceric ammonium nitrate
Cbz	carboxybenzyl
CCDC	Cambridge Crystallographic Data Centre
CoA	coenzyme A
COD	1,5-cyclooctadiene
COSY	homonuclear correlation spectroscopy
CSA	camphorsulfonic acid
Δ	heating (under reflux)
d	doublet (NMR spectroscopy)
d.r.	diastereomeric ratio
DCE	1,2-dichloroethane
DIBALH	diisobutylaluminum hydride
DIPEA	diisopropylethylamine
DIP-Cl	(-)- <i>B</i> -chlorodiisopinocampheylborane
DMA	dimethylacetamide
DMC	dimethylcarbonate
DMAP	4-(dimethylamino)pyridine
DME	1,2-dimethoxyethane
DMF	dimethylformamide
DMP	Dess–Martin periodinane
DMSO	dimethylsulfoxide
dppf	1,1'-bis(diphenylphosphino)ferrocene
dtbpy	2,6-di- <i>tert</i> -butylpyridine
ee	enantiomeric excess

EI	electron impact ionization (mass spectrometry)
<i>epi</i>	epimer
eq	equivalent(s)
ESI	electron spray ionization (mass spectrometry)
Et	ethyl
g	gram(s)
GI	Grubbs catalyst, 1 <sup>st</sup> generation
GII	Grubbs catalyst, 2 <sup>nd</sup> generation
h	hour(s)
HGI	Hoveyda–Grubbs catalyst, 1 <sup>st</sup> generation
HGII	Hoveyda–Grubbs catalyst, 2 <sup>nd</sup> generation
HSQC	heteronuclear single quantum coherence
Hz	Hertz (frequency)
<i>i</i>	<i>iso</i> (isomer)
<i>i</i> -Pr	isopropyl
kb	kilobase(s)
J	coupling constant (NMR)
KHMDS	potassium hexamethyldisilazide
LDA	lithium diisopropylamide
LiHMDS	lithium hexamethyldisilazide
M	molar
m	meter(s)
m	medium (IR spectroscopy)
m	multiplet (NMR spectroscopy)
Me	methyl
min	minute(s)
mL	milliliter
mmol	millimole
MS	mass spectrometry
MS	molecular sieves
MTBE	methyl <i>tert</i> -butyl ether
MVK	methyl vinyl ketone
NADP	nicotinamide adenine dinucleotide phosphate
NIS	<i>N</i> -iodosuccinimide
nm	nanometer(s)
NMO	<i>N</i> -methylmorpholine <i>N</i> -oxide
NMR	nuclear magnetic resonance

## List of Abbreviations

NOESY	nuclear Overhauser effect correlation spectroscopy
NRPS	nonribosomal peptide synthetase
Ns	2-nitrobenzenesulfonyl
<i>o</i>	<i>ortho</i> (isomer)
<i>p</i>	<i>para</i> (isomer)
Ph	phenyl
ppm	parts per million
PPTS	pyridinium <i>para</i> -toluenesulfonate
<i>p</i> -TsOH	<i>para</i> -toluenesulfonic acid
q	quartet (NMR spectroscopy)
R	undefined substituent
R <sub>f</sub>	retardation or retention factor
R <sub>t</sub>	retention time
r.t.	room temperature
s	strong (IR spectroscopy)
s	singlet (NMR spectroscopy)
t	triplet (NMR spectroscopy)
<i>t</i>	( <i>tert</i> -) tertiary (isomer)
TBAF	tetrabutylammonium fluoride
TBAI	tetrabutylammonium iodide
TBDPS	<i>tert</i> -butyldiphenylsilyl
TBS	<i>tert</i> -butyldimethylsilyl
<i>t</i> Bu	<i>tert</i> -butyl
Tf	trifluoromethanesulfonyl
TFA	trifluoroacetic acid
TFAA	trifluoroacetic anhydride
THF	tetrahydrofuran
TLC	thin layer chromatography
TMANO	trimethylamine <i>N</i> -oxide
TMEDA	tetramethylethylenediamine
TMS	trimethylsilyl
Ts	<i>para</i> -toluenesulfonyl
UV	ultraviolet (irradiation)
W	watt (unit of power)
w	weak (IR spectroscopy)
wt%	weight percent
<i>Z</i>	together ( <i>cis</i> )

## Table of Contents

<b>Abstract</b> .....	<b>VII</b>
<b>Acknowledgements</b> .....	<b>IX</b>
<b>List of Abbreviations</b> .....	<b>X</b>
<b>Table of Contents</b> .....	<b>XIII</b>
<b>1. GENERAL INTRODUCTION – ALKALOIDS</b> .....	<b>1</b>
1.1. The Beginning of Alkaloid Chemistry .....	1
1.2. Definition of Alkaloid .....	3
1.3. Significance and Opportunities .....	5
<b>PART I: TOTAL SYNTHESIS AND RACEMIZATION OF (-)-SINORACUTINE</b> .....	<b>7</b>
<b>1. INTRODUCTION</b> .....	<b>8</b>
1.1. Structural Variety of Benzyloquinoline Alkaloids .....	8
1.2. Sinoracutine .....	11
1.1.1. Isolation, Structure and Absolute Stereochemistry .....	11
1.1.2. Biosynthesis .....	12
1.1.3. Bioactivity .....	13
1.3. Project Aims .....	14
<b>2. RESULTS AND DISCUSSION</b> .....	<b>15</b>
2.1. Retrosynthesis .....	15
2.1.1. Synthesis of the Pyrrolidine Coupling Partner .....	16
2.1.2. Synthesis of the Aromatic Coupling Partner .....	18
2.1.3. Cross-Coupling Attempts .....	20
2.1.4. Alternative Fragment Union .....	23
2.1.5. Stepwise Construction of the Pyrroline Ring .....	25
2.2. Revised Retrosynthesis .....	26
2.2.1. Synthesis of the Isovanillin Portion .....	27

*Table of Contents*

2.2.2.	Pauson-Khand Reaction .....	28
2.2.3.	Introduction of the Quaternary Stereocenter .....	30
2.2.4.	Formation of the Pyrrolidine Ring .....	39
2.2.5.	Completion of the Synthesis.....	44
2.2.6.	Asymmetric Synthesis of Sinoracutine.....	46
2.2.7.	Stereochemical Identity and Racemization of Sinoracutine.....	53
<b>3.</b>	<b>SUMMARY .....</b>	<b>56</b>
<b>4.</b>	<b>EXPERIMENTAL PART .....</b>	<b>58</b>
4.1.	General Experimental Details.....	58
4.2.	Experimental Procedures .....	61
4.3.	Experimental Study on the Racemization of (-)-Sinoracutine .....	100
4.4.	Comparison of Natural and Synthetic Sinoracutine .....	105
4.5.	X-Ray Crystallographic Data.....	106
4.6.	NMR Spectra .....	112
	<b>PART II: TOWARDS THE TOTAL SYNTHESIS OF HERQULINES A AND B .....</b>	<b>153</b>
<b>1.</b>	<b>INTRODUCTION .....</b>	<b>154</b>
1.1.	Peptide-derived Natural Products of Nonribosomal Origin.....	154
1.2.	Herqulines A & B.....	157
1.2.1.	Isolation, Structure and Biosynthesis .....	157
1.2.2.	Bioactivity .....	159
1.3.	Previous Synthetic Efforts .....	161
1.4.	Project Aims .....	167
<b>2.</b>	<b>RESULTS AND DISCUSSION .....</b>	<b>168</b>
2.1.	Retrosynthesis: Early Introduction of the Piperazine Ring.....	168
2.1.1.	Synthesis of C <sub>2</sub> -symmetric β,γ-unsaturated Ketone .....	171
2.1.2.	Oxidative Enolate Coupling Reaction.....	177
2.1.3.	Conclusion and Analysis .....	179

<b>2.2. Revised Retrosynthesis: late-stage Piperazine Formation</b> .....	<b>181</b>
2.2.1. Development of a Bifunctional Allylation Reagent .....	183
2.2.2. Exploratory Studies .....	184
2.2.3. Synthesis and Reactivity of Bifunctional Allylboration Reagent (268) .....	185
2.2.4. Application Towards the Synthesis of Herquelines A and B.....	191
<b>3. SUMMARY AND FUTURE WORK</b> .....	<b>196</b>
<b>4. EXPERIMENTAL PART</b> .....	<b>198</b>
4.1. General Experimental Details.....	198
4.2. Experimental Procedures .....	202
4.3. X-Ray Crystallographic Data.....	236
4.4. NMR Spectra .....	243
<b>REFERENCES</b> .....	<b>284</b>

*Table of Contents*

# 1. General introduction – Alkaloids

## 1.1. The Beginning of Alkaloid Chemistry

Although only defined and classified for the first time at the beginning of the 19<sup>th</sup> century, for thousands of years the naturally occurring small molecules known today as “alkaloids” have played a central role in the evolution of human society. The causality link that was recognized between the ingestion of a certain alkaloid-containing plants and the resulting effect on the body was documented as early as 5000 years ago in the form of a Sumerian clay slab from Nagpur (India), which comprised twelve recipes for drug preparation containing over 250 various plants.<sup>[1]</sup> Independently, similar knowledge developed in China, with the drafting of the botanical treaty “Pen T’Sao” (2500 BC), describing the proprieties of 365 medicinal herbs.<sup>[2]</sup> Over the centuries, based on empirical observations, virtually every literate society developed their own compendium of bioactive plants and described their therapeutic (and sometimes toxic) proprieties: from the Ebers papyrus (1550 BC) in Ancient Egypt to the *Historia Plantarum* of Theophrastus of Eresos (372–287 BC), as well as the works of Pliny the Elder (23–79) and Galen (129–199).<sup>[3]</sup>

With the advent of the moveable type printing press in the 15<sup>th</sup> century, several so-called “herbals” based on the abovementioned compendia became widely distributed to inform scholars about the identity and proprieties of hundreds of plants.<sup>[4]</sup> As we know today, many of them owe their bioactivity to the alkaloids they contain. However, the idea that a single molecule can produce a determined effect on the body with perfect cause-effect relationship, the very mechanism on which modern medicine is based, was recognized only in the 17<sup>th</sup> century.

Interestingly, many researchers attribute the paradigm shift to Paracelsus (1493–1541), whose iconoclast ideas revolutionized the medieval conceptions of anatomy and physiology passed down by Avicenna and Galen.<sup>[5]</sup> Paracelsus’ teachings entailed that within every object there was a “spirit”, the so-called quintessence, which was ultimately responsible for the experienced effect. This substance was “contained in the mystery of nature, which is termed “purity”, while the remainder of the body, in which the quintessence was trapped, was termed “impurity”.<sup>[6,7]</sup> For example, searching for the spirit of wine, he was able to isolate its “essence”, ethanol, by distillation.<sup>[8]</sup> Although Paracelsus’ alchemy was guided by astrological and mystical theories, with the ultimate goal of freeing substances from their earthly qualities and to elevate them to a spiritual level, his chemical approach to medicine lived on through the centuries. In the late 18<sup>th</sup> century, the concept of “purity” and of “pure substance”, now more aligned with contemporary meaning, together with the advances in analytical chemistry (specifically the concepts of solubility solvent extraction methods), stimulated pharmacists to analyze vegetable drugs in common use at the time.<sup>[9]</sup>

The most popular among them was opium, the dried latex originating from the seed pods of *Papaver somniferum*, which had a reputation as a panacea (Figure 1). It was used against diarrhea for

its constipating effect, was prescribed as a cough suppressant in cases of bronchitis and tuberculosis, and its sedative proprieties were recognized in the treatment of insomnia and mental illness. It had an exquisite capability to relieve pain and also to induce euphoria, relaxation and dream-like states, which propagated its recreational use.<sup>[10]</sup> However, it was also known that its consumption was accompanied with severe addiction and withdrawal symptoms, while higher doses could lead to unconsciousness and death. Nevertheless, the opium trade became a worldwide operation by the end of 18<sup>th</sup> century, and prompted several investigations into its composition with the aim of finding a way to precisely dose the drug to avoid health risks, as well as discover adulterated batches with inferior quality and potency.<sup>[11]</sup>

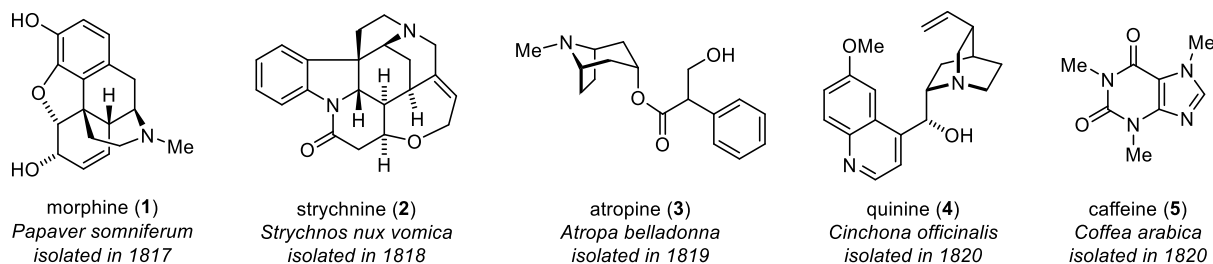


**Figure 1. F. W. A. Sertürner (left), who isolated morphine, the active ingredient from raw opium (middle), the dried latex from the seed pods of *Papaver somniferum* (right).**<sup>[12–14]</sup>

First reports on the successful extraction and purification of opium were carried out between 1803 and 1806 by the pharmacists Friedrich Wilhelm Adam Sertürner (1783–1841), Charles Derosne (1780–1846), Armand Seguin (1767–1835) and Bernard Courtois (1777–1838).<sup>[15]</sup> Although their preparations had similar effect to opium, they did not pose significant advantages and were likely mixtures of compounds. Sertürner continuously experimented with new procedures, and in 1817 he described the successful isolation of a pure compound from raw opium after extraction with hot water and precipitation using ammonia.<sup>[16]</sup> The obtained white crystals were poorly soluble in water, but soluble in alcohol. Most importantly, they reacted with acids to neutralize them and to form fully water-soluble salts. Hence, he had demonstrated the isolation of a compound with “basic” proprieties. Sertürner stated that it was similar to ammonia “in the order of salifiable bases”.<sup>[17]</sup>

This finding was groundbreaking: at the time, only acidic compounds were thought to exist in plants (Sertürner himself isolated meconic acid from *Papaver somniferum* 1805).<sup>[18]</sup> Furthermore, “because experiments on animals do not give exact results”, he also described dosing himself and three young men with the compound.<sup>[19]</sup> The experiment caused confusion and fatigue in the test subjects, one of his friends suffered severe nausea and headaches after being rendered unconscious by the drug for several hours. However, at lower doses Sertürner experienced relief for his toothache, and drowsiness if he doubled the amount of compound.<sup>[20]</sup> He named the compound morphium, in honor of the Greek god of dreams Morpheus, and anticipated that other alkalis were to be found in other plants. In the following years, compounds such as the highly toxic strychnine (2), the cycloplegic atropine (3),

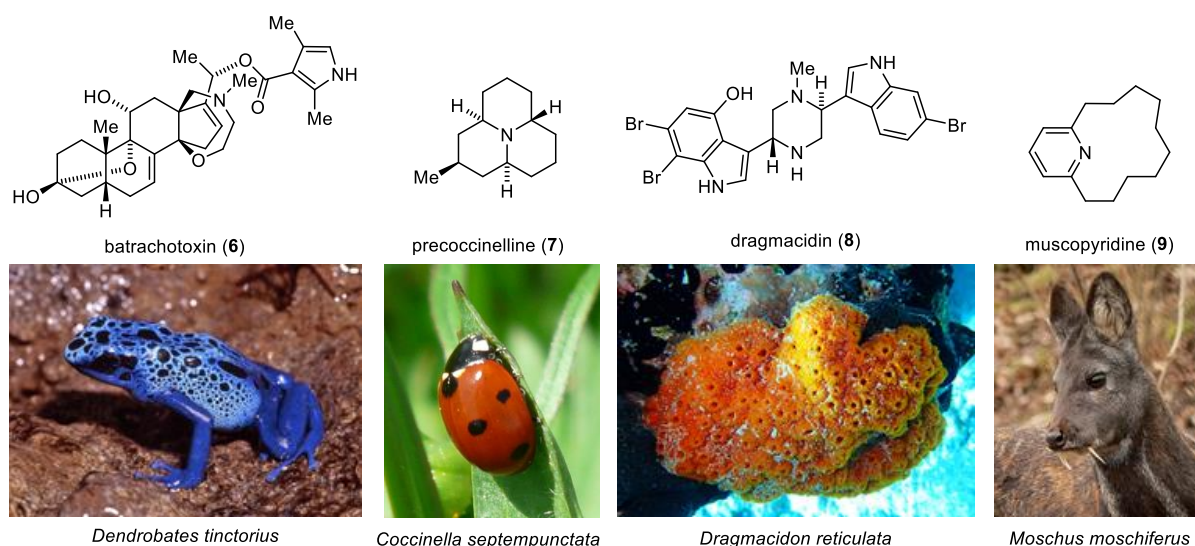
the antimalarial quinine (4), and the stimulant caffeine (5), were isolated in pure form, giving birth to the modern era of alkaloid chemistry, pharmacy, and medicine (Figure 2).<sup>[21]</sup>



**Figure 2. Prominent alkaloids isolated at the beginning of the 19<sup>th</sup> century.**

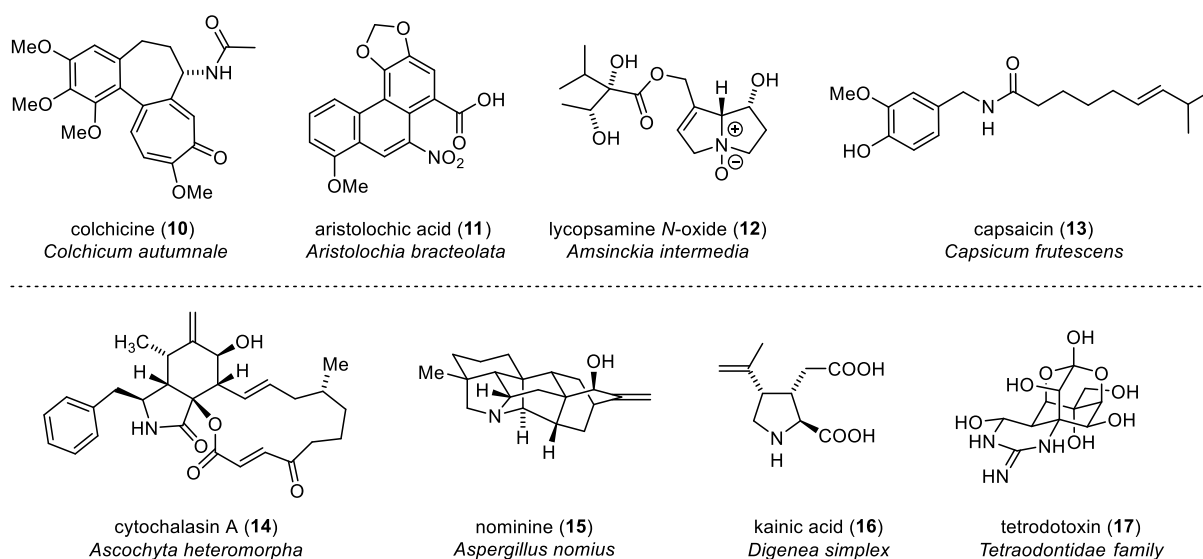
## 1.2. Definition of Alkaloid

The word “alkaloid” was coined in 1818 by the German pharmacist Carl Friedrich Wilhelm Meißner (1792–1853) by merging the Arabic word alkali “*al-quali*”, referring to the calcinated ashes of plants, and the Greek suffix “-oid” meaning “alike”. This name reflects the basic nature of these compounds, but stresses their different chemical composition compared to the known alkalis of the time (essentially potash, soda, and ammonia).<sup>[17]</sup> Anecdotal evidence resulting from the discoveries since 1815 led to the belief that they would only occur in higher plants (see above). Therefore, a first definition of alkaloid was: “the plant component which shows basic properties and a strong biological effect”.<sup>[22]</sup> Over the past decades, as the chemistry of natural products progressed and broadened its hunting ground, it allowed the isolation of compounds with similar properties, but from sources other than plants (Figure 3). For example, the highly toxic batrachotoxin (6) was isolated from the skin of *Dendrobates* “poison dart” frogs, and polycyclic alkaloids such as precoccinelline (7) were found to occur in the ladybug beetle. The cytotoxic dragmacidin A (8) was isolated from a deep sea sponge, and the macrocyclic pheromone muscopyridine (9) is found in the ventral glands of the musk deer.<sup>[23–26]</sup>



**Figure 3. Structurally diverse alkaloids from sources other than plants.**<sup>[27–30]</sup>

Although all the above mentioned molecules react as bases due to the presence of a non-bonding electron pair on the nitrogen atom, other compounds that do not possess such functionality are still classified as alkaloids (Figure 4). Colchicine (**10**) is commonly used for the treatment of gout, and capsaicin (**13**) is responsible for the hot sensation of chili peppers.<sup>[31,32]</sup> Furthermore, biosynthetic processing targeting the nitrogen atom can give rise to oxidized compounds such as the aristolochic acid (**11**), which contains a nitro group, and lycopsamine *N*-oxide (**12**).<sup>[33,34]</sup> However, not all nitrogen-containing metabolites are classified as alkaloids. Early biosynthetic intermediates and primary metabolites indispensable for the organism's survival such as simple amino acids, purines and pyrimidines, as well as complex polypeptides and proteins, do not fall into this category. Nevertheless, amino acids can, through enzymatic processing and the merger of different biosynthetic pathways, give rise to alkaloidal metabolites such as cytochalasin A (**14**), which incorporates phenylalanine into a polyketide-derived alkyl chain. Glutamic acid and a monoterpene unit are the bioprecursors for kainic acid (**16**), while nominine (**15**) contains a C<sub>20</sub>-diterpene scaffold in which a nitrogen atom is introduced.<sup>[29–31]</sup> Furthermore, the notorious pufferfish poison tetrodotoxin (**17**) is likely derived from arginine, although its origin is still under debate despite extensive studies since its isolation in 1909.<sup>[35]</sup>



**Figure 4. Examples of non-basic plant alkaloids (top);**

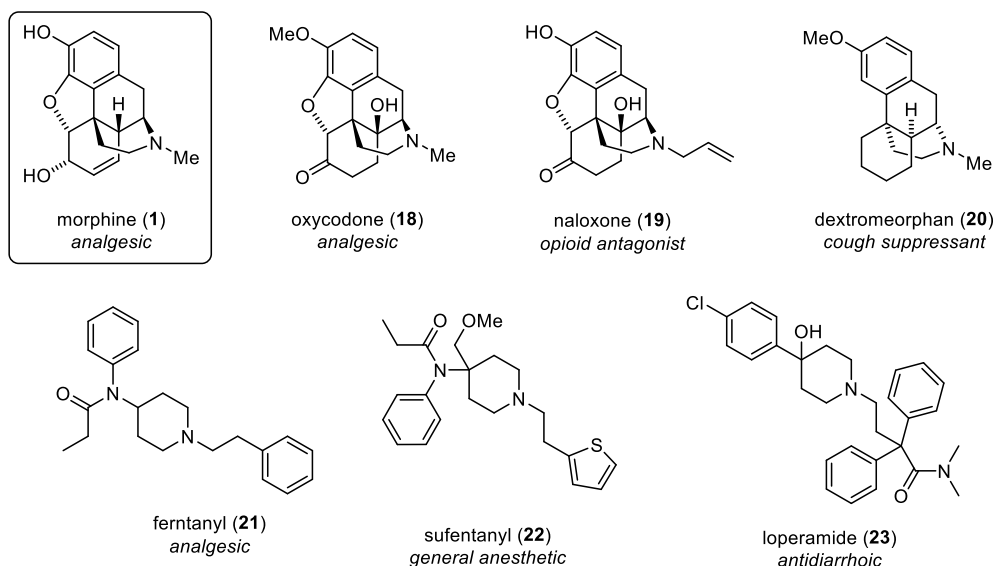
**Alkaloids derived from mixed polyketide or terpenoid biosynthetic pathways (bottom).**

Based on the above examples, structurally diverse compounds originating from all living domains can be classified as alkaloids as long as they contain a nitrogen atom. Despite the fact that this principle might seem vague, if contextualized within the experience accumulated in the past 200 years, a sensible classification of alkaloids is possible. As famously put by natural product isolation chemist Geoffrey Cordell: “You know one when you see one”.<sup>[36]</sup>

### 1.3. Significance and Opportunities

In a series of reviews, Newman and Cragg estimated that about 64% of the all marketed drugs between 1981 and 2014 were either directly or indirectly derived from natural products.<sup>[37]</sup> Although only 6% of these were unmodified natural products, the remaining 58% is made up by: a) semisynthetic modifications of natural products, b) entirely synthetic molecules whose pharmacophore was originally discovered owing to a natural product, or c) synthetic natural product mimics and analogues with the same mode of action as the natural product itself.

The century-long tradition in their use as medicines has been the main source of inspiration for these developments. The advances initiated by the discovery of morphine are a glaring example of this. Not only did it mark the dawn of alkaloid chemistry and their use in therapy, it also sparked several forays into the investigation of its biosynthesis and its structure-activity relationships. It led to the discovery of the complex physiological mechanisms of endogenous opioid regulation and, along with advances in analytical instrumentation and synthetic chemistry, several new drugs. Figure 5 shows how structural modifications (both semi-synthetic and totally synthetic) of morphine (**1**) did lead to several essential therapeutic agents: oxycodone (**18**) is an excellent analgesic that has been widely prescribed in the past 20 years. It also exhibits high addiction potential and often initiates illicit drug abuse.<sup>[38]</sup> The *O*-demethylated and *N*-allylated analogue naloxone (**19**) can counteract its effect, and is a ubiquitous emergency medication in response to an opioid overdose. Removal of functional groups in the optical antipode of morphine leads to the phenantrenoid skeleton of dextromethorphan (**20**), which is used as a cough suppressant and has highly diminished analgesic and anesthetic properties relative to the (*S*)-configured series. Although their structure suggest otherwise, the fully synthetic analogues fentanyl (**21**) and sufentanyl (**22**) are respectively 100 and 500 times more potent than morphine. The former is used for the control of severe pain, and the latter is used as a sedative during general surgical anesthesia.<sup>[39]</sup> The structurally closely related loperamide (**23**) on the other hand, has been used for the past 50 years as an antidiarrhoeic.<sup>[40]</sup> If taken orally, it has very low central nervous system penetration, thereby selectively manifesting only the constipating properties (i.e. promotes intestinal water absorption) of morphine without sedative and euphorizing effects. Most importantly, many other alkaloids have served as inspiration for the development of drugs, either as structural templates or as physiochemical probes. Among them are tubocurarine, atropine, camptothecin, staurosporine, and vinblastine.<sup>[41,42]</sup>



**Figure 5. Morphine and six derivatives with improved therapeutic profiles.**

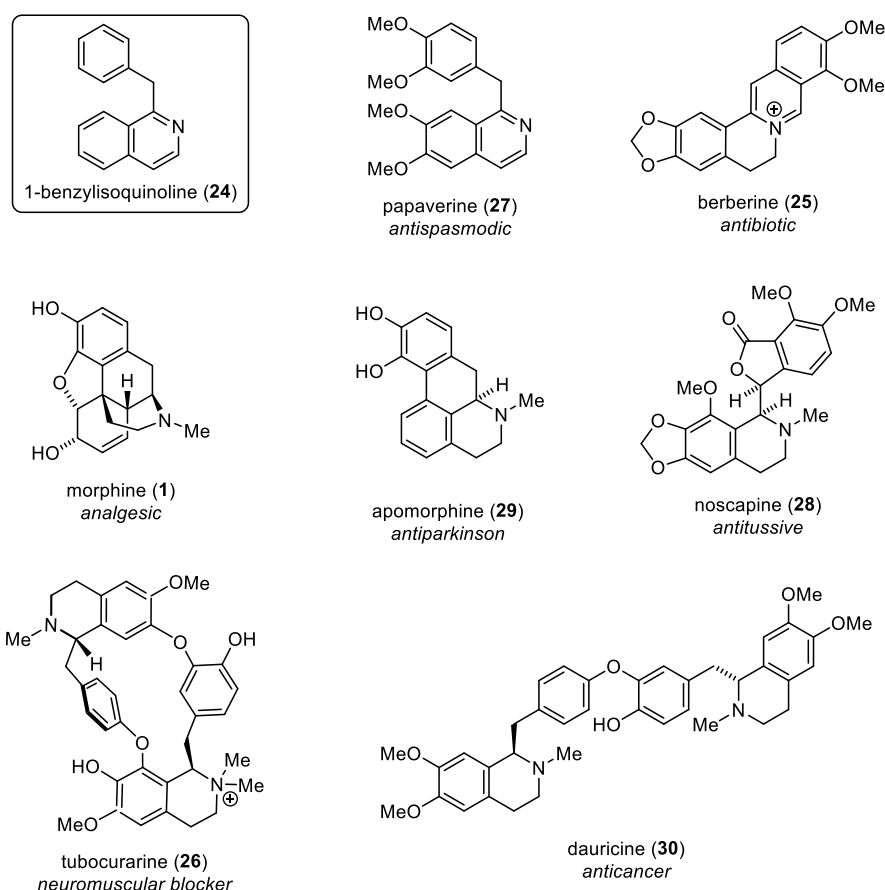
Although alkaloids comprise only about 15% of all the known natural products, they account for 46% of all plant-derived pharmaceuticals.<sup>[43]</sup> While it may be argued that their centennial history and availability have led plants to be investigated in much more detail compared to other sources of natural products (e.g. marine organisms or fungi), this percentage is still remarkably high. Furthermore, a study among the 21.120 known plant-derived alkaloids described in the “Natural Products Alert” database (out of approximately 27000 in total) has shown that only 24% have been evaluated for bioactivity at all.<sup>[44]</sup> Considering these numbers in relation to the historical success of alkaloids in therapy and the nearly limitless possibilities of synthetic chemistry, many more interesting discoveries lie ahead of us.

**Part I:**  
**Total Synthesis and Racemization**  
**of (-)-Sinoracutine**

# 1. Introduction

## 1.1. Structural Variety of Benzyloquinoline Alkaloids

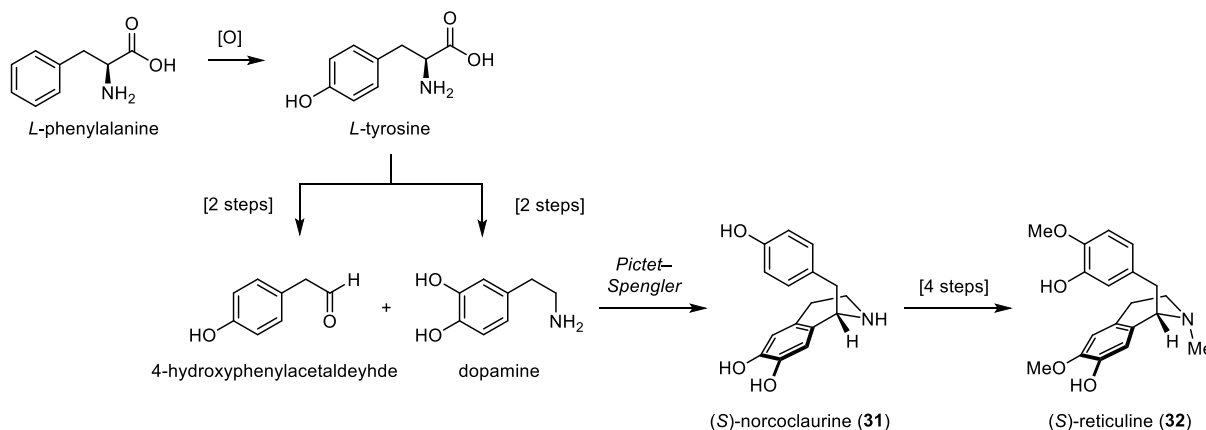
Benzyloquinoline alkaloids (BIAs) are a structurally diverse group of plant metabolites that include more than 2500 structures and share a common benzyloquinoline skeleton (**24**, Figure 6) in different oxidation and substitution patterns.<sup>[45]</sup> Their topological complexity is increased by intramolecular cyclization and ring-opening reactions resulting in diverse structures and biological activity (Figure 6). For example, they include the narcotic analgesic morphine (**1**), the antibiotic berberine (**25**), the muscle relaxants tubocurarine (**26**) and papaverine (**27**), the cough suppressant noscapine (**28**), the antiparkinsonian apomorphine (**29**), and the anticancer drug dauricine (**30**). All these alkaloids stem from the same fundamental biosynthetic pathway using metabolites derived from shikimic acid, and exhibit plant-specific diversity as a result of the enzymatic array present in the producing organism.



**Figure 6. Structural variety of plant-derived alkaloids with benzyloquinoline core structure.**

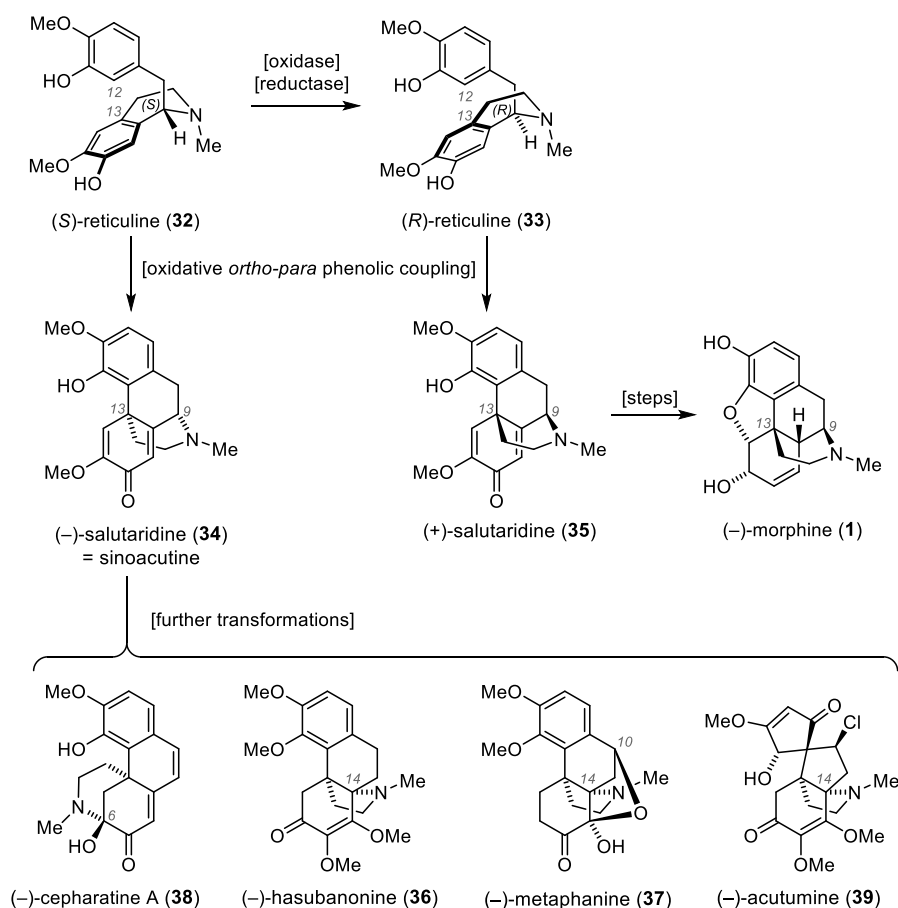
In contrast to woody phenotypes, where the shikimate pathway primarily serves to form cinnamic acids and alcohols necessary for the formation of lignin and condensed tannins, BIAs can be found in herbaceous plant families (Papaveraceae, Ranunculaceae, Berberidaceae and

Menispermaceae). Here, the products of the shikimate pathway are heavily diverted towards phenylalanine, the primary substrate for the biosynthesis of BIAs (Scheme 1). Oxidation of phenylalanine to L-tyrosine followed by oxidative deamination and decarboxylation leads to the formation of 4-hydroxyphenylacetaldehyde. Alternatively, aromatic oxidation of L-tyrosine followed by decarboxylation leads to the synthesis of dopamine.<sup>[46]</sup> Condensation of these two intermediates and Pictet–Spengler reaction forms norcoclaurine (**31**), the first benzyloquinoline alkaloid encountered in the biosynthetic pathway. Four additional enzymatic steps result in the formation of reticuline (**32**), the most important branching point in the formation of several benzyloquinoline alkaloids.



**Scheme 1. Biosynthesis of (*S*)-reticuline from (*S*)-phenylalanine.**

(*S*)-Reticuline (**32**) features an (*S*)-configured benzylic stereocenter at C9. This stereochemical information is retained in further downstream transformations except in cases where aromatization to a benzyloquinoline occurs (e.g. papaverine **27**, Figure 6). In certain plants however, (*S*)-reticuline can be isomerized via oxidation and enzymatic reduction to its antipode (*R*)-reticuline (**33**, Scheme 2).<sup>[47,48]</sup> The dextrorotatory reticuline can also undergo similar downstream transformations with conservation of the benzylic stereocenter (now in (*R*)-configuration). Among the most important enzymatic conversions of reticuline (in either enantiomeric form) is the phenolic *o,o*-coupling between positions 12 and 13 (Scheme 2) that leads to a phenantrenoid ring system. So, starting from (*R*)-reticuline this oxidative coupling forms (+)-salutaridine (**35**), which serves as the gateway to the morphine alkaloids. This pathway is operative in several species of the Papaveraceae family such as *Papaver Somniferum*, which delivers morphine (**1**). Conversely, (*S*)-reticuline can undergo the oxidative coupling to form (–)-salutaridine (**34**), widely referred to as sinoacutine, which is the entry point into the hasubanan alkaloids. This transformation is predominant in the Menispermaceae family, prominently represented by species such as *Sinomenium acutum*. Further plant-specific downstream transformations in either enantiomeric series greatly increase the structural variety of these tetracyclic alkaloids. However, a common denominator is an all-carbon quaternary stereocenter in the benzylic position, from which a two-carbon chain terminating in a nitrogen atom projects. This nitrogen can be connected to the remainder of the skeleton at different positions to provide structures that contain various five- or six-membered heterocycles (Scheme 2).



**Scheme 2. Tetracyclic alkaloids derived from (S)- and (R)-reticuline.**

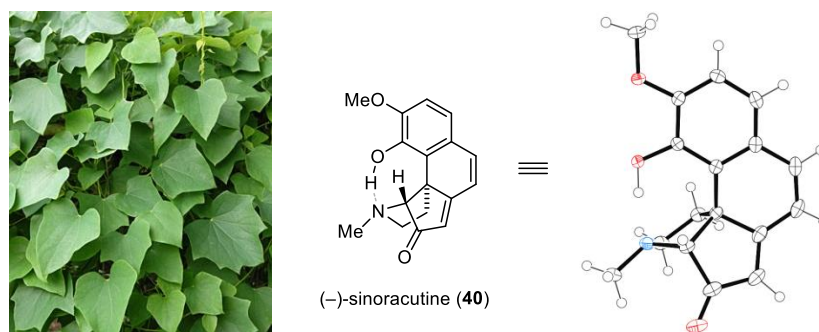
In the morphinan series, exemplified by morphine, the original C–N connection at C9 is preserved to form a piperidine ring. In the hasubanan series, exemplified by hasubanonine (**36**), the nitrogen substituent is moved from the C9 to the C14 position, forming a 5-membered ring and a [4.4.3]aza-propellane.<sup>[49]</sup> Oxidative transformations can lead to hydroxylation at C10 as seen in metaphanine (**37**).<sup>[50]</sup> C–N bond fission can also occur with concomitant ring closure at C6, giving rise to cepharatine-type alkaloids such as cepharatine A (**38**).<sup>[51–53]</sup> Further enzymatic processing of hasubanan-type alkaloids can also lead to skeletal rearrangements and loss of carbon atoms, for example in the acutumine alkaloid series, where the northern aromatic ring is cleaved and rearranged to a cyclopentenone through a Favorskii rearrangement followed by decarboxylation.<sup>[54–56]</sup>

Although most of the skeletal subtypes mentioned above have been known for decades, many of them have succumbed to total synthesis only recently (e.g. acutumine (**39**) was isolated in 1929 and first synthesized in 2009). New compounds belonging to these structural classes are being discovered in present times and continue to capture the attention of organic chemists.<sup>[56,57]</sup> Occasionally, new alkaloids containing unprecedented skeletal subtypes are also discovered. One such alkaloid is sinoracutine, which is the present object of study.

## 1.2. Sinoracutine

### 1.1.1. Isolation, Structure and Absolute Stereochemistry.

In 2009, a structurally unusual alkaloid was isolated from the dried stems of *Sinomenium acutum*. It was termed sinoracutine and was fully characterized by NMR, IR, and mass spectroscopic methods (**40**, Figure 7).<sup>[58]</sup> Additional structural proof was obtained by X-ray crystallographic analysis. Sinoracutine features an unprecedented 6/6/5/5 tetracyclic skeleton with an aromatic ring bearing a methoxy and a hydroxyl group. A benzylic quaternary carbon connects an *N*-methyl pyrrolidine ring to a cyclopentenone moiety which is, in turn, connected to the aromatic ring through a cyclohexene ring. As a result, a highly conjugated  $\pi$ -system ( $\lambda_{n-\pi^*} = 393$  nm) is formed.

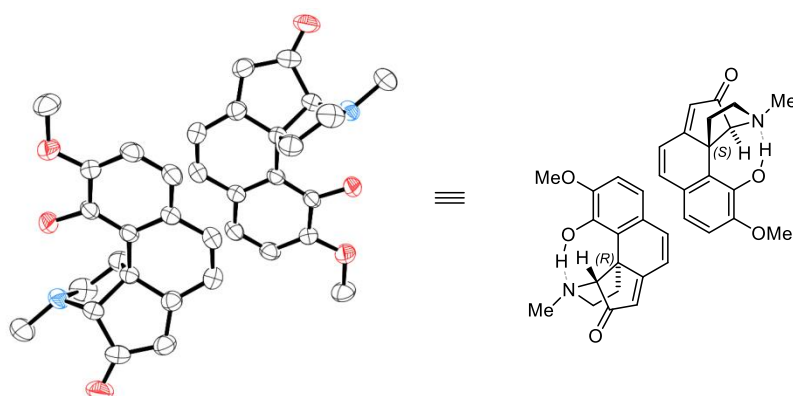


**Figure 7.** Leaves of *Sinomenium acutum* (left); structure and ORTEP plot of sinoracutine (right).

The X-ray structure shows that the phenolic hydroxy group engages in an intramolecular hydrogen bond with the tertiary amine in the pyrrolidine ring. The pyrrolidine ring stands perpendicular to the carbocyclic 6/6/5 system, which assumes a slightly helical conformation. Moreover, the isolated sample exhibited a levorotatory optical power of  $-7.4$  ( $c = 0.35$ ,  $\text{CHCl}_3$ ). In 2010, (-)-sinoracutine was also found to occur in *Stephania cepharantha*, another member of the Menispermaceae family. In this case, the optical rotation was reported to be considerably higher:  $-754.5$  ( $c = 1.14$ ,  $\text{CHCl}_3$ ).<sup>[59]</sup> Interestingly, in 2014, the “optical isomer” of (-)-sinoracutine, namely (+)-sinoracutine, was reportedly isolated from *Sinomenium acutum*.<sup>[60]</sup> The structural assignment was carried out exclusively using X-ray crystallography, and no optical rotation was reported to substantiate this unusual finding.

Interestingly, a closer look at the two available X-ray structures reveals that they depict the same enantiomer, namely the molecule bearing (*R*)-configuration at C13, which was assigned as (-)-sinoracutine by Bao. However, this could be the result of a production error during manuscript preparation. Nevertheless, inspection of the crystallographic data of purported (+)-sinoracutine revealed the centrosymmetric space group *Pbca*, whose unit cell contains both enantiomers. Furthermore, examination of the crystallographic data file for the X-ray structure of purported (-)-sinoracutine also exhibited a centrosymmetric unit cell with both enantiomers present, namely  $P2_1/n$ . It

was erroneously reported in the publication as the chiral space group  $P2_1$ . Taken together, these data suggest that in *Sinomenium acutum* sinoracutine occurs in scalemic form, but that the racemate crystallizes preferentially. Furthermore, the large differences in the absolute values of the optical rotations indicate that (–)-sinoracutine isolated from *Stephania cepharanta* is also scalemic, albeit of higher optical purity than the material derived from *Sinomenium acutum*. This is a very interesting circumstance and hints either to a biosynthetic pathway that operates with imperfect enantioselectivity, which has never been observed in reticuline-derived alkaloids, or to a partial racemization of the natural product either upon storage or isolation. However, no studies to assess the veracity of these hypotheses have been carried out by the isolation teams.

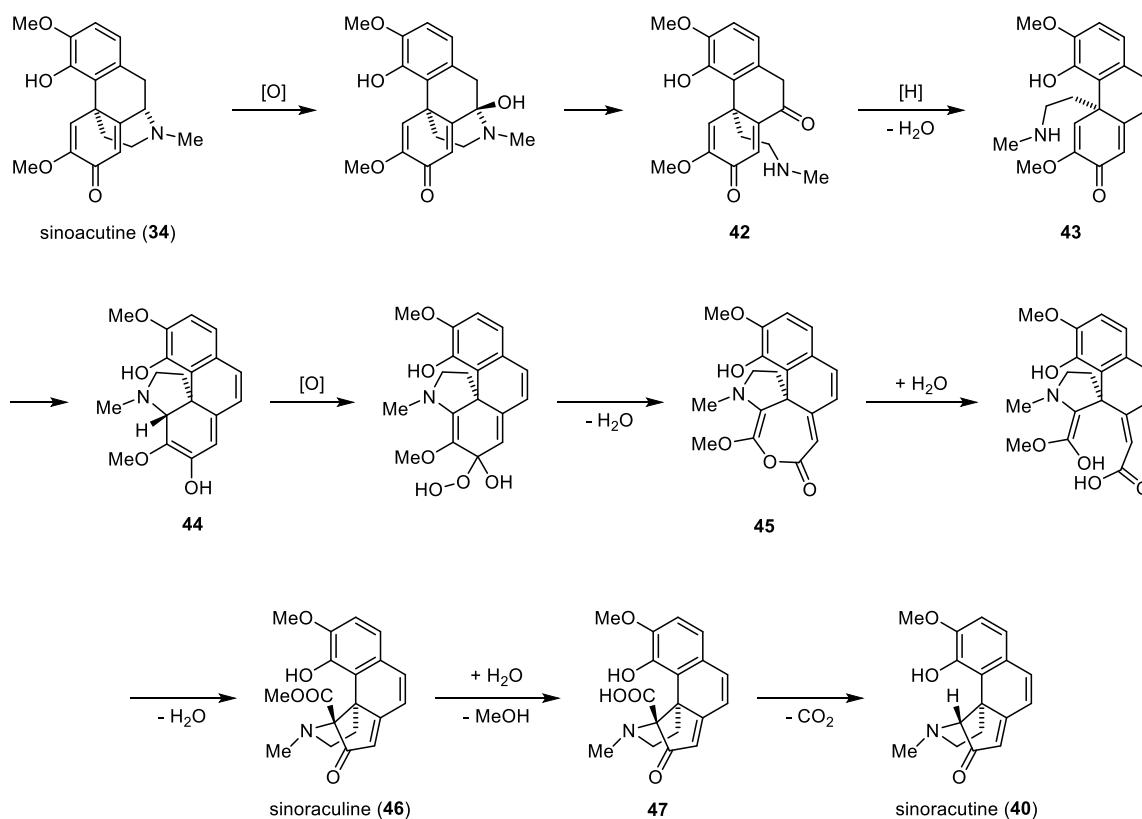


**Figure 8: ORTEP rendering of the crystal structure of sinoracutine reported by Bao, in which the unit cell contains both (*R*)- and (*S*)-sinoracutine (H-atoms omitted for clarity).**

### 1.1.2. Biosynthesis

Several alkaloids that are believed to be biosynthetically related to sinoracutine have been isolated from *Sinomenium acutum* and *Stephania cepharanta*. Although the reported X-ray structures of sinoracutine represent racemic material, the published CD spectrum obtained from a sample originating from *Sinomenium acutum* suggests the configuration at the benzylic quaternary carbon to be (*R*). Thereby in the biosynthesis of sinoracutine, the morphinan-type alkaloid sinoacutine (**34**, Scheme 2) could be enlisted as the first committed biosynthetic intermediate after the phenolic *o,o*-coupling of (*S*)-reticuline. This intermediate has been isolated from both *Sinomenium acutum* and *Stephania cepharanta*.<sup>[59]</sup> A biosynthetic proposal, shown in Scheme 3, was put forth by the isolation team led by Bao. It involves an oxidative deamination of sinoacutine to cleave the piperidine bridge to give ketone **42**.<sup>[58]</sup> Reduction and elimination of the resulting alcohol would give **43** featuring the fully conjugated eastern backbone of sinoracutine. Conjugate addition of the secondary amine to the  $\alpha$ -methoxy enone gives pyrrolidine **44**. Then, Baeyer–Villiger oxidation would furnish 7-membered lactone **45** which upon hydrolysis undergoes a Dieckmann-type condensation to form sinoraculine (**46**), the carboxylated congener of sinoracutine (**40**). This compound was isolated in 2012 from

*Stephania cepharanta* as well and is very likely to occur in *Sinomenium acutum* as well.<sup>[61]</sup> With the 6/6/5/5 system in place, ester hydrolysis to **47** and decarboxylation of the exocyclic carboxylic acid finally results in sinoracutine (**40**).



**Scheme 3. Proposed biosynthesis of sinoracutine (40) from sinoacutine (34).**

### 1.1.3. Bioactivity

*Sinomenium acutum* and *Stephania cepharanta*, from which sinoracutine has been isolated, are commonly used in traditional Chinese medicine for the treatment of inflammatory diseases such as rheumatoid arthritis, neuralgia, and edema.<sup>[62]</sup> A root cause for these diseases is prominently linked to oxidative stress resulting from the surplus of reactive oxygen species ( $\cdot O_2^-$ ,  $\cdot OH$ ,  $H_2O_2$ ) that are either byproducts of cell metabolism or generated by external stimuli (e.g. radiation, metabolism of xenobiotics).<sup>[63]</sup> Increased levels of ROS lead to chronic inflammation that is manifested by the abovementioned pathologies and plays a major role in a variety of other degenerative illnesses including cancer, diabetes, pulmonary hypertension, coronopathy, as well as Alzheimer's or Parkinson's diseases.<sup>[64]</sup>

In this context, sinoracutine has been investigated by Bao and co-workers for its antioxidant and cell-protective effects.<sup>[58]</sup> As a neuronal replacement model, the rat pheochromocytoma derived PC12 cells were treated with hydrogen peroxide to simulate endogenously produced ROS and induce oxidative stress. When PC12 cells were incubated with (–)-sinoracutine prior to exposure to hydrogen peroxide cell viability was increased and the survival rate rose from 59.4% in the control sample to

62.5% in the cultures treated with sinoracutine (1  $\mu\text{M}$ ). These values show the same trend as those obtained for the positive control huperzine A (64.3%, 10  $\mu\text{M}$ ), a lycopodium-type alkaloid first isolated from *Huperzia serrata* which is marketed as a dietary supplement for memory improvement. It has also been demonstrated that it can improve cognitive function and daily living activity in subjects with Alzheimer's disease.<sup>[65,66]</sup>

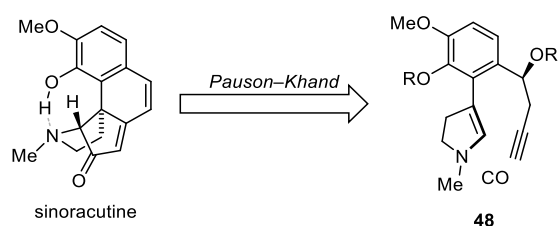
### **1.3. Project Aims**

The unique structure of sinoracutine and the open questions concerning its optical purity, together with the probable biosynthetic and pharmacological implications, prompted us to devise a synthetic route that could access the natural product both in a racemic as well as in enantiopure form. Given its high lipophilicity by virtue of an intramolecular hydrogen bond, that effectively mitigates the polarity of a basic tertiary amine and free phenolic OH, sinoracutine could serve as a template for the synthesis of new neuroprotective agents with central nervous system penetration ability.

## 2. Results and Discussion

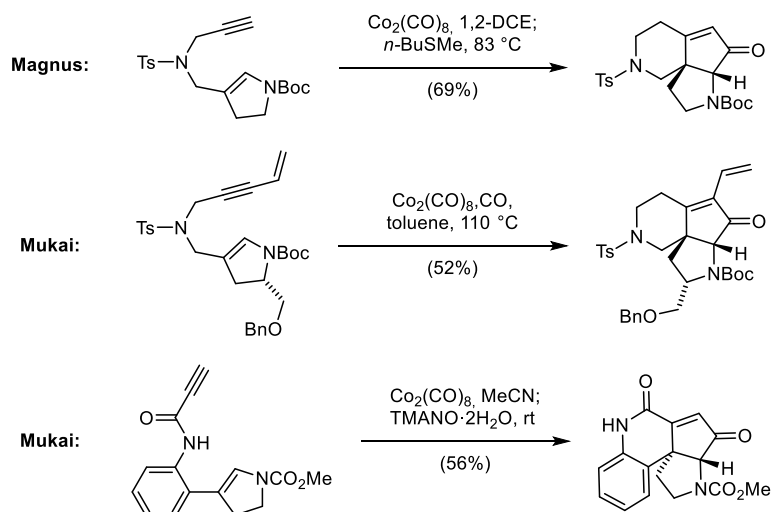
### 2.1. Retrosynthesis

The projected key transformation for the synthesis of sinoracutine was envisaged to be a Pauson–Khand reaction of 3-aryldihydropyrroline **48** bearing a pendant alkyne (Scheme 4). This retrosynthetic disconnection would allow the synthesis of two of the four rings of the natural product in a single step. Completion of the synthesis would then require elimination of the benzylic alcohol.



**Scheme 4. Proposed key disconnection via Pauson–Khand reaction.**

Enamines are known to engage in Pauson–Khand reactions, although the literature precedent is thin (Scheme 5). Interestingly, every example reported employs an *N*-carbamoyl-pyrrolidine and forms a quaternary carbon at the cyclopentenone junction, the same arrangement required for this synthetic plan.<sup>[67–70]</sup>

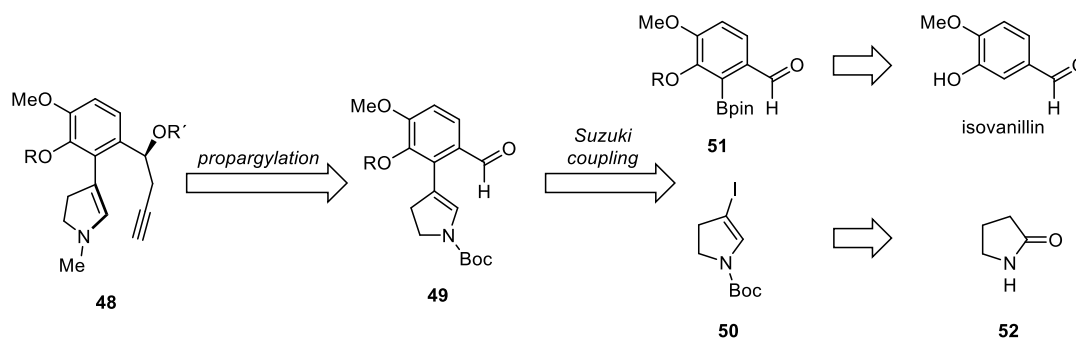


**Scheme 5. Representative Pauson–Khand reaction employing an enamine.**

Additionally, this Pauson–Khand disconnection could enable a stereoselective synthesis of sinoracutine by exploiting the steric bulk of an appropriately protected enantiomerically pure alcohol **48** (Scheme 6). The configuration of the secondary alcohol and its protecting group could conceivably promote the formation of a single diastereoisomer during the Pauson–Khand reaction by imparting a decisive conformational preorganization of the starting enyne. This intermediate could be prepared in enantioenriched form from aldehyde **49**. Several methods for the synthesis of enantiopure **48** could be

employed, such as an asymmetric propargylation of aldehyde **49** or an asymmetric reduction of the ketone derived from racemic secondary alcohol **48** itself.<sup>[71–76]</sup>

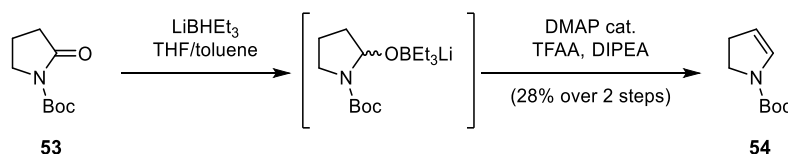
The required aldehyde **49** is the product resulting from a cross-coupling of literature-known iodoenamine **50** with boronate **51**, which is easily derived from inexpensive isovanillin (Scheme 6). Although the steric hindrance of **49** is worthy of note, the coupling of *o,o*-disubstituted arenes has been reported several times in literature, establishing isovanillin as a convenient entry to the aromatic portion of many natural products.<sup>[77–79]</sup> The second building block (**50**) is derived from pyrrolidinone **52** (Scheme 6).<sup>[80]</sup>



**Scheme 6. Retrosynthetic analysis of 1,7-enyne 48.**

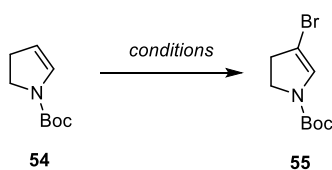
### 2.1.1. Synthesis of the Pyrrolidine Coupling Partner

The synthesis of halogenated enamine **50** commenced from commercially available Boc-protected pyrrolidinone **53** (Scheme 7).<sup>[80]</sup> Reduction of the carbonyl to give a hemiaminal, followed by in situ elimination furnished 2-pyrroline **54**, which was subjected to halogenation conditions.



**Scheme 7. Reduction and elimination of lactam 53.**

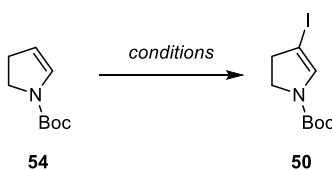
As summarized in Table 1, bromination using NBS in the presence of base gave no reaction, while the use of molecular bromine resulted only in low product yield and partial decomposition of the starting material even at  $-78\text{ }^\circ\text{C}$  (Entries 1 to 3).<sup>[81–83]</sup> The reaction was more successful after the addition of 4 Å MS and bromide **55** could be isolated in moderate yield, provided the reaction was stopped as soon as the disappearance of **54** was observed by TLC (Entry 4).

**Table 1. Bromination of Boc-protected pyrroline 54.**

Entry	Reagent	Base	Solvent	Additive	Temp. (°C)	Time (h)	Yield <sup>a</sup> (%)
1	NBS	Et <sub>3</sub> N	CH <sub>2</sub> Cl <sub>2</sub>	-	rt	16	-
2	Br <sub>2</sub>	Et <sub>3</sub> N	CH <sub>2</sub> Cl <sub>2</sub>	-	0	2	32
3	Br <sub>2</sub>	DIPEA	toluene/CH <sub>2</sub> Cl <sub>2</sub>	-	-78	2	38
4	Br <sub>2</sub>	Et <sub>3</sub> N	CH <sub>2</sub> Cl <sub>2</sub>	4 Å MS	rt	2	47

a) decomposition of **55** was observed;

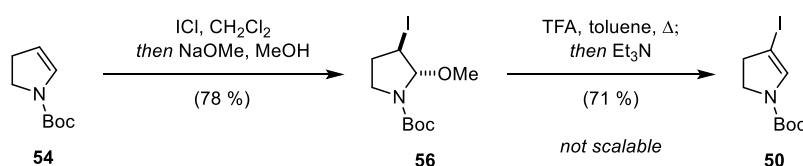
Iodide **50** was synthesized next. Analogous to the synthesis of bromide **55**, a one-step preparation was attempted by direct iodination of **54** (Table 2). Although the reaction is known to proceed on the corresponding Boc-dehydropiperidine, either no conversion at room temperature (Entries 1 to 3) or slow decomposition of the starting material at higher temperatures was observed under the examined conditions (Entries 4 and 5).<sup>[84–86]</sup>

**Table 2. Iodination of Boc-protected pyrroline 54.**

Entry	Reagent	Base	Solvent	Temp. (°C)	Time (h)	Yield <sup>a</sup>
1	NIS	Et <sub>3</sub> N	CH <sub>2</sub> Cl <sub>2</sub>	rt	17	-
2	I <sub>2</sub>	Cs <sub>2</sub> CO <sub>3</sub>	1,4-Dioxane	rt	10	-
3	I <sub>2</sub>	K <sub>2</sub> CO <sub>3</sub>	THF	rt	10	-
4	I <sub>2</sub>	Cs <sub>2</sub> CO <sub>3</sub>	1,4-Dioxane	65	6	-
5	I <sub>2</sub>	K <sub>2</sub> CO <sub>3</sub>	THF	80	6	-

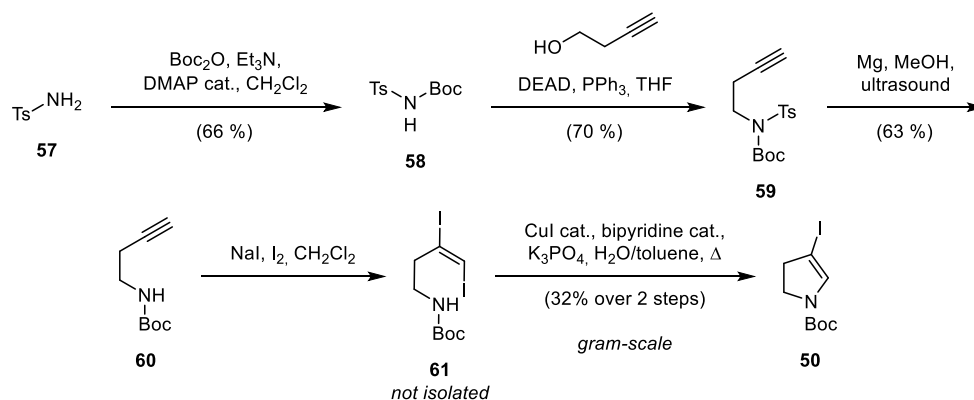
a) decomposition of **54** was observed;

Consequently, we turned to a previously reported two-step preparation of **50** (Scheme 8).<sup>[87]</sup> Pyrroline **54** was treated with ICl in methanol to give addition product **56**. Subsequent acid-mediated elimination of MeOH with citric acid led to decomposition of the starting material. Changing the acid to TFA and reducing its stoichiometry to 0.1 eq provided moderate yields of **50**.<sup>[88]</sup>

**Scheme 8. Synthesis of iodinated pyrroline 50.**

Unfortunately, the TFA-mediated elimination reaction did not prove amendable to scale-up beyond 1.5 mmol. The reaction time increased with scale, which invariably led to lower yields due to

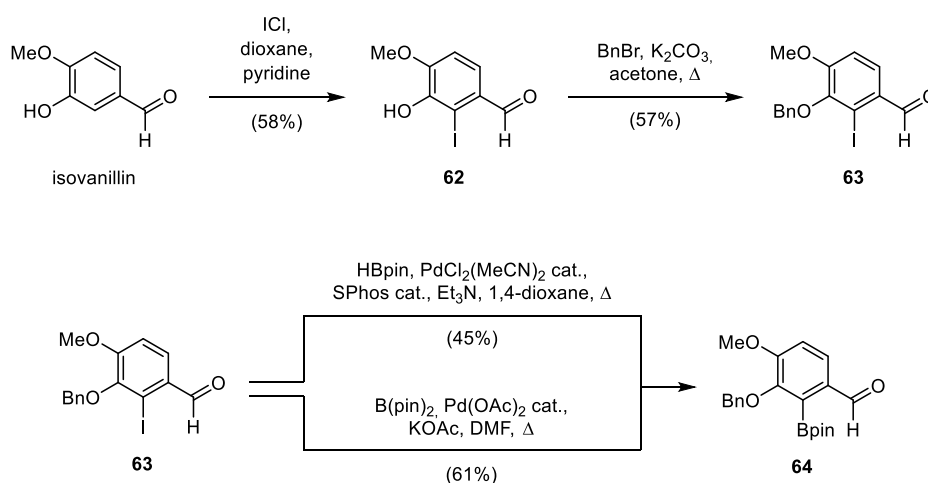
the concomitant decomposition of the product under the reaction conditions. Therefore, the route to iodinated pyrroline was modified (Scheme 9).<sup>[89]</sup> After Boc-protection of *p*-tosyl amine (**57**) and subsequent Mitsunobu reaction of **58** with but-3-yn-1-ol to give **59**, detosylation furnished alkyne **60**. Diiodination and intramolecular Ullman-type reaction afforded vinyl iodide **50**.<sup>[90–93]</sup> With gram-quantities of **50** in hand, we focused on the preparation of different isovanillin type building blocks.



**Scheme 9. Alternative route to iodinated pyrroline 50.**

### 2.1.2. Synthesis of the Aromatic Coupling Partner

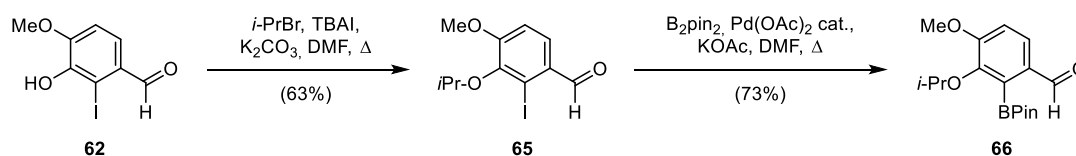
As previously shown by Curran and co-workers, iodide **50** can be successfully coupled to arylboronic esters using the Suzuki reaction.<sup>[87]</sup> Fortunately, the functional group compatibility of this method is excellent and can be carried out in the presence of aldehydes.<sup>[94]</sup> As shown in Scheme 10, iodination of isovanillin followed by benzylation furnished **63**. Borylation using bis(pinacolato)diboron proceeded well, whereas the use of less expensive pinacolborane was found to be slightly inferior.<sup>[78,95,96]</sup>



**Scheme 10. Synthesis of the borylated isovanillin 64.**

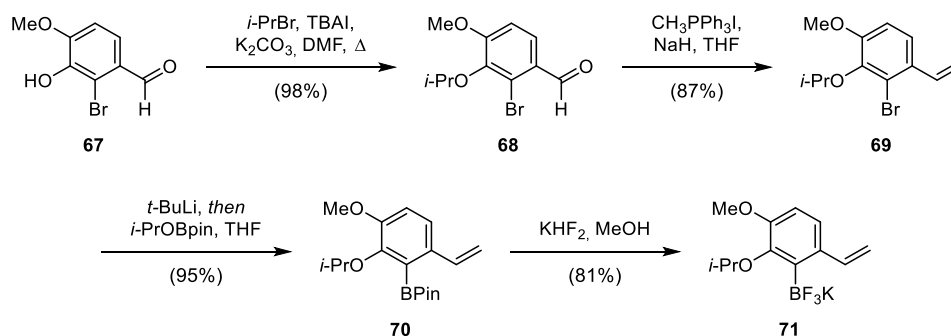
A second substrate, in which the hydroxy group of 2-iodoisovanillin (**62**) was protected as the corresponding isopropoxy ether, was prepared next (**65**, Scheme 11). The isopropoxy group was

chosen because cross-coupling reactions of this building block are known and a selective deprotection of the isopropyl ether in presence of the methyl ether is possible using Lewis acids.<sup>[97]</sup> Using a Miyaura borylation, the corresponding pinacol ester **66** was obtained in good yield (Scheme 11).<sup>[95]</sup>



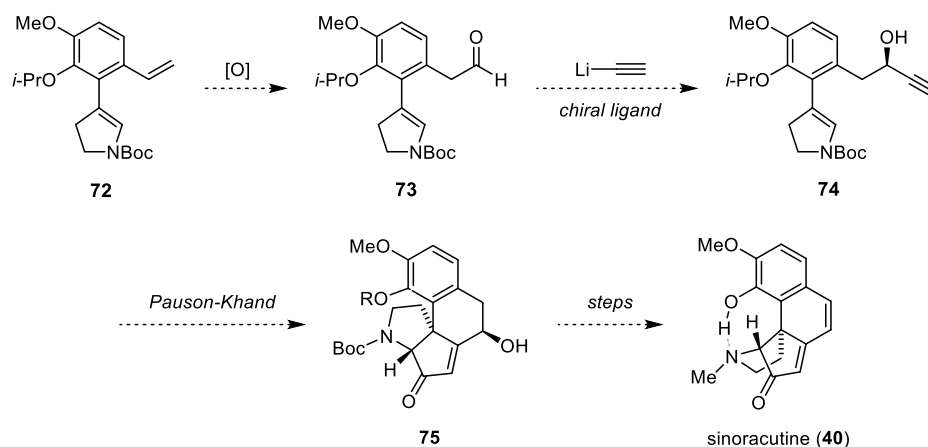
**Scheme 11. Synthetic route to access different isovanillin type building blocks.**

Other borylated building blocks were obtained from 2-bromoisovanillin **67** (Scheme 12): Williamson ether synthesis and olefination delivered styrene **69** which was treated with *n*-BuLi at low temperature followed by addition of isopropoxyboronic acid pinacol ester to give boronic ester **70** in excellent yield. To further increase the options for the cross-coupling reaction, the potassium trifluoroborate analog of **70** was prepared.<sup>[98,99]</sup>



**Scheme 12. Synthetic route to access borylated aromatic building blocks.**

The use of styrene **70** in the cross-coupling could give an alternative precursor for the Pauson–Khand reaction after oxidation to aldehyde **73** and acetylide addition (Scheme 13).<sup>[100–102]</sup> As **74** contains a propargylic alcohol instead of a homopropargylic alcohol (**48**), the effect on diastereoselectivity in the cyclization reaction could be probed.

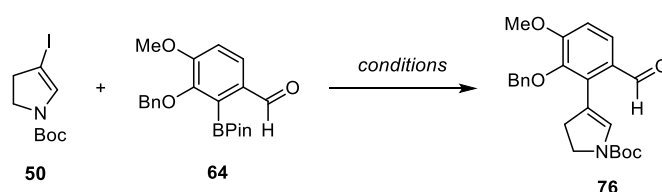


**Scheme 13. Proposed conversion of styrene **72** into sinoracutine.**

### 2.1.3. Cross-Coupling Attempts

With building blocks **50** and **64** in hand, several cross-coupling conditions used successfully for sterically hindered aryl coupling partners as well as for electron-rich heteroatom-bearing vinyl halides were screened.<sup>[87,103–105]</sup> The formation of **76** could not be observed, and protodeborylated **64** was the major byproduct (Table 3). Iodide **50** was completely consumed in every instance, indicating that oxidative addition proceeded well, but the subsequent transmetalation step, even in the presence of alcoholic solvents and water that activate the boron center through formation of a boronate complex, did not proceed at all.<sup>[106]</sup>

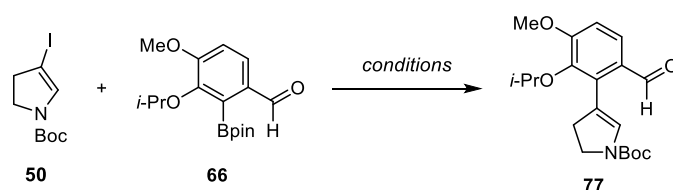
**Table 3. Suzuki cross-coupling of iodoenamine **50** with aldehyde **64**.**



Entry	Pd Source <sup>a</sup>	Ligand <sup>b</sup>	Base	Solvent System	Temp. (°C)	Time (h)	Yield <sup>c</sup>
1	Pd(PPh <sub>3</sub> ) <sub>4</sub>	-	K <sub>2</sub> CO <sub>3</sub>	Benzene/MeOH/H <sub>2</sub> O	70	14	-
2	Pd(PPh <sub>3</sub> ) <sub>4</sub>	-	Na <sub>2</sub> CO <sub>3</sub>	Toluene/EtOH	105	16	-
3	Pd(PPh <sub>3</sub> ) <sub>4</sub>	-	KOH	Toluene/H <sub>2</sub> O	105	16	-
4	Pd(dppf)Cl <sub>2</sub>	-	K <sub>2</sub> CO <sub>3</sub>	DMSO	80	16	-
5	Pd(OAc) <sub>2</sub>	CyJohnPhos	Ba(OH) <sub>2</sub>	1,4-Dioxane	80	2	-
6	Pd(OAc) <sub>2</sub>	CyJohnPhos	K <sub>3</sub> PO <sub>4</sub>	1,4-Dioxane	80	2	-
7	Pd(OAc) <sub>2</sub>	SPhos	K <sub>3</sub> PO <sub>4</sub>	Toluene/H <sub>2</sub> O	80	5	-

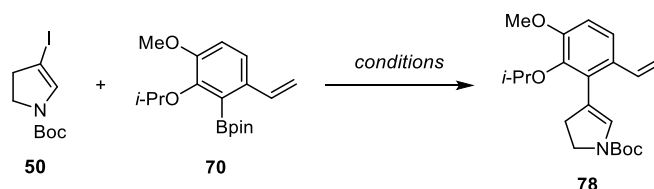
a) 10 mol%; b) 20 mol%; c) decomposition of **50** observed, protodeboronation of **64** as determined by LCMS.

Similar results were observed in the attempted coupling of iodoenamine **50** with isopropoxy-protected aldehyde **66** (Table 4) as well as styrene **70** (Table 5). Using potassium tetrafluoroborate **71** in conjunction with iodide **50** was not successful either (Table 6).<sup>[107–110]</sup> These results suggest that steric hindrance, and not electronic bias, might be the culprit for the failure of this cross-coupling. Additionally, since **66** had been reported to undergo cross-coupling with aryl bromides, the halogenated enamine seems to be the main problem for the unsuccessful reaction outcomes. In fact, using this building block, only one example of cross-coupling can be found in literature.<sup>[87]</sup>

**Table 4. Suzuki cross-coupling of iodoenamine 50 with isopropoxy-protected aldehyde 66.**

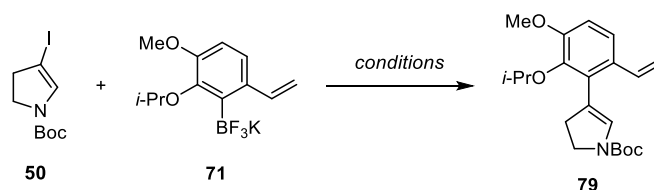
Entry	Pd Source <sup>a</sup>	Ligand <sup>b</sup>	Base	Solvent System	Temp (°C)	Time (h)	Yield <sup>c</sup>
1	Pd(PPh <sub>3</sub> ) <sub>4</sub>	-	K <sub>2</sub> CO <sub>3</sub>	benzene/MeOH/H <sub>2</sub> O	70	14	-
2	Pd(PPh <sub>3</sub> ) <sub>4</sub>	-	Na <sub>2</sub> CO <sub>3</sub>	toluene/EtOH	105	16	-
3	Pd(PPh <sub>3</sub> ) <sub>4</sub>	-	K <sub>3</sub> PO <sub>4</sub>	1,4-dioxane	80	7	-
4	Pd(OAc) <sub>2</sub>	CyJohnPhos	Ba(OH) <sub>2</sub>	1,4-dioxane	60	48	-
5	Pd(OAc) <sub>2</sub>	SPhos	K <sub>3</sub> PO <sub>4</sub>	toluene/H <sub>2</sub> O	100	5	-

a) 10 mol%; b) 20 mol%; c) decomposition of **50** observed, protodeboronation of **66** as determined by LCMS.

**Table 5. Suzuki cross-coupling of iodoenamine 50 with isopropoxy-protected styrene 70.**

Entry	Pd Source <sup>a</sup>	Ligand <sup>b</sup>	Base	Solvent System	Temp (°C)	Time (h)	Yield <sup>c</sup>
1	Pd(PPh <sub>3</sub> ) <sub>4</sub>	none	K <sub>2</sub> CO <sub>3</sub>	benzene/MeOH/H <sub>2</sub> O	70	14	-
2	Pd(PPh <sub>3</sub> ) <sub>4</sub>	none	Na <sub>2</sub> CO <sub>3</sub>	toluene/EtOH	105	16	-
3	Pd(PPh <sub>3</sub> ) <sub>4</sub>	none	K <sub>3</sub> PO <sub>4</sub>	1,4-dioxane	80	16	-
4	Pd(OAc) <sub>2</sub>	CyJohnPhos	Ba(OH) <sub>2</sub>	1,4-dioxane	80	16	-
5	Pd(OAc) <sub>2</sub>	SPhos	K <sub>3</sub> PO <sub>4</sub>	toluene/H <sub>2</sub> O	100	5	-

a) 10 mol%; b) 20 mol%; c) decomposition of **50** observed, protodeboronation of **70** as determined by LCMS.

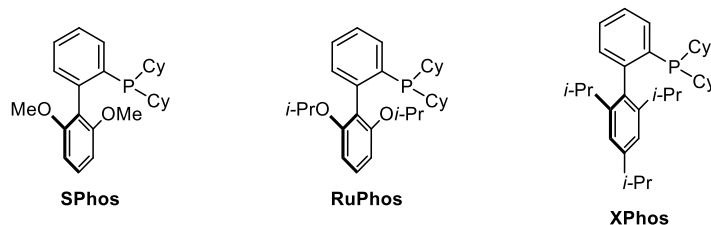
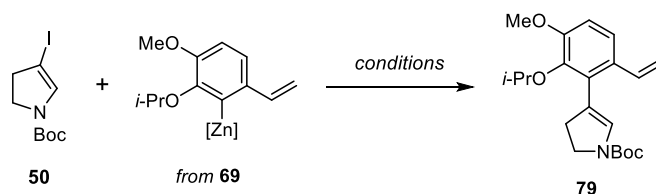
**Table 6. Suzuki cross-coupling of iodoenamine 50 with potassium tetrafluoroborate 71.**

Entry	Pd Source <sup>a</sup>	Ligand <sup>b</sup>	Base	Solvent System	Temp (°C)	Time (h)	Yield <sup>c</sup>
1	Pd(dppf)Cl <sub>2</sub>	none	Ag <sub>2</sub> O	toluene	100	18	-
2	PdCl <sub>2</sub> (PhCN) <sub>2</sub>	none	K <sub>2</sub> CO <sub>3</sub>	1,4-dioxane/H <sub>2</sub> O	80	16	-
3	PdCl <sub>2</sub>	none	K <sub>2</sub> CO <sub>3</sub>	1,4-dioxane/H <sub>2</sub> O	80	16	-
4	Pd(PPh <sub>3</sub> ) <sub>4</sub>	none	K <sub>2</sub> CO <sub>3</sub>	DMF/H <sub>2</sub> O	100	12	-
5	Pd(dppf)Cl <sub>2</sub>	none	CsCO <sub>3</sub>	toluene	100	18	-
6	Pd(OAc) <sub>2</sub>	PPh <sub>3</sub>	K <sub>3</sub> PO <sub>4</sub>	THF/H <sub>2</sub> O	60	24	-

a) 10 mol%; b) 20 mol%; c) decomposition of **50** observed, protodeboronation of **71** as determined by LCMS.

We attempted to overcome the lack of reactivity in the cross-coupling by substituting the boronic ester-based Suzuki reaction with a Negishi reaction of organozinc reagents, which have been shown to participate in cross-coupling reactions even at ambient temperature.<sup>[111]</sup> Styrene **69** was chosen as the substrate this study. After Br/Li exchange with *t*-BuLi, lithiated **69** was treated with ZnCl<sub>2</sub> and subjected to various Pd-mediated cross-coupling protocols (Table 7).<sup>[112]</sup> Although **50** was completely consumed in the reaction, no desired product was formed, and the main side-product was dehalogenated **69** resulting from protolysis of the intermediate organozinc species.

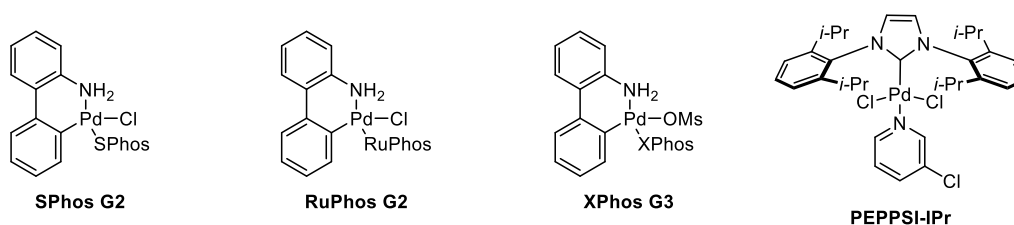
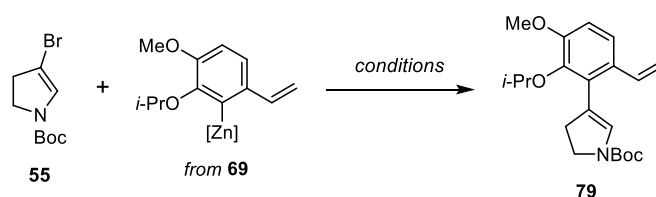
**Table 7. Negishi cross-coupling of **50** and **69** to form enamine **79**.**



Entry	Pd Source <sup>a</sup>	Ligand <sup>b</sup>	Solvent	Temp (°C)	Time (h)	Yield <sup>c</sup>
1	Pd <sub>2</sub> dba <sub>3</sub>	SPhos	THF	60	16	-
2	Pd <sub>2</sub> dba <sub>3</sub>	RuPhos	THF	60	16	-
3	Pd <sub>2</sub> dba <sub>3</sub>	XPhos	THF	60	16	-

a) 5 mol%; b) 20 mol%; c) decomposition of **50**, protodemetalation of **69** observed.

Next, the brominated enamine was examined as cross-coupling partner, as it was believed to be less reactive than the iodide which was evidently too unstable under the reaction conditions (see Table 8, next page). Despite using the very general systems reported by Buchwald and co-workers, the Negishi cross-coupling reaction of **55** and **69** did not lead to product formation.<sup>[113,114]</sup> Examination of H<sub>2</sub>O-quenched reaction aliquots after 2 h indicated only the Br/H exchange of **69** and traces of **55**. After 16 h, **55** was completely consumed and only the Br/H exchange product could be identified in the crude reaction mixture. These disappointing results on the cross-coupling of halogenated enamines **50** and **55** led us to reverse the polarity of the coupling partners.

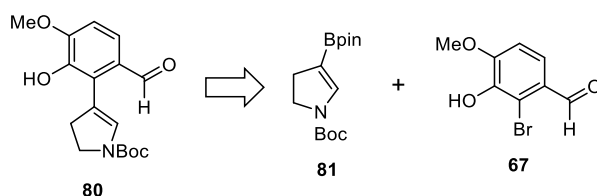
**Table 8. Negishi cross-coupling reaction of bromoenamine **55** and styrene **69**.**

Entry	Pd Source <sup>a</sup>	Ligand <sup>b</sup>	Solvent	Temp. (°C)	Time (h)	Yield <sup>c</sup>
1	SPhos G2	SPhos	THF	60	16	-
2	XPhos G3	XPhos	THF	60	16	-
3	RuPhos G2	RuPhos	THF	60	16	-
4	PEPPSI-IPr	none	THF	60	16	-
5	Pd(P( <i>o</i> -tolyl) <sub>3</sub> ) <sub>2</sub> Cl <sub>2</sub>	none	THF	60	16	-
6	Pd(dppf)Cl <sub>2</sub>	none	THF	60	16	-

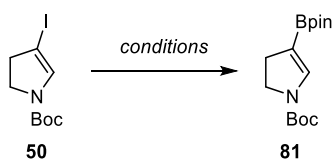
a) 10 mol%; b) 10 mol%; c) decomposition of **55**, protodemetalation of **69** observed.

#### 2.1.4. Alternative Fragment Union

Placement of the halogen on the isovanillin building block, rendered electron-poor by the presence of the aldehyde moiety, should favor oxidative addition during the Pd-catalyzed cross-coupling process (Scheme 14). In fact, similar compounds have shown to engage in cross-coupling reactions.<sup>[115–117]</sup> The electron-rich nature of the enamine should facilitate the introduction of a boron atom and the subsequent Suzuki cross-coupling. Furthermore, we decided to employ unprotected 2-bromo isovanillin **67** in the cross-coupling. The benzyl group was left out to remove any possible steric hindrance during oxidative addition.

**Scheme 14. Envisioned building blocks for the formation of aldehyde **80**.**

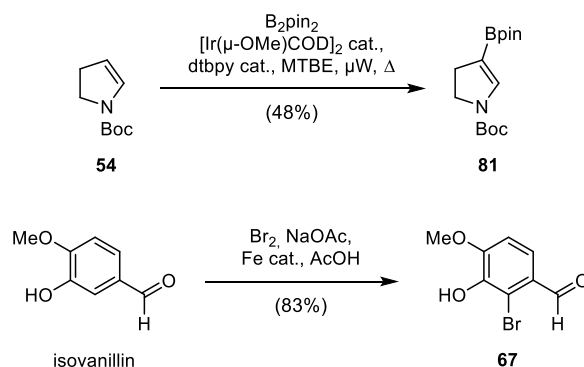
For the synthesis of borylated enamine **81** conditions similar to the Pd-catalyzed borylation of isovanillin were investigated.<sup>[118–121]</sup> As shown in Table 9, all the conditions tested resulted in degradation of vinyl iodide **50**

**Table 9. Formation of borylated enamine **81** using palladium catalysis.**

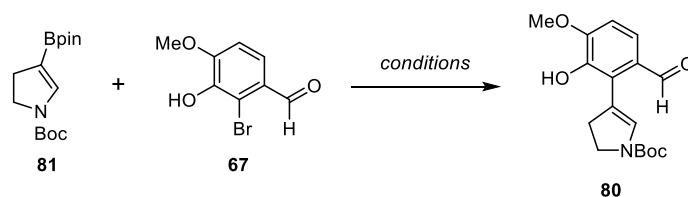
Entry	Pd Source <sup>a</sup>	Ligand <sup>b</sup>	Base	Solvent	Temp. (°C)	Time (h)	Yield <sup>d</sup>
<b>1</b> <sup>c</sup>	Pd(OAc) <sub>2</sub>	CyJohnPhos	Et <sub>3</sub> N	1,4-dioxane	80	1	-
<b>2</b> <sup>d</sup>	Pd(dppf)Cl <sub>2</sub>	none	K <sub>2</sub> CO <sub>3</sub>	1,4-dioxane	80	16	-
<b>3</b> <sup>d</sup>	Pd(dppf)Cl <sub>2</sub>	none	KOAc	DMSO	80	3	-
<b>4</b> <sup>d</sup>	Pd(OAc) <sub>2</sub>	none	KOAc	DMF	80	5	-

**a)** 10 mol%; **b)** 20 mol%; **c)** HBPIn was used as the boron source; **d)** B<sub>2</sub>pin<sub>2</sub> was used as the boron source; **d)** decomposition of **50** was observed.

Therefore, a microwave accelerated C–H borylation of enamine **54** was investigated using the conditions reported by Steel and co-workers for the borylation of pyrrole (Scheme 15).<sup>[122]</sup> This reaction formed the desired borylated enamine in moderate yield and gram-quantities of **81** could be synthesized using sequential reactions on 1 mmol scale. Brominated isovanillin **67** was prepared following a literature procedure (Scheme 15).<sup>[123]</sup>

**Scheme 15. Synthesis coupling partners with reversed polarity.**

With borylated enamine **81** and bromoisovanillin **67** in hand, another screening of conditions for the Suzuki cross-coupling was performed using catalytic systems known to engage boronic esters containing free phenols (Table 10).<sup>[52,82,124]</sup> While reactions carried out at 100 °C resulted in complex mixtures (Entries 1 and 2), a reaction carried out at room temperature did not show appreciable conversion (Entry 3). The use of microwave irradiation, which is routinely used to accelerate challenging Suzuki coupling, also resulted in a complex mixture of products despite the moderate temperature and short reaction time (Entries 5 and 6).<sup>[125,126]</sup>

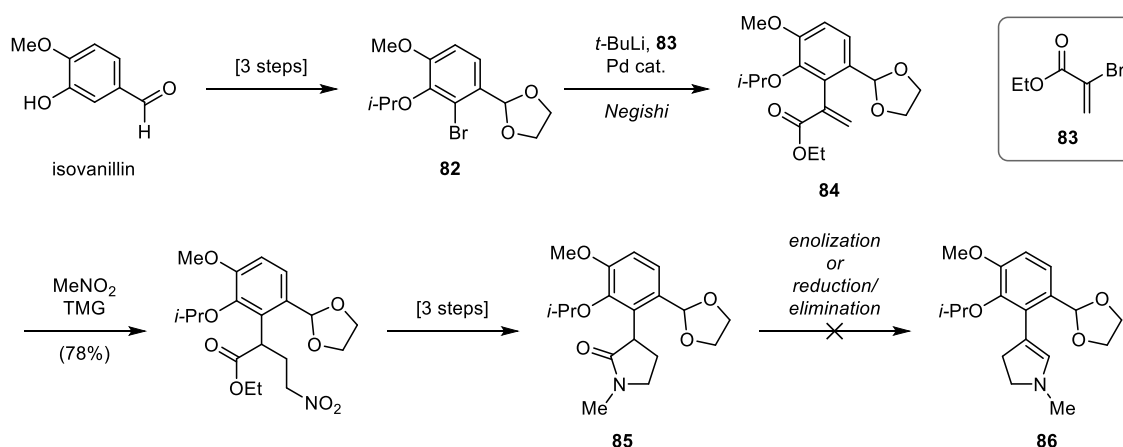
**Table 10. Suzuki cross-coupling of boronate **81** and bromoisovanillin **67**.**

Entry	Pd Source <sup>a</sup>	Ligand <sup>b</sup>	Base	Solvent System	Temp. (°C)	Time(h)	Yield <sup>d</sup>
1	Pd(PPh <sub>3</sub> ) <sub>4</sub>	none	K <sub>2</sub> CO <sub>3</sub>	1,4-dioxane/H <sub>2</sub> O	100	2	-
2	Pd(PPh <sub>3</sub> ) <sub>4</sub>	none	K <sub>3</sub> PO <sub>4</sub>	DMF	100	18	-
3	Pd(OAc) <sub>2</sub>	SPhos	K <sub>3</sub> PO <sub>4</sub>	DMC	r.t.	48	-
4	Pd(OAc) <sub>2</sub>	SPhos	K <sub>3</sub> PO <sub>4</sub>	<i>n</i> -BuOH/H <sub>2</sub> O	100	1	-
5 <sup>c</sup>	Pd(OAc) <sub>2</sub>	SPhos	K <sub>3</sub> PO <sub>4</sub>	MTBE/H <sub>2</sub> O	100	0.15	-
6 <sup>c</sup>	Pd(dppf)Cl <sub>2</sub>	none	KOH	MTBE/H <sub>2</sub> O	80	0.15	-

a) 10 mol%; b) 20 mol%; c) reaction performed in the microwave; d) decomposition of **81** was observed.

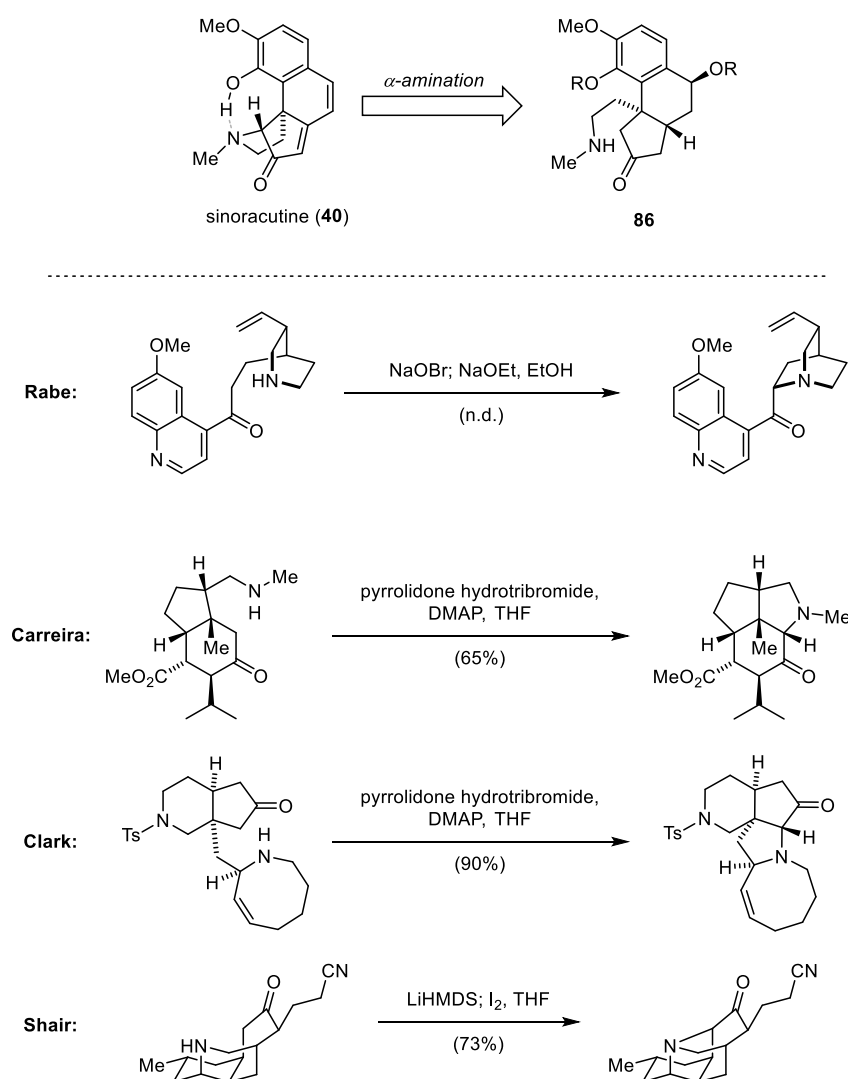
### 2.1.5. Stepwise Construction of the Pyrroline Ring

Our unsuccessful attempts at a convergent cross-coupling of an aromatic building block with a pyrroline unit prompted us to devise a stepwise construction of the pyrroline ring from a substrate that already incorporates the *o,o*-disubstituted aromatic ring. Previous work conducted by Andreas Bellan showed that that a high-yielding Negishi coupling of acetal **82** with bromoacrylate **83** could afford  $\alpha,\beta$ -unsaturated ester **84** (Scheme 16).<sup>[127]</sup> Subsequent 1,4-addition of nitromethane followed by reduction and cyclization gave lactam **85** after *N*-methylation. Efforts to reduce this compound to the desired enamine **86**, or effect enolization to form a vinyl triflate or vinyl phosphonate, remained unsuccessful. Steric hindrance due to the flanking *ortho*-substituents on the aromatic ring severely obstructs productive reactivity of the five-membered ring and forced us to revise our synthetic approach.

**Scheme 16. Stepwise construction of 3-aryl substituted lactam **85**.**

## 2.2. Revised Retrosynthesis

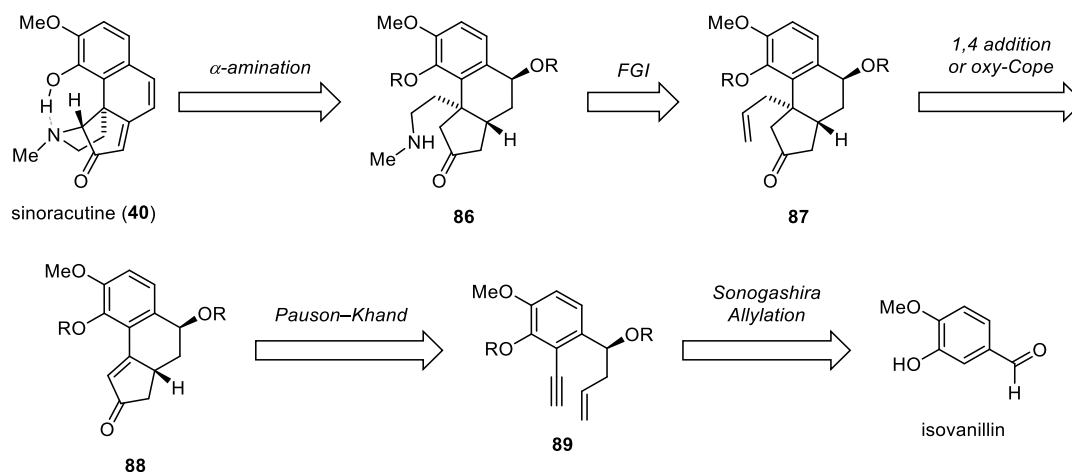
Failure to synthesize a pyrrolidine ring in the sterically hindered position of an *o,o*-disubstituted arene led us to modify our synthetic approach and focus on the introduction of a less bulky substituent, thereby postponing the formation of the pyrrolidine ring at a later stage in the synthesis. As shown in Scheme 17, the ring closure was planned to be performed on ketone **86** bearing a pendant amine following treatment with an amination agent. Pertinent examples for this reaction, that constitutes a formal umpolung of the  $\alpha$ -position of a ketone, have been employed in total synthesis (Scheme 17).<sup>[128–134]</sup>



**Scheme 17. Proposed  $\alpha$ -amination of **86** and relevant literature precedents.**

Formation of the crucial benzylic quaternary stereocenter could be achieved by a [3,3]-sigmatropic rearrangement, i.e. the oxy-Cope rearrangement, in which alkene **87** could be formed in high stereoselectivity after the addition of allylmagnesium bromide to ketone **88** (Scheme 18).<sup>[56]</sup> Alternatively, a 1,4-addition of an allyl or vinyl nucleophile could allow the introduction of the C2-unit after appropriate functional group manipulations. In any case, the required tricycle bearing  $\alpha,\beta$ -unsaturated ketone (**88**) would result from a Pauson–Khand reaction of enyne **89** that could be

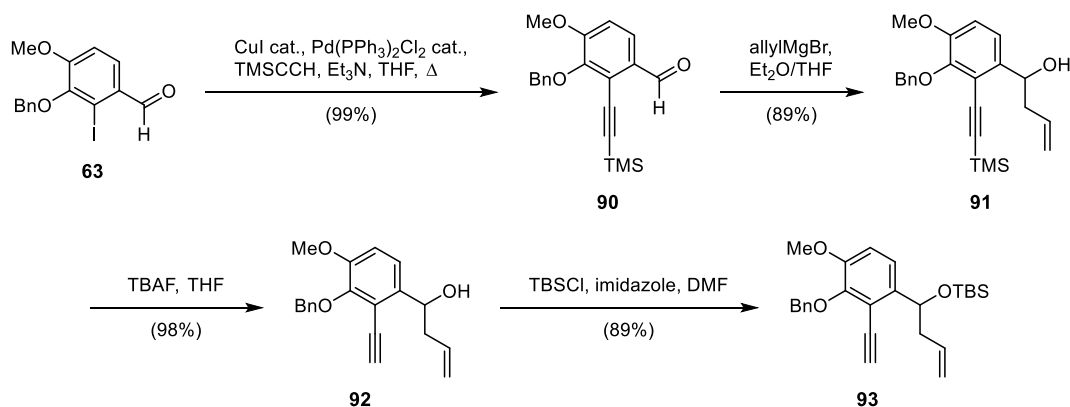
accessed from isovanillin following Sonogashira coupling and allylation. As put forth in Section 2.1, the allylic alcohol may serve as a stereocontrolling element to enable a diastereoselective Pauson–Khand reaction and therefore an enantioselective synthesis of sinoracutine. The rigidity of the formed tricycle should allow for the stereoselective introduction of the allyl group required for the projected oxy-Cope rearrangement and stereochemical relay from **88** to the final product.<sup>[135]</sup>



**Scheme 18. Full retrosynthetic plan for sinoracutine starting from isovanillin.**

### 2.2.1. Synthesis of the Isovanillin Portion

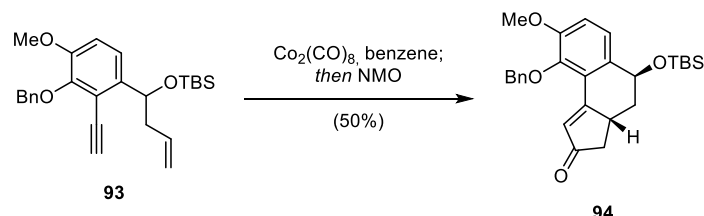
Isovanillin was regioselectively iodinated to give **62**, whose free hydroxyl group was benzylated to afford **63** (shown in Scheme 10).<sup>[136]</sup> Sonogashira cross-coupling of **63** with trimethylsilyl-acetylene and subsequent allylation with allylmagnesium bromide afforded enyne **91** (Scheme 19).<sup>[137]</sup> Cleavage of the terminal TMS group with  $K_2CO_3$  in MeOH proceeded smoothly on small scale, but side products and lower yields were observed during scale-up. Instead, deprotection of **91** using TBAF proceeded in excellent yield and Pauson–Khand precursor **93** was obtained after treatment with TBSCl and imidazole.



**Scheme 19. Synthesis of TBS-protected enyne 93 from protected iodoisovanillin 63.**

## 2.2.2. Pauson–Khand Reaction

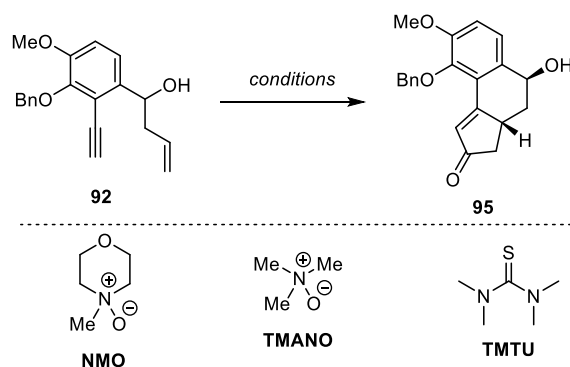
Addition of solid  $\text{Co}_2(\text{CO})_8$  to **93** in  $\text{CH}_2\text{Cl}_2$  led to the formation of an alkyne cobalt complex within 4 hours as determined by TLC analysis. Then, slow addition of NMO delivered the desired tricyclic **94** in moderate yield and as a single diastereoisomer (Scheme 20). The relative configuration could be assigned on the basis of NOE data.



**Scheme 20.** Pauson–Khand reaction to form the 6,6,5-carbocycle (**94**) of sinoracutine.

Assuming that the steric demand of the TBS group might be responsible for the moderate yields, the reaction was performed with free benzylic alcohol **92**. As seen in Table 11, application of the same reaction conditions resulted in only 24% yield (Entry 1). By modification of the reaction parameters, we determined that oxidatively promoted reactions at ambient temperature performed better than thermally promoted cyclizations. Between the oxidative protocols, TMANO consistently showed better results than NMO (Entry 3). Among the thermal protocols, the reaction with  $\text{Co}_2(\text{CO})_8$  in substoichiometric amounts (0.5 eq.) using TMTU as an additive under CO atmosphere (balloon) gave the best result (Entry 9).<sup>[138]</sup>

**Table 11.** Conditions for the Pauson–Khand reaction with free benzylic OH-group.

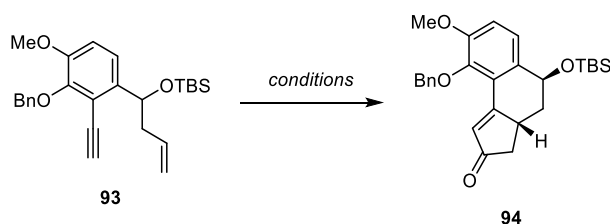


Entry	Solvent	$\text{Co}_2(\text{CO})_8$ (eq.)	Oxidant/Additive	Temp. (°C)	Time (h)	Yield (%)
1	benzene	1.2	NMO (3 eq.)	0 to r.t.	16	24
2	THF	1.2	NMO (3 eq.)	0 to r.t.	16	40
3	benzene	1.2	TMANO (3 eq.)	0 to r.t.	16	52
5	THF	1.2	TMANO (3 eq.)	0 to r.t.	16	53
4	benzene	1.2	TMANO (3 eq.)	70	16	31
6	benzene	1.2	none	70	24	35
7	benzene	1.2	TMTU (3 eq.)	70	24	37
8	benzene	1.2	TMTU (6 eq.)	70	24	24
9 <sup>a</sup>	benzene	0.5	TMTU (3 eq.)	70	24	46

a) under CO pressure (balloon).

Next, reaction conditions for the TBS protected enyne **93** were examined (Table 12). In accordance with the previous results, TMANO proved to be more efficient than NMO, and the reaction showed solvent-specific variability, with DCE being the solvent of choice (Entry 9). Thermal promotion also afforded the desired product in good yields (Entry 12), and commonly employed additives such as *n*-BuSMe, celite or 4 Å molecular sieves did not provide benefit (Entry 13 to 15).<sup>[70,139]</sup> Consistently higher yields were achieved compared to precursor **92** bearing a free benzylic OH group. Upon scale-up, we observed decreased yields (cf. Entries 9 and 10), presumably due to the insolubility of TMANO in DCE and inefficient mixing of the reaction partners. Therefore, continuous and vigorous stirring had to be ensured, and was best realized using round bottom flasks no larger than 250 mL equipped with appropriately sized stirring bars (3 cm length). Scale-up reactions were performed in parallel batches and could be combined for work-up and purification to allow reliable material throughput. Also, the use of a freshly opened bottle of  $\text{Co}_2(\text{CO})_8$  was crucial to achieve reproducibly high yields, whereas bottles that had been opened for longer than 1 week resulted in yield drops in the range of 20 to 25%, despite using every precaution to prologue its shelf-life (storage under a blanket of argon in a  $-25\text{ }^\circ\text{C}$  freezer).

**Table 12. Conditions for the Pauson–Khand reaction with benzylic TBS ether **93**.**

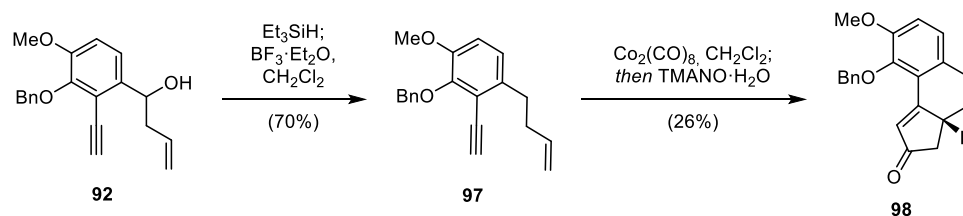


Entry <sup>a</sup>	Solvent	$\text{Co}_2(\text{CO})_8$ (eq.)	Oxidant/Additive	Temp. ( $^\circ\text{C}$ )	time (h)	Yield (%)
1	benzene	1.2	TMANO (3 eq.)	0 to rt	16	41
2	benzene	1.2	NMO (3 eq.)	0 to rt	16	31
3	THF	1.2	TMANO (3 eq.)	0 to rt	16	58
4	THF	1.2	NMO (3 eq.)	0 to rt	16	16
5	THF	1.2	TMANO (6 eq.)	0 to rt	16	50
6	$\text{CH}_2\text{Cl}_2$	1.2	TMANO (3 eq.)	0 to rt	16	50
7	$\text{CH}_2\text{Cl}_2$	1.2	TMANO (6 eq.)	0 to rt	16	66
8	$\text{CH}_2\text{Cl}_2$	1.2	NMO (6 eq.)	0 to rt	16	50
9	DCE	1.2	TMANO (6 eq.)	0 to rt	16	75
10 <sup>b</sup>	DCE	1.2	TMANO (6 eq.)	0 to rt	16	56
11	toluene	1.2	TMANO (6 eq.)	0 to rt	16	68
12	toluene	1.2	-	rt to 70	24	61
13	toluene	1.2	BuSMe (3.5 eq.)	rt to 70	24	60
14	toluene	1.2	Celite (10x w/w)	rt to 70	24	64
15	toluene	1.2	4 Å MS (10x w/w)	rt to 70	24	27

a) all reactions performed on 0.2 mmol scale except Entry 10; b) carried out on 1 mmol scale.

To probe if the presence of coordinating or bulky functionalities had detrimental effect on the yield of the reaction, the TBS ether was removed via ionic reduction and the resulting product **97** was

submitted to Pauson–Khand reaction conditions (Scheme 21). A low yield of cyclization product **98** was obtained, even lower than the reaction of **92** bearing the free benzylic hydroxyl group. This suggests that while a possible coordination site is advantageous to the reaction, a high steric demand of the benzylic position in proximity of the alkene is crucial for optimal reactivity by enforcing a favorable conformation between the alkyne-Cobalt complex and the approaching alkene.<sup>[140]</sup>

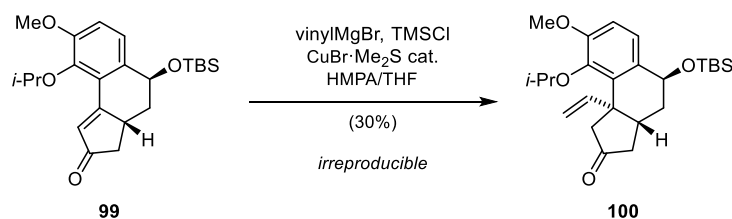


**Scheme 21.** Removal of benzylic alcohol followed by Pauson–Khand reaction.

## 2.2.3. Introduction of the Quaternary Stereocenter

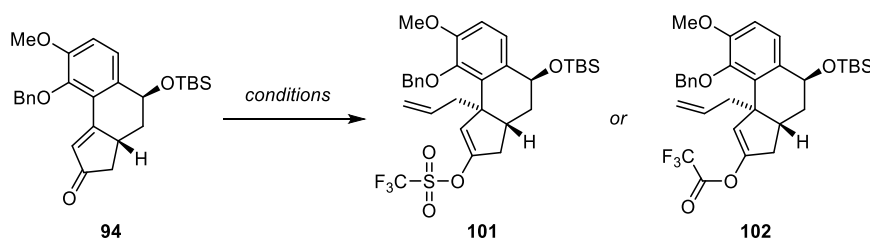
### 2.2.3.1. 1,4-Addition

Having constructed the tricyclic framework of sinoracutine, we proceeded with the introduction of the last ring. The first strategy pursued was analogous to the Mulzer–Trauner morphine synthesis, i.e. vinylcuprate addition to an enone.<sup>[141]</sup> Andreas Bellan showed that Pauson-Khand product **99** could undergo 1,4-addition with vinylmagnesium bromide, but despite several optimization attempts, the reaction was low-yielding and irreproducible, and plagued by the concomitant formation of 1,2-addition product (Scheme 22).<sup>[127]</sup> Therefore, the addition of ionic vinyl- or allylmetal species was not further investigated.



**Scheme 22:** Previously investigated 1,4-addition with vinylcopper reagent.

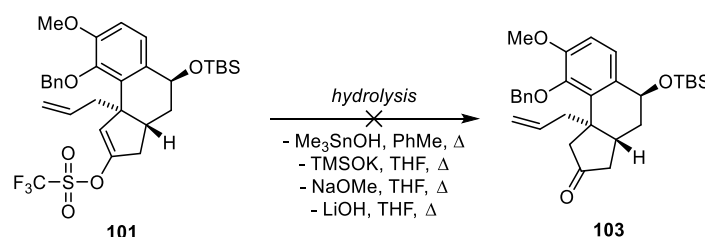
Next, the conjugate addition of allyltributylstannane to enone **94** was investigated in collaboration with Till Reinhardt according to the procedure developed by Trauner and coworkers.<sup>[142]</sup> They reported the successful 1,4-addition to cyclic enones upon prior electrophilic activation of the carbonyl with trifluoroacetic anhydride (TFAA) or trifluoromethanesulfonic anhydride (Tf<sub>2</sub>O).<sup>[143]</sup>

**Table 13. Conditions examined for the 1,4-allylation and enolate trapping.**

Entry	Activating agent	Allyltributyltin	Additives	Solvent	Yield ( <b>101</b> or <b>102</b> ) <sup>a</sup>
1	TFAA (1.2 eq.)	1.2 eq.	DTBP, 4 Å MS	CH <sub>2</sub> Cl <sub>2</sub> /MeCN = 1/1	no reaction
2	TFAA (1.2 eq.)	1.2 eq.	DTBP, 4 Å MS	CH <sub>2</sub> Cl <sub>2</sub>	no reaction
3	Tf <sub>2</sub> O (1.2 eq.)	1.4 eq.	DTBP, 4 Å MS	CH <sub>2</sub> Cl <sub>2</sub> /MeCN = 1/1	<b>101</b> , 47%
4	Tf <sub>2</sub> O (1.2 eq.)	1.4 eq.	DTBP, 4 Å MS	CH <sub>2</sub> Cl <sub>2</sub>	<b>101</b> , 26%

DTBP = 2,6-di-tert-butylpyridine; **a**) stereochemistry of the addition not determined.

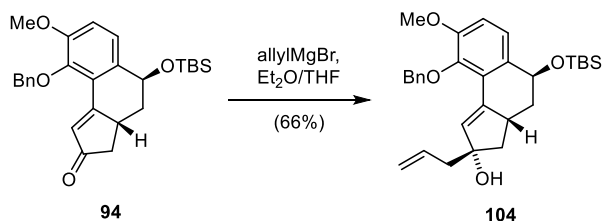
As shown in Table 13, TFAA was not successful in activating enone **94**, and neither the enol trifluoroacetate **102** nor its desired hydrolysis product **103** could be observed. On the other hand, the reaction with Tf<sub>2</sub>O furnished a single intermediate, tentatively assigned as vinyl triflate **101**. Attempted hydrolysis of this compound to the desired ketone **103** could not be effected under several base-mediated conditions (Scheme 23).<sup>[144,145]</sup> Therefore, we explored an alternative strategy that would yield intermediate **103** by intramolecular allyl transfer – namely the anionic oxy-Cope reaction.

**Scheme 23. Attempted hydrolysis of presumed enol triflate to ketone 103.**

### 2.2.3.2. Oxy-Cope Rearrangement

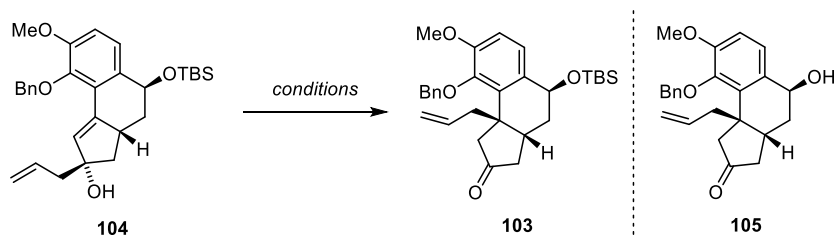
The oxy-Cope reaction has been successfully employed in various alkaloid syntheses that bear a benzylic quaternary stereocenter.<sup>[55,56,105]</sup> In contrast to the neutral variant of the reaction that requires prolonged times at elevated temperature (> 200 °C), the [3,3]-sigmatropic rearrangement of 1,5-diene alkoxides proceeds at very high rates due to the weakening effect by the alkoxide anion on the adjacent carbon-carbon bond.<sup>[146]</sup> This allows the reaction to be performed at cryogenic temperatures within a few hours. A literature review reveals a strong counterion dependence (order of reactivity: K>Na>Li), and that further acceleration can be achieved by addition of appropriate ionophores to generate a more reactive “naked” anion. Additionally, a model study by Evans and co-workers illustrated that maximum yield and rate improvements were achieved using no more than 3.0 eq. of 18-crown-6.<sup>[147]</sup> With these considerations in mind, treatment of **94** with allylmagnesium bromide afforded allylic alcohol **104**, the precursor for the rearrangement, as a single diastereomer (Scheme

24). It proved unstable to silica gel chromatography and was subjected to anionic oxy-Cope reaction conditions immediately after aqueous workup.



**Scheme 24. Preparation of tertiary allylic alcohol 104.**

**Table 14. Conditions applied for the anionic oxy-Cope rearrangement of 104.**



Entry <sup>a</sup>	Base	Additive	Temp. (°C)	Time (h)	Yield (%)
1 <sup>b</sup>	KO <i>t</i> -Bu (2.0 eq.)	18-crown-6 (2.0 eq.)	0 to rt	3	10
2	KHMDS (3.0 eq.)	18-crown-6 (3.0 eq.)	0 to rt	3	41
3	KHMDS (3.0 eq.)	18-crown-6 (3.0 eq.)	-5 to rt	3	48
4	KHMDS (1.5 eq.)	18-crown-6 (1.5 eq.)	-5 to rt	3	43
5	LiHMDS (1.5 eq.)	12-crown-4 (1.5 eq.)	0 to rt to 60	48	-
6	NaHMDS (1.5 eq.)	18-crown-5 (1.5 eq.)	0 to rt to 60	48	-

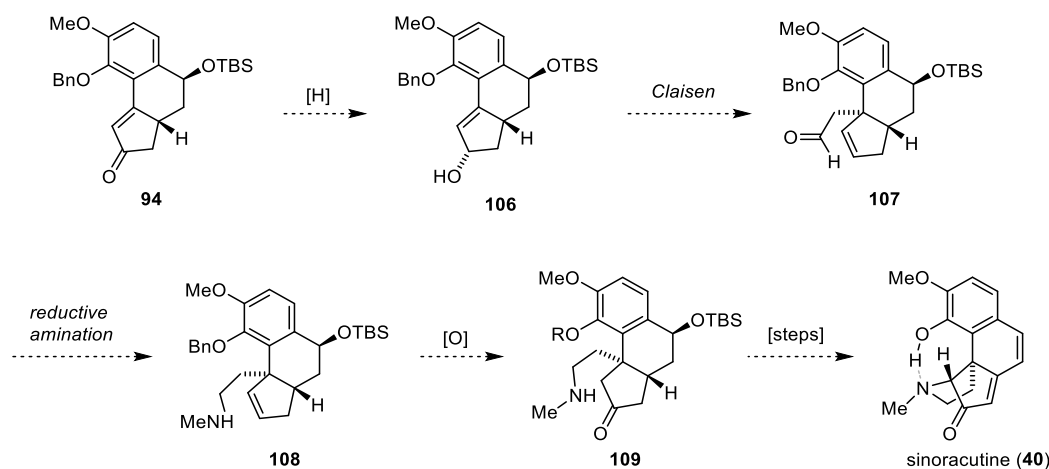
a) all reactions conducted in THF    b) TBS-cleavage product **105** was isolated in 46% yield.

As seen in Table 14, employing KO*t*-Bu as base afforded the desired product **103** only in poor yield. Additionally, cleavage of the TBS group was observed. Under the reaction conditions and in the presence of the crown ether, the naked *t*-butoxy anion was able to attack and cleave the silyl ether. Hence, we decided to employ the non-nucleophilic base KHMDS and were able to improve the yield to 48% (Entry 3). While no TBS-cleavage product was observed in this case, the starting material was completely consumed and gave rise to non-specific decomposition products as evidenced by darkening of the reaction mixture. By comparison, the corresponding lithium and sodium HMDS-bases with the appropriately sized crown ether ionophores were investigated (Entries 5 and 6). Even after prolonged reaction times, no rearrangement product was observed, and the starting allylic alcohol slowly decomposed. Due to these problems and the limited options for improvement, primarily due to the instability of alcohol **103**, we decided to investigate an alternative approach.

### 2.2.3.3. Claisen Rearrangement

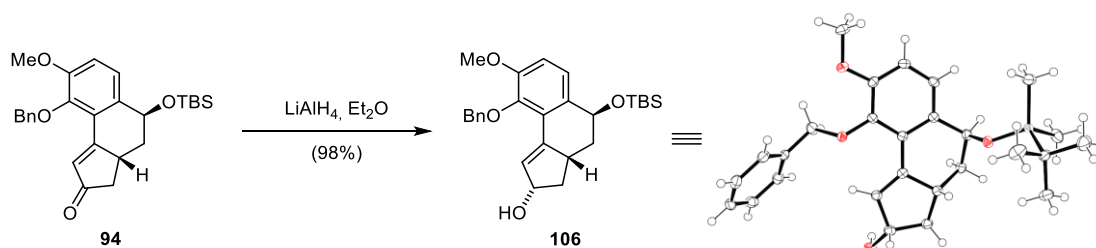
The required allylic alcohol for the introduction of the quaternary carbon at C13 by Claisen rearrangement was envisaged to be accessed diastereoselectively by reduction of **94** (Scheme 25). The

reaction was expected to be highly diastereoselective, as the addition of allylMgBr had proceeded in a completely diastereoselective manner (Scheme 24). After successful rearrangement, the last ring could be formed by cyclization of the pendant amine onto cyclopentene **108** (Scheme 25).



**Scheme 25.** Envisaged synthesis of sinoracutine via Claisen rearrangement of allyl alcohol **106**.

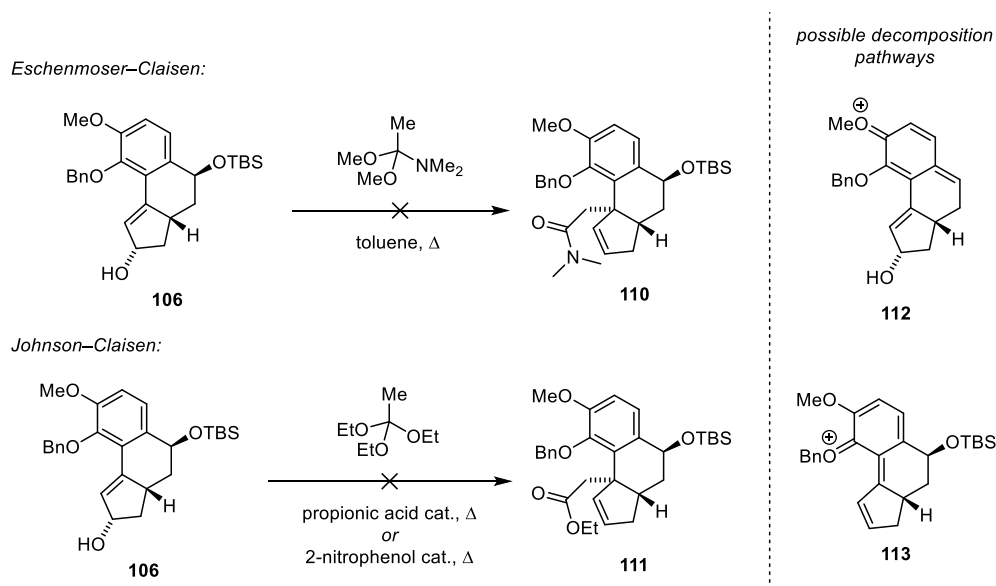
Reduction of **94** was successful using different reducing agents ( $\text{NaBH}_4/\text{CeCl}_3$ , DIBALH), but  $\text{LiAlH}_4$  provided the cleanest reaction profile and most convenient workup, merely necessitating a filtration of the reaction mixture over a pad of silica after quenching with  $\text{H}_2\text{O}$  and  $\text{NaOH}$  (Scheme 26). As anticipated, **106** was formed as a single diastereomer and its relative stereochemistry could be established through X-ray crystallographic analysis by Nynke Vepřek.



**Scheme 26.** Diastereoselective reduction of enone **94** and X-ray structure of allylic alcohol **106**.

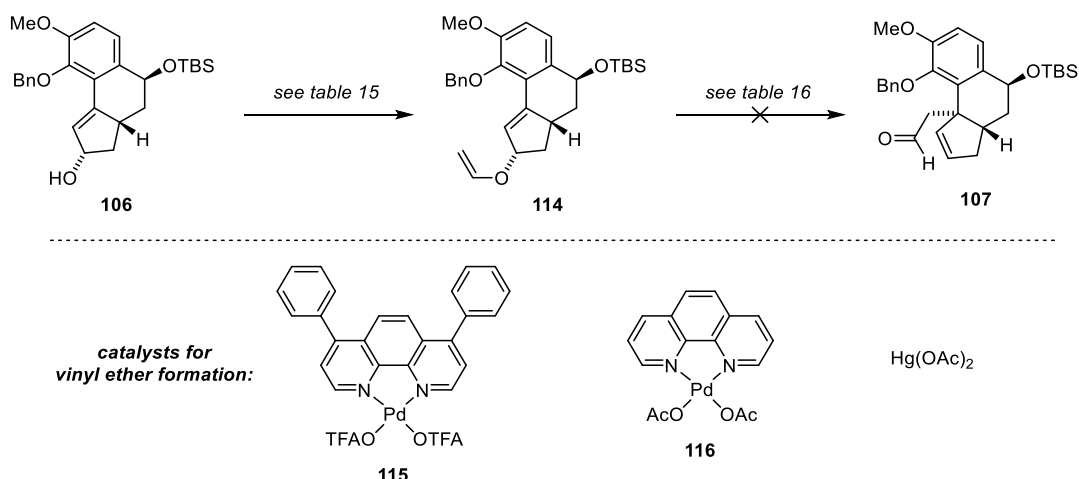
With gram-quantities of alcohol **106** in hand, we turned our attention to the Claisen rearrangement. First, an Eschenmoser–Claisen reaction was attempted (Scheme 27).<sup>[148]</sup> Unfortunately, the starting material decomposed within 5 minutes upon heating to 100 °C and the reaction mixture turned bright red, suggesting that a major decomposition pathway might include quinoidal intermediates likely to be formed after solvolytic removal of the benzylic silyl ether by liberated methanol (**112**) or by ionization of the conjugated allylic alcohol (**113**). The same red color was observed under Johnson–Claisen conditions employing triethyl orthoacetate in the presence of either propionic acid or 2-nitrophenol.<sup>[149]</sup> Control experiments carried out by heating the reaction mixture in the presence of triethyl orthoacetate without acid additive also resulted in decomposition. Another experiment carried out using boiling ethanol, which is liberated by triethyl orthoacetate during the

rearrangement reaction, resulted in the same red color, confirming the instability of intermediate **106** to protic solvent at high temperatures.



**Scheme 27. Attempted Claisen-type rearrangements and possible decomposition intermediates.**

Next, protocols that involve the formation and rearrangement of vinyl ether **114** were examined. As shown in Table 15, palladium-mediated vinyl ether formation was attempted.<sup>[150,151]</sup> Unfortunately, the desired product was not formed (Entries 1 to 4). Therefore, we turned to the well-precedented formation of vinyl ethers assisted by mercury salts.<sup>[152]</sup> As previously shown by Nynke Vepřek, reacting **106** with mercury acetate in the presence of either ethyl vinyl ether or the higher-boiling butyl vinyl ether afforded **114**, which was used after filtration over alumina to remove Hg-salts (Entries 5 and 6). Unfortunately, heating of **114** in either xylene or benzonitrile did not form any aldehyde product and resulted in decomposition (Table 16). We also tested the rearrangement in wet dioxane, which was reported by Grieco to occur at lower temperatures, but this resulted in no product formation and hydrolysis of the labile vinyl ether (Entry 3).<sup>[153]</sup>

**Table 15. Conditions examined for the formation of vinyl ether **114** from alcohol **106**.**

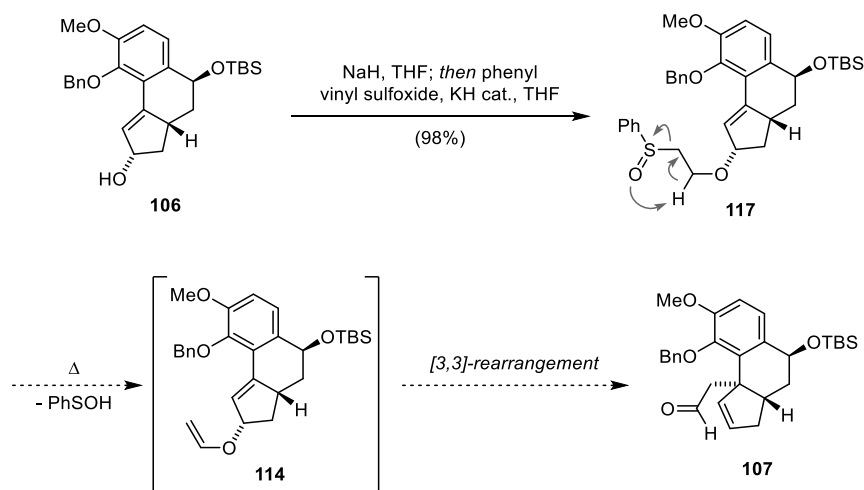
Entry	Catalyst <sup>a</sup>	Vinyl Ether Donor	Temp. (°C)	Yield (%)
1	<b>116</b>	tris(diethyleneglycol) divinyl ether	130	complex mixture
2	<b>116</b>	butyl vinyl ether	75	no reaction
3	<b>115</b>	butyl vinyl ether	75	no reaction
4	<b>115</b>	ethyl vinyl ether	35	no reaction
5	Hg(OAc) <sub>2</sub>	ethyl vinyl ether	35	83 <sup>b</sup>
6	Hg(OAc) <sub>2</sub>	butyl vinyl ether	75	61 <sup>b</sup>

a) 10 mol%    b) crude yield reported; product contaminated with unidentified impurities.

**Table 16. Conditions examined for the thermal rearrangement of vinyl ether **114**.**

Entry	Solvent	Temp. (°C)	Time (h)	Yield	Comment
1	benzonitrile	160	5	n.d.	decomposition
2	xylene	140	5	n.d.	decomposition
3	dioxane/H <sub>2</sub> O	110	48	n.d.	no rearrangement, hydrolysis to <b>106</b>

The results involving the synthesis and isolation of vinyl ether **114** led us to consider a Claisen strategy originally reported by Mandai in which the isolation of hemistable vinyl ether **114** is not necessary.<sup>[154]</sup> Instead, the required intermediate is formed in situ starting from sulfoxide **117** which undergoes Grieco-type elimination with expulsion of a sulfenic acid at elevated temperature (>150 °C), where the subsequent sigmatropic rearrangement occurs readily (Scheme 28). Therefore, we prepared sulfoxide **117** through conjugate addition of **106** to phenyl vinyl sulfoxide using NaH and catalytic KH. The adduct was isolated in very good yield as an inseparable mixture with excess vinyl sulfoxide. Thankfully, subjection of the crude reaction mixture to methylamine in isopropanol scavenged unreacted vinyl sulfoxide and rendered the isolation of pure **117** possible.

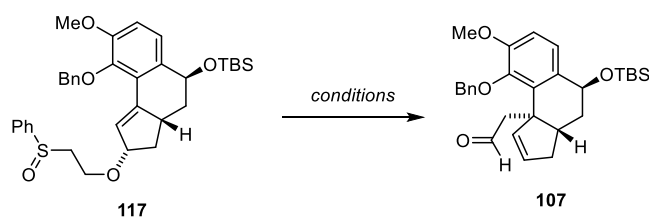


**Scheme 28. Synthesis of sulfoxide **117** and proposed conversion into aldehyde **107**.**

Heating of **117** in *o*-dichlorobenzene showed that the desired product was formed, but yields were variable and longer reaction times were necessary on larger scales, which resulted in side product formation and lower overall yield.<sup>[155]</sup> Attempts to shorten the reaction time by the use of microwave irradiation were also unsuccessful.<sup>[156]</sup> Therefore, we investigated the reaction variables in more detail.

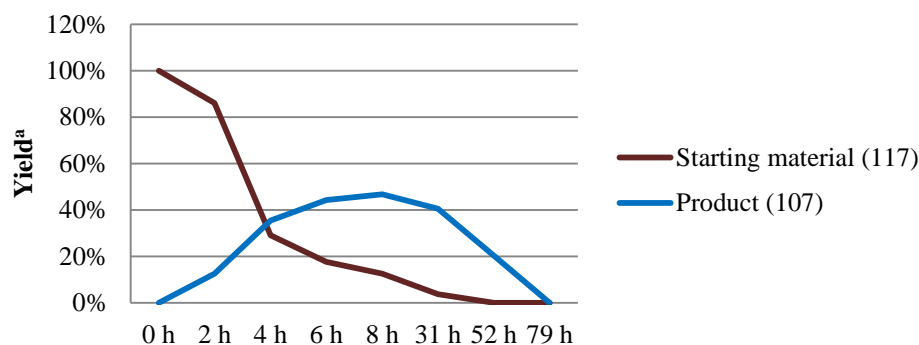
As can be seen in Table 17 the reaction provides variable yields, even if set up in parallel on the same scale (Entries 2 to 5). In line with the original report, NaHCO<sub>3</sub> was the base of choice but we observed higher yields when a large excess of base was used (>50 eq.), as opposed to 30 eq. in the original publication. Furthermore, NaHCO<sub>3</sub> outperformed other bases such as NaOAc and KOAc (Entries 20 and 21). The absence of base resulted in no product formation, whereas the use of a thiophilic scavenger (PPh<sub>3</sub>) to trap liberated sulfenic acid was possible, but not advantageous (Entries 22 and 23).<sup>[157]</sup> For reactions conducted in screw-cap vials using a heated metal block, a temperature of 165 °C was optimal (Entries 24 - 26), while lower temperatures resulted in prolonged reaction times and a slight decrease in yield (entries 6 to 11). Reactions above 200 mg of substrate, exemplified by entry 27, were conducted in a round bottom flask and heated in an oil bath set at a temperature of 10 °C higher than desired to compensate for heat dissipation. The reaction was monitored by <sup>1</sup>H NMR of reaction aliquots withdrawn every hour.

Figure 9 shows that the starting material is consumed at a higher rate compared to the rate of product formation. Additionally, the product aldehyde **107** is not stable under the reaction conditions, resulting in low isolated yields if the reaction is not monitored frequently and stopped after the disappearance of **117**. Taking these findings into account, the reaction reproducibly afforded aldehyde **107** in 60 to 65% isolated yield on scales up to 3 mmol.

**Table 17. Conditions examined for the thermolysis and Claisen rearrangement of sulfoxide 117.**

Entry <sup>a</sup>	Scale (mg)	Base	Eq.	Solvent	Conc. (mM)	Temp. (°C)	Time (h) <sup>b</sup>	Yield (%) <sup>c</sup>
1	8	NaHCO <sub>3</sub>	30	Mesitylene	4	150	8	31
2	10	NaHCO <sub>3</sub>	30	1,2-DCB	4	150	6	42
3	10	NaHCO <sub>3</sub>	30	1,2-DCB	4	150	6	41
4	10	NaHCO <sub>3</sub>	30	1,2-DCB	4	150	6	27
5	10	NaHCO <sub>3</sub>	30	1,2-DCB	4	150	6	28
6	66	NaHCO <sub>3</sub>	30	1,2-DCB	4	150	11	40
7	9	NaHCO <sub>3</sub>	5	1,2-DCB	5	150	8	51
8	9	NaHCO <sub>3</sub>	10	1,2-DCB	5	150	8	55
9	9	NaHCO <sub>3</sub>	25	1,2-DCB	5	150	8	56
10	9	NaHCO <sub>3</sub>	50	1,2-DCB	5	150	8	58
11	9	NaHCO <sub>3</sub>	100	1,2-DCB	5	150	8	49
12	10	NaHCO <sub>3</sub>	50	1,2-DCB	5	170	5	29
13	53	NaHCO <sub>3</sub>	50	1,2-DCB	5	170	2	38
14	48	NaHCO <sub>3</sub>	50	1,2-DCB	5	170	2	37
15	48	NaHCO <sub>3</sub>	50	1,2-DCB	2.5	170	2	29
16	50	NaHCO <sub>3</sub>	83	1,2-DCB	5	170	2	38
17	40	NaHCO <sub>3</sub>	100	1,2-DCB	5	170	2	35
18	40	NaHCO <sub>3</sub>	100	1,2-DCB	5	160	4	35
19	40	NaHCO <sub>3</sub>	100	1,2-DCB	5	160	5	40
20	36	NaOAc	35	1,2-DCB	5	170	2	27
21	36	KOAc	35	1,2-DCB	5	170	2	29
22	36	PPh <sub>3</sub>	3	1,2-DCB	5	170	2	25
23	36	PPh <sub>3</sub>	10	1,2-DCB	5	170	2	36
24	90	NaHCO <sub>3</sub>	80	1,2-DCB	5	165	6	85
25	90	NaHCO <sub>3</sub>	80	1,2-DCB	5	165	4	72
26	90	NaHCO <sub>3</sub>	80	1,2-DCB	5	165	4	81
27 <sup>d</sup>	1818	NaHCO <sub>3</sub>	90	1,2-DCB	5	175	6	73

**a)** all reactions carried out with catalytic amounts of BHT as additive; **b)** time until disappearance of starting material as monitored by <sup>1</sup>H NMR every hour; **c)** NMR yield using phenanthrene as internal standard; **d)** isolated yield: 61%.



a) Product distribution calculated by  $^1\text{H}$  NMR against phenanthrene as internal standard;

**Figure 9. Time-dependent formation and decomposition of aldehyde 107.**

Hoping to improve the yield further, we turned to the reaction of *p*-chloro phenyl sulfone **118**, reported to give higher yields than the parent phenyl sulfone **117**.<sup>[154]</sup> Table 18 shows that, for chloro-substituted arene **118**, KOAc was the best base for the transformation. Although 140 °C was sufficient to effect the rearrangement (Entry 7), shorter reaction times were achieved at 160 °C (Entry 6). Interestingly, NaHCO<sub>3</sub> was ineffective for this substrate (Entries 2 and 14). Nevertheless, yields were lower compared to the parent system using **117**. Given that *p*-chloro phenyl vinyl sulfoxide is not commercially available and requires multistep synthesis, the use of **118** was not implemented.<sup>[158]</sup>

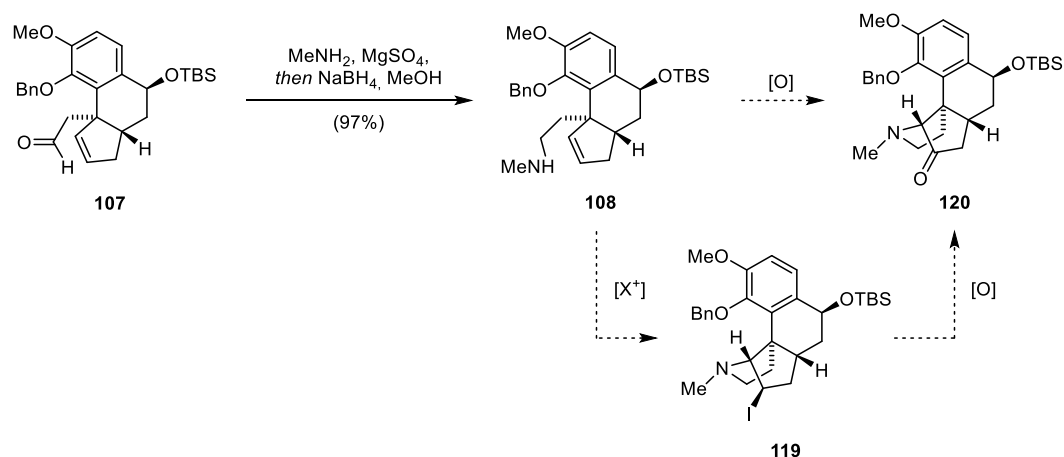
**Table 18. Conditions examined for the thermolysis and Claisen rearrangement of sulfoxide 118.**

Entry <sup>a</sup>	Base	Eq.	Temp. (°C)	Time <sup>b</sup> (h)	Yield (%) <sup>c</sup>
1	no base	10	175	3	0
2	NaHCO <sub>3</sub>	10	175	3	0
3	NaOAc	10	175	3	33
4	KHCO <sub>3</sub>	10	175	3	16
5	KOAc	10	175	3	59
6	KOAc	10	160	2	71
7	KOAc	10	140	16	68
8	KOAc	10	150	18	60
9	BaCO <sub>3</sub>	10	150	3	0
10	no base	10	150	18	35
11	KHCO <sub>3</sub>	10	150	18	73
12	KH <sub>2</sub> PO <sub>3</sub>	10	150	18	0
13	K <sub>2</sub> HPO <sub>3</sub>	10	150	18	0
14	NaHCO <sub>3</sub>	10	150	18	0
15	NaH <sub>2</sub> PO <sub>3</sub>	10	150	18	0
16	Na <sub>2</sub> HPO <sub>3</sub>	10	150	18	0

a) all reactions carried out using 10 mg of **118** in 1,2-DCB (4 mM) and catalytic amounts of BHT; b) time until disappearance of starting material as monitored by  $^1\text{H}$  NMR every hour; c) NMR yield using phenanthrene as internal standard.

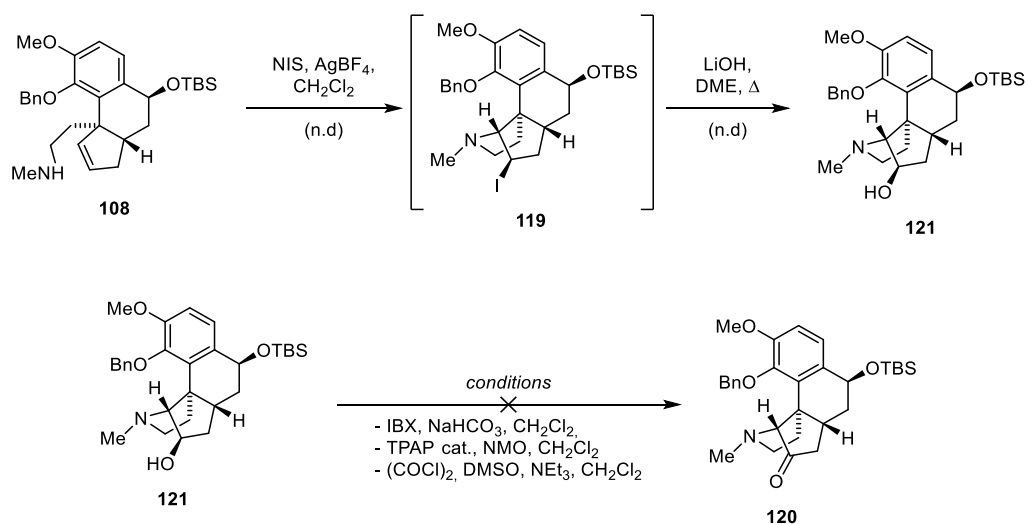
## 2.2.4. Formation of the Pyrrolidine Ring

Reductive amination of aldehyde **107** using an ethanolic solution of methylamine proceeded smoothly to deliver secondary amine **108** (Scheme 29). Since direct oxidative cyclization to **120** was not viable, we decided to activate the alkene electrophilically to effect the attack of the pendant nitrogen and form the pyrrolidine ring. The ketone could then be introduced at a later stage.<sup>[156]</sup>



**Scheme 29. Reductive amination and projected ring closure to ketone 120.**

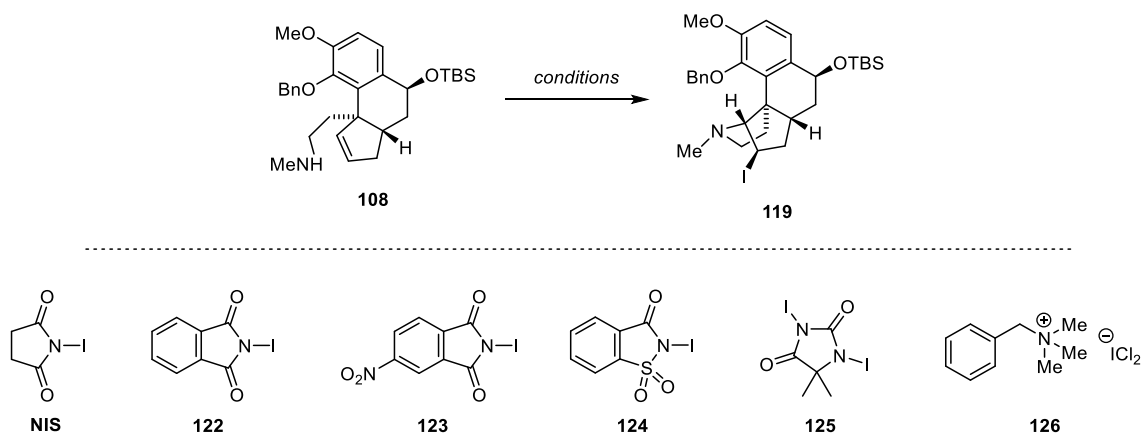
Nynke Vepřek demonstrated that treatment of **108** with NIS resulted in rapid conversion of the starting material to a single intermediate (**119**, Scheme 30). This compound proved to be unstable to aqueous workup, but structural assignment was possible by NMR analysis and mass spectrometry. When crude **119** was treated with 1 M aqueous  $\text{LiOH}$  solution in DME, introduction of a hydroxyl group was effected to give secondary alcohol **121**.<sup>[159]</sup> Unfortunately, the yield for the transformation was low and not reproducible. In addition, secondary alcohol **121** did not deliver ketone **120** under standard alcohol oxidation conditions.



**Scheme 30. Formation of the pyrrolidine ring and introduction of oxygen functionality.**

Although the product derived from the reaction using NIS defied our isolation attempts, we decided to carry on with the formed intermediate and optimize its formation. From a screening of several electrophilic iodination reagents and their stoichiometry, NIS (2 eq.) emerged as the optimal reagent (Table 19).<sup>[160–162]</sup>

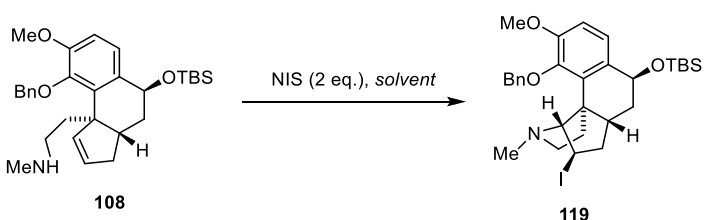
**Table 19. Conditions for the iodocyclization of 108.**



Entry <sup>a</sup>	Reagent	Eq.	Solvent	Yield <sup>b</sup> (%)
1	NIS	2	CH <sub>2</sub> Cl <sub>2</sub>	64
2	122	2	CH <sub>2</sub> Cl <sub>2</sub>	58
3	123	2	CH <sub>2</sub> Cl <sub>2</sub>	43
4	124	2	CH <sub>2</sub> Cl <sub>2</sub>	12
5	125	1	CH <sub>2</sub> Cl <sub>2</sub>	49
6	126	2	CH <sub>2</sub> Cl <sub>2</sub>	12
7	NIS	0.5	CD <sub>2</sub> Cl <sub>2</sub>	7
8	NIS	1	CD <sub>2</sub> Cl <sub>2</sub>	33
9	NIS	1.5	CD <sub>2</sub> Cl <sub>2</sub>	42
11	NIS	2.5	CD <sub>2</sub> Cl <sub>2</sub>	38
12	NIS	2	MeCN	45
13 <sup>c</sup>	NIS	2	MeCN	52

a) Reactions performed at room temperature except entries 12 and 13 (−20 °C) b) determined by <sup>1</sup>H NMR using diphenylmethane as internal standard c) solution of NIS added slowly via syringe pump.

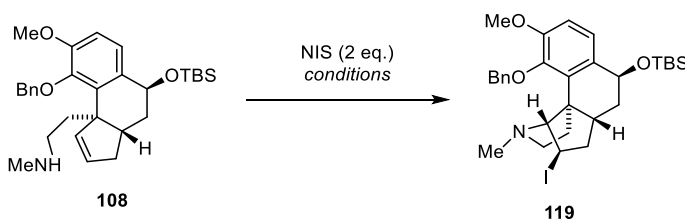
As can be seen in Table 20, treatment of **108** with NIS in different aprotic solvents led to the formation of the product in low to moderate yields. The reaction occurred in all the solvents examined, but CH<sub>2</sub>Cl<sub>2</sub> and MeCN provided the cleanest reaction profile and were selected for further optimization (Entries 1 and 5).

**Table 20. Solvents examined for the iodocyclization of 108 using NIS.**


Entry	Solvent	Yield <sup>a</sup> (%)	Comment
1	CH <sub>2</sub> Cl <sub>2</sub>	47	clean conversion
2	CHCl <sub>3</sub>	56	several side products
3	DCE	42	-
4	DME	40	-
5	MeCN	53	clean conversion
6	THF	42	-
7	DMF	44	several side products
8	benzene	42	-
9	DMSO	27	several side products
10	toluene	42	-

a) determined by <sup>1</sup>H NMR using diphenylmethane as internal standard.

We observed that in all cases the consumption of starting material was very fast (< 10 minutes), but the product yield was moderate. Therefore, we attempted to lower the reaction temperature and decrease the concentration to slow down the reaction, diminish side product formation, and improve the yield of the major product (Table 21).

**Table 21. Variation of reaction conditions for iodocyclization reaction of alkene 108.**


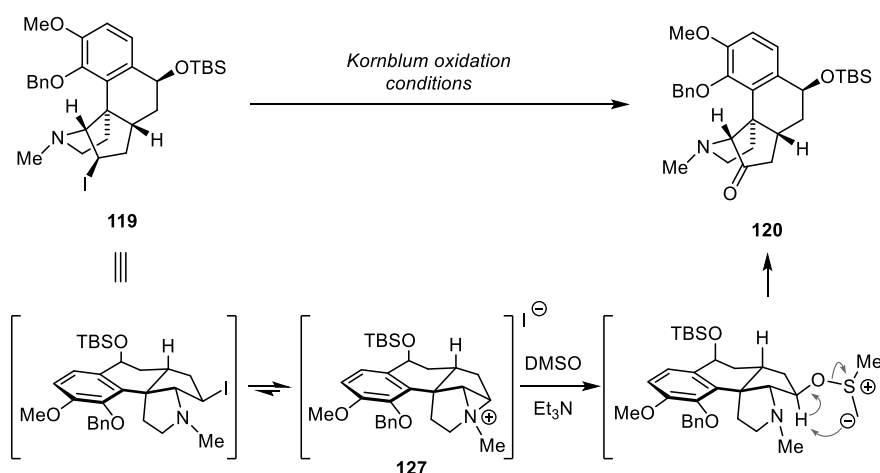
Entry <sup>a</sup>	Solvent	Conc. (mM)	Temp. (°C)	Yield <sup>b</sup> (%)
1	CH <sub>2</sub> Cl <sub>2</sub>	12	-20	55
2	CH <sub>2</sub> Cl <sub>2</sub>	20	-20	49
3	CH <sub>2</sub> Cl <sub>2</sub>	40	-20	56 <sup>c</sup>
4	CH <sub>2</sub> Cl <sub>2</sub>	12	rt	53
5	CH <sub>2</sub> Cl <sub>2</sub>	25	rt	53
6	CH <sub>2</sub> Cl <sub>2</sub>	50	rt	53
7	CH <sub>2</sub> Cl <sub>2</sub>	62	rt	38
8	MeCN	10	-20	54
9	MeCN	20	-20	59
10	MeCN	40	-20	51
11	MeCN	75	-20	48
12	MeCN	150	-20	46

a) reaction time 30 min; b) determined by <sup>1</sup>H NMR of the crude mixture using diphenylmethane as internal standard; c) incomplete consumption of starting material observed.

Although the reaction was complete within 30 minutes even at  $-20\text{ }^{\circ}\text{C}$ , lowering the temperature only gave minimal improvements in yield. For example, a reaction in  $\text{CH}_2\text{Cl}_2$  at 12 mM carried out at  $-20\text{ }^{\circ}\text{C}$  gave the product in 55% yield, while the reaction at room temperature gave the product in 53% yield (cf. Entries 1 and 4). Furthermore, NMR analysis showed that increasing concentration led to several unidentified side products and lower overall yields. Optimum concentrations for the  $\text{CH}_2\text{Cl}_2$  reaction was found to be 12 mM, while in MeCN the best yield was achieved at 20 mM and at ambient temperature.

To displace the iodine atom with an oxygen nucleophile, the reaction mixture containing **119** was diluted with DMSO in the presence of halophilic silver tetrafluoroborate.<sup>[163]</sup> Addition of an amine base (i.e. triethylamine) would then effect deprotonation of the sulfonium ion resulting from substitution of the secondary iodide, lead to the loss of dimethyl sulfide, and give ketone **120** (see Scheme in Table 22). Indeed, the desired ketone could be synthesized in moderate yield. Whereas in typical Kornblum conditions the base is added after several hours in order to complete the substitution reaction of DMSO with the halide, we found that the  $\text{Et}_3\text{N}$  could be added to the reaction from the beginning to achieve the same result. Furthermore, these substitutions in Kornblum oxidations generally require elevated temperatures and are only successful for activated alkyl halides (i.e. primary, or benzylic, allylic).<sup>[164]</sup> In our case, the reaction proceeds readily at room temperature, and is similarly efficient if carried out without silver salts (cf. Entries 1 and 2 or Entries 3 and 4). These results suggest the neighboring group participation of the adjacent amine to form aziridinium **127** that obviates the use of silver salts by internal displacement of the iodide and conformationally locks intermediate **127** to favor the attack by DMSO.

**Table 22. Proposed neighboring-group participation Kornblum reaction of iodide 119.**



Entry <sup>a</sup>	Solvent	Base	Additive	Yield <sup>b</sup>
1	50% DMSO in $\text{CH}_2\text{Cl}_2$	$\text{Et}_3\text{N}$	$\text{AgBF}_4$	54%
2	50% DMSO in $\text{CH}_2\text{Cl}_2$	$\text{Et}_3\text{N}$	none	53%
3	50% DMSO in $\text{CH}_2\text{Cl}_2$	$\text{Et}_3\text{N}$	$\text{AgBF}_4$	53%
4	50% DMSO in MeCN	$\text{Et}_3\text{N}$	none	50%

a) substitution reaction carried out at  $-15\text{ }^{\circ}\text{C}$  to room temperature for 16 hours;  
 b) determined by  $^1\text{H}$  NMR using diphenylmethane as internal standard.

As can be seen in Table 23, the requirement for low concentrations during the oxidation is instrumental for high yield of ketone **120** in both CH<sub>2</sub>Cl<sub>2</sub> and MeCN. Decreasing the temperature for the addition of Et<sub>3</sub>N from room temperature to –20 °C gave similar yields for both solvent mixtures when the reaction was performed in comparable concentrations (Entries 2 and 10).

**Table 23. Reaction conditions for the synthesis of ketone 120 via Kornblum oxidation.**

Entry	Cyclization <sup>a</sup>			Oxidation <sup>b</sup>			Yield <sup>c</sup>
	solvent	Temp. (°C)	Conc. (mM)	solvent	Temp. (°C)	Conc. (mM)	
1	MeCN	–20 °C	20	50% MeCN in DMSO	–15	10	63%
2	MeCN	–20 °C	40	50% MeCN in DMSO	–15	20	52%
3	MeCN	–20 °C	72	50% MeCN in DMSO	–15	38	53%
4	MeCN	–20 °C	150	50% MeCN in DMSO	–15	75	38%
5	MeCN	0 °C	20	50% MeCN in DMSO	rt	10	65%
6	MeCN	–20 °C	40	50% MeCN in DMSO	rt	20	56%
7	MeCN	–20 °C	75	50% MeCN in DMSO	rt	38	48%
8	MeCN	–20 °C	150	50% MeCN in DMSO	rt	75	42%
9	MeCN	–20 °C	20	50% MeCN in DMSO	rt	10	62%
10	CH <sub>2</sub> Cl <sub>2</sub>	–20 °C	40	50% CH <sub>2</sub> Cl <sub>2</sub> in DMSO	–15	20	54%
11	CH <sub>2</sub> Cl <sub>2</sub>	–20 °C	20	50% CH <sub>2</sub> Cl <sub>2</sub> in DMSO	rt	10	58%
12	CH <sub>2</sub> Cl <sub>2</sub>	0 °C	20	50% CH <sub>2</sub> Cl <sub>2</sub> in DMSO	rt	10	61%

a) performed using 2 eq. of NIS; time: 15 min; b) performed using 3 eq. of Et<sub>3</sub>N, time: 24 h; c) isolated yield.

In a last series of experiments we examined the possibility of performing a solvent switch to DMSO after the iodocyclization reaction. As **119** was not stable towards aqueous workup and silica gel chromatography, we feared it would also be unstable during the required manipulations. In fact, we determined that solvent removal had to be performed in the dark while setting the water bath temperature below 25 °C (at 35 °C, 50% of the product decomposed upon redissolution). In doing so, solvent-free **119** could be handled in air for short time and used for the substitution reactions.

As can be seen by the comparison of Table 23 with Table 24, DMSO alone was slightly superior for the Kornblum oxidation to mixtures containing either MeCN or CH<sub>2</sub>Cl<sub>2</sub>. For example, oxidation in DMSO at room temperature in 5 mM solution yielded in 73% (Table 24, Entry 3), whereas the highest yields achieved with 1/1 mixtures of MeCN/DMSO or CH<sub>2</sub>Cl<sub>2</sub>/DMSO were 65% and 61% respectively (Table 23, Entries 5 and 12).

**Table 24 Variation of reaction conditions for the synthesis of ketone 120 in pure DMSO.**

Entry	Cyclization <sup>a</sup>			Oxidation <sup>b</sup>			Yield <sup>c</sup>
	solvent	Temp. (°C)	Conc. (mM)	solvent	Temp. (°C)	Conc. (mM)	
1	CH <sub>2</sub> Cl <sub>2</sub>	–20 °C	12.5	DMSO	rt	5	64
2	CH <sub>2</sub> Cl <sub>2</sub>	rt	12.5	DMSO	rt	5	73
3	CH <sub>2</sub> Cl <sub>2</sub>	–20 °C	12.5	DMSO	rt	10	67
4	CH <sub>2</sub> Cl <sub>2</sub>	rt	25	DMSO	rt	10	65
5	CH <sub>2</sub> Cl <sub>2</sub>	rt	12.5	DMSO	rt	20	45
6	CH <sub>2</sub> Cl <sub>2</sub>	rt	50	DMSO	rt	20	58

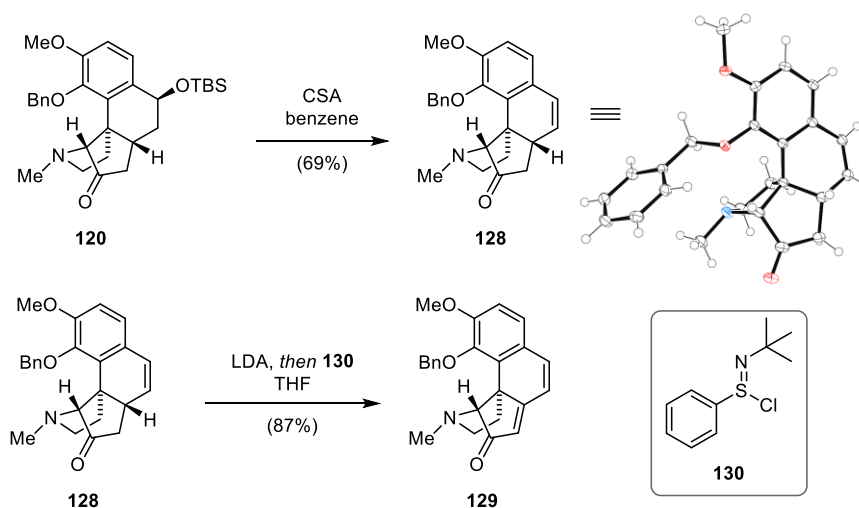
a) performed using 2 eq. of NIS; time: 15 min; b) performed using 3 eq. of Et<sub>3</sub>N, time: 24 h; c) isolated yield.

Additionally, we determined that ketone **120** was heavily retained on regular silica gel, which led to a yield loss of 20%. This issue could be resolved by pretreatment of silica gel with the eluent mixture containing 1% Et<sub>3</sub>N followed by loading and elution with amine-free eluent. Interestingly, purification using Et<sub>3</sub>N in the eluent mixture resulted in lower yields (10%). Using the optimized conditions described above, **120** could reliably be accessed on scales up to 1 mmol in 60 to 70% isolated yield.

### 2.2.5. Completion of the Synthesis

The one-pot iodoamination–Kornblum oxidation sequence successfully installed the tetracyclic ring system of sinoracutine. The fully conjugated eastern backbone required elimination of the benzylic TBS ether and oxidation of the ketone to the  $\alpha,\beta$ -unsaturated ketone.

Styrene **128** could be best accessed by treatment of silyl ether **120** with CSA (Scheme 31). Its structure was established by X-ray crystallographic analysis and confirmed the diastereoselective installation of the quaternary stereocenter and the *anti*-orientation of the pyrrolidine ring with respect to the angular proton of the cyclopentene moiety. For the introduction of unsaturation, we decided to apply the method of Mukaiyama using LDA followed by sulfimidoyl chloride (**130**).<sup>[165–167]</sup> Gratifyingly, this oxidation protocol cleanly afforded benzylsinoracutine **129** in good yield as an intensely yellow oil.

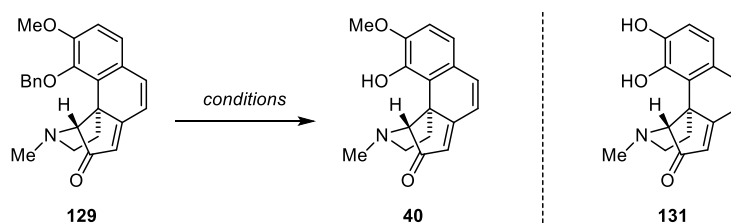


**Scheme 31. Elimination of benzylic alcohol to tetracycle **128** and its Mukaiyama oxidation.**

Final debenylation was attempted using BCl<sub>3</sub> in the presence of pentamethylbenzene, a reagent combination that has shown to selectively remove benzyl groups in presence of methoxy groups and other Lewis basic sites.<sup>[168,169]</sup> As shown in Table 25, BCl<sub>3</sub> did not react with starting material at –40 °C but cleavage of the benzyl ether could be observed at –20 °C. However, significant amounts of demethylated product were observed by LCMS, reflecting the electron-deficient nature of the methoxy group that is in direct conjugation with the carbonyl (Entry 4). When the stronger Lewis

acid  $\text{BBr}_3$  was used, both benzyl- and methyl ethers were cleaved at competing rates even at  $-78\text{ }^\circ\text{C}$  (Entry 5). Trifluoroacetic acid was examined next, as it had been reported to cleave phenolic benzyl groups in complex peptides.<sup>[170]</sup> When used in conjunction with electron-rich aromatic compounds such as trimethoxybenzene or pentamethylbenzene, dramatic rate acceleration and higher yields were observed, likely a result of efficient scavenging of the generated benzylic cation.<sup>[171]</sup> Upon treatment of **129** in neat TFA with pentamethylbenzene for 48 h, selective removal of the benzyl group was effected to afford sinoracutine. The reaction could be carried out at  $40\text{ }^\circ\text{C}$  with comparable efficiency (Entry 7).

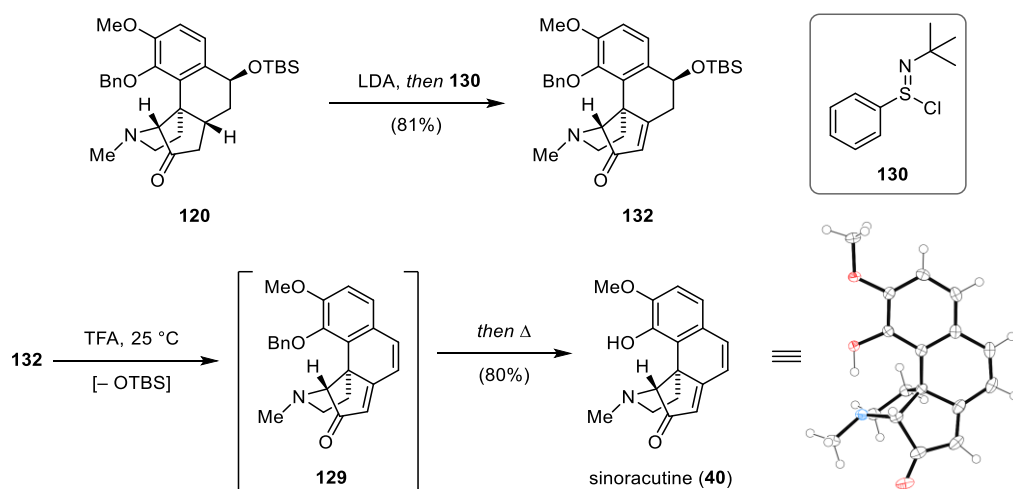
**Table 25. Conditions examined for the debenzylation of 129 to give sinoracutine.**



Entry	Reagent <sup>a</sup>	Temp. ( $^\circ\text{C}$ )	Time (h)	Product distribution (% , HPLC relative peak area)		
				Starting material (129)	Sinoracutine (40)	131 (undesired)
1	$\text{BCl}_3$	$-40$	24	-	no reaction	-
2	$\text{BCl}_3$	$-20$	12	10	80	10
3	$\text{BCl}_3$	$-15$	6	10	85	15
4	$\text{BCl}_3$	0	6	5	50	50
5	$\text{BBr}_3$	$-78$	2	3	0	97
6	TFA	rt	48	15	85	0
7	TFA	40	24	11	89	0

a) All reactions carried out in the presence of pentamethylbenzene (10.0 eq.).

In an effort to shorten the overall reaction sequence, silyl ether **120** was oxidized under Mukaiyama conditions to afford enone **132**, which was subjected to trifluoroacetic acid at  $40\text{ }^\circ\text{C}$  (Scheme 32). The elimination of the benzylic alcohol to **129** could be observed by LCMS within 10 minutes and subsequent debenylation progressed over the course of 16 hours. Sinoracutine could be isolated after extractive workup and chromatography on silica gel to remove excess pentamethylbenzene. We experienced difficulties in obtaining an analytically pure sample of **40**, which is not stable to silica gel as evidenced by two-dimensional TLC analysis and could not be purified on aluminum oxide. Gratifyingly, purification by semipreparative HPLC (reverse phase,  $\text{H}_2\text{O}/\text{MeCN} + 1\% \text{ FA}$ ) followed by direct lyophilization of the product-containing fractions was successful. This material could also be recrystallized from slow diffusion of hexane into a solution of **40** in  $\text{CH}_2\text{Cl}_2$ .



**Scheme 32. Oxidation of silyl ether 120 followed by sequential elimination/debenzylation.**

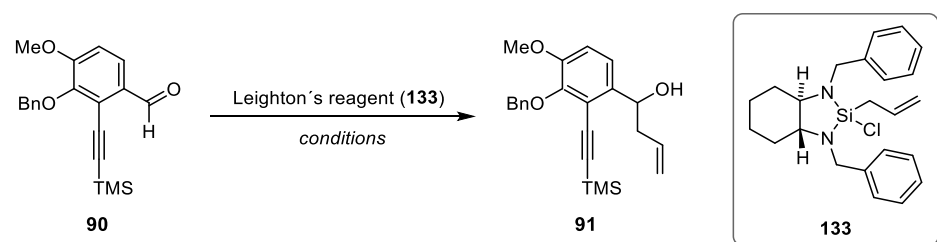
### 2.2.6. Asymmetric Synthesis of Sinoracutine

With a reliable route to racemic sinoracutine in hand, we moved on to render our synthesis asymmetric. As stated in Chapter 2.2, preparation of Pauson–Khand precursor **94** in enantiopure form should allow the enantioselective synthesis of sinoracutine by virtue of the stereoselectivity exhibited by Pauson–Khand reaction, the 1,2-reduction, and by the ensuing Claisen rearrangement.

#### 2.2.6.1. Enantioselective Allylation

A literature review showed that catalytic enantioselective methods for the allylation of *o*-substituted benzaldehydes tend to give low enantioselectivities and are highly substrate dependent.<sup>[172]</sup> Among the methods investigated (chiral *N*-oxide catalysts in conjunction with allyltrichlorosilane, titanium-BINOL complexes with allyltributyltin, chiral phosphoric acids with allylpinacolborane) all exhibited moderate enantioselectivities, especially with *o*-alkynyl-substituted substrates relevant for this project.

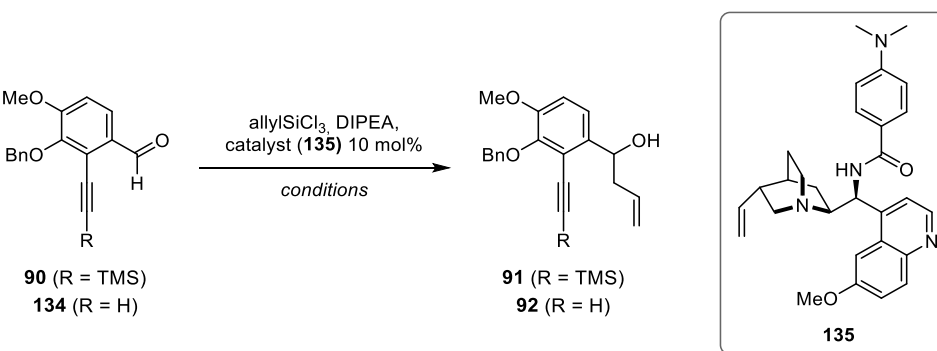
Therefore, we started our investigations using stoichiometric chiral allylation reagents. Among the methods at our disposal, the allylsilane developed by Leighton was tested first.<sup>[173]</sup> The reaction was performed using TMS-protected **90** under standard conditions (Table 26). At room temperature, no reaction took place. Heating did not improve conversion and led to decomposition of the starting material. Also the addition of  $\text{Sc}(\text{OTf})_3$ , reported to improve reactivity in reluctant substrates, was not successful in our hands.<sup>[174]</sup>

**Table 26. Asymmetric allylation of TMS-alkyne **90** with Leighton's chiral allylsilane **133**.**


Entry	Solvent	Additive	Temp. (°C)	Time (h)	Yield <sup>a</sup> (%)	ee (%)
1	CH <sub>2</sub> Cl <sub>2</sub>	none	4	12	-	n.d.
2	CH <sub>2</sub> Cl <sub>2</sub>	none	rt	12	-	n.d.
3	CH <sub>2</sub> Cl <sub>2</sub>	none	rt to 40	36	-	n.d.
4	CH <sub>2</sub> Cl <sub>2</sub>	Sc(OTf) <sub>3</sub> (8 mol%)	rt to 40	100	-	n.d.

a) decomposition of **90** was observed; **n.d.** = not determined.

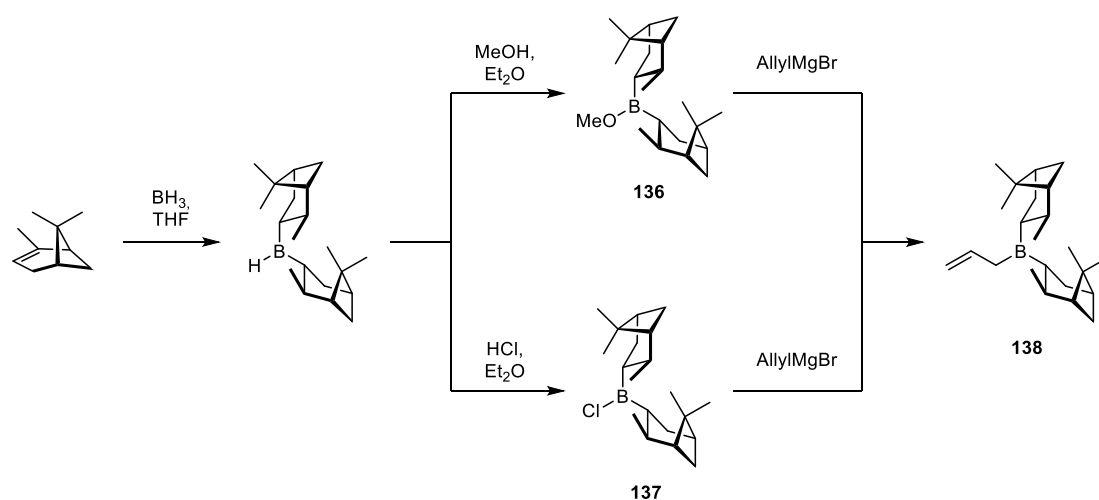
A recent protocol using a cinchona-alkaloid based catalyst in conjunction with allyltrichlorosilane and DIPEA as Lewis-basic activator was examined next.<sup>[175]</sup> To determine the influence of the protecting group on the allylation, in addition to the TMS-protected Sonogashira product (**90**), we also used the free alkyne (**134**), which could easily be accessed by TBAF-promoted desilylation. Unfortunately, both aldehydes did not give the allylated product and decomposed under the reaction conditions (Table 27).

**Table 27. Asymmetric allylation mediated by chiral organocatalyst **135**.**


Entry	Substrate	Solvent	Temp. (°C)	Time (h)	Yield <sup>a</sup> (%)	ee (%)
1	<b>90</b> (R = TMS)	toluene	rt	12	-	n.d.
2	<b>134</b> (R = H)	toluene	rt	12	-	n.d.

a) decomposition of **90** or **134** was observed; **n.d.** = not determined.

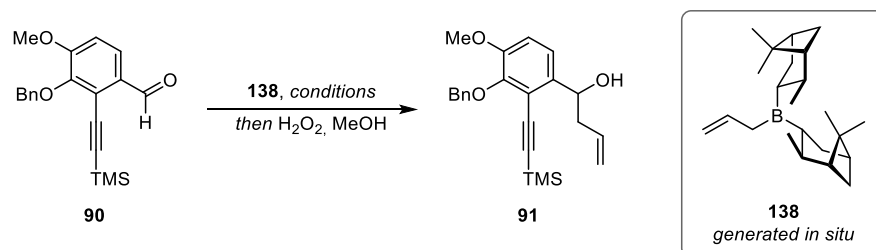
Due to these unsatisfactory results using silicon-based reagents, we turned our attention to the highly powerful and well-established allylboranes derived from terpene-based chiral auxiliaries introduced by Brown and co-workers (**138**, Scheme 33).<sup>[176,177]</sup> They can be prepared in situ from pinene-derived *B*-diisopinocampheylmethoxyborane (**136**) or *B*-chlorodiisopinocampheylborane (**137**) by treatment with allylmagnesium bromide.



**Scheme 33. Synthesis of B-allyldiisopinocampheylborane from  $\alpha$ -pinene.**

Furthermore, treatment of the so-formed reagent with pentane effects complete precipitation of the formed inorganic salts ( $\text{MgCl}_2$  or  $\text{Mg}(\text{OMe})_2$ ) that slow down the reaction by complexation with the allylborane. Filtration through a pre-dried glassfiber filter can increase the reaction rate markedly.<sup>[178]</sup> This is especially important as the reaction is usually performed at  $-100\text{ }^\circ\text{C}$  for several hours resulting in a complicated experimental setup requiring constant monitoring and refrigerant addition.

**Table 28. Brown allylation of 90 by in situ-generated B-allyldiisopinocampheylborane.**



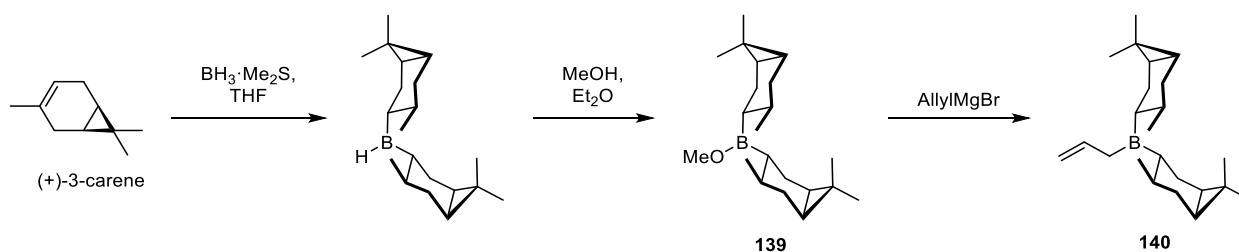
Entry	Filtration	solvent	Temp. ( $^\circ\text{C}$ )	Time (h)	Yield <sup>a</sup> (%)	ee <sup>b</sup> (%)
1	yes	$\text{Et}_2\text{O}$	$-100$ to rt	3.5	76	58.4
2	yes	$\text{Et}_2\text{O}$	$-78$ to rt	3.5	70	19.7
3	no	$\text{Et}_2\text{O}$	$-78$ to rt	3.5	90	89.7
4	no	THF	$-78$ to rt	3.5	91	90.2

a) contaminated with isopinocampheol, component ratio calculated by  $^1\text{H}$  NMR;

b) determined by HPLC analysis on chiral stationary phase.

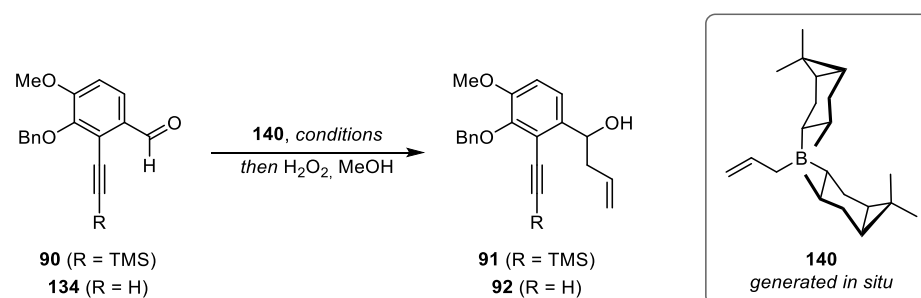
The reactions performed after filtration of the precipitated magnesium salts exhibited lower enantioinduction than the unfiltered experiments (Table 28, Entries 1 and 2). This is probably due to the presence of unreacted allylmagnesium bromide that was preferentially transferred to the reaction flask. Also, Brown's allylation reagent partially decomposed during filtration, thereby increasing the relative ratio of achiral reagent. Although we achieved good yields and enantiomeric excess without filtering the in situ formed allylborane (Entry 4), it was impossible to separate **91** from isopinocampheol, which was formed after the oxidative scission of the pinene-derived chiral auxiliary.

To examine the effect of alternative chiral auxiliaries on optical purity and ease of purification, we decided to substitute the pinene-derived allyldiisopinocampheylborane (**138**, Scheme 33) by allylbis(4-isocaranyl)borane (**140**, Scheme 34), which is reported to achieve higher enantioselectivities.<sup>[179]</sup> Its precursor (**139**) was prepared by hydroboration of (+)-3-carene with  $\text{BH}_3 \cdot \text{SMe}_2$  and subsequent methanolysis (Scheme 34).



**Scheme 34. Preparation of *B*-allyldi-4-isocaranylborane from (+)-3-carene.**

As can be seen in Table 29, decreasing the temperature from  $-78\text{ }^\circ\text{C}$  to  $-100\text{ }^\circ\text{C}$  revealed no improvement but slight deterioration of the enantioselectivity (Entries 1 and 2). The reaction carried out without filtration gave the product with very high enantiomeric excess, albeit with moderate yield (Entry 3). For the unprotected substrate, we determined that THF was inferior to diethyl ether (cf. Entries 4 and 5), likely due to its coordinating ability. Again, the low temperature did not improve the enantioinduction and resulted only in lower yields and a slower reaction. Increasing the stoichiometry of the reagent to 2.2 equivalents was beneficial (entries 8 and 10), but also resulted in a very challenging purification due to the presence of caranyl alcohol. At this point, although we were able to access the desired alcohols in enantioenriched form in moderate yields, we decided to investigate asymmetric reduction methods before implementing the Brown allylation in our synthesis. The better result obtained for the TMS-protected substrate also place the labor- and mass-intensive allylation reaction one step earlier in the synthesis.

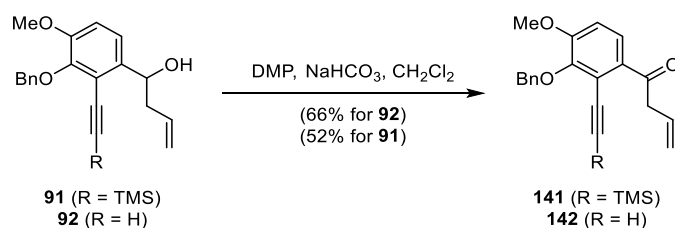
**Table 29. Allylation of aldehyde **90** or **134** with in situ-generated *B*-allyldi-4-isocaranylborane.**


Entry	Filtration	Solvent	Allylborane <b>140</b> generation	Temp. (°C)	Time (h)	Yield <sup>a</sup> (%)	ee <sup>b</sup> (%)
<b>For R = TMS (90)</b>							
<b>1</b>	yes	Et <sub>2</sub> O	2 eq. <b>139</b> 1.5 eq. AllylMgBr	-100 to rt	7	72	84.9
<b>2</b>	yes	Et <sub>2</sub> O	2 eq. <b>139</b> , 1.5 eq. AllylMgBr	-78 to rt	7	67	82.3
<b>3</b>	no	Et <sub>2</sub> O	2 eq. <b>139</b> , 1.5 eq. AllylMgBr	-78 to rt	7	58	95.6
<b>For R= H (134)</b>							
<b>4</b>	no	Et <sub>2</sub> O	1.5 eq. <b>139</b> , 1.5 eq. AllylMgBr	-78 to rt	8	38	93.9
<b>5</b>	no	THF	1.5 eq. <b>139</b> , 1.5 eq. AllylMgBr	-78 to rt	8	61	34.8
<b>6</b>	no	Et <sub>2</sub> O	1.5 eq. <b>139</b> , 1.5 eq. AllylMgBr	-100 to rt	8	22	85.3
<b>7</b>	no	THF	1.5 eq. <b>139</b> , 1.5 eq. AllylMgBr	-100 to rt	8	32	37.8
<b>8</b>	yes	Et <sub>2</sub> O	2.9 eq. <b>139</b> , 2.2 eq. AllylMgBr	-100 to rt	7	67	86.2
<b>9</b>	yes	Et <sub>2</sub> O	2.9 eq. <b>139</b> , 2.2 eq. AllylMgBr	-78 to rt	7	20	89.4
<b>10</b>	no	Et <sub>2</sub> O	2.9 eq. <b>139</b> , 2.2 eq. AllylMgBr	-78 to rt	7	59	93.4

**a)** contaminated with 4-caranol, ratio calculated by <sup>1</sup>H-NMR; **b)** determined by HPLC analysis on chiral stationary phase.

### 2.2.6.2. Asymmetric Reduction of Prochiral Ketones.

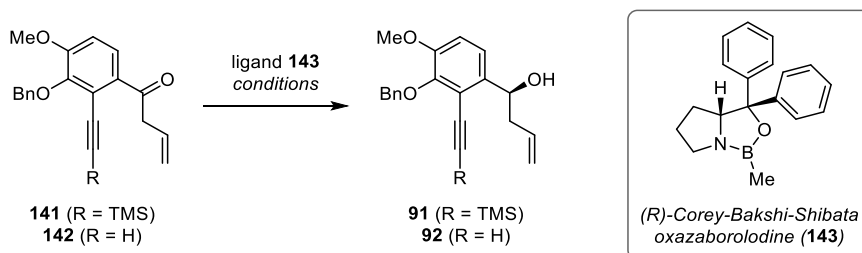
Oxidation of racemic allylation product **91** using Dess–Martin periodinane gave prochiral ketone **141** (Scheme 35). Similarly, ketone **142** bearing a free alkyne group was prepared by DMP-oxidation of deprotected allylation product **92**.

**Scheme 35. Oxidation of allylic alcohol using Dess–Martin periodinane.**

First, asymmetric reduction employing the Corey–Bakshi–Shibata protocol was investigated on both the protected and the free alkyne substrates (Table 30). To determine the maximum achievable enantioselectivity, the reactions were carried out using a stoichiometric amount of chiral borane

(formed by treating oxazaborolidine **143** with a borane source).<sup>[180]</sup> An initial experiment conducted according to a general procedure determined that the TMS-protected substrate **141** produced the corresponding alcohol in lower yield and enantiomeric excess (Table 30, entries 1 and 2).<sup>[181]</sup> Further experiments carried out on free alkyne **142** were not promising: lowering the reaction temperature was detrimental to the yield (Entry 4), while a reaction at ambient temperature resulted in complete decomposition of the starting material (Entry 3). The use of the sterically more hindered and less reactive catecholborane as hydride source was unsatisfactory with respect to yield and enantioinduction both at room temperature and at low temperature (Entries 5 and 6).

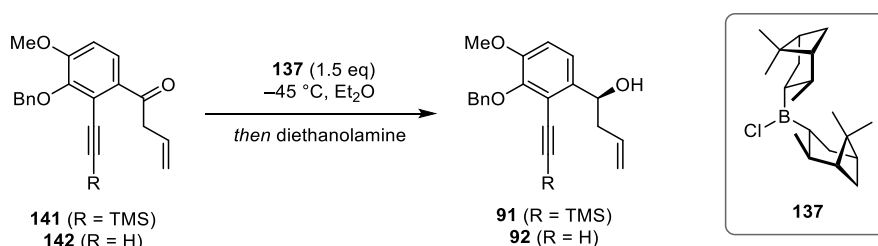
**Table 30. Enantioselective reduction of ketones **141** or **142** with CBS-reagent.**



Entry	Substrate	Conditions	Temp (°C)	Time (h)	Yield (%)	ee <sup>b</sup> (%)
<b>1</b>	<b>141</b> (R = TMS)	1 eq. <b>143</b> , 1.5 eq. BH <sub>3</sub> ·SMe <sub>2</sub>	−20	5	54	73.0
<b>2</b>	<b>140</b> (R = H)	1 eq. <b>143</b> , 1.5 eq. BH <sub>3</sub> ·SMe <sub>2</sub>	−20	5	65	84.6
<b>3</b>	<b>140</b> (R = H)	1 eq. <b>143</b> , 1.5 eq. BH <sub>3</sub> ·SMe <sub>2</sub>	rt	21	- <sup>a</sup>	n.d.
<b>4</b>	<b>140</b> (R = H)	1 eq. <b>143</b> , 1.5 eq. BH <sub>3</sub> ·SMe <sub>2</sub>	−78	21	4	87.0
<b>5</b>	<b>140</b> (R = H)	1 eq. <b>143</b> , 2.3 eq. HBcat	rt	21	38	60.8
<b>6</b>	<b>140</b> (R = H)	1 eq. <b>143</b> , 2.3 eq. HBcat	−78	21	17	73.7

**a)** decomposition of **140** was observed; **n.d.** = not determined; **HBcat** = catecholborane; **b)** determined by HPLC analysis on chiral stationary phase.

Parallel to our efforts in using the CBS-reagent **143**, we investigated the reduction mediated by DIP-Cl.<sup>[182–184]</sup> Exposure of the protected ketone **141** to DIP-Cl (**137**) in THF at −40 °C furnished homoallylic alcohol in 70% yield with an excellent enantiomeric excess of 93% (Table 31). Even better results were achieved by reduction of the free alkyne (cf. Entries 2 and 3). Reduction of **142** delivered multigram quantities of corresponding alcohol **92** in 72% yield and an excellent optical purity approaching 99% ee (Entry 5).

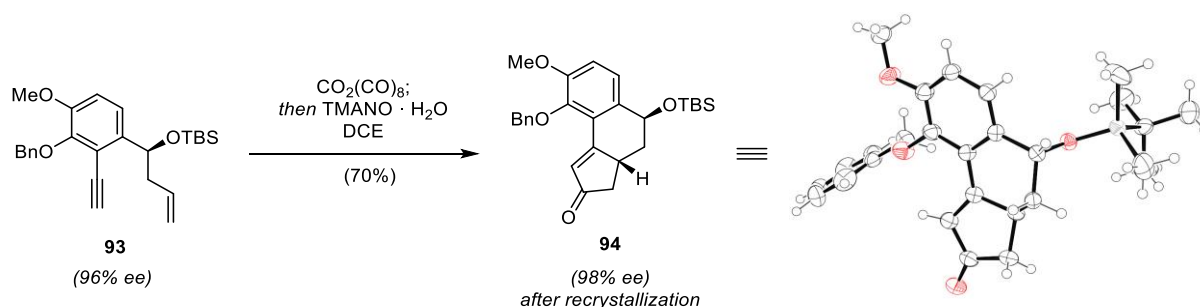
**Table 31. Enantioselective ketone reduction mediated by DIP-Cl.**

Entry	Substrate	Scale (mg)	Yield (%)	ee <sup>a</sup> (%)
1	<b>141</b> (R = TMS)	64	80%	87.7
2	<b>141</b> (R = TMS)	64	70%	93.2
3	<b>142</b> (R = H)	79	76%	97.1
4	<b>142</b> (R = H)	79	73%	96.4
5	<b>142</b> (R = H)	4200	72%	98.7

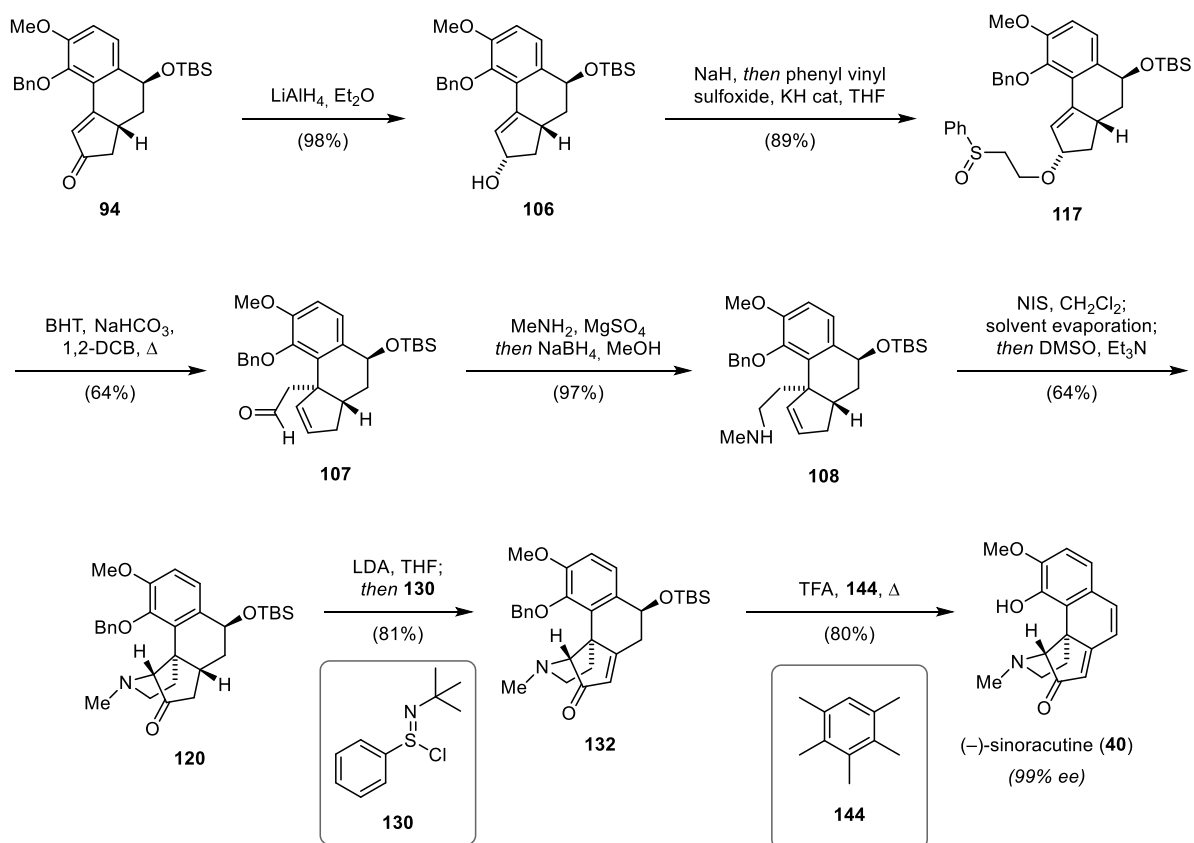
a) determined by HPLC analysis on chiral stationary phase.

### 2.2.6.3. Completion of the Enantioselective Synthesis

Silylation of enantioenriched alcohol **92** delivered enyne **93**, which was subjected to previously optimized conditions for the Pauson–Khand reaction. Tricyclic **94** was obtained in good yield and excellent enantiomeric excess. It could be recrystallized to afford crystals suitable for X-ray analysis, allowing us to assign the absolute configuration (Scheme 36).

**Scheme 36. Pauson-Khand reaction and absolute configuration of enone 94.**

Reduction of **94** followed by Mandai–Claisen rearrangement delivered aldehyde **107** which was treated with methylamine and NaBH<sub>4</sub> to give **108**. Tandem Iodocyclization–Kornblum oxidation delivered Ketone **120** which, under Mukaiyama conditions, was transformed into enone **132**. Elimination and debenzoylation with TFA in the presence of pentamethylbenzene finally afforded (–)-sinoracutine (**40**) in excellent enantiopurity (see Section 2.2.7).



Scheme 37. Completion of the enantioselective synthesis of (-)-sinoracutine.

### 2.2.7. Stereochemical Identity and Racemization of Sinoracutine

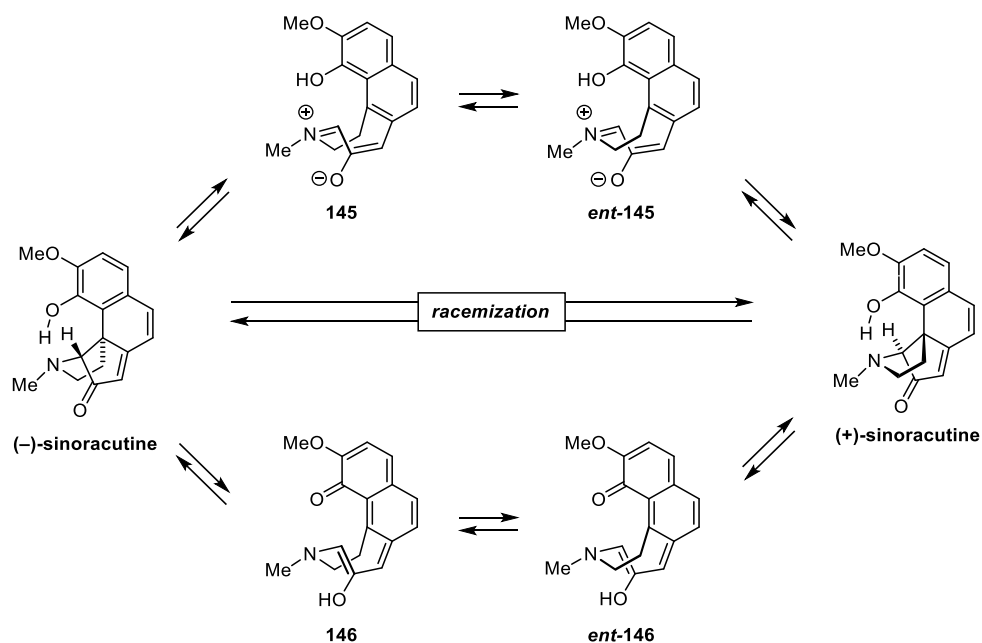
Using a racemic sample of sinoracutine, we developed a method to separate its enantiomers using HPLC on chiral stationary phase. (see Experimental Part for further details). Pleasingly, the material resulting from our asymmetric synthesis showed an enantiomeric excess of 98.9%. This material also exhibited the same levorotatory optical power as the natural isolate from *Sinomonium acutum*. With an optical rotation of  $[\alpha]_{\text{D}}^{25} = -1067.3$  ( $c = 0.35$ ,  $\text{CHCl}_3$ ), the magnitude of the synthetic sample was considerably higher than the value of the original isolation report by Bao:  $[\alpha]_{\text{D}}^{25} = -7.4$  ( $c = 0.35$ ,  $\text{CHCl}_3$ ). Furthermore, the sample of sinoracutine from *Stephania cepharantha* also exhibited a lower optical power:  $[\alpha]_{\text{D}}^{25} = -754.5$  ( $c = 1.14$ ,  $\text{CHCl}_3$ ). Although different factors can influence the value of optical rotation (water content in solvent, pH, presence of nonchiral impurities that interact with the compound of interest), this supports the observation that the enantiopurity of sinoracutine varies in nature. In particular, the X-ray of purported (+)-sinoracutine, where no value for optical rotation was reported, stands in contrast to the original isolation report of (-)-sinoracutine, which also features crystallographic structural proof. Since we had the crystallographic data for racemic sinoracutine available, the three datasets were compared.

**Table 32. Selected crystallographic parameters for available X-ray structures of sinoracutine.**

	This work (2016)	Wang et al. (2014) <sup>[60]</sup>	Bao et al. (2009) <sup>[58]</sup>
net formula	C <sub>17</sub> H <sub>17</sub> NO <sub>3</sub>	C <sub>17</sub> H <sub>17</sub> NO <sub>3</sub>	C <sub>17</sub> H <sub>17</sub> NO <sub>3</sub>
M <sub>r</sub> (g/mol)	283.31	283.31	283.31
crystal size (mm)	0.10 × 0.07 × 0.01	0.20 × 0.43 × 0.50	0.56 × 0.48 × 0.06
T (K)	100.(2)	93	293
crystal system	orthorhombic	orthorhombic	monoclinic
space group	Pbca	Pbca	P2 <sub>1</sub> /n
a (Å)	14.8795(5)	14.888(3)	8.6507 (14)
b (Å)	10.3203(3)	10.331(2)	10.4644(16)
c (Å)	17.7065(6)	17.724(4)	16.078(3)
α (°)	90	90	90
β (°)	90	90	104.9
γ (°)	90	90	90
V (Å <sup>3</sup> )	2719.03	2726.3	1406.5
Z	8	8	4

As can be seen in Table 32, the crystal structure of our racemic compound is identical to the structure reported by Wang and co-workers in 2014. Both crystals have identical cell parameters and belong to the centrosymmetric space group *Pbca* whose unit cell contains both enantiomers. The same goes for the purported structure of (–)-sinoracutine, which belongs to the centrosymmetric P2<sub>1</sub>/n. So far, all crystallographic data in the literature and available to us describe racemic samples of sinoracutine, which might explain the high variability in optical rotation in the different reports.

The existence of racemic sinoracutine in nature and the variable optical rotations raise the question on the origin of these stereochemical differences. It seems very unlikely that the enzymes involved in the biosynthesis of sinoracutine are able to process both enantiomers of every intermediate in the biosynthetic pathway and funnel them towards the final product, which would then appear as a scalemic mixture. Another possibility is that sinoracutine is subject to racemization once formed. Reasonable mechanisms, which could occur without enzymatic assistance, are shown in Scheme 38. They both rely on the planarization of the benzylic all-carbon quaternary stereocenter. Thereby, a retro-Mannich reaction would lead to ring-opening of the pyrrolidine ring to an intermediate eight-membered azocane **145**, in which the benzylic quaternary carbon is destroyed and becomes sp<sup>2</sup>-hybridized. The resulting vinylogous enolate intermediate can undergo a Mannich-type ring-closure to reform the pyrrolidine ring and give sinoracutine, now in racemic form. Alternatively, after proton transfer from the phenolic oxygen to the carbonyl oxygen, a retro-Michael reaction through the intermediacy of *o*-quinone methide **146** occurs to give a ring opened intermediate – again with loss of stereochemical information. Ring closure of the resulting enol to the newly formed, highly electrophilic *o*-quinone methide affords racemic sinoracutine after proton transfer.



**Scheme 38. Racemization mechanisms of sinoracutine via ring-opening and -closure.**

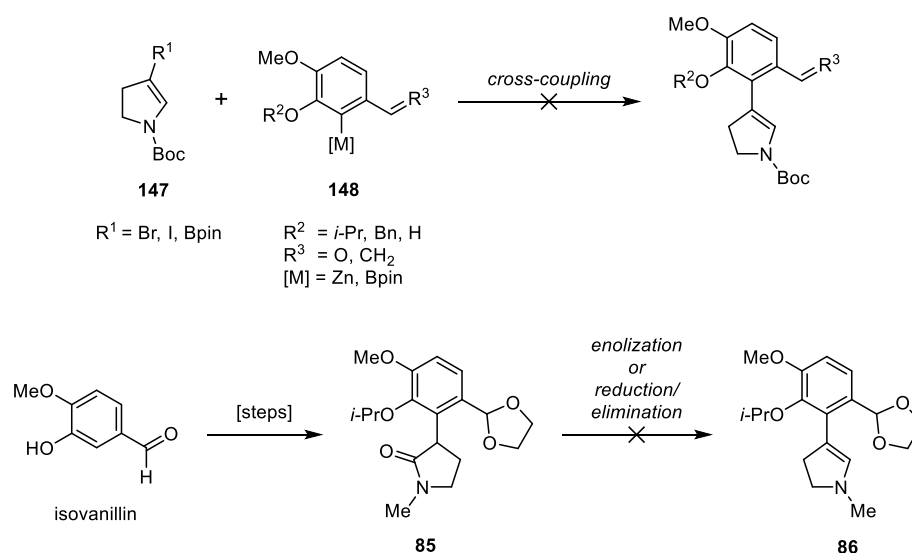
Interestingly, the final reaction in the synthesis uses forcing conditions to achieve debenzoylation of **132** (neat TFA, 40 °C, 14 hours), but delivered an enantiopure sample of sinoracutine. Under these conditions it can be assumed that the nitrogen is fully protonated. This indicates that protonation of the tertiary amine might inhibit a racemization through the indicated mechanisms above either by discouraging the iminium ion formation of **145**, or by preventing proton transfer and ketone enolization to give **146**. Under neutral conditions on the other hand, racemization occurs.

Therefore, we set out to examine the racemization of sinoracutine experimentally under neutral conditions. A protic solvent was added to a sample of enantiopure sinoracutine to encourage proton transfer, as it is a requirement for the proposed mechanisms shown above to be operative. Fascinatingly, when a sample of sinoracutine exhibiting 98.9% ee that had been stored in a solution of heptane/*i*PrOH/MeOH = 6/2/2 was kept at room temperature for 67 days, we noticed a very small but measurable erosion of enantiopurity to 95.7% ee. Heating the same sample to 60 °C for 5 days delivered a nearly racemic product (3.2% ee). A control experiment with a sample that was kept neat at -25 °C for the same time, still showed an enantiomeric excess of 98.7%. Indeed, racemization of sinoracutine does occur slowly at ambient temperature and can be accelerated thermally.

It is likely that during the isolation process (e.g. during solvent evaporation or recrystallization) racemization of sinoracutine might have occurred. Alternatively, during the natural life cycle of the plant, which lasts several years, accumulated sinoracutine might have undergone gradual racemization. Although further studies are necessary to determine the culprit of this erosion of stereochemistry in nature, theoretical calculations are being performed to assess the legitimacy of the mechanisms proposed in Scheme 38. These results represent a highly unusual, and to the best of our knowledge, unique racemization of an all-carbon substituted quaternary stereogenic center.

### 3. Summary

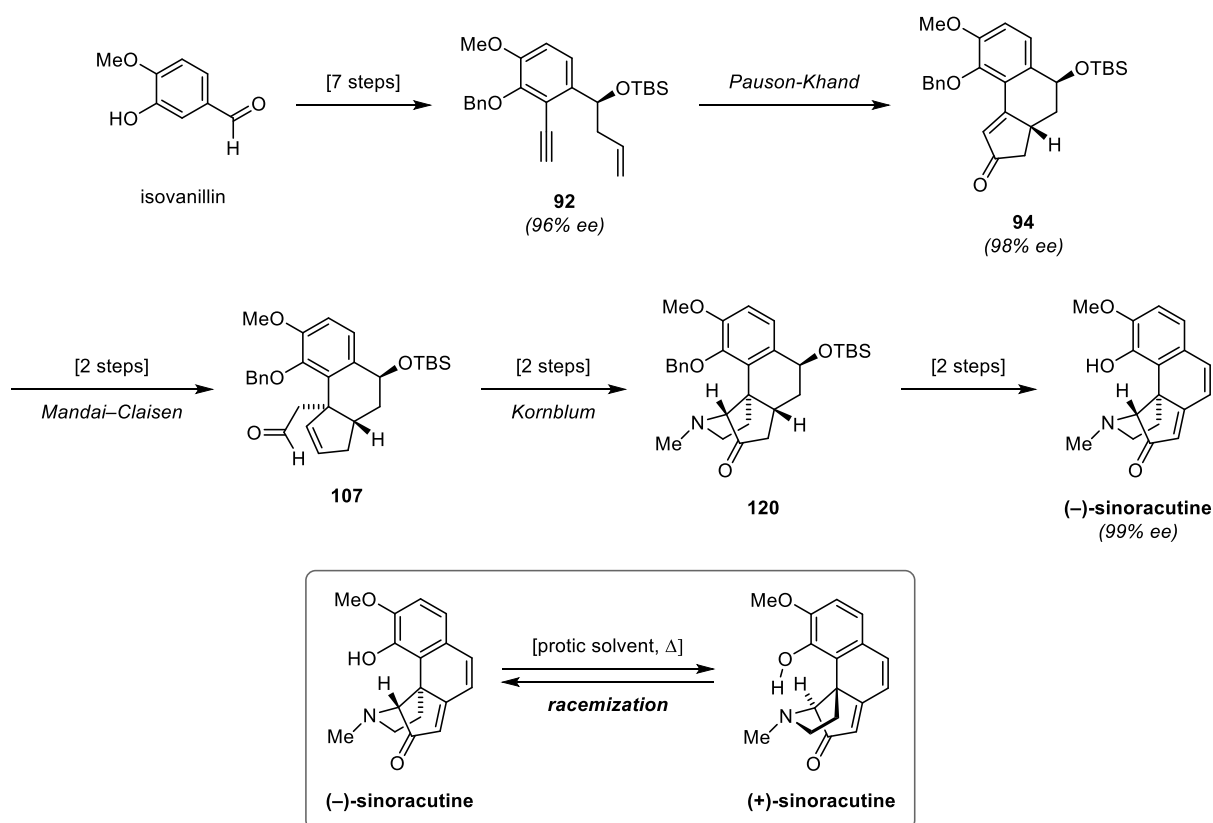
Part I of this thesis described the total synthesis of the tetracyclic alkaloid sinoracutine, which was isolated from *Sinomenium Acutum* and *Stephania cepharanta*. It occurs as a racemic mixture in contrast to the vast majority of reticuline-derived alkaloids, which occur as single enantiomers. Two strategies were pursued to synthesize an appropriately protected 2-arylpyrrolidine bearing a pendant alkyne as substrate for an enamine Pauson–Khand reaction (Scheme 39). A cross-coupling strategy using halogenated dihydropyrroles of type **147** in conjunction with *o,o*-disubstituted aromatic partners (**148**) was not successful. Several possible coupling partners were investigated without success, and the polarity reversal of the partners was also unfruitful. Failure of the approach lies in the steric hindrance of the aromatic substrate and the instability of the pyrroline coupling partner under the reaction conditions examined. A stepwise construction of the pyrrolidine ring was successful and gave rise to *N*-methylated lactam **85**. However, attempted enolization or reduction of the pyrrolidinone in order to introduce the required enamine functionality (**86**), was not possible.



**Scheme 39.** Failed approaches for the synthesis of sinoracutine.

Therefore, the synthetic plan was modified to employ a 1,7-enyne bearing a benzylic silyl ether as a stereocontrolling element and to introduce the pyrrolidine ring at a later stage in the synthesis (Scheme 40). The construction of a 6,6,5-tricycle was achieved by Pauson–Khand reaction. Installation of the quaternary benzylic stereocenter was best accomplished by the Mandai–Claisen protocol after diastereoselective reduction of the allylic alcohol derived from Pauson–Khand product **94**. From this intermediate, reductive amination followed by a tandem iodocyclization–Kornblum oxidation delivered tetracyclic intermediate **120**. Oxidation, elimination and debenylation afforded racemic sinoracutine. The route could be rendered asymmetric by using enantiopure enyne **92**, synthesized by an enantioselective reduction of the corresponding ketone mediated by DIP-Cl. To explain the racemic occurrence of sinoracutine in variable optical purity across different natural

isolates, we set out to determine whether enantiopure (–)-sinoracutine could undergo racemization. While in acidic medium the enantiomeric purity of the natural product remains constant, we were able to demonstrate the exceptionally facile racemization of (–)-sinoracutine in protic solvent. Presumably, the mechanism of racemization involves ring-opening of the cyclopentenone ring followed by ring-closure. Most notably, this results in the loss of stereochemical information of an all-carbon substituted quaternary stereocenter, and represents a highly unusual result that had never been observed in the series of reticuline-derived alkaloids, as well as other natural product classes.



**Scheme 40.** Synthesis of (–)-sinoracutine and its racemization.

## 4. Experimental Part

### 4.1. General Experimental Details

#### 4.1.1. Materials and Methods

Unless noted otherwise, all reactions were performed in flame-dried glassware fitted with rubber septa under a positive pressure of nitrogen. Air- and moisture-sensitive liquids were transferred via syringe or stainless steel cannula through rubber septa. Solids were added under inert gas or were dissolved in appropriate solvents. The reactions were magnetically stirred and monitored by NMR spectroscopy where noted or analytical thin-layer chromatography (TLC) using glass plates precoated with silica gel (0.25 mm, 60-Å pore size, Merck) impregnated with a fluorescent indicator (254 nm). TLC plates were visualized by exposure to ultraviolet light (UV, 254 or 366 nm), were stained by submersion in either aqueous potassium permanganate solution (KMnO<sub>4</sub>), ceric ammonium molybdate solution (CAM) or acidic *p*-anisaldehyde solution (PAA) and were developed by heating with a heat gun. Flash-column chromatography on silica gel (60 Å pore size, 40–63 μm, Merck KGaA) was performed as described by Still<sup>[185]</sup> or using a Biotage Isolera™ Prime Automated Flash Purification system. Triethylamine-deactivated silica was obtained by preparing a slurry of silica gel (20% v/v in the initial eluent mixture + 5% v/v Et<sub>3</sub>N) followed by magnetic stirring for 1 h. The slurry was poured into a chromatography column and flushed with 5 column volumes of amine-free eluent prior to sample loading and elution.

Tetrahydrofuran (THF) and diethyl ether (Et<sub>2</sub>O) were distilled from Na/benzophenone prior to use. Dichloromethane (CH<sub>2</sub>Cl<sub>2</sub>), triethylamine (Et<sub>3</sub>N), *N,N*-diisopropylamine (DIPA) were distilled under nitrogen atmosphere from CaH<sub>2</sub> prior to use. Benzene, 1,2-dichloroethane (DCE), dimethyl sulfoxide (DMSO), 1,2-dichlorobenzene (DCB) were purchased from Acros Organics as 'extra dry' and used as received. All other reagents and solvents were purchased from chemical suppliers (Sigma-Aldrich, Acros Organics, Alfa Aesar, Strem Chemicals, ABCR) and were used as received. Solvents for extraction, crystallization and flash-column chromatography on silica gel were purchased as technical grade and distilled under reduced pressure prior to use. The molarity of *n*-butyllithium solutions was determined by titration to a blue endpoint against *N*-benzylbenzamide<sup>[186]</sup> at -40 °C (average of three determinations).

Unless noted otherwise, yields refer to chromatographically and spectroscopically (<sup>1</sup>H and <sup>13</sup>C NMR) pure material.

#### 4.1.2. Melting Point

Melting points were measured on a Stanford Research Systems MPA120 EZ-Melt apparatus in open glass capillaries.

#### 4.1.3. NMR Spectroscopy

NMR spectra were measured at room temperature (22 °C) on a Bruker Avance III HD 800 MHz spectrometer equipped with a CryoProbe™ operating at 800 MHz for proton nuclei and 200 MHz for carbon nuclei or a Bruker Avance III HD 400 MHz spectrometer equipped with a CryoProbe™ operating at 400 MHz for proton nuclei and 100 MHz for carbon nuclei. Proton chemical shifts are expressed in parts per million (ppm,  $\delta$  scale) and are referenced to residual protium in the NMR solvent ( $\text{CHCl}_3$ :  $\delta$  7.26,  $\text{C}_6\text{HD}_5$ : 7.16). Carbon chemical shifts are expressed in parts per million (ppm,  $\delta$  scale) and are referenced to the carbon resonance of the NMR solvent ( $\text{CDCl}_3$ :  $\delta$  77.16,  $\text{C}_6\text{D}_6$ : 128.06).  $^1\text{H}$  NMR spectroscopic data are reported as follows: Chemical shift in ppm (multiplicity, coupling constants  $J$  (Hz), integration intensity). The multiplicities are abbreviated with s (singlet), d (doublet), t (triplet), q (quartet), app (apparent), broad (br), combinations thereof, and m (multiplet). In case of combined multiplicities, the multiplicity with the larger coupling constant is stated first. Except for complex and overlapping multiplets, where a resonance range is given, the chemical shift of all other symmetric signals is reported as the center of the resonance range.  $^{13}\text{C}$  NMR spectroscopic data are reported as follows: Chemical shift in ppm. Additionally to  $^1\text{H}$  and  $^{13}\text{C}$  NMR measurements, 2D NMR techniques such as homonuclear correlation spectroscopy (COSY), heteronuclear single quantum coherence (HSQC) and heteronuclear multiple bond coherence (HMBC) were used to assist signal assignment. For further elucidation of 3D structures of the products, nuclear Overhauser enhancement spectroscopy (NOESY) was conducted. All raw FID files were processed and the spectra analyzed using the program Mnova 10.0.2 from Mestrelab Research S. L.

#### 4.1.4. Mass Spectrometry

All mass spectra were measured by the Analytical division of the Department of Chemistry, Ludwig-Maximilians-Universität München. Mass spectra were recorded on the following spectrometers (ionisation mode in brackets): MAT 95 (EI) and MAT 90 (ESI) from Thermo Finnigan GmbH and were recorded in high-resolution. The method used is reported in the relevant section of the experimental part.

#### 4.1.5. IR Spectroscopy

IR spectra were recorded on a Perkin Elmer Spectrum BX II FT-IR system and the compound was applied as thin film directly on the ATR unit (either as neat substance or as solution in CH<sub>2</sub>Cl<sub>2</sub>). Data are represented as follows: absorption frequency (expressed in cm<sup>-1</sup>) and intensity of absorption: s (strong), m (medium), w (weak), br (broad).

#### 4.1.6. Optical Rotation

Optical rotation values were recorded on an Anton Paar MCP 200 polarimeter. The specific rotation is calculated as follows:

$$[\alpha]_{\lambda}^{\varphi} = \frac{[\alpha] \cdot 100}{c \cdot d}$$

Thereby, the wavelength  $\lambda$  is reported in nm and the measuring temperature in °C.  $\alpha$  represents the recorded optical rotation,  $c$  the concentration of the analyte in 10 mg/mL and  $d$  the length of the cuvette in dm. Thus, the specific rotation is given in 10<sup>-1</sup>·deg·cm<sup>2</sup>·g<sup>-1</sup>. Use of the sodium D line ( $\lambda = 589$  nm) is indicated by  $D$  instead of the wavelength in nm. The sample concentration as well as the solvent is reported in the relevant section of the experimental part

#### 4.1.7. HPLC Analyses

Analytical HPLC on Chiral Stationary Phase was performed on a computer-operated Shimadzu system (Windows 10, LabSolutions Software, two LC-20AP pumps, manual injection (2 mL sample loop), CTO-20A column oven, SPD-M20A Diode Array detector). Column, oven temperature, solvent system, flow rate, detection mode and retention times are given in the relevant section of the experimental part.

Preparative HPLC was performed on a computer-operated Varian instrument (Windows XP, Galaxie Chromatography Software, two PrepStar SD-1 pumps, manual injection with 2 mL sample loop, ProStar 335 Photo Diode Array Detector, Agilent 440-LC Fraction Collector). Column, solvent system, flow rate, detection mode and retention times are given in the relevant section of the experimental part.

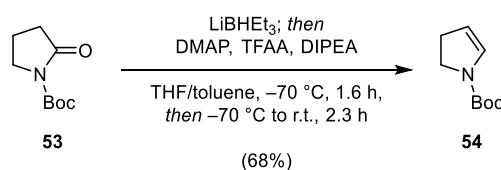
#### 4.1.8. X-ray Diffraction Analysis

Experiments were carried out by Dr. Peter Mayer (Ludwig-Maximilians-Universität München). The data collections were performed on a Bruker D8Venture using MoK $\alpha$ -radiation ( $\lambda = 0.71073$  Å, graphite monochromator). The CrysAlisPro software (version 1.171.33.41) was applied for the integration, scaling and multi-scan absorption correction of the data. The structures were solved by

direct methods with SIR9713 and refined by least-squares methods against F2 with SHELXL-97.14. All nonhydrogen atoms were refined anisotropically. The hydrogen atoms were placed in ideal geometry riding on their parent atoms. Further details are summarized in the tables at the different sections. Plotting of thermal ellipsoids in this document and in the main text was carried out using Ortep-3 for Windows.<sup>[187]</sup>

## 4.2. Experimental Procedures

### *tert*-Butyl 2,3-dihydro-1H-pyrrole-1-carboxylate (**54**)



To a solution of *N*-Boc-pyrrolidin-2-one (10.0 g, 54.0 mmol, 1.00 eq.) in toluene (74 mL) at  $-78\text{ }^\circ\text{C}$  was added lithium triethylborohydride (1 M in THF, 59.0 mmol, 1.10 eq.) over 40 min using a syringe pump. After stirring for 1 h at  $-70\text{ }^\circ\text{C}$  (internal temperature), DMAP (66.0 mg, 0.54 mmol, 0.01 eq.) was added. DIPEA (54.0 mL, 318 mmol, 5.40 eq.) was added dropwise over 10 min. Then TFAA (9.1 mL, 65.0 mmol, 1.20 eq.) was added dropwise over 20 min in order to keep the internal temperature below  $-70\text{ }^\circ\text{C}$ . After complete addition the cooling bath was removed and the mixture was stirred for further 2 h at room temperature. The solution was quenched by dropwise addition of water (80 mL). The phases were separated and the organic layer was washed with water (3 x 30 mL) and brine (3 x 30 mL). The mixture was dried over  $\text{MgSO}_4$ , filtered and the solvent was removed in vacuo. The crude product was submitted to flash column chromatography ( $\text{SiO}_2$ , hexanes/EtOAc = 19/1) to afford **54** as a colorless liquid (6.20 g, 36.7 mmol, 68 %). Spectral data match the previously reported values.<sup>[188]</sup>

$R_f = 0.26$  (hexanes/EtOAc = 19/1).

*Note: NMR spectra are complex due to the presence of rotamers.*

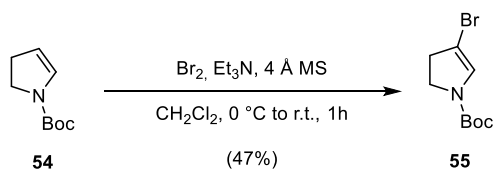
$^1\text{H NMR}$  (400 MHz,  $\text{CDCl}_3$ ):  $\delta = 6.52 - 6.38$  (m, 1H), 4.94 – 4.90 (m, 1H), 3.68 – 3.61 (m, 2H), 2.60 – 2.51 (m, 2H), 1.41 (s, 9H).

$^{13}\text{C NMR}$  (100 MHz,  $\text{CDCl}_3$ ):  $\delta = 130.0, 107.6, 80.1, 45.4, 44.9, 29.9, 28.6$ .

*Note: The carbonyl carbon was not visible in the  $^{13}\text{C}$  spectrum.*

**HRMS (EI)** for  $\text{C}_9\text{H}_{15}\text{NO}_2$   $[\text{M}]^+$ : calcd.: 169.1103, found: 169.1106.

**IR (ATR):**  $\tilde{\nu} = 2976$  (w), 1697 (s), 1618 (w), 1478 (w), 1405 (s), 1378 (s), 1258 (m), 1174 (m), 1132 (s), 1092 (m).

**tert-Butyl 4-bromo-2,3-dihydro-1H-pyrrole-1-carboxylate (55)**

A solution of bromine (30.0  $\mu\text{L}$ , 0.59 mmol, 1.00 eq.) in  $\text{CH}_2\text{Cl}_2$  (1.20 mL) was added over 1 h to a suspension of enamine **54** (0.50 g, 2.95 mmol, 1.00 eq.),  $\text{Et}_3\text{N}$  (1.44 mL, 10.3 mmol, 3.50 eq.) and activated 4  $\text{\AA}$  molecular sieves (114 mg) in  $\text{CH}_2\text{Cl}_2$  (10.0 mL) at 0  $^\circ\text{C}$ . After addition was completed the ice bath was removed and the mixture was stirred for another hour at room temperature. Afterwards the mixture was filtered through a Celite pad, the solvent was removed under reduced pressure and the crude product was purified by flash column chromatography ( $\text{SiO}_2$ , hexane/ $\text{EtOAc}$  = 19/1) to afford **55** as yellow oil (346 mg, 37.0 mmol, 47 %).

*Note: The product was unstable upon storage at room temperature and therefore stored in a benzene matrix at  $-25^\circ\text{C}$  (100 mg/10 mL).*

$R_f$  = 0.46 (hexanes/ $\text{EtOAc}$  = 19/1).

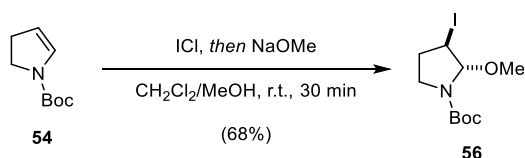
*Note: NMR spectra are complex due to the presence of rotamers.*

$^1\text{H NMR}$  (400 MHz,  $\text{CDCl}_3$ )  $\delta$  = 6.62 (s, 1H), 3.89 – 3.67 (m, 2H), 2.84 (t,  $J$  = 9.1 Hz, 2), 1.45, (s, 9H).

$^{13}\text{C NMR}$  (100 MHz,  $\text{CDCl}_3$ )  $\delta$  = 151.5, 151.0, 129.9, 100.2, 100.0, 80.9, 80.7, 46.2, 45.6, 36.6, 35.6, 29.8, 28.4.

**HRMS (EI)** for  $\text{C}_9\text{H}_{14}\text{BrNO}_2^+ [\text{M}]^+$ : calcd.: 247.0208, found: 247.0207.

**IR (ATR):**  $\tilde{\nu}$  = 2975 (w), 1694 (s), 1628 (w), 1478 (w), 1381 (s), 1366 (s), 1324 (m), 1255 (m), 1007 (s), 962 (m), 918 (m), 876 (s), 844 (m), 772 (m).

**Rac-tert-butyl (2S,3R)-3-iodo-2-methoxypyrrolidine-1-carboxylate (56)**

$\text{ICl}$  (1 M in  $\text{CH}_2\text{Cl}_2$ , 29.25 mmol, 1.1 eq.) was added dropwise to a solution of sodium methoxide (2.87 g, 53.2 mmol, 2.00 eq.) and *N*-Boc-2,3-dihydro-1H-pyrrole **54** (4.5 g, 26.6 mmol, 1.00 eq.) in  $\text{MeOH}$  (95 mL) at room temperature. After stirring for 30 min, a saturated solution of  $\text{Na}_2\text{S}_2\text{O}_3$  (20 mL) was added and the mixture was stirred for further 30 min. The phases were separated and the aqueous phase was extracted three times with  $\text{Et}_2\text{O}$  (40 mL). The combined organic layers were

washed with water (3 x 30 mL) and brine (3 x 30 mL), dried over MgSO<sub>4</sub>, filtered and the solvent was removed in vacuo. The crude product was purified by flash column chromatography (SiO<sub>2</sub>, hexane/EtOAc = 5/1) to afford **56** as beige oil (5.91 g, 18.08 mmol, 68 %). Spectral data match the previously reported values.<sup>[87]</sup>

$R_f = 0.31$  (hexanes/EtOAc = 5/1)

*Note: NMR spectra are complex due to the presence of rotamers.*

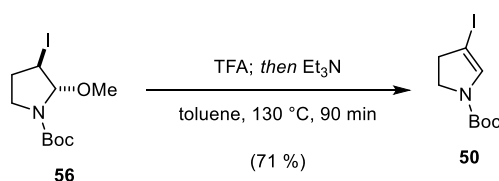
<sup>1</sup>H NMR (400 MHz, CDCl<sub>3</sub>)  $\delta = 5.37$  and  $5.24$  (s, 1H),  $4.21$  (d,  $J = 5$  Hz, 1H),  $3.69 - 3.55$  (m, 1H),  $3.48 - 3.42$  (m, 1H),  $3.40$  and  $3.35$  (s, 3H),  $2.54 - 2.43$  (m, 1H),  $2.15 - 2.07$  (m, 1H),  $1.49$  (s, 9H).

<sup>13</sup>C NMR (100 MHz, CDCl<sub>3</sub>)  $\delta = 155.2$ ,  $154.6$ ,  $96.6$ ,  $96.4$ ,  $80.7$ ,  $80.5$ ,  $56.4$ ,  $56.1$ ,  $45.1$ ,  $44.5$ ,  $33.9$ ,  $33.1$ ,  $28.5$ ,  $27.2$ ,  $26.3$ .

HRMS (EI) for C<sub>10</sub>H<sub>18</sub>INO<sub>3</sub><sup>+</sup> [M]<sup>+</sup>: calcd.: 327.0331, found: 327.0343.

IR (ATR):  $\tilde{\nu} = 2976$  (w),  $1702$  (s),  $1478$  (w),  $1378$  (s),  $1258$  (w),  $1162$  (s),  $1115$  (m),  $1076$  (s),  $1030$  (w).

### **tert-butyl 4-iodo-2,3-dihydro-1H-pyrrole-1-carboxylate (50)**



A solution of *trans*-tert-butyl 3-iodo-2-methoxypyrrolidine-1-carboxylate **56** (700 mg, 2.14 mmol, 1.00 eq.) and TFA (15  $\mu$ L, 0.2 mmol, 0.10 eq.) in toluene (46 mL) was submerged in an oil bath preheated to 130 °C for 90 min. After cooling to room temperature with the aid of an ice bath, Et<sub>3</sub>N (90  $\mu$ L, 0.6 mmol, 0.30 eq.) was added, the solvent was removed in vacuo and the residue was submitted to flash column chromatography (SiO<sub>2</sub>, hexane/EtOAc = 19/1) to afford **50** as colorless oil (450 mg, 1.51 mmol, 71%). Spectral data match the previously reported values.<sup>[87]</sup>

*Note: The product is sensitive towards light and temperature. It can be stored in a benzene matrix at  $-25$  °C in dilute solution (0.1 M). A 0.5 M solution was found to decompose within 14 days even if stored at  $-25$  °C.*

$R_f = 0.29$  (hexanes/EtOAc = 19/1)

*Note: NMR spectra are complex due to the presence of rotamers.*

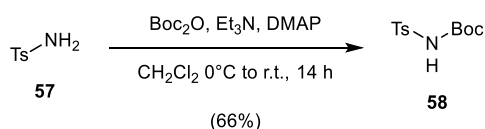
<sup>1</sup>H NMR (400 MHz, CDCl<sub>3</sub>)  $\delta = 6.76$  and  $6.62$  (s, 1H),  $3.76 - 3.71$  (m, 2H),  $2.86 - 2.79$  (m, 2H),  $1.45$  (s, 9H).

<sup>13</sup>C NMR (100 MHz, CDCl<sub>3</sub>)  $\delta = 151.1$ ,  $150.5$ ,  $136.0$ ,  $81.0$ ,  $80.7$ ,  $66.3$ ,  $46.7$ ,  $46.1$ ,  $39.9$ ,  $38.9$ ,  $28.5$ .

**HRMS (EI)** for  $C_9H_{15}O_2N^+$   $[M]^+$ : calcd.: 296.0142, found: 296.0134.

**IR (ATR):**  $\tilde{\nu}$  = 2976 (w), 2931 (w), 1702 (s), 1478 (w), 1455 (w), 1391 (s), 1284 (w), 1243 (m), 1173 (m), 1127 (m).

### ***tert*-butyl tosylcarbamate (58)**



To a solution of 4-methylbenzenesulfonamide **57** (20.03 g, 117.0 mmol, 1.00 eq.), Et<sub>3</sub>N (16.8 mL, 120.5 mmol, 1.03 eq.) and DMAP (1.43 g, 11.70 mmol, 0.10 eq.) in CH<sub>2</sub>Cl<sub>2</sub> (190 mL) at 0 °C was added a solution of Boc<sub>2</sub>O (29.11 g, 133.4 mmol, 1.14 eq.) in CH<sub>2</sub>Cl<sub>2</sub> (100 mL). The reaction mixture was stirred for 14 h. Then, the solvent was removed under reduced pressure and the residue was taken up in EtOAc (200 mL), washed with aqueous HCl (1 M, 100 mL), water (100 mL), brine (100 mL), dried over MgSO<sub>4</sub> and filtered. The solvent was removed in vacuo and the crude product was recrystallized from EtOAc/hexanes (280/100 mL) to afford, after filtration, **58** as white crystalline solid (21.0 g, 77.2 mmol, 66 %). Spectral data match the previously reported values.<sup>[189]</sup>

$R_f$  = 0.19 (hexanes/EtOAc = 7/3).

**Melting point** = 97.0 – 99.2 °C.

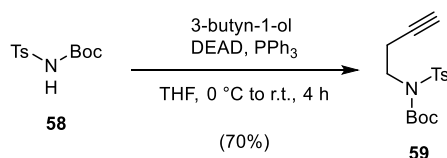
**<sup>1</sup>H NMR** (400 MHz, CDCl<sub>3</sub>)  $\delta$  = 7.90 (d,  $J$  = 8.4 Hz, 2H), 7.34 (d,  $J$  = 8.4 Hz, 2H), 7.08 (br s, 1H), 2.45 (s, 3H), 1.39 (s, 9H).

**<sup>13</sup>C NMR** (100 MHz, CDCl<sub>3</sub>)  $\delta$  = 149.0, 144.9, 136.0, 129.7, 128.4, 84.2, 28.0, 21.8.

**HRMS (EI)** for  $C_{12}H_{17}NO_4S^+$   $[M]^+$ : calcd.: 271.0837, found: 271.0878.

**IR (ATR):**  $\tilde{\nu}$  = 3246 (w), 2982 (w), 1746 (m), 1598 (w), 1435 (w), 1347 (m), 1238 (w), 1147 (s), 1090 (m), 912 (w), 830 (w).

### ***tert*-butyl but-3-yn-1-yl(tosyl)carbamate (59)**



To a solution of *tert*-butyl tosylcarbamate **58** (8.28 g, 30.5 mmol, 1.00 eq.), 3-butyn-1-ol (2.77 mL, 36.6 mmol, 1.20 eq.) and triphenylphosphine (16.0 g, 61.0 mmol, 2.00 eq.) in THF (165 mL) at 0 °C was slowly added diethyl azodicarboxylate (40% in toluene, 9.56 g, 54.9 mmol, 1.80 eq.) was added dropwise via syringe pump. The solution was stirred at 0 °C while slowly warming to room

temperature over 4 h. The solvent was removed in vacuo and the resulting solid was submitted to flash column chromatography (SiO<sub>2</sub>, hexane/EtOAc = 8/2 to 1/1) to afford **59** as a white solid (6.88 g, 21.3 mmol, 70%). Spectral data match the previously reported values.<sup>[190]</sup>

**R<sub>f</sub>** = 0.50 (hexanes/EtOAc = 7/3).

**Melting point** = 77.0 – 79.0 °C

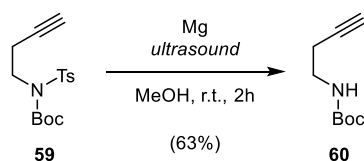
**<sup>1</sup>H NMR** (400 MHz, CDCl<sub>3</sub>) δ = 7.80 (d, *J* = 8.3 Hz, 2H), 7.31 (d, *J* = 8.3 Hz, 2H), 4.00 (t, *J* = 7.4 Hz, 2H), 2.66 (td, *J* = 7.4 Hz, 2.7 Hz, 2H), 2.44 (s, 3H), 2.02 (t, *J* = 2.7 Hz, 1H), 1.35 (s, 6H).

**<sup>13</sup>C NMR** (100 MHz, CDCl<sub>3</sub>) δ = 150.9, 144.4, 137.3, 129.4, 128.1, 84.7, 80.6, 70.6, 45.4, 28.0, 21.8, 20.1.

**HRMS (EI)** for C<sub>16</sub>H<sub>21</sub>NO<sub>4</sub>S<sup>+</sup> [M]<sup>+</sup>: calcd.: 323.1191, found: 323.1301.

**IR (ATR)**:  $\tilde{\nu}$  = 3295 (m), 2982 (w), 1722 (s), 1597 (m), 1494 (w), 1448 (w), 1372 (m), 1355 (s), 1327 (m), 1287 (m), 1167 (s), 1135 (s), 1093 (s), 1077 (m), 970 (w).

### ***tert*-butyl but-3-yn-1-ylcarbamate (**60**)**



To a solution of *tert*-butyl but-3-yn-1-yl(tosyl)carbamate **59** (5.87 g, 18.2 mmol, 1.00 eq.) in MeOH (180 mL) were added magnesium turnings (4.42 g, 182 mmol, 10.00 eq.). The reaction mixture was sonicated for 2 h after which all magnesium has been dissolved. The solvent was removed in vacuo, diluted with CH<sub>2</sub>Cl<sub>2</sub> (100 mL), poured onto aqueous HCl (0.5 M, 100 mL) and the resulting white precipitate was filtered off. The organic phase was separated, washed with saturated aqueous NaHCO<sub>3</sub> (100 mL), brine (100 mL), dried over MgSO<sub>4</sub> and filtered. The solvent was removed in vacuo and the crude product purified by flash column chromatography (SiO<sub>2</sub>, hexanes/Et<sub>2</sub>O = 8/2, to 7/3) to afford **60** as colorless oil (1.93 g, 11.4 mmol, 63 %). Spectral data match the previously reported values.<sup>[191]</sup>

**R<sub>f</sub>** = 0.39 (hexanes/EtOAc = 7/3).

**Melting point** = 77.0 – 79.0 °C

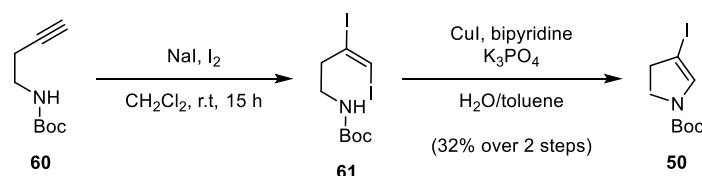
**<sup>1</sup>H NMR** (400 MHz, CDCl<sub>3</sub>) δ = 4.84 (br s, 1H), 3.28 (d, *J* = 6.4 Hz, 2H), 2.38 (td, *J* = 6.4, 2.7 Hz, 2H), 2.00 (t, *J* = 2.7 Hz, 1H), 1.45 (s, 9H)

**<sup>13</sup>C NMR** (100 MHz, CDCl<sub>3</sub>) δ = 155.8, 81.8, 79.6, 70.0, 39.4, 28.5, 20.1.

**HRMS (EI)** for C<sub>9</sub>H<sub>16</sub>NO<sub>2</sub><sup>+</sup> [M]<sup>+</sup>: calcd.: 170.1181, found: 170.1181.

**IR (ATR):**  $\tilde{\nu}$  = 3306 (w), 2979 (w), 2935 (w), 1692 (s), 1513 (m), 1456 (w), 1392 (w), 1366 (m), 1251 (m), 1169 (s), 1074 (w).

**tert-butyl 4-iodo-2,3-dihydro-1H-pyrrole-1-carboxylate (50)**



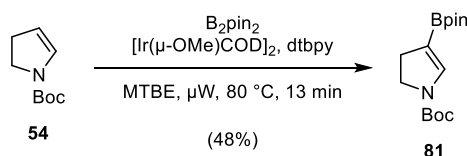
*Note: The following reaction was performed under the exclusion of light: laboratory and fume hood lights were turned off, the reaction flask wrapped in aluminum foil and flasks connected to a rotary evaporator were covered with aluminum foil.*

To a solution of tert-butyl but-3-yn-1-ylcarbamate **60** (1.86 g, 11.0 mmol, 1.00 eq.) in anhydrous CH<sub>2</sub>Cl<sub>2</sub> (76 mL), were added sodium iodide (8.81 g, 58.7 mmol, 5.30 eq.) and iodine (6.00 g, 23.7 mmol, 2.15 eq.). The reaction mixture was stirred for 15 h in and quenched with a saturated aqueous Na<sub>2</sub>S<sub>2</sub>O<sub>3</sub> (120 mL). The phases were separated and the aqueous phase was extracted with CH<sub>2</sub>Cl<sub>2</sub> (3 × 50 mL). The combined organic layers were washed with brine (100 mL), dried over MgSO<sub>4</sub>, filtered and concentrated in vacuo. The resulting crude tert-butyl (E)-(3,4-diiodobut-3-en-1-yl)carbamate **61** appeared as yellow oil and was immediately used for the next step without further purification.

To a solution of crude (E)-(3,4-diiodobut-3-en-1-yl)carbamate (4.65 g, 11.0 mmol, 1.00 eq., based on a hypothetical 100 % yield of the diiodination reaction) toluene (170 mL) was added CuI (1.05 g, 5.50 mmol, 0.50 eq.), K<sub>3</sub>PO<sub>4</sub> (7.01 g, 33.0 mmol, 3.00 eq.), 2,2'-bipyridine (1.72 g, 11.0 mmol, 1.00 eq.) and water (0.178 mL, 9.90 mmol, 0.90 eq.) and the resulting red mixture was heated to reflux for 72 h. The solution was allowed to cool to room temperature, filtered through a pad of celite and concentrated in vacuo. The residue was directly submitted to flash column chromatography (SiO<sub>2</sub>, hexane/EtOAc = 10/1) and afforded **50** as colorless oil (1.04 g, 3.41 mmol, 32%).

Spectral data matched the values reported on page 63.

*Note: The product is sensitive towards light and temperature. It can be stored in a benzene matrix at –25 °C in dilute solution (0.1 M). A 0.5 M solution was found to decompose within 14 days even if stored at –25°C.*

**tert-butyl-4-boropinacolato-2,3-dihydro-1H-pyrrole-1-carboxylate (81)**

A solution of bis(pinacolato)diboron (254 mg, 1.0 mmol, 1.00 eq.), 4,4'-di-*tert*-butyl-2,2'-dipyridyl (8 mg, 30.0  $\mu\text{mol}$ , 0.03 eq.) and (cycloocta-1,5-diene)(methoxy)iridium(I) dimer (9.9 mg, 15.0  $\mu\text{mol}$ , 0.015 eq.) in methyl *tert*-butyl ether (2.4 mL) was degassed (freeze-pump-thaw, three cycles). The resulting solution was added to **54** (169 mg, 1.0 mmol, 1.00 eq.) in a 10 mL glass microwave tube. The vessel was sealed and irradiated in a CEM Discover microwave apparatus (200 Watt, 80  $^\circ\text{C}$ ) for 13 min. The resulting mixture was directly applied onto a chromatography column. After chromatography (SiO<sub>2</sub>, hexanes/EtOAc = 19/1) **81** was obtained as colorless liquid (142 mg, 480  $\mu\text{mol}$ , 48 %).

*Note: The solution of bis(pinacolato)diboron, 4,4'-di-tert-butyl-2,2'-dipyridyl and (cycloocta-1,5-diene)(methoxy)iridium(I) dimer in methyl tert-butyl ether can be prepared and stored in a Schlenk tube under Argon and used for subsequent experiments. This solution was found to be functional after 14 days if stored under the exclusion of light.*

$R_f$  = 0.29 (hexanes/EtOAc = 19/1, UV 254 nm, CAM)

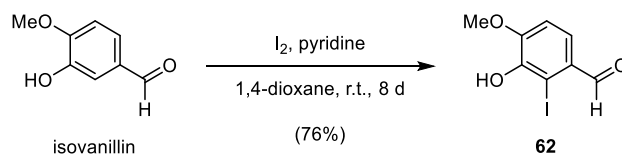
Note: NMR spectra are complex due to the presence of rotamers.

<sup>1</sup>H NMR (400 MHz, CDCl<sub>3</sub>)  $\delta$  = 7.18, 7.03 (s, 1H), 3.77-3.72 (m, 2H), 2.70-2.66 (m, 2H), 1.47 (s, 9H), 1.27 (s, 12H).

<sup>13</sup>C NMR (100 MHz, CDCl<sub>3</sub>)  $\delta$  = 151.2, 141.9, 83.5, 83.1, 80.8, 46.2, 29.8, 28.6, 28.4, 25.1, 24.8.

HRMS (EI) for C<sub>15</sub>H<sub>26</sub>BNO<sub>4</sub> [M]<sup>+</sup>: calcd.: 295.1955, found: 295.1959.

IR (ATR):  $\tilde{\nu}$  = 2976 (w), 1742 (w), 1695 (m), 1610 (w), 1474 (m), 1380 (m), 1368 (s), 1328 (s), 1269 (m), 1140 (s), 983 (m), 851 (s), 774 (m), 676 (s).

**3-hydroxy-2-iodo-4-methoxybenzaldehyde (62)**

An aluminum-foil wrapped dropping funnel was charged with 1,4-dioxane (611 mL) and ICl (100 g, 616 mmol, 1.03 eq.) in 1,4-dioxane (611 mL). This solution was added dropwise to a solution of isovanillin (91.0 g, 598 mmol, 1.00 eq.) in pyridine (340 mL, 4.19 mol, 7.00 eq.) in a 2 L round-bottom flask. The reaction mixture was stirred for 8 d under the exclusion of light. After the solvents

were removed in vacuo, water (500 mL) was added and the aqueous layer was acidified with aqueous HCl (1 M, 800 mL). The aqueous layer was extracted with EtOAc (3 x 1.2 L). The combined organic layers were washed with NaHSO<sub>3</sub> (2 x 600 mL) and brine (600 mL), dried over MgSO<sub>4</sub>, filtered and concentrated under reduced pressure.

The solid residue was filtered over a Büchner funnel and washed with cold EtOAc (3 x 100 mL). Arene **62** was obtained as a light-yellow solid (127 g, 457 mmol, 76%) and as a 9/1 ratio of product and starting material (determined by <sup>1</sup>H NMR) that was used for the next step without further purification. An analytically pure sample was obtained by flash column chromatography (SiO<sub>2</sub>, hexanes/EtOAc = 7/3). Spectral data match the previously reported values.<sup>[137]</sup>

**R<sub>f</sub>** = 0.29 (hexanes/EtOAc = 7/3, UV 254 nm, CAM).

**Melting point** = 171.1 – 173.5 °C.

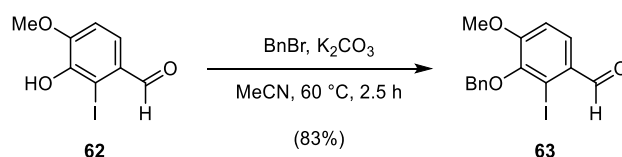
**<sup>1</sup>H NMR** (400 MHz, CDCl<sub>3</sub>) δ = 10.03 (s, 1H), 7.55 (d, *J* = 8.5 Hz, 1H), 6.92 (d, *J* = 8.5 Hz, 1H), 6.32 (s, 1H), 4.00 (s, 3H).

**<sup>13</sup>C NMR** (100 MHz, CDCl<sub>3</sub>) δ = 195.0, 150.8, 145.8, 128.8, 124.0, 111.1, 88.2, 56.7.

**HRMS (ESI)** for C<sub>8</sub>H<sub>6</sub>IO<sub>3</sub><sup>-</sup> [M-H]<sup>-</sup>: calcd.: 276.9367, found: 276.9370.

**IR (ATR)**:  $\tilde{\nu}$  = 4241 (w), 1558 (s), 1584 (m), 1558 (m), 1488 (m), 1460 (m), 1436 (m), 1386 (w), 1330 (w), 1281 (s), 1201 (s), 1166 (m), 1126 (m), 1011 (s), 982 (m), 822 (m), 808 (s), 781 (m), 654 (m).

### 3-(benzyloxy)-2-iodo-4-methoxybenzaldehyde (**63**)



To a solution of iodoisovanillin (**62**) (45.1 g, 162 mmol, 1.00 eq.) in acetonitrile (550 mL) were added potassium carbonate (67.3 g, 487 mmol, 3.00 eq.) and benzyl bromide (21.3 mL, 178 mmol, 1.10 eq.). The resulting yellow suspension was heated to 60 °C and stirred for 2.5 h. The dark orange precipitate was filtered over celite, rinsed with EtOAc (3 x 200 mL) and the filtrate was concentrated under reduced pressure. Upon addition of Et<sub>2</sub>O, the product **63** precipitated as light-yellow solid (47.5 g, 129 mmol, 83%). Spectral data match the previously reported values.<sup>[136]</sup>

**R<sub>f</sub>** = 0.29 (hexanes/EtOAc = 7/3, UV 254 nm, CAM).

**Melting point** = 89.3 – 90.5 °C.

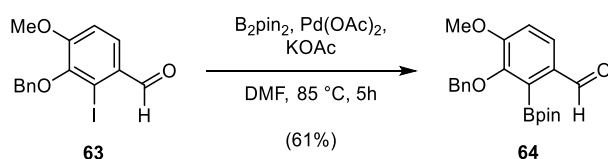
**<sup>1</sup>H NMR** (400 MHz, CDCl<sub>3</sub>) δ = 10.03 (s, 1H), 7.74 (d, *J* = 8.6 Hz, 1H), 7.62 – 7.57 (m, 2H), 7.45 – 7.32 (m, 3H), 7.00 (d, *J* = 8.6 Hz, 1H), 5.04 (s, 2H), 3.97 (s, 3H).

$^{13}\text{C}$  NMR (100 MHz,  $\text{CDCl}_3$ )  $\delta$  = 195.3, 158.0, 147.6, 136.7, 129.2, 128.7, 128.6, 128.4, 127.7, 112.0, 101.1, 74.6, 56.4.

**HRMS (ESI)** for  $\text{C}_{15}\text{H}_{14}\text{IO}_3^+$   $[\text{M}+\text{H}]^+$ : calcd. 368.9982, found: 368.9985.

**IR (ATR):**  $\tilde{\nu}$  = 2944 (w), 2850 (w), 1675 (s), 1574 (m), 1555 (w), 1495 (w), 1479 (m), 1453 (w), 1437 (w), 1382 (w), 1360 (w), 1302 (w), 1278 (s), 1252 (s), 1221 (m), 1177 (w), 1134 (w), 1080 (w), 1021 (s), 1000 (m), 940 (w), 911 (m), 845 (w), 821 (m), 779 (w), 750 (w), 739 (w), 696 (m).

### 3-Benzyloxy-2-boropinacolato-4-methoxybenzaldehyde (**64**)



A solution of aldehyde **63** (200 mg, 0.54 mmol, 1.00 eq.), bis(pinacolato)diboron (152 mg, 0.60 mmol, 1.10 eq.) and KOAc (160 mg, 1.63 mmol, 3.00 eq.) in DMF (2.1 mL) was degassed by subsurface sparging with Ar for 15 min. Then,  $\text{Pd}(\text{OAc})_2$  (3.7 mg, 16  $\mu\text{mol}$ , 0.03 eq.) was added. The mixture was stirred for 5 h at 85  $^\circ\text{C}$ . After cooling to room temperature, water (10 mL) was added and the mixture was extracted using EtOAc. The organic phase was washed with LiCl (10% w/w, 3 x 10 mL), water (3 x 20 mL), brine (20 mL), dried over  $\text{MgSO}_4$  and filtered. The solvent was removed in vacuo and the crude product was purified by flash column chromatography ( $\text{SiO}_2$ , pentane/EtOAc = 9/1) to afford **64** as a colorless solid (103 mg, 0.33 mmol, 61%).

$R_f$  = 0.24 (pentane/EtOAc = 9/1, UV 254 nm,  $\text{KMnO}_4$ )

**Melting point** = 85.6 – 93.1  $^\circ\text{C}$

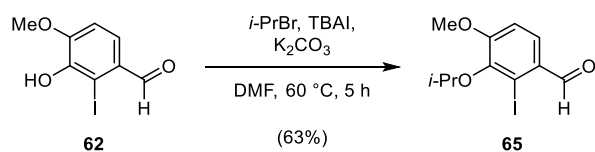
$^1\text{H}$  NMR (200 MHz,  $\text{CDCl}_3$ )  $\delta$  = 9.82 (s, 1H), 7.56 (d,  $J$  = 8.3 Hz, 1H), 7.53-7.48 (m, 2H), 7.39-7.34 (m, 2H), 7.33- 7.28 (m, 1H), 7.02 (d,  $J$  = 8.3 Hz, 1H), 5.04 (s, 2H), 3.92 (s, 3H), 1.34 (s, 12H).

$^{13}\text{C}$  NMR (75 MHz,  $\text{CDCl}_3$ )  $\delta$  = 191.6, 157.5, 151.7, 137.9, 133.7, 130.6, 128.4, 128.2, 127.9, 112.4, 84.4, 75.7, 56.0, 25.1.

*Note: The peak belonging to the boron-bound carbon was not observed due to quadrupolar relaxation.*

**HRMS (FAB)** for  $\text{C}_{21}\text{H}_{26}\text{O}_5\text{B}^+$   $[\text{M}+\text{H}]^+$ : calcd.369.1868, found: 369.1860.

**IR (ATR):**  $\tilde{\nu}$  = 2976 (w), 1683 (m), 1561 (m), 1455 (m), 1435 (m), 1372 (m), 1336 (s), 1312 (s), 1267 (s), 1232 (m), 1169 (w), 1138 (m), 1050 (m).

**2-Iodo-3-isopropoxy-4-methoxybenzaldehyde (65)**

To a solution of 3-hydroxy-2-iodo-4-methoxybenzaldehyde **62** (11.5 g, 41.3 mmol, 1.00 eq.) in DMF (75 mL) were added K<sub>2</sub>CO<sub>3</sub> (8.56 g, 62.0 mmol, 1.50 eq.), tetrabutylammonium iodide (3.81 g, 10.3 mmol, 0.25 eq.) and isopropyl bromide (5.66 mL, 60.3 mmol, 1.46 eq.). The reaction mixture was stirred for 5 h at 60 °C. The mixture was cooled to room temperature, diluted with water (20 mL) and extracted with EtOAc (3 × 50 mL). The combined organic layers were washed with aqueous HCl (1 M, 50 mL) and brine (50 mL), dried over MgSO<sub>4</sub> and filtered. The solvent was removed in vacuo and the crude product was purified by flash column chromatography (SiO<sub>2</sub>, hexanes/EtOAc = 9/1) to afford **65** as light yellow solid (8.37 g, 26.0 mmol, 63%).

**R<sub>f</sub>** = 0.40 (hexanes/EtOAc = 9/1, UV 254 nm, CAM).

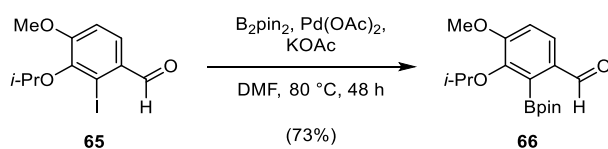
**Melting point** = 34.1 – 35.5 °C.

**<sup>1</sup>H NMR** (400 MHz, CDCl<sub>3</sub>) δ = 10.04 (s, 1H), 7.68 (d, *J* = 8.6 Hz), 6.95 (d, *J* = 8.6 Hz, 1H), 4.71 (sep, *J* = 6.2 Hz, 1H), 3.92 (s, 3H), 1.37 (d, *J* = 6.2 Hz, 6H).

**<sup>13</sup>C NMR** (100 MHz, CDCl<sub>3</sub>) δ = 195.7, 158.0, 147.0, 129.3, 126.7, 111.7, 102.3, 76.3, 56.3, 22.8.

**HRMS (ESI)** for C<sub>11</sub>H<sub>13</sub>IO<sub>3</sub><sup>+</sup> [M]<sup>+</sup>: calcd.: 319.9909, found: 319.9906.

**IR (ATR)**:  $\tilde{\nu}$  = 2973 (w), 2933 (w), 2841 (w), 1675 (s), 1569 (s), 1473 (m), 1369 (m), 1296 (m), 1269 (s), 1203 (m), 1098 (s), 1017 (s).

**3-Isopropoxy-4-methoxy-2-(4,4,5,5-tetramethyl-1,3,2-dioxaborolan-2-yl)benzaldehyde (66)**

To a mixture of 2-iodo-3-isopropoxy-4-methoxybenzaldehyde **65** (1.00 g, 3.13 mmol, 1.00 eq.), KOAc (2.78 g, 9.38 mmol, 3.00 eq.) and bis(pinacolato)diboron (952 mg, 3.75 mmol, 1.20 eq.) in DMF (11.6 mL) was added a solution of Pd(OAc)<sub>2</sub> (42.1 mg, 0.19 mmol, 0.06 eq.) in DMF (11.6 mL). The black suspension was stirred for 48 h at 80 °C. The reaction was diluted with water (20 mL) and EtOAc (20 mL). The layers were separated and the aqueous layer was extracted with EtOAc (5 × 10 mL). The combined organic layers were washed with water (50 mL), brine (50 mL), dried over MgSO<sub>4</sub> and filtered. The solvent was removed under reduced pressure and the crude product was

purified by flash column chromatography (SiO<sub>2</sub>, hexanes/EtOAc = 7/3) to afford **66** as light yellow solid (731.8 mg, 2.28 mmol, 73%).

$R_f = 0.39$  (hexanes/EtOAc = 7/3).

**Melting point** = 80 – 83 °C.

<sup>1</sup>H-NMR (400 MHz, CDCl<sub>3</sub>):  $\delta = 9.79$  (s, 1H), 7.50 (d,  $J = 8.3$  Hz), 6.97 (d,  $J = 8.3$  Hz, 1H), 4.72 (sept,  $J = 6.2$  Hz, 1H), 3.90 (s, 3H), 1.46 (s, 12H), 1.27 (d,  $J = 6.2$  Hz, 6H).

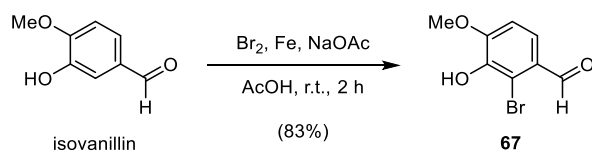
<sup>13</sup>C-NMR (100 MHz, CDCl<sub>3</sub>):  $\delta = 191.8, 157.7, 150.2, 133.7, 130.1, 112.1, 84.3, 74.4, 55.9, 25.3, 22.6$ .

*Note: The peak belonging to the boron-bound carbon was not observed due to quadrupolar relaxation.*

**HRMS (EI)** for C<sub>17</sub>H<sub>25</sub>BO<sub>5</sub><sup>+</sup> [M]<sup>+</sup>: calcd.: 320.1795, found: 320.1798.

**IR (ATR):**  $\tilde{\nu} = 2973$  (w), 1675 (s), 1564 (m), 1438 (m), 1370 (m), 1334 (m), 1302 (s), 1269 (s), 1235 (m), 1108 (m), 1031 (s), 917 (m).

## 2-Bromo-3-hydroxy-4-methoxybenzaldehyde (**67**)



To a suspension of isovanillin (20.0 g, 131.0 mmol, 1.00 eq.), NaOAc (21.6 g, 263 mmol, 2.00 eq.) and iron powder (734 mg, 13 mmol, 0.10 eq.) in acetic acid (131.5 mL), a solution of bromine (7.4 mL, 145 mmol, 1.10 eq.) in acetic acid (20 mL) was added dropwise over 20 min using a syringe pump. After 2 h, the mixture was poured into an ice bath. The resulting precipitate was filtered, washed with cold water (100 mL) and recrystallized from hot ethanol (1 L) to afford, after filtration, **67** as light brown solid (25.1 g, 108.7 mmol, 83%). Spectral data match the previously reported values.<sup>[123]</sup>

$R_f = 0.29$  (hexanes/EtOAc = 2/1).

**Melting point** = 195.0 – 199.2 °C.

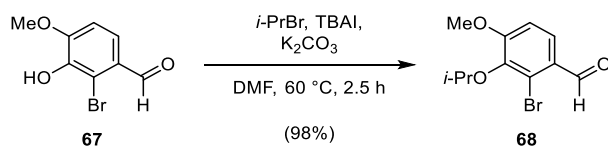
<sup>1</sup>H NMR (400 MHz, CDCl<sub>3</sub>):  $\delta = 10.26$  (s, 1H), 7.58 (d,  $J = 8.5$  Hz, 1H), 6.93 (d,  $J = 8.6$  Hz, 1H), 6.06 (s, 1H), 4.01 (s, 3H).

<sup>13</sup>C NMR (101 MHz, CDCl<sub>3</sub>):  $\delta = 191.0, 151.8, 143.3, 127.4, 122.9, 113.0, 109.4, 56.7$ .

**HRMS (ESI)** for C<sub>8</sub>H<sub>8</sub>BrO<sub>3</sub><sup>+</sup> [M+H]<sup>+</sup>: calcd.: 230.9651, found: 230.9652.

**IR (ATR):**  $\tilde{\nu}$  = 3221 (br, m), 1667 (s), 1592 (m), 1563 (s), 1461 (m), 1385 (w), 1334 (w), 1277 (s), 1233 (m), 1204 (s), 1168 (m), 1131 (m), 1015 (s).

### 2-Bromo-3-isopropoxy-4-methoxybenzaldehyde (**68**)



To a solution of 2-bromo-3-hydroxy-4-methoxybenzaldehyde **67** (7.94 g, 34.3 mmol, 1.0 eq.) in DMF (62 mL) were added  $\text{K}_2\text{CO}_3$  (7.12 g, 51.5 mmol, 1.5 eq.), isopropyl bromide (4.71 mL, 50.2 mmol, 1.46 eq.), and tetrabutylammonium iodide (3.17 g, 8.59 mmol, 0.25 eq.). The reaction mixture was stirred for 2.5 h at 60 °C. The mixture was cooled to room temperature, diluted with water (60 mL) and extracted with EtOAc (4 × 50 mL). The combined organic layers were washed with 1 M HCl (50 mL) and brine (50 mL), dried over  $\text{MgSO}_4$  and filtered. The solvent was removed in vacuo and the residue was purified by flash column chromatography ( $\text{SiO}_2$ , hexanes/EtOAc = 9/1 to 7/3) to afford **68** as slightly yellow solid (9.17 g, 33.6 mmol, 98%). Spectral data match the previously reported values.<sup>[193]</sup>

$R_f$  = 0.41 (hexanes/EtOAc = 7/1).

**Melting point** = 33.0 – 34.0 °C.

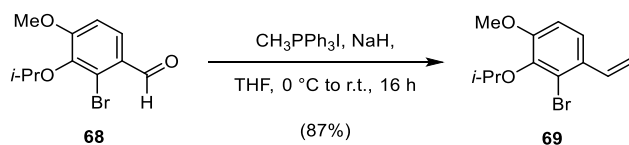
**$^1\text{H NMR}$**  (400 MHz,  $\text{CDCl}_3$ ):  $\delta$  = 10.26 (s, 1H), 7.70 (d,  $J$  = 8.7 Hz, 1H), 6.93 (d,  $J$  = 8.7 Hz, 1H), 4.59 (sep,  $J$  = 6.2 Hz, 1H), 3.92 (s, 3H), 1.34 (d,  $J$  = 6.2 Hz).

**$^{13}\text{C NMR}$**  (101 MHz,  $\text{CDCl}_3$ ):  $\delta$  = 191.5, 158.9, 144.6, 127.6, 126.0, 124.1, 110.8, 76.4, 56.3, 22.6.

**HRMS (EI)** for  $\text{C}_{11}\text{H}_{13}\text{BrO}_3^+ [\text{M}]^+$ : calcd.: 272.0048, found: 272.0037.

**IR (ATR):**  $\tilde{\nu}$  = 2973 (w), 2929 (w), 2863 (w), 1675 (s), 1576 (s), 1482 (m), 1376 (m), 1303 (m), 1275 (s), 1211 (m), 1097 (s), 906 (s).

### 2-Bromo-3-isopropoxy-4-methoxy-1-vinylbenzene (**69**)



To a suspension of NaH (60% w/w in mineral oil, 432 mg, 18.0 mmol, 1.50 eq.) in THF (72 mL) at 0 °C was portionwise added methyltriphenylphosphonium iodide (5.82 g, 14.4 mmol, 1.20 eq.). The mixture was stirred for 5 min at 0 °C and for 25 min at room temperature. 2-Bromo-3-isopropoxy-4-methoxybenzaldehyde **68** (3.28 g, 12.0 mmol, 1.00 eq.) was added portionwise slowly and the

resulting white suspension was stirred for 16 h, quenched by slow addition of water (60 mL) and extracted with EtOAc (3 × 20 mL). The combined organic layers were washed with water (50 mL) and brine (50 mL), dried over MgSO<sub>4</sub> and filtered. The solvent was removed in vacuo and the residue was purified by flash column chromatography (SiO<sub>2</sub>, hexanes/EtOAc = 9/1 to 7/3) to afford **69** as a colorless oil (2.83 g, 10.4 mmol, 87%). Spectral data match the previously reported values.<sup>[193]</sup>

$R_f$  = 0.41 (hexanes/EtOAc = 7/1).

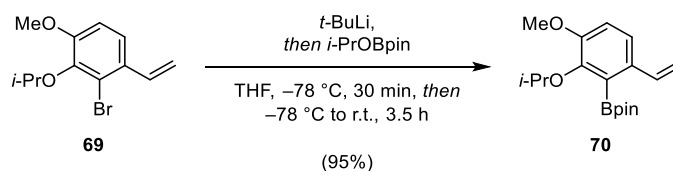
<sup>1</sup>H NMR (400 MHz, CDCl<sub>3</sub>): δ = 7.27-7.24 (m, 1H), 7.03 (dd,  $J$  = 17.4, 10.9 Hz, 1H), 6.84 (d,  $J$  = 8.6 Hz, 1H), 5.56 (dd,  $J$  = 17.4, 1.2 Hz, 1H), 5.24 (dd,  $J$  = 10.9, 1.2 Hz, 1H), 4.56 (sept,  $J$  = 6.2 Hz, 1H), 3.84 (s, 3H), 1.33 (d,  $J$  = 6.2 Hz, 6H).

<sup>13</sup>C NMR (101 MHz, CDCl<sub>3</sub>): δ = 153.4, 144.6, 136.1, 131.5, 121.3, 120.7, 114.9, 111.4, 76.0, 56.2, 22.7.

HRMS (EI) for C<sub>12</sub>H<sub>15</sub>O<sub>2</sub>Br<sup>+</sup>[M]<sup>+</sup>: calcd.: 270.0255, found: 270.0246.

IR (ATR):  $\tilde{\nu}$  = 2973 (w), 2929 (w), 2863 (w), 1675 (s), 1576 (s), 1482 (m), 1376 (m), 1303 (m), 1275 (s), 1211 (m), 1097 (s), 906 (s).

## 2-(2-Isopropoxy-3-methoxy-6-vinylphenyl)-4,4,5,5-tetramethyl-1,3,2-dioxaborolane (**70**)



A solution of **69** (1.00 g, 3.70 mmol, 1.00 eq.) in THF (18.6 mL) was cooled to  $-78$  °C and a solution of *t*-BuLi (2.1 M in heptane, 1.93 mL, 4.07 mmol, 1.10 eq.) was added. The resulting mixture was stirred for 30 min at  $-78$  °C and 1-Isopropoxy-3,3,4,4-tetramethylborolane (1.12 mL, 5.51 mmol, 1.49 eq.) was added dropwise. After stirring for 2 hat  $-78$  °C, the cooling bath was removed and the mixture stirred for additional 90 min. The reaction was quenched with water (20 mL) and extracted with Et<sub>2</sub>O (3 × 30 mL). The combined organic layers were washed with water (50 mL) and brine (50 mL), dried over MgSO<sub>4</sub> and filtered. The solvent was removed under reduced pressure and the crude product was purified by flash column chromatography (SiO<sub>2</sub>, hexanes/Et<sub>2</sub>O = 9/1 to 7/3) to afford **70** as a white solid (1.12 g, 3.51 mmol, 95%). Spectral data match the previously reported values.<sup>[193]</sup>

$R_f$  = 0.16 (hexanes/Et<sub>2</sub>O = 9/1).

Melting point = 73.0 – 75.0 °C.

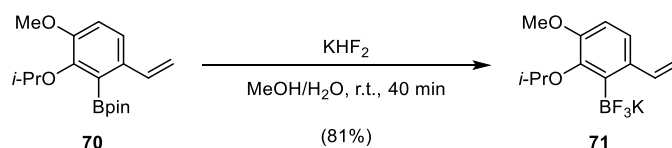
**<sup>1</sup>H NMR** (400 MHz, CDCl<sub>3</sub>): δ = 7.21 (d, *J* = 8.4, 1H), 6.85 (d, *J* = 8.4 Hz, 1H), 6.75 (dd, *J* = 17.4, 10.8 Hz, 1H), 5.56 (dd, *J* = 17.4, 1.2 Hz, 1H), 5.12 (dd, *J* = 10.8, 1.2 Hz, 1H), 4.68 (sept, *J* = 6.2 Hz, 1H), 3.80 (s, 3H), 1.39 (s, 12H), 1.25 (d, *J* = 6.2 Hz, 6H).

**<sup>13</sup>C NMR** (101 MHz, CDCl<sub>3</sub>): δ = 151.6, 149.2, 136.7, 134.7, 120.5, 114.0, 113.4, 84.0, 73.9, 55.9, 25.2, 22.6.

**HRMS (EI)** for C<sub>18</sub>H<sub>27</sub>O<sub>4</sub>B<sup>+</sup> [M]<sup>+</sup>: calcd.: 318.2003, found: 318.1997.

**IR (ATR):**  $\tilde{\nu}$  = 2975 (w), 2933 (w), 1562 (w), 1472 (m), 1430 (m), 1328 (s), 1303 (s), 1261 (s), 1140 (m), 1106 (m), 1045 (s) 991 (m).

### Trifluoro(2-isopropoxy-3-methoxy-6-vinylphenyl)-14-borane, potassium salt (**71**)



To a solution of **70** (101.8 mg, 0.32 mmol, 1.00 eq) in MeOH (1.0 mL) was added aqueous KHF<sub>2</sub> (4.5 M, 2 mL). The reaction mixture was stirred at room temperature for 40 min and the solvent was removed under reduced pressure. The residue was redissolved in methanol/water (3 mL, 50% v/v) and the solvent was removed under reduced pressure. This procedure was repeated three times. The resulting white residue was suspended in hot acetone (2 mL), the supernatant was filtered through a syringe filter (glassfiber, 45 μm) and the solvent was removed in vacuo to afford **71** as white solid (77.3 mg, 0.26 mmol, 81%).

**R<sub>f</sub>** = 0.16 (hexanes/Et<sub>2</sub>O = 9/1).

**Melting point** = > 200 °C (decomposition).

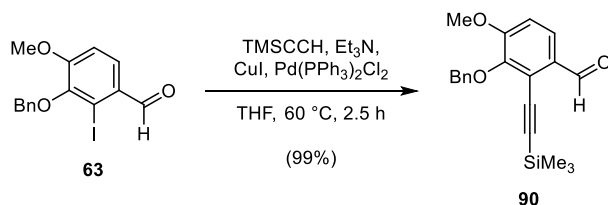
**<sup>1</sup>H NMR** (400 MHz, CDCl<sub>3</sub>): δ = 7.33 (dd, *J* = 17.8, 10.8 Hz, 1H), 7.09 (d, *J* = 8.3 Hz, 1H), 6.66 (d, *J* = 8.3 Hz, 1H), 5.24 (d, *J* = 17.8 Hz, 1H), 4.78 (d, *J* = 10.8 Hz, 1H), 4.18 (sept, *J* = 6.1 Hz, 1H), 3.65 (s, 3H), 1.06 (d, *J* = 6.1 Hz, 6H).

**<sup>13</sup>C NMR** (101 MHz, CDCl<sub>3</sub>): δ = 152.3, 149.6, 141.3, 135.5, 119.2, 109.7, 108.0, 73.8, 55.3, 22.3.

**HRMS (ESI)** for C<sub>12</sub>H<sub>15</sub>BF<sub>3</sub>O<sub>2</sub><sup>-</sup> [M-K]<sup>-</sup>: calcd.: 259.1117, found: 259.1120.

**IR (ATR):**  $\tilde{\nu}$  = 2973 (w), 2936 (w), 1563 (w), 1458 (m), 1417 (w), 1285 (m), 1207 (m), 1117 (m), 966 (s).

### 3-(benzyloxy)-4-methoxy-2-((trimethylsilyl)ethynyl)benzaldehyde (**90**)



To a solution of benzyl iodoisovanillin (**63**) in THF (130 mL) was added triethylamine (26.3 mL, 189 mmol, 6.00 eq.), giving a dark-brown solution. CuI (0.30 g, 1.58 mmol, 0.05 eq.), Pd(PPh<sub>3</sub>)<sub>2</sub>Cl<sub>2</sub> (0.55 g, 0.79 mmol, 0.025 eq.) and TMS-acetylene (11.2 mL, 78.8 mmol, 2.50 eq.) were added. The reaction was stirred at 60 °C for 12 h under air. The reaction was cooled to room temperature, filtered over celite and the filter cake rinsed with EtOAc (3 x 50 mL). The solvent was removed under reduced pressure and the crude product was purified by flash column chromatography (SiO<sub>2</sub>, Hex/EtOAc = 9/1 to 8/2), giving **90** as orange crystalline solid (10.6 g, 31.3 mmol, 99%).

Crystals suitable for X-ray analysis were grown from EtOAc.

$R_f$  = 0.61 (hexanes/EtOAc = 9/1, UV 254 nm, PAA).

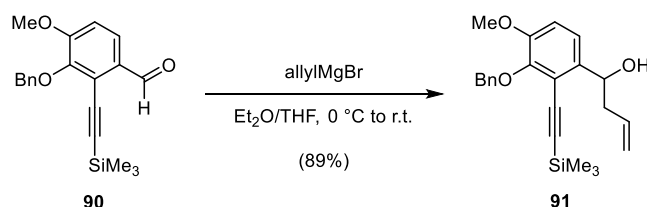
<sup>1</sup>H NMR (CDCl<sub>3</sub>, 400 MHz)  $\delta$  = 10.40 (s, 1H), 7.72 (d,  $J$  = 8.7 Hz, 1H), 7.61 – 7.53 (m, 2H), 7.45 – 7.28 (m, 3H), 6.98 (d,  $J$  = 8.7 Hz), 5.13 (s, 2H), 3.92 (s, 3H), 0.26 (s, 9H).

<sup>13</sup>C NMR (CDCl<sub>3</sub>, 100 MHz)  $\delta$  = 190.9, 158.0, 137.2, 130.0, 128.4, 128.4, 128.2, 124.4, 122.2, 112.3, 107.1, 96.2, 75.3, 56.3, 56.3, –0.12.

HRMS (ESI) for C<sub>20</sub>H<sub>23</sub>O<sub>3</sub>Si<sup>+</sup> [M+H]<sup>+</sup>: calcd.: 339.1411, found: 339.1412.

IR (ATR):  $\tilde{\nu}$  = 3032 (w), 2959 (w), 2899 (w), 2841 (w), 2744 (w), 2151 (w), 1687 (s), 1580 (s), 1497 (w), 1482 (m), 1455 (w), 1438 (m), 1386 (w), 1373 (w), 1307 (m), 1280 (s), 1251 (s), 1194 (w), 1167 (w), 1080 (s), 1016 (w), 962 (w), 904 (w), 840 (s), 786 (m), 760 (m), 731 (m), 697 (m).

### 1-(3-(benzyloxy)-4-methoxy-2-((trimethylsilyl)ethynyl)phenyl)but-3-en-1-ol (**91**)



Sonogashira product **90** (9.97 g, 29.5 mmol, 1.00 eq.) was dissolved in benzene and concentrated in vacuo. The residue was dissolved in THF (120 mL) and cooled to 0 °C. A solution of allylmagnesium bromide (1 M in diethyl ether, 35.3 mL, 35.3 mmol, 1.20 eq.) was added dropwise to the reaction. After 1 h, the reaction was quenched with saturated aqueous NH<sub>4</sub>Cl (100 mL). After the addition of EtOAc (50 mL) the layers were separated and the aqueous phase was extracted with EtOAc

(2 x 100 mL). The combined organic layers were dried over  $\text{MgSO}_4$ , filtered and concentrated under reduced pressure. Purification of the crude product by flash column chromatography ( $\text{SiO}_2$ , hexanes/EtOAc = 9/1) gave **91** as a yellow oil (10.6 g, 27.9 mmol, 89%).

$R_f$  = 0.5 (hexanes/EtOAc = 9/1, UV 254 nm, PAA).

$^1\text{H NMR}$  ( $\text{CDCl}_3$ , 400 MHz)  $\delta$  = 7.58 – 7.56 (m, 2H), 7.39 – 7.29 (m, 3H), 7.18 (d,  $J$  = 8.56 Hz, 1H), 6.92 (d,  $J$  = 8.56 Hz), 5.86 (dddd,  $J$  = 16.9 Hz, 10.1 Hz, 7.6 Hz, 6.5 Hz, 1H), 5.21 – 5.06 (m, 3H, H-10), 5.11 (s, 2H), 3.85 (s, 3H), 2.71 – 2.58 (m, 1H), 2.47 – 2.36 (m, 1H), 2.30 (d,  $J$  = 4.2 Hz, 1H), 0.25 (s, 9H).

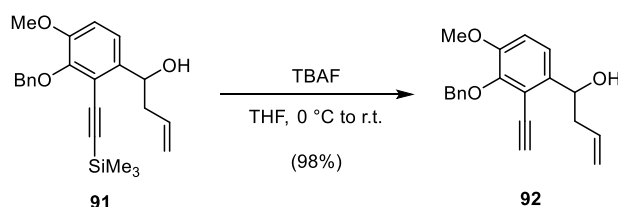
$^{13}\text{C NMR}$  ( $\text{CDCl}_3$ , 100 MHz)  $\delta$  = 151.9, 149.5, 139.5, 137.7, 135.1, 128.4, 128.3, 128.0, 121.0, 118.1, 116.0, 113.2, 104.7, 98.9, 75.1, 71.3, 56.2, 42.8, 0.0.

**HRMS (ESI)** for  $\text{C}_{23}\text{H}_{27}\text{O}_2\text{Si}^+$  [ $\text{M}-\text{OH}]^+$ : calcd.: 363.1775, found: 363.1779.

**IR (ATR)**:  $\tilde{\nu}$  = 3404 (w), 2957 (m), 2150 (w), 1598 (w), 1482 (m), 1433 (m), 1372 (w), 1272 (m), 1249 (s), 1085 (s), 1025 (w), 914 (w), 843 (s), 759 (w), 696 (w).

**Enantiomeric excess of 91** was determined by HPLC analysis on chiral stationary phase (DAICEL CHIALPAK IC, 4.6 x 250 mm, 25 °C, 1 mL/min, 3% *i*-PrOH in heptane, detection at 254 nm);  $t_R$  first enantiomer = 11.390 min,  $t_R$  second enantiomer = 14.840 min.

### **Rac-1-(3-(benzyloxy)-2-ethynyl-4-methoxyphenyl)but-3-en-1-ol (92)**



A solution of alcohol **91** (10.6 g, 27.9 mmol, 1.00 eq.) in THF (220 mL) was cooled to 0 °C and a solution of TBAF (1 M in THF, 33.4 mL, 33.4 mmol, 1.20 eq.) was added dropwise over 15 minutes. The brown reaction was stirred for 45 min at 0 °C, quenched with saturated aqueous  $\text{NH}_4\text{Cl}$  (70 mL) and diluted with EtOAc (70 mL). The two layers were separated and the aqueous phase was extracted with EtOAc (3 x 70 mL). The combined organic layers were washed with brine, dried over  $\text{MgSO}_4$  and concentrated under reduced pressure. Purification by flash column chromatography ( $\text{SiO}_2$ , hexanes/EtOAc = 8/2 to 6/4) gave **92** as a yellow oil (5.50 g, 17.8 mmol, 98%).

$R_f$  = 0.35 (hexanes/EtOAc = 7/3, UV 254 nm, PAA).

$^1\text{H NMR}$  (100 MHz,  $\text{CDCl}_3$ )  $\delta$  = 7.57 – 7.51 (m, 1H), 7.40 – 7.28 (m, 3H), 7.21 (d,  $J$  = 8.6 Hz, 1H), 6.95 (d,  $J$  = 8.6 Hz, 1H), 5.85 (dddd,  $J$  = 16.9, 10.2, 7.7, 6.5, 1H), 5.19 – 5.09 (m, 3H), 5.10 (s, 2H), 3.85 (s, 3H), 3.51 (s, 1H), 2.69 – 2.56 (m, 1H), 2.49 – 2.39 (m, 1H), 2.21 (d,  $J$  = 3.4 Hz, 1H).

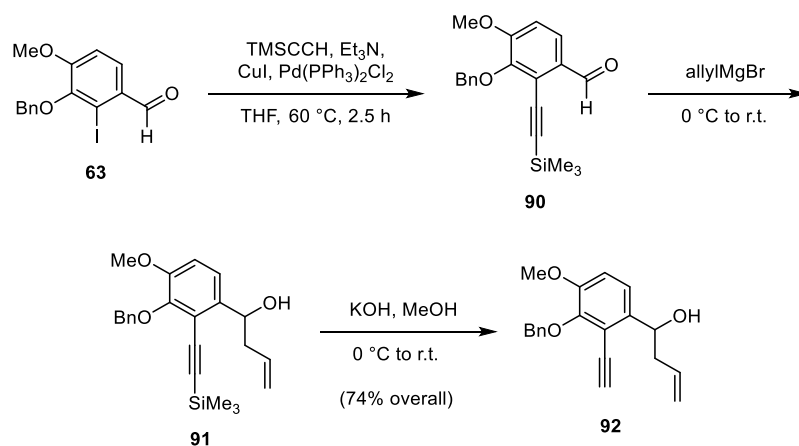
$^{13}\text{C}$  NMR (100 MHz,  $\text{CDCl}_3$ )  $\delta$  = 151.8, 149.7, 139.2, 137.4, 134.8, 128.4, 128.2, 128.0, 121.1, 118.2, 115.2, 113.3, 86.6, 77.6, 75.1, 70.8, 56.0, 42.7.

HRMS (ESI) for  $\text{C}_{20}\text{H}_{19}\text{O}_2^+ [\text{M}-\text{OH}]^+$ : calcd.: 291.1380, found: 291.1381.

IR (ATR):  $\tilde{\nu}$  = 3280 (m), 3065 (w), 3031 (w), 2939 (w), 2837 (w), 1740 (w), 1642 (w), 1601 (w), 1570 (w), 1480 (s), 1454 (m), 1374 (m), 1321 (w), 1293 (m), 1267 (s), 1249 (s), 1218 (s), 1193 (m), 1169 (w), 1117 (w), 1066 (s), 1021 (m), 994 (m), 981 (s), 930 (w), 913 (s), 891 (m), 871 (s), 842 (m), 809 (s), 791 (w), 747 (s), 700 (s).

Enantiomeric excess of **92** was determined by HPLC analysis on chiral stationary phase. Conditions for the separation of the enantiomers are reported on page 80.

### Telescoped Procedure for the synthesis of *Rac*-**92**.



To a solution of benzyl iodoisovanillin (**63**) (10.5 g, 28.5 mmol, 1.00 eq.) in THF (120 mL) were added triethylamine (23.8 mL, 171 mmol, 6.00 eq.), CuI (0.27 g, 1.42 mmol, 0.05 eq.),  $\text{Pd}(\text{PPh}_3)_2\text{Cl}_2$  (0.5 g, 0.71 mmol, 0.025 eq.) and TMS-acetylene (10.1 mL, 71.2 mmol, 2.50 eq.) in sequence. The reaction flask was sealed with a plastic cap and heated to  $60\text{ }^\circ\text{C}$  for 12 h.

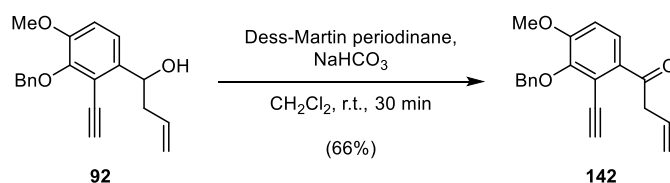
After full conversion of the starting material **63** ( $R_f$  = 0.53 in hexanes/EtOAc = 7/3) to the intermediate Sonogashira product **90** ( $R_f$  = 0.61 in hexanes/EtOAc = 9/1), the solution was cooled to  $0\text{ }^\circ\text{C}$  (ice-acetone bath) and allylmagnesium bromide (1 M in diethyl ether, 71.2 mL, 71.2 mmol, 2.50 eq.) was added dropwise to the reaction via cannula.

After stirring for 2 h, the dark grey reaction mixture was cooled to  $0\text{ }^\circ\text{C}$  (ice-acetone bath) and MeOH (117 mL, 2.88 mol, 100 eq.) was added dropwise. Then, KOH pellets (7.99 g, 142 mmol, 9.29 eq.) were added. After 7 h, TLC showed incomplete consumption of the starting material **S4** ( $R_f$  = 0.5 in hexanes/EtOAc = 9/1), and a second charge of KOH pellets (7.99 g, 142 mmol, 9.29 eq.) was added. After further 3 h the reaction was complete, and the mixture was filtered over a pad of celite and washed with MeOH (300 mL). The solvent was evaporated under reduced pressure, and the black residue was taken up in water (100 mL), saturated aqueous  $\text{NH}_4\text{Cl}$  (100 mL) and EtOAc (100 mL).

The layers were separated and the aqueous phase was extracted with EtOAc (2 x 100 mL). The combined organic layers were dried over MgSO<sub>4</sub>, filtered and concentrated under reduced pressure. Purification of the crude product by flash column chromatography (SiO<sub>2</sub>, hexanes/EtOAc = 8/2) gave **92** as a clear yellow oil (6.47 g, 21.0 mmol, 74%).

Spectral data matched the ones reported on page 76.

### 1-(3-(benzyloxy)-2-ethynyl-4-methoxyphenyl)but-3-en-1-one (**142**)



A solution of allylic alcohol **92** (6.47 g, 21.0 mmol, 1.00 eq.) in CH<sub>2</sub>Cl<sub>2</sub> (213 mL) was cooled to 0 °C and powdered NaHCO<sub>3</sub> (7.93 g, 94.5 mol, 4.50 eq.) was added, followed by Dess-Martin periodinane (10.1 g, 23.7 mmol, 1.13 eq.). After 1 h, a half-saturated solution of Na<sub>2</sub>SO<sub>3</sub> (100 mL) was added and the reaction mixture was vigorously stirred for 30 minutes. The reaction was diluted with water (100 mL) and CH<sub>2</sub>Cl<sub>2</sub> (100 mL). The layers were separated and the aqueous layer was extracted with CH<sub>2</sub>Cl<sub>2</sub> (2 x 100 mL). The combined organic layers were washed with aqueous NaOH (1 M, 150 mL), brine (150 mL), dried over MgSO<sub>4</sub>, filtered and concentrated under reduced pressure. Purification of the crude product by flash column chromatography (SiO<sub>2</sub>, hexanes/EtOAc = 20/1 to 6/4) gave **142** as a white solid (4.20 g, 13.7 mmol, 66%).

$R_f$  = 0.57 (hexanes/EtOAc = 7/3, UV 254 nm, CAM).

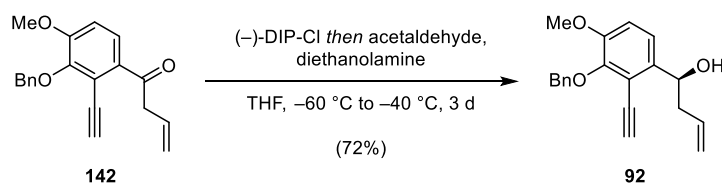
**Melting point** = 61.0 – 62.3 °C.

**<sup>1</sup>H NMR** (400 MHz, CDCl<sub>3</sub>)  $\delta$  = 7.57 – 7.48 (m, 3H), 7.41 – 7.29 (m, 3H), 6.94 (d,  $J$  = 8.7 Hz, 1H), 6.05 (ddt,  $J$  = 17.1, 10.4, 6.8 Hz, 1H), 5.25 – 5.14 (m, 2H), 5.10 (s, 2H), 3.89 (s, 3H), 3.85 (dt,  $J$  = 6.7, 1.5 Hz, 2H), 3.59 (s, 1H).

**<sup>13</sup>C NMR** (CDCl<sub>3</sub>, 100 MHz)  $\delta$  = 198.9, 155.9, 150.8, 137.2, 134.3, 131.4, 128.5, 128.5, 128.4, 128.4, 128.3, 128.2, 125.9, 118.6, 116.5, 112.0, 87.7, 78.3, 77.4, 75.2, 56.1, 46.3.

**HRMS (EI)**: for C<sub>20</sub>H<sub>18</sub>O<sub>3</sub><sup>+</sup> [M<sup>+</sup>]: calcd.: 306.1256, found: 306.1250.

**IR (ATR)**:  $\tilde{\nu}$  = 3273 (w), 3030 (w), 2841 (w), 2357 (w), 1650 (m), 1582 (m), 1562 (m), 1453 (m), 1269 (s), 1246 (s), 1171 (m), 1096 (m), 1072 (s), 991 (m), 809 (m), 697 (s).

**(S)-1-(3-(benzyloxy)-2-ethynyl-4-methoxyphenyl)but-3-en-1-ol (92)**

Ketone **4** (4.20 g, 13.7 mmol, 1.00 eq.) was dissolved in THF (14.6 mL) and cooled to  $-60\text{ }^\circ\text{C}$ . A solution of (-)-B-Chlorodiisopinocampheylborane (60% in heptane, 12.4 mL, 20.6 mmol, 1.50 eq.) was added at  $-60\text{ }^\circ\text{C}$ . The mixture solidified and was placed in a  $-40\text{ }^\circ\text{C}$  cooling bath (dry ice/isopropanol) connected to a cryostat and was stirred at this temperature for 3 days. After complete consumption of the starting material (TLC taken directly from the reaction mixture), acetaldehyde (3.46 mL, 61.7 mmol, 4.50 eq.) was added dropwise and the solution was warmed to room temperature over the course of 1 h. The solvent was removed under reduced pressure and the residue was dissolved in  $\text{Et}_2\text{O}$  (47 mL) and diethanolamine (2.89 mL, 30.2 mmol, 2.20 eq.) was added at room temperature. The formation of a white precipitate was observed. The suspension was stirred for 2 h before it was filtered over a silica plug (d = 5 cm, h = 2 cm) and the filter cake was rinsed with EtOAc (4 x 50 mL). Removal of the volatiles in vacuo and purification by flash column chromatography ( $\text{SiO}_2$ , hexanes/EtOAc = 8/2) afforded alcohol **92** as a yellow oil (3.05 g, 9.88 mmol, 72%).

$R_f = 0.35$  (hexanes/EtOAc = 7/3, UV 254 nm, PAA).

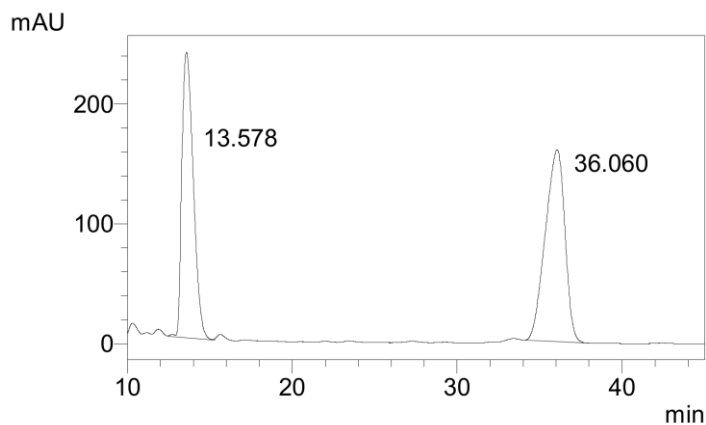
**Melting point** =  $79.4 - 81.7\text{ }^\circ\text{C}$ .

$[\alpha]_D^{20} = -58.2^\circ$  (c = 2.60,  $\text{CH}_2\text{Cl}_2$ ).

Spectral data matched the racemic sample prepared according to the procedure reported on page 76.

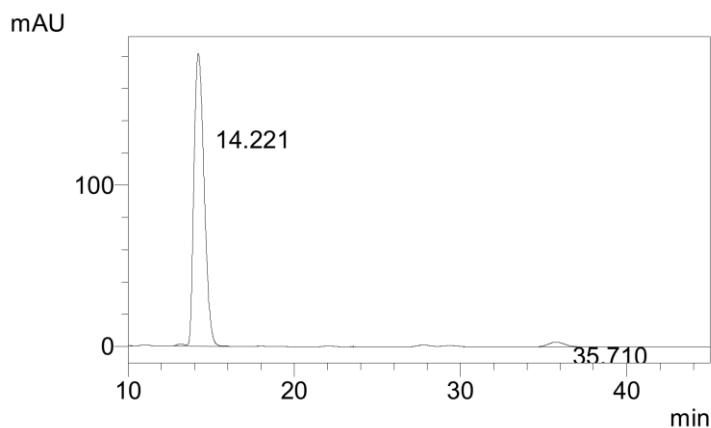
**Enantiomeric excess of 92** was determined by HPLC analysis on chiral stationary phase (DAICEL CHIALPAK IC, 4.6 x 250 mm), 25 °C, 1 mL/min, 15% *i*-PrOH in heptane, detection at 269 nm) to be 95.5% by comparison with a racemic sample and coinjection;  $t_R$  major enantiomer = 14.221 min,  $t_R$  minor enantiomer = 35.710 min.

- *Racemic sample of 92:*



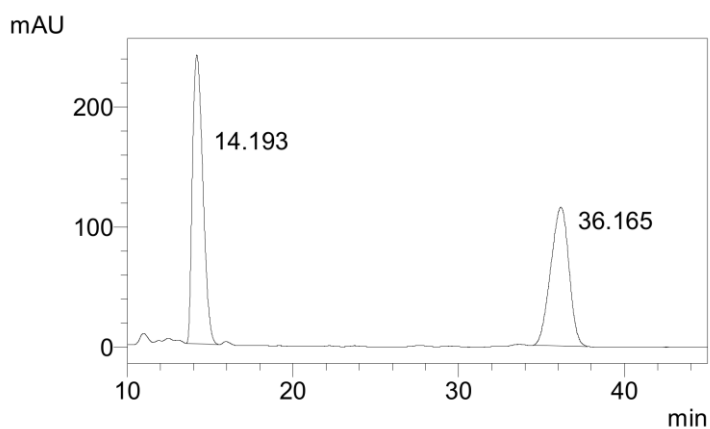
PDA Ch5 269nm		
Peak#	Ret. Time	Area%
1	13.578	46.363
2	36.060	53.637
Total		100.000

- *Enantioenriched sample of 92:*

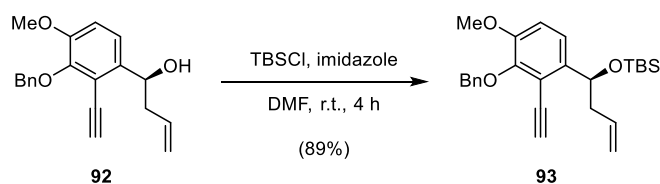


PDA Ch5 269nm		
Peak#	Ret. Time	Area%
1	14.221	97.730
2	35.710	2.270
Total		100.000

- *Coinjection:*



PDA Ch5 269nm		
Peak#	Ret. Time	Area%
1	14.193	54.298
2	36.165	45.702
Total		100.000

**(S)-((1-(3-(benzyloxy)-2-ethynyl-4-methoxyphenyl)but-3-en-1-yl)oxy)(tert-butyl)dimethylsilane (93)**

To a stirred solution of **92** (5.74 g, 18.6 mmol, 1.00 eq.) in DMF (87 mL) imidazole (3.17 g, 46.5 mmol, 2.50 eq.) and TBSCl (3.37 g, 22.3 mmol, 1.20 eq.) were added. Stirring was continued for 4 h at room temperature before the reaction was quenched with saturated aqueous  $\text{NH}_4\text{Cl}$ . The layers were separated and the aqueous layer was extracted with EtOAc (3 x 80 mL). The combined organic layers were washed with aqueous LiCl (10% w/w, 4 x 50 mL), dried over  $\text{MgSO}_4$ , filtered and concentrated under reduced pressure. Purification of the crude product was performed by flash column chromatography ( $\text{SiO}_2$ , hexanes/EtOAc = 9/1) to afford **93** as a yellow oil (7.02 g, 16.6 mmol, 89%).

$R_f = 0.54$  (hexanes/EtOAc = 9/1, UV 254 nm, CAM).

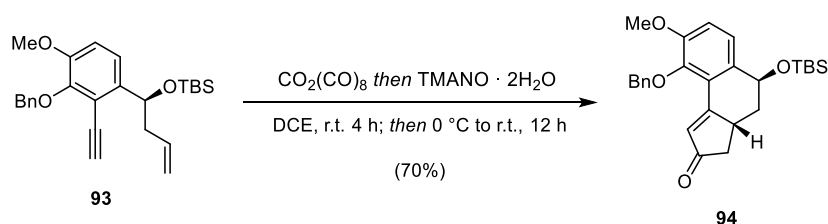
$^1\text{H NMR}$  (400 MHz,  $\text{CDCl}_3$ )  $\delta = 7.56 - 7.51$  (m, 2H), 7.40 – 7.27 (m, 3H), 7.22 (d,  $J = 8.6$  Hz, 1H), 6.93 (d,  $J = 8.6$  Hz, 1H), 5.84 (ddt,  $J = 19.1, 9.3, 7.1$ , 1H), 5.16 – 5.09 (m, 2H), 5.11 (s, 2H), 5.05 – 5.01 (m, 1H), 5.00 – 4.97 (m, 1H), 3.84 (s, 3H), 3.48 (s, 1H), 2.48 – 2.28 (m, 2H), 0.88 (s, 9H), 0.03 (s, 2H), –0.13 (s, 3H).

$^{13}\text{C NMR}$  (100 MHz,  $\text{CDCl}_3$ )  $\delta = 151.4, 149.1, 140.9, 137.6, 135.6, 128.6, 128.3, 128.1, 121.9, 116.9, 114.8, 113.3, 86.2, 77.8, 75.1, 72.0, 56.1, 44.4, 26.0, 18.4, -4.6, -4.8$ .

**HRMS (ESI)** for  $\text{C}_{26}\text{H}_{38}\text{O}_3\text{NSi}^+ [\text{M}+\text{NH}_4]^+$ : calcd.: 440.2615, found: 440.2623.

**IR (ATR):**  $\tilde{\nu} = 3287$  (w), 2929 (m), 2856 (m), 1598 (w), 1483 (s), 1432 (m), 1372 (w), 1294 (m), 1256 (s), 1077 (s), 1002 (m), 912 (m), 835 (s), 811 (m), 776 (m), 740 (w), 698 (w).

$[\alpha]_D^{20} = -40.0$  ( $c = 1.35, \text{CH}_2\text{Cl}_2$ ).

**(3aR,5S)-9-(benzyloxy)-5-((tert-butyldimethylsilyl)oxy)-8-methoxy-3,3a,4,5-tetrahydro-2H-cyclopenta[a]naphthalen-2-one (94)**

*Note: Due to a 15% yield drop upon further scale-up, the following procedure was performed in two separate flasks with identical amounts of substrate, which were combined for purification. The use of a new bottle of  $\text{Co}_2(\text{CO})_8$  provided better and more reproducible results.*

In a 250 mL round-bottom flask, enyne **93** (1.64 g, 3.88 mmol, 1.00 eq.) was dissolved in DCE (78 mL) and stirred at room temperature. Under exclusion of light,  $\text{Co}_2(\text{CO})_8$  (1.59 g, 4.66 mmol, 1.20 eq.) was added in one portion and the reaction was stirred in the dark. After successful complexation (monitored by TLC in hexanes/ $\text{Et}_2\text{O}$  = 9/1;  $R_f$  of **93** = 0.32;  $R_f$  of Co-complex = 0.9; approx. 4 h) the reaction was cooled to 0 °C and trimethylamine N-oxide dihydrate (2.59 g, 23.3 mmol, 6.00 eq.) was added portionwise to the light-protected brown reaction mixture. Stirring was continued for 12 h and the reaction was allowed to warm to room temperature while a color change to dark violet was observed. The reactions were filtered over silica ( $\phi$  = 6 cm, h = 4 cm) and the filter pad was rinsed with EtOAc until only colorless filtrate was obtained. Concentration of the filtrate under reduced pressure and purification by flash column chromatography ( $\text{SiO}_2$ , dry loading by adsorption on  $\text{SiO}_2$ , hexanes/EtOAc = 98/2 to 5/5) afforded tricycle **94** as an off-white solid (2.46 g, 5.46 mmol, 70%). Crystals suitable for X-ray analysis were grown from EtOAc by slow evaporation.

$R_f$  = 0.11 (hexanes/EtOAc = 95/5, UV 366 nm, CAM).

**Melting point** = 128.3 – 132.7 °C.

$^1\text{H NMR}$  (400 MHz,  $\text{CDCl}_3$ )  $\delta$  = 7.42 – 7.37 (m, 2H), 7.37 – 7.27 (m, 3H), 7.04 (d,  $J$  = 5.5 Hz, 1H), 7.01 (d,  $J$  = 4.5 Hz, 1H), 6.90 (d,  $J$  = 1.9 Hz, 1H), 5.06 (d,  $J$  = 10.7 Hz, 1H), 4.97 (d,  $J$  = 10.7 Hz, 1H), 4.86 (t,  $J$  = 2.8 Hz, 1H), 3.90 (s, 3H), 3.55 – 3.44 (m, 1H), 2.67 (dd,  $J$  = 18.5, 6.7 Hz, 1H), 2.24 – 2.18 (m, 1H), 2.07 (dd,  $J$  = 18.5, 3.3, 1H), 1.73 (td,  $J$  = 13.1, 3.0 Hz, 1H), 0.88 (s, 9H), 0.17 (s, 3H), 0.10 (s, 3H).

$^{13}\text{C NMR}$  (100 MHz,  $\text{CDCl}_3$ )  $\delta$  = 209.9, 171.0, 152.6, 147.0, 136.8, 133.2, 129.7, 128.7, 128.5, 128.3, 126.3, 124.8, 115.0, 74.6, 68.4, 56.1, 41.0, 39.0, 34.9, 25.9, 18.2, –4.1, –4.2.

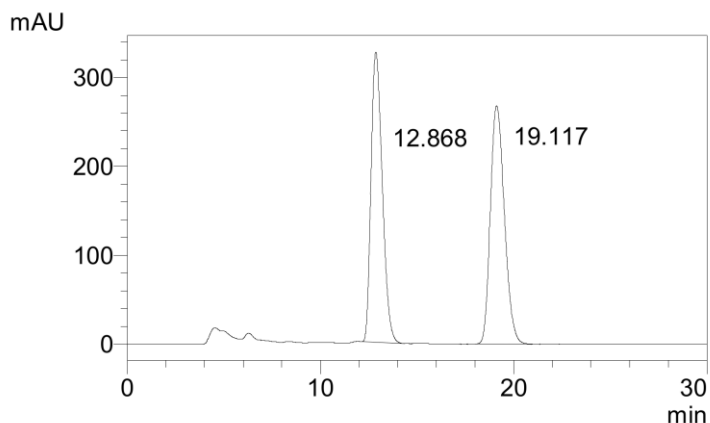
**HRMS (ESI)** for  $\text{C}_{20}\text{H}_{24}\text{O}_2\text{N}^+$  [ $\text{M}+\text{NH}_4$ ] $^+$ : calcd.: 310.1802, found: 310.1806.

**IR (ATR):**  $\tilde{\nu}$  = 2953 (m), 2927 (m), 2875 (w), 2855 (m), 1699 (m), 1676 (s), 1592 (m), 1480 (m), 1470 (m), 1454 (m), 1442 (m), 1404 (w), 1358 (w), 1346 (w), 1333 (w), 1315 (w), 1302 (m), 1261 (s), 1246 (s), 1232 (m), 1215 (w), 1206 (w), 1178 (m), 1112 (m), 1060 (s), 1041 (s), 1006 (m), 968 (s), 944 (m), 911 (w), 898 (m), 874 (w), 831 (s), 811 (m), 795 (s), 771 (s), 762 (s), 725 (m), 700 (s).

$[\alpha]_D^{20}$  = –29.9 (c = 1.5,  $\text{CH}_2\text{Cl}_2$ ).

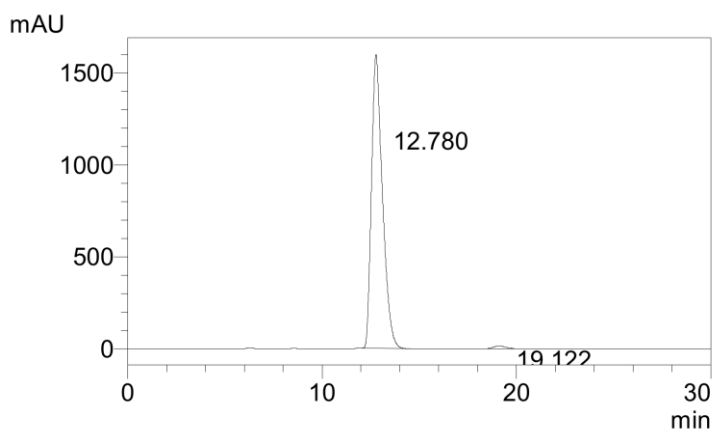
**Enantiomeric excess of 94** was determined by HPLC analysis on chiral stationary phase (DAICEL CHIALPAK IC, 4.6 x 250 mm, 25 °C, 1mL/min, 30% *i*-PrOH in heptane, detection at 254 nm) to be 97.7% by comparison with a racemic sample and coinjection;  $t_R$  major enantiomer = 12.780 min,  $t_R$  minor enantiomer = 19.122 min.

- *Racemic sample of 94:*



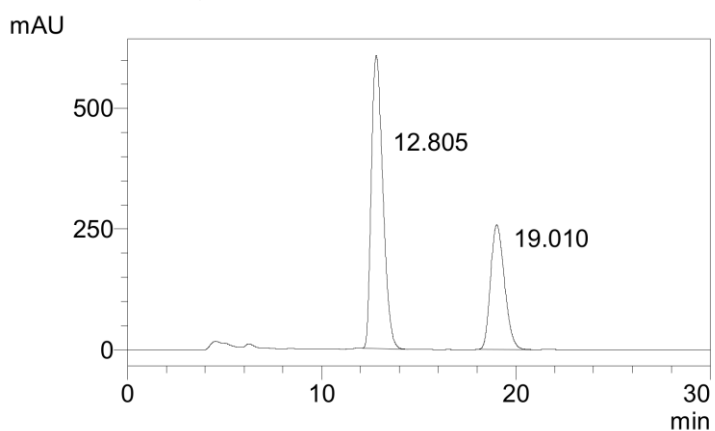
PDA Ch6 254nm		
Peak#	Ret. Time	Area%
1	12.868	49.546
2	19.117	50.454
Total		100.000

- *Enantioenriched sample of 94:*



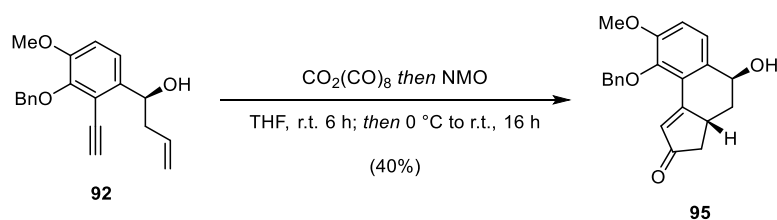
PDA Ch6 254nm		
Peak#	Ret. Time	Area%
1	12.780	98.883
2	19.122	1.117
Total		100.000

- *Coinjection:*



PDA Ch6 254nm		
Peak#	Ret. Time	Area%
1	12.805	66.091
2	19.010	33.909
Total		100.000

### Rac-9-(benzyloxy)-5-hydroxy-8-methoxy-3,3a,4,5-tetrahydro-2H-cyclopenta[a]naphthalen-2-one (**95**)



To a solution of enyne **92** (60.0 mg, 195  $\mu\text{mol}$ , 1.00 eq.) in THF (3.2 mL) was added  $\text{Co}_2(\text{CO})_8$  (79.8 mg, 223  $\mu\text{mol}$ , 1.20 eq.) in one portion and the reaction was stirred in the dark. After successful complexation (monitored by TLC, 6h) the reaction was cooled to 0  $^\circ\text{C}$  and *N*-methylmorpholine *N*-oxide (68.4 mg, 584  $\mu\text{mol}$ , 3.00 eq.) was added portionwise to the light-protected brown reaction mixture. After 16 h, the reaction mixture was filtered over silica ( $\varnothing = 2$  cm,  $h = 2$  cm) and the filter pad was rinsed with EtOAc until only colorless filtrate was obtained. Concentration of the filtrate under reduced pressure and purification by flash column chromatography ( $\text{SiO}_2$ , dry loading by adsorption on  $\text{SiO}_2$ , hexanes/EtOAc = 1/1 to 3/7) afforded tricycle **95** as a colorless oil (26.0 mg, 77.3  $\mu\text{mol}$ , 40%).

$R_f = 0.10$  (hexanes/EtOAc = 1/1, UV 254 nm,  $\text{KMnO}_4$ )

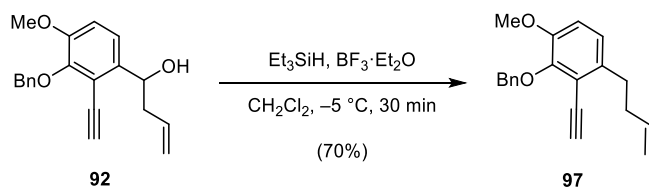
$^1\text{H NMR}$  (400 MHz,  $\text{CDCl}_3$ )  $\delta = 7.40$  (d,  $J = 6.8$  Hz, 2H), 7.37 – 7.29 (m, 3H), 7.16 (d,  $J = 8.4$  Hz, 1H), 7.04 (d,  $J = 8.4$  Hz, 1H), 6.88 (s, 1H), 5.04 (d,  $J = 10.6$  Hz, 1H), 4.94 (d,  $J = 10.6$  Hz, 1H), 4.89 (t,  $J = 2.5$  Hz, 1H), 3.89 (s, 3H), 3.50 – 3.40 (m, 1H), 2.68 (dd,  $J = 18.6$  Hz, 6.6 Hz, 1H), 2.35 (d,  $J = 13.1$  Hz, 1H), 2.28 (br s, 1H), 2.07 (dd,  $J = 18.6, 3.2$  Hz, 1H), 1.75 (td,  $J = 13.1$  Hz, 3.2 Hz, 1H).

$^{13}\text{C NMR}$  (100 MHz,  $\text{CDCl}_3$ )  $\delta = 209.8, 170.3, 153.0, 147.1, 136.7, 132.4, 129.9, 128.6, 128.5, 128.4, 126.3, 124.7, 115.3, 74.7, 67.7, 56.1, 40.9, 37.8, 34.8$ .

**HRMS (ESI)** for  $\text{C}_{21}\text{H}_{21}\text{O}_4^+$   $[\text{M}+\text{H}]^+$ : calcd.: 337.1434, found: 337.1436.

**IR (ATR)**:  $\tilde{\nu} = 3386$  (br, m), 3031 (w), 2938 (w), 2839 (w), 2361 (s), 1699 (m), 1665 (s), 1583 (s), 1479 (s), 1454 (m), 1439 (m), 1406 (w), 1374 (w), 1340 (s), 1304 (m), 1263 (s), 1196 (m), 1178 (m), 1112 (s), 1056 (m), 1035 (s), 1002 (m), 964 (w), 921 (w), 876 (m), 846 (w), 820 (m), 752 (w), 733 (w), 697 (m), 682 (w).

### 2-(benzyloxy)-4-(but-3-en-1-yl)-3-ethynyl-1-methoxybenzene (**97**)



Allylic alcohol **92** (100 mg, 324  $\mu\text{mol}$ , 1.00 eq.) was dissolved in  $\text{CH}_2\text{Cl}_2$  (1.70 mL) and the solution cooled to  $-5\text{ }^\circ\text{C}$ . Triethylsilane (210  $\mu\text{L}$ , 1.30 mmol, 4.00 eq.) was added, followed by the dropwise addition of boron trifluoride etherate (80.0  $\mu\text{L}$ , 649  $\mu\text{mol}$ , 2.00 eq.). After 30 minutes, the reaction was quenched with sat.  $\text{NaHCO}_3$  (5 mL) and the layers were separated and the aqueous phase was extracted with  $\text{CH}_2\text{Cl}_2$  (3 x 10 mL). The combined organic phases washed with brine (20 mL) and dried over  $\text{MgSO}_4$ . The crude product was purified by flash column chromatography ( $\text{SiO}_2$ , hexanes/ $\text{Et}_2\text{O}$  = 20/1) to afford **97** as a pale yellow oil (66.0 mg, 226  $\mu\text{mol}$ , 70%).

$R_f$  = 0.50 (hexanes/ $\text{Et}_2\text{O}$  = 9/1, UV 254 nm, CAM).

**Melting point** = 171.1 – 173.5  $^\circ\text{C}$ .

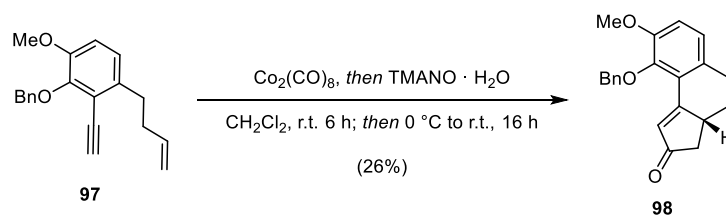
$^1\text{H NMR}$  (400 MHz,  $\text{CDCl}_3$ )  $\delta$  = 7.57 (d,  $J$  = 7.0 Hz, 2H), 7.42 – 7.29 (m, 3H), 6.91 (d,  $J$  = 8.4 Hz, 1H), 6.86 (d,  $J$  = 8.4 Hz, 1H), 5.88 (ddt,  $J$  = 17.0, 10.2, 6.6 Hz, 1H), 5.12 (s, 2H), 5.05 (dd,  $J$  = 17.0, 1.7 Hz, 1H), 4.99 (dd,  $J$  = 10.2, 1.7 Hz, 1H), 3.83 (s, 3H), 3.46 (s, 1H), 2.83 (t,  $J$  = 8.0, 6.6 Hz, 2H), 2.39 (q,  $J$  = 8.0, 6.6 Hz, 2H).

$^{13}\text{C NMR}$  (100 MHz,  $\text{CDCl}_3$ )  $\delta$  = 151.0, 150.1, 138.3, 137.7, 128.5, 128.3, 128.0, 124.3, 117.3, 114.9, 113.2, 85.2, 78.6, 75.2, 56.2, 34.7, 33.5.

**HRMS (ESI)** for  $\text{C}_{20}\text{H}_{24}\text{O}_2\text{N}^+$  [ $\text{M}+\text{NH}_4$ ] $^+$ : calcd.: 310.1802, found: 310.1806.

**IR (ATR)**:  $\tilde{\nu}$  = 3286 (w), 3065 (w), 3031 (w), 3001 (w), 2935 (w), 2837 (w), 2361 (w), 2101 (w), 1639 (w), 1598 (w), 1570 (w), 1482 (s), 1463 (m), 1453 (m), 1433 (m), 1372 (m), 1335 (w), 1265 (s), 1221 (m), 1162 (w), 1105 (w), 1074 (s), 1026 (s), 996 (m), 909 (s), 806 (m), 735 (s), 697 (s).

### **Rac-9-(benzyloxy)-8-methoxy-3,3a,4,5-tetrahydro-2H-cyclopenta[*a*]naphthalen-2-one (98)**



To a solution of enyne **97** (180 mg, 615  $\mu\text{mol}$ , 1.00 eq.) in  $\text{CH}_2\text{Cl}_2$  (24 mL) was added  $\text{Co}_2(\text{CO})_8$  (252 mg, 738  $\mu\text{mol}$ , 1.20 eq.) in one portion and the reaction was stirred in the dark. After successful complexation (monitored by TLC, 2 h) the reaction was cooled to  $0\text{ }^\circ\text{C}$  and trimethylamine *N*-oxide dihydrate (410 mg, 3.69 mmol, 6.00 eq.) was added portionwise to the light-protected brown reaction mixture. After 16 h, the reaction mixture was filtered over silica ( $\phi$  = 3 cm, h = 4 cm) and the filter pad was rinsed with  $\text{EtOAc}$  until only colorless filtrate was obtained. Concentration of the filtrate under reduced pressure and purification by flash column chromatography ( $\text{SiO}_2$ , dry loading by adsorption

on SiO<sub>2</sub>, hexanes/EtOAc = 9/1 to 1/1) afforded tricycle **98** as a colorless oil (52.0 mg, 162 μmol, 26%).

$R_f$  = 0.30 (hexanes/EtOAc = 8/2).

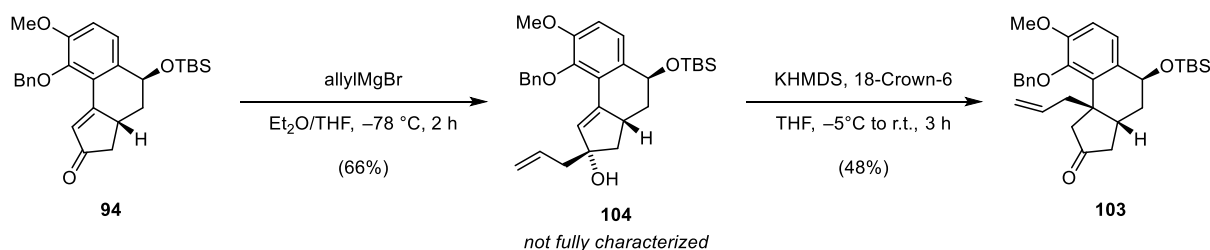
<sup>1</sup>H NMR (CDCl<sub>3</sub>, 400 MHz): δ = 7.42 (d, *J* = 6.6 Hz, 2H), 7.37 – 7.28 (m, 3H), 6.98 (d, *J* = 8.4 Hz, 1H), 6.93 (d, *J* = 8.4 Hz, 1H), 6.88 (d, *J* = 1.7 Hz, 1H), 5.04 (d, *J* = 10.7 Hz, 1H), 4.96 (d, *J* = 10.7 Hz, 1H), 3.88 (s, 3H), 2.99 – 2.88 (m, 3H), 2.67 (dd, *J* = 18.5, 6.6 Hz, 1H), 2.25 – 2.18 (m, 1H), 2.07 (dd, *J* = 18.5, 3.2 Hz, 1H), 1.63 – 1.53 (m, 1H).

<sup>13</sup>C NMR (CDCl<sub>3</sub>, 100 MHz): δ = 209.8, 171.2, 151.2, 147.5, 136.9, 132.4, 129.2, 128.6, 128.5, 128.2, 125.1, 124.9, 115.4, 74.5, 56.3, 41.4, 41.0, 30.2, 29.8.

HRMS (ESI) for C<sub>21</sub>H<sub>21</sub>O<sub>3</sub><sup>+</sup> [M+H]<sup>+</sup>: calcd.: 321.1485, found: 321.1487.

IR (ATR):  $\tilde{\nu}$  = 2938 (w), 2906 (s), 2836 (s), 2361 (w), 2340 (w), 1701 (s), 1678 (s), 1584 (s), 1479 (s), 1455 (m), 1439 (m), 1375 (s), 1298 (m), 1275 (s), 1263 (s), 1171 (m), 1111 (s), 1053 (m), 1022 (m), 997 (m), 963 (s), 911 (w), 845 (s), 804 (w), 747 (w), 698 (w).

### 9b-allyl-9-(benzyloxy)-5-((*tert*-butyldimethylsilyl)oxy)-8-methoxy-1,3,3a,4,5,9b-hexahydro-2H-cyclopenta[*a*]naphthalen-2-one (**103**)



The Pauson–Khand product **94** (200 mg, 444 μmol, 1.00 eq.) was dissolved in benzene (10 mL) and the solvent was removed under reduced pressure. The residue was dissolved in THF (16 mL) and the solution was cooled to  $-78$  °C. Allylmagnesium bromide (1.06 M in Et<sub>2</sub>O, 460 μL, 488 μmol, 1.1 eq.) was added dropwise, the yellow solution was stirred for 2 h. Subsequently, the reaction was quenched with saturated aqueous NH<sub>4</sub>Cl (10 mL). The aqueous layer was extracted with EtOAc (3 x 20 mL) and the combined organic phases were washed with saturated aqueous NaHCO<sub>3</sub> (30 mL), brine (30 mL), dried over MgSO<sub>4</sub> and filtered. The solvent was removed in vacuo to afford **104** (143.8 mg, 292 μmol, 66%) that was directly subjected to the next step without further purification.

*Note:* **104** could be stored for several weeks in a benzene matrix at  $-25$  °C (100 mg/5 mL). Attempts to purify it by silica gel chromatography resulted in decomposition.

To a solution of tertiary alcohol **104** (100 mg, 203 μmol, 1.0 eq.) in THF (4 mL) at  $-5$  °C was added 18-crown-6 (161 mg, 609 μmol, 3.00 eq.) followed by KHMDS (1M in THF, 609 μL, 609 μmol, 3.00 eq.). The orange solution was stirred for 3 h and was slowly allowed to warm to room

temperature in the cooling bath. The reaction mixture was cooled to 0 °C and quenched with pH 7 buffer. The solution was extracted with EtOAc (3 x 20 mL), successively washed with saturated aqueous KCl (2 x 20 mL), brine (20 mL) and dried over MgSO<sub>4</sub>. After filtration the crude product was purified by flash column chromatography (SiO<sub>2</sub>, hexanes/EtOAc = 9/1) to yield the rearrangement product **103** as a yellow oil (40.8 mg, 82.8 μmol, 48%).

$R_f = 0.42$  (hexanes/Et<sub>2</sub>O = 8/2)

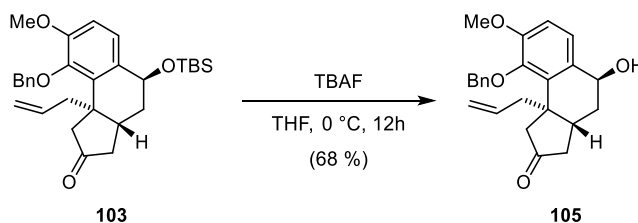
<sup>1</sup>H NMR (CDCl<sub>3</sub>, 400 MHz): δ = 7.48 (d, *J* = 7.3 Hz, 2H), 7.40 (t, *J* = 7.3 Hz, 2H), 7.33 (t, *J* = 7.3 Hz, 1H), 6.97 – 6.90 (m, 1H), 6.89 – 6.83 (m, 1H), 5.60 – 5.47 (m, 1H), 5.16 (d, *J* = 11.3 Hz, 1H), 5.04 (d, *J* = 11.3 Hz, 1H), 4.97 (d, *J* = 17.1 Hz, 1H), 4.91 (d, *J* = 10.5 Hz, 1H), 4.79 – 4.72 (m, 1H), 3.87 (s, 3H), 3.18 – 3.02 (m, 2H), 2.82 (d, *J* = 19.2 Hz, 1H), 2.78 – 2.66 (m, 1H), 2.53 – 2.42 (m, 1H), 2.41 – 2.28 (m, 1H), 2.04 (d, *J* = 19.2 Hz, 1H), 1.92 – 1.80 (m, 1H), 1.70 – 1.56 (m, 1H), 0.89 (s, 9H), 0.17 (s, 3H), 0.15 (s, 3H).

<sup>13</sup>C NMR (CDCl<sub>3</sub>, 100 MHz): δ = 220.2, 152.6, 146.7, 138.0, 136.0, 135.2, 132.3, 128.6, 127.8, 127.4, 124.9, 117.0, 111.0, 73.6, 68.6, 55.8, 50.5, 44.6, 43.3, 43.0, 36.6, 32.6, 25.9, 18.1, -4.1, -4.4.

HRMS (ESI) for C<sub>30</sub>H<sub>44</sub>O<sub>4</sub>NSi<sup>+</sup> [M+NH<sub>4</sub>]<sup>+</sup>: calcd.: 510.3034, found: 510.3043.

IR (ATR):  $\tilde{\nu}$  = 3069 (w), 3032 (w), 2953 (m), 2928 (m), 2855 (w), 2361 (w), 2252 (w), 1737 (s), 1638 (w), 1598 (w), 1577 (w), 1483 (m), 1463 (m), 1434 (m), 1403 (w), 1353 (m), 1324 (w), 1297 (m), 1270 (s), 1251 (s), 1201 (w), 1172 (m), 1136 (w), 1079 (s), 1055 (s), 1025 (m), 1002 (s), 974 (s), 947 (m), 910 (m), 878 (w), 833 (s), 815 (m), 795 (m), 773 (s), 732 (s), 696 (s).

### *Rac*-(3*aR*,5*S*,9*bR*)-9*b*-allyl-9-(benzyloxy)-5-hydroxy-8-methoxy-1,3,3*a*,4,5,9*b*-hexahydro-2*H*-cyclopenta[*a*]naphthalen-2-one (**105**)



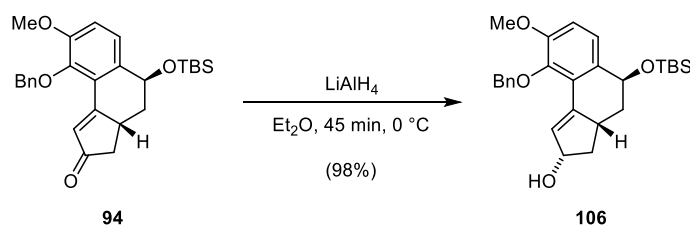
To a solution of the rearrangement product **103** (23.0 mg, 46.7 μmol, 1.00 eq.) in THF (1.70 mL) was added tetrabutylammonium fluoride hydrate (1 M in THF, 100 μL, 0.10 mmol, 2.14 eq.) at 0 °C. The reaction mixture was stirred at room temperature for 12 h and subsequently quenched with saturated aqueous NH<sub>4</sub>Cl (5 mL). The aqueous layer was extracted with EtOAc (3 x 10 mL) and combined organic phases were washed with brine (20 mL) and dried over MgSO<sub>4</sub>. The crude product was purified by flash column chromatography (SiO<sub>2</sub>, hexanes/EtOAc = 1/1) to yield the rearrangement product **105** as a pale yellow oil (12.0 mg, 31.7 μmol, 68 %).

$R_f = 0.26$  (hexanes/EtOAc = 1/1).

<sup>1</sup>H NMR (CDCl<sub>3</sub>, 400 MHz): δ (ppm) = 7.43 (d, *J* = 7.5 Hz, 2H), 7.20 (t, *J* = 7.5 Hz), 7.11 (t, *J* = 7.4 Hz, 1H), 6.88 – 6.77 (m, 1H), 6.50 (d, *J* = 8.3 Hz, 1H), 5.52 – 5.35 (m, 1H), 5.19 (d, *J* = 11.2 Hz, 1H), 4.89 – 4.74 (m, 3H), 4.50 (s, 1H), 3.26 (s, 3H), 3.14 (dd, *J* = 13.0, 5.6 Hz), 2.85 – 2.75 (m, 2H), 2.42 – 2.29 (m, 2H), 2.07 – 1.97 (m, 1H), 1.76 (d, *J* = 19.0 Hz, 1H), 1.70 – 1.60 (m, 1H), 1.24 (t, *J* = 13.6 Hz, 1H).

<sup>13</sup>C NMR (C<sub>6</sub>D<sub>6</sub>, 100 MHz): δ (ppm) = 216.5, 153.1, 147.3, 138.5, 136.2, 135.5, 132.6, 128.8, 128.1, 125.3, 117.5, 111.6, 74.0, 68.2, 55.4, 50.6, 44.7, 43.0, 35.3, 32.6.

**(2*S*,3*aS*,5*S*)-9-(benzyloxy)-5-((*tert*-butyldimethylsilyl)oxy)-8-methoxy-3,3*a*,4,5-tetrahydro-2*H*-cyclopenta[*a*]naphthalen-2-ol (106)**



Enone **94** (1.56 g, 3.47 mmol, 1.00 eq.) was added portionwise to a stirred suspension of LiAlH<sub>4</sub> (92.3 mg, 2.43 mmol, 0.70 eq.) in Et<sub>2</sub>O (30 mL) placed in an ice-acetone bath (0 °C). The reaction was stirred for 45 minutes and quenched by sequential slow addition of water (125 μL), aqueous NaOH (2.5 M, 125 μL) and water (375 μL). The yellow suspension was filtered over a pad of silica (d = 5 cm, h = 3 cm) and the filter cake rinsed with EtOAc (200 mL). Evaporation of the filtrate gave a white foam, which was triturated with EtOAc and hexanes under sonication to afford **7** as white solid (1.55 g, 3.44 mmol, 98%).

In the racemic series, crystals suitable for X-ray analysis were grown from EtOAc by slow evaporation.

*R<sub>f</sub>* = 0.23 (hexanes/EtOAc = 8/2, UV 254 nm, CAM).

**Melting point** = 111.8 – 113.5 °C.

<sup>1</sup>H NMR (400 MHz, CDCl<sub>3</sub>) δ = 7.51 – 7.45 (m, 2H), 7.41 – 7.29 (m, 3H), 6.98 (d, *J* = 8.4 Hz, 1H), 6.86 (d, *J* = 8.4 Hz, 1H), 6.64 (t, *J* = 2.1 Hz, 1H), 5.01 (d, *J* = 10.6 Hz, 1H), 4.97 (d, *J* = 10.8 Hz, 1H), 4.76 (t, *J* = 3.0 Hz, 1H), 3.86 (s, 3H), 3.21 – 3.08 (m, 1H), 2.62 (dt, *J* = 12.5, 7.2 Hz, 1H), 2.07 (dt, *J* = 13.0, 3.7 Hz, 1H), 1.64 (s, 1H), 1.59 (dt, *J* = 13.2, 3.4 Hz, 1H), 1.31 – 1.18 (m, 1H), 0.88 (s, 9H), 0.15 (s, 3H), 0.06 (s, 3H).

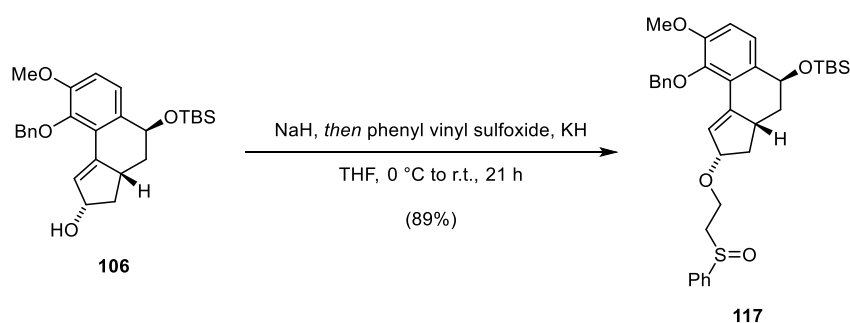
<sup>13</sup>C NMR (100 MHz, CDCl<sub>3</sub>) δ = 152.5, 146.2, 140.2, 137.8, 132.7, 131.9, 128.4, 128.4, 128.0, 125.9, 125.6, 112.0, 78.0, 73.6, 69.3, 56.1, 41.2, 39.3, 37.7, 26.0, 18.2, –4.1, –4.2.

**HRMS (ESI)** for C<sub>27</sub>H<sub>33</sub>O<sub>3</sub>Si<sup>–</sup> [M–H<sub>3</sub>O<sup>+</sup>]: calcd.: 433.2215, found: 433.2209.

**IR (ATR):**  $\tilde{\nu}$  = 3343 (br, w), 2952 (m), 2928 (m), 2883 (m), 2866 (m), 2361 (w), 1597 (w), 1571 (w), 1479 (s), 1440 (m), 1408 (w), 1377 (m), 1350 (m), 1327 (m), 1303 (m), 1267 (s), 1255 (s), 1220 (m), 1164 (w), 1124 (m), 1109 (m), 1052 (s), 977 (s), 920 (m), 832 (s), 808 (m), 795 (m), 773 (s), 752 (m), 731 (m), 696 (m), 677 (m).

$[\alpha]_D^{20} = -17.2$  (c = 2.95, CH<sub>2</sub>Cl<sub>2</sub>).

**(((2S,3aS,5S)-9-(benzyloxy)-8-methoxy-2-(2-(phenylsulfinyl)ethoxy)-3,3a,4,5-tetrahydro-2H-cyclopenta[a]naphthalen-5-yl)oxy)(tert-butyl)dimethylsilane (117)**



To a suspension of NaH (60% w/w in mineral oil, 103 mg, 2.58 mmol, 1.00 eq.) in THF (30 mL) was added dropwise a solution of alcohol **106** (1.13 g, 2.58 mmol, 1.00 eq.) in THF (8 mL). The reaction was stirred for 30 minutes and phenyl vinyl sulfoxide (1.09 mL, 7.73 mmol, 3.00 eq.) was added, followed by catalytic amount of washed KH (oil free, stored under argon, tip of a Pasteur pipette). The reaction was stirred at room temperature for 21 h and then quenched at 0 °C with saturated aqueous NH<sub>4</sub>Cl (50 mL). After separation of the layers, the aqueous layer was extracted with EtOAc (3 x 50 mL) and the combined organic layers were washed with brine, dried over MgSO<sub>4</sub>, filtered and concentrated in vacuo to afford a mixture of **117** and unreacted phenyl vinyl sulfoxide. Although remaining phenyl vinyl sulfoxide does not interfere with the subsequent reaction, spectral analysis, was facilitated if it was removed. To this end, the crude reaction mixture was dissolved in *i*-PrOH, and a solution of methylamine was added (33% in EtOH, 33.2 mmol, 3.63 mL, 10.00 eq.). The light orange solution was stirred for 3 h at room temperature, upon which time TLC analysis indicated complete disappearance of phenylvinyl sulfoxide ( $R_f = 0.48$  in hexanes/EtOAc = 6/4, stains very strongly with KMnO<sub>4</sub>). The solvent was removed in vacuo and the crude reaction mixture was purified by flash column chromatography (SiO<sub>2</sub>, hexanes/EtOAc = 9/1 to 2/8) to give **117** as a colorless oil (1.74 g, 2.95 mmol, 89%).

$R_f = 0.52$  (hexanes/EtOAc = 6/4, UV 254 nm, CAM).

*Note: NMR spectra are complex due to the presence of diastereoisomers resulting from the sulfoxide moiety.*

**<sup>1</sup>H NMR** (400 MHz, CDCl<sub>3</sub>) δ = 7.74 – 7.58 (m, 2H), 7.48 (ddt, *J* = 7.6, 5.8, 1.6 Hz, 5H), 7.42 – 7.28 (m, 3H), 6.97 (dd, *J* = 8.4, 3.0 Hz, 1H), 6.85 (dd, *J* = 8.4, 1.7 Hz, 1H), 6.71 – 6.59 (m, 1H), 5.30 (s, 1H), 4.99 (d, *J* = 1.9 Hz, 2H), 4.84 – 4.59 (m, 2H), 4.02 – 3.79 (m, 4H), 3.62 (ddt, *J* = 18.0, 10.2, 5.1 Hz, 1H), 3.13 (d, *J* = 9.8 Hz, 1H), 3.07 – 2.85 (m, 2H), 2.52 (ddt, *J* = 26.8, 12.3, 7.2 Hz, 1H), 2.24 – 1.97 (m, 1H), 1.63 (ddd, *J* = 12.7, 7.2, 3.1 Hz, 2H), 1.47 – 1.19 (m, 2H), 0.87 (s, 9H), 0.14 (d, *J* = 1.7 Hz, 3H), 0.05 (d, *J* = 2.3 Hz, 3H).

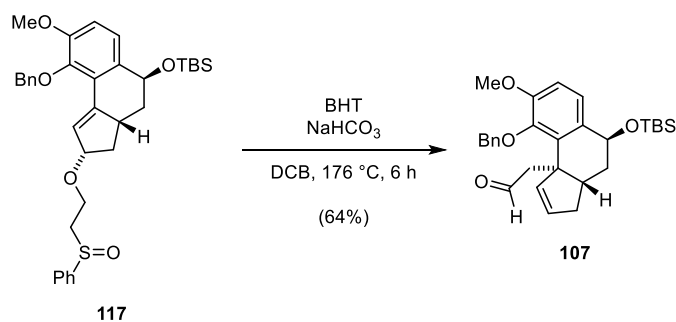
**<sup>13</sup>C NMR** (100 MHz, CDCl<sub>3</sub>) δ = 152.5, 152.4, 146.3, 146.2, 144.2, 144.2, 140.7, 140.7, 138.0, 137.8, 132.7, 132.6, 131.1, 129.3, 128.6, 128.5, 128.5, 128.4, 128.3, 128.0, 127.9, 125.9, 125.8, 125.5, 124.1, 124.1, 112.1, 112.1, 85.8, 85.7, 73.7, 73.6, 69.3, 61.6, 61.2, 60.5, 58.8, 58.7, 56.1, 39.2, 39.1, 37.5, 37.3, 37.3, 26.0, 21.2, 18.2, 14.3, -4.1, -4.2.

**HRMS (ESI)** for C<sub>35</sub>H<sub>44</sub>NaO<sub>5</sub>SSi<sup>+</sup> [M+H]<sup>+</sup>: calcd.: 627.2576, found: 627.258.

**IR (ATR):**  $\tilde{\nu}$  = 3403 (br, w), 2953 (m), 2928 (m), 2855 (m), 1596 (w), 1570 (w), 1479 (m), 1442 (m), 1339 (m), 1305 (m), 1269 (s), 1221 (w), 1164 (w), 1129 (m), 1085 (s), 1049 (s), 980 (m), 932 (m), 834 (s), 809 (m), 796 (m), 775 (m), 747 (m), 695 (m).

$[\alpha]_D^{20}$  = +18.0° (c = 0.66, CH<sub>2</sub>Cl<sub>2</sub>).

**2-((3*aS*,5*S*,9*bS*)-9-(benzyloxy)-5-((*tert*-butyldimethylsilyl)oxy)-8-methoxy-3,3*a*,4,5-tetrahydro-9*bH*-cyclopenta[*a*]naphthalen-9*b*-yl)acetaldehyde (107)**



A 500 mL three-neck round-bottom flask fitted with a water-cooled Liebig-type reflux condenser, an internal thermometer and a rubber septum was charged with **117** (1.67 g, 2.83 mmol, 1.00 eq.), DCB (115 mL), NaHCO<sub>3</sub> (21.34 g, 254 mmol, 90.0 eq.), and 3,5-di-*tert*-4-butylhydroxytoluene (31.1 mg, 141 μmol, 0.05 eq.). Phenanthrene (262 mg, 1.47 mmol, 0.52 eq.) was added as internal standard and nitrogen was bubbled through the reaction mixture for 20 minutes via a 22-gauge steel needle under vigorous stirring (800 rpm). The needle was retracted from below the solvent surface and the setup was lowered in a preheated oil bath (197 °C). In the next hour, the clear reaction mixture foams and vapor accumulates in the head of the reflux condenser. After 2 h, the internal temperature reaches and stabilizes at 176 °C under moderate refluxing and occasional fizzing.

Every hour, a 0.1 mL aliquot is withdrawn with a syringe from the hot reaction mixture, diluted with  $\text{CDCl}_3$  and analyzed by  $^1\text{H}$  NMR (integration of signals against phenanthrene). After disappearance of the starting material **117** (6 h), the reaction is lifted from the oil bath, left to cool for one hour while stirring and filtered (porosity 3 glass frit covered with a thin layer of sand). The filter cake is washed with  $\text{CHCl}_3$  (2 x 100 mL) and the resulting orange solution is concentrated on a rotary evaporator (40 °C water bath, 10 mbar) followed by distillation in a short-path apparatus (50 °C water bath, 3 mbar) to remove residual DCB. The brown residue was purified via flash column chromatography ( $\text{SiO}_2$ , hexanes/ $\text{Et}_2\text{O}$  = 100/1 to 85/15) to afford aldehyde **107** as light brown oil (838 mg, 1.80 mmol, 64%).

*Note: The reaction must be stopped as soon as the starting material is fully converted as judged by NMR analysis. Longer reaction times invariably lead to lower isolated yields.*

$R_f$  = 0.52 (hexanes/ $\text{EtOAc}$  = 9/1, CAM).

$^1\text{H}$  NMR (400 MHz,  $\text{CDCl}_3$ )  $\delta$  = 9.63 (t,  $J$  = 3.3 Hz, 1H), 7.53 – 7.47 (m, 2H), 7.44 – 7.37 (m, 2H), 7.36 – 7.31 (m, 1H), 7.22 (dd,  $J$  = 8.5, 0.9 Hz, 1H), 6.89 (d,  $J$  = 8.6 Hz, 1H), 6.87 – 6.82 (m, 1H), 5.93 (ddd,  $J$  = 5.9, 3.0, 1.6 Hz, 1H), 5.26 (d,  $J$  = 11.2 Hz, 1H), 4.94 (ddd,  $J$  = 7.2, 2.0, 0.9 Hz, 1H), 4.84 (d,  $J$  = 11.2 Hz, 1H), 3.86 (s, 3H), 2.58 – 2.47 (m, 1H), 2.36 – 2.18 (m, 4H), 2.03 – 1.92 (m, 2H), 0.95 (s, 9H), 0.19 (s, 3H), 0.18 (s, 3H).

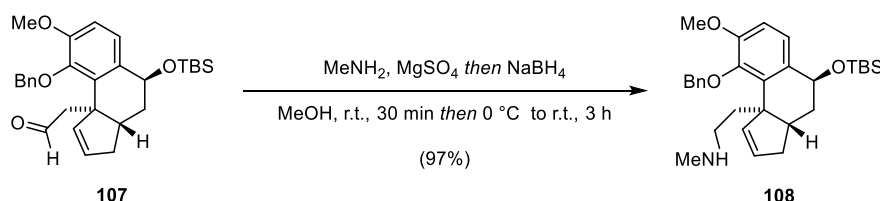
$^{13}\text{C}$  NMR (100 MHz,  $\text{CDCl}_3$ )  $\delta$  = 204.1, 151.7, 143.8, 138.0, 137.9, 136.5, 132.9, 132.4, 128.9, 127.8, 127.6, 125.7, 111.0, 74.5, 68.1, 55.9, 51.4, 50.2, 45.1, 33.6, 32.9, 26.1, 18.3, -4.0, -4.4.

HRMS (ESI) for  $\text{C}_{29}\text{H}_{42}\text{O}_4\text{NSi}^+$  [ $\text{M}+\text{NH}_4$ ] $^+$ : calcd.: 496.2878, found: 496.2886.

IR (ATR):  $\tilde{\nu}$  = 2929 (s), 2855 (s), 2740 (w), 2359 (w), 1718 (s), 1601 (w), 1573 (w), 1497 (w), 1474 (s), 1439 (m), 1374 (m), 1345 (w), 1301 (m), 1256 (s), 1219 (m), 1165 (w), 1145 (m), 1130 (m), 1100 (m), 1076 (m), 1049 (s), 987 (m), 938 (m), 910 (m), 832 (s), 812 (m), 775 (s), 732 (m), 697 (m).

$[\alpha]_{\text{D}}^{20}$  = -18.2 ( $c$  = 0.66,  $\text{CH}_2\text{Cl}_2$ ).

## 2-((3a*S*,5*S*,9*bS*)-9-(benzyloxy)-5-((*tert*-butyldimethylsilyl)oxy)-8-methoxy-3,3a,4,5-tetrahydro-9*bH*-cyclopenta[*a*]naphthalen-9*b*-yl)-*N*-methylethan-1-amine (108)



Claisen rearrangement product **107** (836 mg, 1.80 mmol, 1.00 eq.) was dissolved in methanol (45 mL) and  $\text{MgSO}_4$  (867 mg, 7.20 mmol, 4.00 eq.) was added in one portion. Then a solution of methylamine (33% in  $\text{EtOH}$ , 1.97 mL, 18.00 mmol, 10.0 eq.) was added dropwise to the reaction. Upon

disappearance of the starting material (monitored by  $^1\text{H}$  NMR following withdrawal of a 0.1 mL aliquot of the reaction mixture, evaporation, and dissolution in  $\text{CDCl}_3$ ), the reaction was cooled to  $0^\circ\text{C}$  and  $\text{NaBH}_4$  (204.0 mg, 5.40 mmol, 3.00 eq.) was added in one portion. After stirring at room temperature for 3 h the reaction was quenched by the addition of water (20 mL) and diluted with brine (50 mL) and  $\text{CHCl}_3$  (50 mL). The layers were separated and the aqueous phase was extracted with  $\text{CHCl}_3$  (4 x 50 mL). The combined organic layers were washed with brine, dried over  $\text{MgSO}_4$ , filtered and concentrated under reduced pressure to afford a brown oil. Purification was performed by flash column chromatography ( $\text{SiO}_2$ ,  $\text{CHCl}_3/\text{MeOH} = 95/5 + 1\% \text{Et}_3\text{N}$  to  $9/1 + 1\% \text{Et}_3\text{N}$ ) and the reductive amination product **108** was obtained as a brown foam (865 mg, 1.75 mmol, 97%).

$R_f = 0.47$  ( $\text{CHCl}_3/\text{MeOH} = 9/1 + 1\% \text{Et}_3\text{N}$ , UV 254 nm, CAM).

$^1\text{H}$  NMR (400 MHz,  $\text{CDCl}_3$ )  $\delta = 7.43 - 7.39$  (m, 2H),  $7.34 - 7.28$  (m, 2H),  $7.26 - 7.21$  (m, 1H),  $7.16$  (dd,  $J = 8.6, 0.9$  Hz, 1H),  $6.74$  (d,  $J = 8.6$  Hz, 1H),  $6.68$  (d,  $J = 6.0$  Hz, 1H),  $5.75$  (ddd,  $J = 6.0, 2.9, 1.5$  Hz, 1H),  $5.07$  (d,  $J = 11.0$  Hz, 1H),  $4.9$  (td,  $J = 5.5, 1.0$  Hz, 1H),  $4.59$  (d,  $J = 11.0$  Hz, 1H),  $3.76$  (s, 3H),  $2.57$  (td,  $J = 11.4, 5.2$  Hz, 1H),  $2.45$  (td,  $J = 11.5, 5.1$  Hz, 1H),  $2.31 - 2.25$  (m, 2H),  $2.20$  (s, 3H),  $2.18 - 2.10$  (m, 1H),  $1.99 - 1.88$  (m, 1H),  $1.85 - 1.77$  (m, 1H),  $1.50$  (td,  $J = 11.8, 5.2$  Hz, 1H),  $1.36$  (td,  $J = 11.7, 5.0$  Hz, 1H),  $0.86$  (s, 9H),  $0.08$  (s, 3H),  $0.06$  (s, 3H).

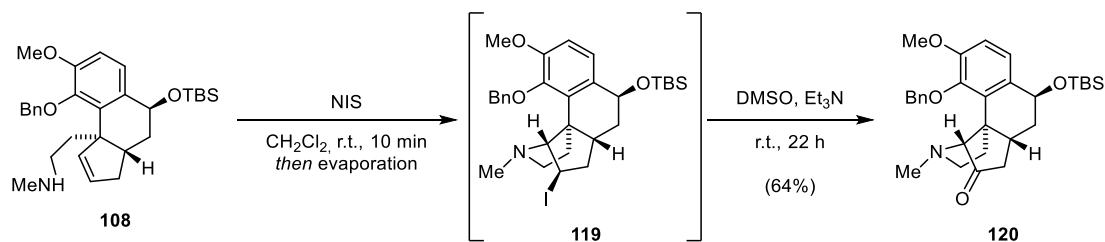
$^{13}\text{C}$  NMR (100 MHz,  $\text{CDCl}_3$ )  $\delta = 151.3, 143.9, 138.8, 138.2, 138.0, 132.9, 131.8, 128.5, 127.8, 127.7, 124.6, 74.5, 67.6, 55.8, 52.0, 48.4, 46.0, 35.9, 35.6, 33.7, 33.6, 26.1, 18.3, -4.00, -4.5$ .

HRMS (ESI) for  $\text{C}_{30}\text{H}_{44}\text{O}_3\text{NSi}^+ [\text{M}+\text{H}]^+$ : calcd.: 494.3085, found: 494.3091.

IR (ATR):  $\tilde{\nu} = 2929$  (m),  $2884$  (w),  $2855$  (m),  $1600$  (w),  $1573$  (w),  $1472$  (m),  $1439$  (m),  $1374$  (m),  $1300$  (m),  $1253$  (s),  $1167$  (w),  $1144$  (w),  $1116$  (m),  $1076$  (m),  $1048$  (s),  $990$  (m),  $937$  (m),  $909$  (m),  $813$  (s),  $773$  (s),  $729$  (s),  $697$  (m).

$[\alpha]_{\text{D}}^{20} = +22.6$  ( $c = 0.21$ ,  $\text{CH}_2\text{Cl}_2$ ).

**(3aR,5aR,7S,11bS)-11-(benzyloxy)-7-((tert-butyldimethylsilyl)oxy)-10-methoxy-3-methyl-1,2,3,3a,5,5a,6,7-octahydro-4H-benzo[6,7]indeno[1,7a-b]pyrrol-4-one (120)**



*Note: The following reaction was performed under the exclusion of light: laboratory and fume hood lights were turned off, the reaction flask wrapped in aluminum foil and flasks connected to a rotary evaporator were covered with aluminum foil.*

Reductive amination product **108** (350 mg, 0.709  $\mu\text{mol}$ , 1.00 eq.) was dissolved in  $\text{CH}_2\text{Cl}_2$  (64 mL). NIS (319 mg, 1.42 mmol, 2.00 eq.) was added in one portion at room temperature and the mixture was stirred for 10 min. The flask was moved to a rotary evaporator and the solvent was removed in vacuo (25 °C water bath, 5 mbar) followed by drying on high vacuum for 5 min (0.5 mbar). The resulting rusty brown foam (**119**) was dissolved in DMSO (143 mL) and stirred for 5 min at room temperature before  $\text{Et}_3\text{N}$  (296  $\mu\text{L}$ , 2.13 mmol, 3.00 eq.) was added. The reaction was sealed with a polyethylene cap and stirred for 22 h at room temperature. The solution was cooled to 0 °C and water (100 mL) was added. After the mixture was stirred for 5 min, it was diluted with EtOAc (100 mL) and 10% LiCl (200 mL). The aqueous layer was extracted with EtOAc (3 x 100 mL) and the combined organic layers were washed with 10% LiCl (3 x 100 mL), brine, dried over  $\text{MgSO}_4$  and filtered. The solvent was removed in vacuo and the resulting brown oil was purified by flash column chromatography ( $\text{Et}_3\text{N}$ -deactivated  $\text{SiO}_2$ , hexanes/EtOAc = 9/1 to 8/2) to afford **120** as light yellow oil (231 mg, 455  $\mu\text{mol}$ , 64%).

$R_f = 0.39$  (hexanes/EtOAc = 8/2, UV 254 nm, CAM).

$^1\text{H NMR}$  (400 MHz,  $\text{C}_6\text{D}_6$ )  $\delta = 7.61\text{--}7.53$  (m, 2H), 7.42 (dd,  $J = 8.5, 1.0$  Hz, 1H), 7.25 (dd,  $J = 8.3, 6.9$  Hz, 3H), 6.60 (d,  $J = 8.5$  Hz, 1H), 5.14 (d,  $J = 11.1$  Hz, 1H), 4.91 (d,  $J = 11.1$  Hz, 1H), 4.80 (ddd,  $J = 7.7, 4.6, 1.1$  Hz, 1H), 3.98 (s, 1H), 3.29 (s, 3H), 2.90 (dt,  $J = 8.4, 6.8$  Hz, 1H), 2.48 (s, 3H), 2.42 (td,  $J = 7.6, 5.1$  Hz, 1H), 2.17 – 2.04 (m, 1H), 2.03 – 1.79 (m, 5H), 1.44 (ddd,  $J = 12.2, 6.7, 5.2$  Hz, 1H), 1.07 (s, 9H), 0.20 (s, 3H), 0.15 (s, 3H).

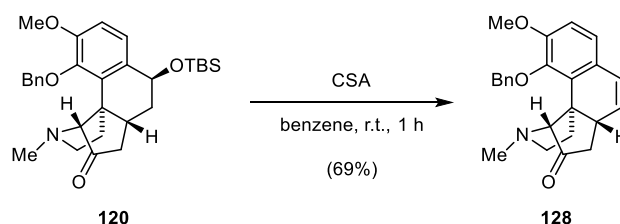
$^{13}\text{C NMR}$  (100 MHz,  $\text{C}_6\text{D}_6$ )  $\delta = 213.4, 152.4, 144.3, 139.1, 138.8, 132.7, 128.6, 128.5, 123.5, 110.5, 75.1, 73.9, 67.8, 55.4, 55.2, 53.7, 39.2, 37.0, 35.4, 35.0, 26.2, 18.4, -4.1, -4.6$ .

**HRMS (ESI)** for  $\text{C}_{30}\text{H}_{42}\text{O}_4\text{NSi}$   $[\text{M}+\text{H}]^+$ : calcd.: 508.2878, found: 508.2874.

**IR (ATR):**  $\tilde{\nu} = 2929$  (w), 2886 (m), 2856 (w), 2794 (w), 1736 (m), 1600 (w), 1576 (w), 1472 (m), 1375 (w), 1304 (m), 1253 (s), 1156 (w), 1125 (m), 1077 (m), 1052 (m), 986 (m), 929 (m), 833 (s), 774 (s), 733 (m), 697 (m), 678 (w).

$[\alpha]_{\text{D}}^{20} = -99.3$  (c = 0.22,  $\text{CH}_2\text{Cl}_2$ ).

***Rac*-(3*aR*,5*aS*,11*bS*)-11-(benzyloxy)-10-methoxy-3-methyl-1,2,3,3*a*,5,5*a*-hexahydro-4*H*-benzo[6,7]indeno[1,7*a-b*]pyrrol-4-one (**128**)**



Kornblum oxidation product **120** (120 mg, 237  $\mu\text{mol}$ , 1.00 eq.) was dried on high vacuum for 5 min before it was dissolved in benzene (25 mL). Camphor-10-sulfonic acid (165 mg, 71.0  $\mu\text{mol}$ , 3.00 eq.) was added at room temperature and the flask was sealed with a polypropylene cap. After stirring for 1 h, saturated aqueous  $\text{NaHCO}_3$  (50 mL) was added and the mixture was diluted with EtOAc (50 mL). The aqueous layer was extracted with EtOAc (3 x 30 mL) and the combined organic layers were washed with brine, dried over  $\text{MgSO}_4$  and concentrated under reduced pressure. Purification by flash column chromatography ( $\text{Et}_3\text{N}$ -deactivated  $\text{SiO}_2$ , hexanes/EtOAc = 8/2) gave the elimination product **128** as a colorless oil that solidified upon standing (61.2 mg, 163  $\mu\text{mol}$ , 69%)

Crystals suitable for X-ray analysis were grown from benzene by slow evaporation.

$R_f$  = 0.8 (hexanes/EtOAc = 8/2, UV 254 nm, CAM).

**Melting point** = 111.8 – 113.5  $^\circ\text{C}$ .

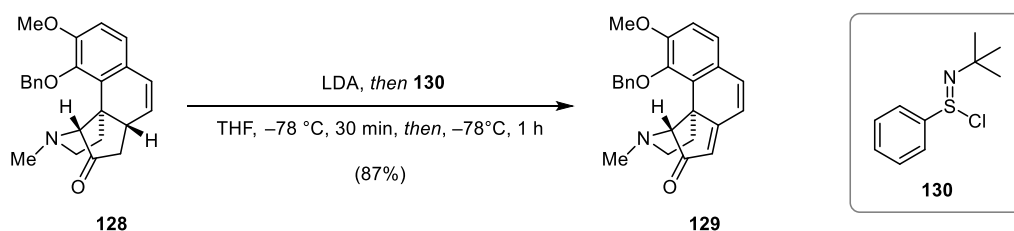
$^1\text{H NMR}$  (400 MHz,  $\text{CDCl}_3$ )  $\delta$  = 7.61 – 7.45 (m, 2H), 7.43 – 7.28 (m, 3H), 6.92 (d,  $J$  = 8.2 Hz, 1H), 6.78 (d,  $J$  = 8.3 Hz, 1H), 6.53 (dd,  $J$  = 9.3, 3.0 Hz, 1H), 6.02 (dd,  $J$  = 9.2, 2.5 Hz, 1H), 5.23 (d,  $J$  = 10.7 Hz, 1H), 4.92 (d,  $J$  = 10.8 Hz, 1H), 3.88 (s, 3H), 3.77 (s, 1H), 2.93 (ddt,  $J$  = 14.7, 7.8, 2.8 Hz, 1H), 2.74 (td,  $J$  = 8.5, 6.0 Hz, 1H), 2.55 (ddd,  $J$  = 8.6, 6.8, 4.2 Hz, 1H), 2.51 – 2.30 (m, 2H), 2.35 (s, 3H), 1.65 (ddd,  $J$  = 13.0, 6.1, 4.3 Hz, 1H).

$^{13}\text{C NMR}$  (100 MHz,  $\text{CDCl}_3$ )  $\delta$  = 216.8, 152.8, 143.8, 137.8, 137.3, 130.2, 128.5, 128.4, 128.2, 128.0, 127.1, 123.7, 109.7, 75.3, 72.3, 55.8, 54.7, 54.2, 39.9, 39.9, 39.1, 35.1.

**HRMS (ESI)** for  $\text{C}_{24}\text{H}_{26}\text{O}_3\text{N}^+$  [ $\text{M}+\text{H}$ ] $^+$ : calcd.: 376.1907, found: 376.1911.

**IR (ATR)**:  $\tilde{\nu}$  = 3032 (w), 2933 (m), 2840 (w), 2793 (w), 1735 (s), 1596 (w), 1562 (w), 1471 (s), 1438 (m), 1305 (m), 1292 (w), 1259 (s), 1188 (w), 1161 (w), 1136 (m), 1081 (m), 1061 (m), 1050 (m), 1029 (m), 929 (w), 909 (w), 816 (m), 735 (m), 697 (m).

**Rac-(3*a*R,11*b*S)-11-(benzyloxy)-10-methoxy-3-methyl-1,2,3,3*a*-tetrahydro-4*H*-benzo[6,7]indeno[1,7*a*-*b*]pyrrol-4-one (129)**



A solution of ketone **128** (33.0 mg, 87.9  $\mu\text{mol}$ , 1.00 eq., dried by 3 times by azeotropic removal of water with benzene) in THF (1.8 mL) was cooled to  $-78\text{ }^\circ\text{C}$ . A solution of LDA (0.2 M in THF, 132  $\mu\text{mol}$ , 659  $\mu\text{L}$ , 1.5 eq., prepared 30 minutes prior from DIPEA in THF and *n*-BuLi (2.3 M in hexane) at  $0\text{ }^\circ\text{C}$ ) was added and the resulting yellow solution was stirred for 30 min at the same temperature. Then, a freshly prepared solution of *N*-*tert*-butylbenzenesulfinimidoyl chloride (**130** handled and stored in a freezer inside an Ar-filled glovebox) in THF (0.25 M, 132  $\mu\text{mol}$ , 529  $\mu\text{L}$ , 1.50 eq.) was added dropwise and stirring was continued for 1 h at  $-78\text{ }^\circ\text{C}$ . A solution of AcOH in THF (0.1 M, 879  $\mu\text{mol}$ , 879  $\mu\text{L}$ , 10.00 eq.) was injected into the cold, bright yellow reaction mixture. After 10 minutes, the reaction was placed in an ice-water bath and saturated aqueous  $\text{NaHCO}_3$  (4 mL) was slowly added dropwise (bubbling). After 10 minutes, the reaction was diluted with EtOAc (20 mL) and the aqueous phase was extracted with EtOAc (3 x 20 mL). The combined organic layers were washed with brine (50 mL), dried over  $\text{MgSO}_4$ , filtered and evaporated. The crude product was purified by flash column chromatography ( $\text{SiO}_2$ , hexanes/EtOAc = 95/5 to 1/1) to deliver benzyl-sinoracutine **129** as an intensely yellow oil (22.0 mg, 58.9  $\mu\text{mol}$ , 87%).

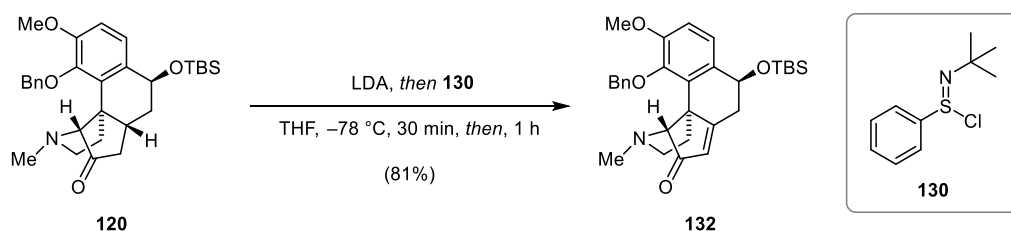
$R_f = 0.21$  (hexanes/EtOAc = 7/3, UV 254 nm, UV 366 nm, CAM).

$^1\text{H NMR}$  (400 MHz,  $\text{C}_6\text{D}_6$ )  $\delta = 7.73 - 7.50$  (m, 2H), 7.33 - 7.23 (m, 2H), 6.63 (d,  $J = 8.3$  Hz, 1H), 6.35 (d,  $J = 8.3$  Hz, 1H), 6.28 (d,  $J = 9.4$  Hz, 1H), 6.10 - 5.98 (m, 1H), 5.80 - 5.70 (m, 1H), 5.18 (d,  $J = 10.4$  Hz, 1H), 4.88 (d,  $J = 10.3$  Hz, 1H), 4.36 (s, 1H), 3.22 (s, 3H), 2.63 (s, 3H), 2.52 (ddd,  $J = 10.3, 9.1, 5.4$  Hz, 1H), 2.17 (ddd,  $J = 12.2, 5.4, 2.0$  Hz, 1H), 1.79 (ddd,  $J = 12.2, 10.3, 6.8$  Hz, 1H).

$^{13}\text{C NMR}$  (100 MHz,  $\text{C}_6\text{D}_6$ )  $\delta = 205.8, 173.3, 154.8, 146.0, 138.8, 137.5, 135.2, 130.4, 128.7, 126.6, 126.3, 125.5, 119.8, 110.5, 74.7, 70.9, 56.6, 55.4, 50.8, 41.5, 38.0$ .

**HRMS (ESI)** for  $\text{C}_{24}\text{H}_{24}\text{NO}_3^+$   $[\text{M}+\text{H}]^+$ : calcd.: 374,1751, found: 374,1747.

**IR (ATR):**  $\tilde{\nu} = 3790$  (w), 3061 (w), 2934 (w), 2841 (w), 2360 (w), 1682 (s), 1610 (s), 1576 (m), 1475 (m), 1440 (m), 1375 (w), 1336 (w), 1264 (s), 1260 (w), 1176 (w), 1096 (w), 1061 (w), 986 (w), 892 (w), 858 (w), 764 (w), 741 (m).

**(3aR,7S,11bS)-11-(benzyloxy)-7-((tert-butyl dimethylsilyl)oxy)-10-methoxy-3-methyl-1,2,3,3a,6,7-hexahydro-4H-benzo[6,7]indeno[1,7a-b]pyrrol-4-one (132)**

A solution of ketone **120** (213 mg, 420  $\mu\text{mol}$ , 1.00 eq., dried 3 times by azeotropic removal of water with benzene) in THF (8.5 mL) was cooled to  $-78\text{ }^\circ\text{C}$ . LDA (0.2 M in THF, 139  $\mu\text{mol}$ , 694  $\mu\text{L}$ , 1.5 eq., prepared 30 minutes prior by addition of *n*-BuLi (2.3 M in hexanes) to DIPEA in THF at  $0\text{ }^\circ\text{C}$ ) was added and the resulting yellow solution was stirred for 30 min at the same temperature. Then, a freshly prepared solution of *N*-*tert*-butylbenzenesulfinimidoyl chloride (stored in a freezer and handled inside an Ar-filled glovebox) in THF (0.25 M, 139  $\mu\text{mol}$ , 557  $\mu\text{L}$ , 1.50 eq.) was added dropwise and stirring was continued for 1 h at  $-78\text{ }^\circ\text{C}$ . A solution of AcOH in THF (0.1 M, 926  $\mu\text{mol}$ , 926  $\mu\text{L}$ , 10.00 eq.) was injected into the cold reaction mixture. After 10 minutes, the reaction was placed in an ice-water bath and saturated aqueous  $\text{NaHCO}_3$  (4 mL) was slowly added dropwise (bubbling). After 10 minutes, the reaction was diluted with EtOAc (20 mL) and the aqueous phase was extracted with EtOAc (3 x 20 mL). The combined organic layers were washed with brine (50 mL), dried over  $\text{MgSO}_4$ , filtered and evaporated under reduced pressure. The crude product was purified by flash column chromatography ( $\text{Et}_3\text{N}$ -deactivated  $\text{SiO}_2$ , hexanes/EtOAc = 95/5 to 6/4) and furnished the title compound **132** as light yellow oil (38.0 mg, 75.1  $\mu\text{mol}$ , 81%).

$R_f = 0.43$  (hexanes/EtOAc = 7/3, UV 254 nm, CAM).

$^1\text{H NMR}$  (400 MHz,  $\text{C}_6\text{D}_6$ )  $\delta = 7.61 - 7.50$  (m, 2H), 7.25 (t,  $J = 7.5$  Hz, 2H), 7.19 – 7.05 (m, 3H), 6.92 (d,  $J = 8.4$  Hz, 1H), 6.54 (d,  $J = 8.4$  Hz, 1H), 6.25 – 5.94 (m, 1H), 5.10 (d,  $J = 11.0$  Hz, 1H), 4.78 (t,  $J = 3.7$  Hz, 1H), 4.72 (d,  $J = 11.0$  Hz, 1H), 3.69 (s, 1H), 3.26 (s, 3H), 2.82 (ddd,  $J = 9.0, 7.0, 2.3$  Hz, 1H), 2.60 (s, 3H), 2.58 – 2.36 (m, 3H), 2.22 (ddd,  $J = 12.0, 9.8, 7.0$  Hz, 1H), 1.66 (ddd,  $J = 12.0, 5.7, 2.3$  Hz, 1H), 0.90 (s, 9H), 0.08 (s, 3H), 0.02 (s, 3H).

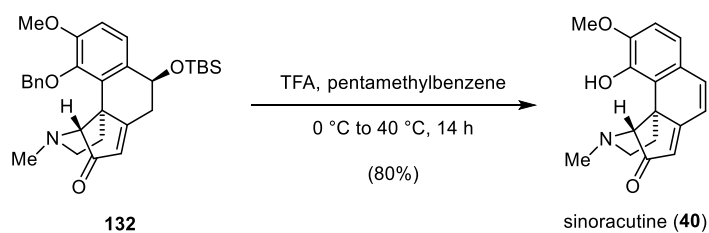
$^{13}\text{C NMR}$  (100 MHz,  $\text{C}_6\text{D}_6$ )  $\delta = 203.7, 175.7, 153.5, 146.8, 139.1, 136.1, 131.6, 131.1, 127.6, 124.8, 111.7, 74.1, 73.9, 70.8, 57.1, 55.4, 53.6, 38.4, 37.8, 36.3, 26.0, 18.3, -4.1, -4.1$ .

**HRMS (ESI)** for  $\text{C}_{30}\text{H}_{40}\text{NO}_4\text{Si}^+$   $[\text{M}+\text{H}]^+$ : calcd.: 506.2721, found: 506.2719.

**IR (ATR)**:  $\tilde{\nu} = 3854$  (w), 3746 (w), 3676 (w), 2955 (m), 2929 (m), 2856 (m), 2360 (w), 1734 (w), 1695 (s), 1635 (m), 1599 (w), 1481 (m), 1300 (m), 1275 (m), 1154 (m), 1095 (m), 1047 (m), 834 (s).

$[\alpha]_D^{20} = +23.0$  (c = 0.17,  $\text{CH}_2\text{Cl}_2$ ).

**Sinoracutine - (3a*R*,11*bS*)-11-hydroxy-10-methoxy-3-methyl-1,2,3,3a-tetrahydro-4*H*-benzo[6,7]indeno[1,7a-b]pyrrol-4-one (40)**



A 25 mL-round bottom flask was charged with **132** (122 mg, 241  $\mu$ mol, 1.00 eq.), pentamethylbenzene (2.41 mmol, 358 mg, 10 eq.) and placed in an ice-water bath. Then, TFA (181 mmol, 13.4 mL, 750 eq.) was added dropwise under heavy stirring (800 rpm), resulting in a dark orange solution. The flask was sealed with a polypropylene cap, lifted from the ice bath, and placed in a 40 °C oil bath. After 14 h, excess TFA was removed by rotary evaporation (100 mbar, 40 °C). The dark brown residue was dissolved in DCM (50 mL) and water (25 mL) was added. Aqueous  $\text{NH}_3$  (10 M, 5 mL) was added dropwise and the biphasic mixture was stirred for 5 minutes. The bright yellow organic layer was separated and the aqueous layer was extracted with  $\text{CH}_2\text{Cl}_2$  (4 x 25 mL). The combined organic layers were washed with brine, dried over  $\text{MgSO}_4$ , filtered and concentrated in vacuo. Purification of the resulting orange oil by flash column chromatography ( $\text{SiO}_2$ , hexanes/ $\text{CH}_2\text{Cl}_2$  = 1/1 to  $\text{CH}_2\text{Cl}_2$  to  $\text{CH}_2\text{Cl}_2/\text{MeOH}$  = 95/5) afforded **sinoracutine (40)** as an orange solid that was contaminated with slight impurities. Based on NMR integration against tetrachloroethane as internal standard, the yield for this step amounts to 80% (0.196  $\mu$ mol, 54 mg).

*Note: Sinoracutine is not stable to silica as evidenced by two-dimensional TLC analysis. Purification on  $\text{Et}_3\text{N}$ -deactivated silica or Davisil (eluents used: hexanes/ $\text{CHCl}_3$ , hexanes/acetone, hexanes/ $\text{EtOAc}$ ,  $\text{CH}_2\text{Cl}_2/\text{MeOH}$ ) did not improve the purity of the product, while chromatography on basic Alumina (Macherey Nagel, 50–200  $\mu\text{m}$ , Brockmann I grade) resulted in complete degradation.*

Spectroscopically pure **sinoracutine** was isolated by purification of the abovementioned sample by semipreparative HPLC (Dynamax Microsorb 60-8 C18, 250 x 21.4 mm;  $\text{H}_2\text{O}/\text{Acetonitrile}$  containing 0.1% formic acid; gradient: 10% to 90% acetonitrile over 30 minutes; flow rate 20 mL/min; detection at 254 nm;  $t_{\text{R}} = 12.2$  min). The product-containing fractions were combined and freeze-dried on a Christ Alpha 2-4 LDplus lyophilizer to afford **sinoracutine** as a yellow powder (91% recovery)

*Note: Attempted extraction of the purified product (dissolved in  $\text{H}_2\text{O}/\text{MeCN}$  + 0.1% FA) with aqueous  $\text{NH}_3$  and  $\text{CH}_2\text{Cl}_2$  resulted in impure product. In another attempt, removal of the purified product dissolved in the HPLC solvent mixture on a rotary evaporator (10 mbar, 35 °C) resulted in partial decomposition.*

When this protocol was applied to **132** on a 59  $\mu$ mol scale, racemic **sinoracutine (40)** could be obtained in 72% isolated yield after HPLC purification (42  $\mu$ mol, 12 mg).

In the racemic series, orange crystals suitable for X-ray analysis were grown from a CH<sub>2</sub>Cl<sub>2</sub> solution by slow vapor diffusion of pentane at room temperature.

**R<sub>f</sub>** = 0.28 (hexanes/EtOAc = 1/1, visibly yellow, UV 254 nm, UV 366 nm, CAM)

**<sup>1</sup>H NMR** (800 MHz, CDCl<sub>3</sub>) δ = 6.78 (d, *J* = 9.4 Hz, 1H), 6.75 (d, *J* = 8.2 Hz, 1H), 6.74 (d, *J* = 8.2 Hz, 1H), 6.54 (d, *J* = 9.4 Hz, 1H), 5.84 (s, 1H), 3.91 (s, 3H), 3.77 (s, 1H), 3.17 (app tt, *J* = 9.7, 8.5, 1.0 Hz), 2.92 (s, 3H), 2.86 – 2.78 (m, 1H), 2.37 (ddd, *J* = 13.6, 8.0, 1.3 Hz, 1H), 2.10 (ddd, *J* = 13.6, 10.8, 8.5 Hz, 1H).

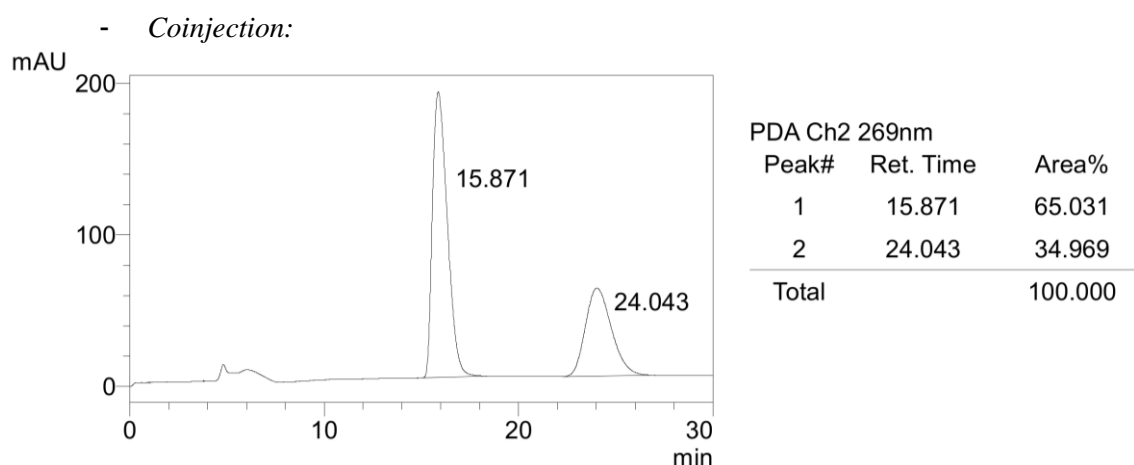
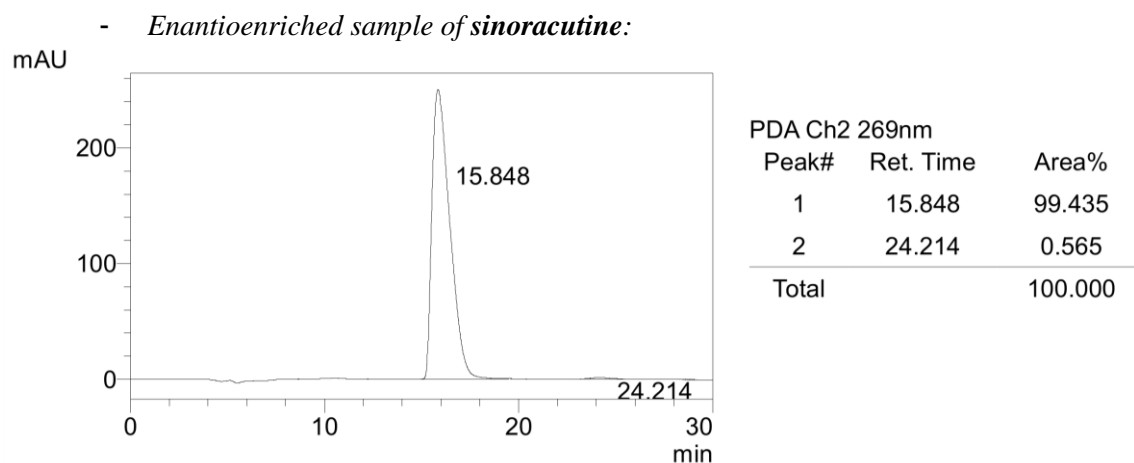
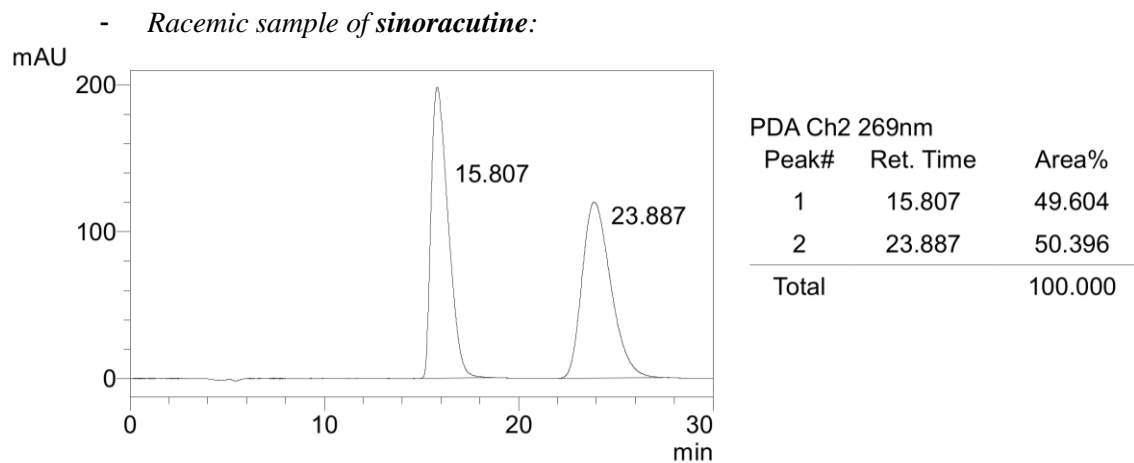
**<sup>13</sup>C NMR** (200 MHz, CDCl<sub>3</sub>) δ = 206.77, 175.06, 151.22, 145.74, 138.31, 127.75, 124.25, 123.40, 121.36, 118.14, 109.54, 72.48, 56.01, 53.85, 51.60, 41.69, 36.49.

**HRMS (ESI)** for C<sub>17</sub>H<sub>18</sub>NO<sub>3</sub><sup>+</sup> [M+H]<sup>+</sup>: calcd.: 284.1281, found: 284.1284.

**IR (ATR):**  $\tilde{\nu}$  = 3554 (br, w), 3057 (w), 2944 (w), 2834 (w), 2582 (br, w) 1680 (s), 1600 (s), 1569 (s), 1547 (s), 1503 (w), 1453 (s), 1437 (s), 1401 (s), 1339 (s), 1293 (w), 1254 (s), 1228 (m), 1202 (m), 1158 (m), 1099 (m), 1086 (m), 1058 (m), 986 (w), 948 (w), 886 (w), 840 (m), 810 (w), 759 (w), 751 (w), 675 (w).

**[ $\alpha$ ]<sub>D</sub><sup>25</sup>** = -1067.3 (c = 0.35, CHCl<sub>3</sub>).

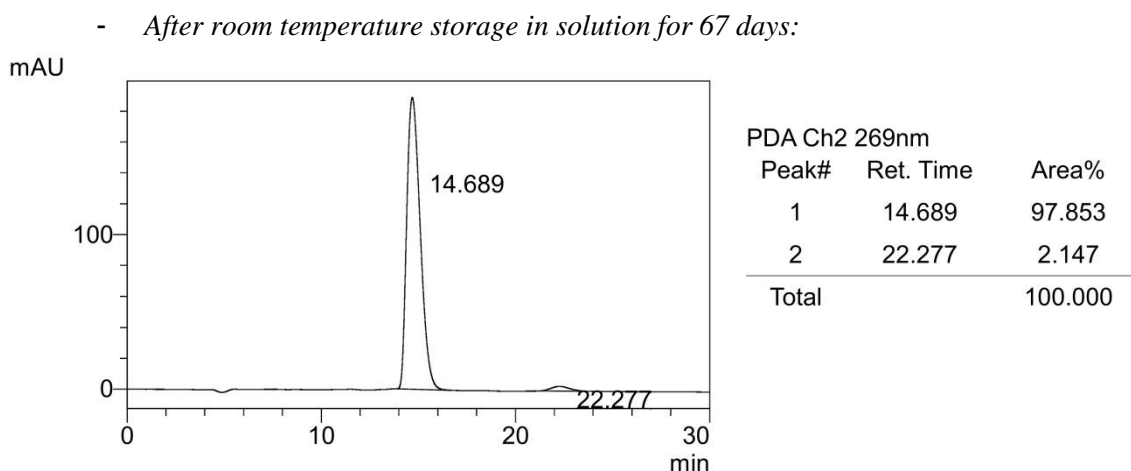
**Enantiomeric excess of sinoracutine** was determined by HPLC analysis on chiral stationary phase (DAICEL CHIALPAK ID, 4.6 x 250 mm), 25 °C, 1 mL/min, 40% *i*-PrOH in heptane + 0.1% diethylamine, detection at 269 nm) to be 98.9% by comparison with a racemic sample and coinjection;  $t_R$  major enantiomer = 15.848 min,  $t_R$  minor enantiomer = 24.214 min.



### 4.3. Experimental Study on the Racemization of (-)-Sinoracutine

A sample of (-)-sinoracutine, synthesized and purified according to the procedure reported on page 97, was dissolved in 60% heptane, 20% *i*-PrOH and 20% MeOH at a concentration of 1.2 mg/ml in a borosilicate glass vial. Aliquots were withdrawn and directly injected into the HPLC instrument.

After three days of storage at room temperature without precautions to exclude air or ambient light, the enantiomeric excess was determined to be 98.9%. After 67 days of storage at room temperature, the same sample was found to have an enantiomeric excess of 95.7%.

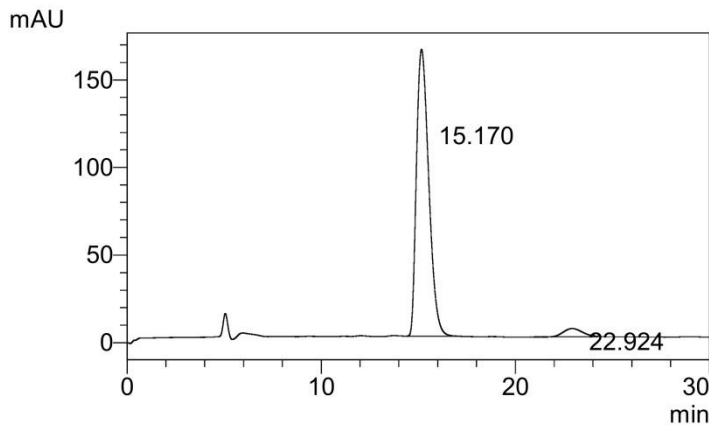


To accelerate the racemization, the same sample was then placed in an aluminum heating block thermostated to 60 °C. After the stated timepoints (see table below), the vial was cooled to room temperature, an aliquot was injected into the HPLC instrument, and heating was continued until the next withdrawal.

Time (h)	ee (%)
0	95.7
16	91.2
30	51.7
46	35.7
60	20.2
84	11.2
100	6.2
124	3.2

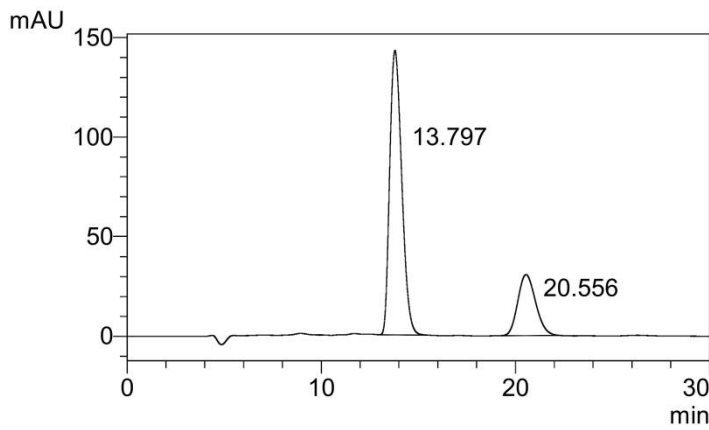
*Note: Retention times vary slightly due to the high volatility of diethylamine (0.1%) used as additive in the mobile phase, which was manually added via microsyringe to the *i*-PrOH/heptane mixture (also prepared manually using graduated cylinders).*

- After room temperature storage for 67 days, followed by heating to 60 °C for 16h:



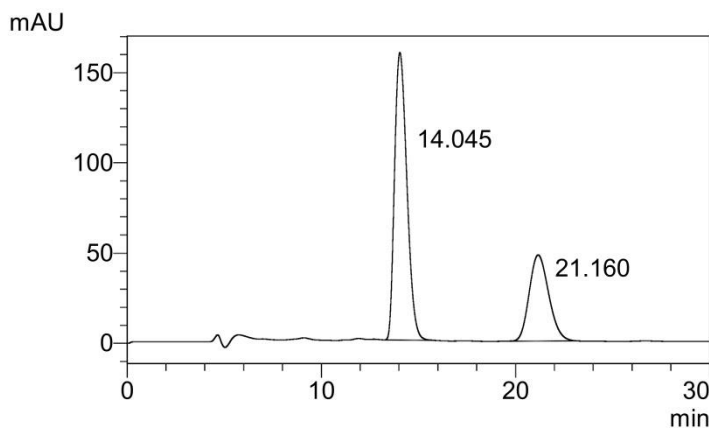
PDA Ch2 269nm		
Peak#	Ret. Time	Area%
1	15.170	95.621
2	22.924	4.379
Total		100.000

- After room temperature storage for 67 days, followed by heating to 60 °C for a total of 30h:



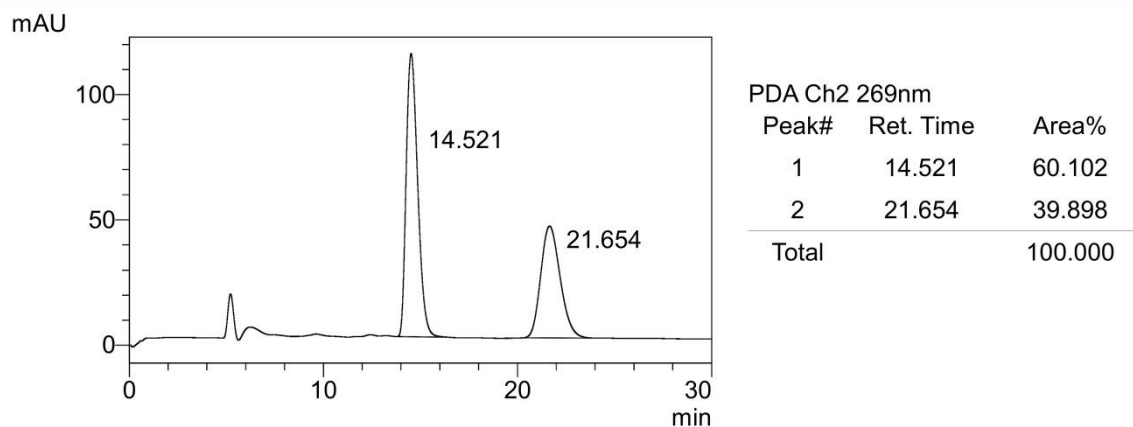
PDA Ch2 269nm		
Peak#	Ret. Time	Area%
1	13.797	75.871
2	20.556	24.129
Total		100.000

- After room temperature storage for 67 days, followed by heating to 60 °C for a total of 46h:

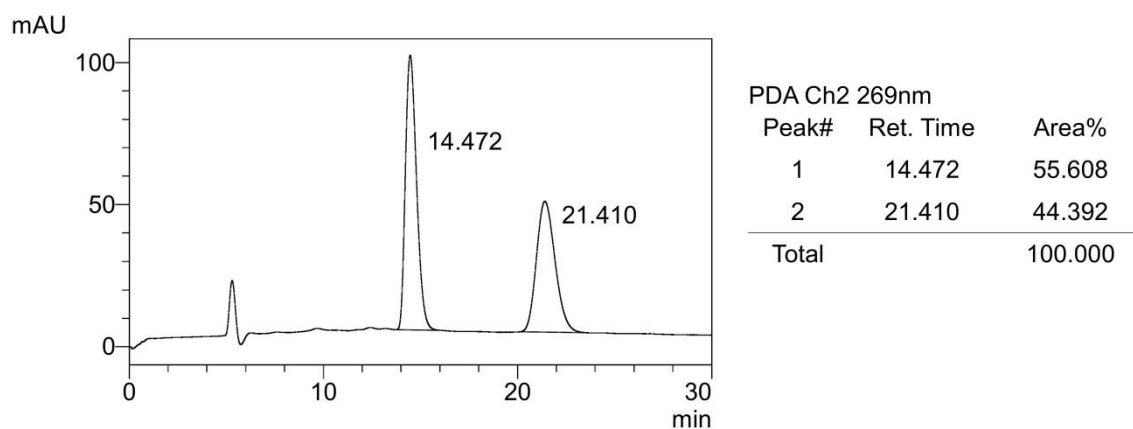


PDA Ch2 269nm		
Peak#	Ret. Time	Area%
1	14.045	67.864
2	21.160	32.136
Total		100.000

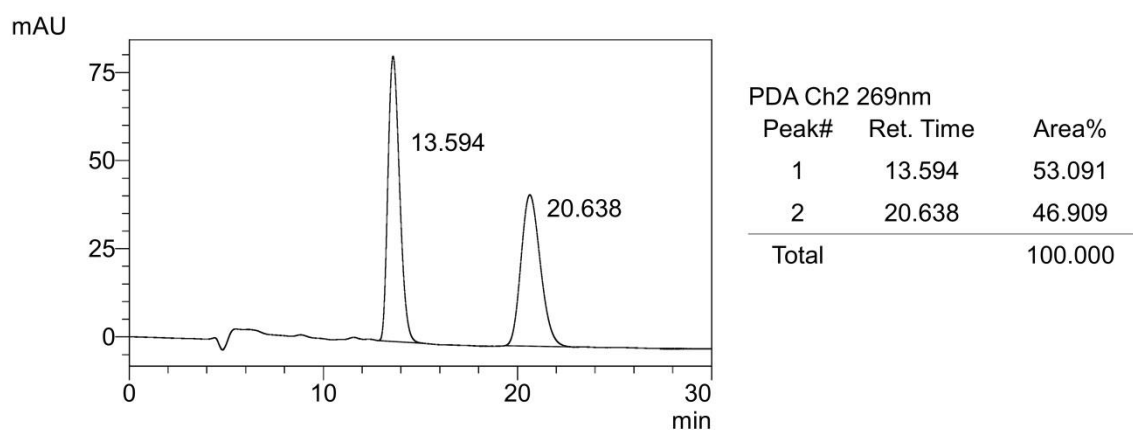
After room temperature storage for 67 days, followed by heating to 60 °C for a total of 60h:



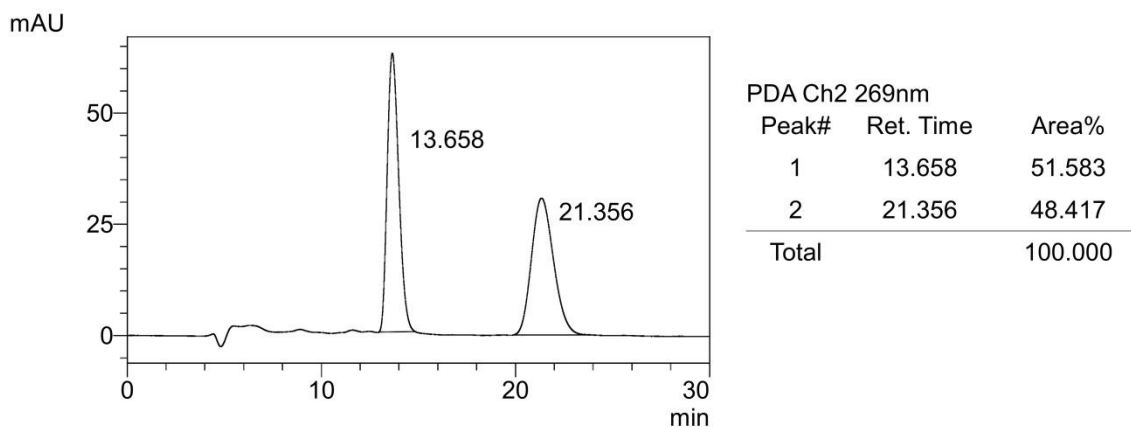
- After room temperature storage for 67 days, followed by heating to 60 °C for a total of 84h:



- After room temperature storage for 67 days, followed by heating to 60 °C for a total of 100h:

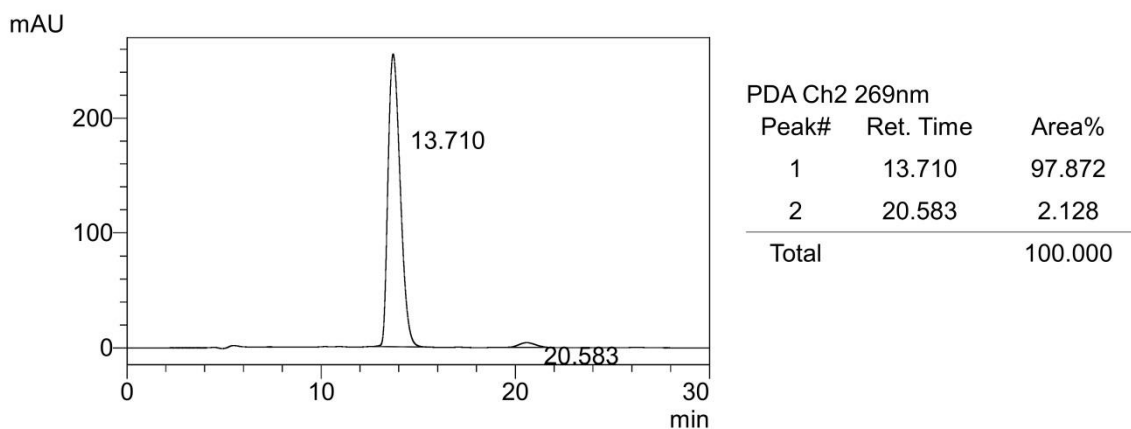


- After room temperature storage for 67 days, followed by heating to 60 °C for a total of 124h:



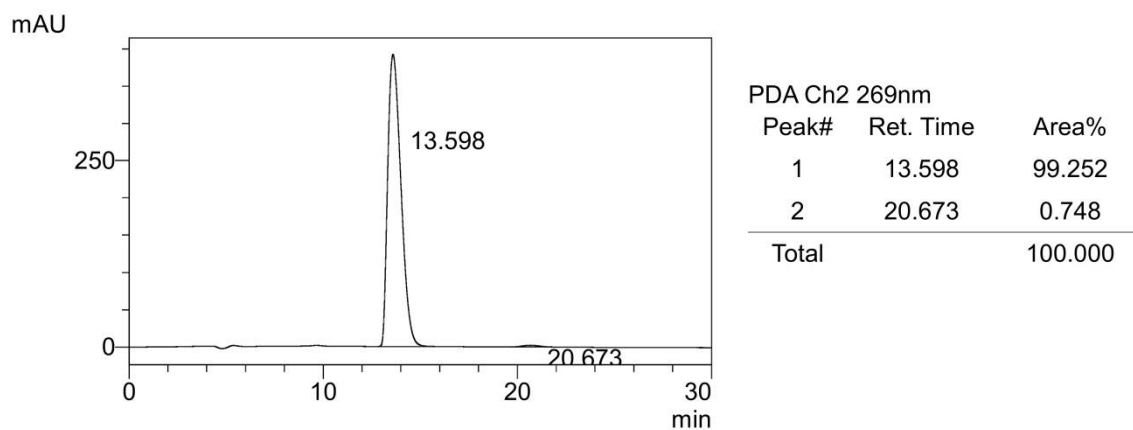
By comparison, an aliquot of the sample that was withdrawn prior to heating at 60 °C and stored at room temperature while the bulk of the sample underwent thermal treatment, still showed an enantiomeric excess of 95.7%.

- After room temperature storage for 73 days:

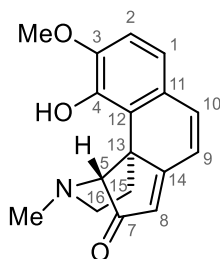


Meanwhile, a sample originating from the same batch of synthetic (-)-sinoracutine used for the experiments at ambient temperature and at 60°C was stored in a freezer (-25 °C) for 67 days as a solution in CH<sub>2</sub>Cl<sub>2</sub>. After evaporation of the solvent and dissolution in 60% heptane, 20% *i*-PrOH and 20% MeOH at a concentration 1.9 mg/ml. The enantiomeric excess of this sample was determined to be 98.5%.

- After storage in solution for 67 days at -25 °C



## 4.4. Comparison of Natural and Synthetic Sinoracutine



sinoracutine

pos.	<sup>1</sup> H NMR (δ in ppm, multiplicity, <i>J</i> in Hz)			<sup>13</sup> C NMR (δ in ppm)		
	Natural <sup>[58]</sup> (500 MHz)	Natural <sup>[59]</sup> (400 MHz)	Synthetic (800 MHz)	Natural <sup>[58]</sup> (125 MHz)	Natural <sup>[59]</sup> (100 MHz)	Synthetic (200 MHz)
<b>1</b>	6.75 (d, 8.2)	6.75 (d, 8.2)	6.75 (d, 8.2)	121.24	121.2	121.36
<b>2</b>	6.73 (d, 8.2)	6.73 (d, 8.2)	6.74 (d, 8.2)	109.42	109.3	109.54
<b>3</b>	-	-	-	151.07	151.0	151.22
<b>4</b>	-	-	-	145.58	145.5	145.74
<b>5</b>	3.77 (s)	3.77 (s)	3.77 (s)	72.31	72.3	72.48
<b>7</b>	-	-	-	206.56	206.6	206.77
<b>8</b>	5.84 (s)	5.84 (s)	5.84 (s)	123.27	123.2	123.4
<b>9</b>	6.54 (d, 9.4)	6.55 (d, 9.4)	6.54 (d, 9.4)	118.00	117.9	118.14
<b>10</b>	6.78 (d, 9.4)	6.78 (d, 9.4)	6.78 (d, 9.4)	138.11	138.1	138.31
<b>11</b>	-	-	-	124.11	124.0	124.25
<b>12</b>	-	-	-	127.59	127.5	127.75
<b>13</b>	-	-	-	53.71	53.6	53.85
<b>14</b>	-	-	-	174.94	174.9	175.06
<b>15</b>	2.73 (m) 2.10 (m)	2.78 (m) 2.14 (m)	2.37 (ddd, 13.6, 8.0, 1.3) 2.10 (ddd, 13.6, 10.8, 8.5)	41.52	41.5	41.69
<b>16</b>	3.18 (dd, 9.7, 8.7) <i>not tabulated</i>	3.18 (m) <i>not tabulated</i>	3.17 (app tt, 9.7, 8.5, 1.0) 2.86 – 2.78 (m)	51.46	51.4	51.60
<b>OCH<sub>3</sub></b>	3.91 (s)	3.91 (s)	3.91 (s)	55.87	55.8	56.01
<b>NCH<sub>3</sub></b>	2.92 (s)	2.92 (s)	2.92 (s)	36.35	36.3	36.49

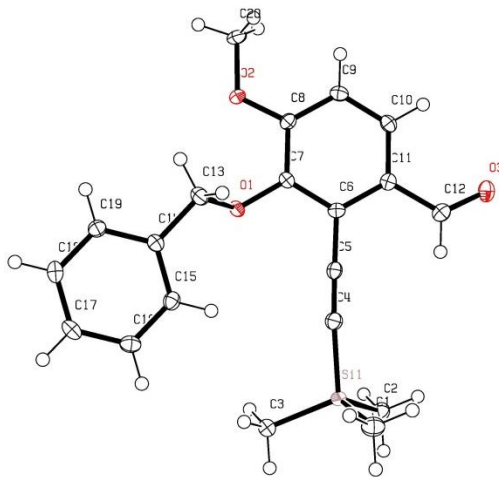
Notes: NMR spectra were recorded in CDCl<sub>3</sub>.

The slight downfield drift in the δ-values of the <sup>13</sup>C spectrum is attributed to different standards in spectral referencing (SiMe<sub>4</sub> in the isolation papers and CHCl<sub>3</sub> in this work).

The atom numbering follows the isolation paper in which the canonical numbering for morphinan and hasubanan structures is used. Since C6 is believed to be lost during biosynthesis, this atom is not reported in the table.

## 4.5. X-Ray Crystallographic Data

### Data for Alkyne **90**.



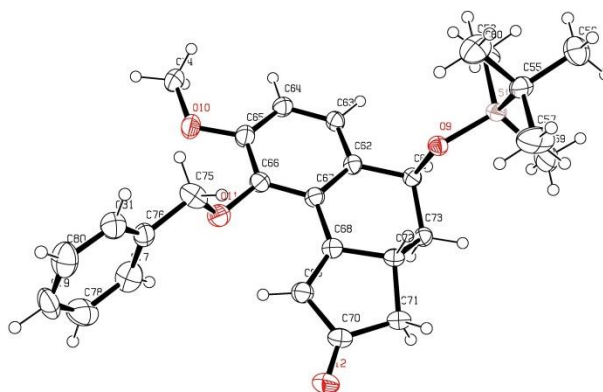
**Figure 10. ORTEP plot of the molecular structure of alkyne **90**.**

CCDC 1499487 contains the supplementary crystallographic data for **90**. These data can be obtained free of charge from The Cambridge Crystallographic Data Centre via [www.ccdc.cam.ac.uk/data\\_request/cif](http://www.ccdc.cam.ac.uk/data_request/cif)

net formula	$C_{20}H_{22}O_3Si$
$M_r/g\ mol^{-1}$	338.46
crystal size/mm	$0.100 \times 0.070 \times 0.020$
$T/K$	100.(2)
radiation	MoK $\alpha$
diffractometer	'Bruker D8 Venture TXS'
crystal system	monoclinic
space group	'P 1 21/c 1'
$a/\text{\AA}$	11.1809(4)
$b/\text{\AA}$	12.2862(5)
$c/\text{\AA}$	13.8451(6)
$\alpha/^\circ$	90
$\beta/^\circ$	107.4580(10)
$\gamma/^\circ$	90
$V/\text{\AA}^3$	1814.30(13)
$Z$	4
calc. density/ $g\ cm^{-3}$	1.239
$\mu/mm^{-1}$	0.144
absorption correction	Multi-Scan
transmission factor range	0.9414–0.9705
refls. measured	34131
$R_{int}$	0.0482
mean $\sigma(I)/I$	0.0258
$\theta$ range	3.085–26.414
observed refls.	3252
$x, y$ (weighting scheme)	0.0320, 1.1010
hydrogen refinement	constr
refls in refinement	3705

parameters	221
restraints	0
$R(F_{\text{obs}})$	0.0328
$R_w(F^2)$	0.0834
$S$	1.052
shift/error <sub>max</sub>	0.001
max electron density/e $\text{\AA}^{-3}$	0.279
min electron density/e $\text{\AA}^{-3}$	-0.267

### Data for Ketone 94.



**Figure 11. ORTEP plot of the molecular structure of ketone 94.**

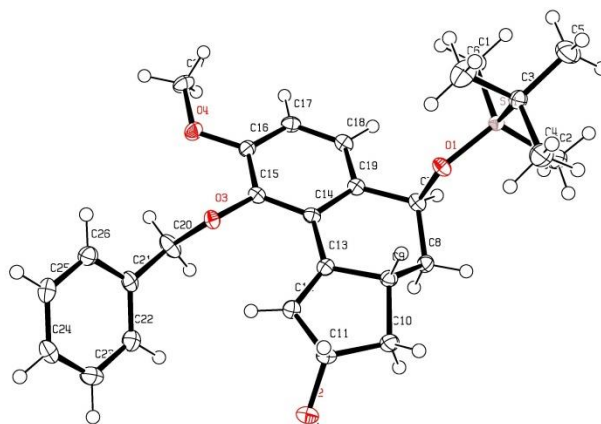
CCDC 1499488 contains the supplementary crystallographic data for **94**. These data can be obtained free of charge from The Cambridge Crystallographic Data Centre via [www.ccdc.cam.ac.uk/data\\_request/cif](http://www.ccdc.cam.ac.uk/data_request/cif)

net formula	$\text{C}_{27}\text{H}_{34}\text{O}_4\text{Si}$
$M_r/\text{g mol}^{-1}$	450.63
crystal size/mm	$0.100 \times 0.080 \times 0.040$
$T/\text{K}$	153.(2)
radiation	$\text{MoK}\alpha$
diffractometer	'Bruker D8 Venture TXS'
crystal system	orthorhombic
space group	'P 21 21 21'
$a/\text{\AA}$	12.5438(4)
$b/\text{\AA}$	14.0646(4)
$c/\text{\AA}$	42.9806(11)
$\alpha/^\circ$	90
$\beta/^\circ$	90
$\gamma/^\circ$	90
$V/\text{\AA}^3$	7582.8(4)
$Z$	12
calc. density/ $\text{g cm}^{-3}$	1.184
$\mu/\text{mm}^{-1}$	0.122
absorption correction	Multi-Scan
transmission factor range	0.8767–0.9705
refls. measured	55451
$R_{\text{int}}$	0.0385
mean $\sigma(I)/I$	0.0419

$\theta$ range	3.191–27.482
observed refls.	14643
<i>x, y</i> (weighting scheme)	0.0512, 2.6535
hydrogen refinement	constr
Flack parameter	0.03(3)
refls in refinement	17251
parameters	913
restraints	0
$R(F_{\text{obs}})$	0.0492
$R_w(F^2)$	0.1196
<i>S</i>	1.044
shift/error <sub>max</sub>	0.001
max electron density/e $\text{\AA}^{-3}$	0.503
min electron density/e $\text{\AA}^{-3}$	-0.335

Partially disordered. Split models applied. Underoccupied regions refined isotropically. The asymmetric unit contains three formula units. The figure shows all formula units in their most probable orientation, as well as in a further figure the only non-disordered molecule.

### Data for Alcohol 106.



**Figure 12. ORTEP plot of the molecular structure of alcohol 106.**

CCDC 1499486 contains the supplementary crystallographic data for **106**. These data can be obtained free of charge from The Cambridge Crystallographic Data Centre via [www.ccdc.cam.ac.uk/data\\_request/cif](http://www.ccdc.cam.ac.uk/data_request/cif)

net formula	$\text{C}_{27}\text{H}_{36}\text{O}_4\text{Si}$
$M_r/\text{g mol}^{-1}$	452.65
crystal size/mm	$0.100 \times 0.080 \times 0.060$
<i>T</i> /K	100(2)
radiation	MoK $\alpha$
diffractometer	'Bruker D8Venture'
crystal system	triclinic
space group	'P -1'
<i>a</i> / $\text{\AA}$	6.3389(3)
<i>b</i> / $\text{\AA}$	8.0829(4)
<i>c</i> / $\text{\AA}$	26.1368(11)
$\alpha$ / $^\circ$	81.4534(12)

$\beta/^\circ$	88.7849(12)
$\gamma/^\circ$	67.2793(11)
$V/\text{\AA}^3$	1220.56(10)
$Z$	2
calc. density/ $\text{g cm}^{-3}$	1.232
$\mu/\text{mm}^{-1}$	0.127
absorption correction	multi-scan
transmission factor range	0.7996–0.9585
refls. measured	11997
$R_{\text{int}}$	0.0285
mean $\sigma(I)/I$	0.0399
$\theta$ range	2.366–26.44
observed refls.	4111
$x, y$ (weighting scheme)	0.0314, 0.8752
hydrogen refinement	mixed
refls in refinement	4865
parameters	299
restraints	0
$R(F_{\text{obs}})$	0.0456
$R_w(F^2)$	0.1036
$S$	1.096
shift/error <sub>max</sub>	0.001
max electron density/ $\text{e \AA}^{-3}$	0.342
min electron density/ $\text{e \AA}^{-3}$	–0.291

C-H: constr. O-H: refall.

### Data for Tetracycline 128.

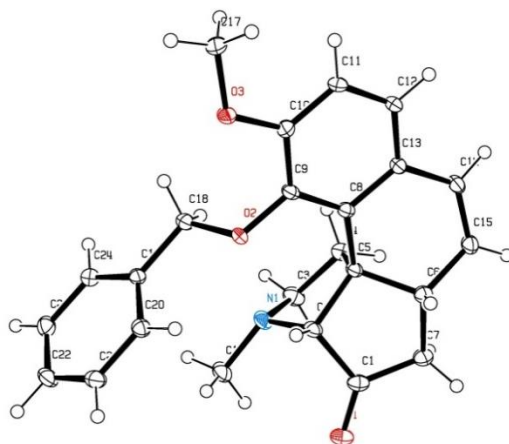


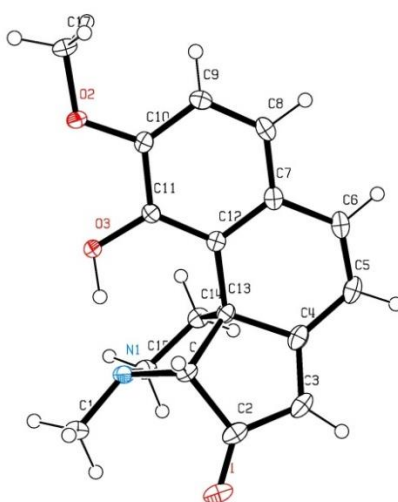
Figure 13. ORTEP plot of the molecular structure of tetracycline 128.

CCDC 1499484 contains the supplementary crystallographic data for **128**. These data can be obtained free of charge from The Cambridge Crystallographic Data Centre via [www.ccdc.cam.ac.uk/data\\_request/cif](http://www.ccdc.cam.ac.uk/data_request/cif)

net formula	$\text{C}_{24}\text{H}_{25}\text{NO}_3$
$M_r/\text{g mol}^{-1}$	375.45
crystal size/mm	$0.060 \times 0.050 \times 0.040$
$T/\text{K}$	100.(2)
radiation	$\text{MoK}\alpha$

diffractometer	'Bruker D8 Venture TXS'
crystal system	triclinic
space group	'P -1'
$a/\text{\AA}$	9.7230(4)
$b/\text{\AA}$	9.8365(4)
$c/\text{\AA}$	10.4360(4)
$\alpha/^\circ$	80.7375(14)
$\beta/^\circ$	79.5349(15)
$\gamma/^\circ$	74.6194(14)
$V/\text{\AA}^3$	939.63(7)
$Z$	2
calc. density/ $\text{g cm}^{-3}$	1.327
$\mu/\text{mm}^{-1}$	0.087
absorption correction	Multi-Scan
transmission factor range	0.8879–0.9590
refls. measured	10343
$R_{\text{int}}$	0.0411
mean $\sigma(I)/I$	0.0531
$\theta$ range	3.179–27.482
observed refls.	3318
$x, y$ (weighting scheme)	0.0482, 0.4974
hydrogen refinement	constr
refls in refinement	4298
parameters	255
restraints	0
$R(F_{\text{obs}})$	0.0491
$R_w(F^2)$	0.1275
$S$	1.033
shift/error $_{\text{max}}$	0.001
max electron density/ $\text{e \AA}^{-3}$	0.340
min electron density/ $\text{e \AA}^{-3}$	-0.255

### Data for Racemic Sinoracutine.



**Figure 14. ORTEP plot of the molecular structure of racemic sinoracutine (40).**

CCDC 1499485 contains the supplementary crystallographic data for racemic sinoracutine (40). These data can be obtained free of charge from The Cambridge Crystallographic Data Centre via [www.ccdc.cam.ac.uk/data\\_request/cif](http://www.ccdc.cam.ac.uk/data_request/cif)

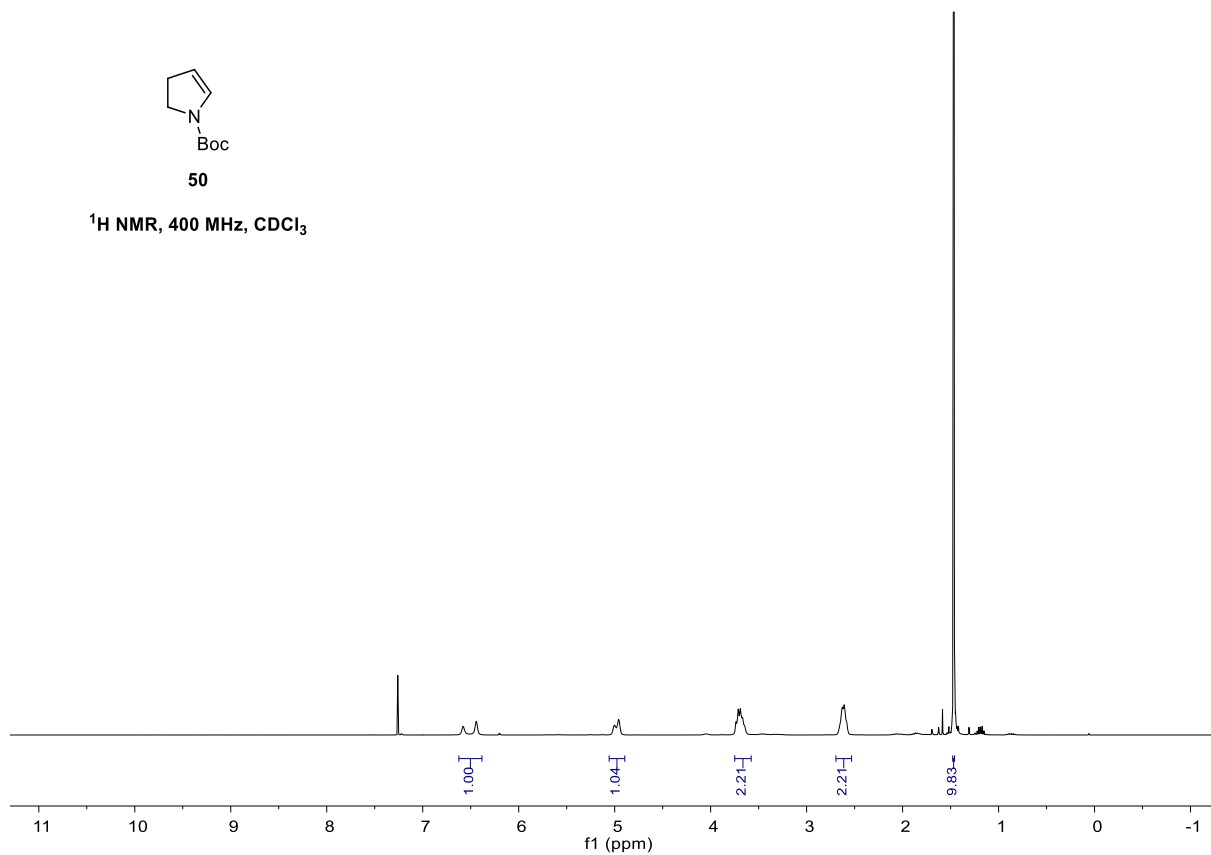
net formula	C <sub>17</sub> H <sub>17</sub> NO <sub>3</sub>
<i>M<sub>r</sub></i> /g mol <sup>-1</sup>	283.31
crystal size/mm	0.100 × 0.070 × 0.010
<i>T</i> /K	100.(2)
radiation	MoK $\alpha$
diffractometer	'Bruker D8 Venture TXS'
crystal system	orthorhombic
space group	'P b c a'
<i>a</i> /Å	14.8795(5)
<i>b</i> /Å	10.3203(3)
<i>c</i> /Å	17.7065(6)
$\alpha$ /°	90
$\beta$ /°	90
$\gamma$ /°	90
<i>V</i> /Å <sup>3</sup>	2719.03(15)
<i>Z</i>	8
calc. density/g cm <sup>-3</sup>	1.384
$\mu$ /mm <sup>-1</sup>	0.095
absorption correction	Multi-Scan
transmission factor range	0.8819–0.9593
refls. measured	29303
<i>R</i> <sub>int</sub>	0.0827
mean $\sigma(I)/I$	0.0460
$\theta$ range	3.327–28.280
observed refls.	2556
<i>x</i> , <i>y</i> (weighting scheme)	0.0364, 2.0197
hydrogen refinement	C-H constr. O-H refall
refls in refinement	3364
parameters	196
restraints	0
<i>R</i> ( <i>F</i> <sub>obs</sub> )	0.0537
<i>R</i> <sub>w</sub> ( <i>F</i> <sup>2</sup> )	0.1194
<i>S</i>	1.080
shift/error <sub>max</sub>	0.001
max electron density/e Å <sup>-3</sup>	0.255
min electron density/e Å <sup>-3</sup>	-0.236

## 4.6. NMR Spectra



50

$^1\text{H}$  NMR, 400 MHz,  $\text{CDCl}_3$



129.96

107.64

80.13

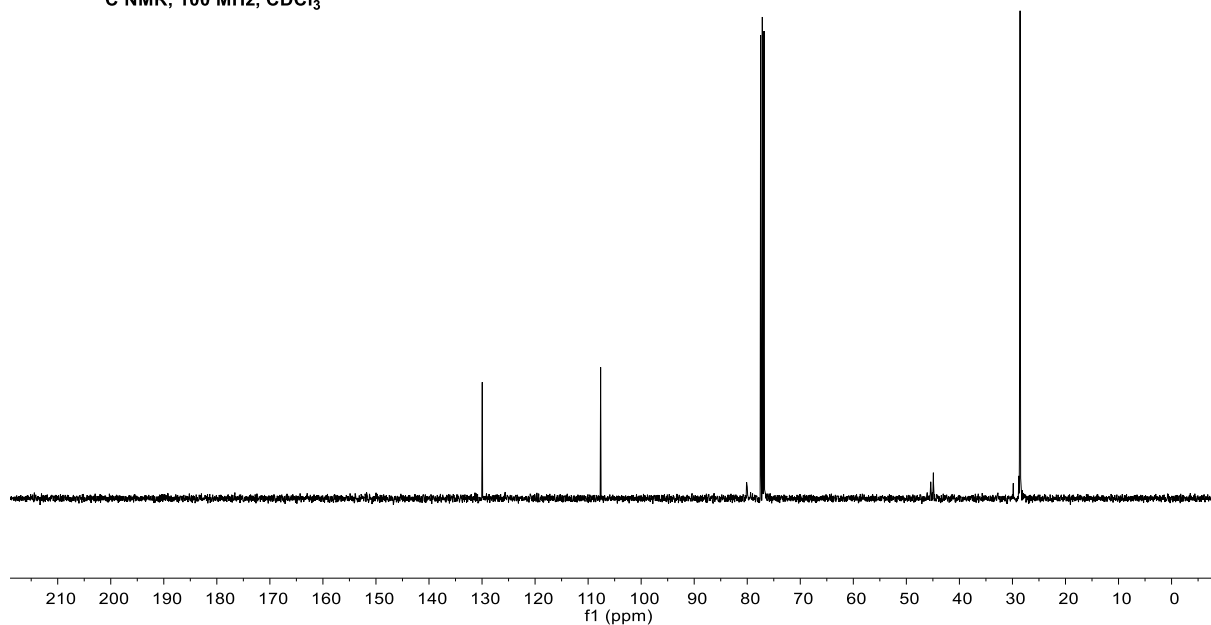
45.41

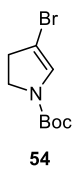
44.91

29.85

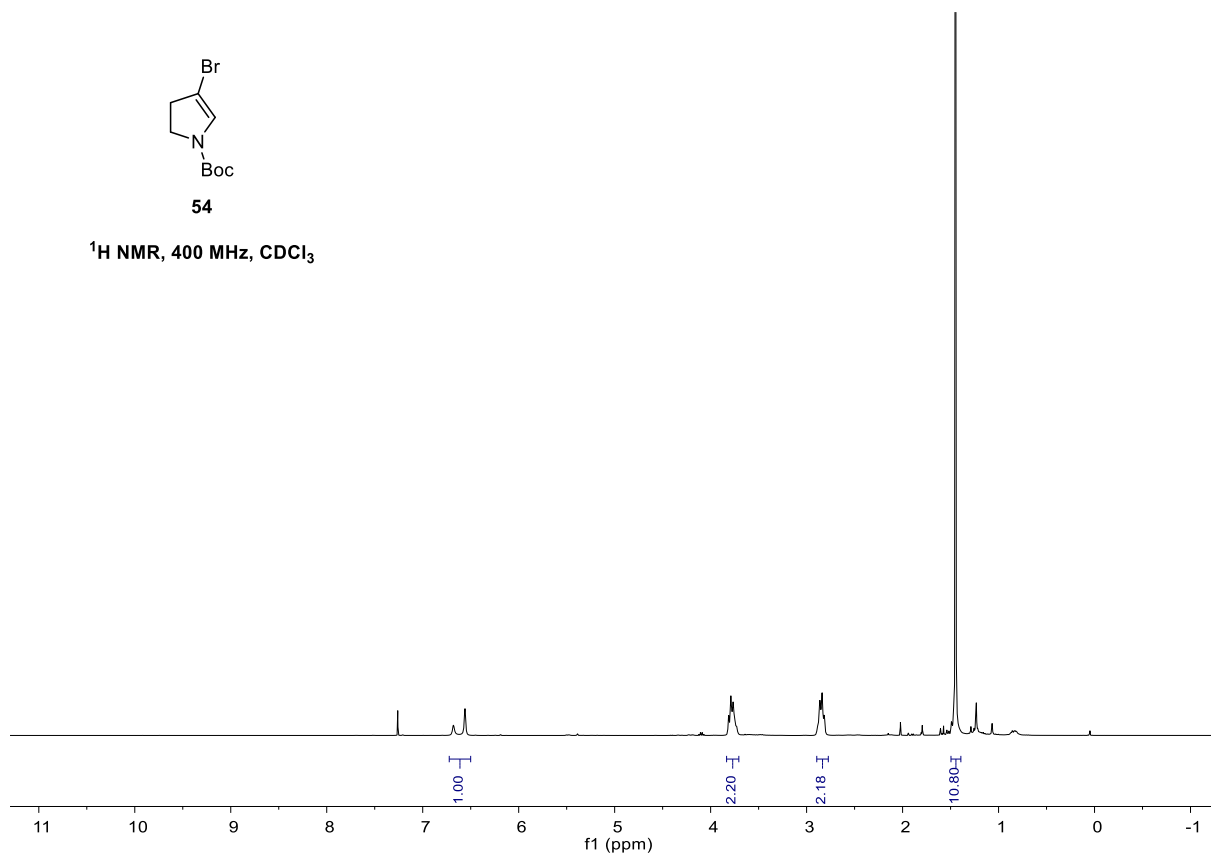
28.56

$^{13}\text{C}$  NMR, 100 MHz,  $\text{CDCl}_3$

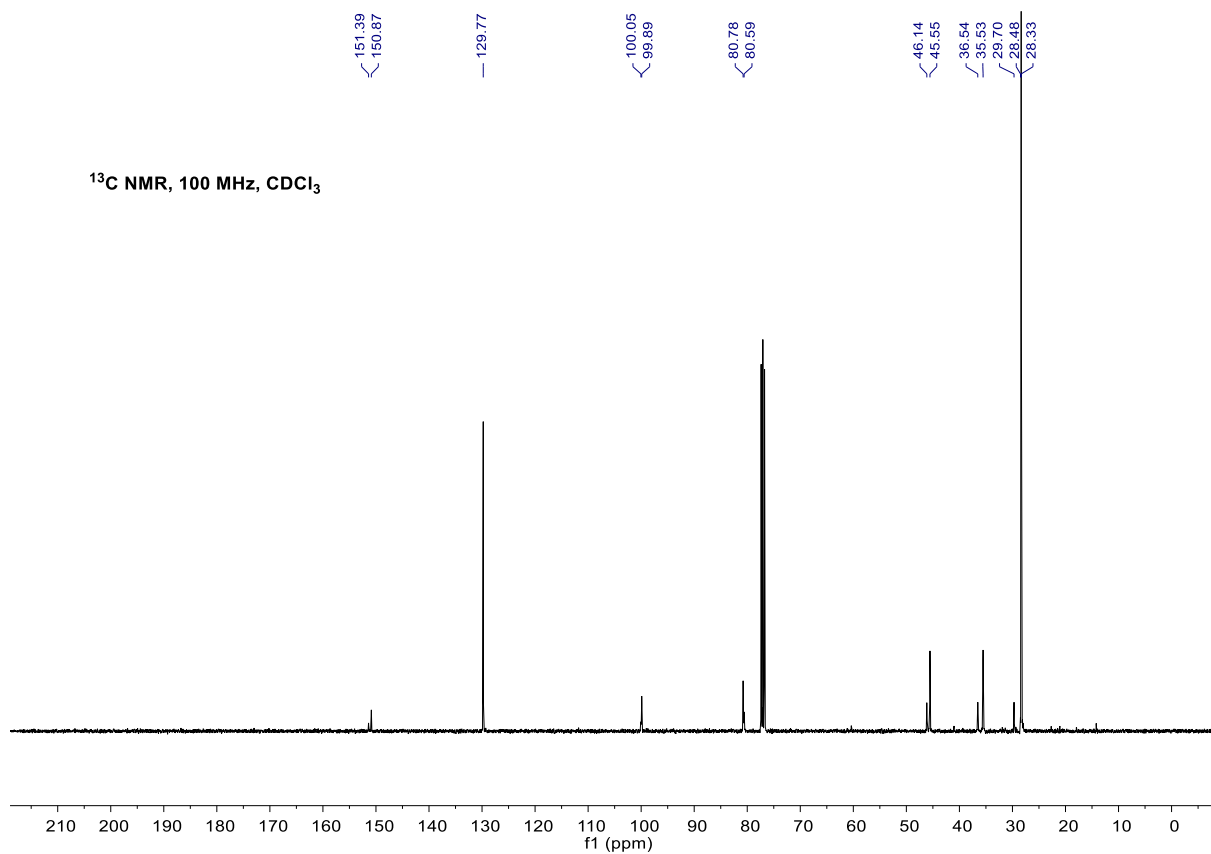


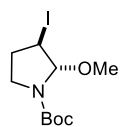


$^1\text{H}$  NMR, 400 MHz,  $\text{CDCl}_3$



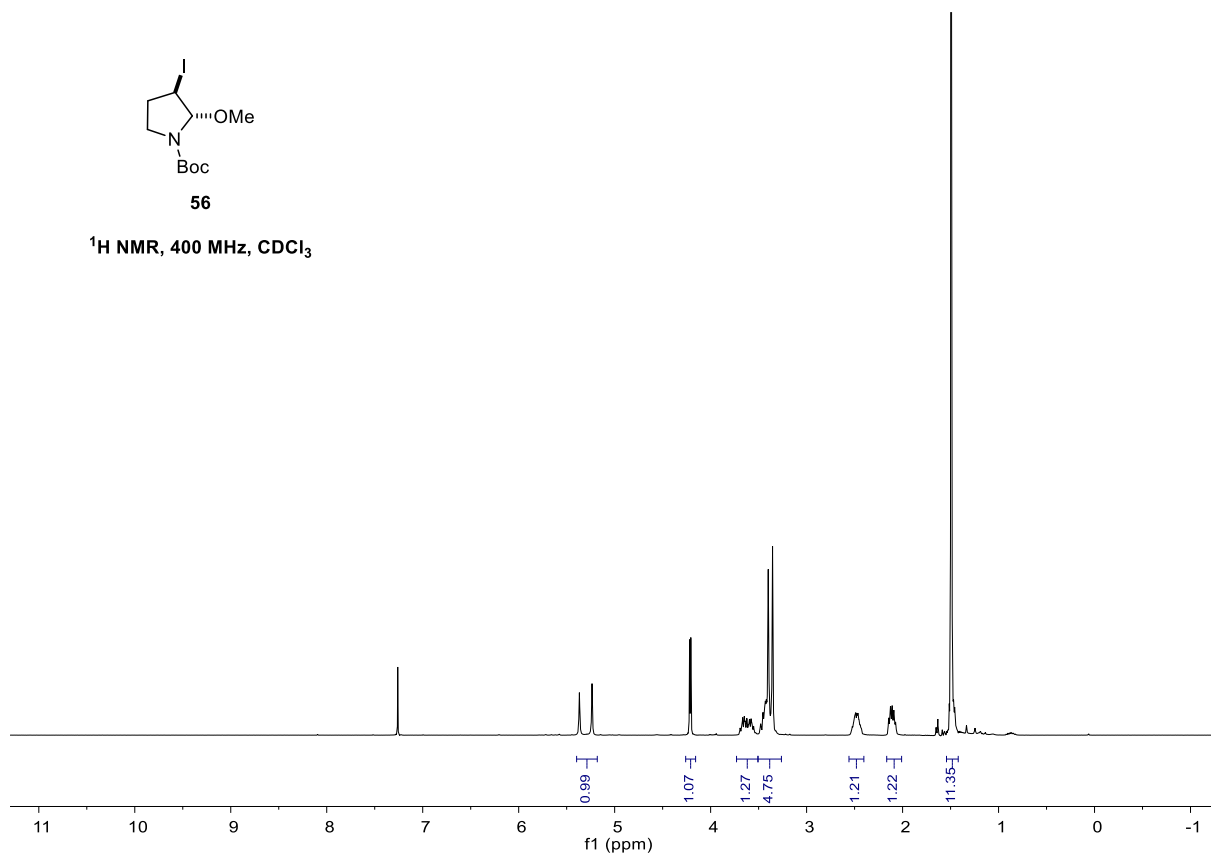
$^{13}\text{C}$  NMR, 100 MHz,  $\text{CDCl}_3$



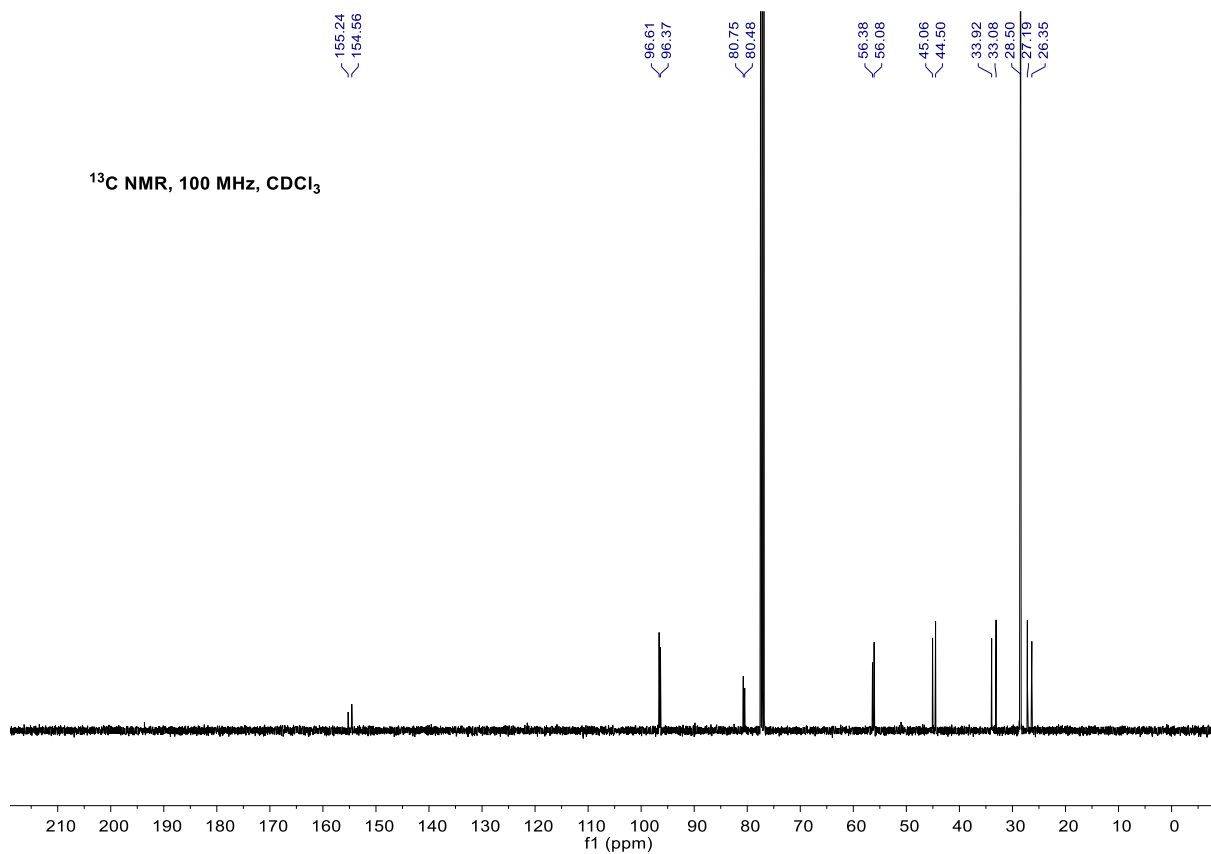


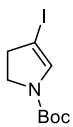
56

$^1\text{H}$  NMR, 400 MHz,  $\text{CDCl}_3$

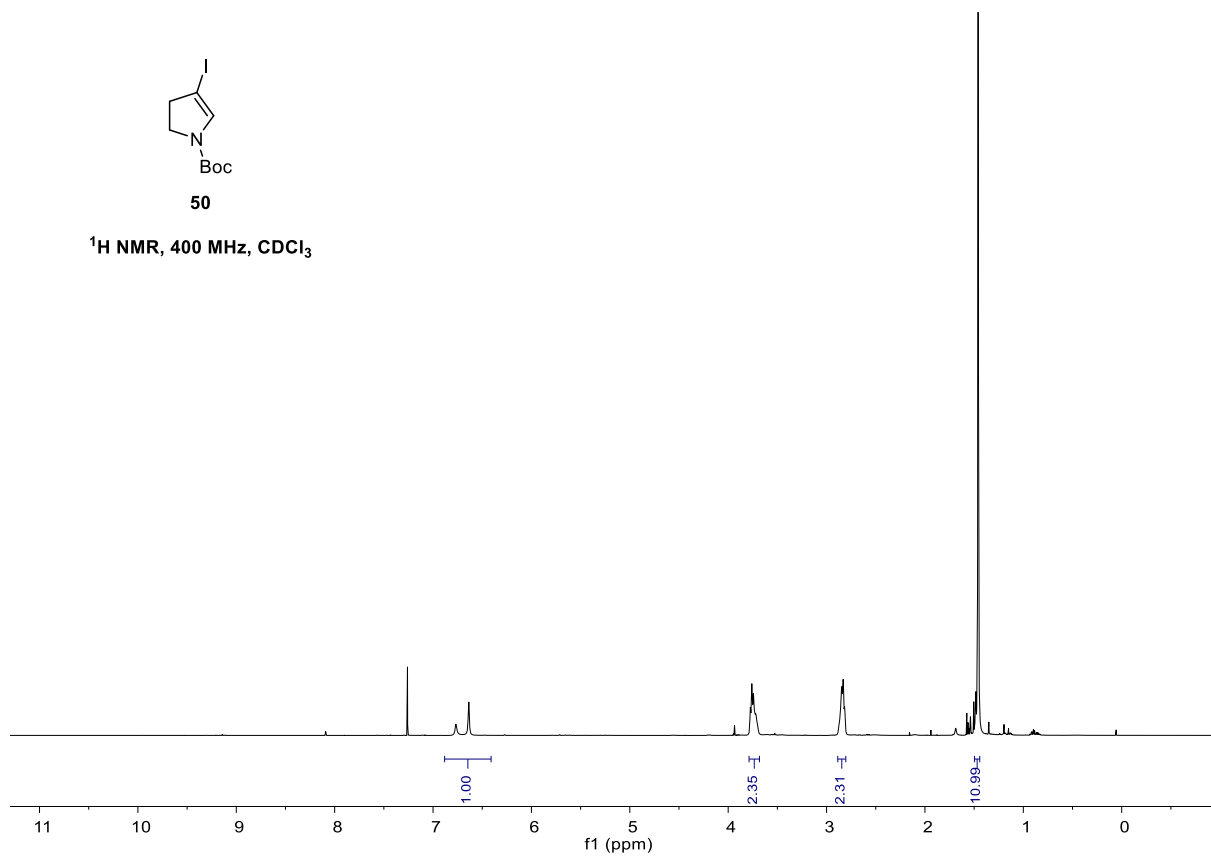
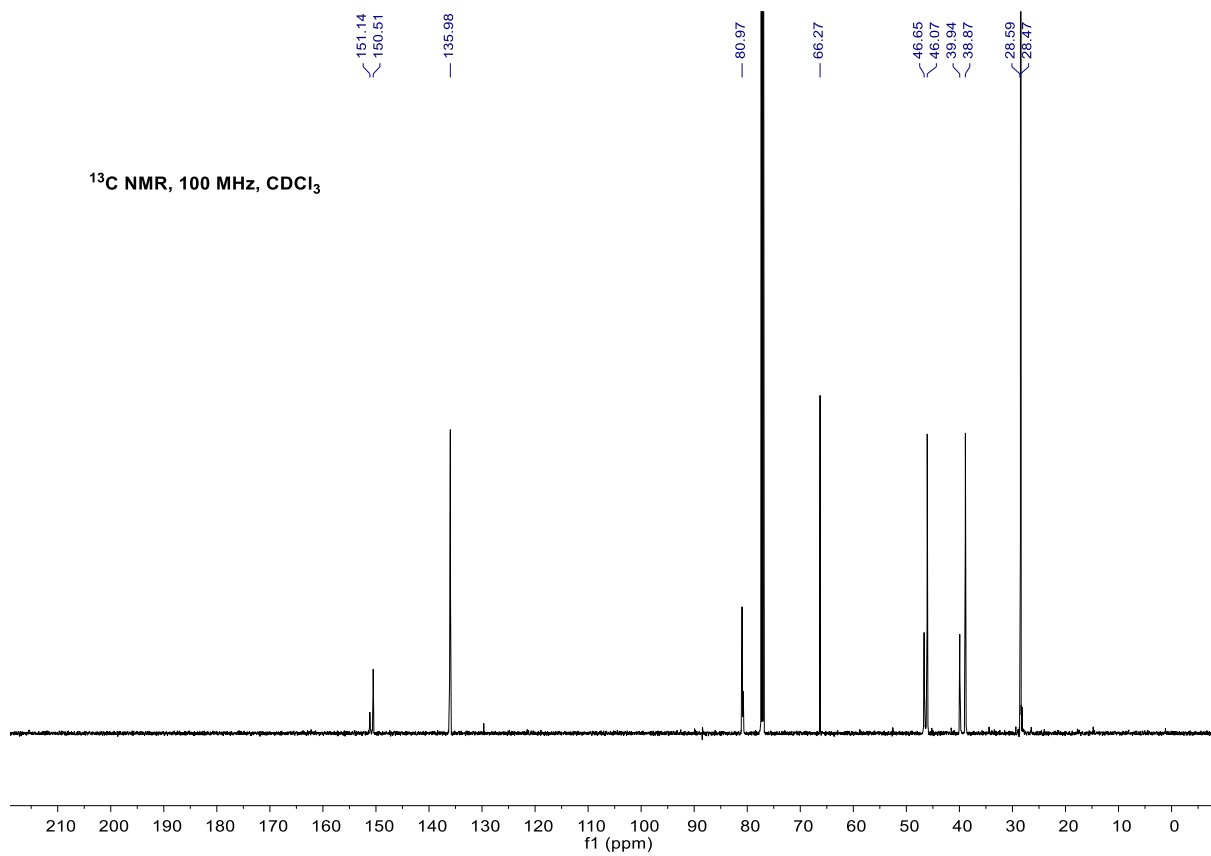


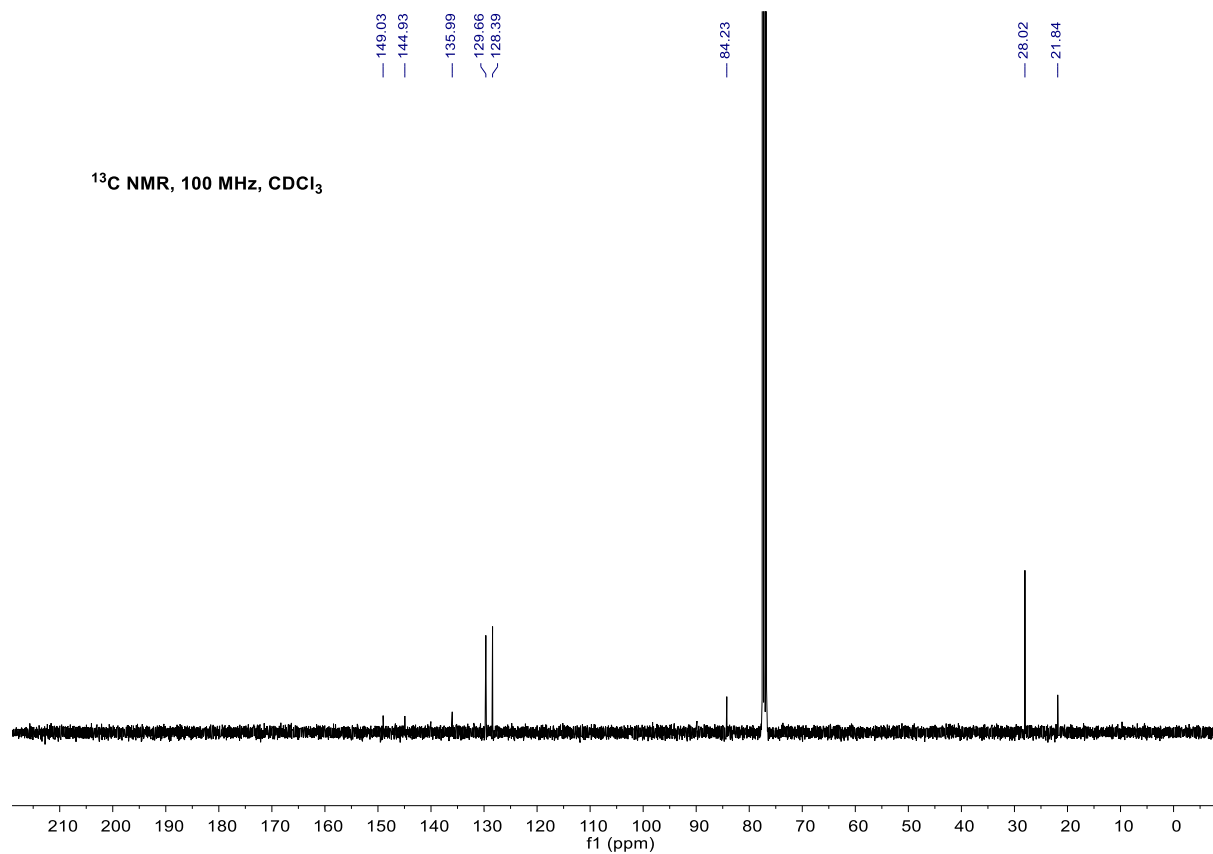
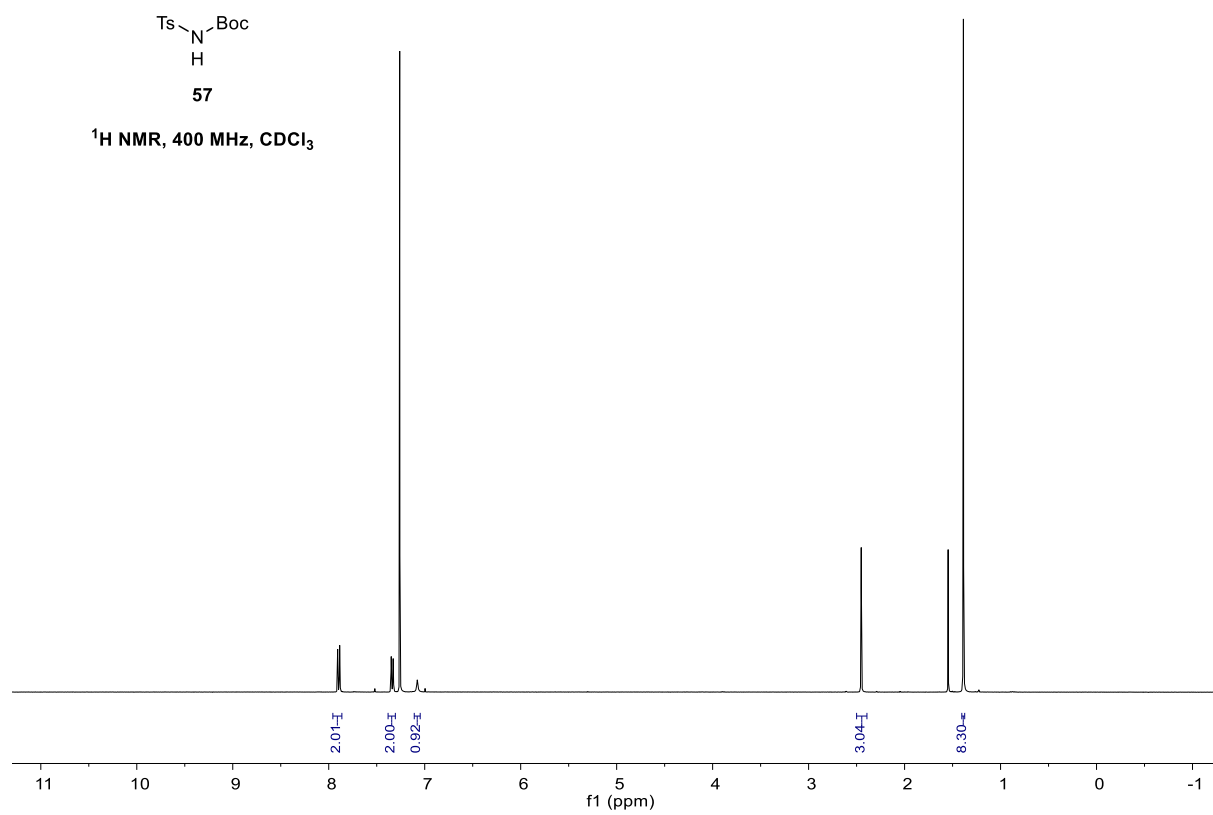
$^{13}\text{C}$  NMR, 100 MHz,  $\text{CDCl}_3$

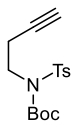




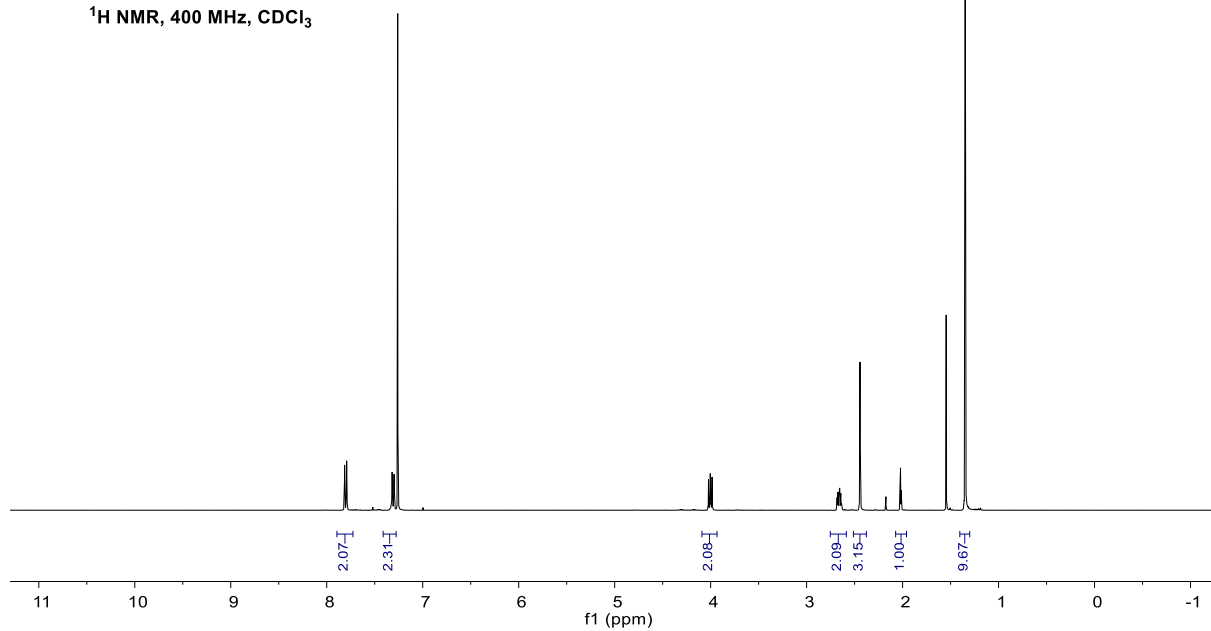
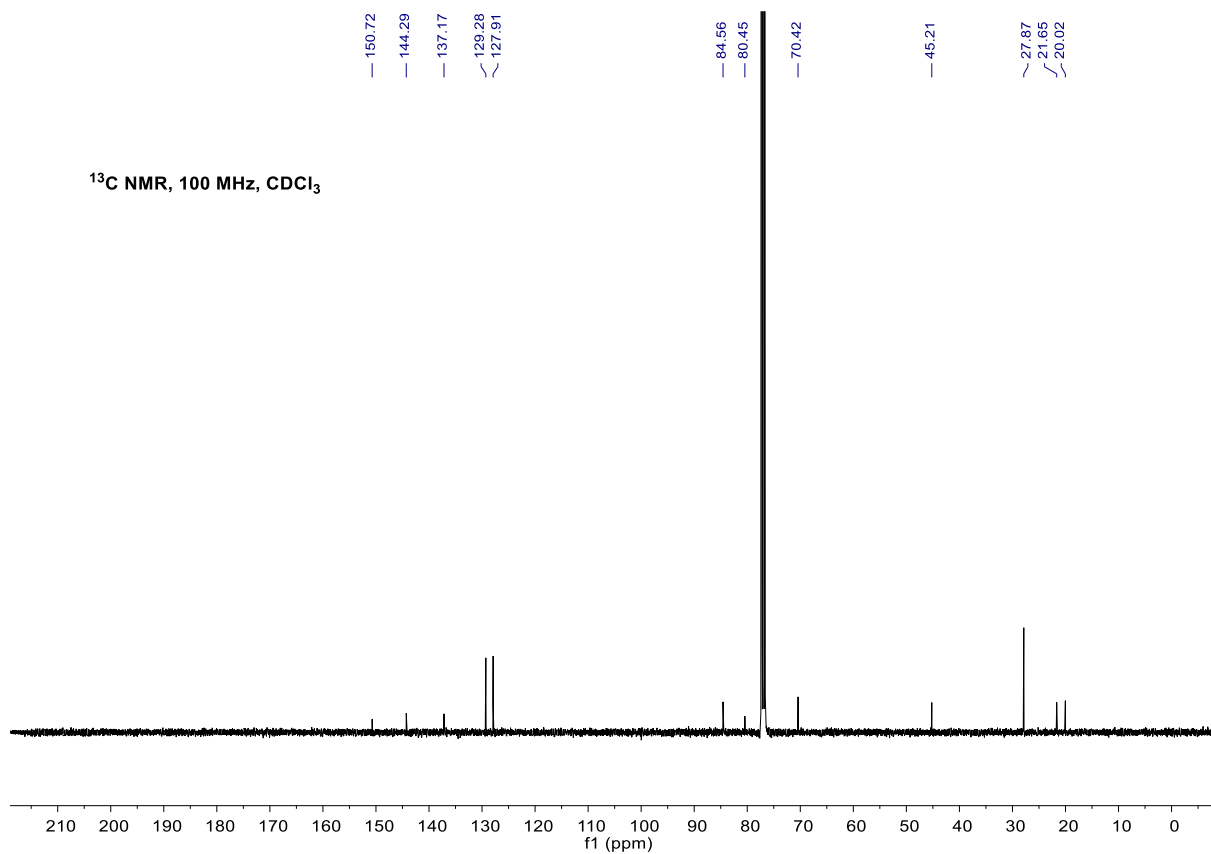
50

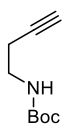
 $^1\text{H}$  NMR, 400 MHz,  $\text{CDCl}_3$  $^{13}\text{C}$  NMR, 100 MHz,  $\text{CDCl}_3$ 





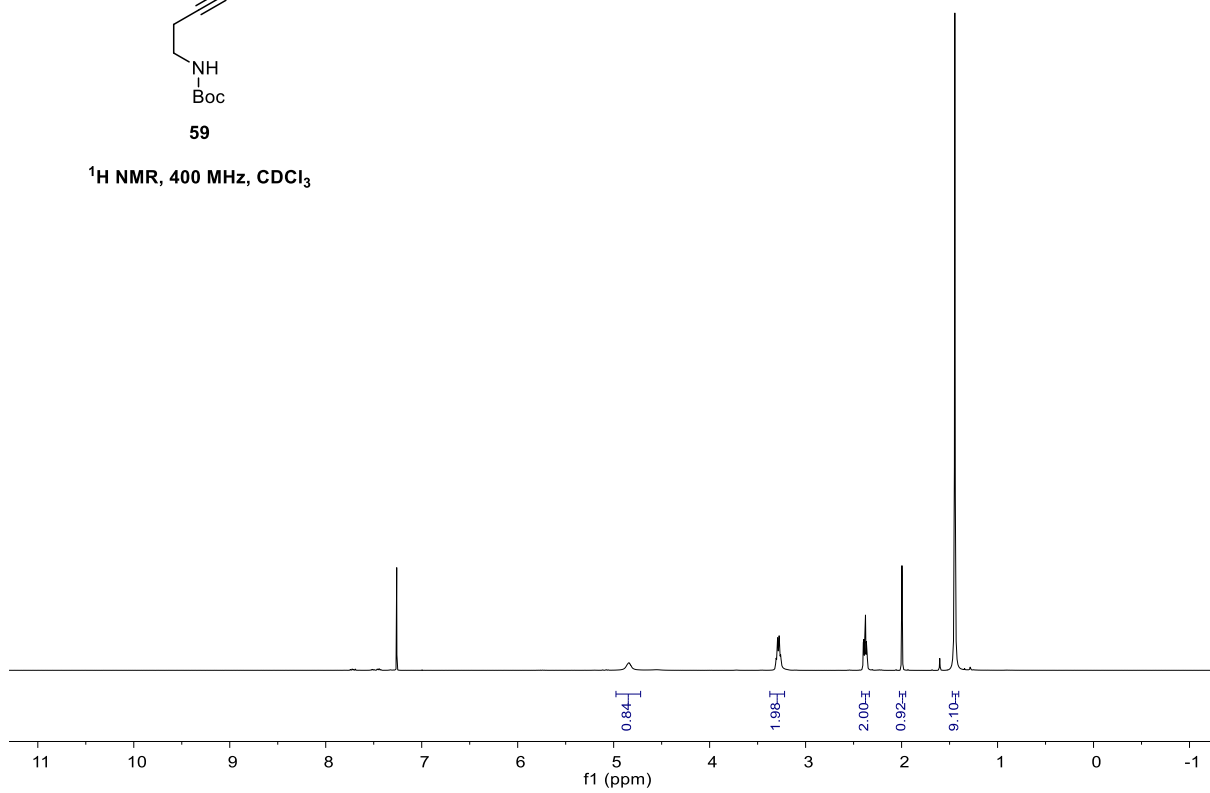
58

 $^1\text{H}$  NMR, 400 MHz,  $\text{CDCl}_3$  $^{13}\text{C}$  NMR, 100 MHz,  $\text{CDCl}_3$ 

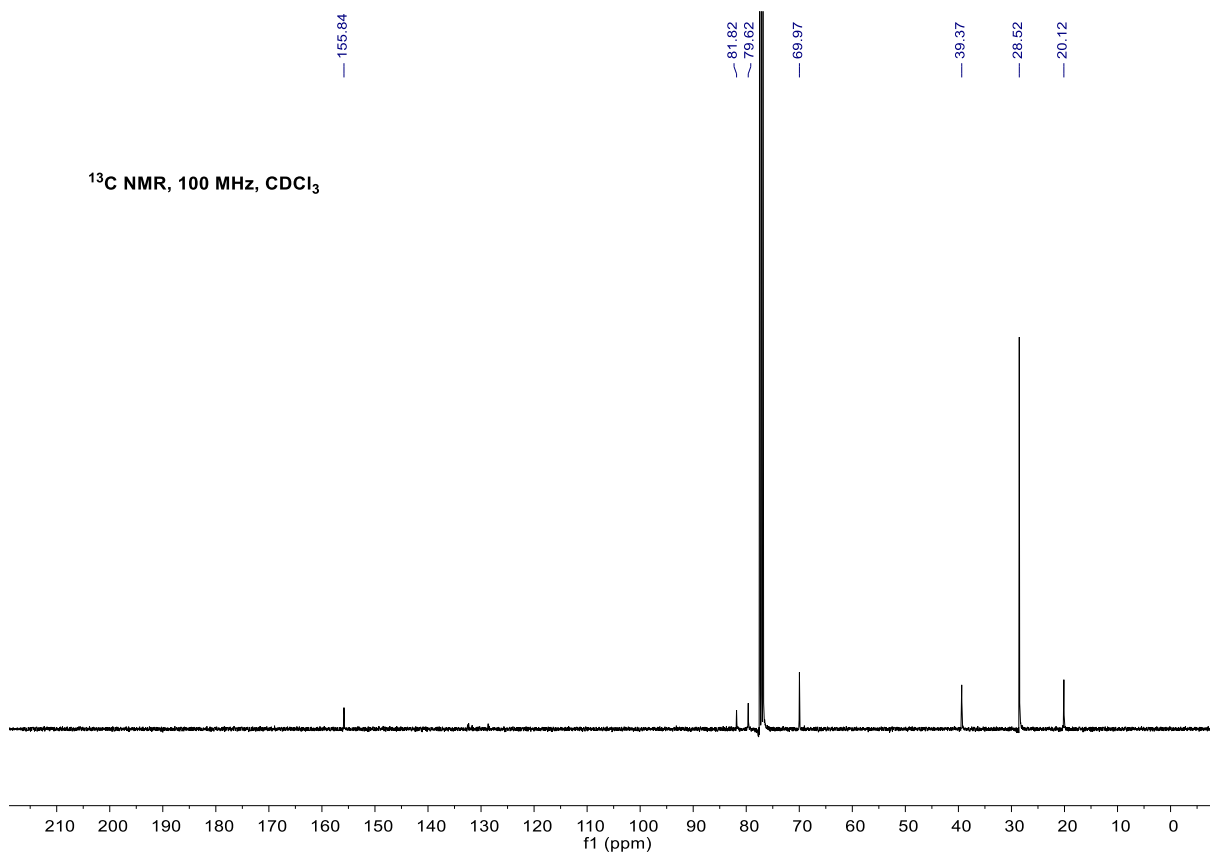


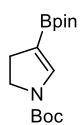
59

$^1\text{H}$  NMR, 400 MHz,  $\text{CDCl}_3$

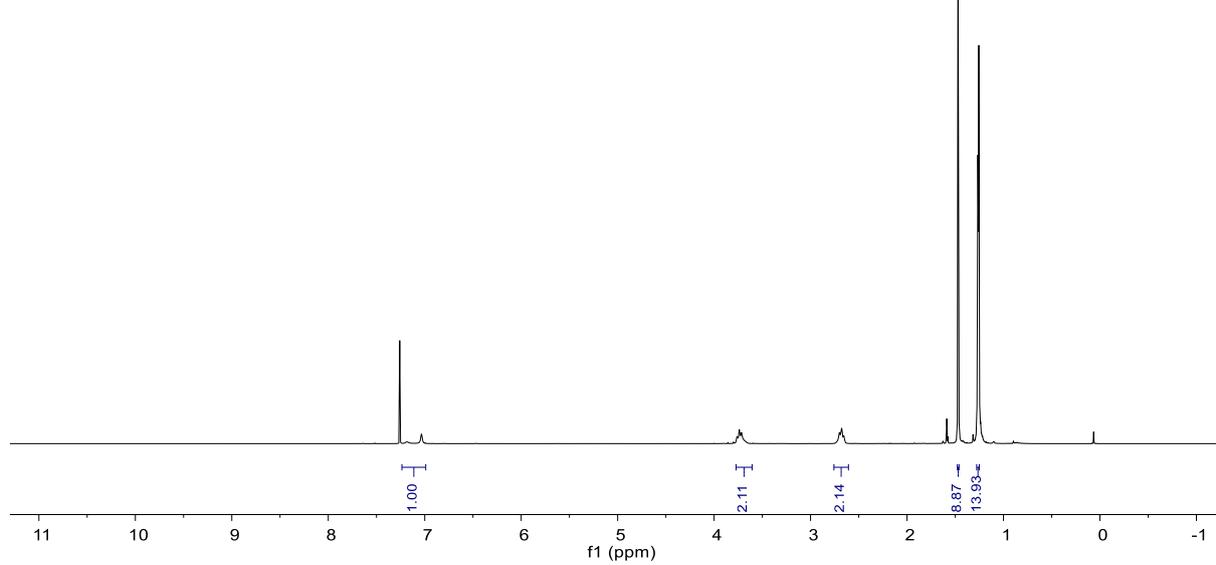
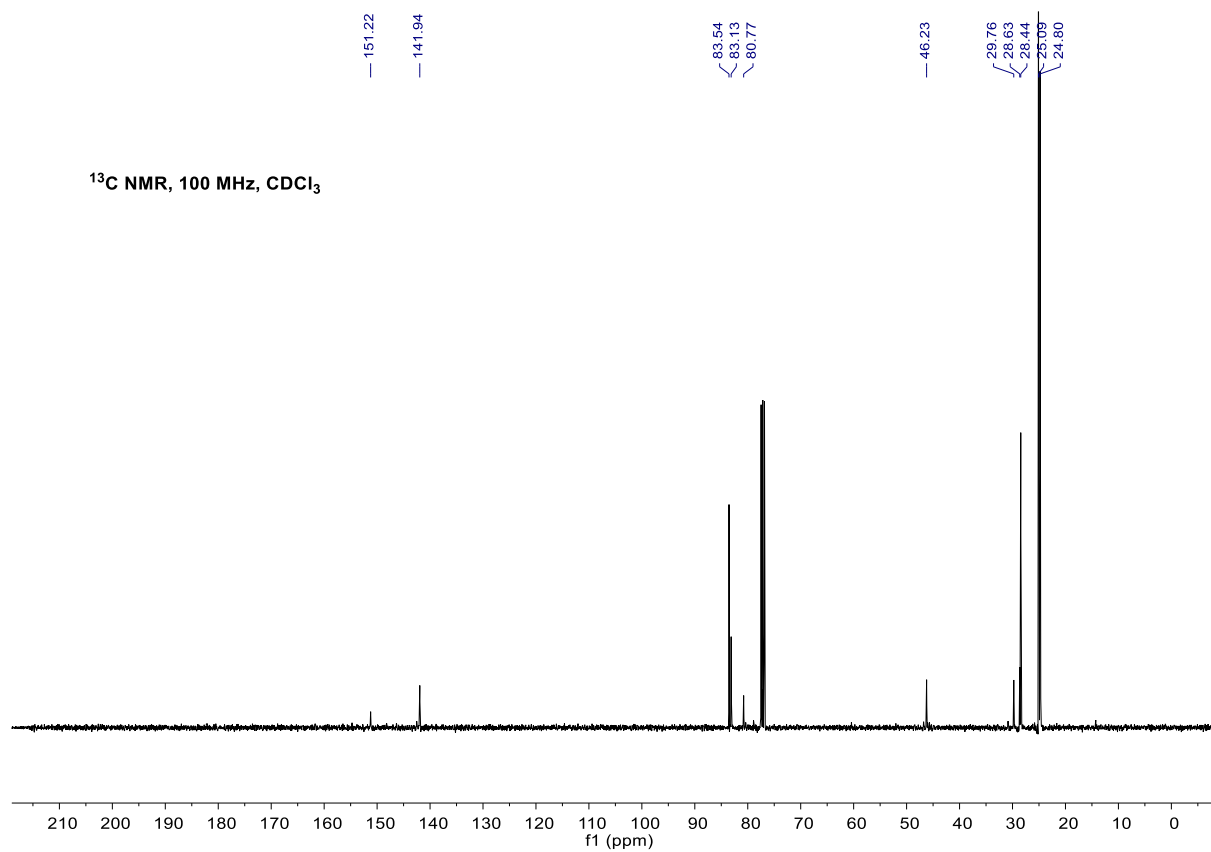


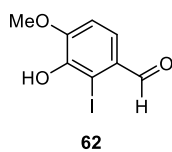
$^{13}\text{C}$  NMR, 100 MHz,  $\text{CDCl}_3$



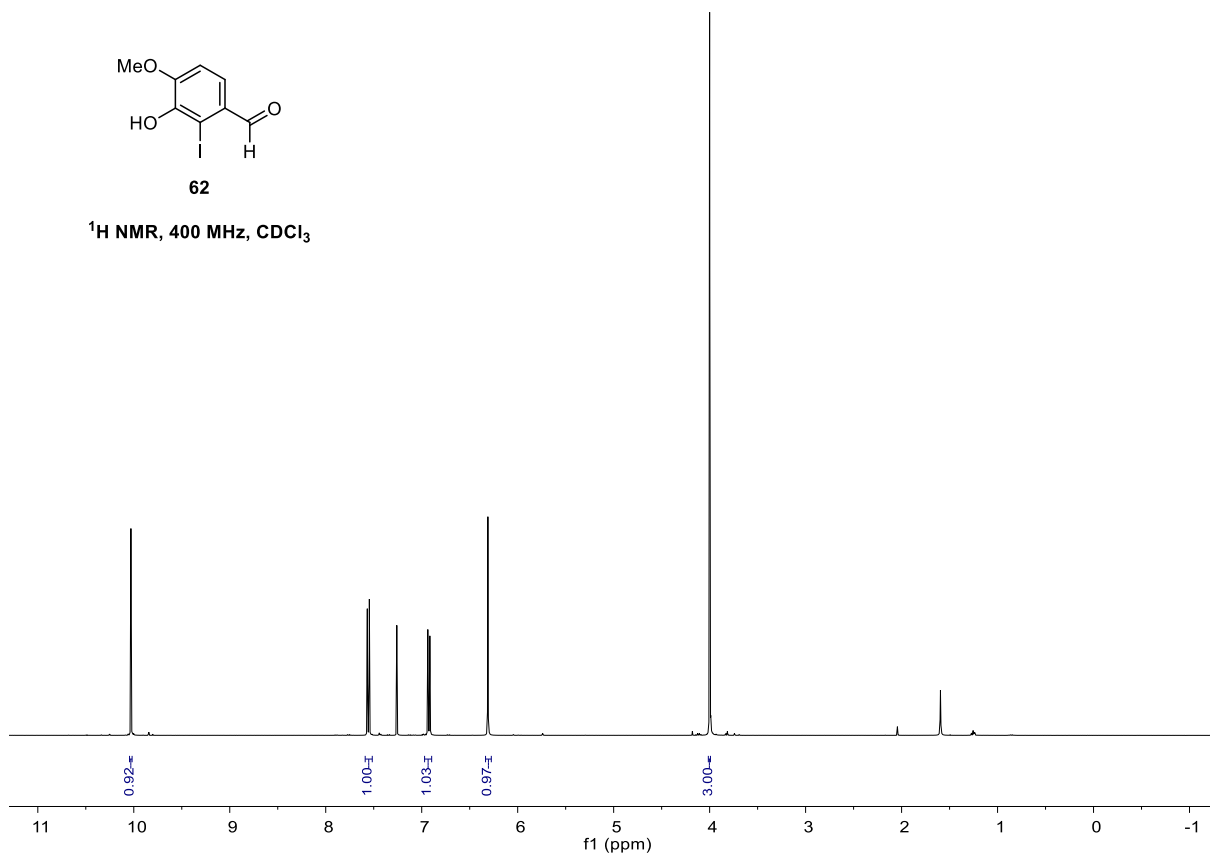


81

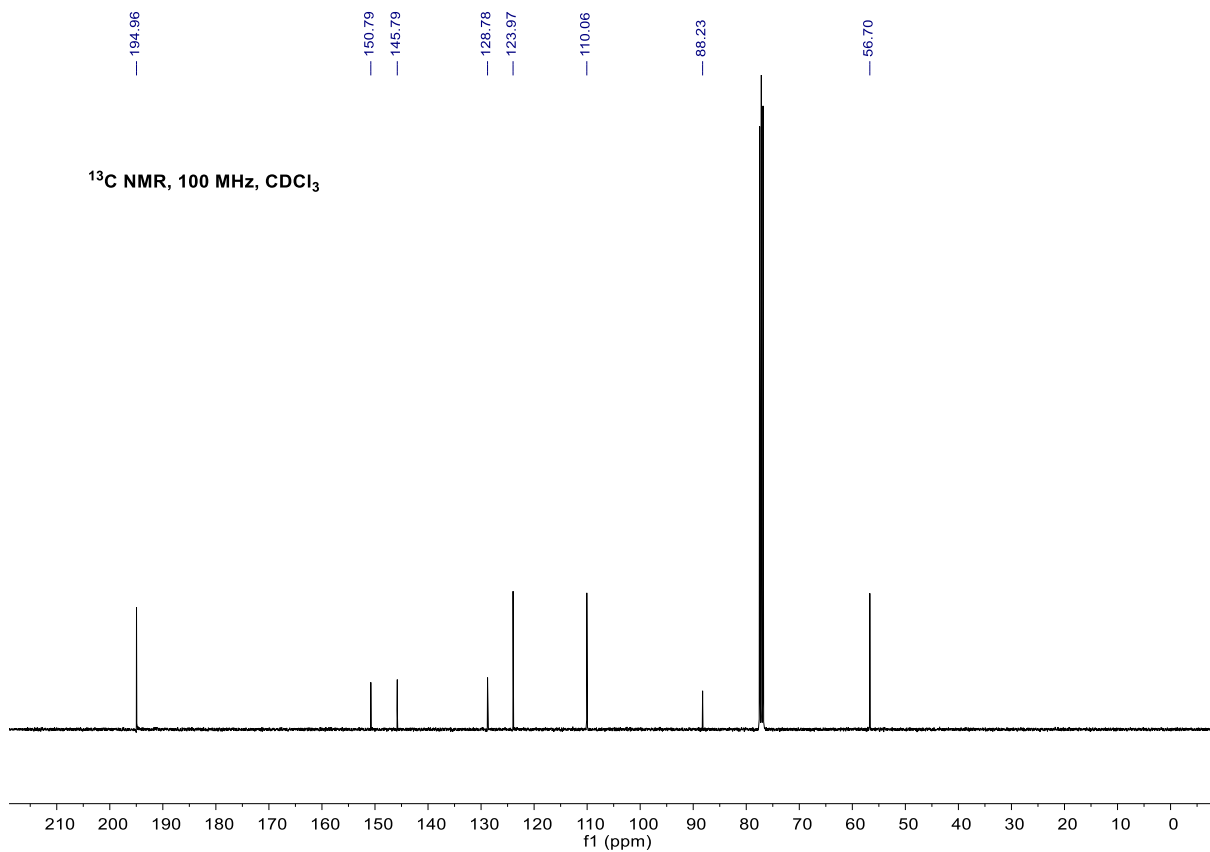
 $^1\text{H}$  NMR, 400 MHz,  $\text{CDCl}_3$  $^{13}\text{C}$  NMR, 100 MHz,  $\text{CDCl}_3$ 

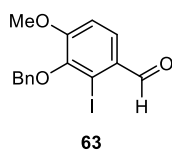


$^1\text{H}$  NMR, 400 MHz,  $\text{CDCl}_3$

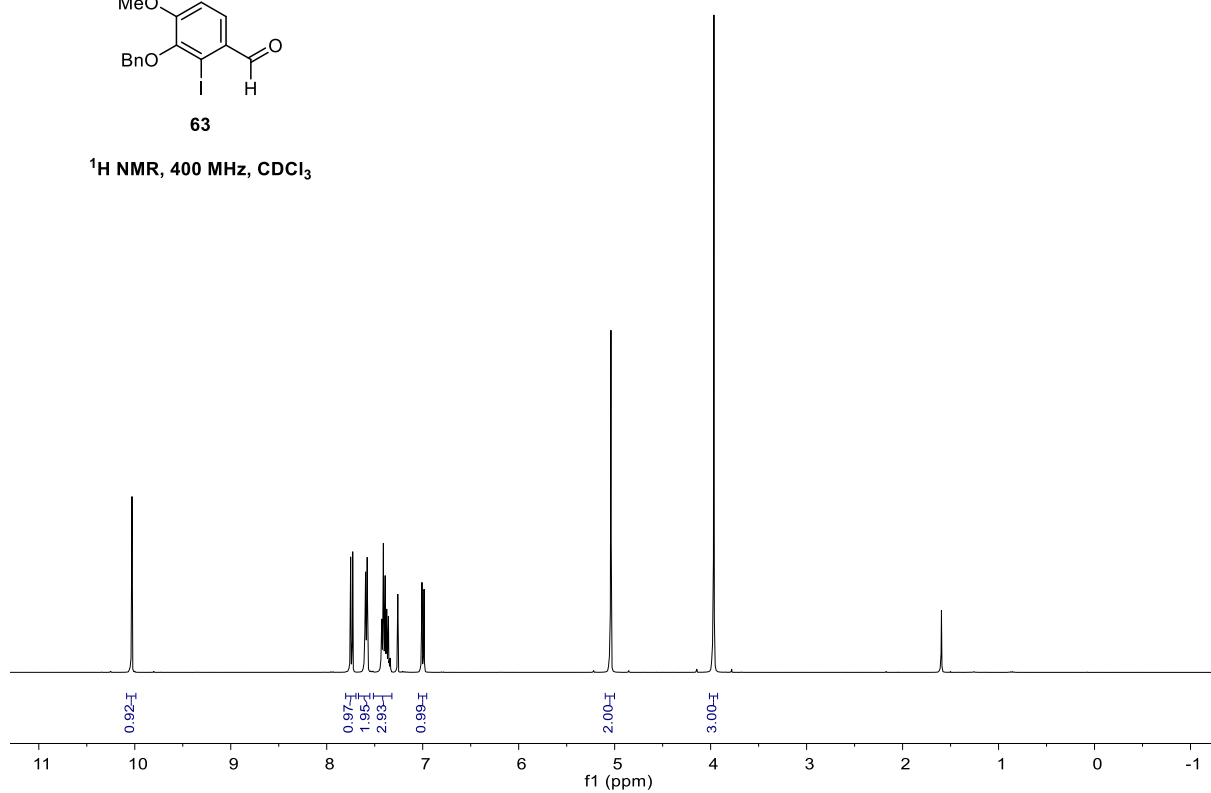


$^{13}\text{C}$  NMR, 100 MHz,  $\text{CDCl}_3$

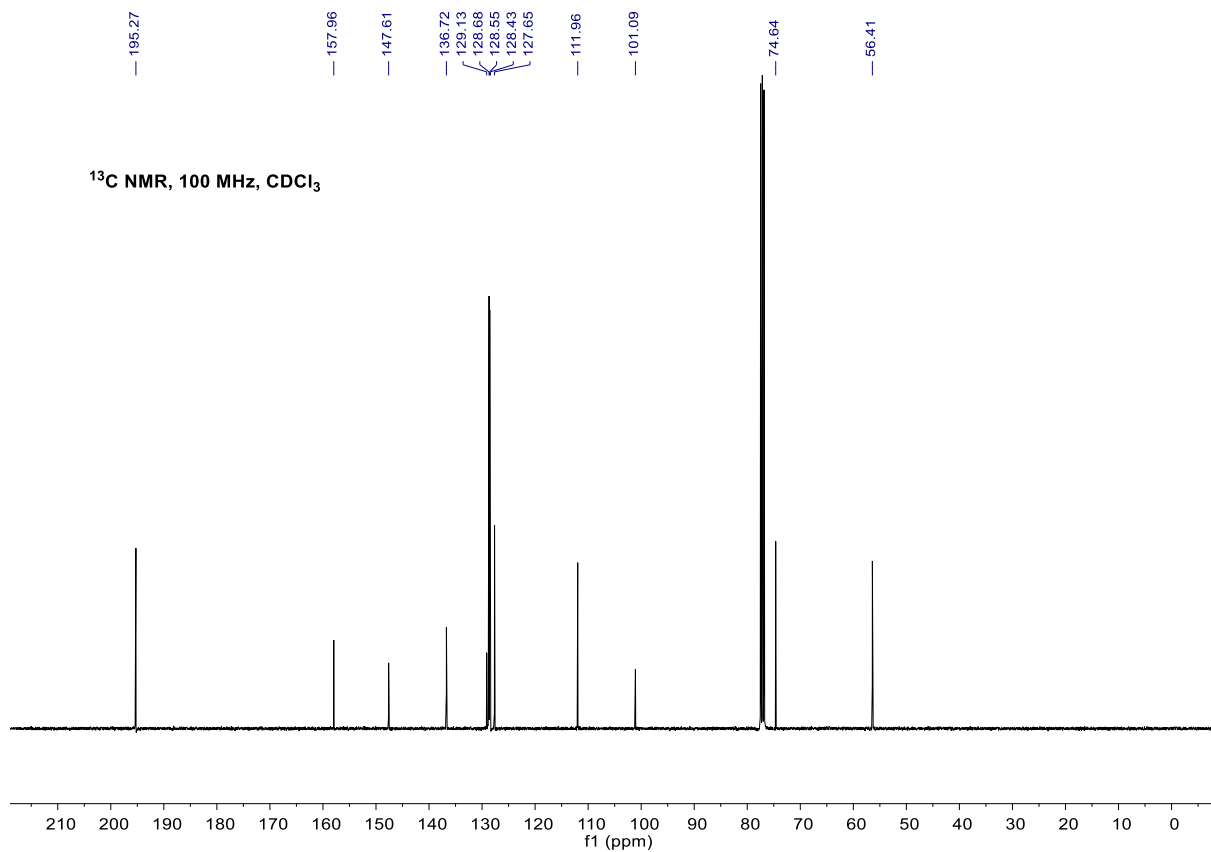


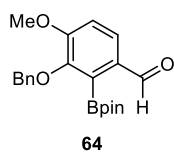


$^1\text{H}$  NMR, 400 MHz,  $\text{CDCl}_3$

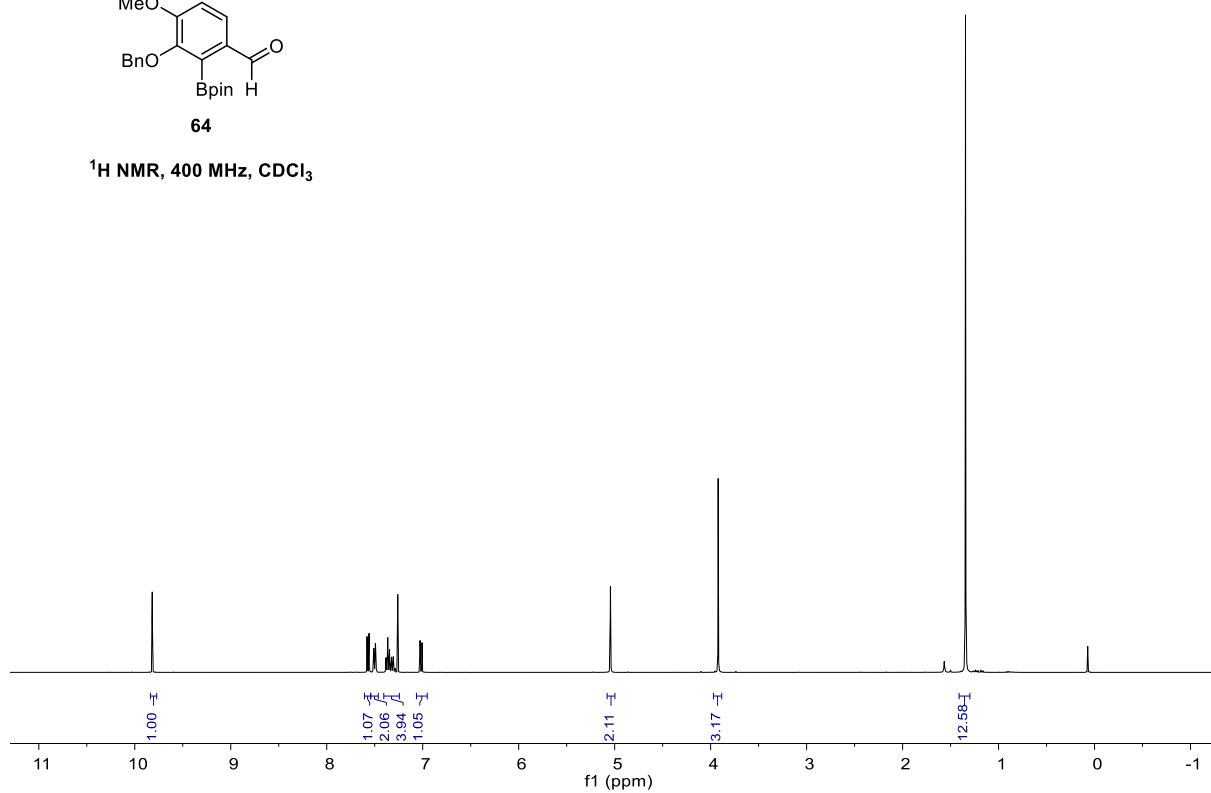


$^{13}\text{C}$  NMR, 100 MHz,  $\text{CDCl}_3$

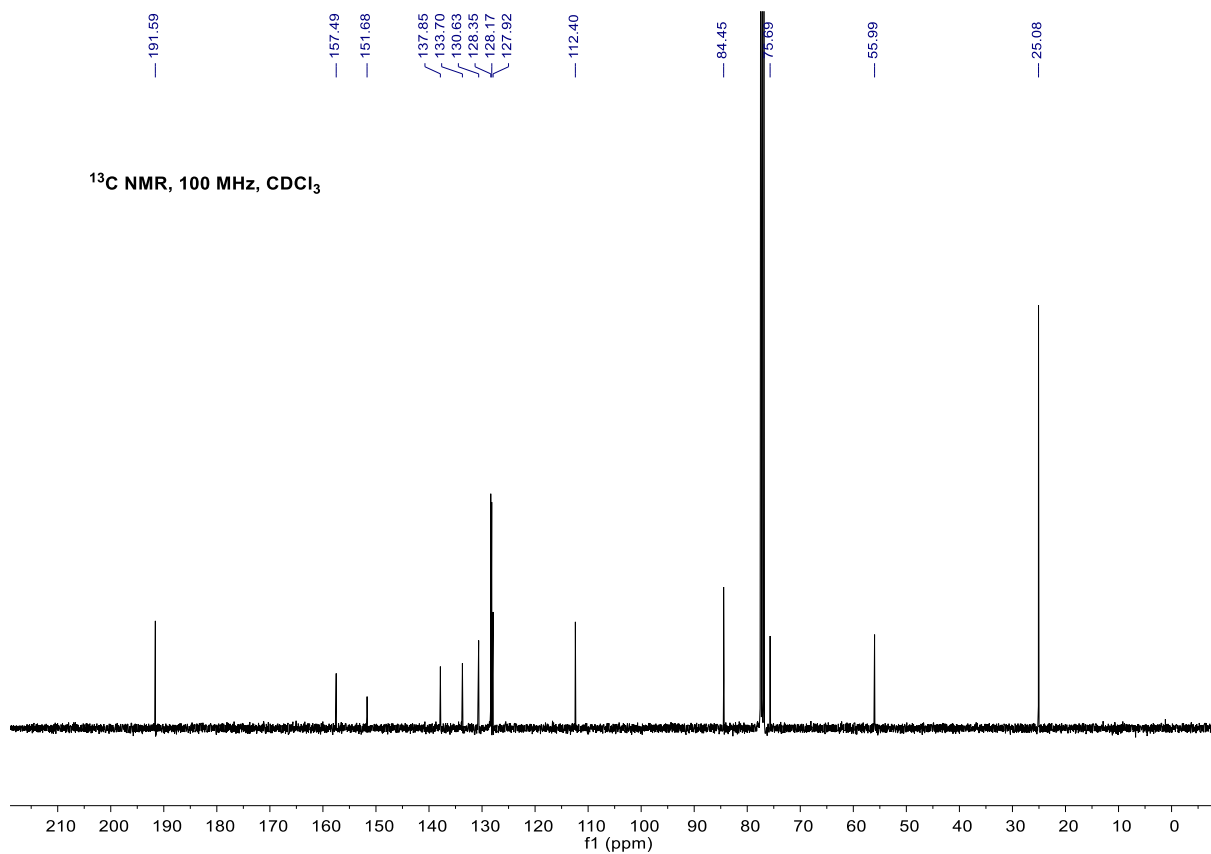


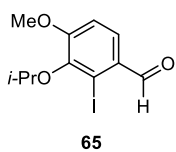


$^1\text{H}$  NMR, 400 MHz,  $\text{CDCl}_3$

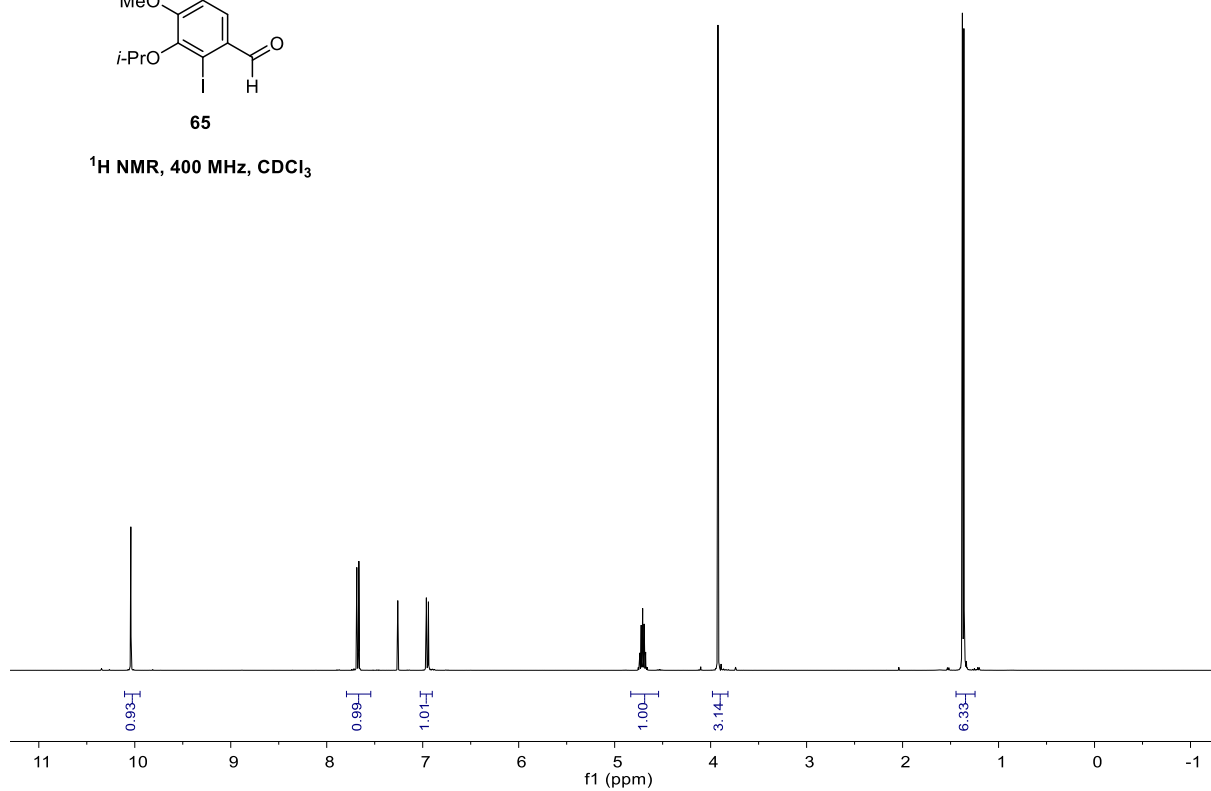


$^{13}\text{C}$  NMR, 100 MHz,  $\text{CDCl}_3$

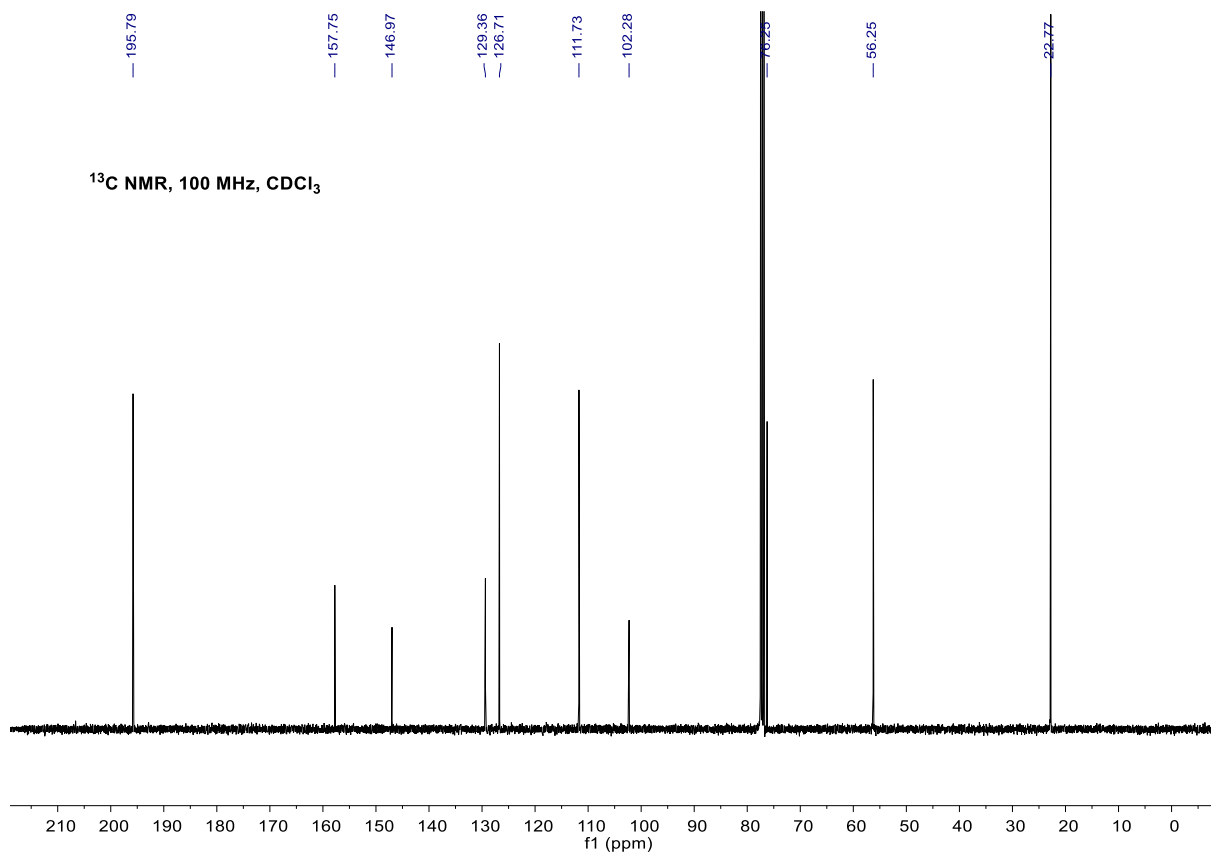


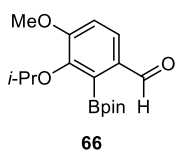


$^1\text{H}$  NMR, 400 MHz,  $\text{CDCl}_3$

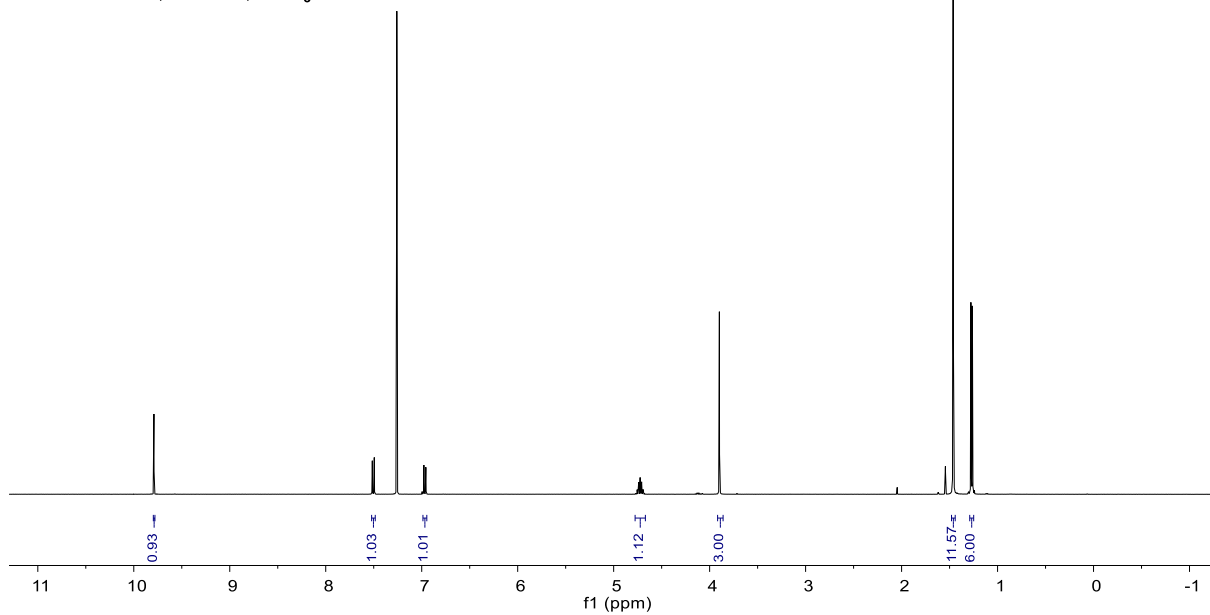


$^{13}\text{C}$  NMR, 100 MHz,  $\text{CDCl}_3$

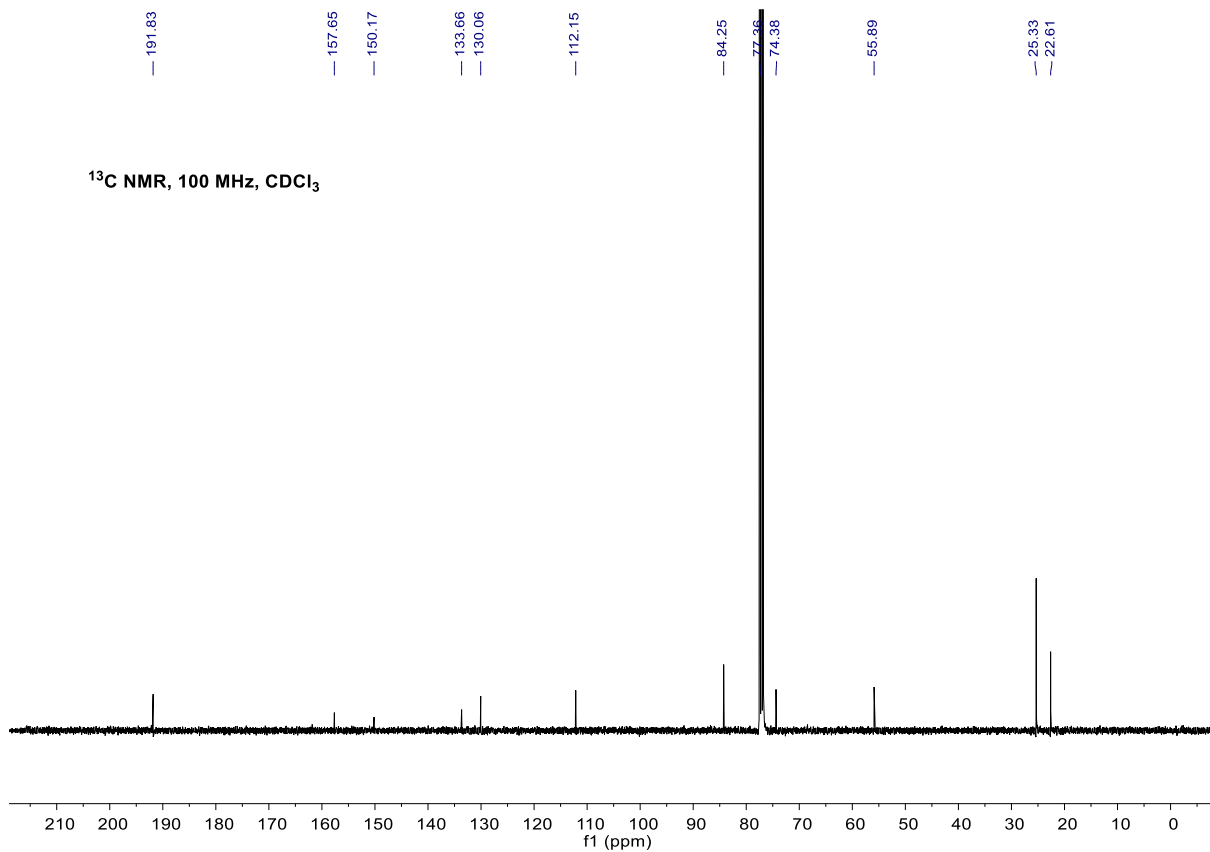


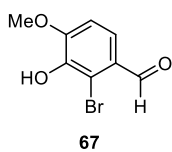


<sup>1</sup>H NMR, 400 MHz, CDCl<sub>3</sub>

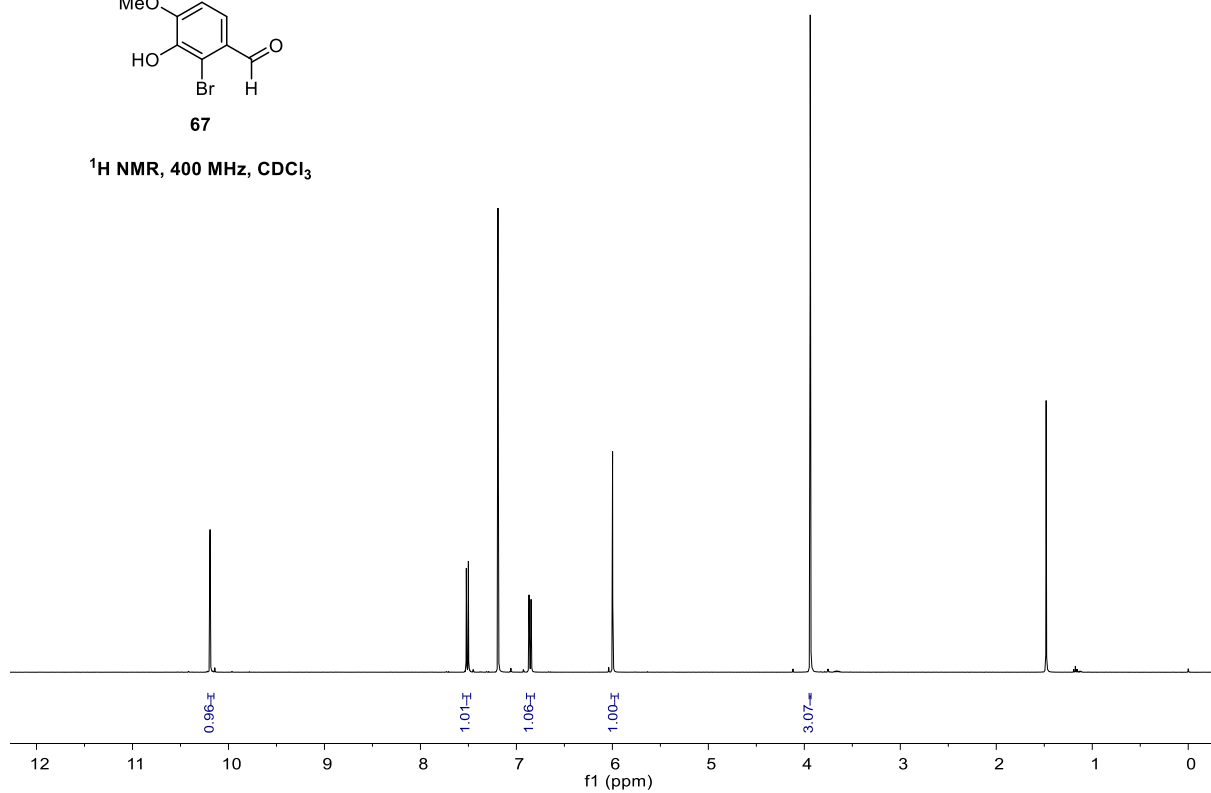


<sup>13</sup>C NMR, 100 MHz, CDCl<sub>3</sub>

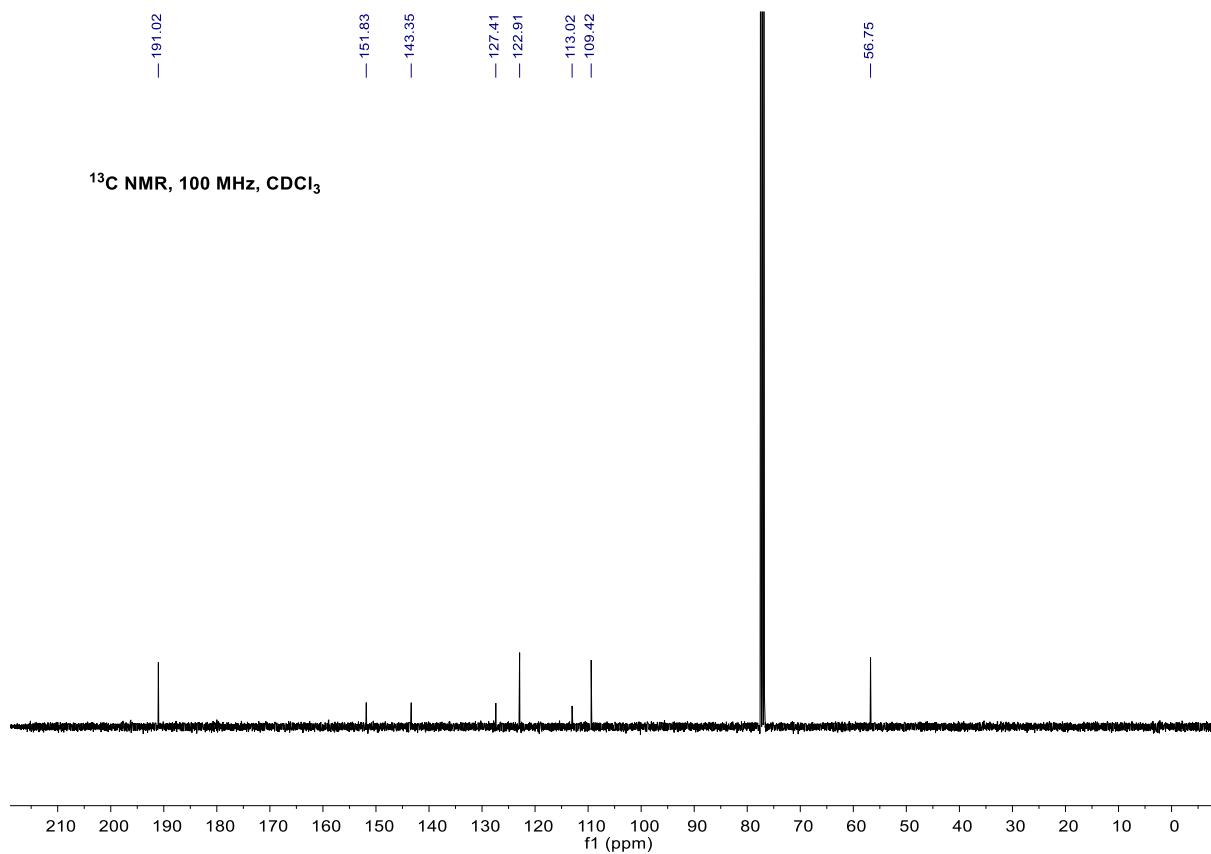


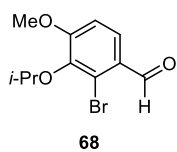


$^1\text{H}$  NMR, 400 MHz,  $\text{CDCl}_3$

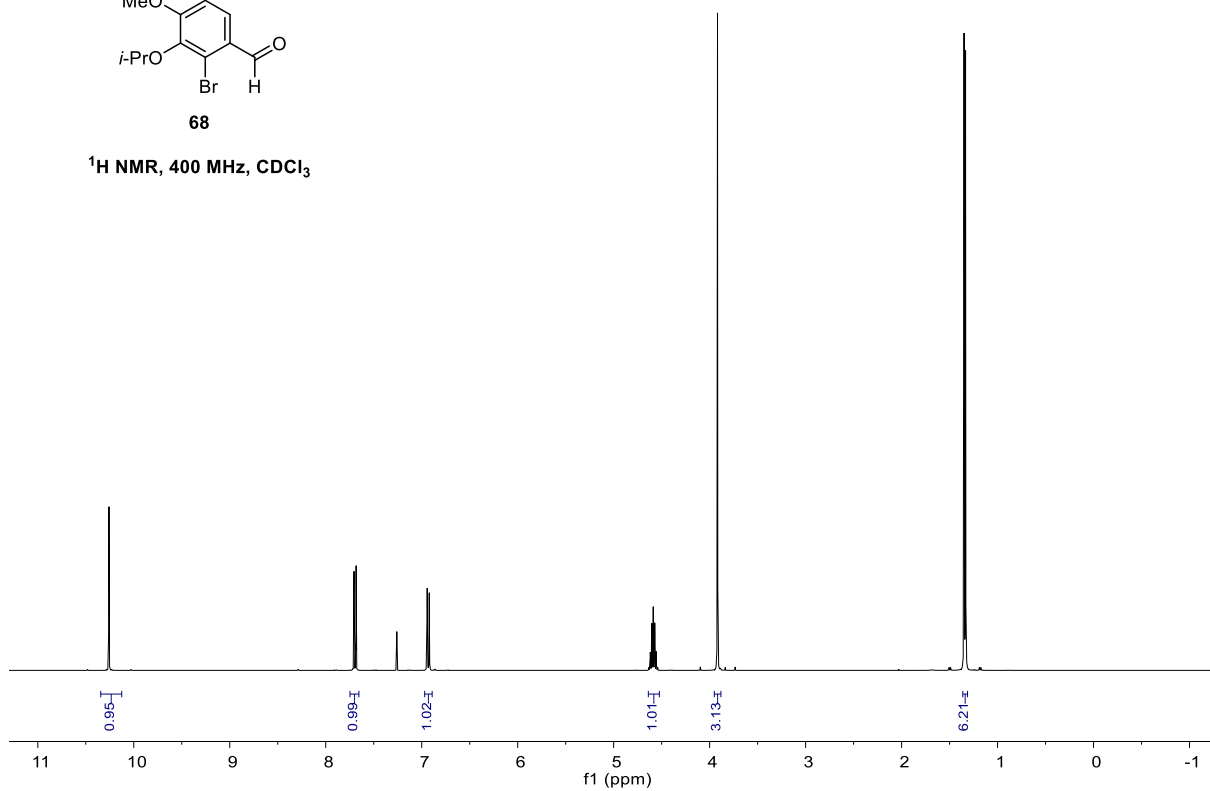


$^{13}\text{C}$  NMR, 100 MHz,  $\text{CDCl}_3$

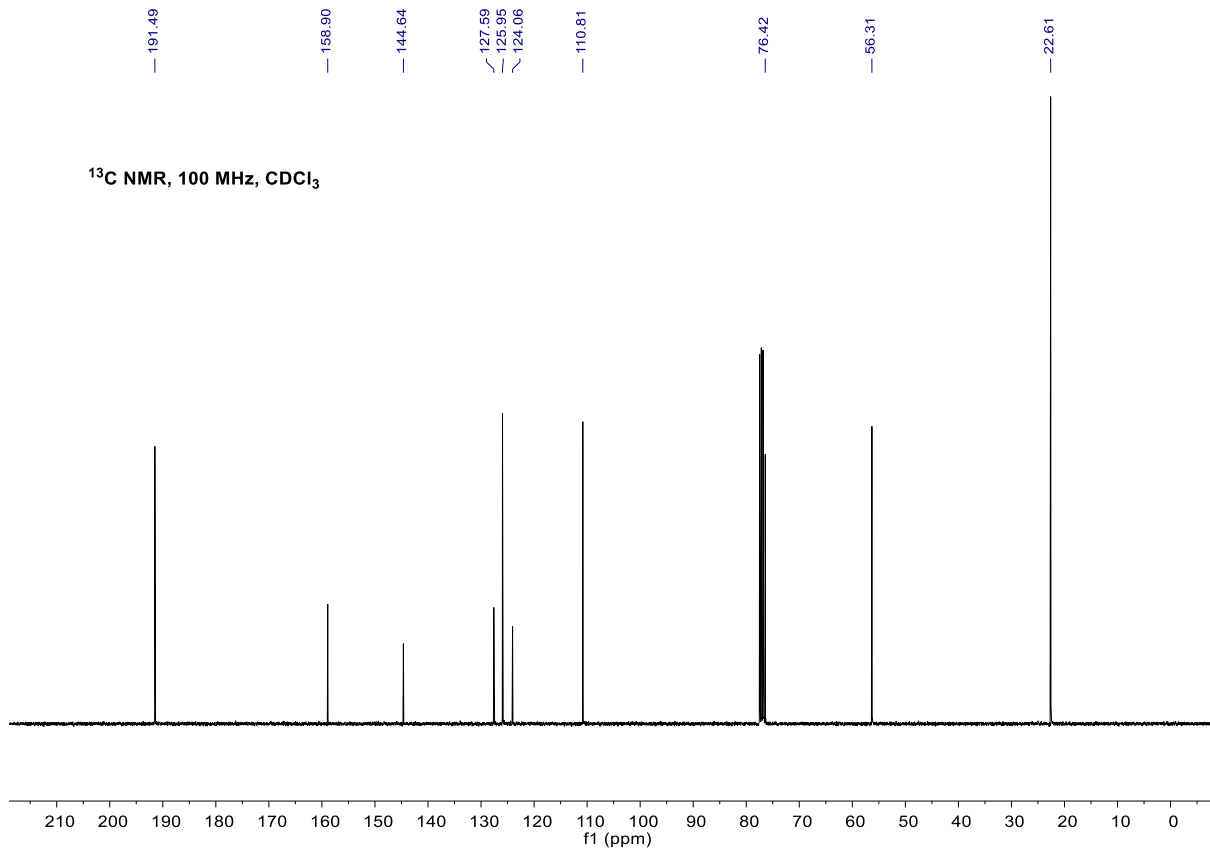


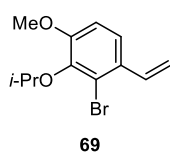


<sup>1</sup>H NMR, 400 MHz, CDCl<sub>3</sub>

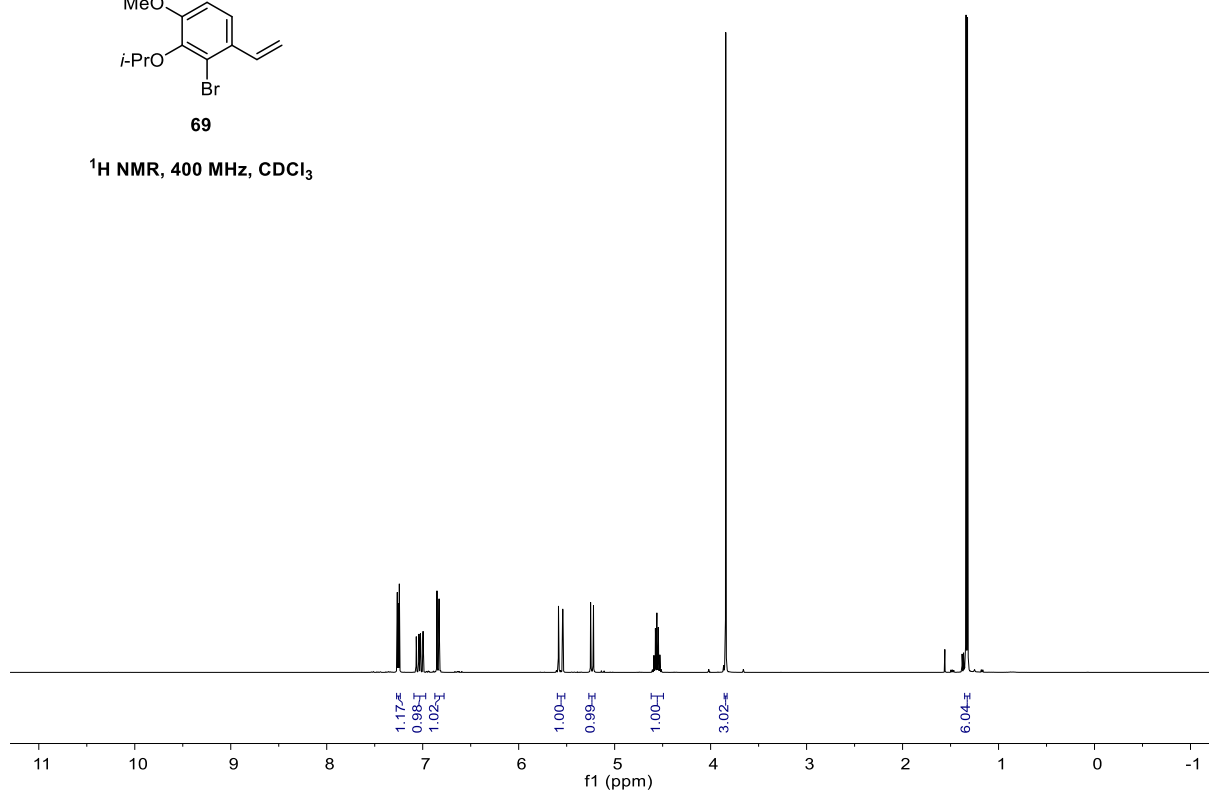


<sup>13</sup>C NMR, 100 MHz, CDCl<sub>3</sub>

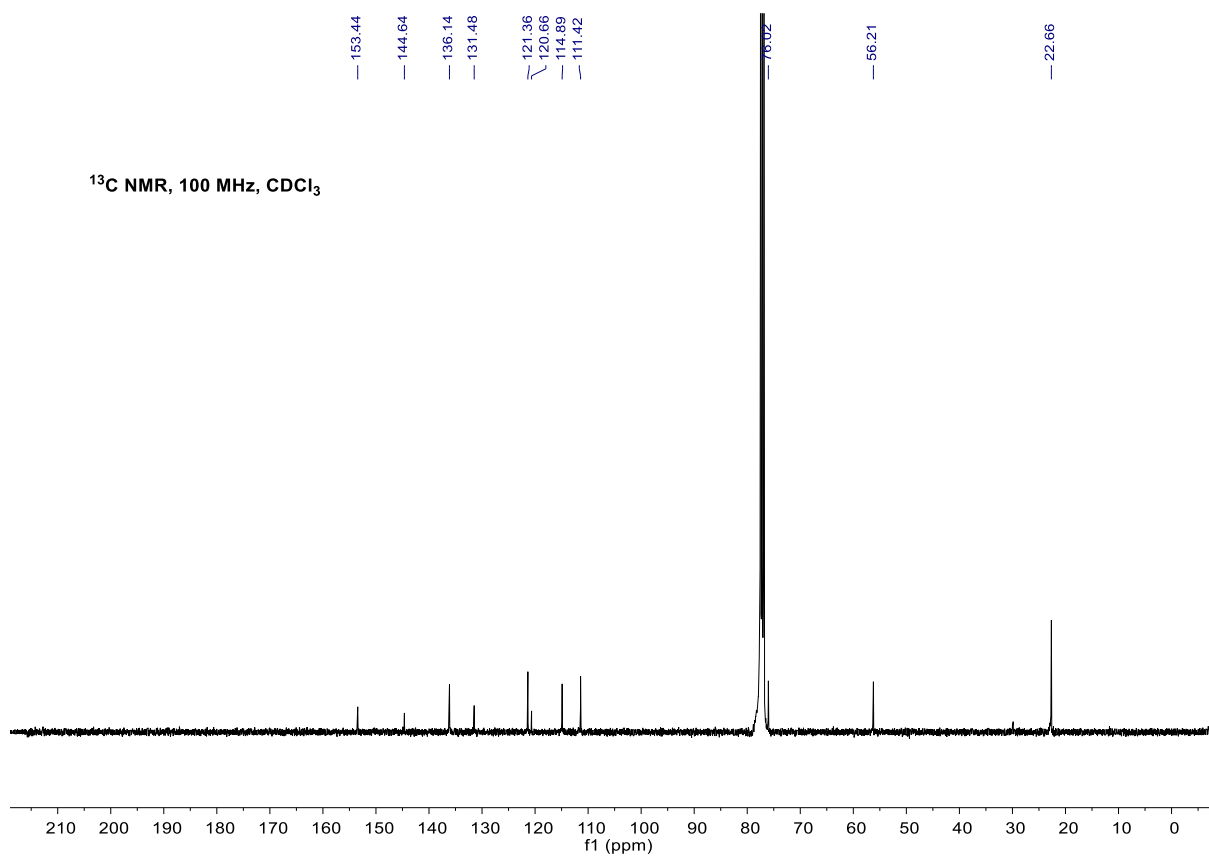


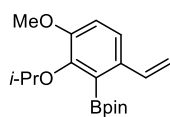


$^1\text{H}$  NMR, 400 MHz,  $\text{CDCl}_3$



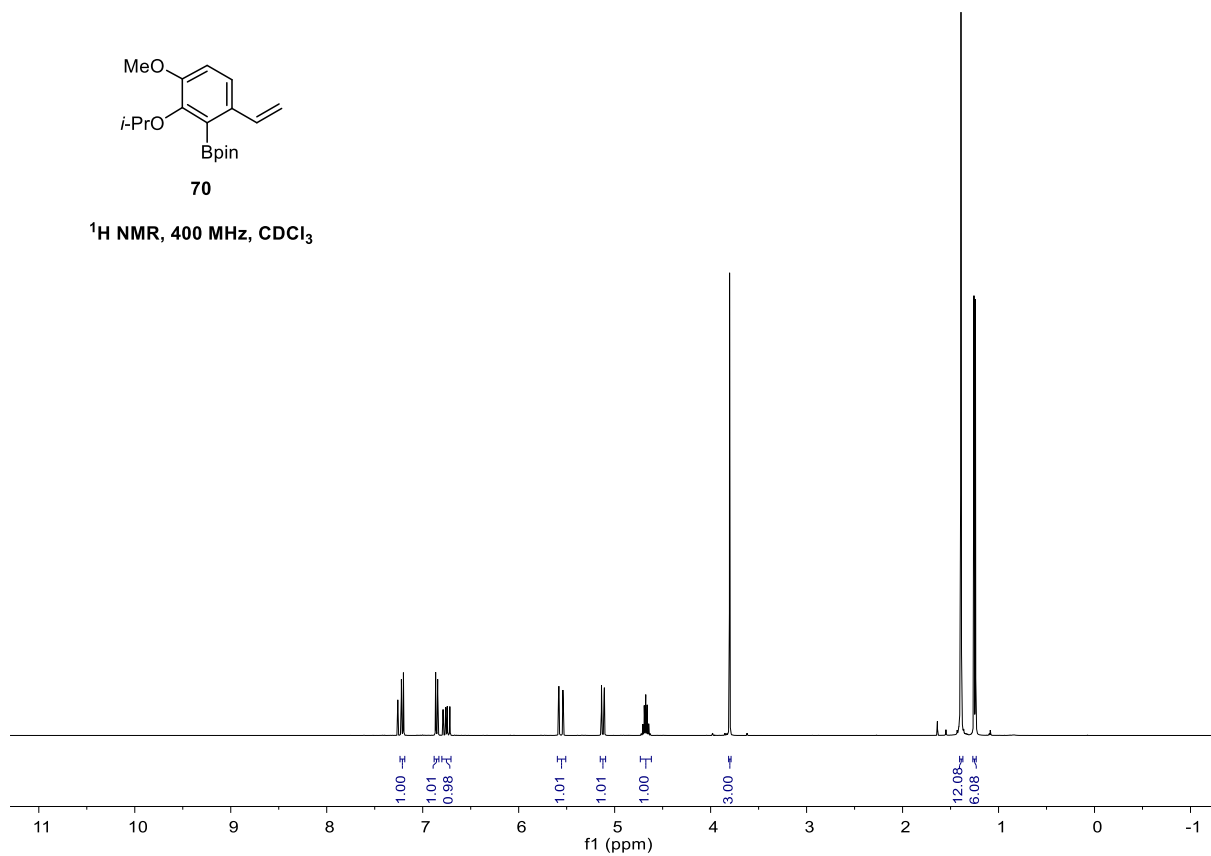
$^{13}\text{C}$  NMR, 100 MHz,  $\text{CDCl}_3$



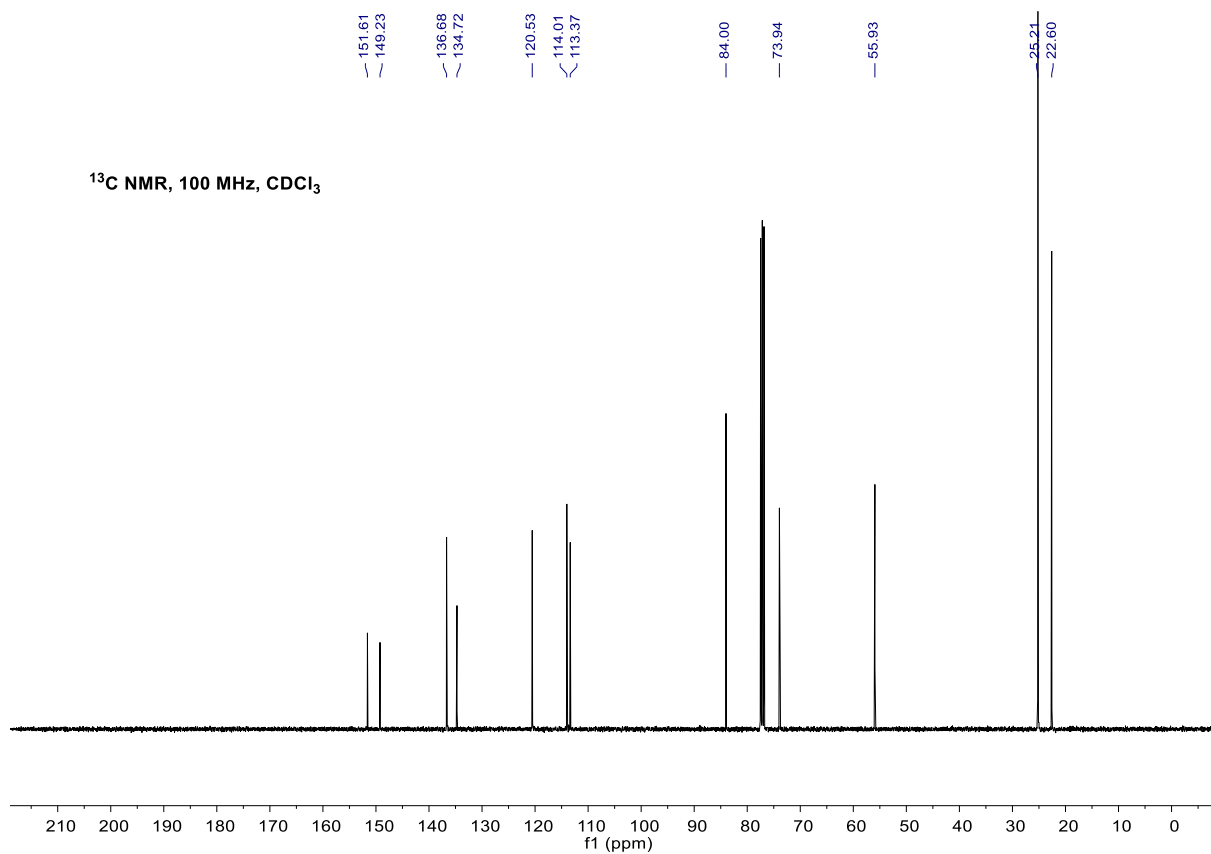


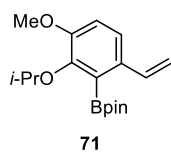
70

<sup>1</sup>H NMR, 400 MHz, CDCl<sub>3</sub>

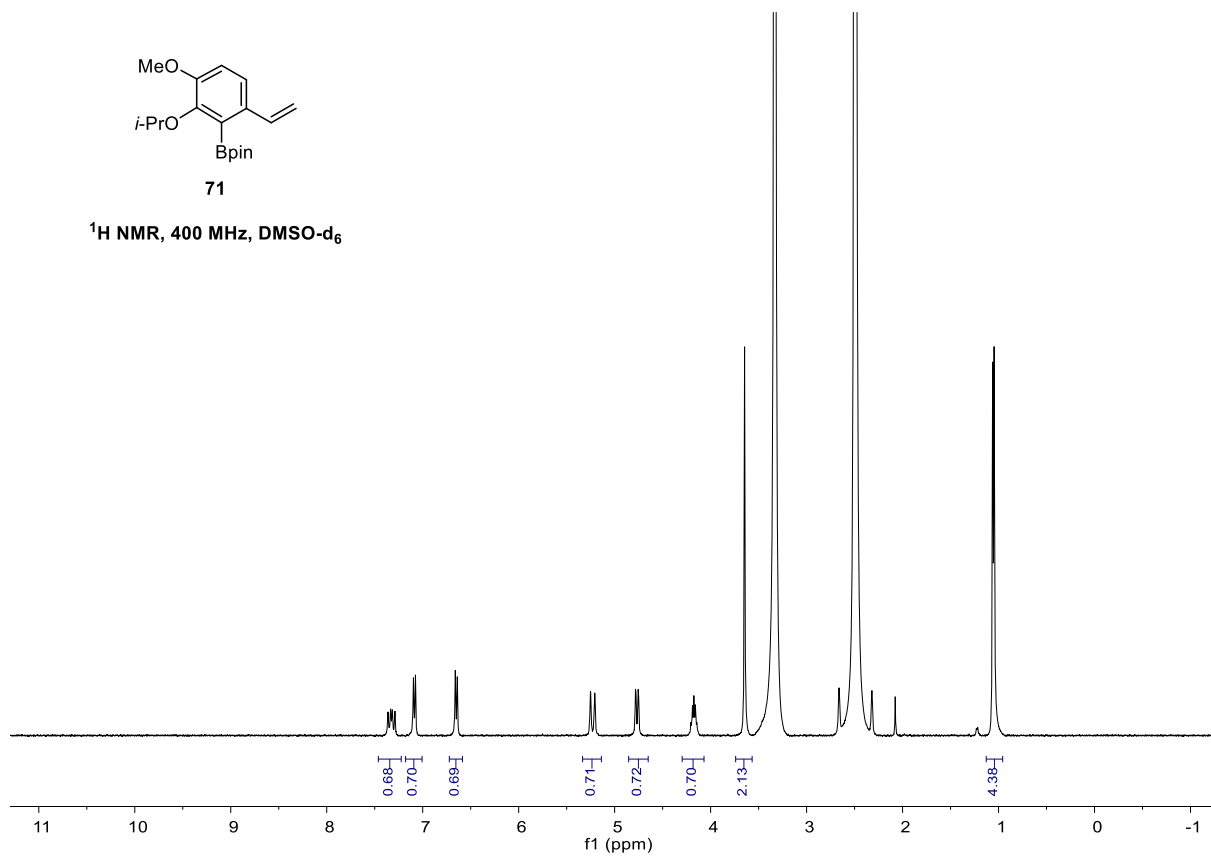


<sup>13</sup>C NMR, 100 MHz, CDCl<sub>3</sub>

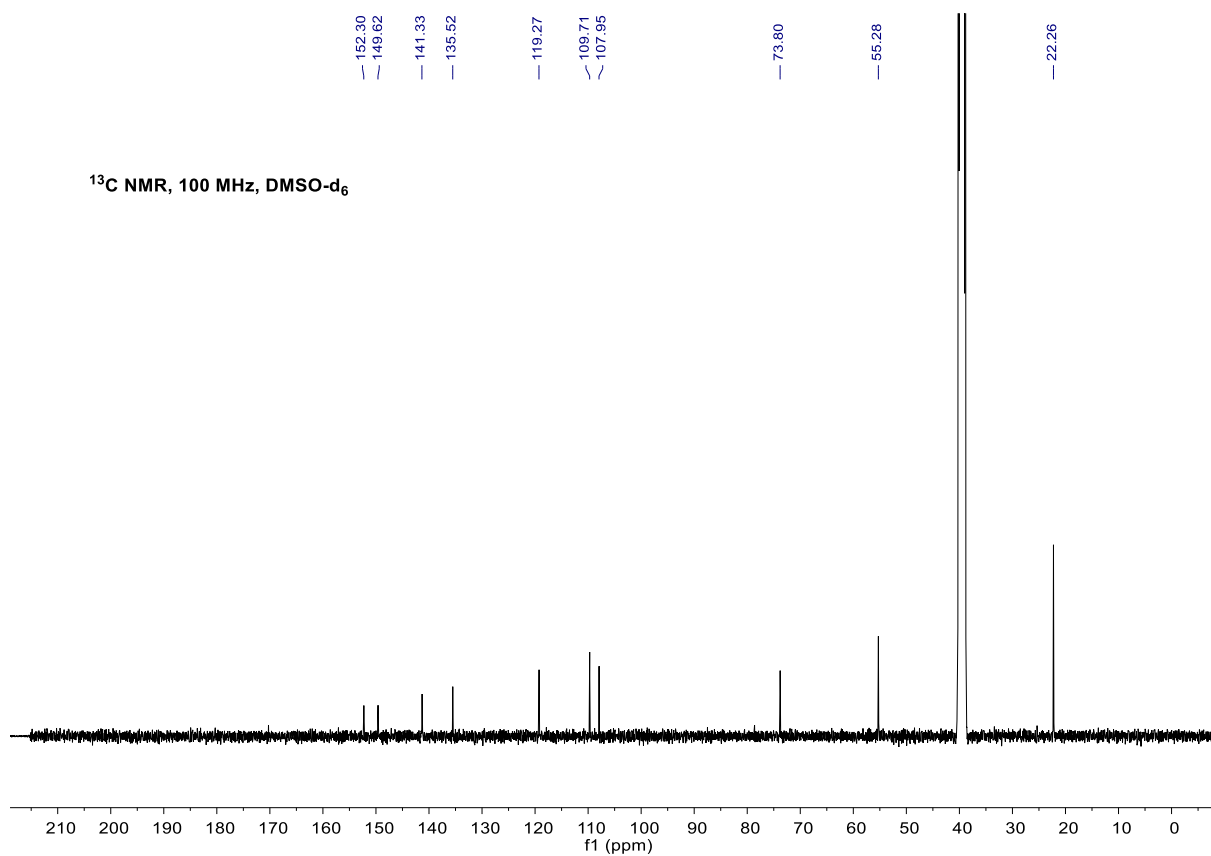


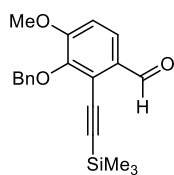


$^1\text{H}$  NMR, 400 MHz,  $\text{DMSO-d}_6$



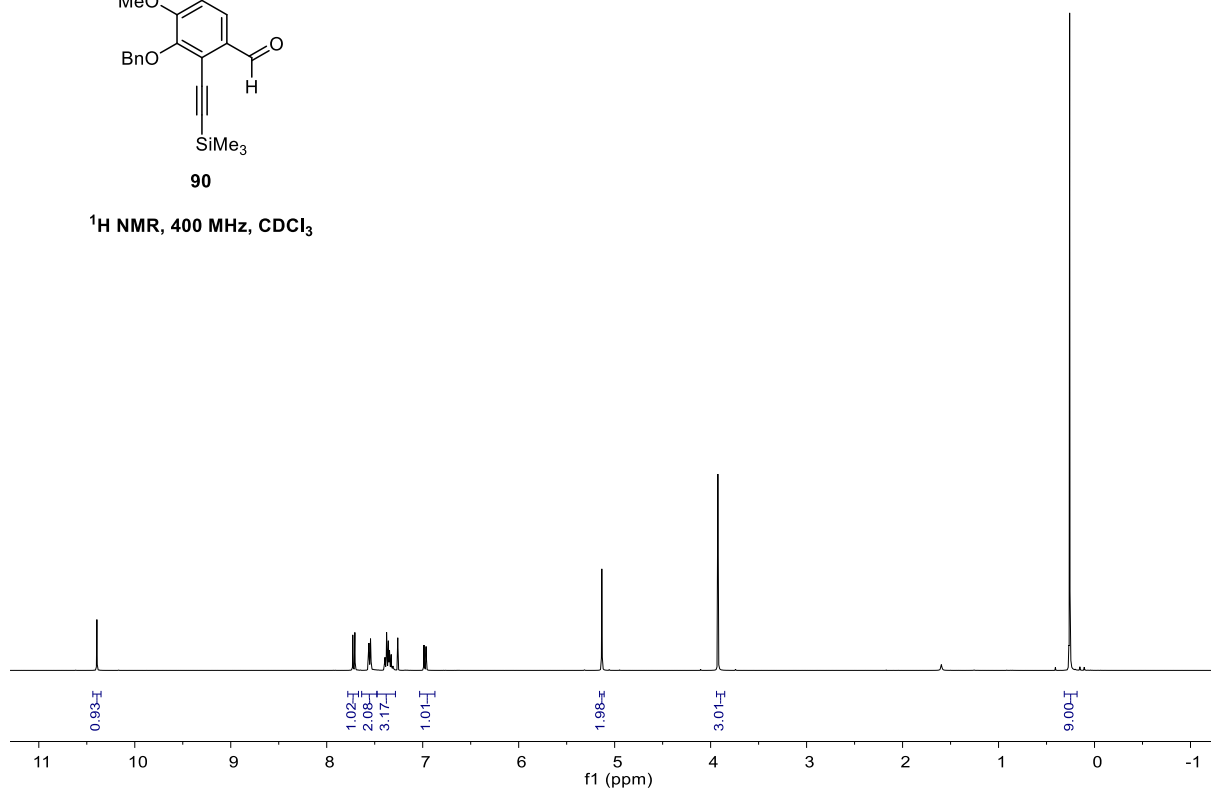
$^{13}\text{C}$  NMR, 100 MHz,  $\text{DMSO-d}_6$



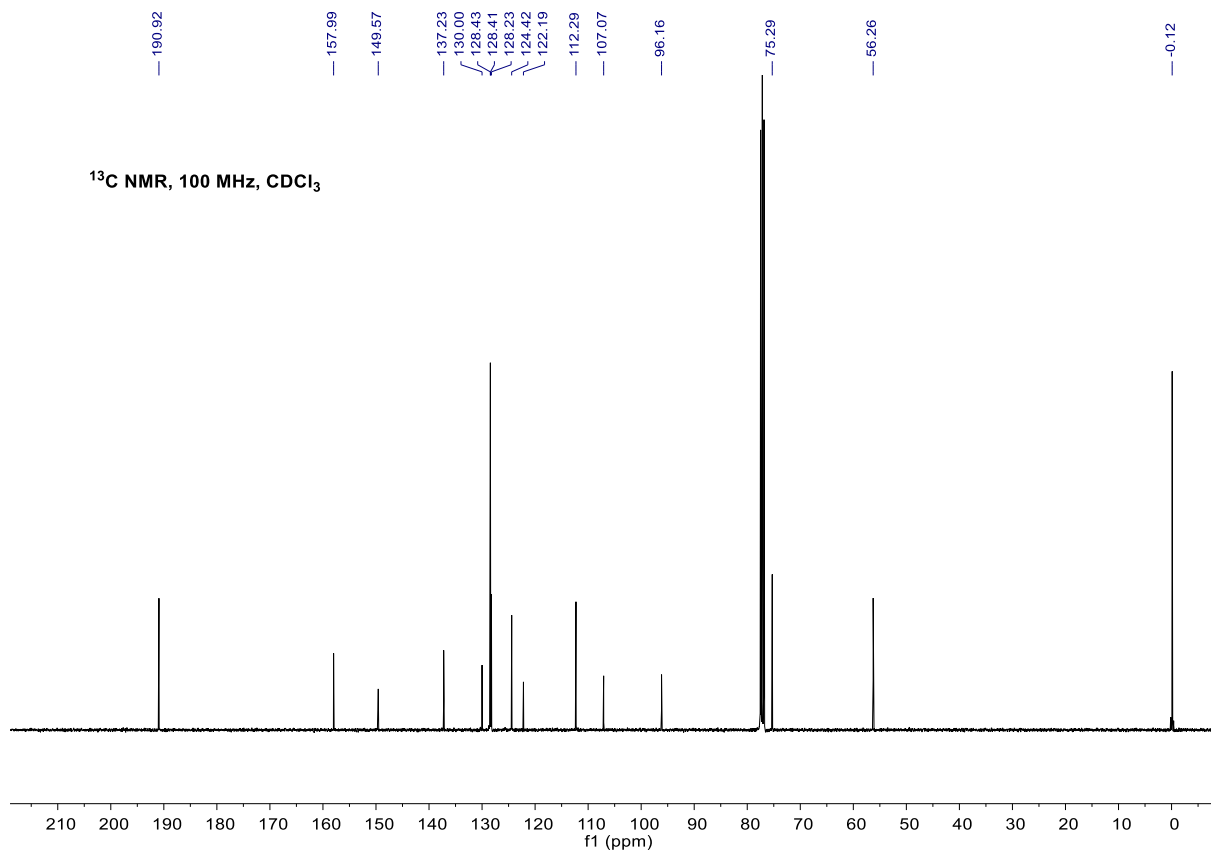


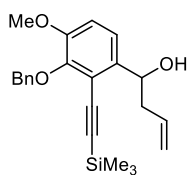
90

<sup>1</sup>H NMR, 400 MHz, CDCl<sub>3</sub>

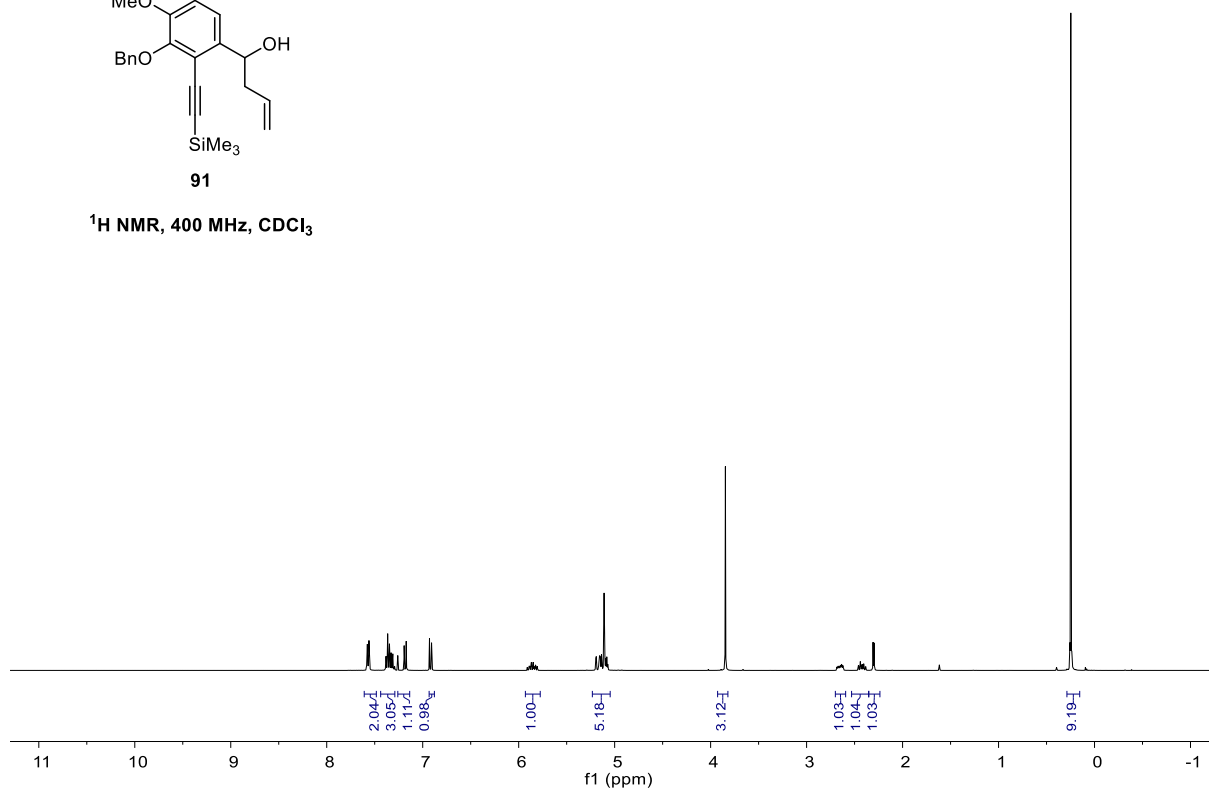


<sup>13</sup>C NMR, 100 MHz, CDCl<sub>3</sub>



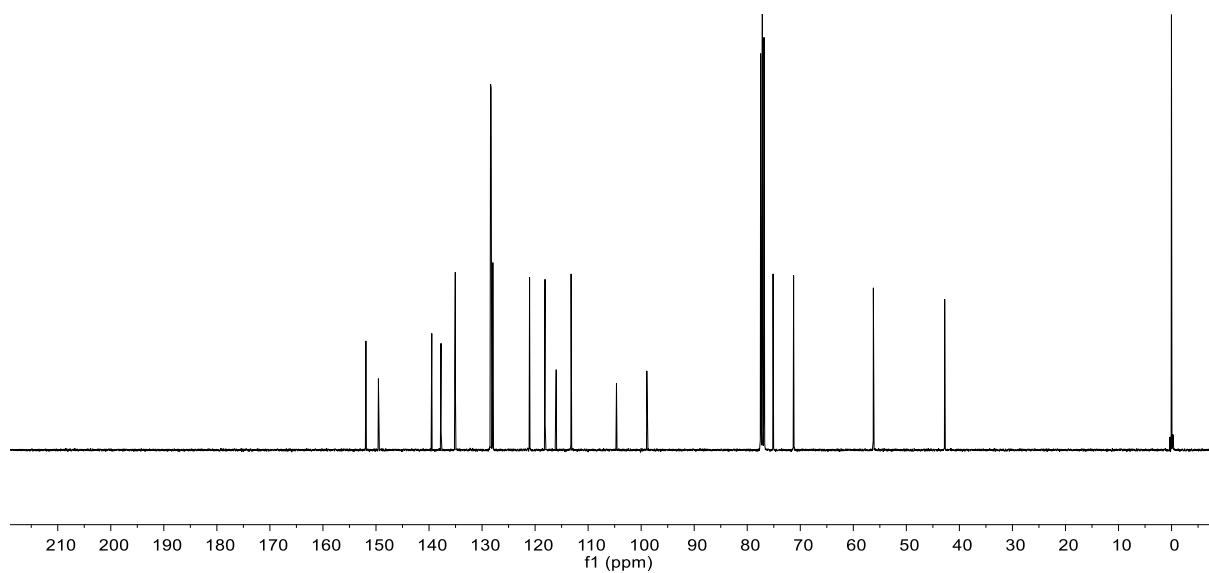


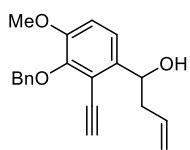
91

 $^1\text{H}$  NMR, 400 MHz,  $\text{CDCl}_3$ 

Chemical shift values (ppm) for  $^{13}\text{C}$  NMR spectrum:

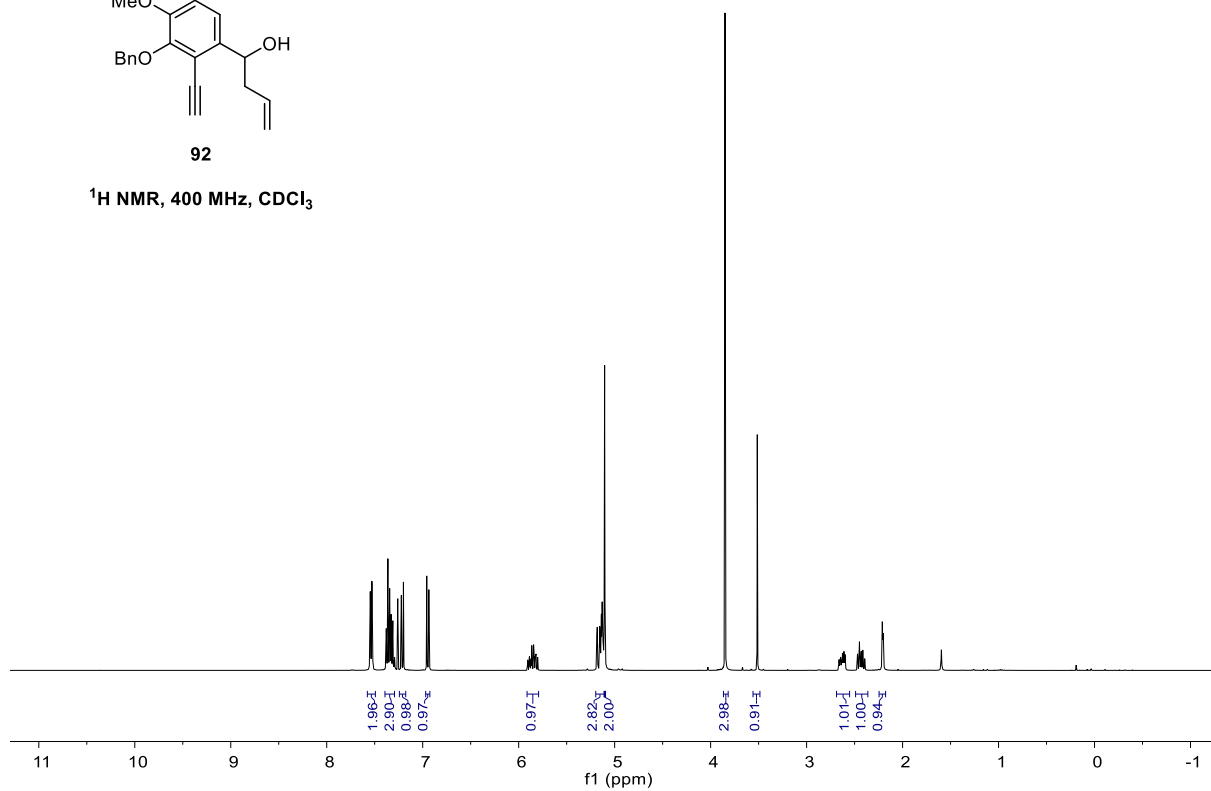
- 151.90
- 149.54
- 139.48
- 137.74
- 135.05
- 128.40
- 127.96
- 121.04
- 118.12
- 116.02
- 113.21
- 104.65
- 98.94
- 75.13
- 71.26
- 56.22
- 42.77
- 0.02

 $^{13}\text{C}$  NMR, 100 MHz,  $\text{CDCl}_3$ 

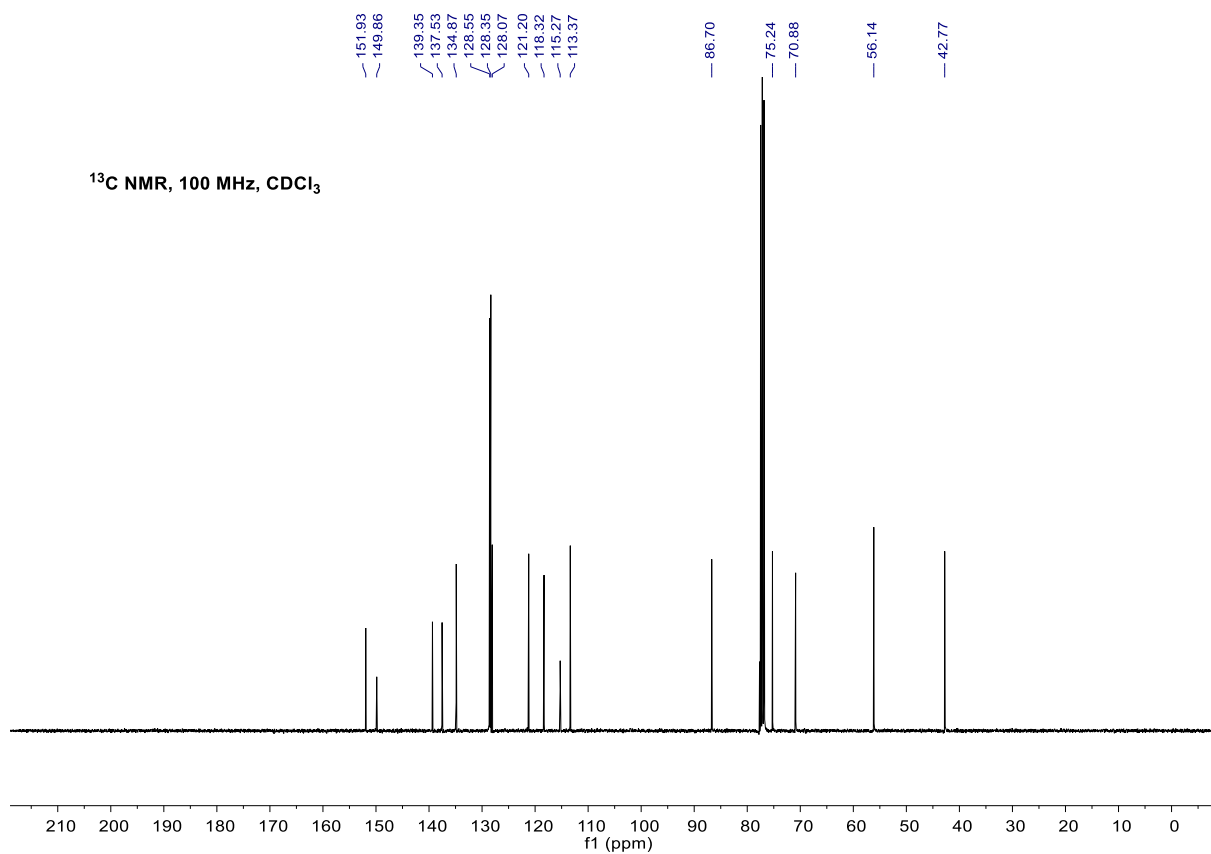


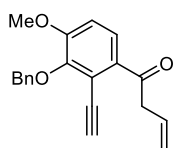
92

$^1\text{H}$  NMR, 400 MHz,  $\text{CDCl}_3$

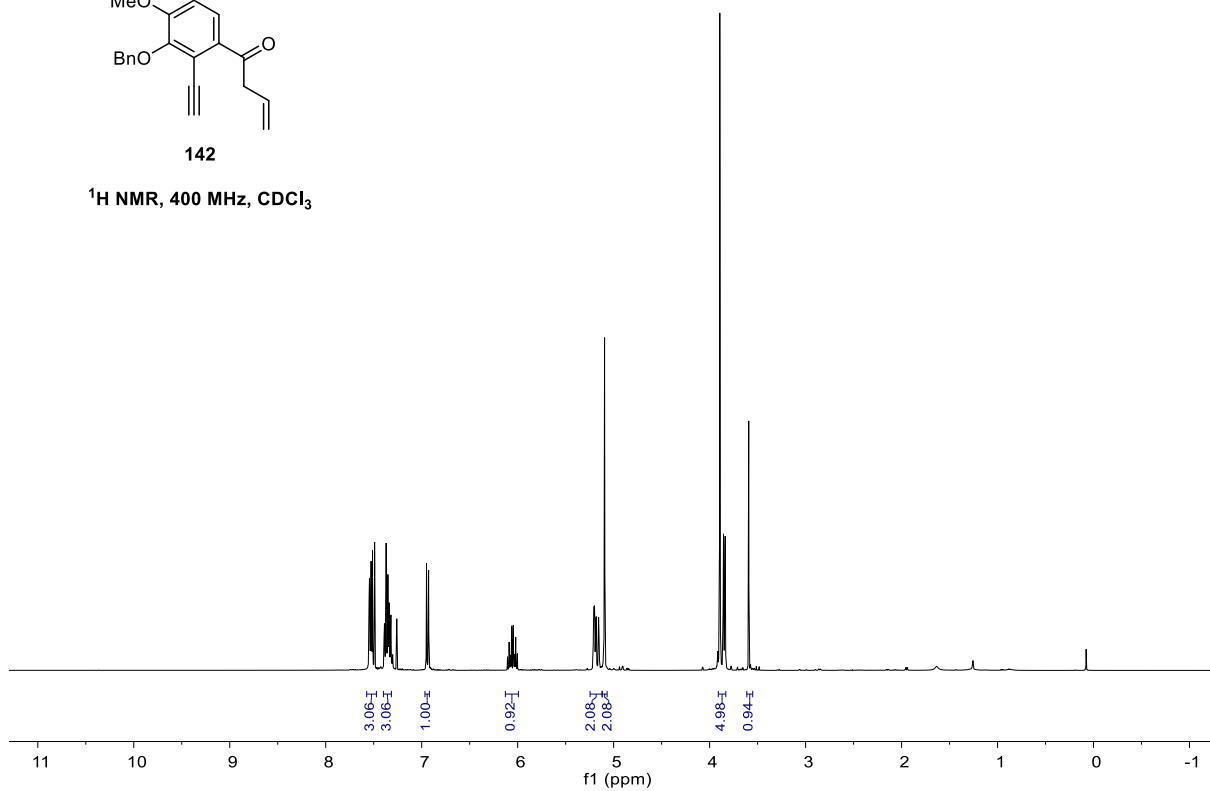
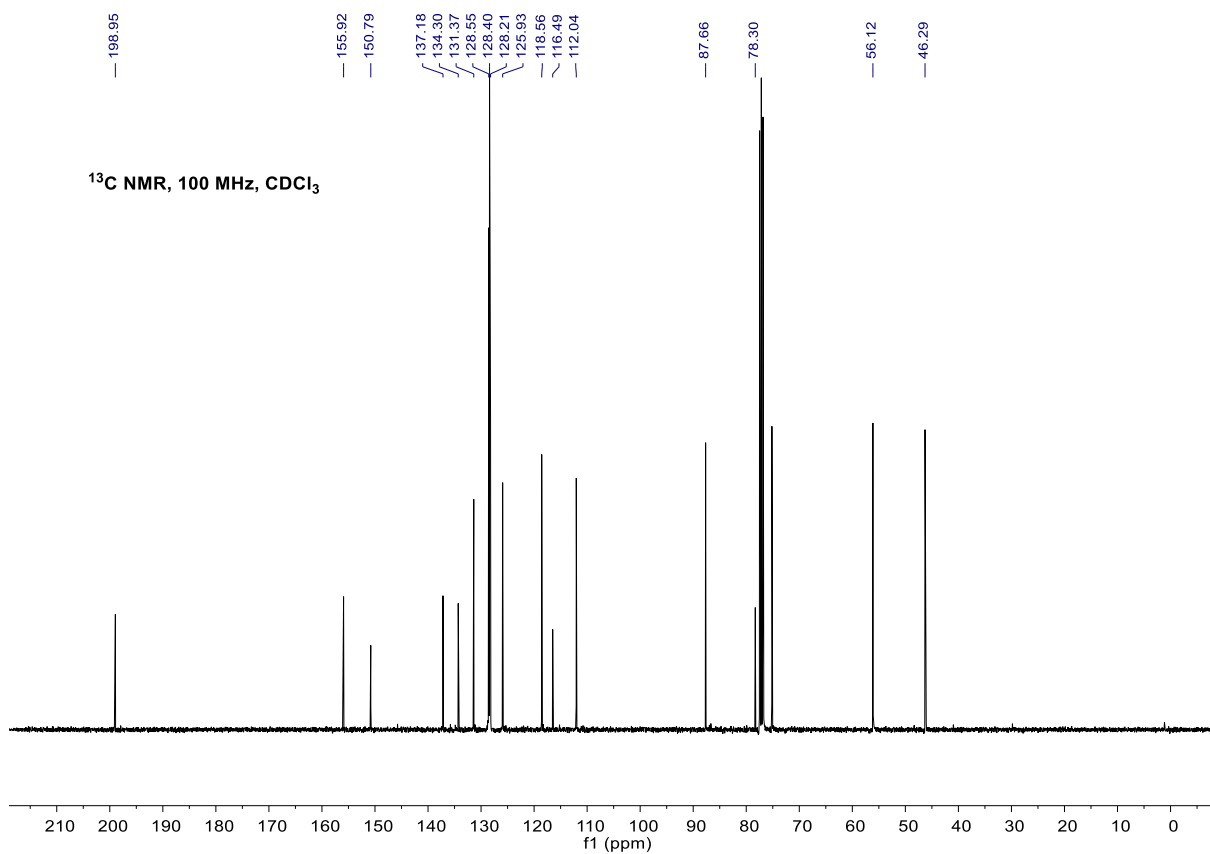


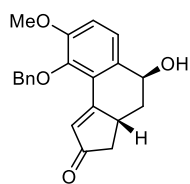
$^{13}\text{C}$  NMR, 100 MHz,  $\text{CDCl}_3$





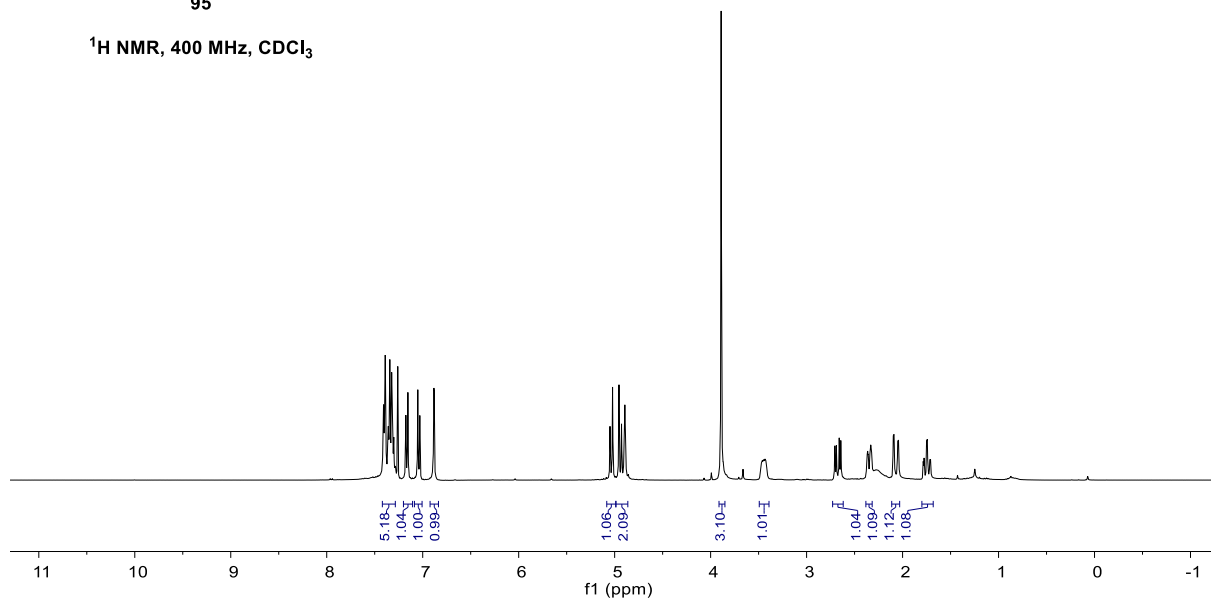
142

 $^1\text{H}$  NMR, 400 MHz,  $\text{CDCl}_3$  $^{13}\text{C}$  NMR, 100 MHz,  $\text{CDCl}_3$ 

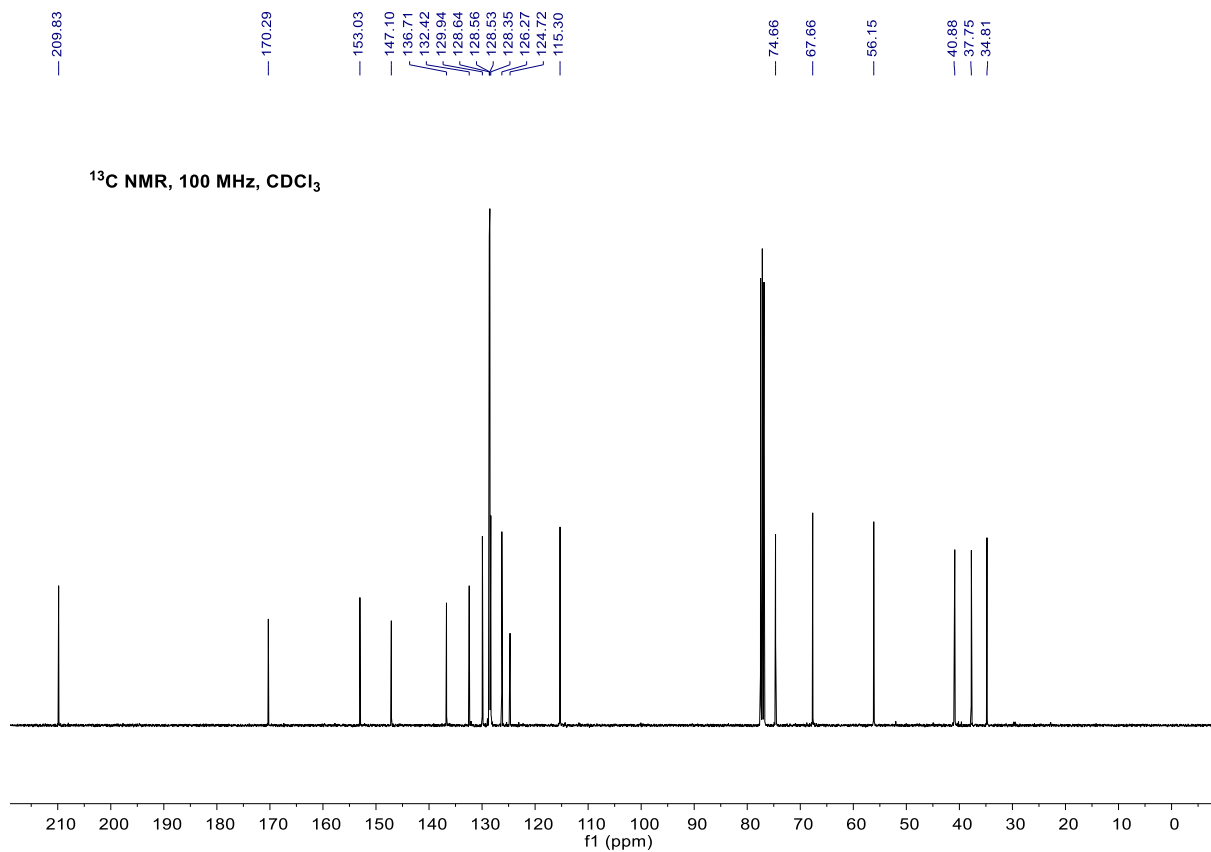


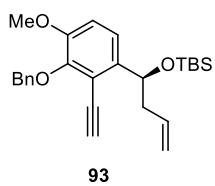
95

$^1\text{H}$  NMR, 400 MHz,  $\text{CDCl}_3$

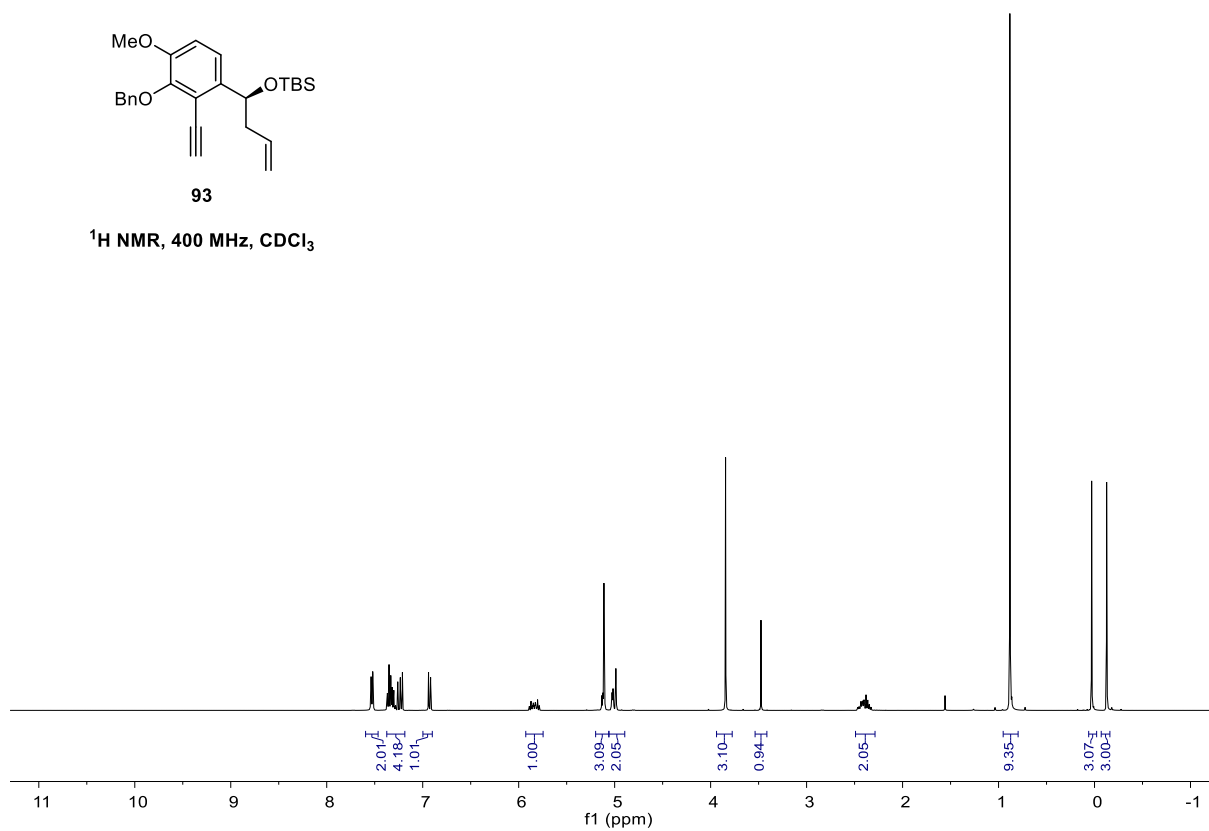
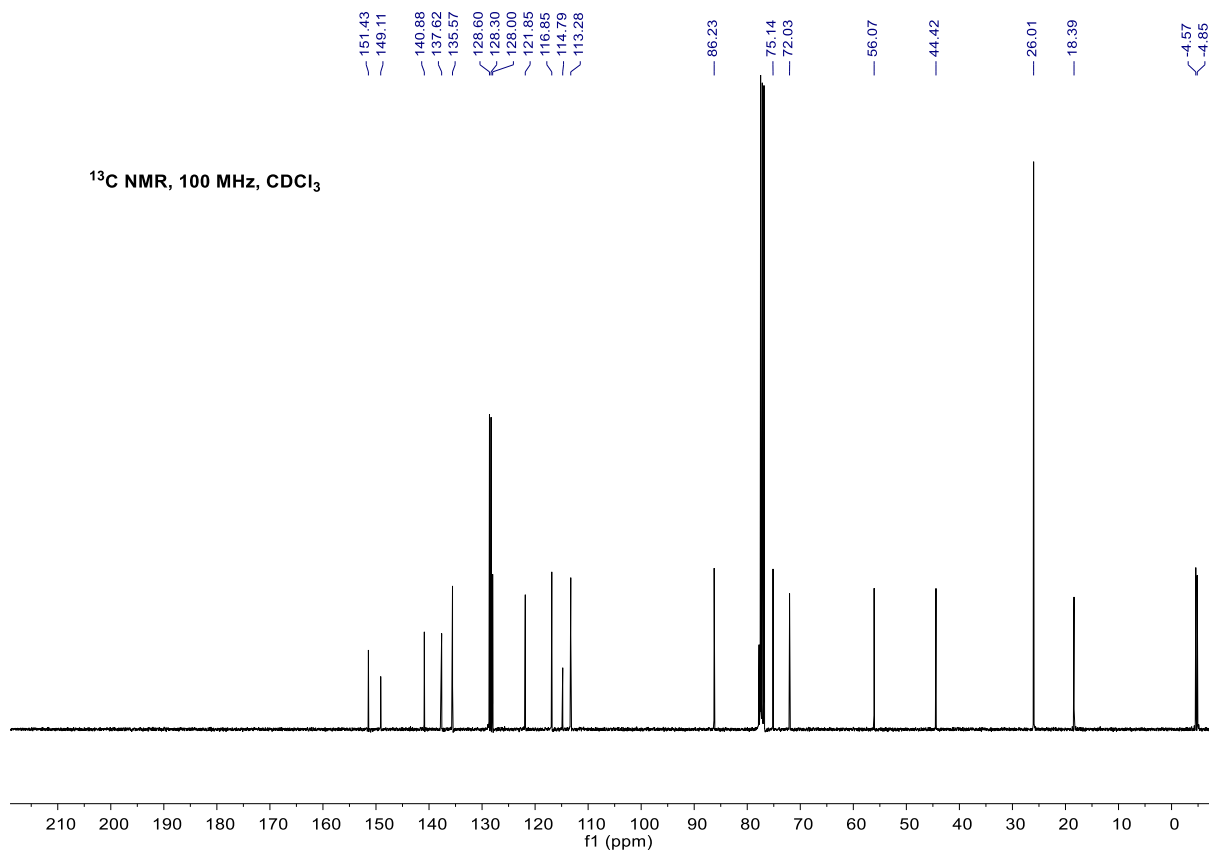


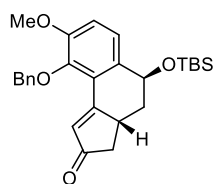
$^{13}\text{C}$  NMR, 100 MHz,  $\text{CDCl}_3$





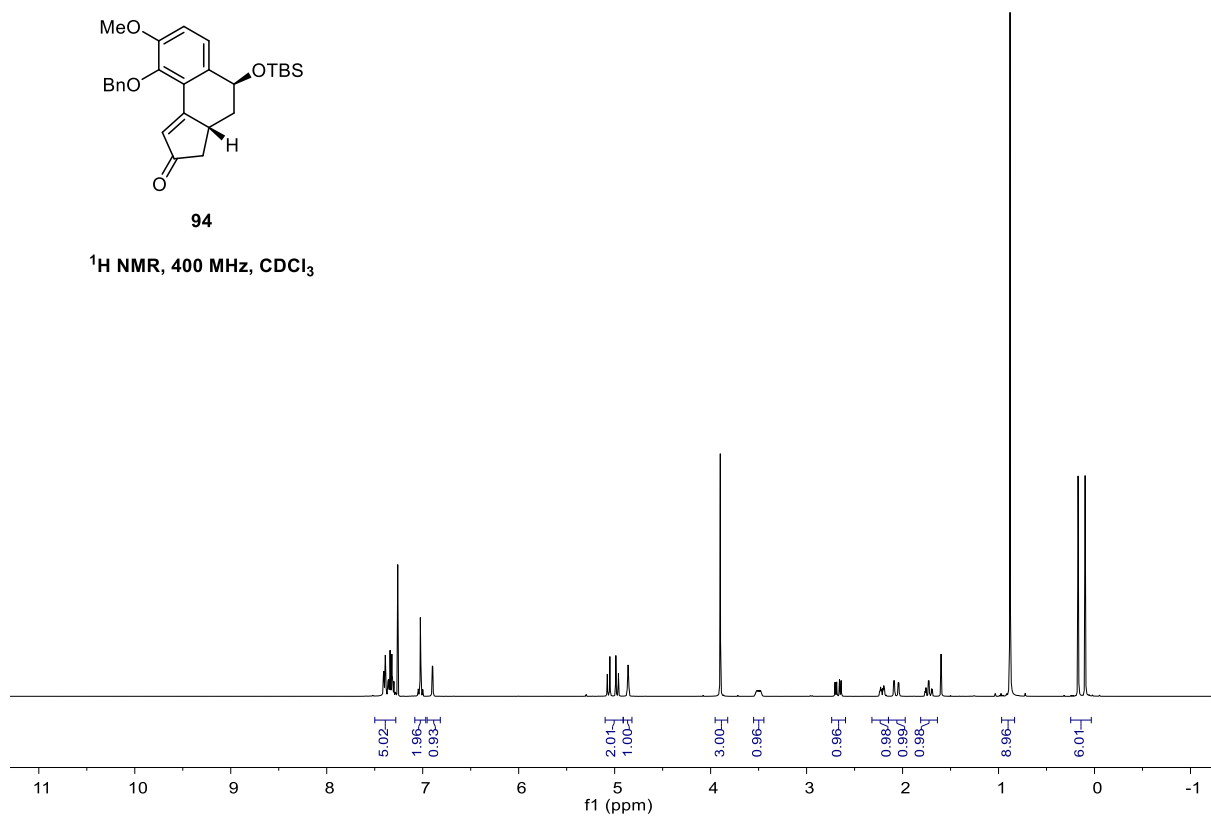
93

 $^1\text{H}$  NMR, 400 MHz,  $\text{CDCl}_3$  $^{13}\text{C}$  NMR, 100 MHz,  $\text{CDCl}_3$ 

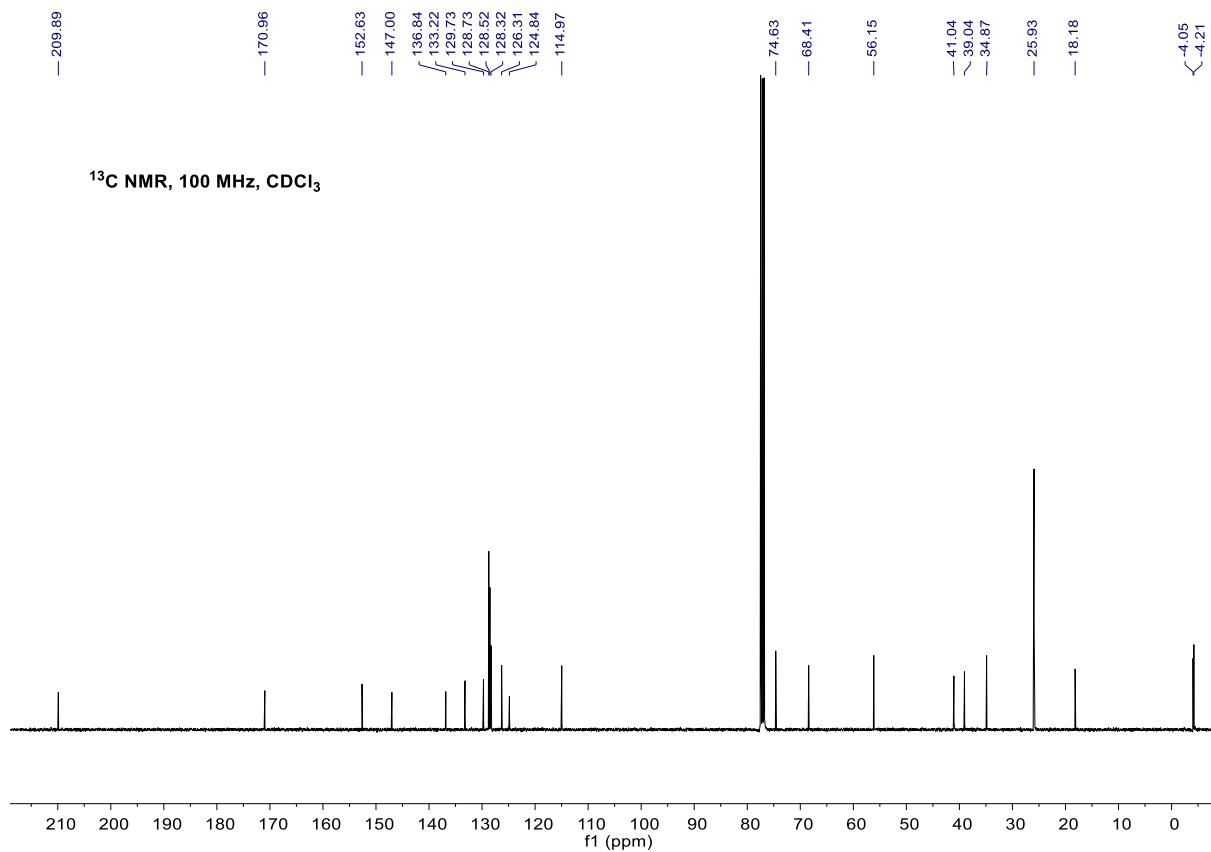


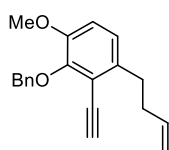
94

$^1\text{H}$  NMR, 400 MHz,  $\text{CDCl}_3$

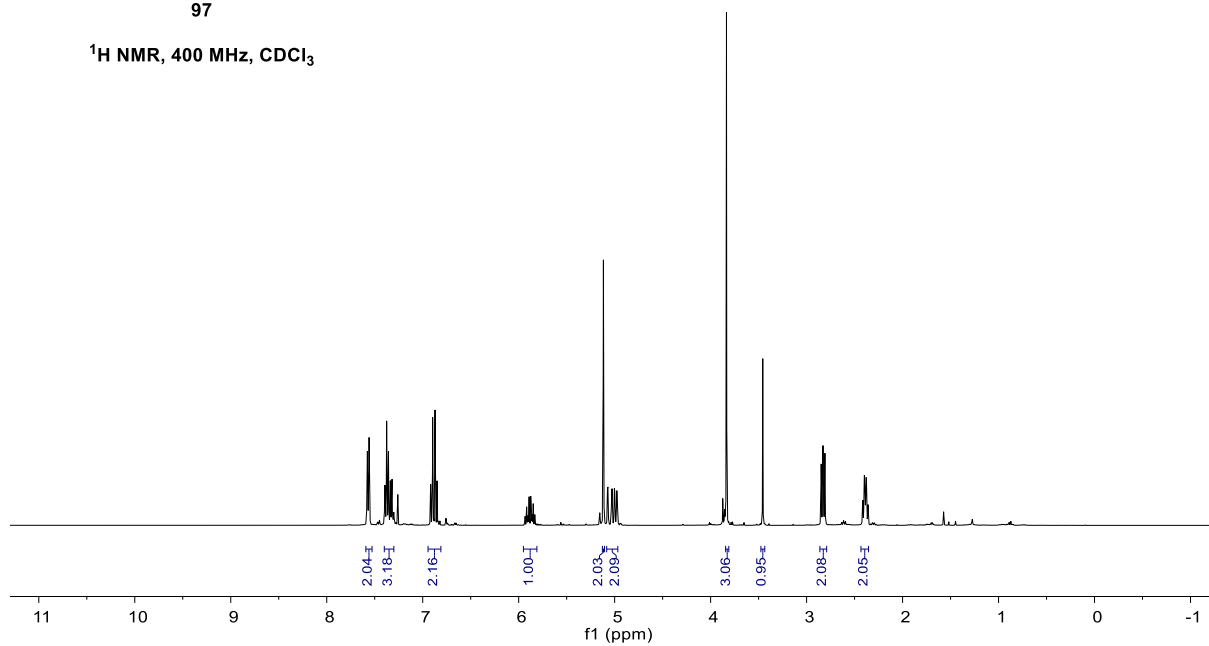


$^{13}\text{C}$  NMR, 100 MHz,  $\text{CDCl}_3$



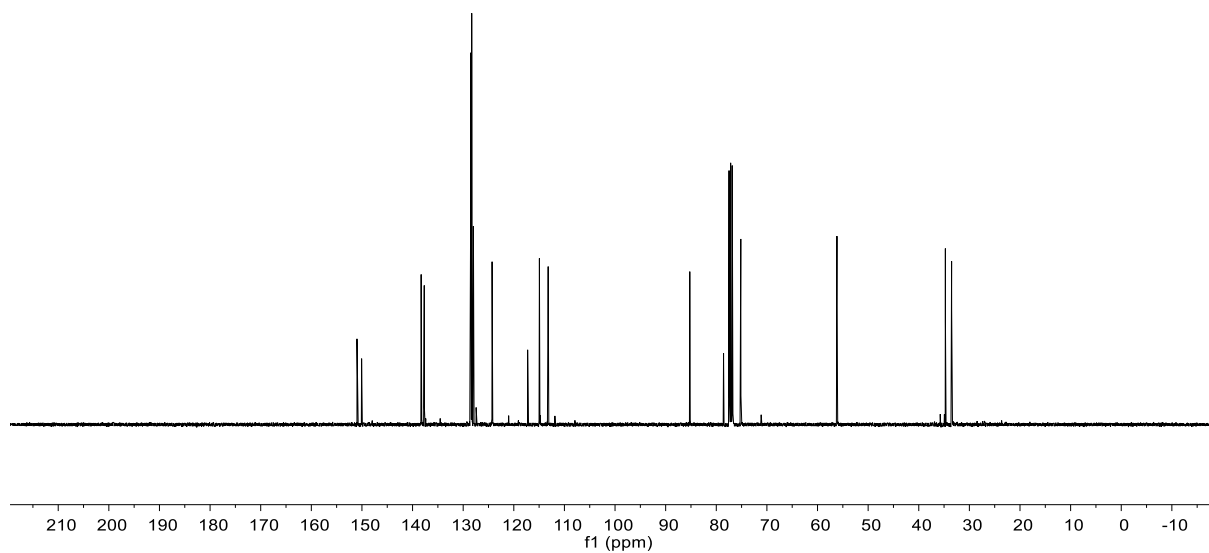


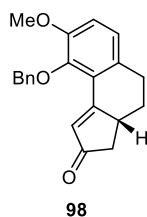
97

 $^1\text{H}$  NMR, 400 MHz,  $\text{CDCl}_3$ 

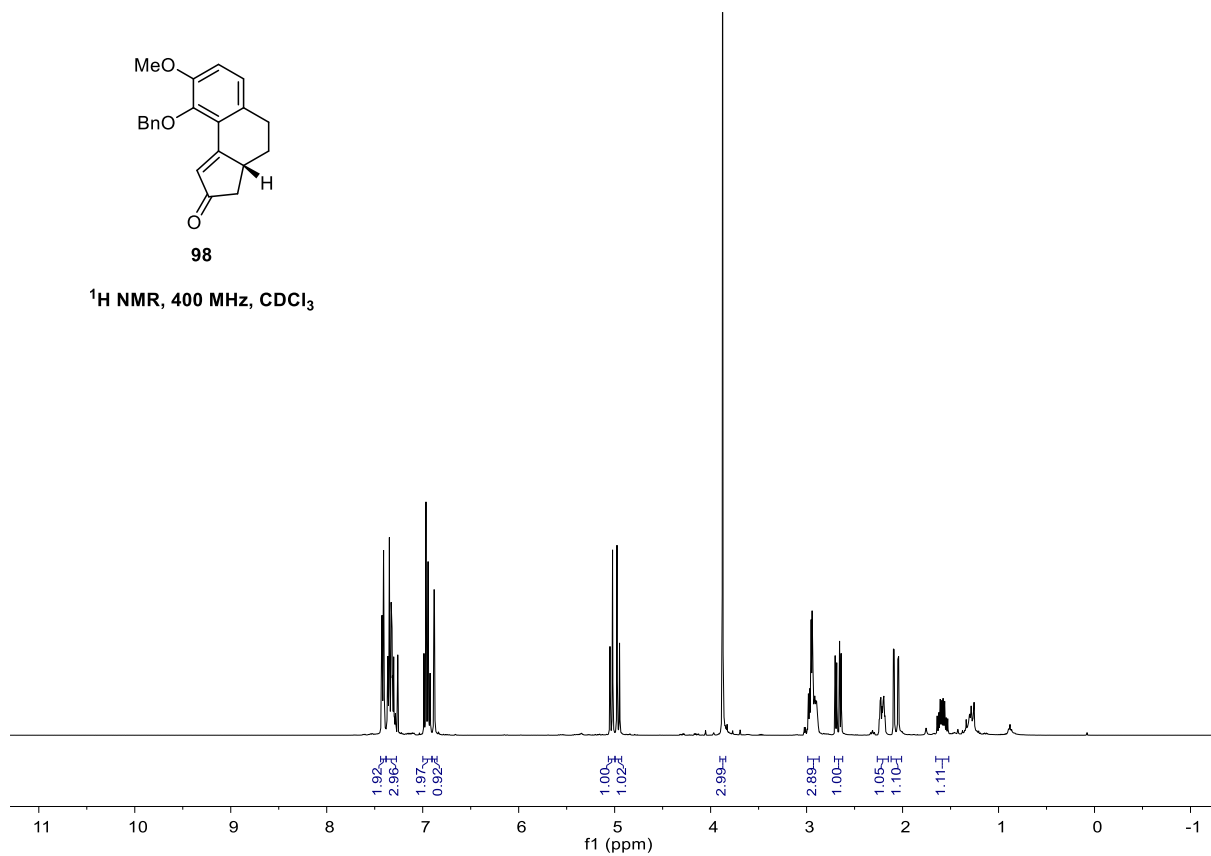
$^{13}\text{C}$  NMR chemical shifts (ppm):

150.98	150.07
138.31	137.68
128.52	128.29
127.98	114.95
113.20	85.22
78.56	75.15
56.16	34.74
33.50	

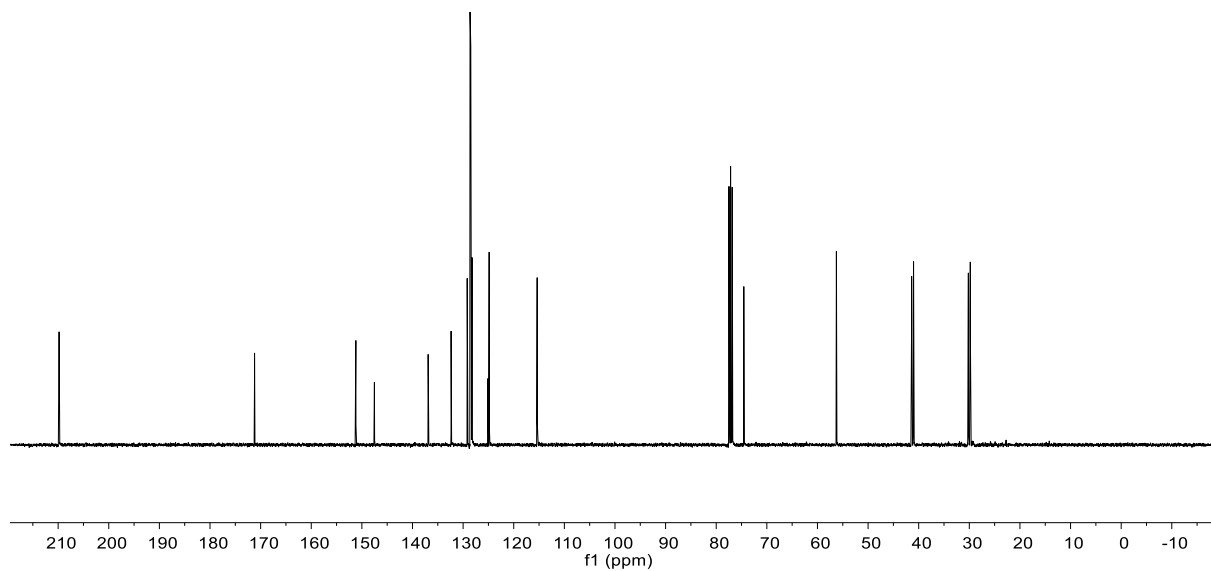
 $^{13}\text{C}$  NMR, 100 MHz,  $\text{CDCl}_3$ 

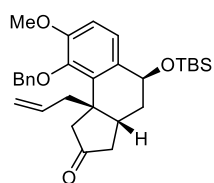


$^1\text{H}$  NMR, 400 MHz,  $\text{CDCl}_3$

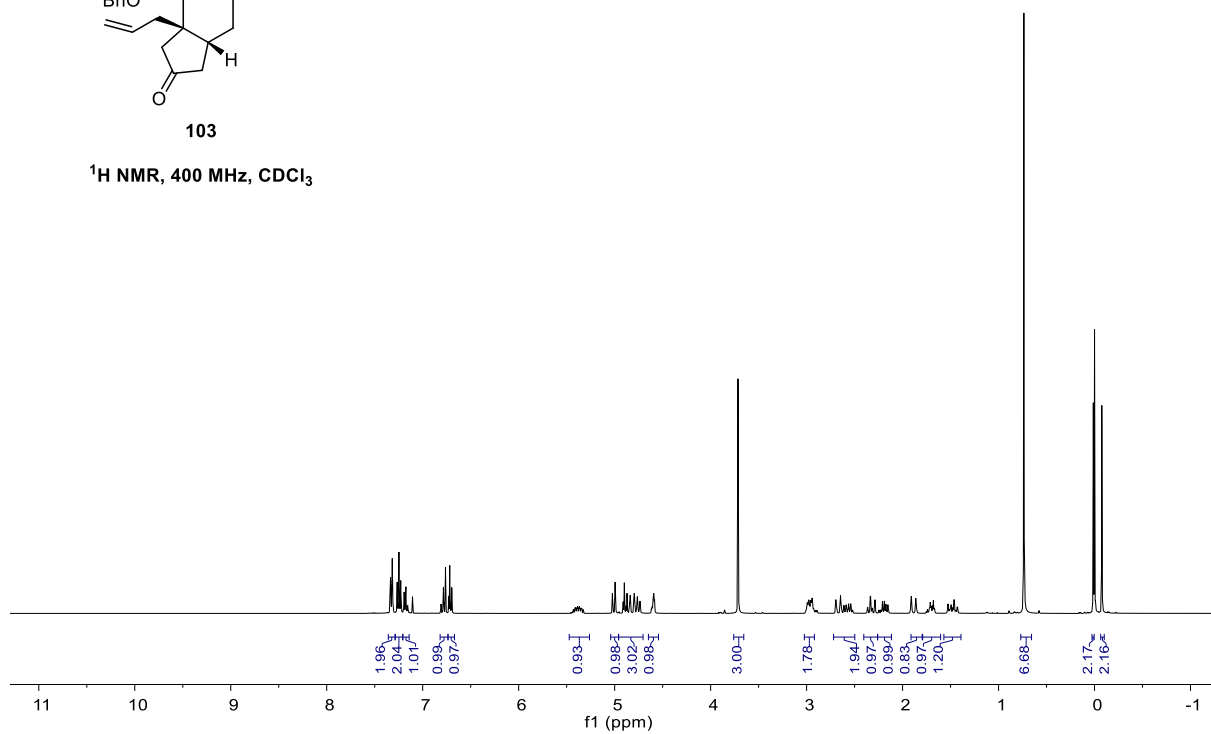


$^{13}\text{C}$  NMR, 100 MHz,  $\text{CDCl}_3$





103

 $^1\text{H}$  NMR, 400 MHz,  $\text{CDCl}_3$ 

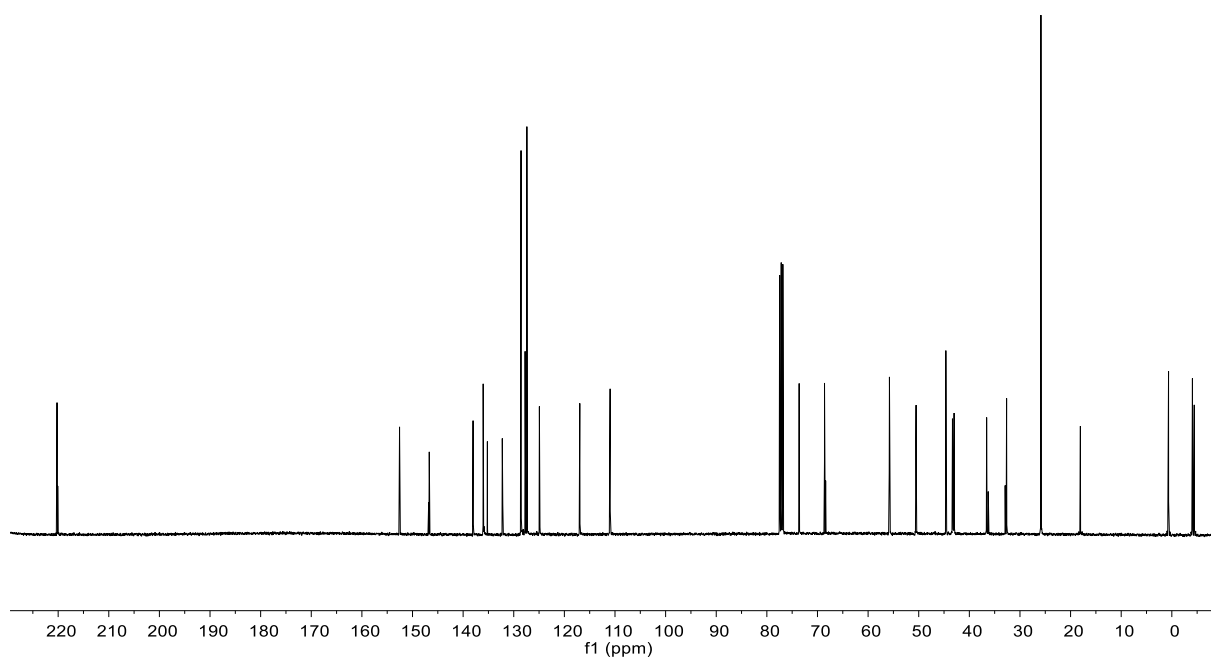
— 220.22

— 152.56  
 — 146.69  
 — 138.04  
 — 136.04  
 — 135.21  
 — 132.26  
 — 128.56  
 — 127.76  
 — 124.94  
 — 116.95  
 — 110.96

— 73.62  
 — 68.61

— 55.83  
 — 55.79  
 — 50.52  
 — 44.66  
 — 44.64  
 — 43.34  
 — 43.01  
 — 36.86  
 — 32.64  
 — 25.86  
 — 18.07

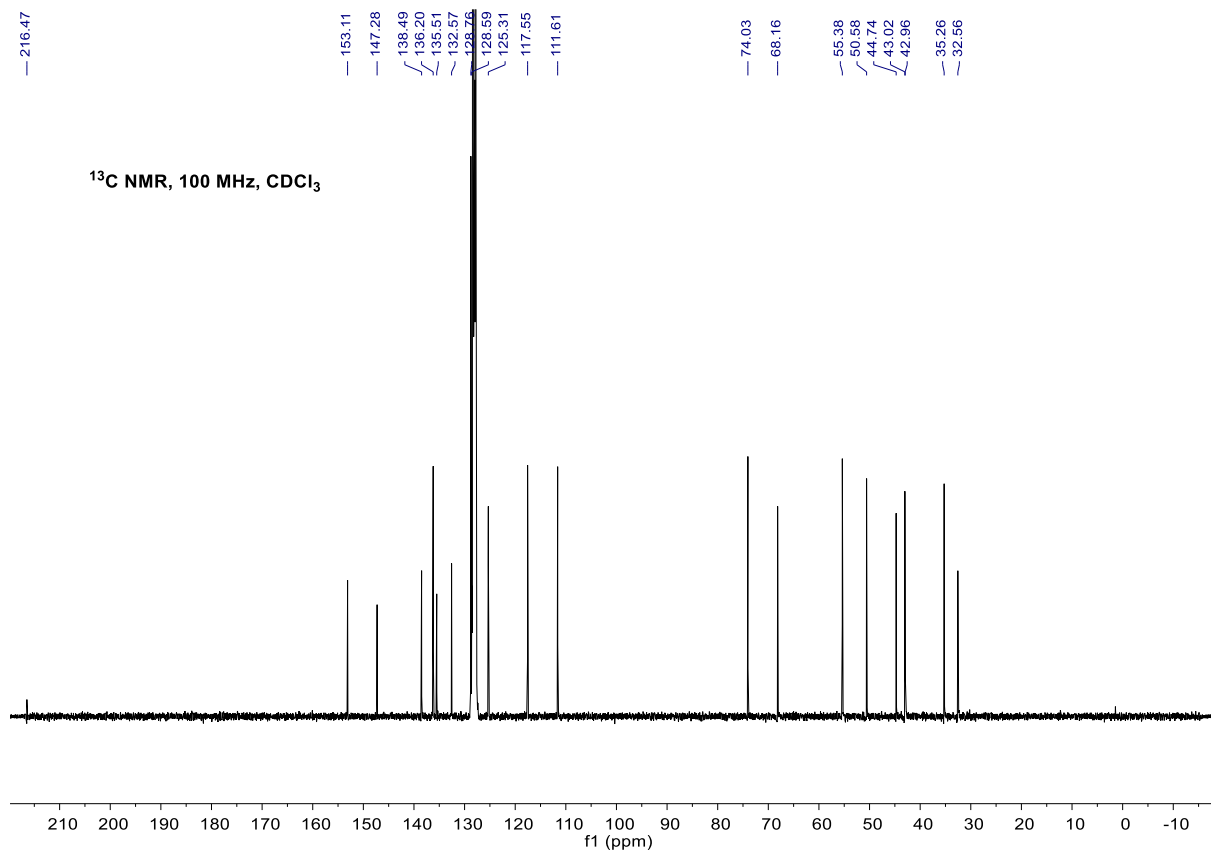
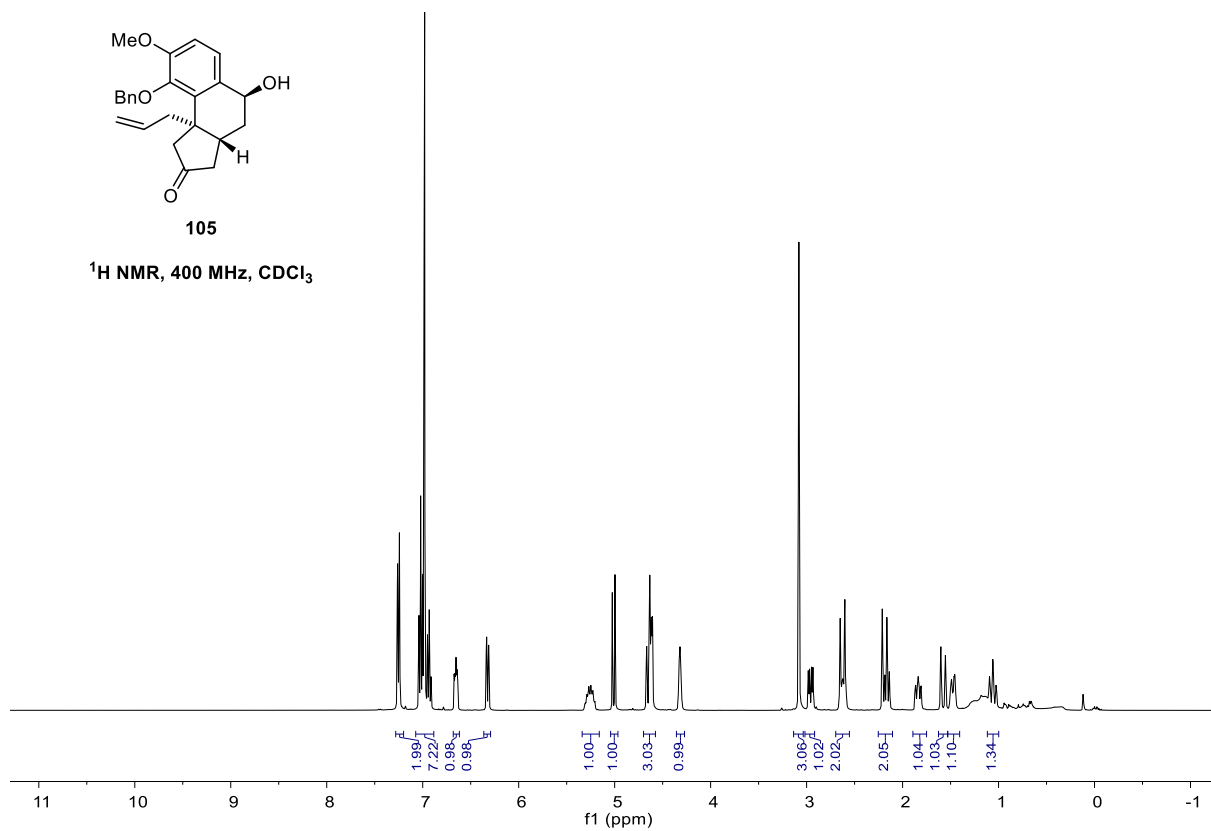
— 0.65  
 — 4.07  
 — 4.43

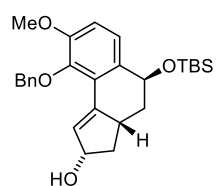
 $^{13}\text{C}$  NMR, 100 MHz,  $\text{CDCl}_3$ 



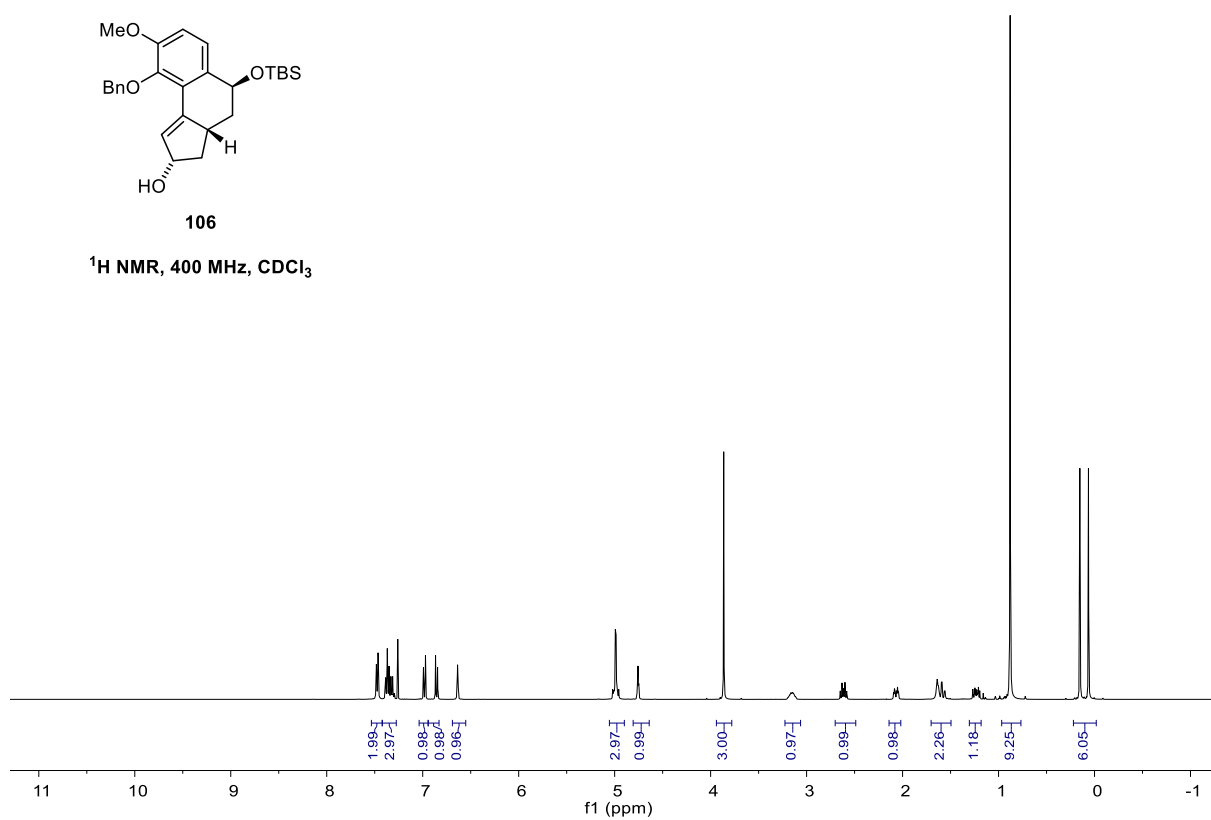
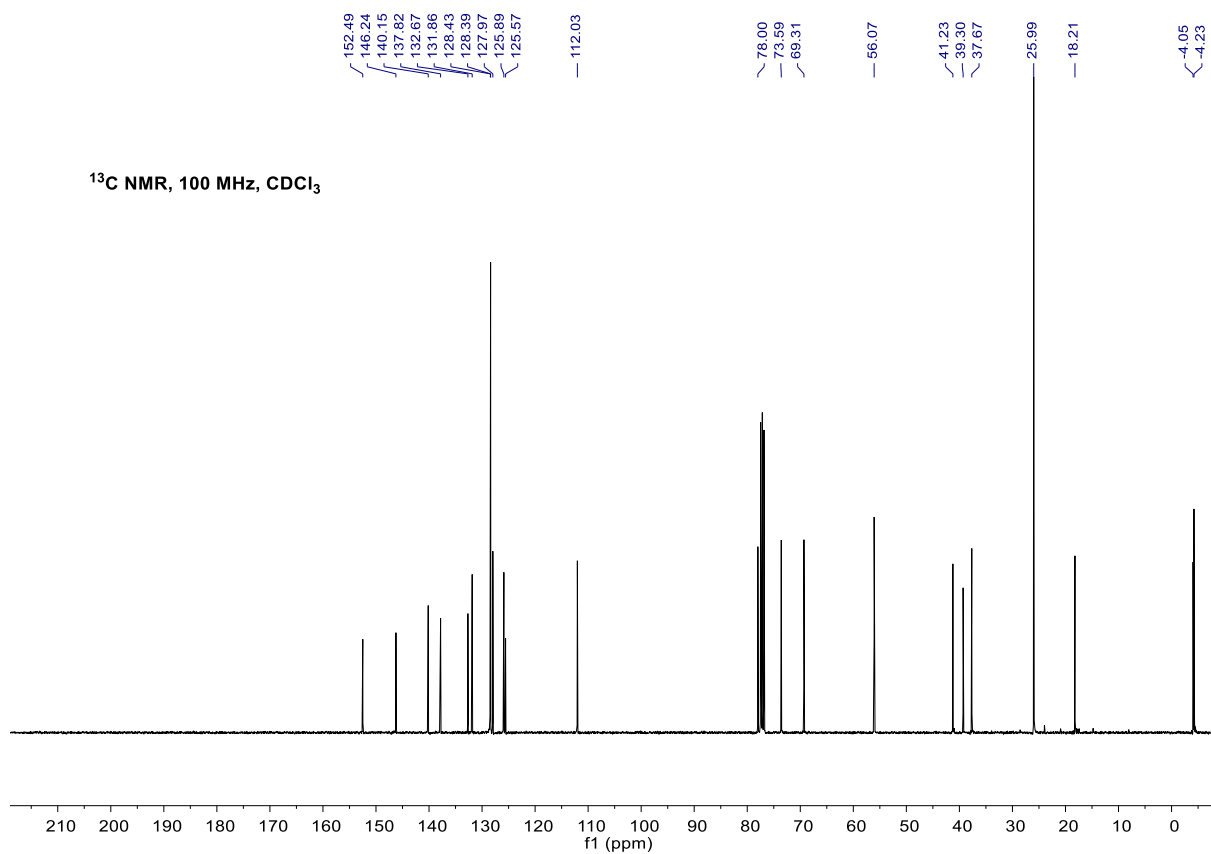
105

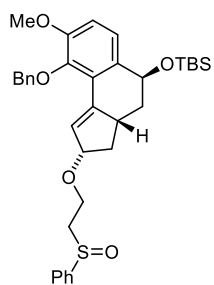
$^1\text{H}$  NMR, 400 MHz,  $\text{CDCl}_3$





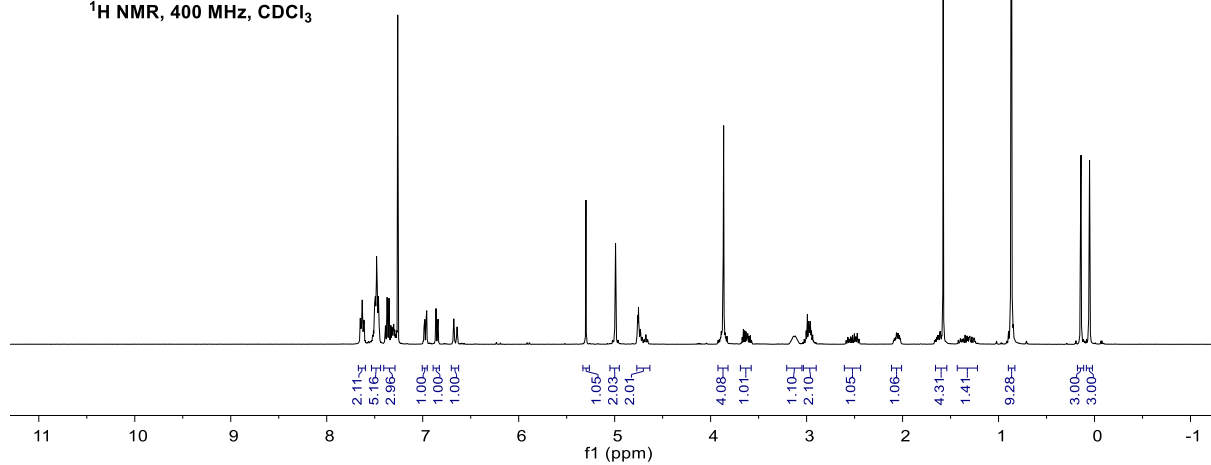
106

 $^1\text{H}$  NMR, 400 MHz,  $\text{CDCl}_3$  $^{13}\text{C}$  NMR, 100 MHz,  $\text{CDCl}_3$ 

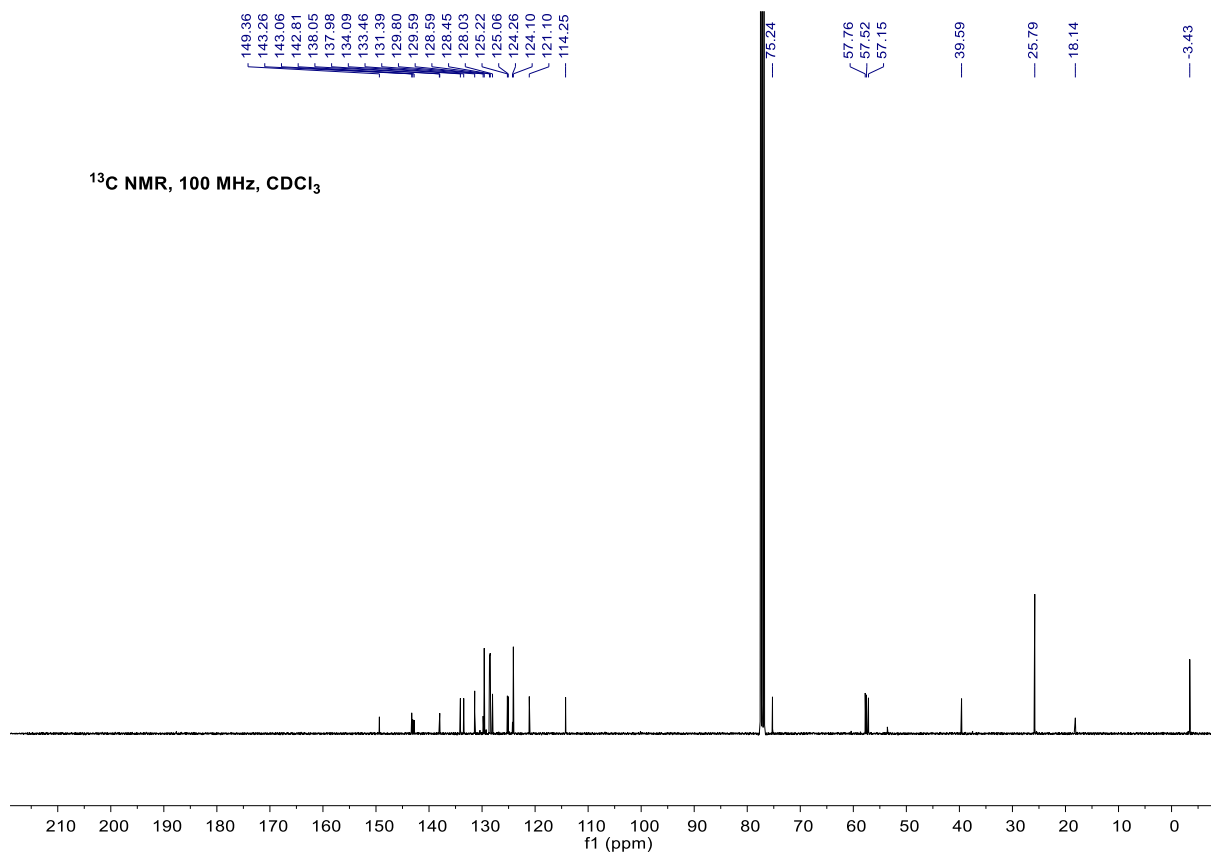


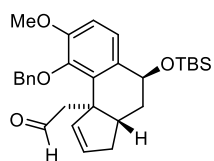
117

<sup>1</sup>H NMR, 400 MHz, CDCl<sub>3</sub>

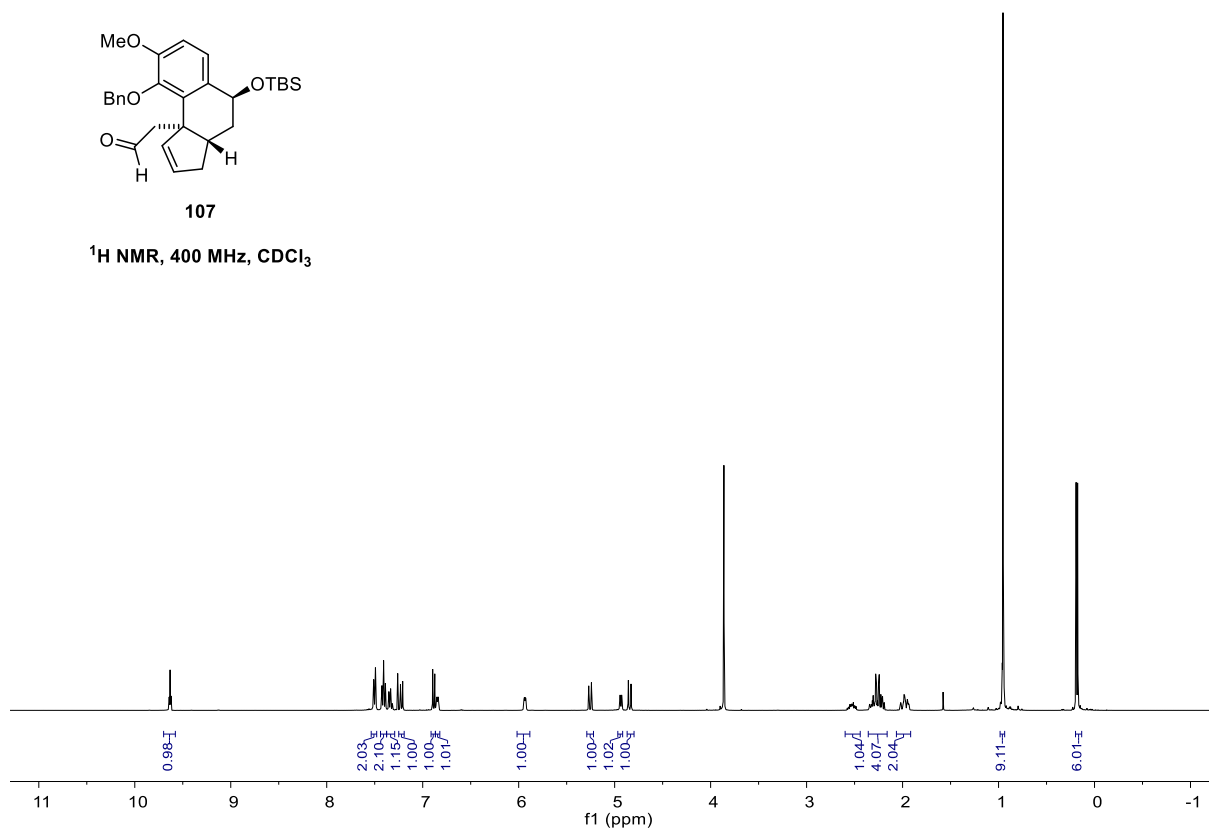


<sup>13</sup>C NMR, 100 MHz, CDCl<sub>3</sub>

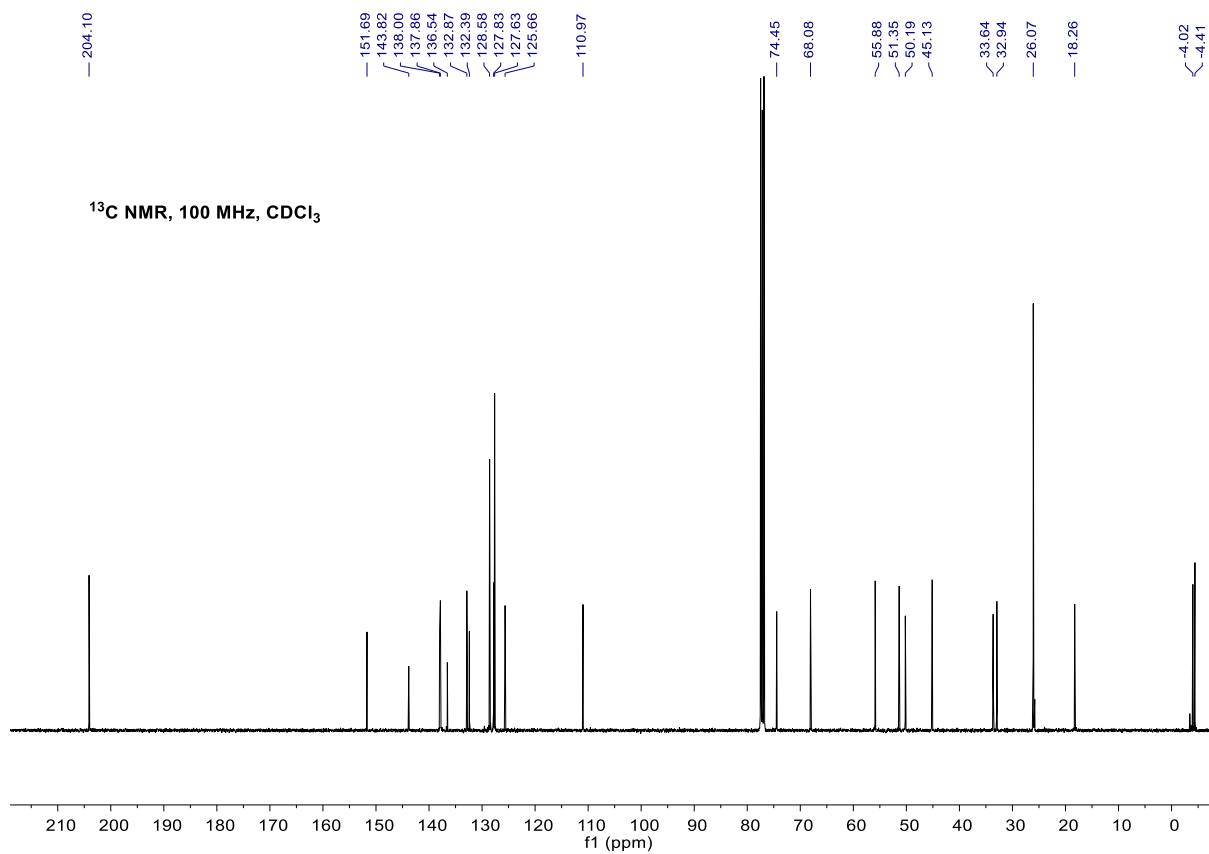


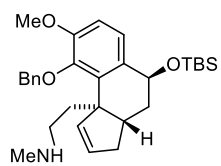


107

 $^1\text{H}$  NMR, 400 MHz,  $\text{CDCl}_3$ 

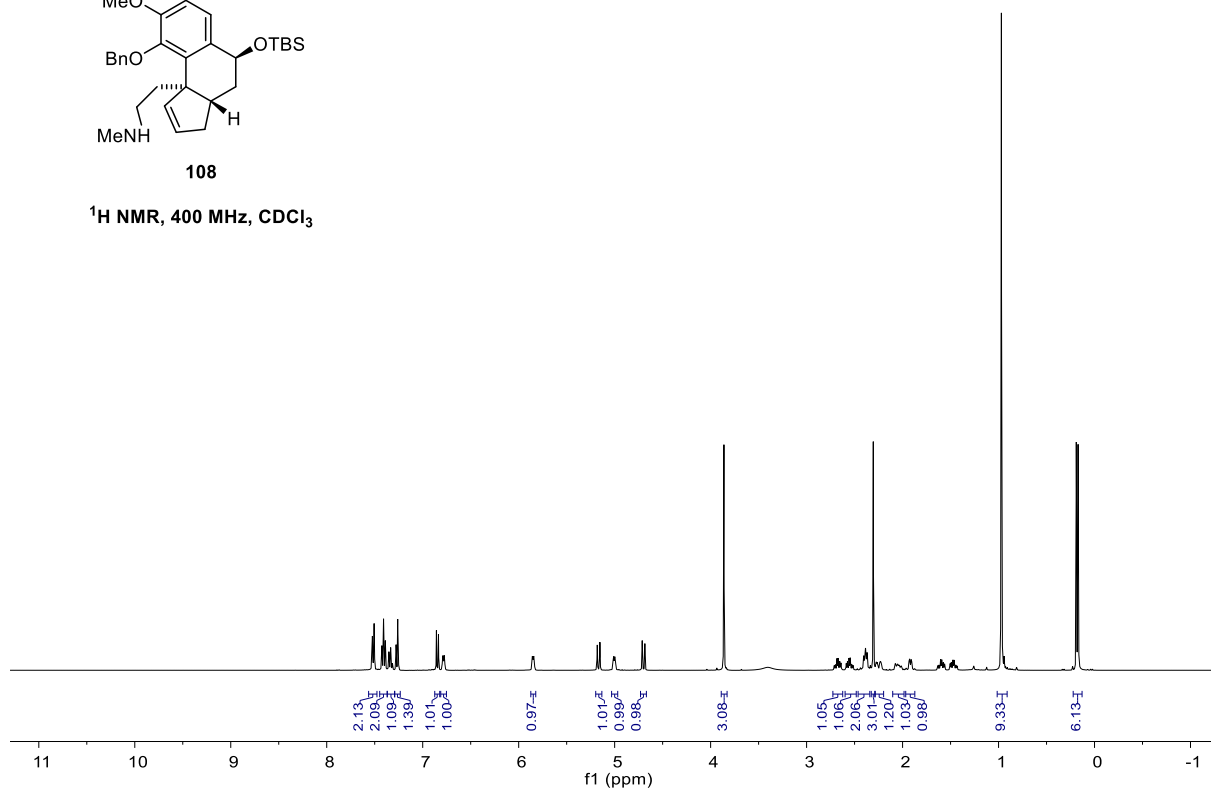
-204.10

 $^{13}\text{C}$  NMR, 100 MHz,  $\text{CDCl}_3$ 

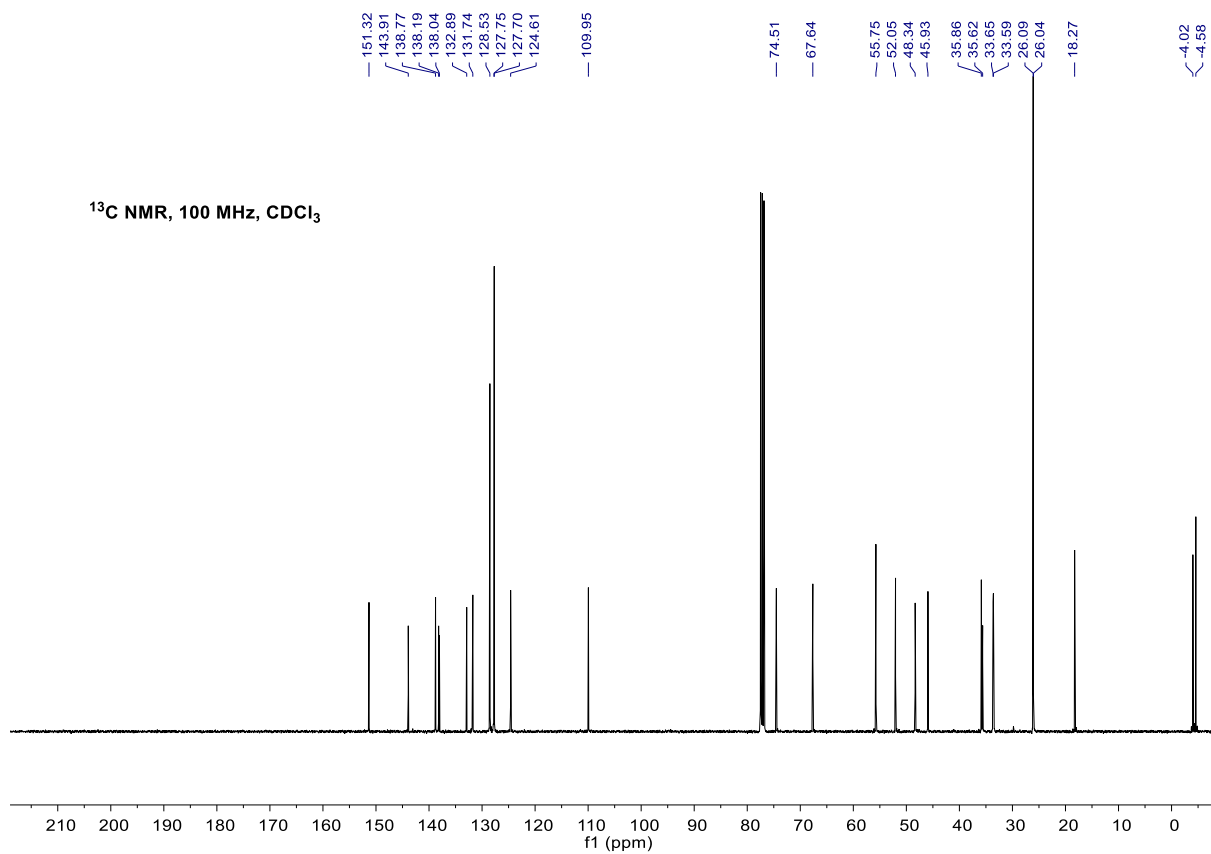


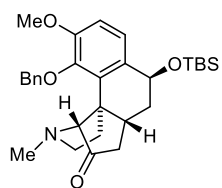
108

$^1\text{H}$  NMR, 400 MHz,  $\text{CDCl}_3$

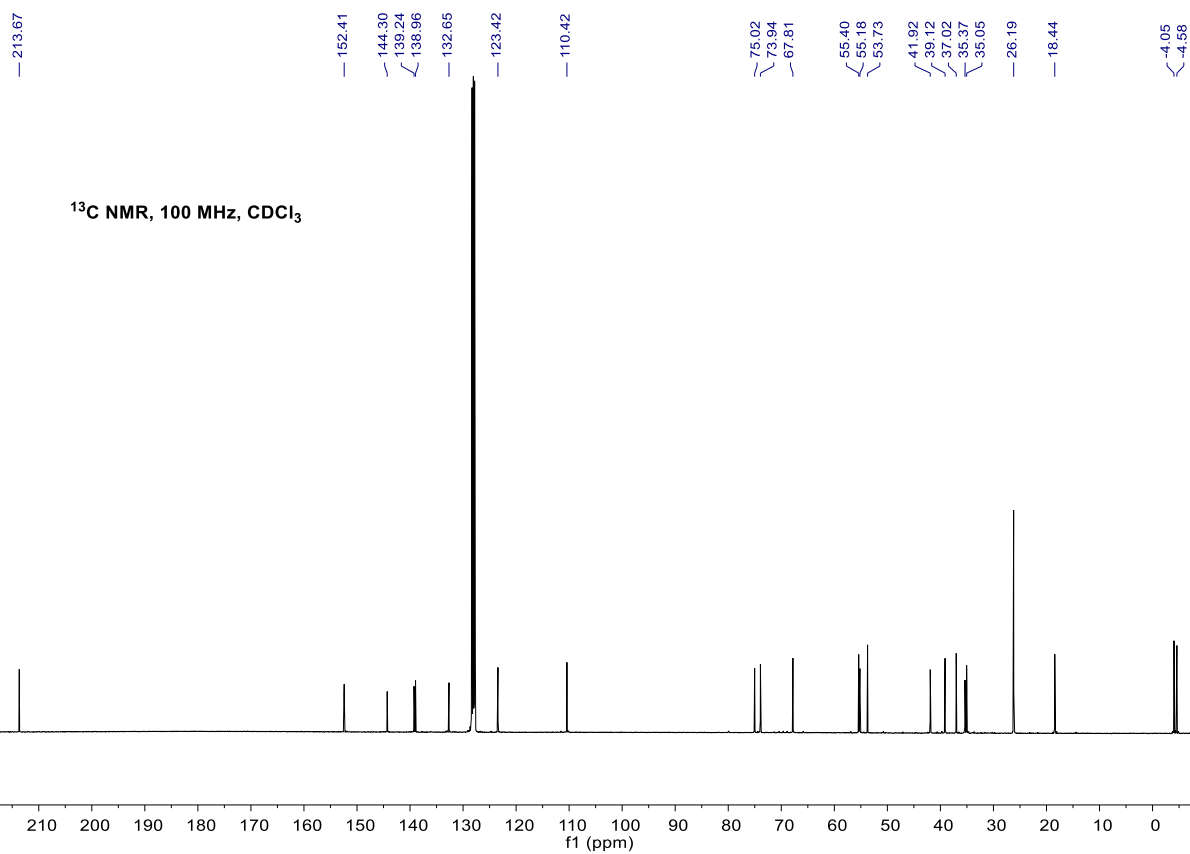
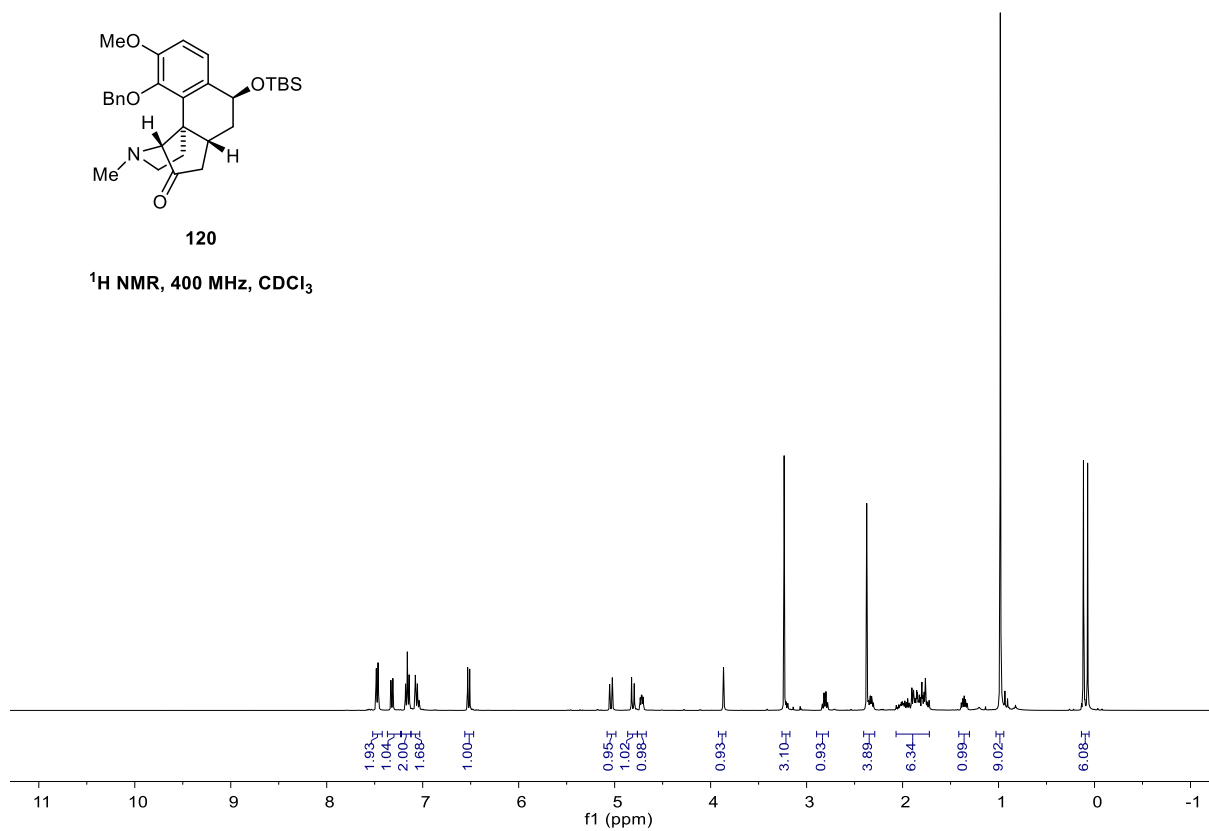


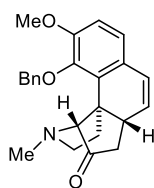
$^{13}\text{C}$  NMR, 100 MHz,  $\text{CDCl}_3$





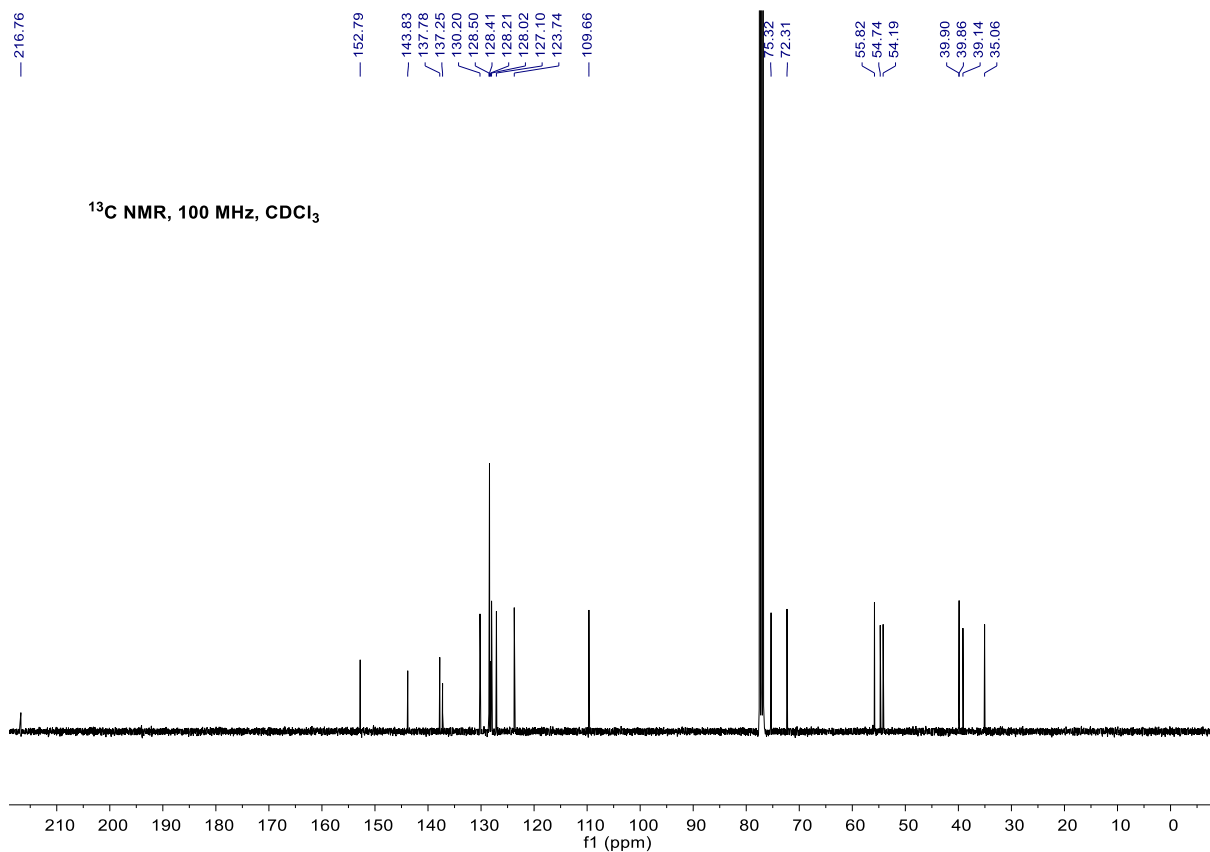
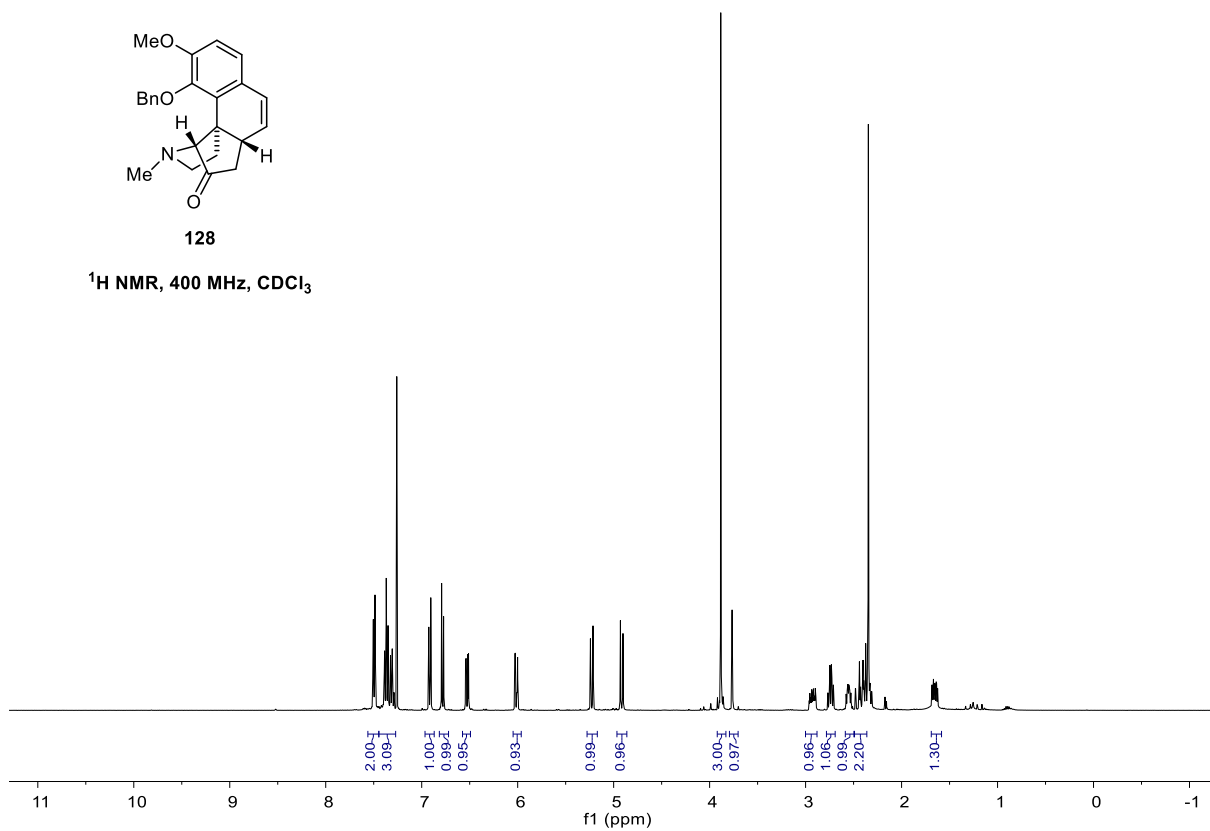
120

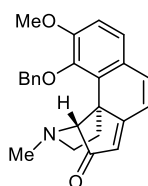
 $^1\text{H}$  NMR, 400 MHz,  $\text{CDCl}_3$ 



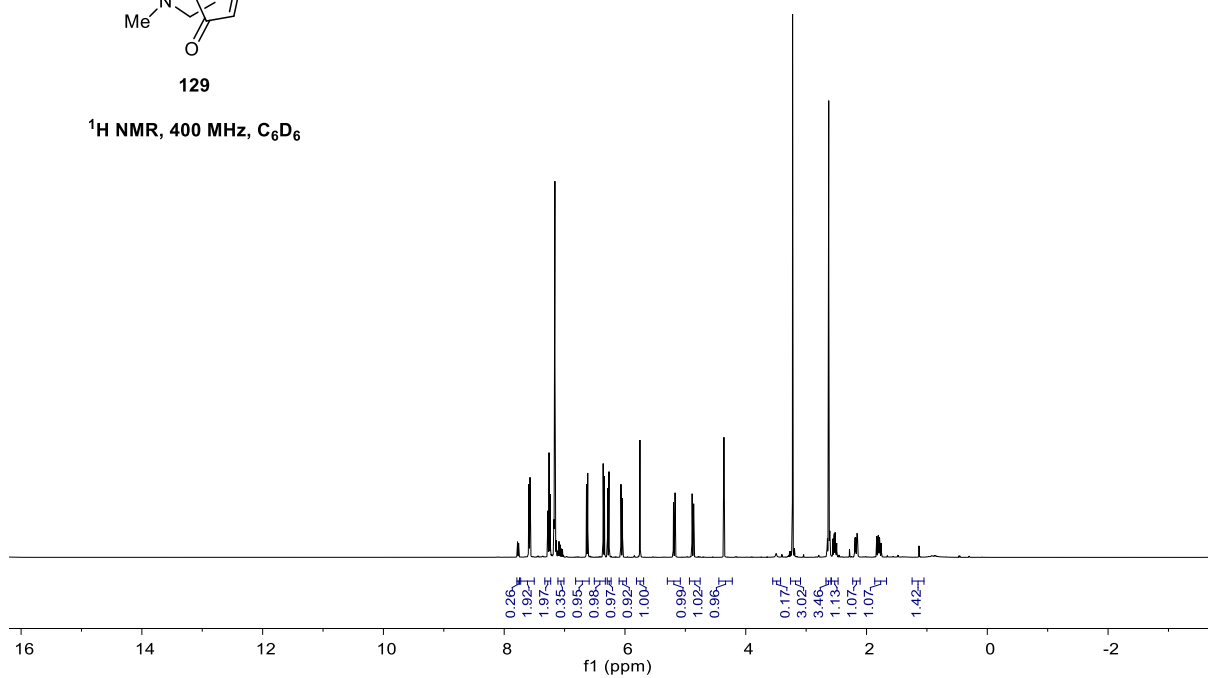
128

$^1\text{H}$  NMR, 400 MHz,  $\text{CDCl}_3$



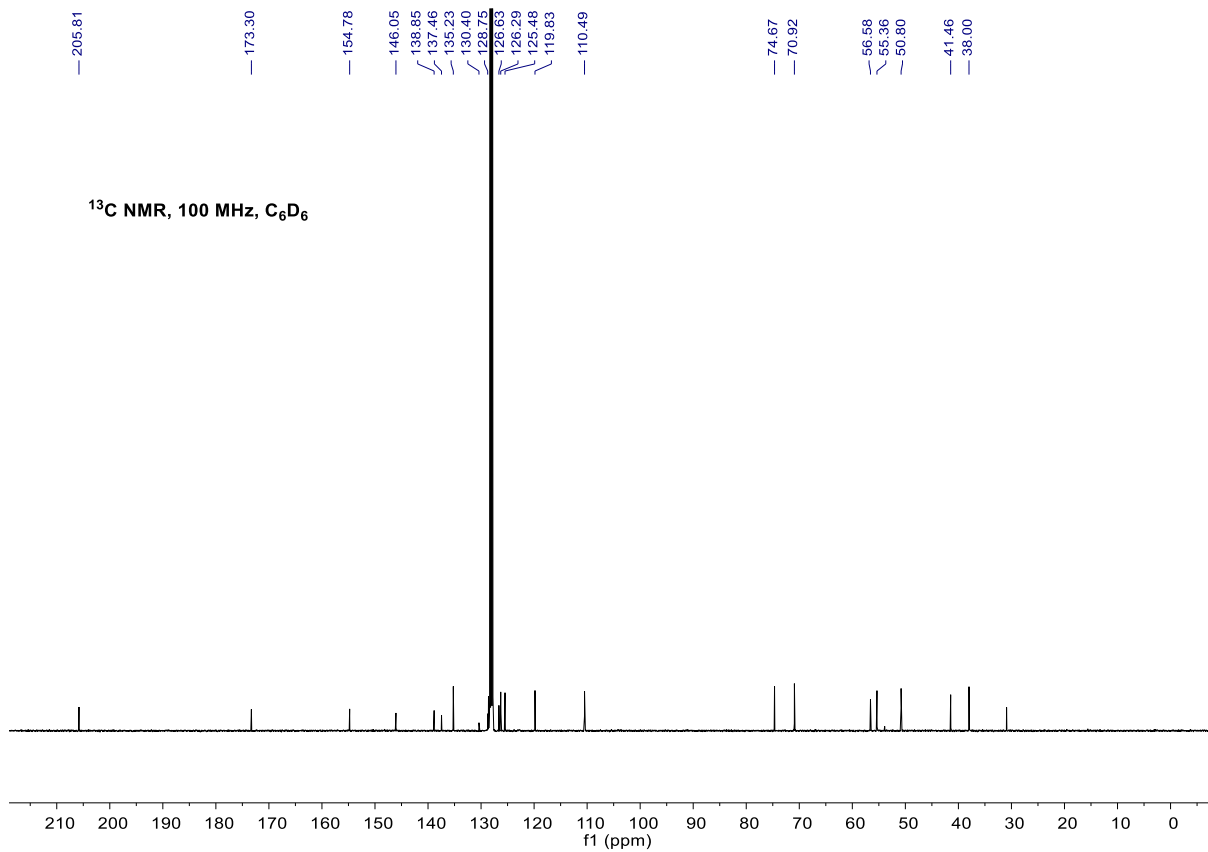


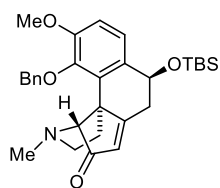
129

 $^1\text{H}$  NMR, 400 MHz,  $\text{C}_6\text{D}_6$ 

Chemical Shifts (ppm) for  $^{13}\text{C}$  NMR spectrum:

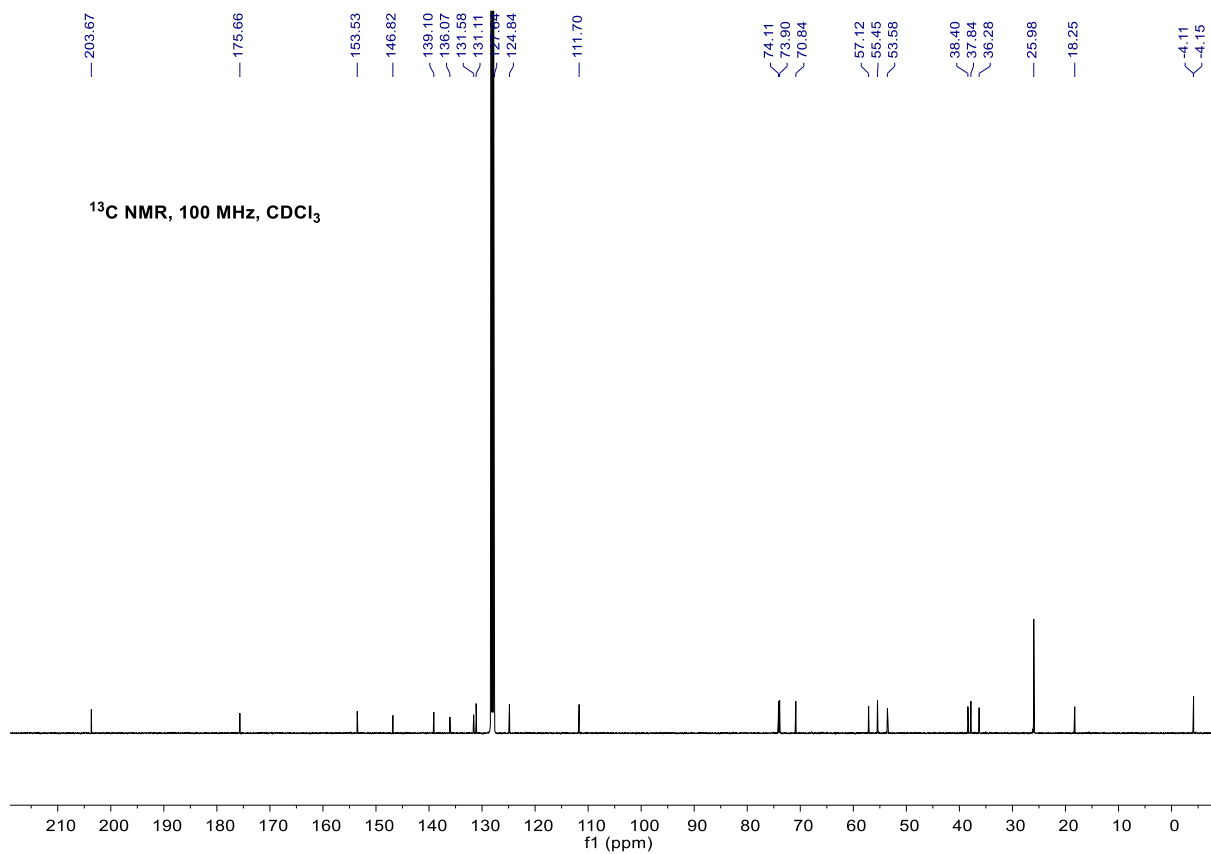
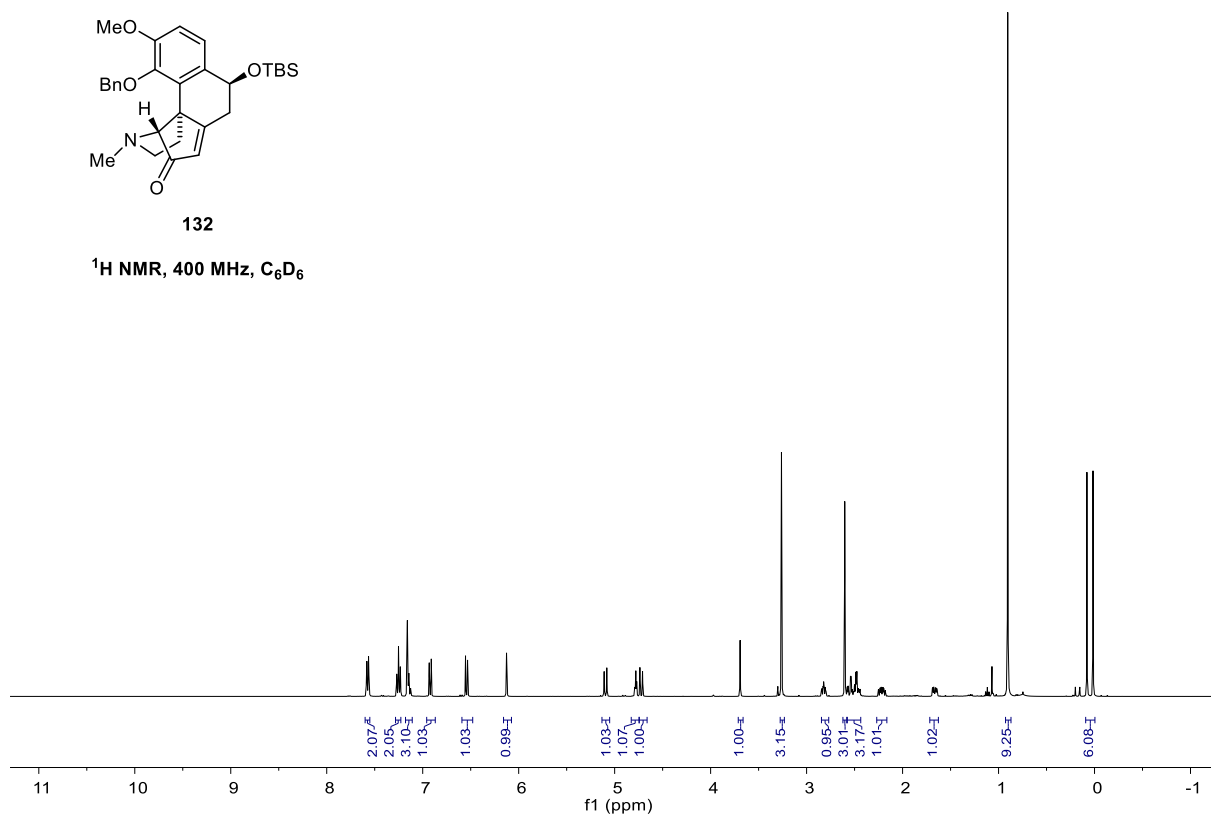
205.81	173.30	154.78	146.05	138.85	137.46	135.23	130.40	128.75	126.63	126.29	125.48	119.83	110.49	74.67	70.92	56.58	55.36	50.80	41.46	38.00
--------	--------	--------	--------	--------	--------	--------	--------	--------	--------	--------	--------	--------	--------	-------	-------	-------	-------	-------	-------	-------

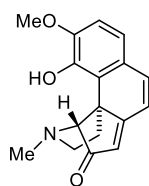
 $^{13}\text{C}$  NMR, 100 MHz,  $\text{C}_6\text{D}_6$ 



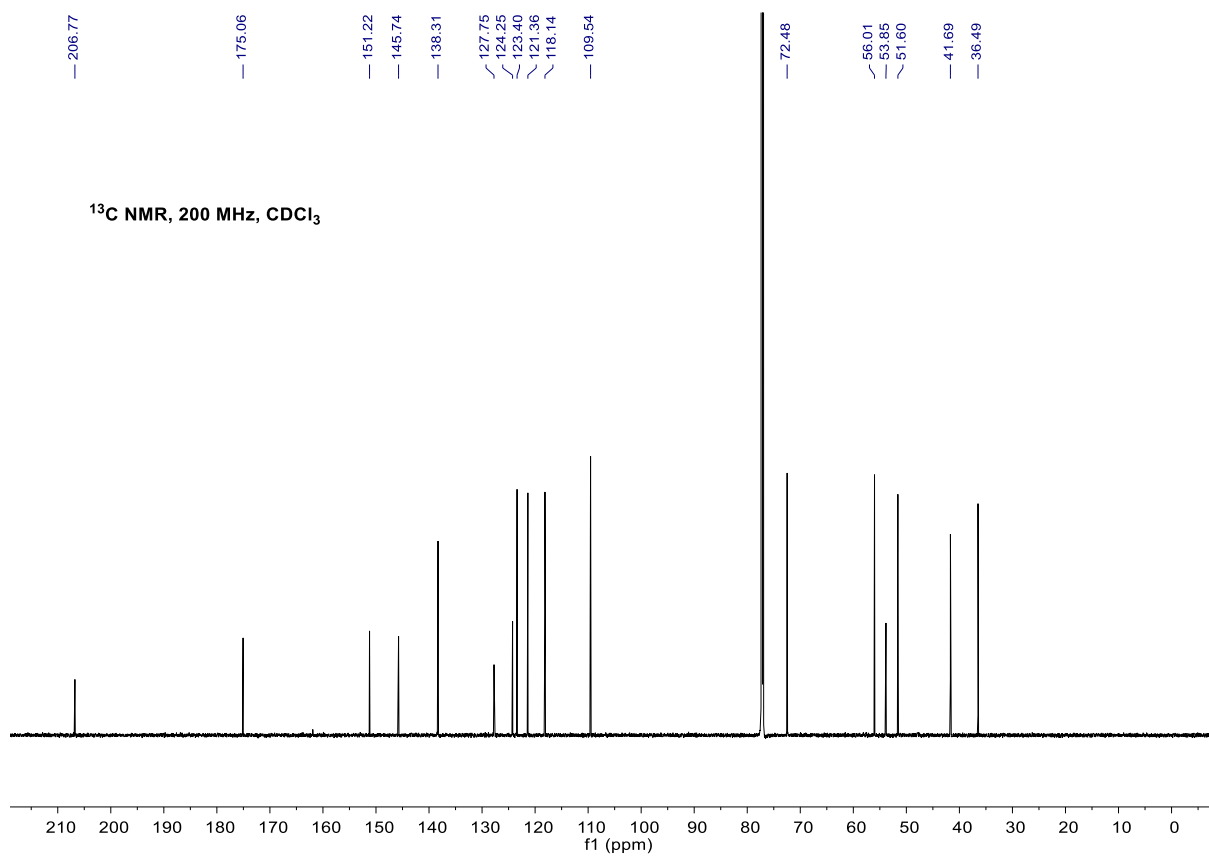
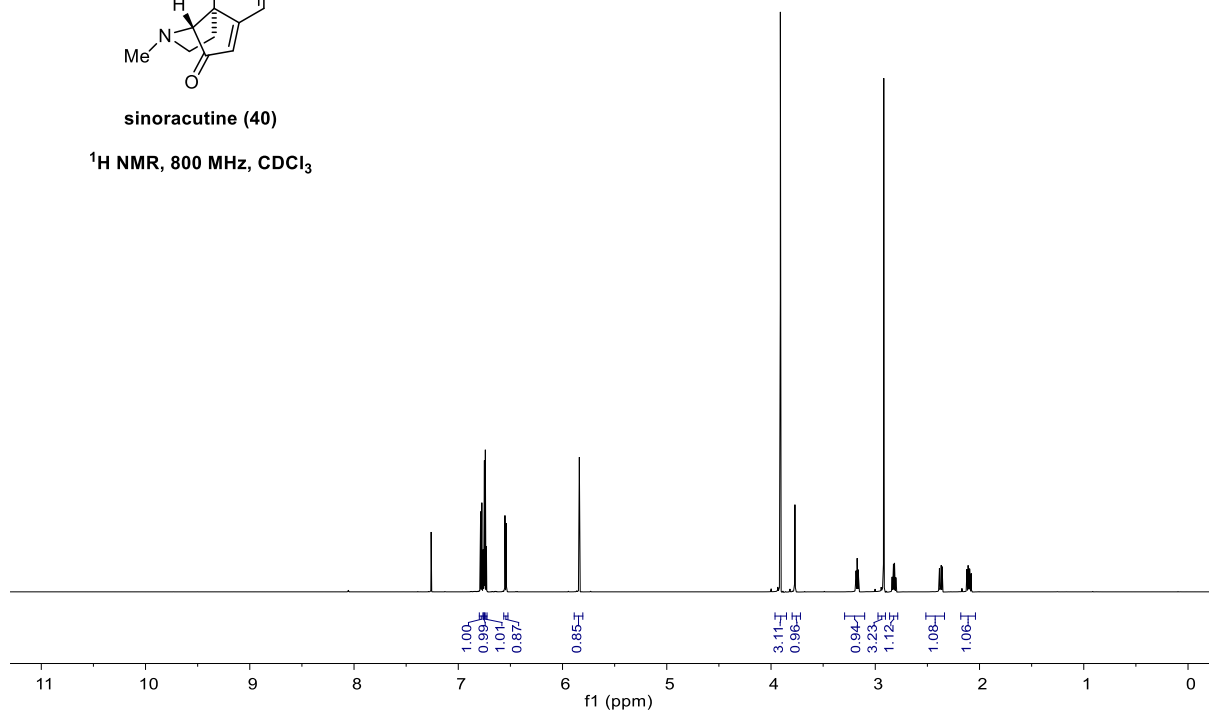
132

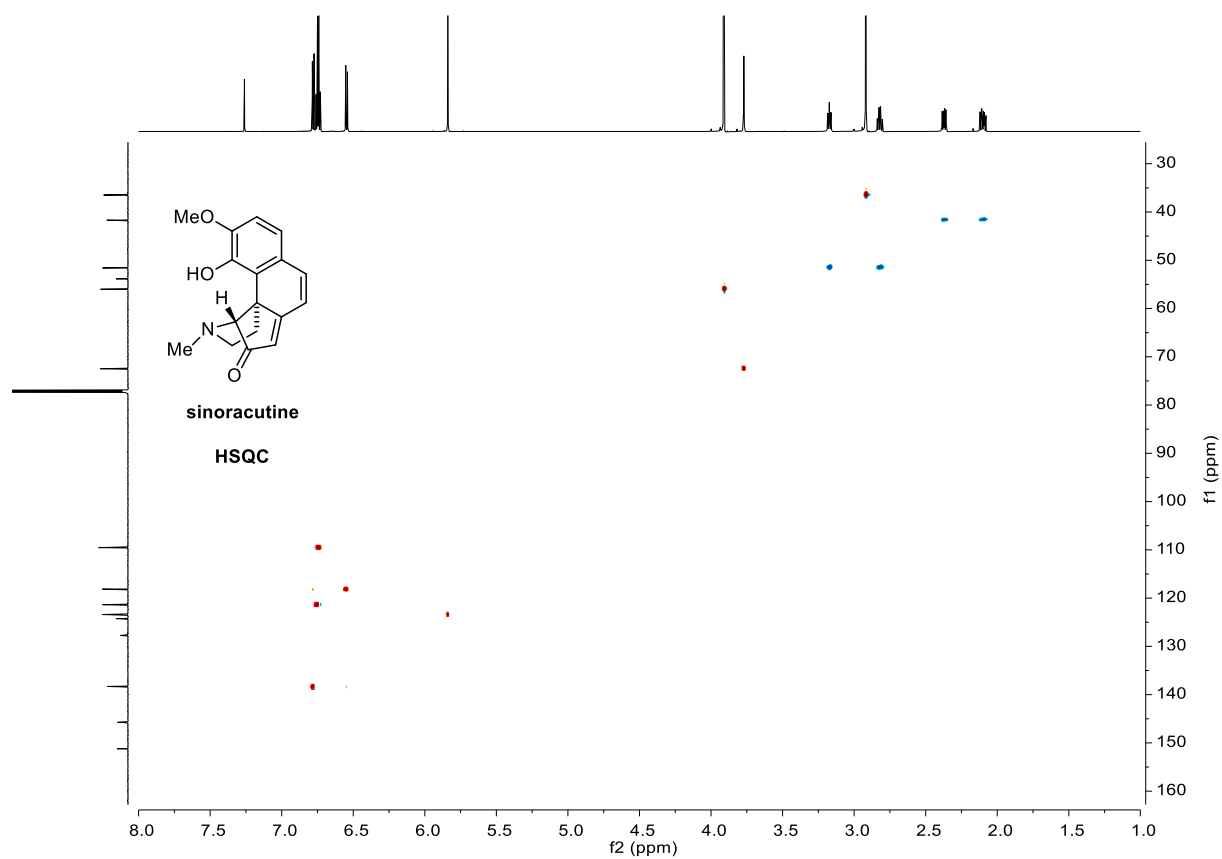
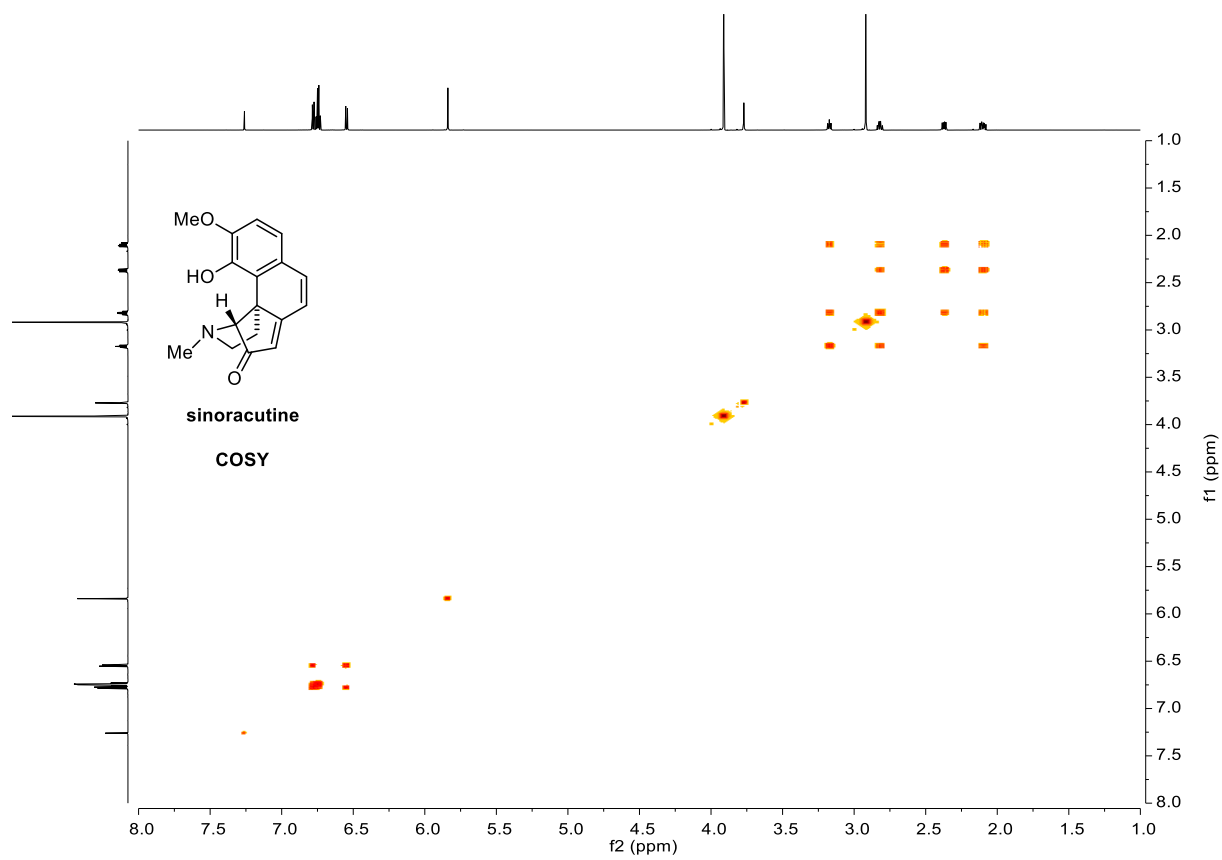
$^1\text{H}$  NMR, 400 MHz,  $\text{C}_6\text{D}_6$

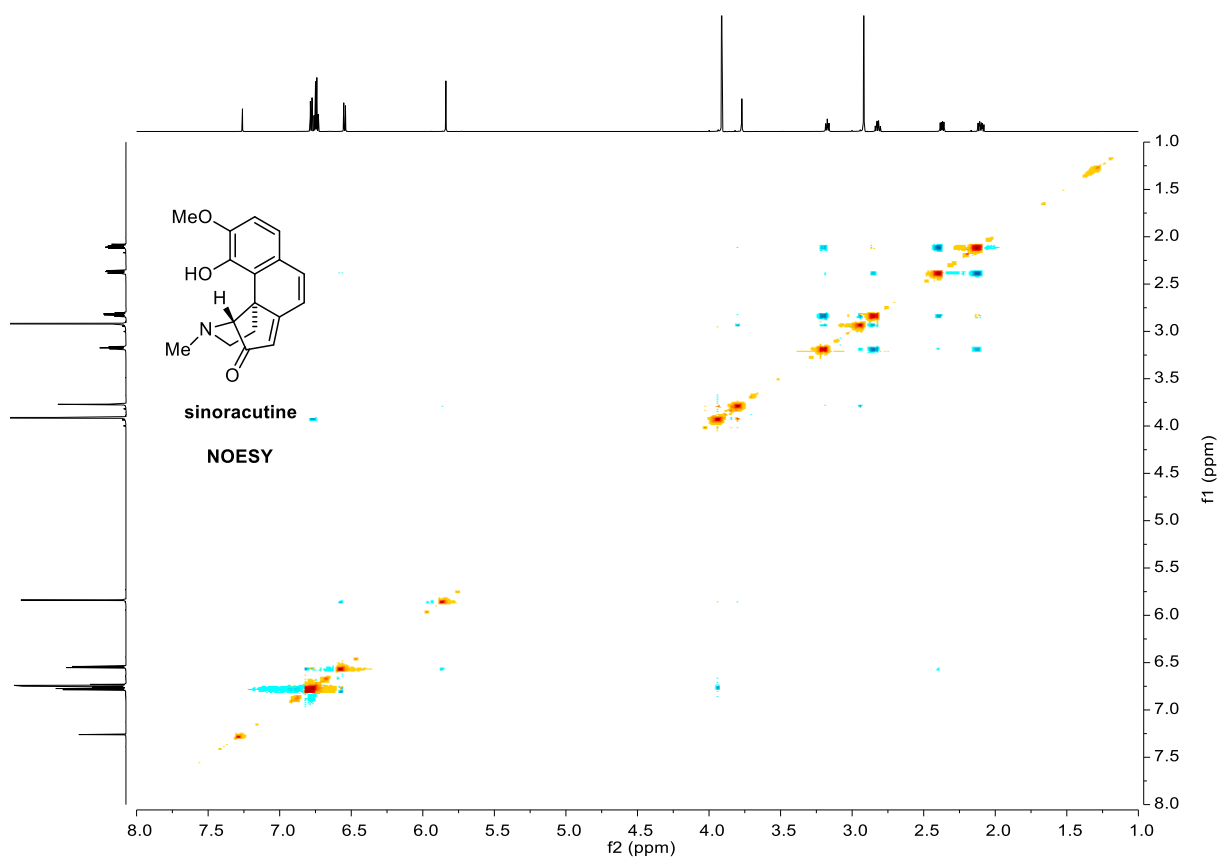
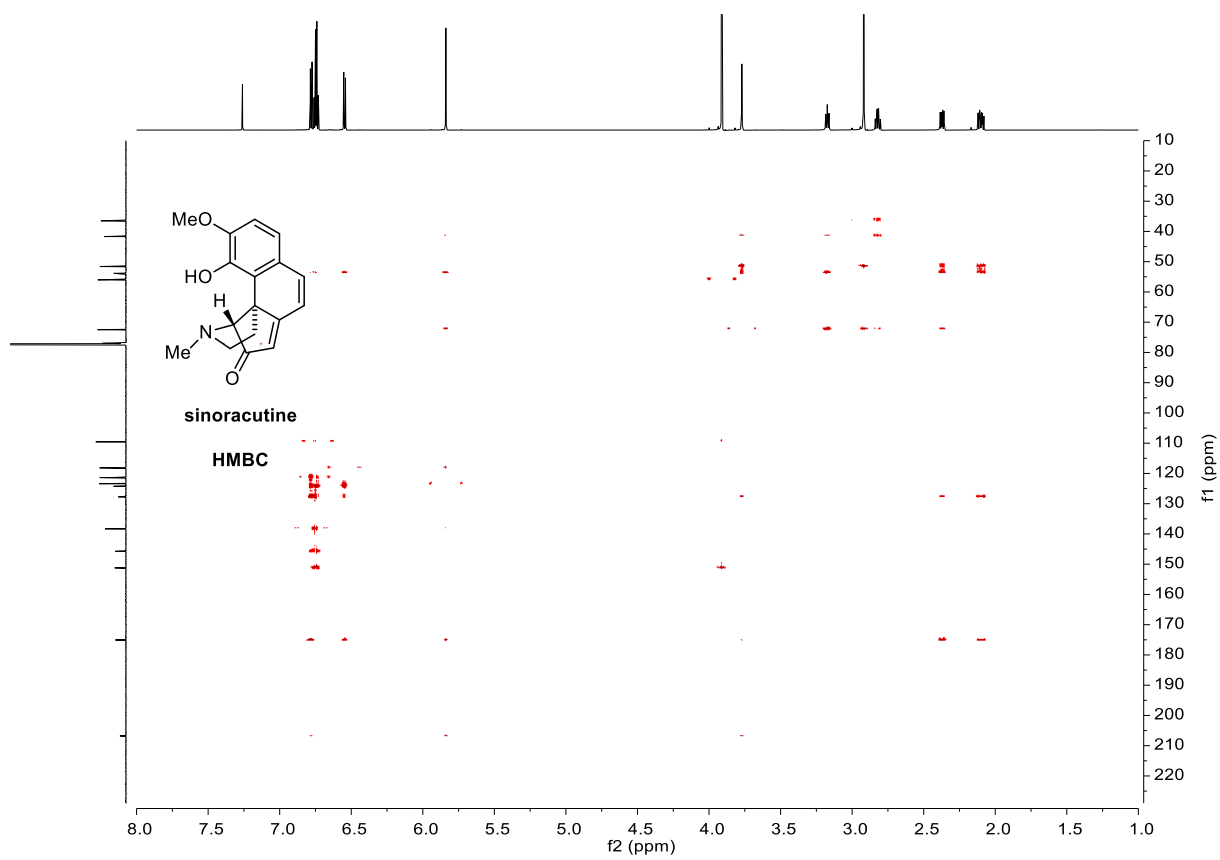




sinoracutine (40)

 $^1\text{H}$  NMR, 800 MHz,  $\text{CDCl}_3$ 







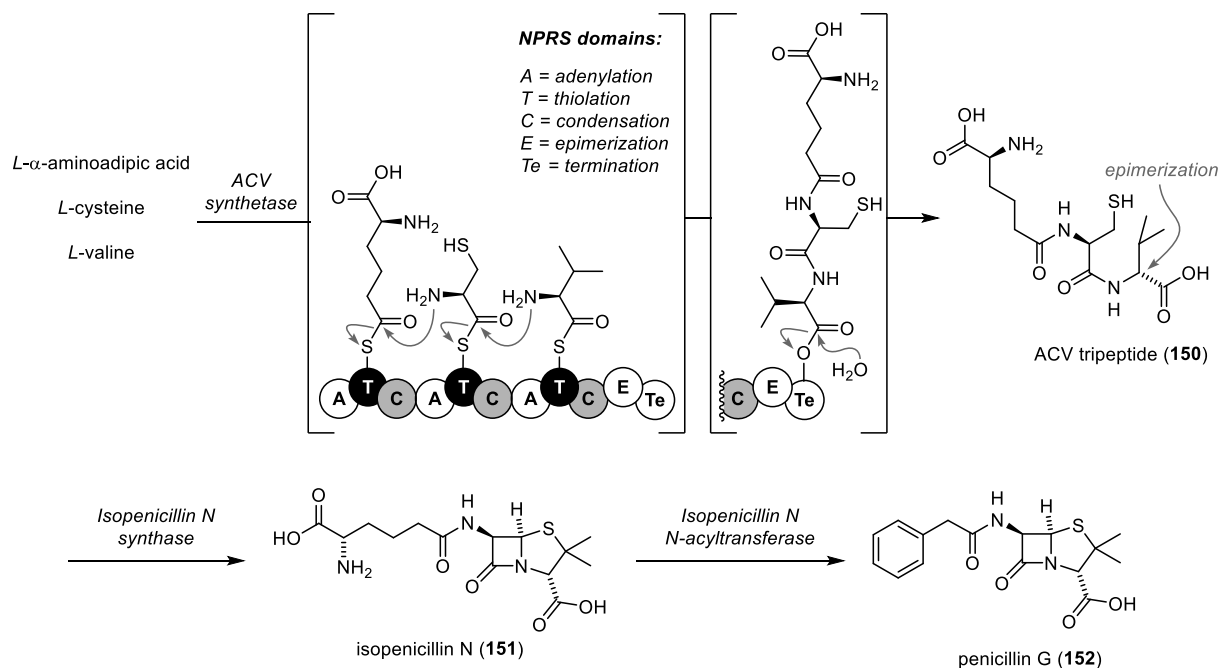
**Part II:**  
**Towards the Total Synthesis**  
**of Herqulines A and B**

# 1. Introduction

## 1.1. Peptide-derived Natural Products of Nonribosomal Origin

The serendipitous discovery of penicillin and its antibiotic activity in 1928 represented one of the greatest medical advances in human history.<sup>[194]</sup> This small molecule, produced by the fungal strain *Penicillium notatum*, not only pioneered the widespread use of antibiotics to universally improve healthcare from surgical outcomes to epidemic control, but also fostered several technological advancements in microbiology, chemical engineering, and synthetic organic chemistry. It also promoted the exploration of metabolites originating from microorganisms as a new source of pharmaceutical agents, which led to the discovery of numerous compounds with antimicrobial, immunosuppressive, antiviral, and antitumor activities. Interestingly, a large fraction of their structures can be traced back to a simple peptidic chain.<sup>[195]</sup>

Although these natural products are based on amino acids, from a structural standpoint their makeup goes far beyond the 20 standard amino acids that are genetically encoded in eukaryotic cells and used by the ribosome to synthesize proteins.<sup>[196]</sup> Penicillin G, for example, stems from a tripeptide containing two proteinogenic amino acids, cysteine and valine. The third building block, however, is the nonproteinogenic L- $\alpha$ -aminoadipic acid. Additionally, valine is present in its unnatural D-configuration. Early on, the biosynthetic origin of penicillin was proposed to be completely independent from the ribosome. In fact, large enzyme complexes, referred to as nonribosomal peptide synthetases (NRPS), have been identified as the biosynthetic machinery of penicillin as well as the large portion of peptide-derived natural product of fungal origin.<sup>[197]</sup> They rely on a thiotemplation mechanism to produce polypeptide chains from single  $\alpha$ -amino acids in an assembly-line process, similar to polyketide synthetases. As seen in Scheme 41, such an enzyme generates the precursor for penicillin termed ACV-tripeptide.<sup>[198]</sup> Other than effecting the union of the three amino acids, this enzyme also subjects the Val-residue to epimerization. After release of ACV (**150**) from the NRPS, so-called tailoring enzymes process the linear peptide: **150** undergoes oxidative cyclization to thiazolidine containing **151** mediated by isopenicillin N synthase, and an acyltransferase enzyme then exchanges the adipic acid side-chain with a phenacetyl moiety to generate penicillin G (**152**), the archetypical penicillin that was discovered first.

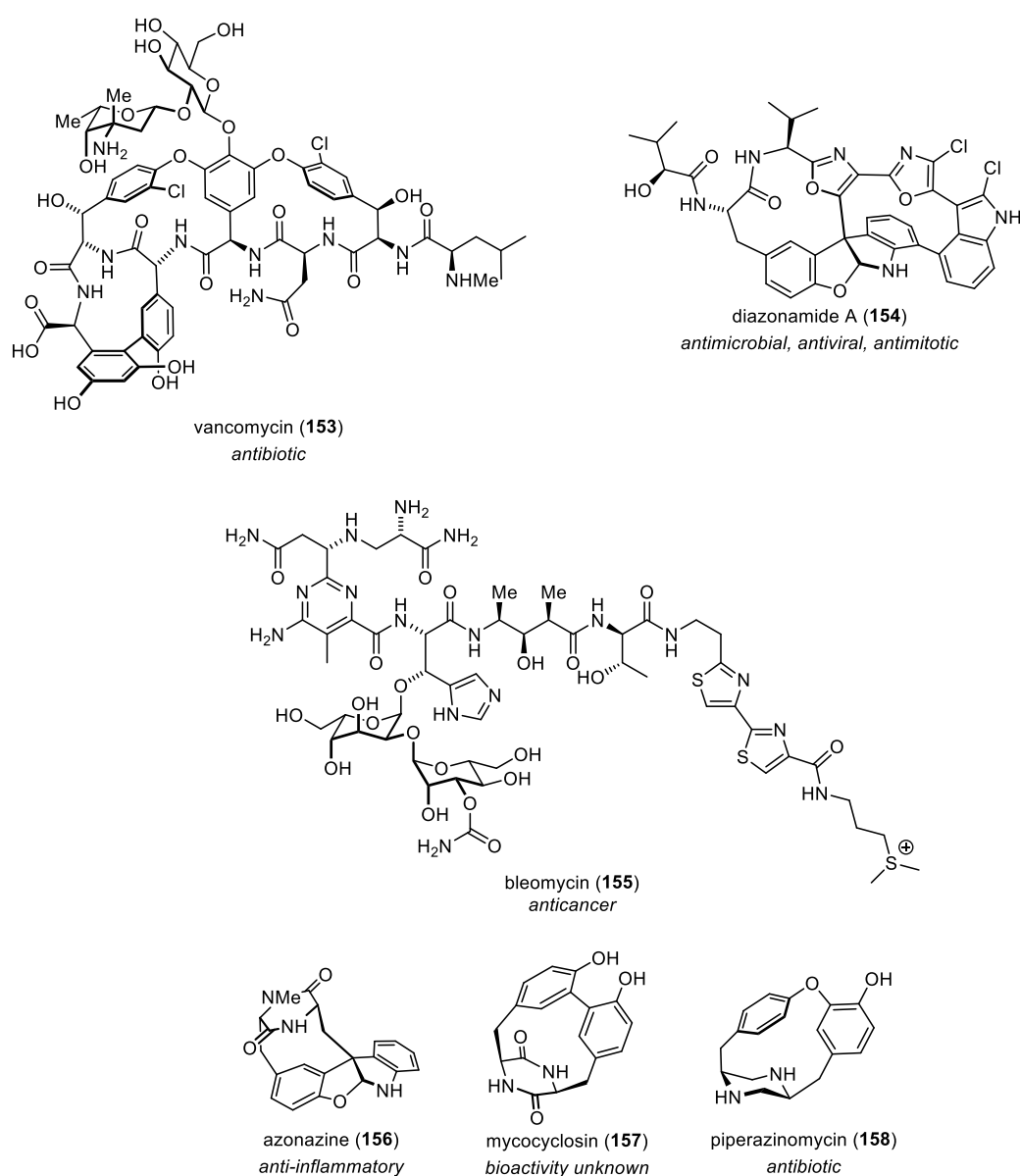


**Scheme 41. Biosynthesis of penicillin G.**

In general, the incorporation of several non-natural amino acids in the NRPS assembly line is common. Cyclization, dehydration, racemization and epimerization are also frequently encountered. Moreover, the NRPS-derived products are often macrocyclic, because along with hydrolysis, intramolecular cyclization is a standard release mechanism for the peptide chain from the thiol anchor on the NRPS.<sup>[196]</sup> Ulterior processing by a variety of enzymes (e.g. methyltransferases, oxidases, reductases, cyclases, dehydrogenases, halogenases, acyltransferases, sulfotransferases, glycosyltransferases) that are either embedded in the NRPS multidomain or stand alone as tailoring enzymes makes the possibilities of diversification virtually limitless.<sup>[199]</sup>

Figure 15 shows a small selection of natural products that derive from nonribosomal peptide synthetases.<sup>[200]</sup> Besides penicillin, the most notorious nonribosomal peptide is vancomycin (**153**, from the bacterium *Amycolatopsis orientalis*), which is used as a last resort to fight antibiotic-resistant bacterial strains. It features five non-natural amino acids produced either by halogenation or hydroxylation.<sup>[201–203]</sup> Additionally, oxidatively generated C-C and C-O biaryl rings and glycosylation patterns heavily modify the structure of this heptapeptide. The potent antimetabolic agent diazonamide A (**154**, from the ascidian *Diazona chinensis*) can originally be traced back to a TyrValTrpTrp tetrapeptide, but extensive oxidative crosslinking, halogenation, and oxidation/cyclodehydration reactions generate a highly complex structure which could be verified only by total synthesis.<sup>[204–206]</sup> Molecules incorporating both polyketide and peptide building blocks are also associated with NRPS enzymatic machineries, such as bleomycin (**155**, from the bacterium *Streptomyces verticillus*), which is used to treat testicular, ovarian, and cervical cancer.<sup>[207,208]</sup> Additionally, structures consisting of as few as two amino acids are also encountered. Often, they are classified as alkaloids. As such, azonazine (**156**, from *Aspergillus insulicola*) features a highly strained 10-membered ring resembling

diazonamide A and is derived from tyrosine and tryptophan.<sup>[209,210]</sup> Mycocyclusin (**157**, from *Mycobacterium tuberculosis*) is derived from two molecules of tyrosine, and features an *o,o*-phenolic linkage between the aromatic rings to assemble a cyclophane-like 12-membered ring.<sup>[211]</sup> Apart from oxidative transformations, which are ubiquitous in NRPS-derived products, reductive transformations are also sometimes encountered. It is the case for the antibiotic piperazinomicin (**158**, from *Streptoverticillium neoenacticus*), also derived from two molecules of tyrosine.<sup>[212–215]</sup> It features an oxidative phenolic C–O linkage (similar to vancomycin), but displays a piperazine ring resulting from reduction of a diketopiperazine moiety. In the following sections, we present our studies towards the related alkaloids herquiline A and B, which are also biosynthetically derived from two molecules of tyrosine but have undergone extensive reductive metabolic processing.



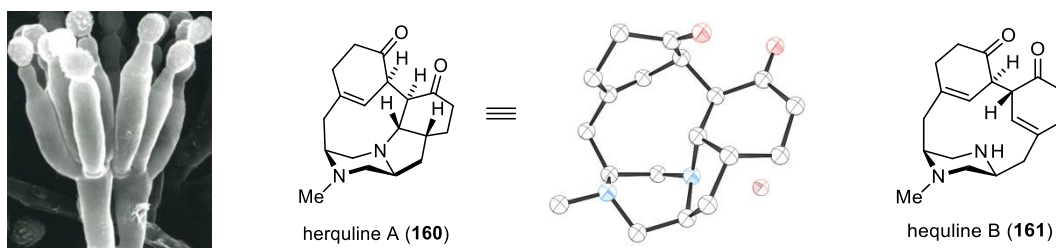
**Figure 15.** Natural products derived from nonribosomal peptide synthetases.

## Herqulines A & B

### 1.1.1. Isolation, Structure and Biosynthesis

Herquline A (**160**) was isolated in 1979 from the culture broth of *Penicillium herquei* (strain FG 372).<sup>[216]</sup> The isolation team, led by Prof. Satoshi Omura at the Kitasato Institute of Tokyo, classified it as an alkaloid due to positive reaction to Draggendorff's stain. Judging by its IR, UV-Vis and mass spectrum it was structurally not related to other known alkaloid classes known to be produced by penicillium strains. This hypothesis was confirmed one year later, when the X-ray structure of its hydrobromide derivative was obtained (Figure 16).<sup>[217]</sup> Despite its low molecular weight of 314 g/mol, herquline A features five rings including a central and highly strained nine membered ring that is nestled between a southern dodecahydropyrazino[1,2-a]indole core and a northern cyclohex-2-ene ring. The six stereocenters, of which four are contiguous, are all tertiary, and contribute to the bowl-like shape of this unique natural product.

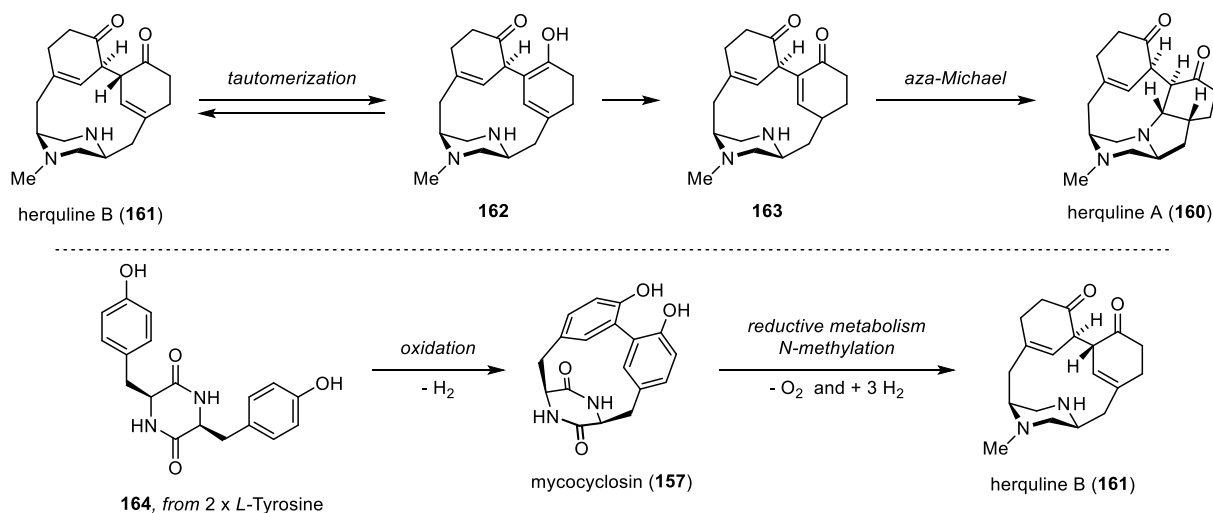
Continuing their search for other alkaloids from *Penicillium herquei*, Omura and co-workers discovered a novel compound in the fermentation broth.<sup>[218]</sup> This molecule, which was termed herquline B (**161**), was isolated as a minor component during the isolation process (5.2 mg in comparison to 110 mg of herquline A, which was reisolated in the same campaign). It was found to be a structural isomer of herquline A, differing in the cleavage of the pyrrolidine ring and the concomitant introduction of a second alkene group, resulting in a twelve-membered ring (Figure 16).



**Figure 16.** Scanning electron micrograph of *Penicillium herquei* (left); molecular and X-ray structures of herquline A (middle, HBr salt), and molecular structure of herquline B (right).

Early on, it was postulated that herquline B could serve as a biosynthetic precursor for herquline A.<sup>[218]</sup> As shown in Scheme 42, enolization of the ketone and tautomerization via dienolate **162** followed by protonation in  $\gamma$ -position could reveal transient  $\alpha,\beta$ -unsaturated ketone **163**. Intramolecular 5-*exo*-trig attack by the pendant secondary amine would then give **160**. Feeding experiments also showed that herquline A is overproduced in tyrosine-enriched medium. A plausible biosynthesis would begin with the condensation of two molecules of L-tyrosine to cyclodityrosine (**164**), followed by an oxidative phenolic coupling to yield mycocyclosin (**157**, Scheme 42). *N*-Methylation and two reductive events need to take place to convert mycocyclosin into herquline B. While the reduction of a diketopiperazine is possible as seen in piperazinomycin (also produced by a

fungus), the dearomatization of the phenolic moiety to yield a cyclohex-2-one by formal addition of an  $H_2$ -equivalent is rare.<sup>[219]</sup> This reductive dearomatization could be facilitated by the high strain of the 12-membered macrocycle, which can be relieved by pyramidalization of the  $sp^2$ -carbon atoms in the ring after dearomatization and isomerization.<sup>[220]</sup>



#### Scheme 42. Formation of herquiline A from herquiline B and biosynthetic proposal.

In October 2016, while this thesis was in preparation, Tang, Houk and co-workers were able to defuse any doubts surrounding the biosynthesis of these alkaloids by isolating the gene cluster responsible for the production of the herquelines from *Penicillium herquei*.<sup>[221]</sup> As shown in Figure 17, this cluster contains six genes that encode one nonribosomal peptide synthetases (*hqlA*), one *N*-methyltransferase (*hqlE*), one CYP450-dependent oxidase (*hqlC*), and three short-chain NADP-dependent dehydrogenases (*hqlB*, *hqlD*, *hqlF*).

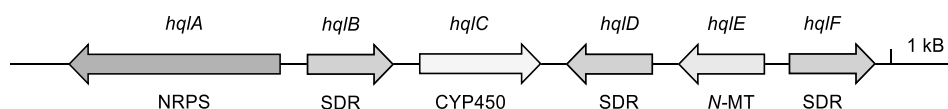
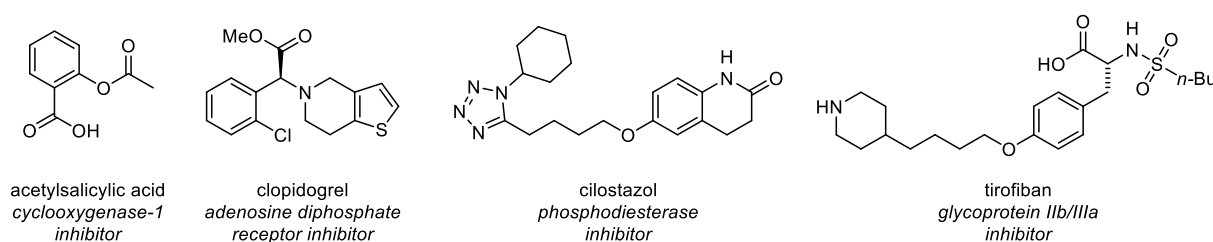


Figure 17. Gene cluster from *Penicillium herquei* involved in herquiline biosynthesis.

Through a series of heterologous expression experiments in *Aspergillus nidulans*, it was demonstrated that *hqlA* activates tyrosine as the thioester and mediates the reduction to aminoaldehyde **165**, which spontaneously condenses to **166** (Scheme 43). Then, *hqlB* reduces the diimine **166** to piperazine **167**. Without this reductase, pyrazine **168** is formed by spontaneous air oxidation. Under the influence of the *hqlC*, oxidative radical coupling to **169** can be effected. This intermediate, which represents a doubly dearomatized phenol tautomer, has been proven to be highly unstable and to spontaneously convert to biaryl piperazine **170**. However, in the presence of *hqlF* and NADH, twofold reduction of the cyclohexadienone to bis- $\beta,\gamma$ -unsaturated ketone **171** is possible to give desmethyl-herquiline B (**171**). This twofold reduction is very remarkable, and most likely facilitated by the macrocyclic framework of **169**, which considerably slows down rearomatization to **170**. Nevertheless, minor quantities of monoreduced product **172**, resulting from incomplete reduction of **169**, are also



already formed clots (thrombolytics) as well as to prevent blood coagulation are available, such as antithrombotics, anticoagulants, and antiplatelet drugs (for a small collection, see Scheme 44).<sup>[223]</sup> The different therapeutic options, based on distinct mechanism of action, are often used in combination to effectively treat underlying conditions that could be exacerbated by a constitutionally upregulated clotting mechanism.<sup>[224]</sup> For example, patients that have suffered ischemic events are treated with both acetylsalicylic acid to inhibit COX-mediated production of proinflammatory prostaglandins, as well as the selective compound clopidogrel, which blocks the so-called P2Y<sub>12</sub> receptor (whose endogenous ligand is ADP) found on the cell membrane of thrombocytes that play a key role in activation of platelets.<sup>[225]</sup>



#### Scheme 44. Drugs with anti-platelet aggregation activity having different mechanisms of action.

In an essay conducted with rabbit blood, herquelines A and B showed promising activity against platelet aggregation induced by both PAF and ADP, which are released at sites of inflammation and vascular injury.<sup>[218]</sup> In both cases, herquiline B was demonstrated to be roughly 50 times more active in the PAF-promoted, and 100 times more active in the ADP-promoted pathways. The molecular target and exact mechanism of action have yet to be elucidated, but the non-selective blocking of two major aggregation pathways implies that a downstream receptor might be the actual target of the herquelines, and might open new therapeutic avenues for thrombosis-related diseases.

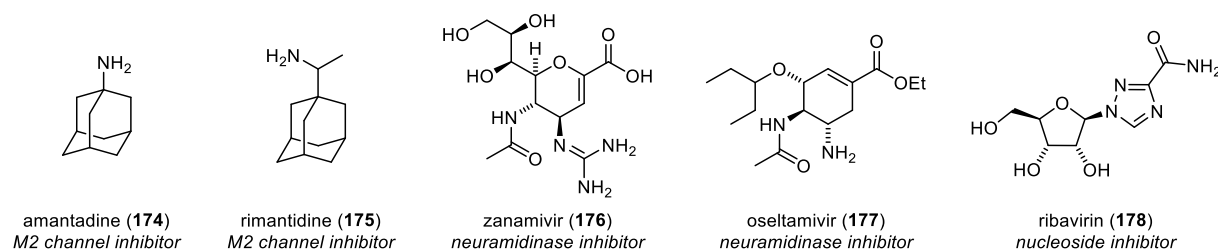
**Table 33. Antiplatelet activity of herquelines A and B.**

compound	IC <sub>50</sub> (μM)	
	PAF aggregation	ADP aggregation
herquiline A	240.0	180.0
herquiline B	5.0	1.6

In 2016, during the course of an activity-based screening campaign for new anti-influenza compounds derived from fungal cultures, herquiline A was found to inhibit replication of the influenza A virus (H1N1 subtype, “swine flu”).<sup>[226]</sup> Between 1918 and 1920, this virus killed more than 50,000,000 people (between three and five percent of the world population) during a worldwide pandemic and reemerged prominently in 2009, causing roughly 17,000 deaths by early 2010.<sup>[227]</sup> Although vaccines for common seasonal influenza infections are available, zoonotic variants of the virus have been shown to be particularly deadly. In these cases, vaccination cannot be implemented quickly enough to prevent a pandemic, and antiviral drugs are the only other treatment option.<sup>[228]</sup> Due to the relatively simple viral architecture, only three mechanisms of action for antiviral drugs are

currently exploited in therapy - the inhibition of neuraminidase, the M2 proton channel, and viral replication.<sup>[229]</sup> However, resistance to M2 channel inhibitors such as amantadine (**174**) and rimantidine (**175**) has widely been reported, limiting treatment options to very few candidates: the neuraminidase inhibitors zanamivir (**176**) and oseltamivir (**177**), and the replication inhibitor ribavirin (**178**, Table 34).<sup>[230,231]</sup> In a plaque assay, herquiline A was shown to inhibit viral replication of the A/PR/8/34 strain (responsible for the 2009 influenza pandemic) with comparable potency to ribavirin and amantadine. It exhibited very interesting subtype selectivity, as it tested inactive against several other influenza strains to which the drugs shown in Table 34 respond. This suggest that the molecular target of **160** might be different from that of the other influenza drugs, and holds promise for developing new lead compounds against influenza pandemics.

**Table 34. Known antiinfluenza drugs and selected activities against influenza subtypes.**

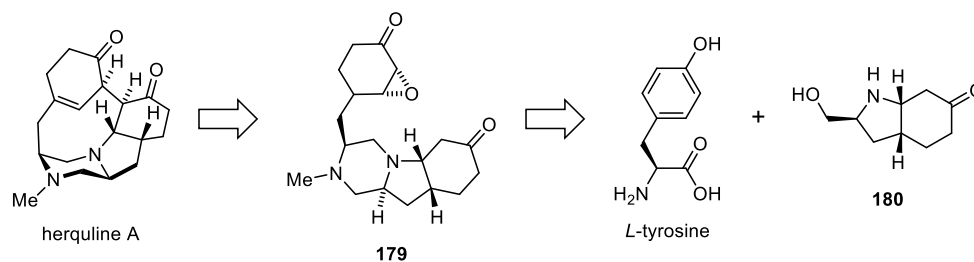


Strain	Subtype	IC <sub>50</sub> (μM)			
		herquiline A	amantadine	zanamivir	ribavirin
A/PR/8/34	H1N1	<b>10</b>	60	0.0002	13
A/WSN/33	H1N1	> <b>300</b>	18	0.0010	42
A/Guizhou/54/89	H3N2	> <b>300</b>	87	0.0010	60
A/Aichi/2/68	H3N2	> <b>300</b>	4	0.0100	38
B/Ibaraki/2/85	B	> <b>300</b>	100	0.0020	69

## 1.2. Previous Synthetic Efforts

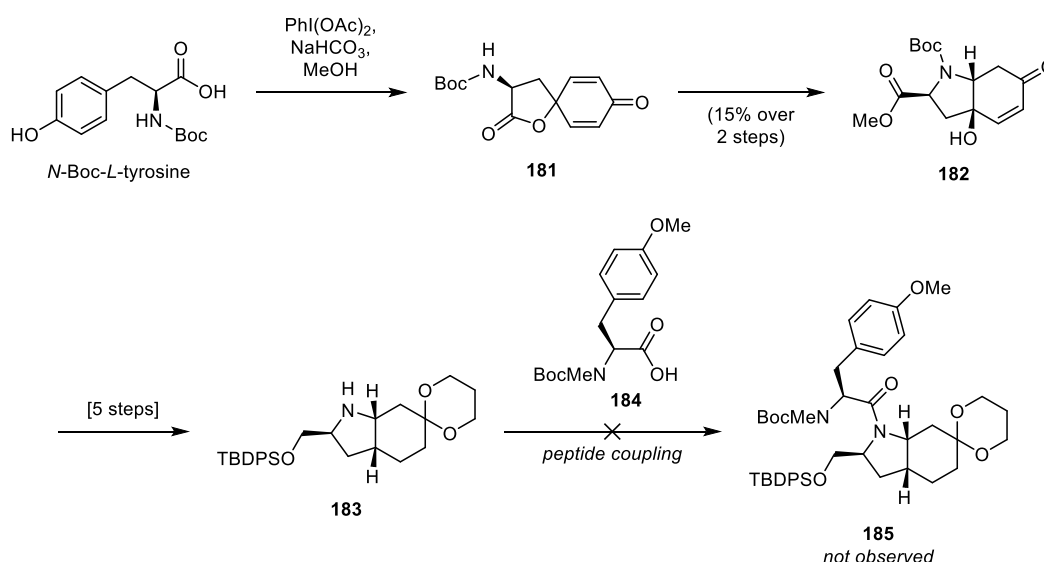
Several synthetic approaches towards the total synthesis of herquelines have been reported in the past 20 years, a testimony to the active pursuit of a target that has yet to surrender to total synthesis 37 years after its original isolation.

In 1997, Kim reported an approach towards herquiline A relying on an epoxide opening reaction of intermediate **179** to form the 9-membered ring of herquiline A, followed by elimination of the resulting secondary alcohol to introduce the  $\beta,\gamma$ -unsaturated ketone moiety (Scheme 45).<sup>[232]</sup> Epoxide **179** could be accessed through coupling of an *N*-methyl tyrosine derivative with a protected version of octahydroindole **180**, which is also derived from tyrosine.



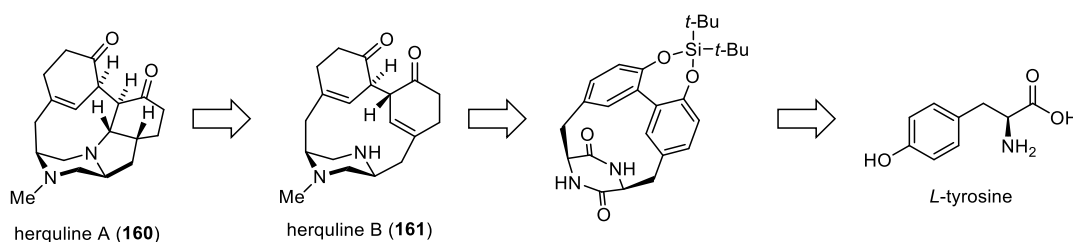
**Scheme 45. Retrosynthesis of herquiline A by Kim and co-workers.**

Bicycle **182** was formed in low yield via oxidative dearomatization of tyrosine to **181** followed by base-mediated transesterification and aza-Michael addition (Scheme 46).<sup>[233]</sup> Reductive manipulations and alcohol protection furnished bicycle **183** which was submitted to peptide coupling with *N*- and *O*-methylated tyrosine derivative **184**. Unfortunately, the desired product **185** was not observed and no further progress on this route was reported.



**Scheme 46. Synthesis of octahydroindole 183 by Kim and attempted peptide coupling.**

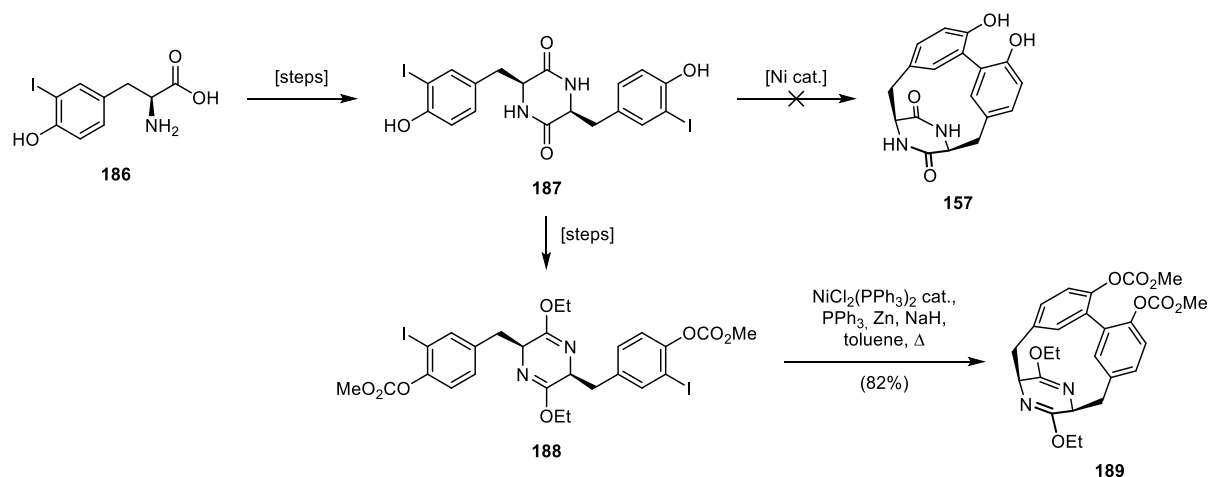
In 2003, a poster abstract from the “Conference of the Chemical Society of Japan” outlined a synthetic approach by Kawai and co-workers following the biosynthetic origin starting from two tyrosine molecules. It relied on an intramolecular Ni-catalyzed Ullman-type coupling to form the 12-membered ring (Scheme 47).



**Scheme 47. Retrosynthesis of herquelines A and B by Kawai and co-workers.**

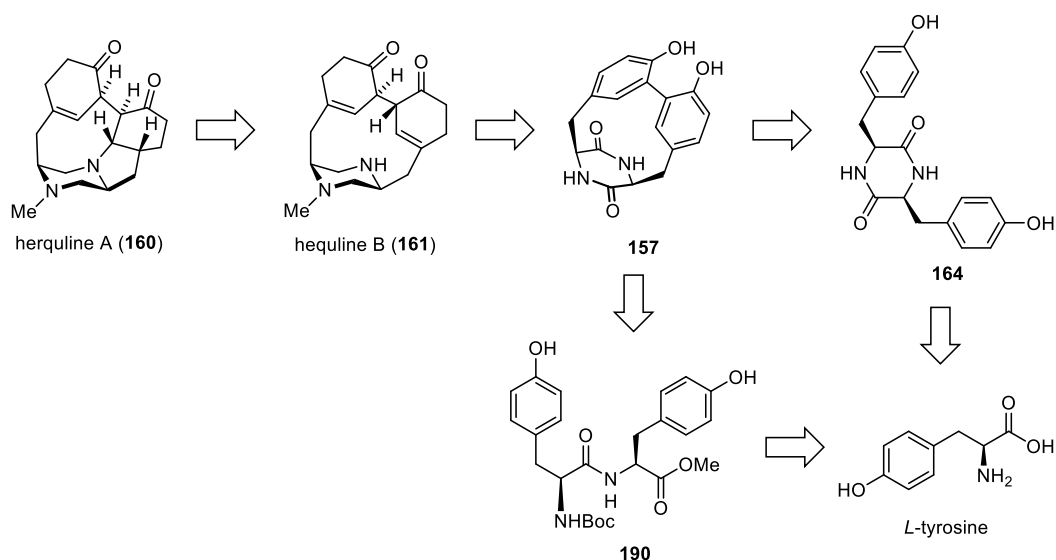
Iodotyrosine **186** was chosen as the starting material and was converted to cyclic diketopiperazine dimer **187**. Subsequent intramolecular aryl coupling of **187** using transition metals

did not proceed (Scheme 48). However, they converted **187** into imino ether **188**. Reductive intramolecular homocoupling of the aromatic iodides gave the desired target compound **189** in good yield.<sup>[234]</sup> Although this product features the required atom connectivity (with exception of an *N*-methyl group) and is only two reductive manipulations away from herquiline B, completion of the synthesis was not possible.



**Scheme 48. Synthesis and macrocyclization via bislactim ether 188.**

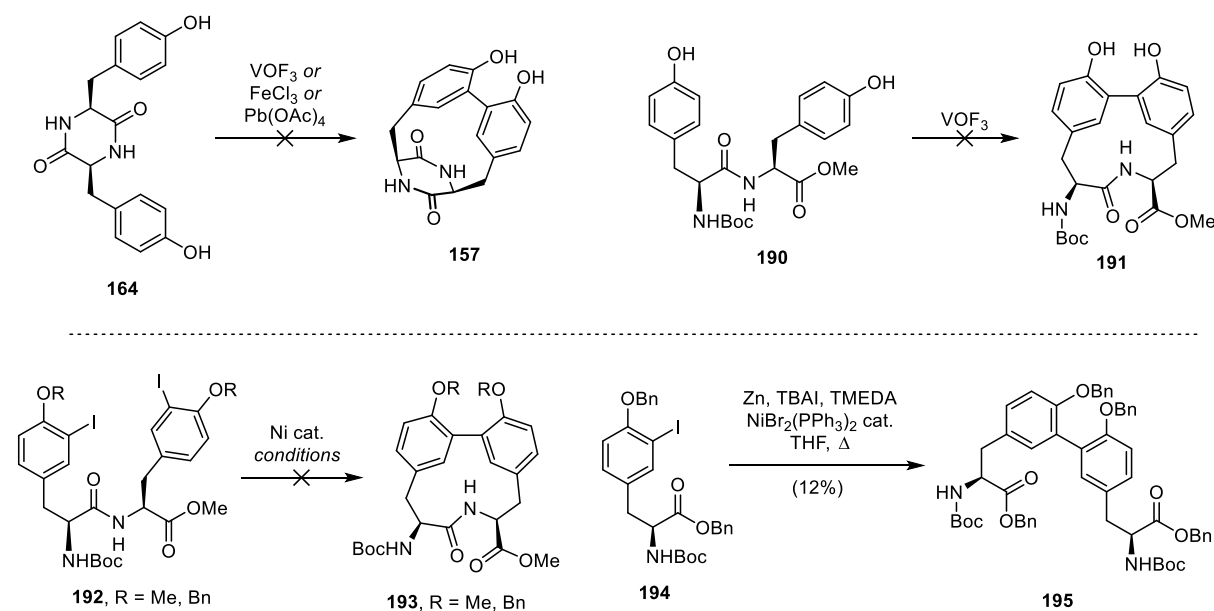
In 2004, Hart described several strategies towards the herquilines based on the reduction of macrocyclic diketopiperazine **157**, identical to the structure of mycocyclosin (see Figure 15).<sup>[235]</sup> This key intermediate was planned to be formed either by direct phenolic coupling of cyclic tyrosine dimer **164** or linear tyrosine dimer **190** followed by formation of the six-membered ring (Scheme 49).



**Scheme 49. Retrosynthetic plan by Hart and Johnson.**

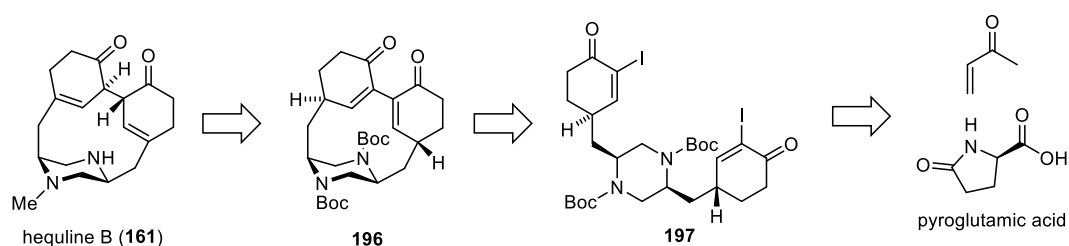
As shown in Scheme 50, several direct oxidative intramolecular phenolic coupling reactions of diketopiperazine **164** were not successful. Similarly, the cyclization of protected dityrosine **190** to give 12-membered ring **191** was not possible under conditions reported by Evans and co-workers.<sup>[236]</sup> A nickel-mediated intramolecular coupling of iodinated dityrosine **192** was also not feasible.

Interestingly, similar reaction conditions did furnish, albeit in low yield, biaryl-linked tyrosine dimer **194** starting from protected iodotyrosine **195**. Clearly, conformational bias prevented the cyclizations from proceeding. Furthermore, several model studies on 4-alkyl substituted phenols were also undertaken, but none of the strategies and methods could successfully be rerouted towards the target molecules (not depicted).



**Scheme 50. Attempted direct oxidative phenolic coupling (top), and transition-metal catalyzed homocoupling of iodoarenes (bottom).**

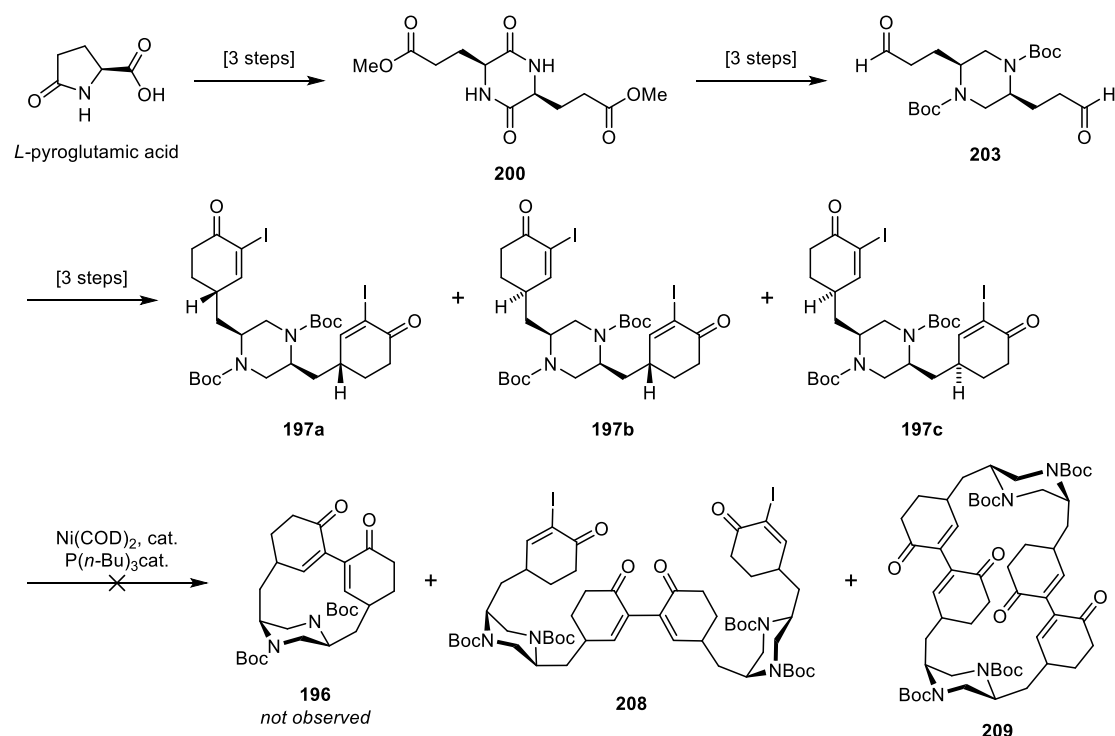
In 2012, Philipp Stawski reported an approach towards the synthesis of herquines A and B using a two-directional strategy starting from a low-oxidation state building block derived from glutamic acid (Scheme 51).<sup>[237]</sup> Herquiline B was the primary target, to be accessed via isomerization of the  $C_2$ -symmetrical enone **196**. Macrocyclization was envisaged to be achieved by homocoupling of  $\alpha$ -iodo cyclohexenone **197**.



**Scheme 51. Retrosynthetic analysis via  $\alpha,\beta$ -unsaturated ketone by Stawski and Trauner.**

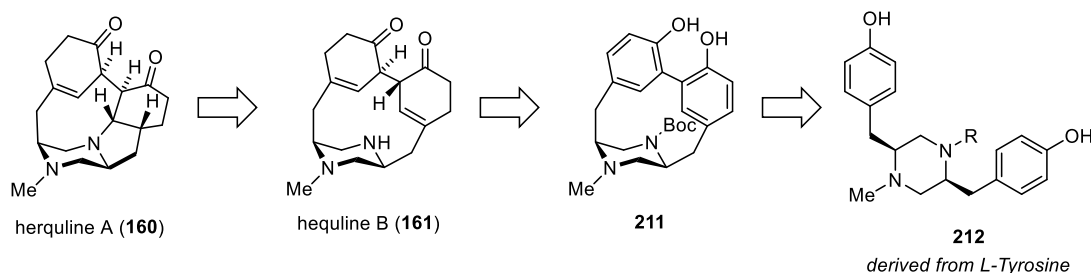
Dimerization of pyroglutamic acid to the 2,5-diketopiperazine followed by hydrolysis and esterification gave **200** (Scheme 52). Dialdehyde **203** was obtained after redox-adjustments and *N*-protection. Twofold 1,4-addition of methyl vinyl ketone, intramolecular aldol condensation and iodination gave rise to macrocyclization precursor **197**. Separation of the three possible isomers (**197a** to **c**) by preparative HPLC set the stage for the key metal-mediated homocoupling reactions. Although several conditions for the formation of the 12-membered ring were investigated, the desired product

**196** could not be isolated, and only dimers such as **208** or **209** were formed as only identifiable products.



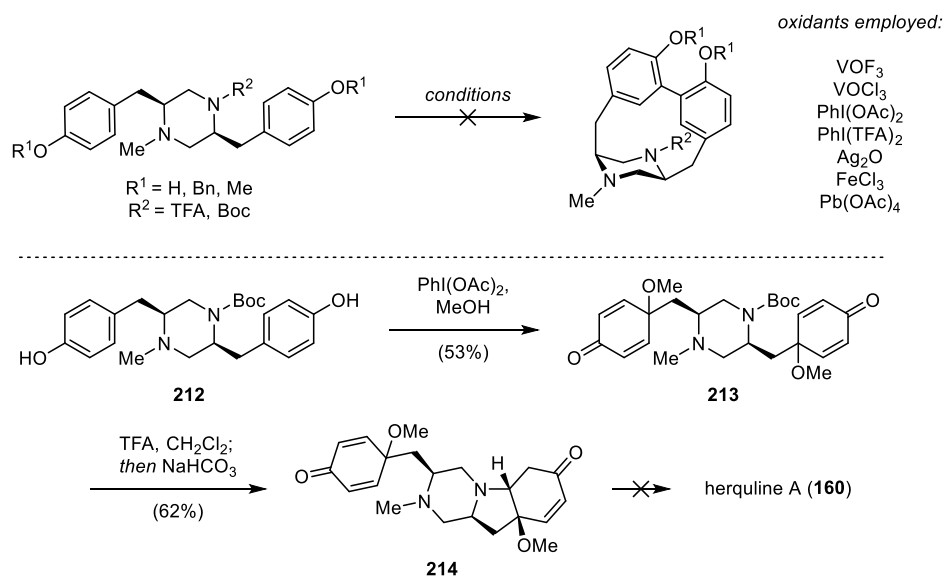
**Scheme 52. Intramolecular cross-coupling approach by Stawski and Trauner.**

Through a private communication with Prof. Nigel Simpkins, we were able to access a PhD thesis by his student He Yang, who completed his doctorate in 2015.<sup>[238]</sup> The retrosynthetic plan relied on the conversion of herquiline B into herquiline A (Scheme 53). Herquiline B would be accessed from reductive dearomatization of *N*-methylated biaryl **211**.



**Scheme 53. Retrosynthesis by Yang and Simpkins.**

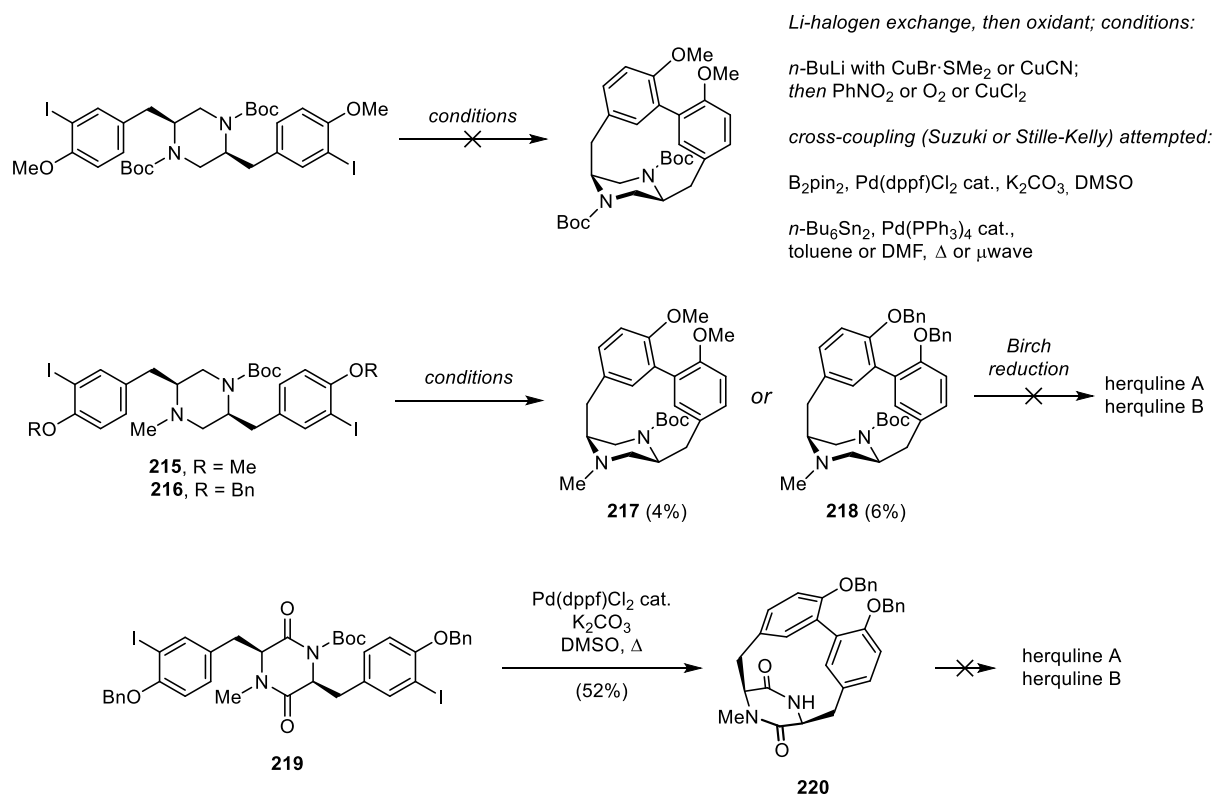
Several intermediates with different protecting group patterns were prepared and subjected to attempted ring closure under a variety of conditions (Scheme 54). First, the phenolic coupling of cyclodityrosine-derived piperazines was investigated without success. Then, an oxidative dearomatization strategy of the same intermediate (**212**) was pursued, which delivered the tricyclic 6,5,6-motif (**214**) found in herquiline A (**160**). Unfortunately, ring closure to form the nine-membered ring was not successful.



### Scheme 54. Attempted oxidative transformation of tyrosine-derived piperazine.

Additionally, metal-mediated cyclization reactions were attempted on functionalized congeners of **212** (see Scheme 55). While the desired ring was formed on several occasions, the prohibitively low yield (4 to 6%) of the cyclization products **217** and **218** prevented further progress. Interestingly, on the related diketopiperazine substrate **219**, the cyclization proceeded in good yield (**220**). This clearly indicates that the  $\text{sp}^2$ -hybridized atoms in the boat-shaped diketopiperazine favor the ring closure by enforcing close proximity between the aromatic rings. On piperazine substrates **215** and **216**, which reside in a chair conformation, the cyclization is highly disfavored and very low yields of **217** or **218** were obtained. Nevertheless, after preparation of an appropriately protected macrocycle **220**, both the reduction of the aromatic ring with Birch conditions, as well as the reduction of the diketopiperazine to the piperazine were not successful, thereby stopping the advancement of the synthesis a mere three steps before its completion.

An additional strategy based on an oxidative enolate coupling is also featured. A very similar approach was investigated independently in our laboratories. The discussion of this last approach, together with our results, can be found in Chapters 2.1.2 and 2.1.3.



**Scheme 55.** Attempted intramolecular coupling of iodoarenes for 12-membered ring formation.

### 1.3. Project Aims

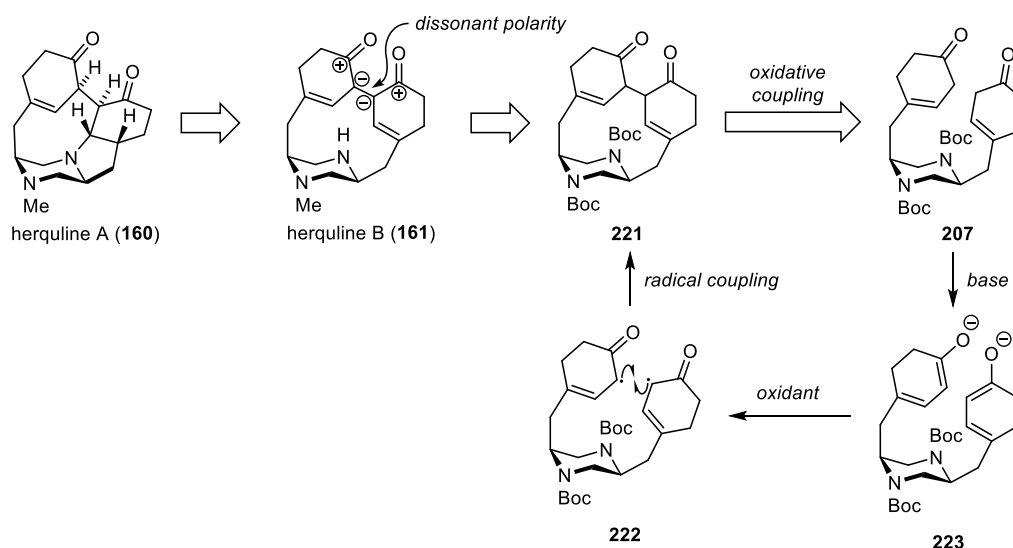
The polycyclic strained architectures of herquelines A and B are unique among natural products. Despite their low molecular weight, they have never been synthesized. Several synthetic approaches were unsuccessful due to the difficulties in accessing either the 9-membered macrocycle of herquiline A, or the 12-membered ring of herquiline B. Moreover, the nonconjugated cyclohexenone moiety represents a very rarely encountered motif in natural products. The idiosyncratic relationship between the highly reduced piperazine ring and the northern cyclohexenone rings add to the synthetic challenge. Together with an interesting, but largely unexplored bioactivity, they are worthy targets for total synthesis.

## 2. Results and Discussion

### 2.1. Retrosynthesis: Early Introduction of the Piperazine Ring

Following the biosynthetic considerations outlined in Chapter 1.2.1, herquiline A can be accessed from herquiline B. Clearly, the  $\beta,\gamma$ -unsaturated ketone (featured in herquiline B) and the corresponding  $\alpha,\beta$ -unsaturated ketone (**163**, Scheme 43), the necessary intermediate in the biosynthesis of herquiline A, are comparable from an energetic point of view, as isomerization occurs under mildly basic conditions at ambient temperature.<sup>[221]</sup> Within the macrocyclic framework provided by the 12-membered ring, the stability gained through conjugation is similar to the presence of trisubstituted, albeit nonconjugated olefin.<sup>[239]</sup>

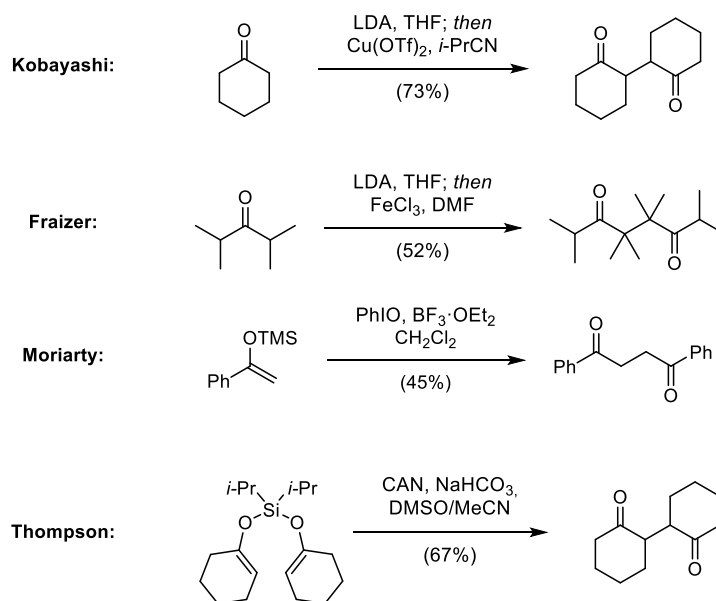
Previous approaches by the Trauner group investigated the intramolecular homocoupling of  $\alpha,\beta$ -unsaturated ketones (see Scheme 52), which would then be subjected to isomerization. This strategy was not successful, and instead we decided to directly target the  $\beta,\gamma$ -unsaturated ketone. To exploit the  $C_2$ -symmetry of the product, a two-directional approach can be pursued, where the key disconnection is the central C–C bond between the 1,4-dicarbonyl moiety of the two cyclohexenones. This substitution pattern requires the application of an “umpolung” strategy such as an oxidative enolate coupling reaction, in which a ketone enolate is oxidized by one-electron oxidation and the resulting diradical (**222**, Scheme 56) undergoes dimerization.<sup>[240]</sup> Regioselective enolate generation on the  $\beta,\gamma$ -unsaturated ketone **207** should be feasible by taking advantage of the higher stability of the resulting dienolate **223** through conjugation.<sup>[241]</sup>



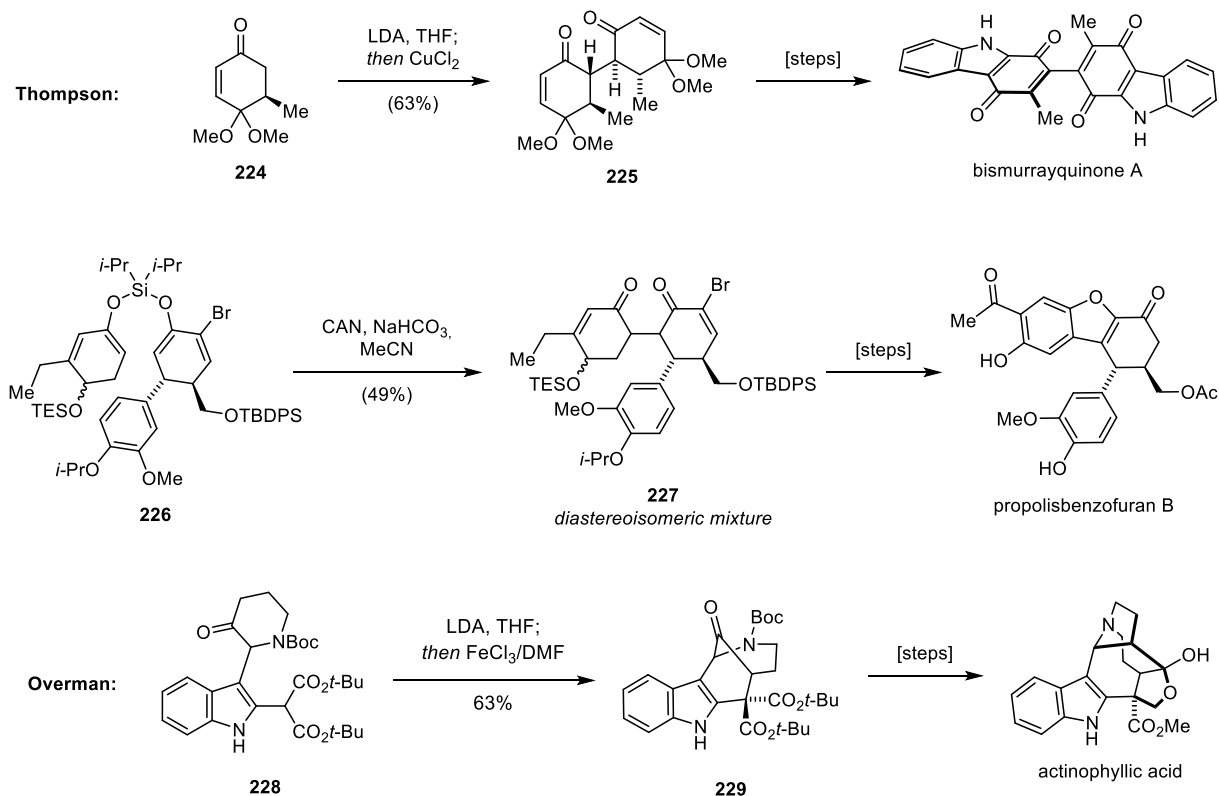
Scheme 56. Umpolung strategy for the synthesis of the herquelines via oxidative enolate coupling.

The one-electron oxidation and resulting “unpoled” reactivity of enolate anions has been used in synthetic chemistry since the 1970’s.<sup>[242]</sup> Deprotonated esters, amides, carboxylic acids, and malonates have been shown to undergo efficient radical coupling to assemble 1,4-dicarbonyl compounds in a convergent manner. Based on the same mechanistic fundament, several experimental protocols have been developed. For example, ketones, predominantly via their lithium enolates, undergo dimerization upon treatment with Fe or Cu salts (Scheme 57).<sup>[243,244]</sup> Silyl enol ethers have also been shown to undergo coupling both in intermolecular fashion as well as intramolecular fashion, most notably starting from a silyl-tethered dienol ether.<sup>[245,246]</sup>

Several applications of the reaction in complex molecule synthesis have been reported to date, and three are shown below (Scheme 58). In the first example, the homodimerization of the enolate derived from **224** gives symmetrical product **225**.<sup>[247]</sup> If non-symmetrical products need to be synthesized, the reaction can be modified by synthesizing silyl dienol ethers such as **226** from the corresponding ketones.<sup>[248]</sup> Intramolecular oxidative coupling gives the desired 1,4-dicarbonyl **227**. In a third example, the intramolecular coupling with formation of a 6-membered ring leading to bicycle **229** was effected starting from a ketone and a malonate as reaction partners (**228**).<sup>[249]</sup> This result especially demonstrates that oxidative coupling is, in principle, possible in intramolecular fashion as required for the realization of our synthetic design.

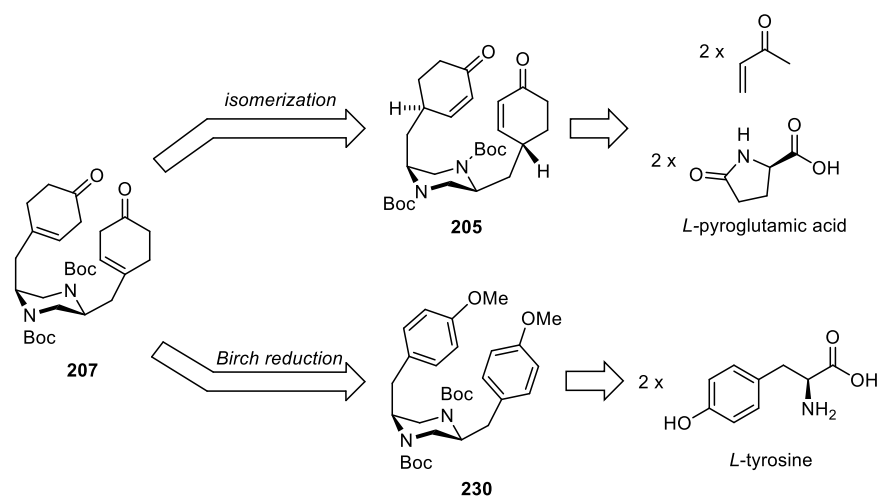


**Scheme 57. Representative methods for oxidative enolate coupling.**



**Scheme 58. Recent applications of oxidative ketone coupling in natural product synthesis.**

As shown in Scheme 59, the required nonconjugated ketone **207** could arise from isomerization of enone **205**, traced back to inexpensive pyroglutamic acid and methyl vinyl ketone. This compound was previously synthesized in the group.<sup>[237]</sup> Alternatively, **207** could be synthesized from a protected tyrosine dimer bearing a piperazine ring (**230**) following partial reduction of the aryl rings using a Birch reduction.

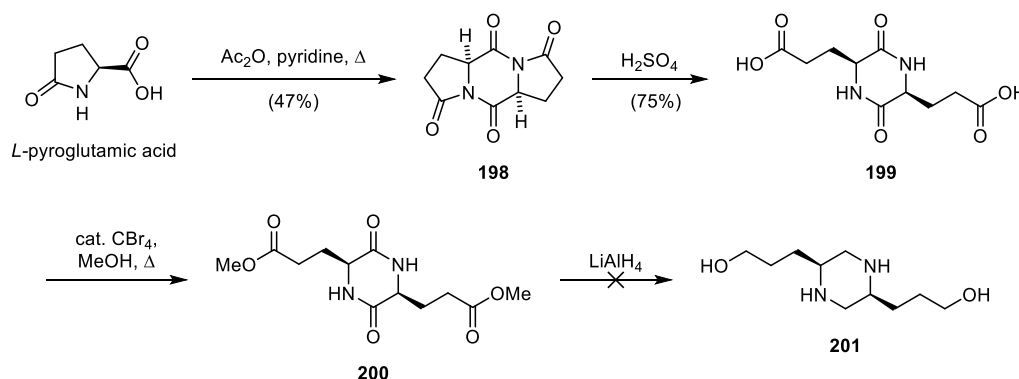


**Scheme 59. Strategies for the synthesis of  $\beta,\gamma$ -unsaturated ketone **207**.**

## 2.1.1. Synthesis of C<sub>2</sub>-symmetric β,γ-unsaturated Ketone

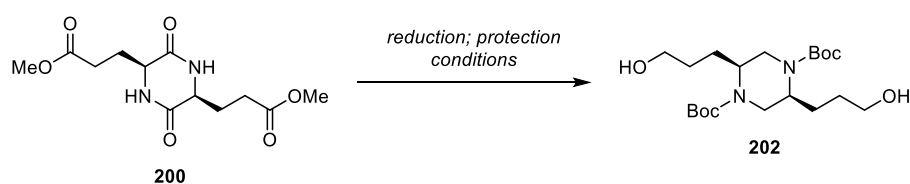
### 2.1.1.1. From L-Pyroglutamic Acid

L-Pyroglutamic acid was treated with acetic anhydride in pyridine to furnish diketopiperazine **198**, which was hydrolyzed in neat sulfuric acid to yield glutamic diketopiperazine **199**.<sup>[250]</sup> Esterification under previously optimized conditions furnished the methyl ester **200** which was taken on towards reduction.<sup>[251]</sup> After several attempts at complete reduction using LiAlH<sub>4</sub>, we were unable to isolate the intermediate piperazine-diol (**201**, Scheme 60).



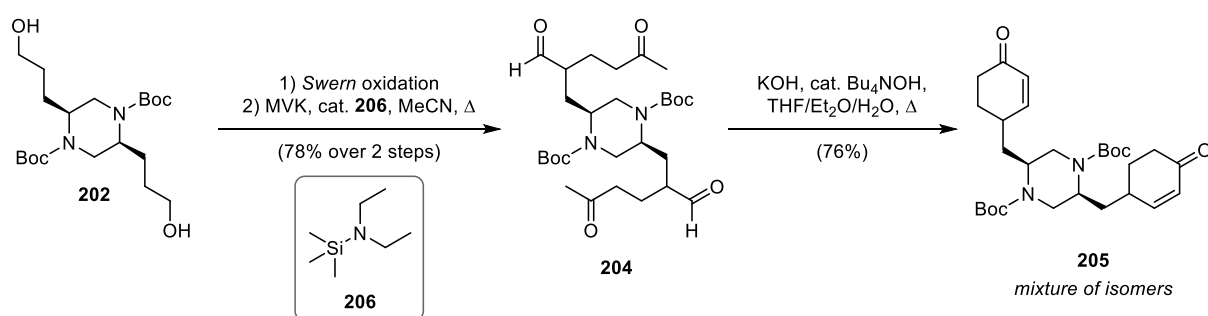
**Scheme 60.** Synthesis and attempted reduction of glutamic diketopiperazine **200**.

Quenching the reaction with a minimal amount of water followed by in situ protection was possible to afford **202**, whose structure could be proven by X-ray crystallographic analysis. This procedure was found to be highly irreproducible on larger scale (> 10 mmol) and called for alternative reaction conditions (Table 35). In situ generated AlH<sub>3</sub> was also ineffective (Entry 6), whereas LiBH<sub>4</sub> (Entry 5) afforded a mixture of products.<sup>[252]</sup> The use of borane, previously reported by Jung as the reagent of choice for reduction of simple diketopiperazines, was investigated next.<sup>[253]</sup> While the use of in situ generated BH<sub>3</sub> and its commercially available dimethyl sulfide adduct was not effective (Entries 7 and 8), the use of borane-THF complex was instrumental to obtaining a high yield, although we observed batch-related variabilities. Excess borane could be quenched with methanolic HCl, which allowed for the isolation of piperazine-alcohol **201** as its HCl salt, whose structure could also be verified by X-ray crystallographic analysis (see Page 236). Subjection of this compound to Boc-protection then gave **202** (see Page 237 for X-ray analysis). Swern oxidation delivered dialdehyde **203** which was reacted with methyl vinyl ketone using aminocatalyst **204**.<sup>[254]</sup> Robinson annulation of the so-obtained ketoaldehyde **204** under phase-transfer conditions and high dilution afforded **205** on a multigram scale as a mixture of diastereoisomers.<sup>[255,256]</sup>

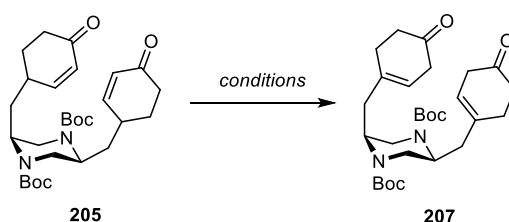
**Table 35. Conditions for the reduction and *N*-Boc protection of diketopiperazine 200.**

Entry	Reagent	Solvent	Temp. (°C)	Time (h)	Quenching method	Yield of 202 (%)
1	LiAlH <sub>4</sub> (15.0 eq.)	THF	0 to 60	30	Fieser Workup <sup>a</sup>	37% <sup>b</sup>
2	LiAlH <sub>4</sub> (15.0 eq.)	THF	0 to 60	30	Rochelle's Salt	-
4	LiAlH <sub>4</sub> (15.0 eq.)	THF	0 to 60	24	Na <sub>2</sub> SO <sub>4</sub> ·10H <sub>2</sub> O	-
5	LiBH <sub>4</sub> (10.0 eq.)	THF	0 to rt	24	aq. NH <sub>4</sub> Cl	-
6	AlH <sub>3</sub> (20.0 eq.) <sup>c</sup>	THF	0 to 60	24	aq. NH <sub>4</sub> Cl	-
7	BH <sub>3</sub> (16.0 eq.) <sup>d</sup>	THF	0 to 60	14	conc. HCl	-
8	BH <sub>3</sub> ·SMe <sub>2</sub> (16.0 eq.)	THF	0 to 60	14	conc. HCl	-
9	BH <sub>3</sub> ·THF (16.0 eq.)	THF	0 to 60	13	conc. HCl	27% <sup>e</sup>
10	BH <sub>3</sub> ·THF (16.0 eq.)	THF	0 to 60	13	HCl in MeOH	49% <sup>e</sup>
11	BH <sub>3</sub> ·THF (13.0 eq.)	THF	0 to 60	17	HCl in MeOH	40% <sup>e</sup>
12	BH <sub>3</sub> ·THF (10.0 eq.)	THF	0 to 60	17	HCl in MeOH	67% <sup>e</sup>
13	BH <sub>3</sub> ·THF (10.0 eq.)	THF	0 to 60	11	HCl in MeOH	63% <sup>f</sup>

**a)** Fieser workup: for every 1 g LiAlH<sub>4</sub>, 1 g H<sub>2</sub>O, 1 g aq. NaOH (10%), and 3 g H<sub>2</sub>O were added in sequence; **b)** after protection using Boc<sub>2</sub>O (2.2 eq), NaHCO<sub>3</sub>, H<sub>2</sub>O/THF, 24 h; **c)** generated from LiAlH<sub>4</sub> (15.0 eq) and AlCl<sub>3</sub> (5.0 eq); **d)** generated from NaBH<sub>4</sub> (16.0 eq.) and I<sub>2</sub> (8.0 eq.) **e)** after protection using Boc<sub>2</sub>O (2.2 eq), Et<sub>3</sub>N (4.5 eq), CH<sub>2</sub>Cl<sub>2</sub>, 16 h; **f)** after Boc-protection using Boc<sub>2</sub>O (2.2 eq), NaOH (4.5 eq), 1,4-dioxane, 18 h.

**Scheme 61. Synthesis of *N*-protected C<sub>2</sub>-symmetric  $\alpha,\beta$ -unsaturated cyclohexenone.**

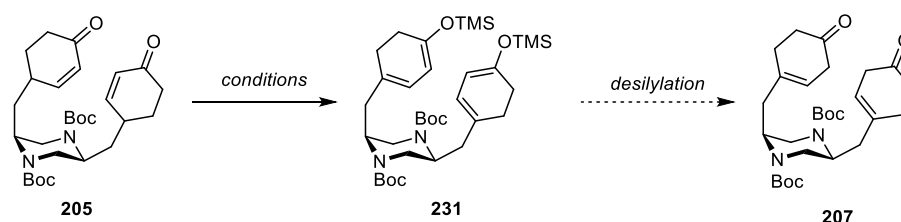
Several strategies to effect the direct alkene isomerization of **205** to the desired trisubstituted  $\beta,\gamma$ -position were investigated (Table 36). Unfortunately, the use of acid catalysts that had been successfully used in olefin isomerization did not deliver any product (Entries 1 to 5).<sup>[257–259]</sup> Basic conditions resulted in the reisolation of starting material when a weak base was used (Entries 6 or 7), whereas stronger bases (e.g. *t*-BuOK) resulted in rapid degradation of **205** (Entries 8 and 9). Formation of the dienolate using various bases followed by kinetic protonation in the  $\alpha$ -position was also not possible (Entries 11 to 14).

**Table 36. Attempted direct isomerization reactions for ketone 205.**

Entry	Reagent(s)	Solvent	Temp. (°C)	Time (h)	Outcome
1	RhCl <sub>3</sub> (0.1 eq.)	EtOH	rt	8	no reaction
2	RhCl <sub>3</sub> (0.1 eq.)	EtOH	80	1	complex mixture
3	HCl (0.1 eq.)	Et <sub>2</sub> O	rt	24	no reaction
4	HCl (0.1 eq.)	EtOH	rt to 60	24	complex mixture
5	<i>p</i> -TSA (0.2 eq.)	toluene	rt to 80	16	no reaction
6	DBU (2 eq.)	toluene	rt	24	no reaction
7	DBU (2 eq.)	toluene	80	24	no reaction
8	<i>t</i> -BuOK (6 eq.)	<i>t</i> -BuOH	rt	1	complex mixture
9	<i>t</i> -BuOK (1 eq.)	DMSO	rt	0.1	complex mixture
10 <sup>a</sup>	LDA (2 eq.), then AcOH (4 eq.)	THF	-78 to rt	1	no reaction
11 <sup>a</sup>	LiHMDS, (2 eq.), then AcOH (4 eq.)	THF	-78 to rt	1	no reaction
12 <sup>a</sup>	LiHMDS, (2 eq.), then AcOH (4 eq.)	THF/HMPA	-78 to rt	1	complex mixture
13 <sup>a</sup>	NaH (2 eq.), then AcOH (4 eq.)	THF	0 to rt	1	no reaction
14 <sup>a</sup>	NaH (2 eq.), then AcOH (4 eq.)	THF	rt to 60	1	complex mixture

a) addition of AcOH was performed at -78 °C;

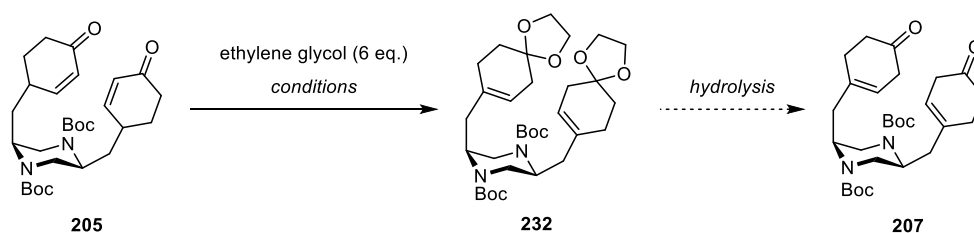
We next investigated two-step protocols for olefin isomerization through intermediate silyl dienol ether **231**, which could be unmasked to the  $\beta,\gamma$ -unsaturated ketone after desilylation.<sup>[260]</sup> As can be seen in Table 37, deprotonation using lithium amide bases (LDA or LiHMDS) followed by trapping with TMSCl or TBSOTf did not result in the desired product even after addition of HMPA (Entries 1 to 3). Application of the Kharash–Grignard reagent was examined next, in which the addition of catalytic FeCl<sub>3</sub> to MeMgBr allows for the generation of an iron “ate” complex that engages in  $\gamma$ -selective deprotonation of  $\alpha,\beta$ -unsaturated ketones.<sup>[261,262]</sup> Unfortunately, the desired product was not observed. Similarly, the use of an amidocuprate reagent generated in situ from LDA and CuCN was also not fruitful.<sup>[263]</sup> Next, we employed thermodynamic conditions to enforce formation of the desired product with TMSI or TMSBr (generated in situ).<sup>[264]</sup> The reactions gave a complex mixture of products and low overall mass balance (Entries 7 to 10).

**Table 37. Attempted formation of silyl dienol ether 231.**

Entry	Reagent(s)	Solvent	Temp. (°C)	Time (h)	Outcome
1	LiHMDS (2 eq.), then TMSCl (2.2 eq.)	THF	-78 to rt	3	mainly <b>205</b>
2	LiHMDS (2 eq.), then TBSOTf (2.2 eq.)	THF	-78 to rt	3	complex mixture
3	LDA (2 eq.), then TMSCl (2.2 eq.)	THF/HMPA	-78 to rt	3	complex mixture
4	LDA (4 eq.), LiCl (2 eq.), CuCN (2 eq.), then TMSCl, (4 eq.) Et <sub>3</sub> N (4 eq.)	THF	-78		complex mixture
5	FeCl <sub>3</sub> (0.1 eq), MeMgBr (2.5 eq.), then TMSCl, Et <sub>3</sub> N (3 eq. each)	Et <sub>2</sub> O	-78	2	no reaction
6	FeCl <sub>3</sub> (0.1 eq), MeMgBr (2 eq.), then TMSCl, Et <sub>3</sub> N (3 eq. each)	THF/DMPU	0	12	complex mixture
7	TMSCl (2 eq.) NaI (2 eq.), Et <sub>3</sub> N (2.2 eq.)	MeCN	-78 to rt	12	complex mixture
8	TMSCl (2 eq.) NaI (2 eq.), Et <sub>3</sub> N (2.2 eq.)	THF	-78 to rt	12	mainly <b>205</b>
9	TMSCl (2 eq.) LiBr (2 eq.), Et <sub>3</sub> N (2.2 eq.)	MeCN	0 to 60	12	complex mixture
10	TMSCl (2 eq.) LiBr (2 eq.), Et <sub>3</sub> N (2.2 eq.)	THF	0 to 60	12	complex mixture

Previous attempts at thermodynamic deprotonation only returned starting material, and none of the desired nonconjugated isomer. Evidently, there is no energetic advantage to the formation a trisubstituted, albeit nonconjugated olefin at the expense of a conjugated ketone, and the stability gain through conjugation is too high to allow isomerization to occur. However, by masking the ketone functionality and removing this possibility for mesomeric stabilization, the desired double bond isomerization should be more facile and lead to the thermodynamically more stable olefin with a higher degree of substitution (Table 38). Afterwards, mild acidic hydrolysis could unmask the desired deconjugated product **207**. This method, in the form of acid-mediated ketal formation, has been applied on decalin systems and steroidal carbocycles to effect deconjugation of an  $\alpha,\beta$ -unsaturated ketone.<sup>[265–267]</sup>

When **205** was treated with ethylene glycol at elevated temperature, we could indeed observe formation of isomeric olefin products by NMR spectroscopy (Table 38, entry 3). However, we also observed the product of direct ketal formation without double bond isomerization. Concomitant decomposition of the substrate was evident by darkening of the reaction mixture and resulted in very low overall yield. Exploratory studies conducted on the isomeric mixture of **232** indicated that either oxalic acid or diluted HCl could liberate the ketone functionality.<sup>[268,269]</sup> Unfortunately, the products **207** and **205** were found to be chromatographically inseparable in a variety of solvent systems. Paired with the long reaction times and low overall yield for the two step sequence, we were forced to abandon the glutamate-based route to cyclohexanone **207** in favor of an alternative approach.

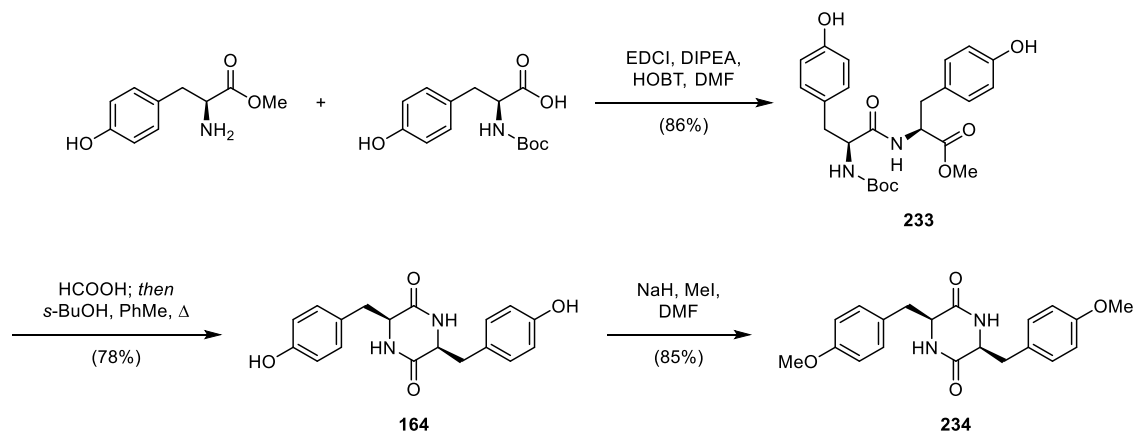
**Table 38. Ketal formation and alkene isomerization.**

Entry	Catalyst	Solvent	Additive	Temp. (°C)	Time (h)	Outcome
1	<i>p</i> -TSA (0.2 eq.)	toluene	none	40	16	no reaction
2	<i>p</i> -TSA (0.2 eq.)	toluene	MgSO <sub>4</sub>	rt to 100	24	decomposition
3	<i>p</i> -TSA (0.2 eq.)	toluene	trimethyl orthoformate	rt to 100	24	mixture, 13% overall <sup>a</sup>
3	<i>p</i> -TSA (0.2 eq.)	toluene	trimethyl orthoformate	rt to 100	72	decomposition
4	(+)-CSA (0.2 eq.)	toluene	MgSO <sub>4</sub>	rt to 100	24	decomposition

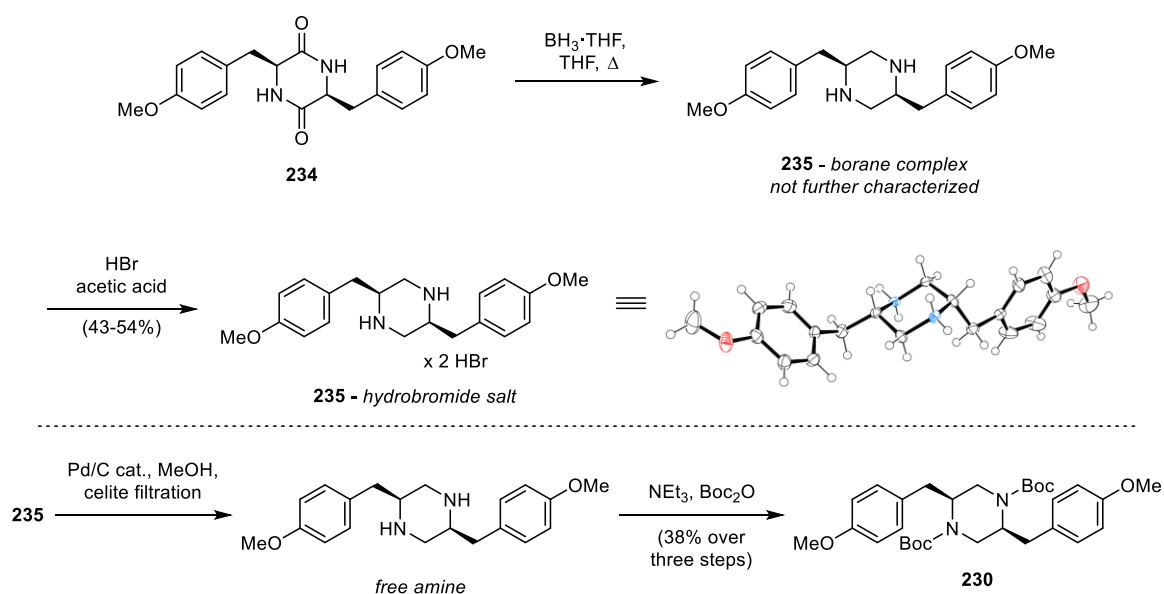
a) 205/207 = 1.5/1, inseparable by chromatography;

### 2.1.1.2. From L-Tyrosine

According to Scheme 59, an alternative route to  $\beta,\gamma$ -unsaturated ketone from L-tyrosine was investigated (Scheme 62). L-tyrosine methyl ester was coupled with Boc-protected tyrosine to yield the dipeptide **233**.<sup>[211]</sup> Removal of the Boc group followed by basification and heating in an *s*-butanol/toluene mixture led to cyclization and afforded the highly insoluble diketopiperazine **164**, which could be isolated in good yield after centrifugation. The phenolic hydroxyl group was selectively methylated to yield **234**.<sup>[270]</sup>

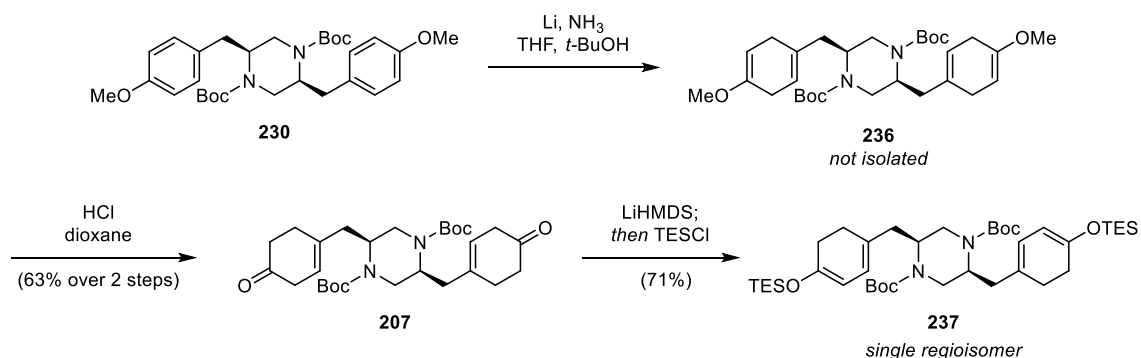
**Scheme 62. Synthesis of *O*-methylated diketopiperazine **234**.**

Reduction of **234** was performed according Jung and co-workers to give, after quenching with HBr, piperazine **235** as the bishydrobromide salt.<sup>[253]</sup> An X-ray structure was obtained, confirming the *cis*-stereochemistry and that no racemization had occurred during the previous synthetic manipulations (Scheme 63). To avoid the use of corrosive HBr, the reaction mixture following the borane reduction was quenched with MeOH, and the solvent could be evaporated to give the piperazine-monoborane complex as determined by LCMS. Pd/C was added to a methanolic solution of **235** to effect decomplexation. After filtration over celite, the solution containing the free secondary amine could be protected in situ and gave Boc-protected piperazine **230** in moderate yield.<sup>[271]</sup>



**Scheme 63. Reduction and protection of *O*-methylated cyclo-TyrTyr (**234**).**

Piperazine **230** was subjected to Birch reduction using elemental lithium in liquid ammonia.<sup>[272]</sup> Success of the reaction was confirmed by NMR, but isolation of the enol ether **236** was not possible and resulted in partial rearomatization during chromatography. Instead, treatment of the crude reaction mixture with diluted HCl afforded ketone **207**, which could be purified by column chromatography and was found to be stable upon storage in a benzene matrix. With a reliable route to the  $\beta,\gamma$ -unsaturated ketone **207** in hand, the regioselectivity of deprotonation of  $\beta,\gamma$ -unsaturated ketone **207** was assessed. Gratifyingly, treatment with LiHMDS at  $-78^\circ\text{C}$  followed by addition with TESCl delivered conjugated dienol ether **237** as the only observed product.

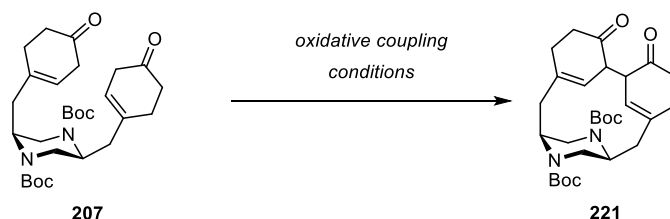


**Scheme 64. Synthesis and deprotonation of the oxidative enolate coupling precursor.**

### 2.1.2. Oxidative Enolate Coupling Reaction

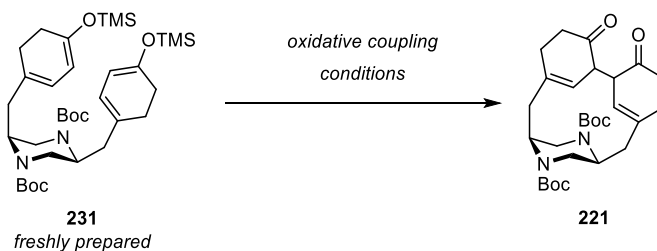
A systematic investigation of reaction conditions for the oxidative enolate coupling of ketone **207** was performed. As shown in Table 39, the use of lithium amide bases with several Fe<sup>3+</sup> salts was examined, as well as the influence of solvent additives such as DMF and HMPA, which are shown to improve the solubility of the oxidant and allow for productive reaction (entries 1 to 9).<sup>[273]</sup> In every case, the desired coupling product could not be isolated. Similarly, Cu<sup>2+</sup> salts were also ineffective in the formation of **221**.<sup>[274]</sup> Direct coupling of **207** without formation of the enolate was attempted using Cu(OAc)<sub>2</sub> but did not convert the starting material, whereas NiO<sub>2</sub> at elevated temperatures led to rapid degradation (Entry 20).<sup>[275,276]</sup> In the majority of cases, we could determine that a mixture of products were formed, judging by the multitude of olefinic and aromatic signals present in the <sup>1</sup>H NMR spectra. The use of alternative oxidants which are used for the oxidative coupling of oxazolidinone enolates (TiCl<sub>4</sub>) or ketone-indole systems (I<sub>2</sub>) were also investigated without success (Entries 10 and 11).<sup>[277]</sup>

**Table 39. Conditions examined for the intramolecular oxidative coupling of ketone 207.**



Additionally, the silyl enol ether **231** could be prepared by treatment with TBSOTf/Et<sub>3</sub>N (Table 40). It was immediately subjected to oxidative coupling conditions due to its instability upon storage. The addition of several oxidants known to promote the intermolecular coupling of silyl enol ethers was not successful and resulted in degradation of **231** or desilylation to give ketone **207**.<sup>[278–281]</sup> The conditions reported by Thompson or Wirth for the intermolecular reaction of tethered silyl bis-enol ethers were also ineffective (Entries 6, 7 and 10, 11).<sup>[245,282]</sup>

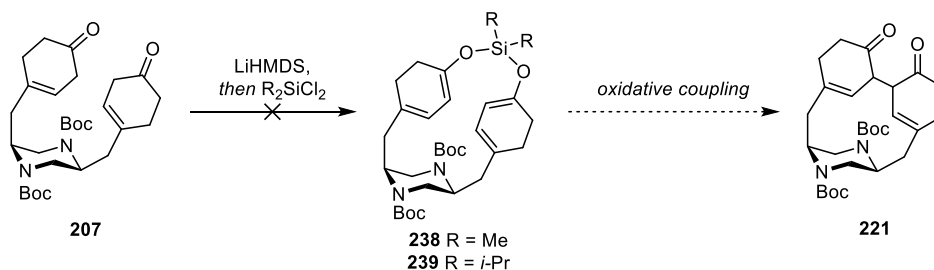
**Table 40. Conditions examined for the intramolecular coupling of silyl dienol ether **231**.**



Entry	Reagent	Solvent	Temp. (°C)	Time (h)	Outcome
1	Ag <sub>2</sub> O (2.2 eq.)	DMSO	100	4	complex mixture
2	Ag <sub>2</sub> O (2.2 eq.)	MeCN	100	4	complex mixture
3	VOCl <sub>3</sub> (3.0 eq.)	CH <sub>2</sub> Cl <sub>2</sub>	-78 to rt	1	complex mixture
4 <sup>a</sup>	VOCl <sub>3</sub> (3.0 eq.)	CH <sub>2</sub> Cl <sub>2</sub>	-78	4	desilylation of <b>231</b>
5 <sup>a</sup>	PhI(OAc) <sub>2</sub> (2.1 eq.)	CH <sub>2</sub> Cl <sub>2</sub>	-10	1	desilylation of <b>231</b>
6	PhI(OAc) <sub>2</sub> (2.1 eq.), BF <sub>3</sub> ·OEt <sub>2</sub> (3.0 eq.)	MeCN	-10	2	complex mixture
7	PhI(OAc) <sub>2</sub> (2.1 eq.), BF <sub>3</sub> ·OEt <sub>2</sub> (3.0 eq.)	CH <sub>2</sub> Cl <sub>2</sub>	-10	2	complex mixture
8 <sup>a</sup>	Cu(OTf) <sub>2</sub> (2.2 eq.)	CH <sub>2</sub> Cl <sub>2</sub>	rt	12	desilylation of <b>231</b>
9	Pb(OAc) <sub>4</sub> (2.1 eq.)	CH <sub>2</sub> Cl <sub>2</sub> /THF	-78 to rt	1	complex mixture
10	CAN (2.2 eq.), NaHCO <sub>3</sub> (4.4 eq.)	DMSO/MeCN	-10 to rt	16	complex mixture
11	CAN (2.2 eq.), NaHCO <sub>3</sub> (4.4 eq.)	MeCN	-10 to rt	16	complex mixture

a) desilylation of **231** resulted in mixtures of **205** and **207**;

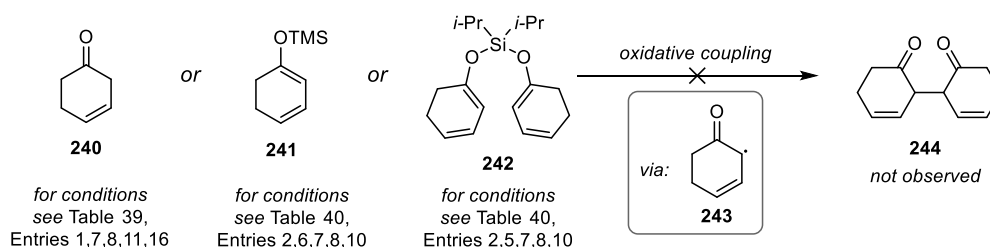
Next, we planned to preorganize the two reactive sites for oxidative coupling by tethering them to give **238**, and perform the coupling on this precursor (Scheme 65). Unfortunately, only starting material could be reisolated after deprotonation and addition of silyl-biselectrophiles.<sup>[245]</sup> As silyl tethered bis-enol ethers have been shown to be stable upon aqueous workup, we suspect that cyclization to **238/239** did not occur at all, and conformational constraints prevented substrate **207** from adapting a conformation necessary to allow the formation of 17-membered dioxasilacycle **238**.



**Scheme 65. Attempted formation of macrocyclic silyl dienol ether **238**.**

Intermolecular coupling experiments on model substrates were carried out to investigate whether the  $\beta,\gamma$ -unsaturated ketone **207** might be at fault for the failure of the reaction (Scheme 66).

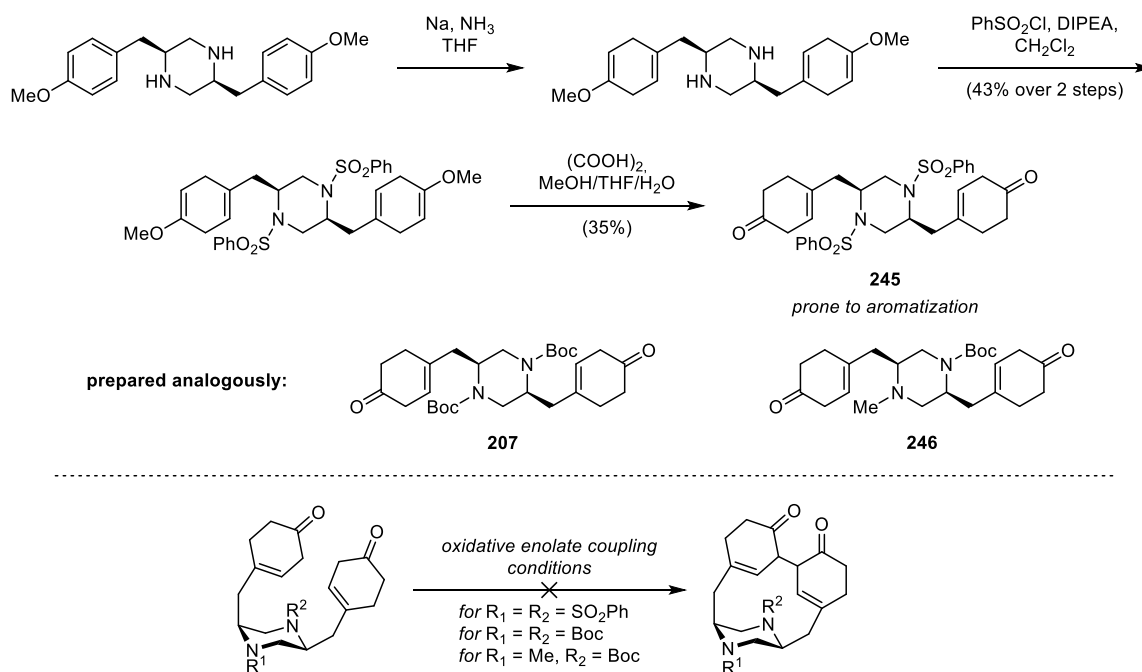
Treatment of the literature-known cyclohexenone **240** under several conditions only resulted in decomposition of the starting material or isomerization to the  $\alpha,\beta$ -unsaturated ketone. The use of the extended silyl enol ether **241**, or its silicon-tethered congener **242** also did not afford any coupling product. Clearly, enolate-derived radicals that benefit from allylic stabilization such as **243** are not able to undergo productive formation of **244** and allow for the synthesis of herquelines A and B.



**Scheme 66.** Attempted oxidative coupling of model  $\beta,\gamma$ -unsaturated ketone or silyl enol ether.

### 2.1.3. Conclusion and Analysis

Starting from inexpensive and readily available amino acids, we prepared the desired *N*-protected  $\beta,\gamma$ -unsaturated ketone **221** and subjected it to oxidative coupling conditions. The desired cyclization product could not be observed either by using its enolate, or **221** itself. Similarly, the preformed silyl dienol ether **231** could also not be converted into the desired 12-membered ring. Tethering the reactive sites by formation of cyclic bis-enol ethers **238** or **239** was also not possible. As previously mentioned in chapter 1.3, we became aware of the work by Yang and Simpkins, who also investigated an oxidative enolate coupling in one of their approaches towards herquelines A and B.<sup>[238]</sup> They prepared sulfonyl-protected dienone **245** (see Scheme 67) and attempted the oxidative coupling reaction using conditions similar to those reported in Table 39. Unfortunately, no cyclization product was formed. Both the direct enolate coupling as well as the coupling of preformed silyl enol ethers was not possible. The reaction was also investigated on related substrates, such as the monomethylated compound **246** and the Boc-protected piperazine **207** (Scheme 67). On the sulfonylated substrate **245** however, a product bearing the required mass of cyclization product was found to be present in trace quantities, but no spectral data were reported to confirm its identity.



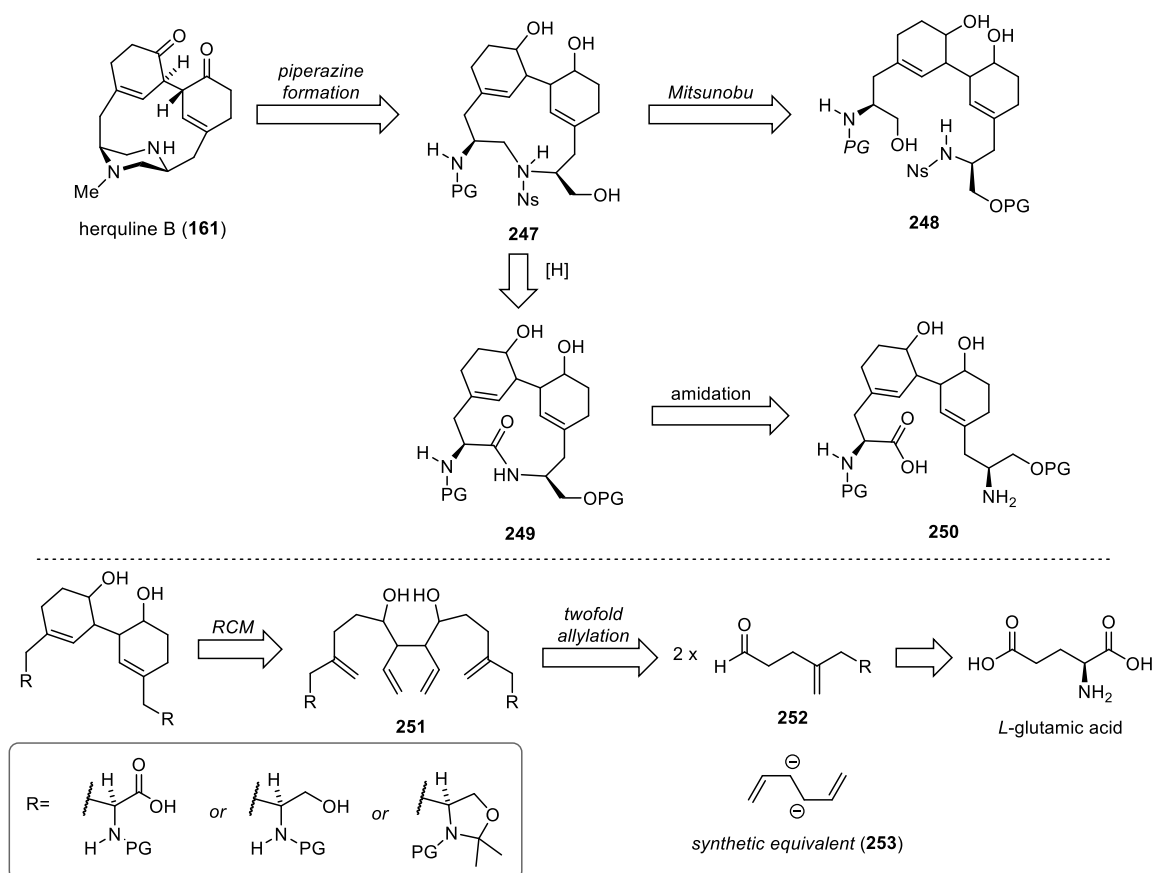
**Scheme 67. Oxidative enolate coupling strategy pursued by Simpkins and Yang.**

Taken together, these independently obtained results reinforced our conviction that  $\beta,\gamma$ -unsaturated ketones with an isolated double bond are not competent substrates in oxidative enolate coupling. Although the formation of a 12-membered ring via intramolecular dimerization of two radicals represents a considerable challenge, model studies showed that the inability of  $\beta,\gamma$ -unsaturated ketones to undergo radical coupling even in intermolecular fashion is at fault.

A main reason for the failure of previously reported approaches based on 12-membered ring formation via the union of two cyclohexene rings through C–C bond formation (e.g. via transition-metal catalyzed coupling) lies in the preference of piperazines to adopt a chair conformation and the difficulty in bringing about a ring-flip to a boat or twist-boat conformation required for the junction of the two cyclohexenone fragments. To solve this problem, the synthesis of a cyclization precursor in which the piperazine ring adopts a boat conformation was thought to solve this issue. Literature precedent showed that  $\text{sp}^2$ -hybridization of the ring atoms (as seen in a 2,5-diketopiperazine or bislactim ether **188**) can allow the formation of a 12-membered ring (see Section 1.2, Scheme 48).<sup>[211]</sup> However, after following this insight, the reduction of either the aryl ring or the diketopiperazine moiety has proven challenging (see Section 1.2, Scheme 48 and Scheme 55). Although masking strategies for the double bond could be imagined, we decided to redesign our approach to avoid the late-stage formation of the central C–C bond of the 1,4-dicarbonyl moiety.

## 2.2. Revised Retrosynthesis: late-stage Piperazine Formation

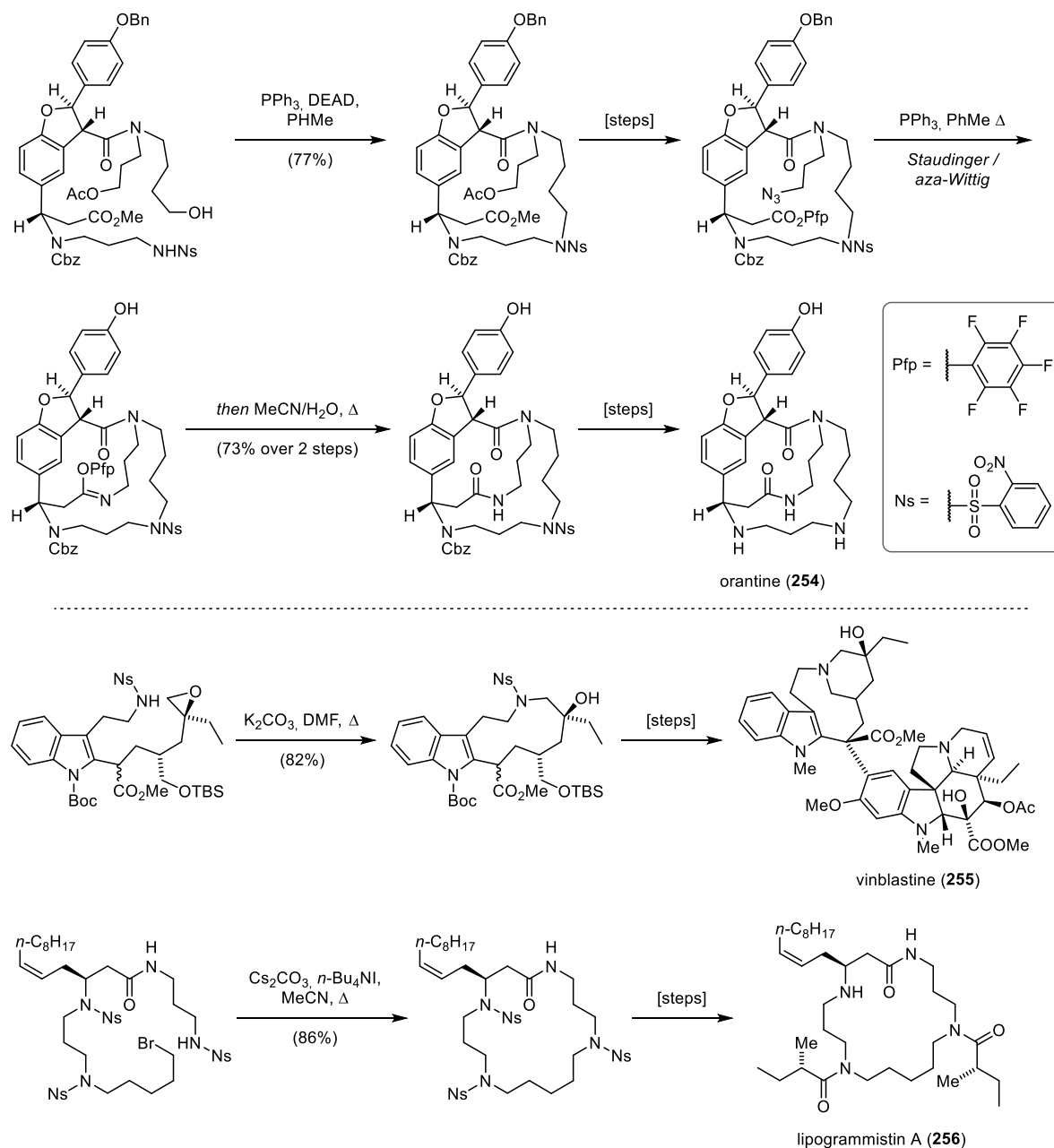
Until now, efforts from our and other research groups have relied on the early introduction of the piperazine ring and the construction of the 1,4-diketone moiety – and the required macrocycle – by joining the  $\alpha$ -position of two cyclohexene ring. In the following sections, a strategically opposite approach is discussed. The two cyclohexenone rings are put in place early on in the synthesis, the 12-membered macrocycle is closed thereafter, and the piperazine ring is formed last. Epimerization of the stereogenic center  $\alpha$  to the ketone moiety, as well as the possibility of enforcing a favorable conformation of the cyclohexenone rings by templation of the 1,4-diol, should allow ring closure to the 12-membered ring either via Mitsunobu reaction or peptide bond formation (Scheme 68). A twofold ring-closing metathesis disconnection could afford the bis-cyclohexenone motif starting from **251**, which results from the twofold allylation of an aldehyde (**252**) with the synthetic equivalent of a hexadienyl anion that bears two adjacent nucleophilic sites (**253**). The aldehyde coupling partner could be prepared from readily available L-glutamic acid and allows the introduction of several different oxidation and protecting group patterns (highlighted in the grey box, Scheme 68).



**Scheme 68. Retrosynthesis of herquiline B using a late-stage piperazine formation strategy.**

For the formation of the 12-membered ring (**247**), literature precedent suggests that an intramolecular Mitsunobu–Fukuyama type reaction of an aminoalcohol of type **248** using the highly nucleophilic nosyl amine could be employed (Scheme 68). Beside amide bond formation, an intramolecular aza-

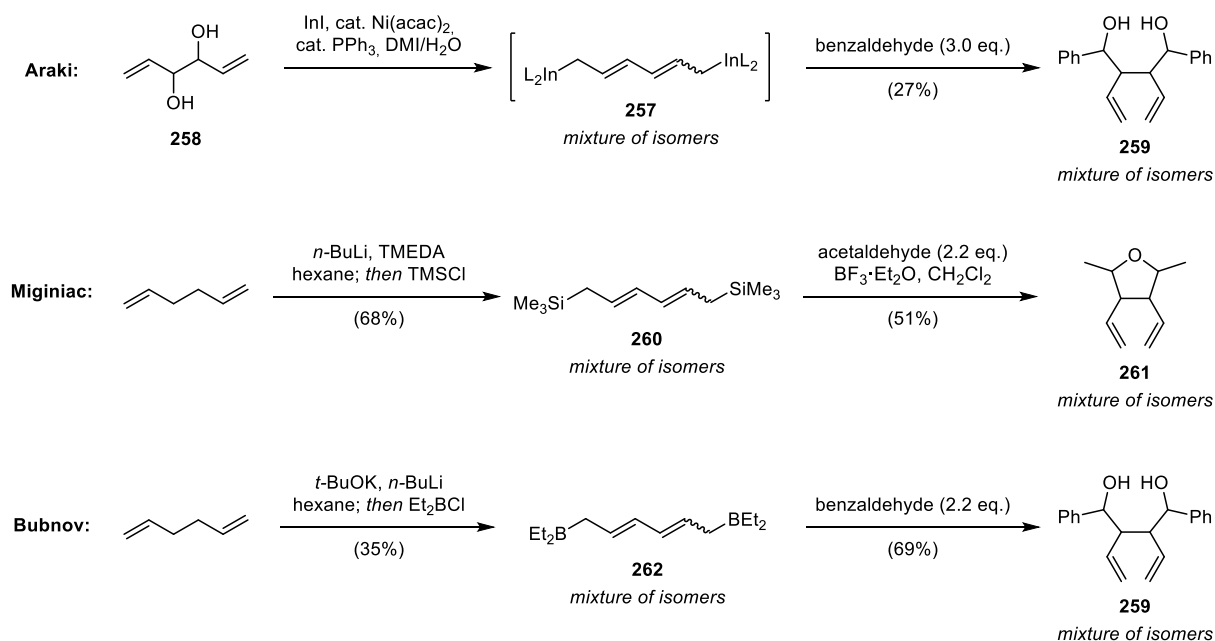
Wittig reaction using an electrophilic pentafluorophenyl ester derived from **250** could also be investigated.<sup>[283,284]</sup> The combination of the two strategies has, for example, been demonstrated by Fukuyama and co-workers in the total synthesis of orantine (**254**, Scheme 69), while the intramolecular cyclization of a Ns-amide is featured in the synthesis of the northern fragment of vinblastine (**255**, 11-membered ring formation), and lipogrammistin A (**256**, 18-membered ring formation).<sup>[285–287]</sup>



**Scheme 69** Macrocyclization via Mitsunobu reaction or intramolecular aza-Wittig reaction (top), or via epoxide opening or nucleophilic substitution using Ns-protected amines (bottom).

### 2.2.1. Development of a Bifunctional Allylation Reagent

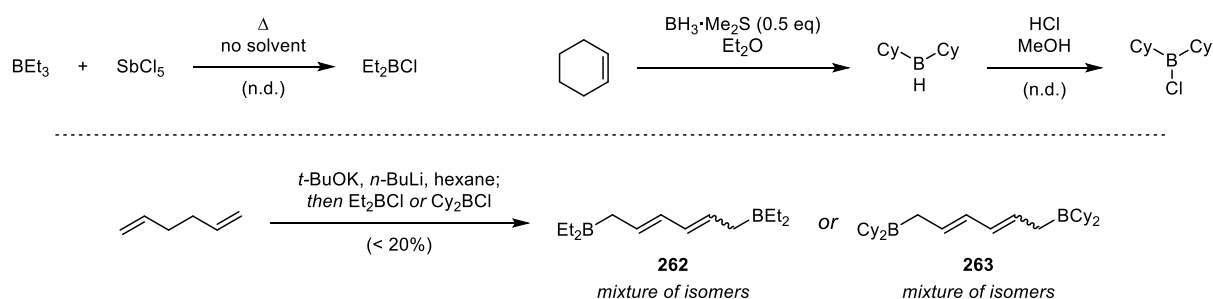
The substitution pattern of **251** (Scheme 68) has rarely been accessed using a short and convergent reaction sequence.<sup>[288]</sup> One pertinent example pertains to the in situ generation of allylindium compound **257** (Scheme 70) starting from 1,2-diol **258**, which gives the desired bis-homoallylic 1,4-diol (**259**) in low yield, and as a diastereoisomeric mixture due to prominent side-reactions (protodemetalation and 1,6 diol formation).<sup>[289]</sup> Using a covalent allylic metal species, such as bisallylic silane **260**, the same type of reaction can be imagined. Reagent **260** is obtained as an isomeric mixture by reaction of hexadiene with *n*-BuLi/TMEDA and addition of 2 eq. of TMSCl to the previously formed dianion.<sup>[290]</sup> It was shown to react with 2 eq. of aldehyde under activation by Lewis acids to form tetrahydrofuran **261**.<sup>[291]</sup> Evidently, the desired 1,4-diol of type **259** is formed during the reaction, but suffered intramolecular nucleophilic substitution induced by the added Lewis acid (BF<sub>3</sub> or TiCl<sub>4</sub>). Circumventing the use of a Lewis acid would require an inherently more Lewis-acidic reagent that would not ionize the just formed alcohol. Along these lines, Bubnov and co-workers developed an allylboron analog to silane **260**.<sup>[292]</sup> It is also synthesized by deprotonation of hexadiene followed by quenching with an electrophilic boron source (Et<sub>2</sub>BCl). The pyrophoric reagent **262**, which is isolated as a mixture of olefin isomers, reacts readily with aldehydes without the necessity for external Lewis acid activation, and ionization of the allylic alcohol to tetrahydrofuran **261** is not observed (Scheme 70).<sup>[293]</sup> Although the product is obtained as a mixture of diastereoisomers, it represented a good starting point for our investigations, as the stereochemistry of the 1,4-diol could be corrected at a later stage in the synthesis.



Scheme 70. Synthetic approaches to 1,4-divinyl alcohols.

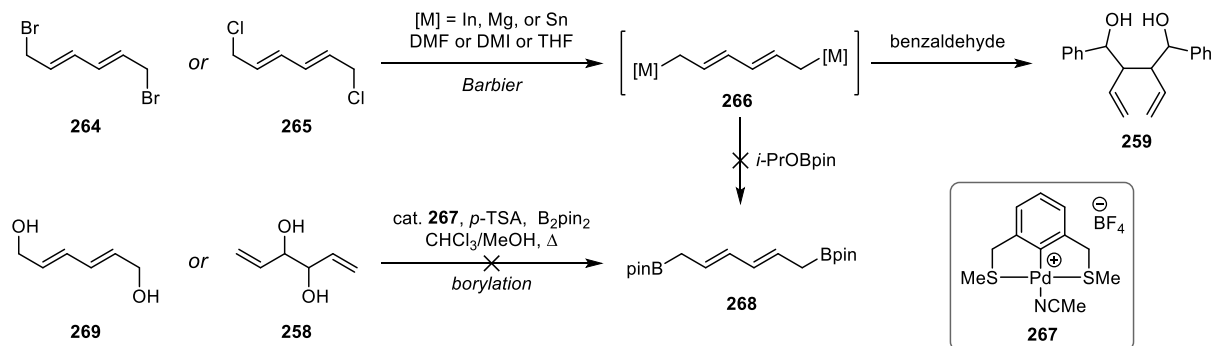
### 2.2.2. Exploratory Studies

The synthesis of diallylborane **262** was attempted from freshly prepared diethyl chloroborane according to Bubnov's procedure (Scheme 71).<sup>[293,294]</sup> Although the desired product was observed after reaction of benzaldehyde, the reagent was found to be inactive two days later in our hands, despite being stored at  $-20\text{ }^{\circ}\text{C}$  under inert atmosphere. In an attempt to increase the ease of synthesis, diethylchloroborane was substituted with dicyclohexylchloroborane, a non-pyrophoric reagent widely used in aldol reactions.<sup>[295]</sup> Application of the same reaction conditions led to the isolation of a colorless oil (**263**) that also proved competent in the double allylation reaction, albeit in low yield (< 20%). However, also in this case, the reagent lost its activity within two days, both when stored neat and as solution in hexane.



**Scheme 71. Preparation of dialkylchloroboranes and reaction with hexadienyl anion.**

Alternative approaches that involved the formation of highly reactive allylmetal reagents without the necessity for isolation of reactive intermediates were evaluated. First, Barbier-type reaction of dialkyl halides (**264** or **265**) with elemental In, Sn, and Mg followed by treatment with benzaldehyde did not furnish the desired product, and resulted in decomposition of the starting materials.<sup>[296–299]</sup> Confirming the presence of allylmetal species **266** by treatment of the reaction mixture with an electrophilic boron source to generate **268** were not successful. Protocols for the in-situ formation of allylboronic esters were also explored following literature precedent by Szabo and co-workers.<sup>[300,301]</sup> Although two possible precursors, the isomeric diols **258** and **269** were evaluated, **268** was not formed and the reaction delivered a mixture of products.

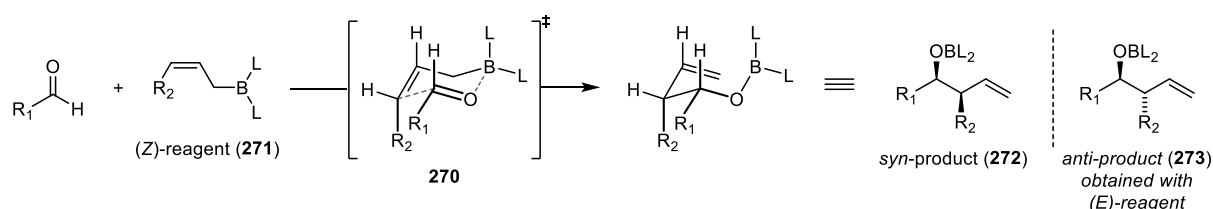


**Scheme 72. Alternative approaches to bifunctional allylation reagents 266 and 268.**

So far, our experiments did not lead to a practical synthesis of the desired 1,4 diol motif. Further developments and optimization efforts were discouraged by the lack of isolable and characterizable reaction intermediates, as well as the absence of any distinct side-products resulting from unwanted reaction pathways. However, we were convinced that it should be possible to find a more stable analog to trialkylborane **262** that would still be able to react in the desired manner. Hoping that the structural variety of allylboron reagents, whose reactivity can be modulated by the substituents on the boron atom, might allow us to find a suitable candidate, we examined this possibility in more detail.

### 2.2.3. Synthesis and Reactivity of Bifunctional Allylboration Reagent (**268**)

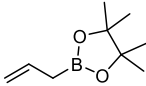
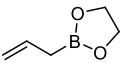
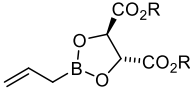
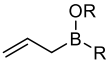
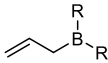
Allylboron reagents are among the most popular organometallic compounds for the synthesis of homoallylic alcohols.<sup>[302]</sup> Their most important feature is that, despite a great structural diversity conferred to them by different ligands on the boron atom (*vide infra*), the same well-established mechanistic rationale applies to explain their reactivity in carbonyl addition. In fact, the majority of allylboron reagents react via a chair-like, rigid transition state.<sup>[301]</sup> As shown in Scheme 73, minimization of 1,3-diaxial interactions paired with the inherent Lewis acidity of the boron atom lead to a Zimmerman–Traxler transition state (**270**) in which the aldehyde residue is placed in the equatorial position. By virtue of this assembly, the reaction is highly stereospecific. So, (*Z*)-allylboranes (**271**) provide the *syn*-product **272**, and the (*E*)-allylborane generates the corresponding *anti*-homoallylic alcohol **273** (Scheme 73).<sup>[303]</sup>



**Scheme 73. Diastereospecific allylboration reaction via chair-like transition state**

Several structural classes of allylboron reagents, which differ in the nature of the ligands on the boron atom, are used in the addition to carbonyl compounds (Scheme 74). The substitution pattern modulates the Lewis acidity of the boron center, and therefore the reactivity towards aldehydes. For example, difluoroallylboranes and alkylboranes react with aldehydes at very low temperatures.<sup>[176]</sup> Due to their high Lewis acidity, they also suffer from rapid 1,3-borotropic shift resulting from intramolecular attack of the pendant allyl group to the boron atom that leads to the loss of stereoisomeric purity. To avoid the necessity for careful monitoring of the reaction conditions, heteroatom-substituted allylboron reagents have been developed, in which the empty p orbital of the boron atom can be populated with electron density from adjacent alkoxy or amido substituents.<sup>[302]</sup> So, if one alkoxy ligand is present, the resulting allylboronic ester (**276**, Scheme 74) reacts with aldehydes

at  $-78\text{ }^{\circ}\text{C}$ , but undergoes 1,3-borotropic shift only upon warming to ambient temperature.<sup>[304]</sup> Allylboronic esters of type **274** bearing two alkoxy ligands, however, do not undergo 1,3-shift even at elevated temperatures and are usually slower to react with aldehydes. Minimization of the steric environment on the boron atom can enhance their reactivity, as does the manipulation of electronic properties on the diol backbone. For example, electron-withdrawing groups (e.g. tartaric esters, **275**) allow similar reactivity to trialkylboron compounds due to enhanced Lewis-acidity and enable enantioselective addition with formation of chiral homoallylic alcohols.<sup>[305]</sup>

					
	allylboronic ester (sterically hindered)	allylboronic ester ( <b>274</b> )	allylboronic ester (electron-poor, <b>275</b> )	allylboronic ester ( <b>276</b> )	trialkylborane ( <b>277</b> )
aldehyde addition:					
temperature / time (with acid catalyst)	rt, several days ( $-78\text{ }^{\circ}\text{C}$ to rt, hours)	$-78\text{ }^{\circ}\text{C}$ to rt, hours (/)	$-78\text{ }^{\circ}\text{C}$ to rt, hours (/)	$-78\text{ }^{\circ}\text{C}$ , hours (/)	$-78\text{ }^{\circ}\text{C}$ , minutes (/)
1,3-borotropic shift:	not observed	not observed	not observed	$-78\text{ }^{\circ}\text{C}$ to rt, 14 h	$-78\text{ }^{\circ}\text{C}$ , 6 h
isolation:	aqueous workup $\text{SiO}_2$ chromatography	aqueous workup distillation	aqueous workup distillation	distillation	distillation

#### Scheme 74. Reactivity and stability of various hydroxyl-substituted allylboron reagents.

In general, reactivity towards carbonyl compound is proportional to the instability of the reagent towards hydrolysis and oxidation. Trialkylboranes (**277**) for instance are usually prepared and reacted in situ, and purification can be carried out exclusively by distillation under inert atmosphere. Only boronate esters of bulky diols (pinacol, pinanediol, benzopinacol) are stable towards routine manipulations, and can even be purified by column chromatography.<sup>[306]</sup> The higher stability makes their addition to aldehydes less facile, with reaction times of several days, sometimes requiring elevated temperatures and ultrahigh pressure. Recently, it has been demonstrated that Lewis or Brønsted acids enhance the rate of allylboration while maintaining high diastereoselectivities (e.g. pinacol allylboronates react under the influence of  $\text{AlCl}_3$  even at  $-78\text{ }^{\circ}\text{C}$ ).<sup>[307,308]</sup> Moreover, the advent of BINOL-derived chiral Lewis and Brønsted acids can impart high enantioselectivity and avoid using reagents that incorporate chiral auxiliaries, further increasing the synthetic utility of reagents of type **274**.<sup>[74,309–312]</sup>

We wanted to address the challenge of synthesizing 1,4-bishomoallylic diols with an isomerically pure and structurally well-defined bifunctional allylation reagent. It should be readily prepared, amendable to storage, and easy to handle at room temperature. As discussed above, allylboronic esters (i.e. pinacolboronates) should provide the necessary stability upon storage and allow for the synthesis of a stereoisomerically pure reagent not suffering from 1,3-borotropic shift, while still allowing productive reaction with aldehydes – if needed under activation by Brønsted or Lewis acid catalysts. The mechanistic rationale of allylboration presented in Scheme 73 led us to maintain the 1,6-diborylhexadiene structural motif employed by Bubnov and Miginiac.<sup>[290,293]</sup>

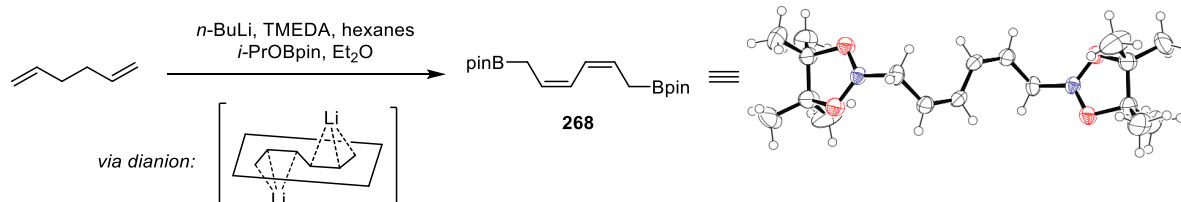
We started our investigations with the implementation of the conditions for hexadiene deprotonation using the mixed alkyllithium/potassium alkoxide system developed by Schlosser (Table 41).<sup>[313]</sup> As already observed in the reactions towards the synthesis of allylborane **262**, upon addition of hexadiene to the base, the reaction turned to a rusty red, unstirrable slurry, indicating formation of a highly conjugated carbanion. Cooling of the reaction mixture and addition of *i*-PrOBpin led to complete solidification of the mixture and partial discoloration. After standard aqueous extractive workup, we obtained a complex mixture of products. Clearly, the formation of the hexadienyl anion was successful, but the heterogeneous reaction conditions prohibited a selective incorporation of boron into the terminal position due to the formation of concentration gradients within the reaction flask. The deprotonation conditions using alkyllithiums in the presence of TMEDA were investigated next, with the hope that the resulting dianion would be better solvated by the diamine.<sup>[290]</sup> The resulting rusty red mixture was then treated with different trialkoxyboron species as electrophiles. In the case of (*i*-PrO)<sub>3</sub>B, transesterification with pinacol was performed to facilitate comparison with the other reactions (Entries 5 and 6). Although all experiments yielded the desired product, the use of *i*-PrOBpin was preferred as it favored the formation of a single predominant product, while the other electrophiles gave unselective addition leading to product mixtures.

**Table 41. Conditions investigated for the synthesis of hexadienyl pinacolboronate**

Entry	Base/Additive <sup>a</sup>	Temp. (°C)	Time (h)	Electrophile addition	Outcome/Yield
1	<i>n</i> -BuLi (2.1 eq.), KO <sup>t</sup> -Bu (2.1 eq.)	0 to rt	6	<i>i</i> -PrOBpin (2.5 eq.) in Et <sub>2</sub> O, -78 °C to rt, 18 h	complex mixture
2	<i>n</i> -BuLi (2.1 eq.), TMEDA (2.1 eq.)	-30 to rt	2	MeOBpin (2.1 eq.) in Et <sub>2</sub> O, -78 °C to rt, 3 h	mixture of isomers
3	<i>n</i> -BuLi (2.1 eq.), TMEDA (2.1 eq.)	-30 to rt	6	MeOBpin (2.5 eq.) in Et <sub>2</sub> O, -78 °C to rt, 3 h	mixture of isomers
4	<i>n</i> -BuLi (2.1 eq.), TMEDA (2.1 eq.)	-30 to rt	6	MeOBpin (2.5 eq.) in Et <sub>2</sub> O, -78 °C to rt, 10 h	mixture of isomers
5	<i>n</i> -BuLi (2.1 eq.), TMEDA (2.1 eq.)	-30 to rt	2	B( <i>i</i> -PrO) <sub>3</sub> (2.2 eq.) in Et <sub>2</sub> O, -78 °C to rt, 8 h	mixture of isomers <sup>b</sup>
6	<i>n</i> -BuLi (2.1 eq.), TMEDA (2.1 eq.)	-30 to rt	2	B( <i>i</i> -PrO) <sub>3</sub> (2.2 eq.) in Et <sub>2</sub> O, -30 °C to rt, 8 h	mixture of isomers <sup>b</sup>
7	<i>s</i> -BuLi (2.1 eq.), TMEDA (2.1 eq.)	-30 to rt	12	<i>i</i> -PrOBpin (2.5 eq.) in Et <sub>2</sub> O, -78 °C to rt, 24 h	one major isomer (>80% purity)
8	<i>n</i> -BuLi (2.1 eq.), TMEDA (2.1 eq.)	-30 to rt	12	<i>i</i> -PrOBpin (2.5 eq.) in Et <sub>2</sub> O, -78 °C to rt, 24 h	one major isomer (>80% purity)
9	<i>n</i> -BuLi (2.1 eq.), TMEDA (2.1 eq.)	-30 to rt	24	<i>i</i> -PrOBpin (2.5 eq.) in Et <sub>2</sub> O, -78 °C to rt, 24 h	one major isomer (85% purity) / 42% <sup>c</sup>
10	<i>n</i> -BuLi (2.1 eq.), TMEDA (2.1 eq.)	-30 to rt	24	<i>i</i> -PrOBpin (2.5 eq.) in Et <sub>2</sub> O, <sup>d</sup> -78 °C to rt, 24 h	one major isomer (94% purity) / 39% <sup>e</sup>

<sup>a</sup>) hexane was used as solvent; <sup>b</sup>) after aqueous workup and transesterification with pinacol; <sup>c</sup>) after aqueous workup and Kugelrohr distillation; <sup>d</sup>) precooled to -78 °C; <sup>e</sup>) after aqueous workup and crystallization.

After acidic aqueous workup and extraction using diethyl ether, **268** could be isolated as a mixture with *n*-BuBpin resulting from incomplete consumption of hexadiene and direct addition of *n*-BuLi to *i*-PrOBpin. Removal of this byproduct was successful via chromatography, but **268** slowly decomposed on all the stationary phases examined (Al<sub>2</sub>O<sub>3</sub>, SiO<sub>2</sub>, Davisil, B(OH)<sub>2</sub>-modified SiO<sub>2</sub>, Et<sub>3</sub>N-treated SiO<sub>2</sub>).<sup>[314]</sup> Nevertheless, isolation of a pure sample of the major product formed during the reactions was possible, and definitive structural proof was obtained by X-Ray analysis. As shown in Scheme 75, The (*Z,Z*)-stereochemistry of the product **268** suggests that in the hydrocarbon solvent TMEDA stabilizes the hexadienyl dianion in an S-shaped conformation that is retained to a high degree during the addition of *i*-PrOBpin even in the more coordinating Et<sub>2</sub>O. In a final optimization round, conducted in collaboration with Marius Schmicker, we realized that complete deprotonation of hexadiene was slow and required longer (at least 24 h) to reach appreciable conversion.<sup>[315]</sup> Furthermore, **268** could be purified via Kugelrohr distillation to with an isomeric purity of 85:7:7 (*Z,Z*):(*E,E*):(*E,Z*) (Table 41, entry 9). This additional purification step could be avoided with cautious monitoring or the reaction temperature and by slow addition of a precooled (−78 °C) solution of *i*-PrOBpin, together with vigorous stirring to ensure adequate mixing of the reaction partners. In doing so, **268** solidified directly after aqueous workup and removal of the solvent, and could be isolated on a 110 mmol scale in 94% isomeric purity and 38% yield after precipitation from hexane at −25 °C (Table 41, entry 10).



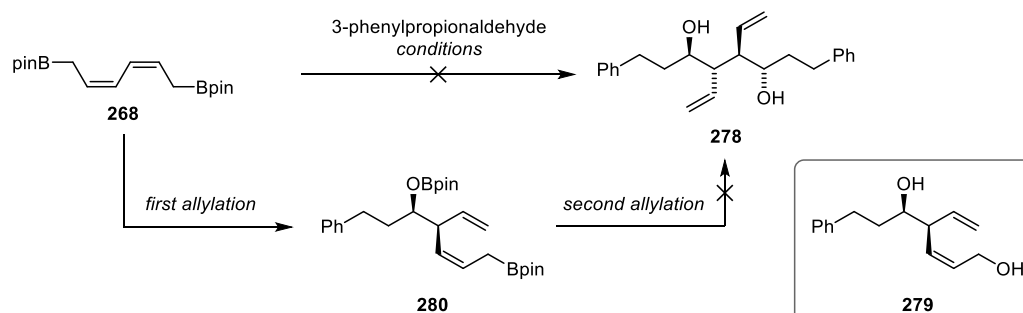
**Scheme 75. Synthesis of (*Z,Z*)-bisallylboronic acid pinacol ester **268**.**

Both (*Z*)- and (*E*)-pinacol crotylboronates are reported to react with equimolar amounts of aldehydes in non-polar, aprotic solvents to afford homoallylic alcohols in good yield.<sup>[303]</sup> We expected that the C<sub>2</sub>-symmetrical bifunctional allylation reagent **268** should afford a twofold addition product. Compared to the pioneering work by Bubnov (see Scheme 70), the diastereoselectivity should be enhanced for reagent **268** given its higher isomeric purity compared to **262**, which exists as mixture of interconverting stereoisomers.

Dienyl boronate **268** was treated with an excess of phenylpropionaldehyde at room temperature for 48 h (Table 42, Entry 1). An oxidative workup was performed to facilitate product isolation by destruction of the intermediate *O*-bound pinacolboronate. Unfortunately, no double allylation product (**278**) was obtained. The major product was determined to be the 1,5-diol **279** resulting from single addition of **268**. Interestingly, it was isolated as a 9 to 1 mixture of diastereoisomers and thorough purification and spectroscopic analysis by Belinda Hetzler showed that the major product formed is the *syn*-product (in accordance with the Zimmerman-Traxler transition

state depicted in Scheme 73).<sup>[316]</sup> Twofold addition product **278** could not be observed at higher temperatures either (Entry 3). The addition of Brønsted and Lewis acid catalysts was investigated by Belinda Hetzler and did not change the outcome, although it did improve the rate of *single* allylboration at ambient temperature (Entries 6 and 7). Under more forcing conditions, complex mixtures were obtained (Entry 8). Evidently, the additional steric hindrance of the pinacolboronate ester transferred in the first allylation step combined with the branched substitution adjacent to the pendant allylboronic ester discourage compound **280** from undergoing a second allylboration reaction to give **278**.

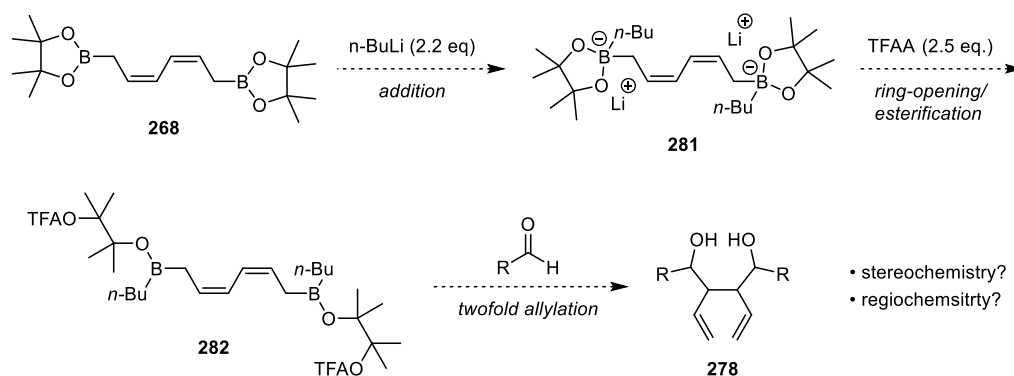
**Table 42. Screening of conditions for the allylation of phenylpropionaldehyde with 268.**



Entry <sup>a</sup>	Catalyst <sup>b</sup>	Solvent	Temp (°C)	Time (h)	Outcome/Yield (%)
1	none	CH <sub>2</sub> Cl <sub>2</sub>	rt	48	only <b>279</b> / n.d.
2	none	toluene	rt	72	only <b>279</b> / 67
3	none	toluene	100	24	only <b>279</b> / n.d.
4	Sc(OTf) <sub>3</sub>	toluene	rt	24	decomposition
5	In(OTf) <sub>3</sub>	toluene	rt	24	decomposition
6	AlCl <sub>3</sub>	toluene	rt	24	only <b>279</b> / n.d.
7	TFA	CH <sub>2</sub> Cl <sub>2</sub>	rt	24	only <b>279</b> / 57
8	TFA	toluene	100	24	decomposition

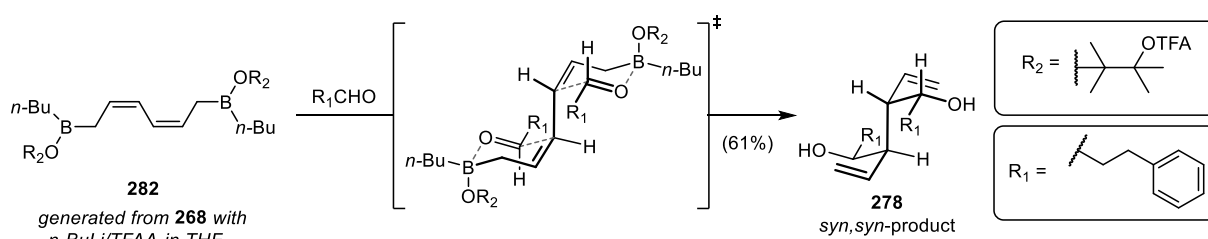
a) all reactions performed with 3.0 eq. of phenylpropionaldehyde; b) 10 mol %;  
c) after oxidative workup with NaOH/H<sub>2</sub>O<sub>2</sub>.

A similar difficulty was faced by Aggarwal and co-workers in their investigation of sterically hindered 3,3-disubstituted allylpinacolboronates.<sup>[317,318]</sup> By converting the boronic ester to the more reactive borinic ester, the desired addition to aldehydes was found to take place. The mechanism of this activation mode, together with its intended application to **268**, is shown in Scheme 76. At low temperature, alkyllithium reagents can add to the electrophilic boron center to form intermediate borate **281**. Addition of an oxophilic electrophile such as TFAA leads to ring-opening of **281** with scission of the B–O bond, and the expelled alkoxide is trapped to form a trifluoroacetyl ester. This effectively generates the tricoordinated borinic ester **282**, a more Lewis acidic species that is markedly more reactive towards carbonyl compounds. If **282** could indeed be generated, it might be reactive enough to undergo a second allylation to give **278** despite the added steric bulk imparted by the first carbonyl addition.

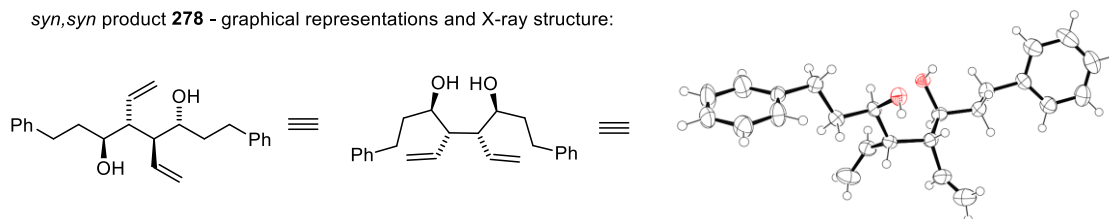


**Scheme 76. Projected activation of 268 via borinic ester and twofold aldehyde allylation.**

After treatment of **268** with *n*-BuLi (2 eq.) at  $-78$  °C for 15 minutes, TFAA was added. After 30 minutes at  $-78$  °C, phenylpropionaldehyde (2 eq.) was added and the mixture was allowed to reach ambient temperature (Scheme 77). Following aqueous workup, one major product was obtained in 62% yield. Its structure could be confirmed by X-ray crystallography, indicating that the desired allylation does indeed proceed as desired. The plane of symmetry exhibited by **278** reflects the stereospecific reactivity of  $C_2$ -symmetric reagent **268** via a chair-like transition state. Additionally, the *syn*-stereochemistry of the homoallylic alcohol product confirms that the (*Z*)-allylboron species underwent allylation without isomerization via 1,3-borotropic shift. Having successfully developed a more practical preparation of the desired 1,4-diol motif, we moved to apply the reaction to the synthesis of herquines A and B.



*syn,syn* product **278** – graphical representations and X-ray structure:



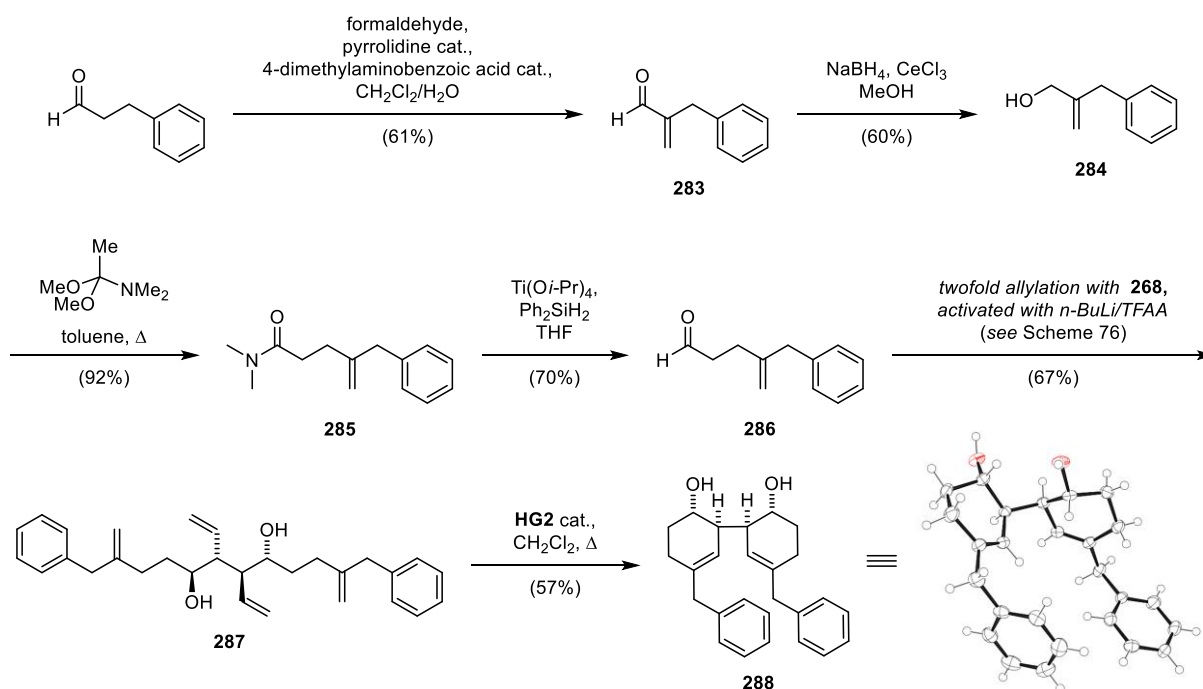
**Scheme 77. Diastereoselective double allylation of borinic ester 282 with phenylpropionaldehyde.**

## 2.2.4. Application Towards the Synthesis of Herquines A and B.

### 2.2.4.1. Model Studies

Before submitting an elaborated aldehyde partner to the abovementioned double allylation reaction, we wanted to systematically assess eventual limitations and functional group compatibility of the method. In this context, Lewis-basic protecting groups might inhibit the desired reactivity towards the aldehydes in both the allylation as well as the metathesis reactions. Therefore, a model substrate was prepared with the intent to test the suitability and robustness of the planned sequence.

Phenylpropionaldehyde was chosen as starting material, and allylic alcohol **284** was obtained after  $\alpha$ -methenylation to **283** and reduction (Scheme 78).<sup>[319]</sup> Chain extension via Eschenmoser–Claisen rearrangement and reduction furnished aldehyde **286**, which was subjected to the allylation protocol with in situ generated borinic ester **282** to give **287**.<sup>[148,320]</sup> Ring closing metathesis reaction of **286** was successful using the Hoveyda–Grubbs' 2<sup>nd</sup> generation catalyst.<sup>[321]</sup> The relative configuration of the product (**288**) could be assigned by X-ray crystallographic analyses. Analogous to the model reaction with phenylpropionaldehyde, the twofold allylation reaction proceeded without isomerization of the allylborinic ester to give *syn*-homoallylic alcohol **287**.

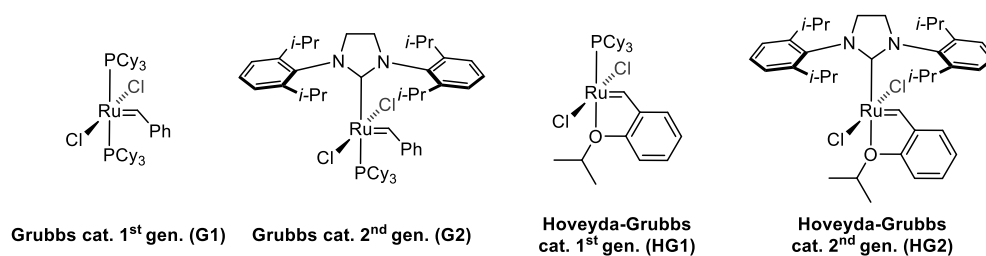
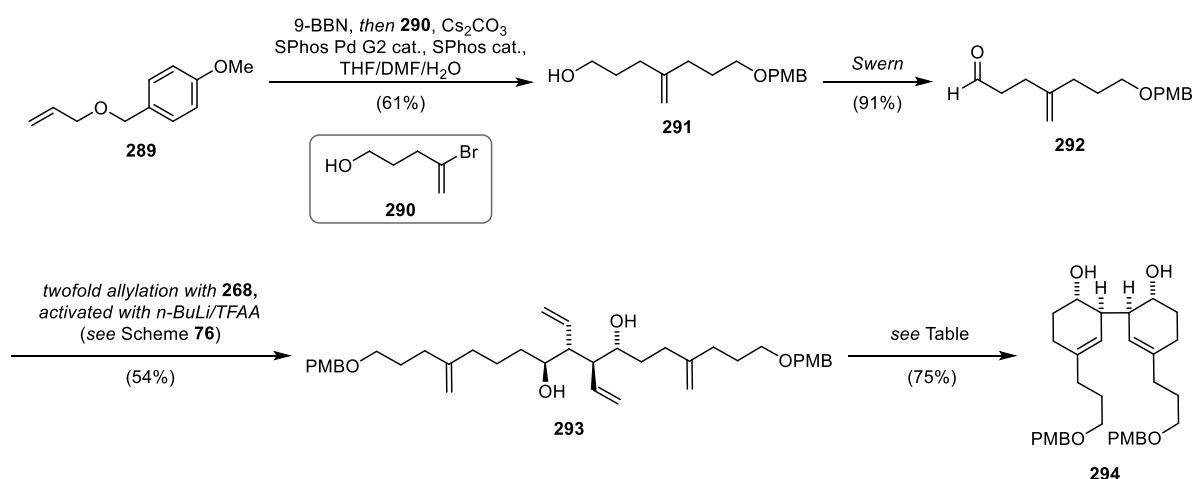


**Scheme 78.** Model study for the double allylation / ring closing metathesis sequence.

A second substrate bearing a protected hydroxyl functionality as a handle for amino acid synthesis was synthesized starting from PMB-protected allyl alcohol (**289**). After hydroboration using 9-BBN, Suzuki cross-coupling with alkenyl bromide **290**, derived from 4-pentynol, delivered the allylic alcohol **291**.<sup>[322,323]</sup> Swern oxidation to the aldehyde followed by double allylation delivered diol **293**, which was subjected to RCM conditions. Interestingly, this substrate proved more reluctant to

participate in metathesis reaction than **287**. While first-generation metathesis catalysts converted the product even at high temperature (Entries 2 and 6), second-generation catalysts bearing an NHC-ligand delivered the tandem metathesis product, although the reaction did not exhibit a clean reaction profile with Grubbs' 2<sup>nd</sup> generation catalyst (Entry 4). The use of phosphine-free Hoveyda–Grubbs' 2<sup>nd</sup> generation catalyst, on the other hand, delivered the desired product **294** in good yield but required elevated temperatures. (Entries 11 and 12).<sup>[324]</sup>

### Scheme 79. Synthesis of long-chain model study via twofold allylation and metathesis.



Entry	Catalyst <sup>a</sup>	Solvent <sup>b</sup>	Conc. (mM)	Temp (°C)	Time (h)	Yield <sup>c</sup> (%)
1	G1	toluene	0.01	rt	7	no reaction
2	G1	toluene	0.01	90	7	no reaction
3	G2	toluene	0.01	rt	3	<5%
4	G2	toluene	0.01	90	7	18%
5	HG1	toluene	0.01	rt	7	no reaction
6	HG1	toluene	0.01	90	7	no reaction
7	HG2	benzene	0.025	40	16	38%
8	HG2	CH <sub>2</sub> Cl <sub>2</sub>	0.025	40	16	<5%
9	HG2	1,2-DCE	0.025	40	16	<5%
10	HG2	toluene	0.01	rt	7	no reaction
11	HG2	toluene	0.025	40	16	39%
12	HG2	toluene	0.01	90	4	75% <sup>d</sup>

a) 10 mol%; b) solvents were deoxygenated by purging with N<sub>2</sub> for 20 min; c) determined by NMR using tetrachloroethane as external standard, except for entry **12**; d) isolated yield after silica gel chromatography.

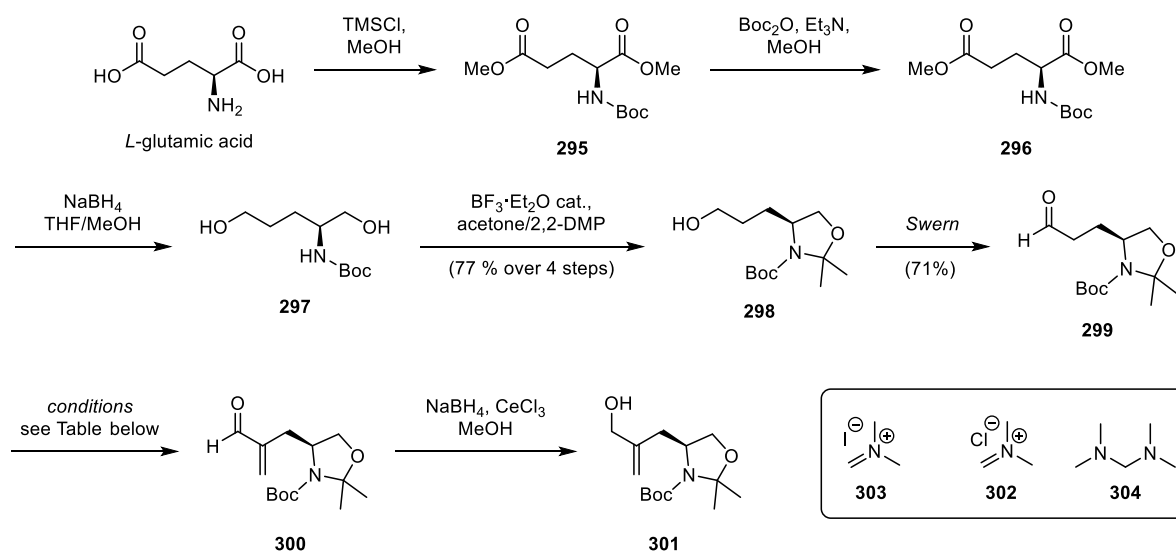
### 2.2.4.2. Synthesis of Amino Acid-derived Coupling partners

Both model substrates **292** and **286** underwent allylation and ring-closing metathesis reaction, but the reaction conditions for the formation of the cyclohexenone rings needed to be adjusted for the more sterically hindered and more coordinating PMB-protected **293**. Further aldehyde substrates exhibiting variation of oxidation state and protecting group patterns on the amino acid-derived terminus were prepared next.

#### 2.2.4.2.1. Aminoalcohol Oxidation Level

L-glutamic acid was treated with TMSCl in MeOH to give **295**, which was Boc-protected to afford **296**. After ester reduction to alcohol **297**, the Boc-protected amine and the proximal hydroxyl group were protected as the *N,O*-acetonide (**298**).<sup>[325]</sup> Then, the primary alcohol was oxidized under Swern conditions to give aldehyde **299**. Organocatalytic methylenation gave **300**, but proceeded only in moderate yield (see Table in Scheme 80, entry 1), analogous to reactions using Bohme's salt (**302**) or Eschenmoser's salt (**303**).<sup>[326]</sup> The in situ generation of the electrophilic iminium intermediate was more successful, and best results were obtained using TFAA as the activating agent for the 1,3-diamine **304**.<sup>[327,328]</sup> Next, aldehyde **300** reduced to corresponding alcohol **301**.<sup>[329]</sup>

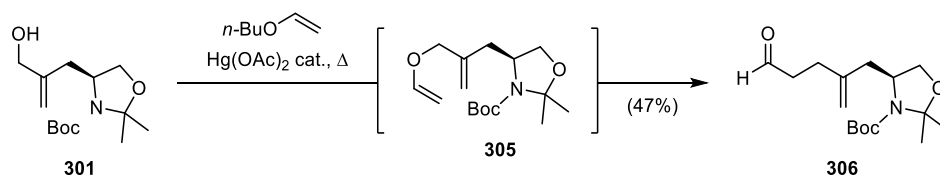
**Scheme 80. Synthesis of Claisen rearrangement precursor from L-glutamic acid.**



Entry	Reaction conditions	Solvent	Temp (°C)	Time (h)	Yield (%)
1	Formaldehyde (1.0 eq.), pyrrolidine (0.1 eq.), 4-dimethylaminobenzoic acid (0.2 eq.)	CH <sub>2</sub> Cl <sub>2</sub>	45	2	47
2	DIPEA (1.0 eq.), TFA (1.0 eq), 1,3,5-Trioxane (2.0 eq.)	THF	60	6	29
3	Eschenmoser's salt ( <b>303</b> ) (2.0 eq.), Et <sub>3</sub> N (3.0 eq.)	CH <sub>2</sub> Cl <sub>2</sub>	0 to rt	2	48
4	Böhme's salt ( <b>302</b> ) (2.0 eq.), Et <sub>3</sub> N (3.0 eq.)	CH <sub>2</sub> Cl <sub>2</sub>	0 to rt	4.5	51
5	AcOH (2.4 eq), <b>304</b> (4.2 eq)	THF	0 to rt	18	56
6	TFAA (1.1 eq.), <b>304</b> (1.1 eq)	CH <sub>2</sub> Cl <sub>2</sub>	0 to rt	18	66

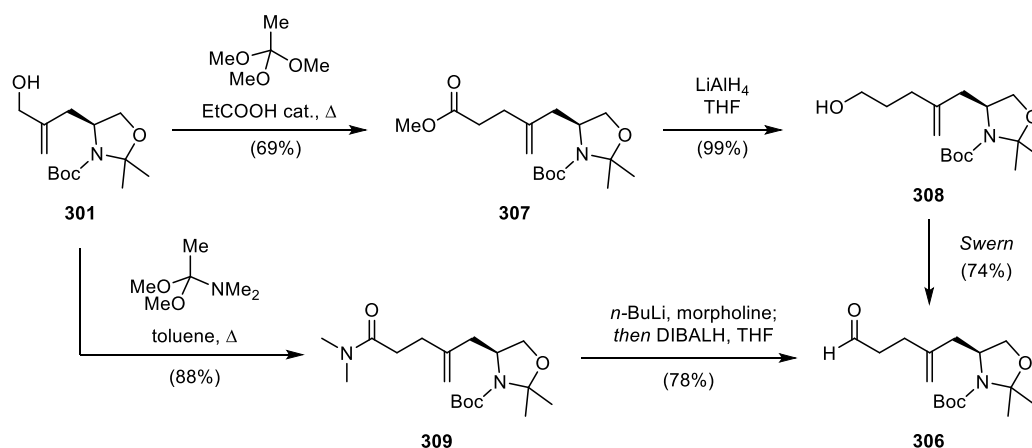
Direct access to the desired aldehyde required a two-carbon homologation, which was attempted via Claisen rearrangement of vinyl ether **305**. The desired product was best synthesized

using conditions reported by Fukuyama and coworker's using the high-boiling *n*-butyl vinyl ether (Scheme 81).<sup>[330]</sup>



**Scheme 81. Mercury-catalyzed Claisen rearrangement to give aldehyde 306.**

Nevertheless, the low yield prompted us to examine different Claisen protocols (Scheme 82). While Ireland–Claisen rearrangement of allylic acetate derived from **301** was not successful (not depicted), Aylin Hirschvogel has shown that Johnson–Claisen protocol afforded the product in acceptable yield, provided the reaction was carried out under microwave irradiation (8 min at 150 °C).<sup>[331]</sup> Unfortunately, material throughput was only possible using sequential reactions carried out on 150 mg scale, as larger reaction volumes led to longer reaction times and lower yields due to slow decomposition of the acid-sensitive substrate (e.g. a reaction carried out on 1.99 gram scale gave **307** in only 34 % yield). Reduction of the ester followed by oxidation afforded the target aldehyde (**306**). In an effort to avoid redox manipulations, we conducted an Eschenmoser–Claisen rearrangement to obtain tertiary amide **309**. The reduction to aldehyde **306** using the conditions that were successful on the model systems ( $\text{Ti}(\text{O}i\text{-Pr})_4/\text{Ph}_2\text{SiH}_2$ ) afforded the product in 30% yield, but better results were obtained using a hydridic aluminate complex generated in situ from DIBALH and lithium morpholide (Scheme 82).<sup>[332]</sup>

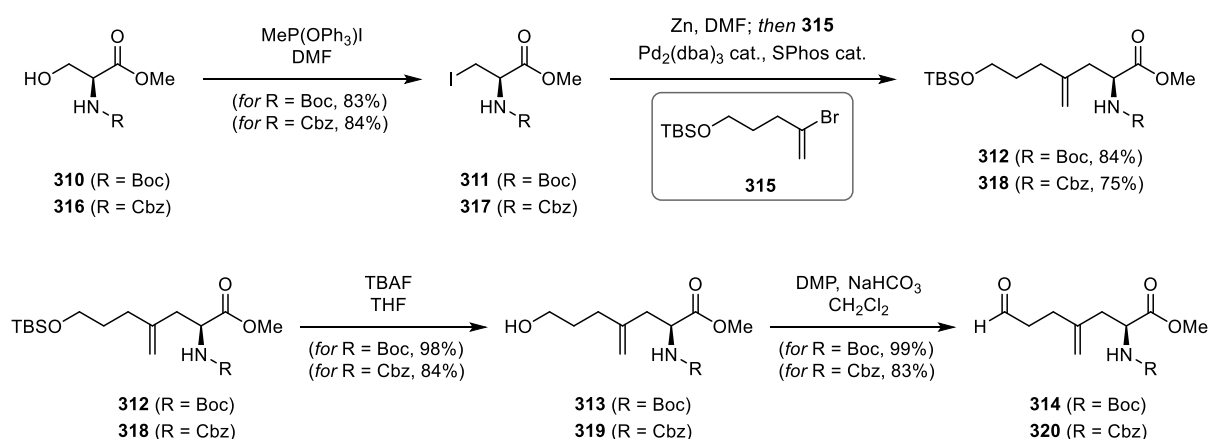


**Scheme 82. Synthesis of allylation precursor with aminoalcohol oxidation level.**

#### 2.2.4.2.2. Amino Acid Oxidation Level

For the synthesis of aldehyde **306** described above, a linear synthetic route starting with the reduction of both the ester functions of L-glutamic acid was used, wherein the side-chain was oxidized as at a later stage while the 1,2-aminoalcohol group was protected as the acetonide. If the desired product was an  $\alpha$ -amino acid, the synthesis would require additional protection and oxidation steps.

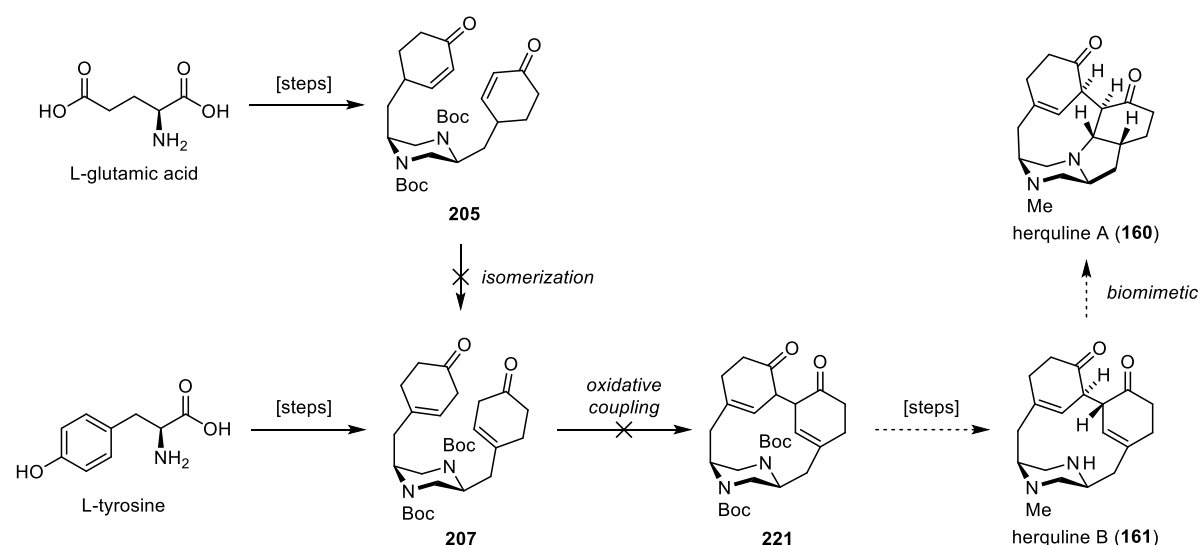
Alternatively, a synthesis starting from L-glutamic acid featuring the selective reduction of the side chain is conceivable. However, literature precedent suggests that a judicious choice of protecting groups would be necessary to differentiate the two ester portions of L-glutamate.<sup>[333]</sup> This would invariably add additional steps to the synthesis. Therefore, we decided to pursue a cross-coupling strategy of an amino acid-derived building block with a pre-reduced side chain. Jackson and co-workers demonstrated that serine-derived organozinc reagents can be coupled with alkenyl and aryl halides under palladium catalysis to deliver unnatural amino acids, and we chose this method to access the desired substrates.<sup>[167,334]</sup> Synthesis of protected iodoalanines **311** and **317** was carried out via iodination of the respective serine derivatives (**310** and **316**).<sup>[335,336]</sup> The side chain was synthesized from TBS-protected 4-pentynol followed by Ni-catalyzed branch-selective alkyne hydroalumination-bromination reaction.<sup>[323]</sup> Formation of the organozinc reagent from the iodide, followed by Negishi coupling with **315**, delivered TBS protected methallylglycine derivative **312**. Desilylation to afford the free alcohol **313** and Dess–Martin oxidation gave aldehyde **314**. The same sequence was also applied to the Cbz-derived substrate to afford, **320** in a similar overall efficiency.



**Scheme 83.** Synthesis of two allylation precursors bearing amino acid oxidation level.

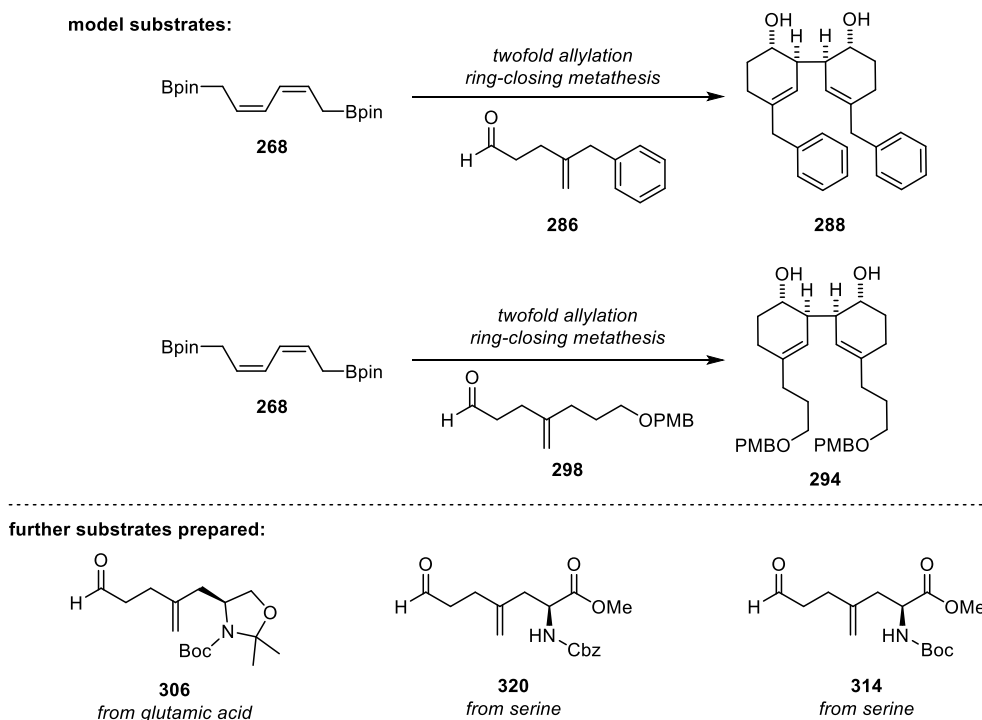
### 3. Summary and Future Work

In summary, two strategies for the synthesis of the alkaloids herquiline A and B were pursued. Following previous work carried out in the Trauner group, L-glutamic acid could be converted into  $\alpha,\beta$ -unsaturated ketone **205**. Attempted isomerization to the  $\beta,\gamma$ -unsaturated isomer **207** required for an intramolecular oxidative enolate coupling reaction was not possible. However, **207** could be prepared from L-tyrosine. Several reaction conditions for the formation of the 12-membered ring in **221** were examined. Unfortunately, the desired product could not be isolated, and control experiments suggest that  $\beta,\gamma$ -unsaturated ketones are not viable substrates for oxidative coupling reaction both in intra-, as well as intermolecular fashion.



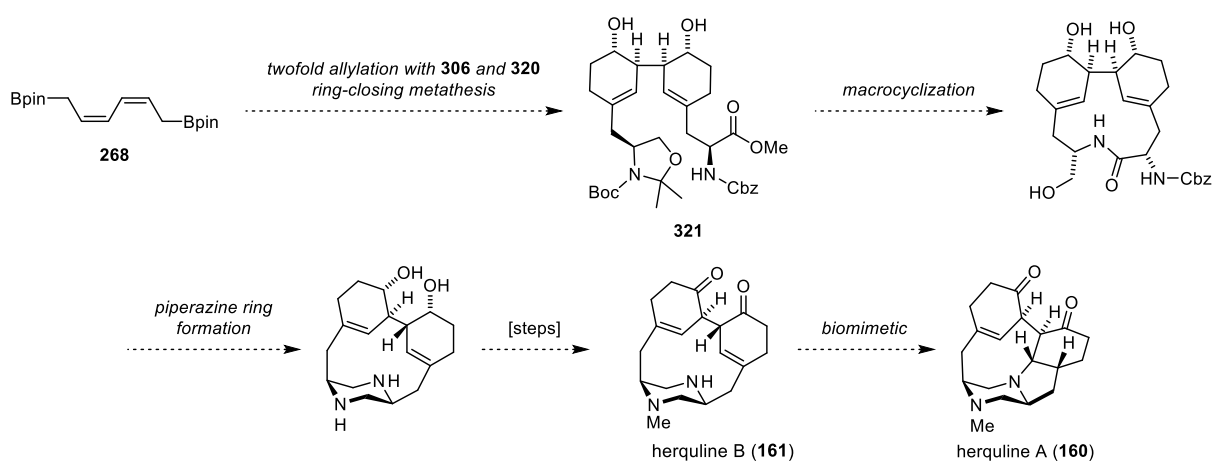
**Scheme 84. Oxidative enolate coupling approach starting from glutamic acid or tyrosine.**

All previous synthetic efforts that relied on the early formation of a piperazine (or diketopiperazine) ring were thwarted by the inability to form the required 12-membered ring by C-C bond formation. This prompted us to redesign our approach and carry out the piperazine formation at a later stage in the synthesis. Inspired by the pseudosymmetrical nature of herquiline B, a twofold allylation-metathesis approach was devised. Using an isomerically pure bifunctional allylboron reagent (**268**) activated in situ by formation of a borinic ester, several aldehydes were shown to undergo sequential double allylation to deliver 1,4-divinyl alcohol in a diastereospecific manner. Ring-closing metathesis on model systems could afford the bis-cyclohexenone core of herquiline B. Additionally, several aldehyde precursors bearing different oxidation states and protecting groups were prepared.



**Scheme 85. Model studies towards the cyclohexenone moiety of herquiline B via allylation.**

In future, they will be subjected to the twofold allylation conditions using **268**. Two different aldehyde substrates bearing either different oxidation states or protecting group patterns could be added sequentially to the allylboron reagent **268** to afford unsymmetrical products of type **321** in order to facilitate intramolecular macrocyclization after ring-closing metathesis. Formation of the 12-membered ring could be achieved by alkylation or amide bond formation, and the six-membered ring could be formed thereafter. After routine manipulations and *N*-methylation, herquiline B could be formed and herquiline A could be formed by olefin isomerization and aza-Michael reaction.



**Scheme 86. Planned fragment union of two different aldehydes via double allylation for the total synthesis of herquelines A and B.**

## 4. Experimental Part

### 4.1. General Experimental Details

#### 4.1.1. Materials and Methods

Unless noted otherwise, all reactions were performed in flame-dried glassware fitted with rubber septa under a positive pressure of nitrogen. Air- and moisture-sensitive liquids were transferred via syringe or stainless steel cannula through rubber septa. Solids were added under inert gas or were dissolved in appropriate solvents. The reactions were magnetically stirred and monitored by NMR spectroscopy where noted or analytical thin-layer chromatography (TLC) using glass plates precoated with silica gel (0.25 mm, 60-Å pore size, Merck) impregnated with a fluorescent indicator (254 nm). TLC plates were visualized by exposure to ultraviolet light (UV, 254 or 366 nm), were stained by submersion in aqueous potassium permanganate solution (KMnO<sub>4</sub>), ceric ammonium molybdate solution (CAM) or acidic *p*-anisaldehyde solution (PAA) and were developed by heating with a heat gun. Flash-column chromatography on silica gel (60 Å pore size, 40–63 μm, Merck KGaA) was performed as described by Still<sup>[185]</sup> or using a Biotage Isolera™ Prime Automated Flash Purification system. Triethylamine-deactivated silica was obtained by preparing a slurry of silica gel (20% v/v in the initial eluent mixture + 5% v/v Et<sub>3</sub>N) followed by magnetic stirring for 1 h. The slurry was poured into a chromatography column and flushed with 5 column volumes of amine-free eluent prior to sample loading and elution. Tetrahydrofuran (THF) and diethyl ether (Et<sub>2</sub>O) were distilled from Na/benzophenone prior to use. Dichloromethane (CH<sub>2</sub>Cl<sub>2</sub>), triethylamine (Et<sub>3</sub>N), *N,N*-diisopropylamine (DIPA) were distilled under nitrogen atmosphere from CaH<sub>2</sub> prior to use. Benzene, 1,2-dichloroethane (DCE), dimethyl sulfoxide (DMSO), 1,2-dichlorobenzene (DCB) were purchased from Acros Organics as 'extra dry' and used as received. All other reagents and solvents were purchased from chemical suppliers (Sigma-Aldrich, Acros Organics, Alfa Aesar, Strem Chemicals, ABCR) and were used as received. Solvents for extraction, crystallization and flash-column chromatography on silica gel were purchased as technical grade and distilled under reduced pressure prior to use. The molarity of *n*-butyllithium solutions was determined by titration to a blue endpoint against *N*-benzylbenzamide<sup>[186]</sup> at –40 °C (average of three determinations).

Unless noted otherwise, yields refer to chromatographically and spectroscopically (<sup>1</sup>H and <sup>13</sup>C NMR) pure material.

#### 4.1.2. Melting Point

Melting points were measured on a Stanford Research Systems MPA120 EZ-Melt apparatus in open glass capillaries.

#### 4.1.3. NMR Spectroscopy

NMR spectra were measured at room temperature (22 °C) on a Bruker Avance III HD 800 MHz spectrometer equipped with a CryoProbe™ operating at 800 MHz for proton nuclei and 200 MHz for carbon nuclei or a Bruker Avance III HD 400 MHz spectrometer equipped with a CryoProbe™ operating at 400 MHz for proton nuclei and 100 MHz for carbon nuclei. Proton chemical shifts are expressed in parts per million (ppm,  $\delta$  scale) and are referenced to residual protium in the NMR solvent (CHCl<sub>3</sub>:  $\delta$  7.26, C<sub>6</sub>D<sub>6</sub>: 7.16, CH<sub>3</sub>SOCD<sub>2</sub>H: 2.50, MeOH: 3.31). Carbon chemical shifts are expressed in parts per million (ppm,  $\delta$  scale) and are referenced to the carbon resonance of the NMR solvent (CDCl<sub>3</sub>:  $\delta$  77.16, C<sub>6</sub>D<sub>6</sub>: 128.06, CH<sub>3</sub>SOCD<sub>2</sub>H: 39.52, MeOH: 49.0). <sup>1</sup>H NMR spectroscopic data are reported as follows: Chemical shift in ppm (multiplicity, coupling constants *J* (Hz), integration intensity). The multiplicities are abbreviated with s (singlet), d (doublet), t (triplet), q (quartet), app (apparent), broad (br), combinations thereof, and m (multiplet). In case of combined multiplicities, the multiplicity with the larger coupling constant is stated first. Except for complex and overlapping multiplets, where a resonance range is given, the chemical shift of all other symmetric signals is reported as the center of the resonance range. <sup>13</sup>C NMR spectroscopic data are reported as follows: Chemical shift in ppm. Additionally to <sup>1</sup>H and <sup>13</sup>C NMR measurements, 2D NMR techniques such as homonuclear correlation spectroscopy (COSY), heteronuclear single quantum coherence (HSQC) and heteronuclear multiple bond coherence (HMBC) were used to assist signal assignment. For further elucidation of 3D structures of the products, nuclear Overhauser enhancement spectroscopy (NOESY) was conducted. All raw FID files were processed and the spectra analyzed using the program Mnova 10.0.2 from Mestrelab Research S. L.

#### 4.1.4. Mass Spectrometry

All mass spectra were measured by the Analytical division of the Department of Chemistry, Ludwig-Maximilians-Universität München. Mass spectra were recorded on the following spectrometers (ionisation mode in brackets): MAT 95 (EI) and MAT 90 (ESI) from Thermo Finnigan GmbH and were recorded in high-resolution. The method used is reported in the relevant section of the experimental part.

#### 4.1.5. IR Spectroscopy

IR spectra were recorded on a Perkin Elmer Spectrum BX II FT-IR system and the compound was applied as thin film directly on the ATR unit (either as neat substance or as solution in CH<sub>2</sub>Cl<sub>2</sub>). Data are represented as follows: absorption frequency (expressed in cm<sup>-1</sup>) and intensity of absorption: s (strong), m (medium), w (weak), br (broad).

#### 4.1.6. Optical Rotation

Optical rotation values were recorded on an Anton Paar MCP 200 or a Krüss Optronic P8000-T polarimeter. The specific rotation is calculated as follows:

$$[\alpha]_{\lambda}^{\varphi} = \frac{[\alpha] \cdot 100}{c \cdot d}$$

Thereby, the wavelength  $\lambda$  is reported in nm and the measuring temperature in °C.  $\alpha$  represents the recorded optical rotation,  $c$  the concentration of the analyte in 10 mg/mL and  $d$  the length of the cuvette in dm. Thus, the specific rotation is given in 10<sup>-1</sup>·deg·cm<sup>2</sup>·g<sup>-1</sup>. Use of the sodium D line ( $\lambda = 589$  nm) is indicated by  $D$  instead of the wavelength in nm. The sample concentration as well as the solvent is reported in the relevant section of the experimental part

#### 4.1.7. HPLC Analyses

Analytical HPLC on Chiral Stationary Phase was performed on a computer-operated Shimadzu system (Windows 10, LabSolutions Software, two LC-20AP pumps, manual injection (2 mL sample loop), CTO-20A column oven, SPD-M20A Diode Array detector). Column, oven temperature, solvent system, flow rate, detection mode and retention times are given in the relevant section of the experimental part.

Preparative HPLC was performed on a computer-operated Varian instrument (Windows XP, Galaxie Chromatography Software, two PrepStar SD-1 pumps, manual injection with 2 mL sample loop, ProStar 335 Photo Diode Array Detector, Agilent 440-LC Fraction Collector). Column, solvent system, flow rate, detection mode and retention times are given in the relevant section of the experimental part.

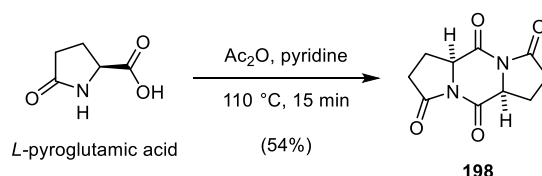
#### 4.1.8. X-ray Diffraction Analysis

Experiments were carried out by Dr. Peter Mayer (Ludwig-Maximilians-Universität München). The data collections were performed on a Bruker Nonius KappaCCD, Bruker D8Venture, or an Oxford Xcalibur diffractometer using MoK $\alpha$ -radiation ( $\lambda = 0.71073$  Å, graphite monochromator). The CrysAlisPro software (version 1.171.33.41) was applied for the integration, scaling and multi-scan

absorption correction of the data. The structures were solved by direct methods with SIR9713 and refined by least-squares methods against F2 with SHELXL-97.14. All nonhydrogen atoms were refined anisotropically. The hydrogen atoms were placed in ideal geometry riding on their parent atoms. Further details are summarized in the tables at the different sections. Plotting of thermal ellipsoids in this document and in the main text was carried out using Ortep-3 for Windows.<sup>[187]</sup>

## 4.2. Experimental Procedures

### (5a*S*,10a*S*)-tetrahydro-3*H*,5*H*-dipyrrolo[1,2-*a*:1',2'-*d*]pyrazine-3,5,8,10(2*H*,5a*H*)-tetraone (**198**)



To a preheated (110 °C) solution of acetic anhydride (442 mL, 4.70 mol, 6.10 eq) and pyridine (82 mL, 1.00 mol, 1.30 eq) was added (*S*)-pyroglutamic acid (99.5 g, 771 mmol, 1.00 eq) portionwise. After 5 min, **198** began to precipitate and a slight orange discoloration of the reaction mixture was observed. After 10 min, the vessel was cooled to 0 °C (ice bath), the precipitate was collected by filtration and transferred to an Erlenmeyer flask containing cold MeOH (200 mL). The solid was filtered on and washed with cold water (200 mL). The product was dried overnight under vacuum to give **198** (45.9 g, 208 mmol, 54%) as a colorless crystalline solid. Spectral data match the previously reported values.<sup>[250]</sup>

$R_f$  = not determined.

**Melting point** = 284 °C (decomposition).

$^1\text{H NMR}$  (400 MHz, DMSO)  $\delta$  = 4.84 (*t*,  $J$  = 8.5 Hz, 2H), 2.64 – 2.38 (m, 4H, partially obscured by solvent), 2.27 – 2.13 (m, 4H).

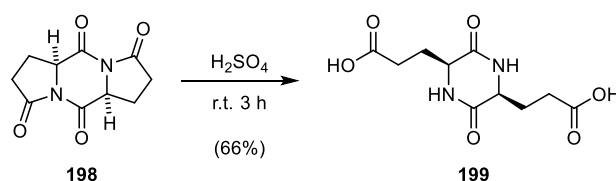
$^{13}\text{C NMR}$  (100 MHz, DMSO)  $\delta$  = 172.7, 165.7, 58.4, 31.2, 18.9.

**HRMS (EI)** for  $\text{C}_{10}\text{H}_{10}\text{N}_2\text{O}_4$   $^+ [\text{M}]^+$ : calcd.: 222.0641, found: 222.0634.

**IR (ATR)**:  $\tilde{\nu}$  = 2941 (w), 1764 (s), 1690 (m), 1463 (w), 1353 (m), 1273 (s), 1247 (s), 1148 (m), 927 (m).

$[\alpha]_{\text{D}}^{25}$  = -96.1 ( $c$  = 1.00, DMSO).

### 3,3'-((2*S*,5*S*)-3,6-dioxopiperazine-2,5-diyl)dipropionic acid (**199**)



Pyroglutamic diketopiperazine (**198**) (45.9 g, 207 mmol, 1 eq) was added portionwise and under rapid magnetic stirring to H<sub>2</sub>SO<sub>4</sub> (96% w/w 166 mL, 15 eq). The reaction mixture was stirred until complete dissolution of **198** (3 hours). The resulting solution was cooled to 0 °C and H<sub>2</sub>O (300 mL) was added slowly dropwise. The mixture was stirred for 1 hour and the resulting precipitate was collected by filtration to afford **199** as white solid (35 g, 136 mmol, 66%). Spectral data match the previously reported values.<sup>[250]</sup>

**R<sub>f</sub>** = not determined.

**Melting point** = 242 °C (decomposition).

**<sup>1</sup>H NMR** (400 MHz, DMSO) δ = 12.13 (s, 2H), 8.20 (s, 2H), 3.88 (t, *J* = 5.3 Hz, 2H), 2.38 – 2.23 (m, 4H), 2.01 – 1.77 (m, 4H).

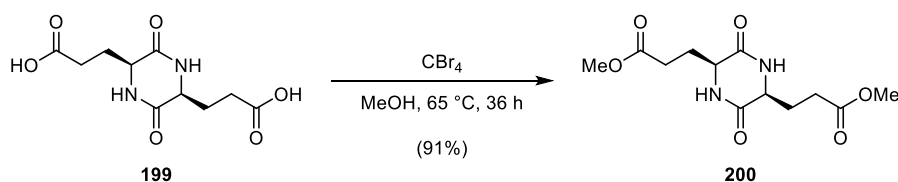
**<sup>13</sup>C NMR** (100 MHz, DMSO) δ = 173.9, 167.9, 53.2, 39.5, 29.3, 28.1.

**HRMS (EI)** for C<sub>10</sub>H<sub>14</sub>N<sub>2</sub>O<sub>6</sub><sup>+</sup> [M]<sup>+</sup>: calcd.: 258.0852, found: 258.0831.

**IR (ATR)**:  $\tilde{\nu}$  = 3200 (b, w), 2822 (b, w), 2518 (b, w), 1677 (s), 1640 (s), 1402 (s), 1291 (s), 1266 (s), 1192 (s), 887 (m), 814 (s).

**[α]<sub>D</sub><sup>25</sup>** = –41.9 (c = 1.00, DMSO).

### dimethyl 3,3'-((2*S*,5*S*)-3,6-dioxopiperazine-2,5-diyl)dipropionate (**200**)



A suspension of **199** (6.25 g, 24.2 mmol, 1.00 eq), MeOH (300 mL) and CBr<sub>4</sub> (803 mg, 2.42 mmol, 0.10 eq) was heated to reflux for 36 hours under. The resulting solution was cooled to room temperature and concentrated in vacuo to ca. 50 mL, at which point a white solid formed. Et<sub>2</sub>O (150 mL) was added and the reaction flask was stored overnight at –25 °C to ensure complete precipitation. Filtration of the solid afforded, after drying at 60 °C for 2 hours, **200** as a white solid (6.33 g, 22.0 mmol, 91%). Spectral data match the previously reported values.<sup>[250]</sup>

**R<sub>f</sub>** = 0.17 (CH<sub>2</sub>Cl<sub>2</sub>/MeOH = 95/5, CAM).

**Melting point** = 183.2 – 186.6 °C.

**<sup>1</sup>H NMR** (400 MHz, DMSO) δ = 4.84 (t, *J* = 8.5 Hz, 2H), 2.64 – 2.38 (m, 4H, partially obscured by solvent), 2.27 – 2.13 (m, 4H).

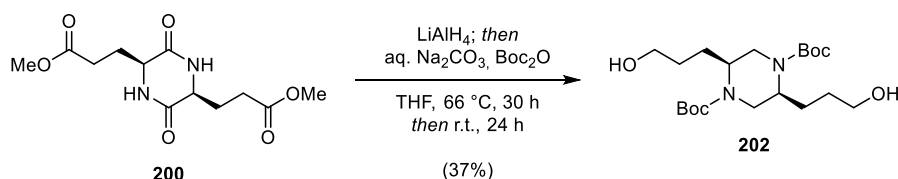
**<sup>13</sup>C NMR** (100 MHz, DMSO) δ = 172.7, 165.7, 58.4, 31.2, 18.9.

**HRMS (ESI)** for  $C_{12}H_{18}N_2O_6Na [M+Na]^+$ : calcd.: 309.1057, found: 309.1058.

**IR (ATR):**  $\tilde{\nu}$  = 2941 (w), 1764 (s), 1690 (m), 1463 (w), 1353 (m), 1273 (s), 1247 (s), 1148 (m), 927 (m).

$[\alpha]_D^{25} = -42.5$  ( $c = 1.00$ , DMSO).

**(2S,5S)-di-tert-butyl 2,5-bis(3-hydroxypropyl)piperazine-1,4-dicarboxylate (202)**



A suspension of **200** (1.11 g, 3.88 mmol, 1.00 eq.) in THF was cooled to 0 °C and  $\text{LiAlH}_4$  (2.21 g, 58.2 mmol, 15.00 eq) was added in five portions. The grey suspension was refluxed for 30 h under  $\text{N}_2$  atmosphere and then cooled to 0 °C. Then,  $\text{H}_2\text{O}$  (2.2 mL) was added dropwise, followed by aqueous  $\text{NaOH}$  (10% w/w, 2.2 mL), and  $\text{H}_2\text{O}$  (6.6 mL). The reaction mixture was heated to reflux for 30 min, cooled to ambient temperature and filtered over a glass sintered funnel (Por. 3). To the resulting clear filtrate was added 10 mL sat aqueous  $\text{NaHCO}_3$ , and the resulting biphasic mixture with precipitate formed was cooled to 0 °C.  $\text{Boc}_2\text{O}$  (1.78 g, 8.14 mmol, 2.10 eq) was added in one portion and the reaction was stirred for 24 h at room temperature. The solvent was evaporated and the crude oil was redissolved in water and extracted with  $\text{EtOAc}$  (5 x 50 mL). The combined organic layers were washed with brine (200 mL), dried over  $\text{Na}_2\text{SO}_4$ , filtered, and the solvent was evaporated. Purification of the crude material by silica gel flash chromatography ( $\text{SiO}_2$ ,  $\text{EtOAc}$ ) afforded **202** as a colorless oil, which solidified upon trituration with  $\text{Et}_2\text{O}$  (577 mg, 1.44 mmol, 37%).

Crystals suitable for X-ray analysis were grown from  $\text{Et}_2\text{O}$ .

$R_f = 0.34$  ( $\text{EtOAc}$ , CAM).

**Melting point** = 103 – 104 °C.

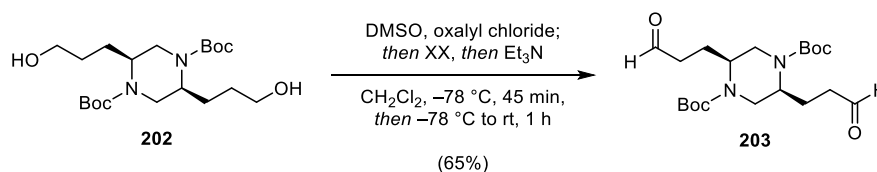
$^1\text{H NMR}$  (600 MHz,  $\text{CHCl}_3$ )  $\delta$  = 3.97 (br s, 4H), 3.64–3.55 (m, 4H), 2.63 – 2.53 (m, 2H), 1.57 – 1.49 (m, 6H), 1.40 (br s, 18 H).

$^{13}\text{C NMR}$  (150 MHz,  $\text{CHCl}_3$ )  $\delta$  = 155.6, 80.2, 62.4, 53.1, 42.06, 28.6, 28.5.

**HRMS (ESI)** for  $C_{20}H_{39}N_2O_6 [M+H]^+$ : calcd.: 403.2808; found: 403.2808.

**IR (ATR):**  $\tilde{\nu}$  = 3450 (m), 2941 (w), 2866 (w), 1669 (s), 1419 (s), 1366 (m), 1151(s), 1052 (s), 993 (w), 878 (m), 767 (m).

$[\alpha]_D^{25} = +84.2$  ( $c = 0.50$ ,  $\text{CH}_2\text{Cl}_2$ ).

**(2S,5S)-di-tert-butyl 2,5-bis(3-oxopropyl)piperazine-1,4-dicarboxylate (203)**

To solution of DMSO (0.81 mL, 11.4 mmol, 5.00 eq.) in  $\text{CH}_2\text{Cl}_2$  (15 mL) at  $-78^\circ\text{C}$  was added oxalyl chloride (2.0 M in  $\text{CH}_2\text{Cl}_2$ , 2.86 mL, 5.71 mmol, 2.50 eq.) dropwise. After complete addition, the reaction mixture was stirred at  $-78^\circ\text{C}$  for 15 min. Then a solution of **202** (920 mg, 2.29 mmol, 1.00 eq.) in dry  $\text{CH}_2\text{Cl}_2$  (10 mL) was added dropwise. After complete addition the reaction mixture was stirred at  $-78^\circ\text{C}$  for 45 min, followed by the dropwise addition of  $\text{Et}_3\text{N}$  (3.18 mL, 22.9 mmol, 10.00 eq.) at the same temperature. The cooling bath was removed, and the reaction was stirred for 1 h. Water (20 mL) was added, and the aqueous phase was extracted with  $\text{CH}_2\text{Cl}_2$  (2 x 20 mL). The combined organic phases were washed successively with aqueous HCl (1 M, 30 mL) saturated aqueous  $\text{NaHCO}_3$  (30 mL) and brine (30 mL), dried over  $\text{Na}_2\text{SO}_4$  filtered, and concentrated in vacuo. Purification by flash column chromatography ( $\text{SiO}_2$ , hexanes/ $\text{EtOAc}$  = 6/4) afforded aldehyde **203** (590 mg, 7.41 mmol, 65%) as a clear oil.

$R_f$  = 0.53 (hexanes/ $\text{EtOAc}$  = 1/1, PAA).

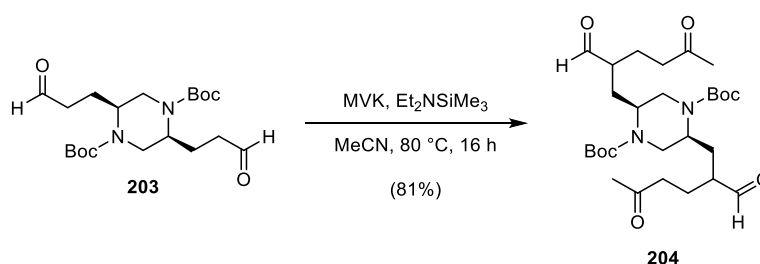
$^1\text{H NMR}$  (400 MHz,  $\text{CDCl}_3$ )  $\delta$  = 9.83 – 9.71 (m, 2H), 4.16 – 3.83 (m, 4H), 2.56 – 2.44 (m, 6H), 1.78 – 1.62 (m, 4 H), 1.43 (s, 18H).

$^{13}\text{C NMR}$  (100 MHz,  $\text{CDCl}_3$ )  $\delta$  = 201.5, 155.7, 80.6, 52.7, 42.0, 40.4, 28.5, 24.0.

**HRMS (EI)** for  $\text{C}_{20}\text{H}_{34}\text{N}_2\text{O}_6^+$   $[\text{M}]^+$ : calcd.: 398.2411, found: 398.2410.

**IR (ATR)**:  $\tilde{\nu}$  = 2973 (w), 2712 (w), 1773 (m), 1684 (s), 1403 (b, m), 1364 (s), 1247 (m), 1153 (s), 866 (m), 770 (m).

$[\alpha]_D^{25}$  = +71.3 (c = 1.00,  $\text{CH}_2\text{Cl}_2$ ).

**di-tert-butyl (2S,5S)-2,5-bis(2-formyl-5-oxohexyl)piperazine-1,4-dicarboxylate (204)**

To solution of aldehyde **203** (3.00 g, 7.53 mmol, 1.00 eq.) in MeCN (100 mL) was  $\text{Et}_2\text{NSiMe}_3$  (713  $\mu\text{L}$ , 3.77 mmol, 0.50 eq.). The resulting solution was heated to 80 °C for 16 h. The resulting orange solution was cooled to room temperature and concentrated in vacuo. Purification of the crude product by flash column chromatography ( $\text{SiO}_2$ , hexanes/EtOAc = 1/1) afforded ketoaldehyde **204** (3.30 g, 6.13 mmol, 81%) as a light yellow oil and as a 1/1 mixture of diastereoisomers. Spectral data match the previously reported values.<sup>[237]</sup>

$R_f = 0.40$  (hexanes/EtOAc = 3/7, CAM).

*Note: NMR spectra are complex due to the presence of diastereoisomers.*

$^1\text{H NMR}$  (600 MHz,  $\text{CHCl}_3$ )  $\delta = 9.60$  (t,  $J = 2.5$  Hz, 1H), 9.54 (t,  $J = 3.3$  Hz, 1H), 4.28 – 3.82 (m, 4H), 2.55 – 2.36 (m, 8H), 2.13 (d,  $J = 2.2$  Hz, 6H), 1.99 – 1.85 (m, 3H), 1.84 – 1.74 (m, 3H), 1.47 – 1.39 (m, 20H).

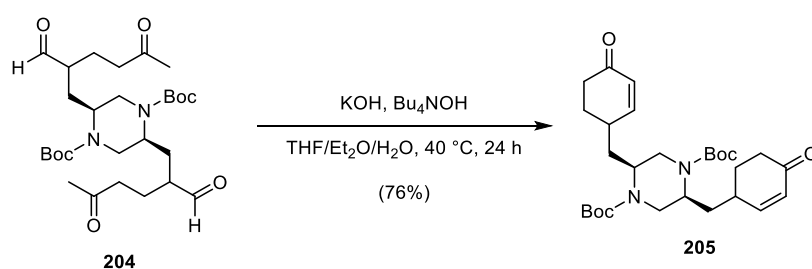
$^{13}\text{C NMR}$  (150 MHz,  $\text{CHCl}_3$ )  $\delta = 207.6, 203.5, 203.2, 155.5, 80.8, 51.8, 51.5, 48.0, 47.3, 42.2, 40.5, 40.4, 31.2, 30.8, 30.7, 30.2, 28.5, 23.1, 22.8$ .

**HRMS (EI)** for  $\text{C}_{28}\text{H}_{46}\text{N}_2\text{O}_8^+ [\text{M}]^+$ : calcd.: 538.3254, found: 538.3264.

**IR (ATR):**  $\tilde{\nu} = 2975$  (w), 2931 (w), 1686 (s), 1478 (w), 1413 (m), 1365 (m), 1247 (w), 1153 (m), 1108 (m), 875 (w), 789 (w).

$[\alpha]_{\text{D}}^{24} = +42.6$  (c = 1.0,  $\text{CH}_2\text{Cl}_2$ ).

### di-tert-butyl (2S,5S)-2,5-bis((4-oxocyclohex-2-en-1-yl)methyl)piperazine-1,4-dicarboxylate (**205**)



To a mixture of ketoaldehyde **204** (3.86 g, 7.17 mmol, 1.00 eq.) in THF (700 mL),  $\text{Et}_2\text{O}$  (1500 mL) and aqueous KOH (0.1 M, 700 mL) was added  $n\text{-Bu}_4\text{NOH}$  (1 M in MeOH, 1.43 mL, 1.43 mmol, 0.20 eq.) at 0 °C and the mixture was heated to 40 °C for 24 h. The organic layer was separated and saturated aqueous  $\text{NH}_4\text{Cl}$  (500 mL) was added, followed by EtOAc (400 mL). The organic layer was separated and the aqueous layer was extracted with EtOAc (2 x 400 mL). The combined organic layers were washed with brine (400 mL), dried over  $\text{MgSO}_4$  and concentrated in vacuo. The crude product was purified by flash column chromatography ( $\text{SiO}_2$ , hexanes/EtOAc = 1/1) to afford  $\alpha,\beta$ -unsaturated

ketone **205** as an inseparable diastereoisomeric mixture and as colorless oil (2.74 g, 5.45 mmol, 76%). Spectral data match the previously reported values.<sup>[237]</sup>

$R_f = 0.21$  (hexanes/EtOAc = 4/6, CAM).

*Note: NMR spectra are complex due to the presence of diastereoisomers.*

$^1\text{H NMR}$  (400 MHz,  $\text{CDCl}_3$ )  $\delta = 7.03 - 6.89$  (m, 2H), 6.81 (ddd,  $J = 10.4, 2.9, 1.2$  Hz, 1H), 5.99 (ddd,  $J = 10.0, 5.3, 2.3$  Hz, 2H), 4.27 (s, 2H), 4.05 (s, 3H), 2.65 – 2.43 (m, 4H), 2.43 – 2.26 (m, 2H), 2.22 – 2.06 (m, 1H), 1.84 – 1.52 (m, 5H), 1.52 – 1.39 (m, 18H), 1.40 – 1.25 (m, 1H), 1.03 – 0.79 (m, 1H).

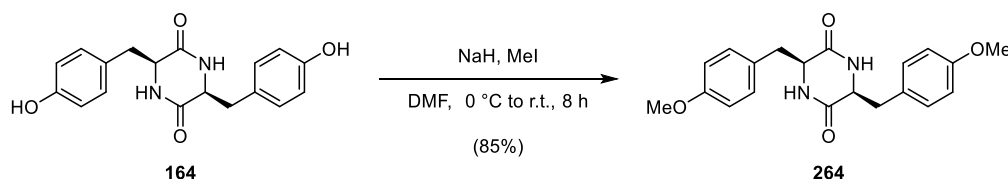
$^{13}\text{C NMR}$  (100 MHz,  $\text{CDCl}_3$ )  $\delta = 199.3, 199.2, 155.5, 155.4, 153.7, 129.4, 129.1, 80.7, 51.2, 51.1, 50.8, 50.7, 36.7, 36.6, 33.0, 32.5, 29.0, 28.9, 28.4$ .

**HRMS (EI)** for  $\text{C}_{28}\text{H}_{42}\text{N}_2\text{O}_6^+$   $[\text{M}]^+$ : calcd.: 502.3037, found: 502.3032.

**IR (ATR):**  $\tilde{\nu} = 3353$  (w), 2973 (w), 2929 (w), 1737 (w), 1676 (s), 1392 (w), 1665 (m), 1245 (m), 1153 (m), 1033 (w).

$[\alpha]_{\text{D}}^{24} = -6.2$  ( $c = 1.0, \text{CH}_2\text{Cl}_2$ ).

### (3S,6S)-3,6-bis(4-methoxybenzyl)piperazine-2,5-dione (**264**)



NaH (60% w/w in mineral oil, 515 mg, 12.9 mmol, 2.10 eq.) in DMF (47 mL) was cooled to 0 °C and diketopiperazine **164** (2.00 g, 6.13 mmol, 1.00 eq.; prepared according to Hutton and co-workers)<sup>[211]</sup> was added. After 30 minutes, MeI (1.14 mL, 18.4 mmol, 3.00 eq.) was added dropwise and the reaction mixture was stirred for 6 h while warming to room temperature. Then, it is cooled to 0 °C and saturated aqueous  $\text{NH}_4\text{Cl}$  (30 mL) was added, followed by  $\text{CHCl}_3$  (50 mL) and *i*-PrOH (10 mL). The layers are separated and the aqueous layer is extracted with an 8/2 mixture of  $\text{CHCl}_3$ /*i*-PrOH (2 x 50 mL). The combined organic layers are washed with LiCl (10% w/w, 3 x 30 mL), brine (30 mL), dried over  $\text{MgSO}_4$  and filtered. The solvent is removed in vacuo and the resulting solid is triturated with MeOH (20 mL) and filtered to afford **234** as a white solid (1.85 g, 5.22 mmol, 85%).

$R_f$  = not determined.

**Melting point** = 295 °C (decomposition).

$^1\text{H NMR}$  (400 MHz, DMSO)  $\delta = 7.85$  (d,  $J = 2.5$  Hz, 2H), 6.95 (d,  $J = 8.3$  Hz, 4H), 6.84 (d,  $J = 8.5$  Hz, 4H), 4.00 – 3.84 (m, 2H), 3.69 (s, 6H), 2.58 – 2.45 (m, 2H), 2.21 (dd,  $J = 13.7, 6.2$  Hz, 2H).

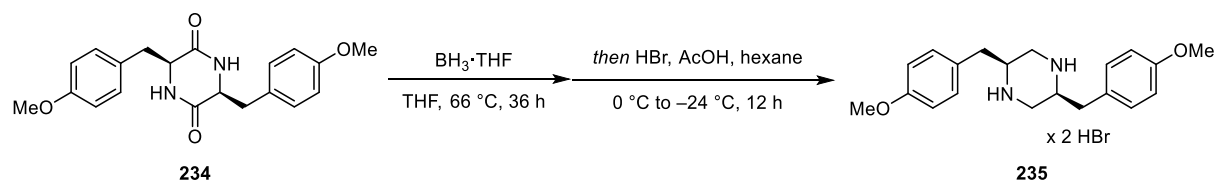
$^{13}\text{C NMR}$  (100 MHz, DMSO)  $\delta = 166.2, 158.0, 130.8, 128.4, 113.7, 55.5, 55.0, 38.4$ .

**HRMS (ESI)** for  $C_{20}H_{23}N_2O_4^+$   $[M+H]^+$ : calcd.: 355.1652, found 355.1651.

**IR (ATR):**  $\tilde{\nu}$  = 3210 (w), 3051 (w), 2933 (w), 1674 (s), 1656 (s), 1612 (m), 1512 (s), 1456 (s), 1338 (m), 1245 (m), 1179 (m), 1037 (m), 925 (w), 834 (m), 686 (w).

$[\alpha]_D^{20}$  = -114.4 (c = 0.5, DMSO)

### (2*S*,5*S*)-2,5-bis(4-methoxybenzyl)piperazine (**235**)



Diketopiperazine **234** (2.00 g, 5.64 mmol, 1.00 eq) was added to THF (46 ml) followed by  $BH_3 \cdot THF$  complex (1 M in THF, 33.9 mL, 33.9 mmol, 6.00 eq.). The suspension was stirred for 1 h at room temperature. Then, the resulting solution was heated to reflux for 36 h. The hot solution was filtered (por. 4 glass frit) into a separate flask containing a teflon-coated stir bar and cooled to 0 °C. Then, HBr (30% in AcOH, 30.6 ml, 169 mmol, 30.0 eq) was added dropwise (gas evolution!), followed by hexane (50 mL). The resulting slurry was aged in a freezer (-24 °C for 12 h). The suspension was filtered, and the resulting light yellow solid was recrystallized from EtOH to afford **235** as light tan crystals (1.19 g, 2.44 mmol, 43%).

Crystals suitable for X-ray analysis were grown from EtOH.

$R_f$  = not determined.

$^1H$  NMR (400 MHz, MeOD)  $\delta$  = 7.41 – 7.31 (m, 4H), 7.01 – 6.91 (m, 4H), 4.00 (dtd,  $J$  = 9.2, 6.7, 4.2 Hz, 2H), 3.79 (s, 6H), 3.48 (qd,  $J$  = 14.3, 5.4 Hz, 4H), 3.31 – 3.17 (m, 4H).

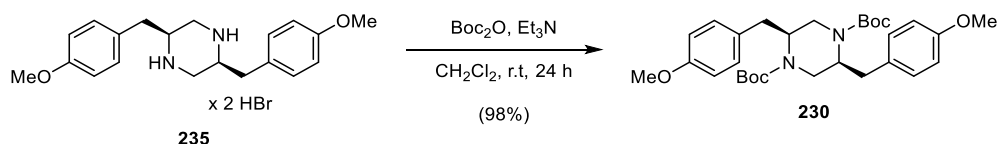
$^{13}C$  NMR (100 MHz, MeOD)  $\delta$  = 160.98, 131.62, 126.80, 115.73, 55.77, 54.12, 42.32, 34.67

**HRMS (ESI)** for  $C_{20}H_{27}N_2O_2^+$   $[M+H]^+$ : calcd.: 327.2076, found: 327.2068

**IR (ATR):**  $\tilde{\nu}$  = 2902 (w), 2718 (m), 1612 (m), 1551 (w), 1514 (s), 1454 (m), 1433 (m), 1257 (s), 1177 (s), 1097 (m), 1064 (m), 1034 (m), 961 (w), 838 (m), 740 (w), 666 (m).

$[\alpha]_D^{25}$  = -3.0 (c = 0.2, MeOH)

### di-*tert*-butyl (2*S*,5*S*)-2,5-bis(4-methoxybenzyl)piperazine-1,4-dicarboxylate (**230**)



Hydrobromide salt **235** (50 mg, 102  $\mu\text{mol}$ , 1.00 eq.) was suspended in  $\text{CH}_2\text{Cl}_2$  (650  $\mu\text{L}$ ) and  $\text{Et}_3\text{N}$  was added (62.6  $\mu\text{L}$ , 45.6  $\mu\text{mol}$ , 4.40 eq.), followed by  $\text{Boc}_2\text{O}$  (49.2 mg, 225  $\mu\text{mol}$ , 2.20 eq.). After stirring for 24 hours, the reaction was diluted with  $\text{CH}_2\text{Cl}_2$  (5 mL) and saturated aqueous  $\text{NH}_4\text{Cl}$  (5 mL). The layers were separated and the aqueous layer was extracted with  $\text{CH}_2\text{Cl}_2$  (2 x 10 mL). The combined organic layers were washed with brine (20 mL), dried over  $\text{MgSO}_4$ , filtered and concentrated under reduced pressure. Purification of the crude product by flash column chromatography ( $\text{SiO}_2$ , hexanes/ $\text{EtOAc}$  = 9/1) gave **230** as a colorless oil (50 mg, 101  $\mu\text{mol}$ , 98%).

$R_f$  = 0.69 (hexanes/ $\text{EtOAc}$  = 8/2, UV 254 nm, CAM).

$^1\text{H}$  NMR (400 MHz,  $\text{CDCl}_3$ )  $\delta$  = 7.03 – 6.97 (m, 4H), 6.83 – 6.76 (m, 4H), 4.04 (d,  $J$  = 7.7 Hz, 2H), 3.79 (overlap, app s, 6H), 2.78 (dd,  $J$  = 13.4, 4.0 Hz, 2H), 2.59 (td,  $J$  = 13.1, 8.7 Hz, 4H), 1.43 (s, 18H).

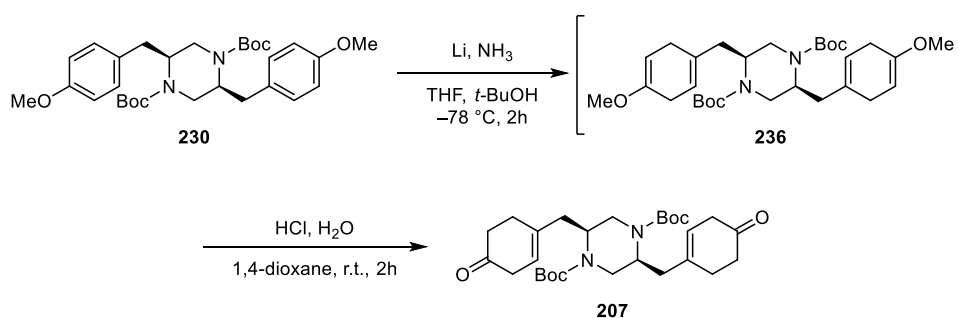
$^{13}\text{C}$  NMR (100 MHz,  $\text{CDCl}_3$ )  $\delta$  = 158.3, 155.1, 130.3, 129.1, 113.9, 80.0, 55.3, 54.5, 41.1, 37.1, 28.4.

HRMS (ESI) for  $\text{C}_{30}\text{H}_{43}\text{N}_2\text{O}_6^+$   $[\text{M}+\text{H}]^+$ : calcd.: 527.3116, found: 527.3124.

IR (ATR):  $\tilde{\nu}$  = 2973 (w), 2933 (m), 2936 (m), 1688 (s), 1512 (s), 1456 (w), 1404 (m), 1392 (m), 1365 (m), 1300 (m), 1246 (s), 1113 (m), 1035 (m), 944 (w), 879 (w), 767 (m).

$[\alpha]_D^{25}$  = +33.4 ( $c$  = 2.11,  $\text{CH}_2\text{Cl}_2$ ).

### di-*tert*-butyl-(2*S*)-2,5-bis((4-oxocyclohex-1-en-1-yl)methyl)piperazine-1,4-dicarboxylate (**207**)



Liquid ammonia (170 mL) was condensed into a three-neck round bottom flask fitted with a teflon-coated stirbar and a dry ice condenser placed in a  $-78^\circ\text{C}$  cooling bath. A solution of **230** (2.10 g, 3.99 mmol 1.00 eq) in  $t\text{-BuOH}$  (15 mL) and THF (50 mL) was added slowly. Lithium chips (553 mg, 79.7 mmol, 20.00 eq.) with vigorous stirring. The dark blue solution was stirred at  $-78^\circ\text{C}$  and the reaction progress was monitored by  $^1\text{H}$  NMR after evaporation of withdrawn reaction aliquots and dissolution in  $\text{CDCl}_3$ . After 2 h the reaction was deemed complete and  $\text{H}_2\text{O}$  was added until disappearance of the blue color. The cooling bath was removed and excess ammonia was allowed to evaporate under an  $\text{N}_2$  stream (ca. 6 h). The orange residue was taken up in water (200 mL) and extracted with  $\text{Et}_2\text{O}$  (3 x 200 mL). The combined organic layers were washed with water (2 x 100

mL), brine (100 mL), dried over  $\text{MgSO}_4$ , filtered and concentrated in vacuo to afford the intermediate methyl enol ether (**236**), which was used directly for the next step.

To a stirred solution of the intermediate methyl enol ether in dioxane (30 mL) was added aqueous HCl (1 M, 4 mL). After 2 h, pH 7 buffer (50 mL) and  $\text{Et}_2\text{O}$  (50 mL) are added. The layers are separated and the aqueous layer was extracted with  $\text{Et}_2\text{O}$  (3 x 50 mL). The combined organic layers were washed with water (2 x 100 mL), brine (100 mL), dried over  $\text{MgSO}_4$ , filtered and concentrated in vacuo. The resulting crude product was purified by flash column chromatography ( $\text{SiO}_2$ , hexanes/ $\text{EtOAc}$  = 8/2) to afford **207** as colorless oil (1.31 g, 2.61 mmol, 66%).

*Note: 207 is sensitive to air oxidation and decomposes if stored at room temperature within 3 days. It can be stored in a benzene matrix at  $-25\text{ }^\circ\text{C}$  for  $> 1$  year, and routine manipulations can be performed.*

$R_f$  = 0.29 (hexanes/ $\text{EtOAc}$  = 6/4,  $\text{KMnO}_4$ ).

$^1\text{H NMR}$  (400 MHz,  $\text{CDCl}_3$ )  $\delta$  = 5.48 (t,  $J$  = 3.6 Hz, 2H), 4.15 – 3.89 (m, 4H), 2.81 (d,  $J$  = 3.6 Hz, 4H), 2.65 (dd,  $J$  = 14.2, 10.5 Hz, 2H), 2.56 – 2.28 (m, 10H), 2.06 (dd,  $J$  = 13.3, 8.3 Hz, 2H), 1.41 (s, 18H).

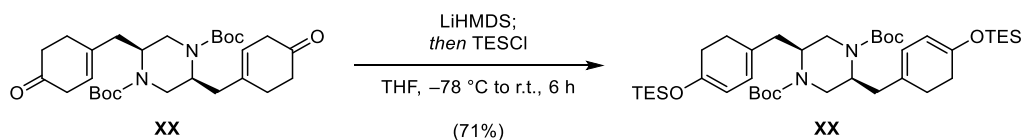
$^{13}\text{C NMR}$  (100 MHz,  $\text{CDCl}_3$ )  $\delta$  = 210.1, 155.0, 134.9, 121.2, 80.3, 51.6, 41.8, 39.7, 38.7, 28.5.

**HRMS (ESI)** for  $\text{C}_{28}\text{H}_{46}\text{N}_3\text{O}_6^+ [\text{M}+\text{NH}_4]^+$ : calcd.: 520.3387, found: 520.3398.

**IR (ATR)**:  $\tilde{\nu}$  = 3419 (w), 3052 (w), 2929 (w), 2341 (w), 2177 (w), 2159 (s), 1690 (s), 1478 (w), 1405 (m), 1366 (m), 1337 (m), 1264 (m), 1161 (m), 1114 (m), 1062 (m), 734 (m)

$[\alpha]_D^{25}$  = +37.7 (c = 0.60,  $\text{CH}_2\text{Cl}_2$ ).

**di-tert-butyl (2S,5S)-2,5-bis((4-((triethylsilyl)oxy)cyclohexa-1,3-dien-1-yl)methyl)piperazine-1,4-dicarboxylate (**237**)**



A solution of **207** (107 mg, 213  $\mu\text{mol}$ , 1.00 eq.) in THF (2 mL) was cooled to  $-78\text{ }^\circ\text{C}$  and a solution of LiHMDS (1M in THF, 468  $\mu\text{L}$ , 468  $\mu\text{mol}$ , 2.20 eq.) was added dropwise. After 45 min,  $\text{Et}_3\text{SiCl}$  was introduced and the reaction was allowed to warm to room temperature over the course of 8 hours. Then, pH 7 buffer (4 mL) was added, followed by  $\text{EtOAc}$  (10 mL). The organic layer was separated and the aqueous layer was extracted with  $\text{EtOAc}$  (2 x 10 mL). The combined organic layers were washed with brine (10 mL), dried over  $\text{Na}_2\text{SO}_4$  and filtered over a plug of silica gel (2 x 2 cm, elution with  $\text{EtOAc}$ ). The solvent was removed in vacuo to afford **237** (110 mg, 150  $\mu\text{mol}$  71%).

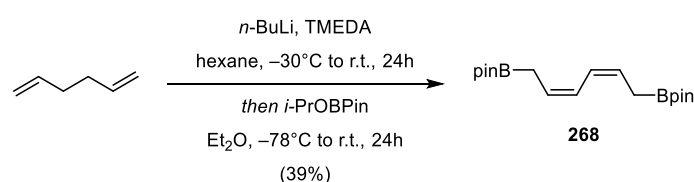
Note: **237** degrades upon storage at room temperature neat and in solution ( $\text{CDCl}_3$ ) within 3 days.

$R_f = 0.81$  (hexanes/EtOAc = 9/1, UV 254 nm,  $\text{KMnO}_4$ ).

$^1\text{H NMR}$  (400 MHz,  $\text{CDCl}_3$ )  $\delta$  5.54 (d,  $J = 5.9$  Hz, 2H), 5.02 (d,  $J = 5.9$  Hz, 2H), 4.00 (s, 4H), 2.68 (d,  $J = 14.2$  Hz, 2H), 2.43 – 2.31 (m, 2H), 2.31 – 2.14 (m, 7H), 2.05 (dd,  $J = 13.2, 9.0$  Hz, 2H), 1.45 (s, 18H), 0.97 (t,  $J = 7.9$  Hz, 18H), 0.72 – 0.59 (m, 12H).

$^{13}\text{C NMR}$  (100 MHz,  $\text{CDCl}_3$ )  $\delta = 166.2, 158.0, 130.8, 128.4, 113.7, 55.5, 55.0, 40.1, 39.9, 39.7, 39.5, 39.3, 39.1, 38.9, 38.4$ .

### (2Z,4Z)-1,6-bis(4,4,5,5-tetramethyl-1,3,2-dioxaborolan-2-yl)hexa-2,4-diene (**268**)



A solution of TMEDA (35 mL, 231 mmol, 2.10 eq.) in hexanes (40 mL) was cooled to  $-30^\circ\text{C}$  and  $n\text{-BuLi}$  (11 M in hexanes, 20.5 mL, 225 mmol, 2.05 eq.) was added dropwise and the resulting light yellow slurry was vigorously stirred until homogeneous. Hexadiene (13.1 mL, 110 mmol, 1.00 eq.) was added dropwise. After complete addition, the flask was sealed with a glass stopper and allowed to warm to room temperature over the course of 24 hours. The resulting dark red mixture was shaken manually to triturate solid aggregates and is cooled to  $-78^\circ\text{C}$  while  $\text{Et}_2\text{O}$  (114 mL) was added under vigorous stirring. A precooled ( $-78^\circ\text{C}$ , jacketed addition funnel) solution of  $i\text{-PrOBpin}$  (50 mL, 242 mmol, 2.20 eq.) in  $\text{Et}_2\text{O}$  (57 mL) was added dropwise under vigorous stirring (700 rpm). The reaction mixture solidifies after addition of approx. 75% of the solution. The setup is allowed to reach room temperature over the course of 24 h. Then, saturated aqueous  $\text{NH}_4\text{Cl}$  (200 mL) and  $\text{Et}_2\text{O}$  (300 mL) were added and the mixture was vigorously shaken and triturated with a glass rod to ensure adequate mixing. The mixture is filtered through a glass frit (por. 3), the aqueous phase is separated and extracted with  $\text{Et}_2\text{O}$  (2 x 200 mL). The combined organic layers are washed with brine (300 mL), dried over  $\text{MgSO}_4$  and filtered. The solvent is removed in vacuo and the crude product is dissolved in hexanes (50 mL) and left to crystallize at  $-24^\circ\text{C}$ . The mother liquor is removed by syringe and hexane (30 mL) is added. After aging at  $-24^\circ\text{C}$  for further 6 h, the resulting off-white solid is collected by filtration (14.06 g, 42.0 mmol, 39%).

Crystals suitable for X-ray analysis were obtained from pentane by slow evaporation under  $\text{N}_2$ .

Note: **268** degrades upon prolonged exposure to silica gel. It can be purified in a Kugelrohr apparatus (oven temperature = 163 to  $245^\circ\text{C}$  at  $2.5 \times 10^2$  mbar)

$R_f = 0.6$  (hexanes/ $\text{Et}_2\text{O}$  = 8/2, UV 254 nm, CAM).

Melting point =  $67.1^\circ\text{C}$ .

$^1\text{H NMR}$  (400 MHz,  $\text{CDCl}_3$ )  $\delta$  = 6.31 – 6.21 (m, 1H), 5.56 (dt,  $J$  = 9.7, 7.6 Hz, 1H), 1.82 (d,  $J$  = 8.2 Hz, 2H), 1.24 (s, 21H).

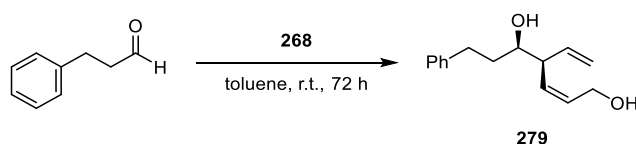
$^{13}\text{C NMR}$  (150 MHz,  $\text{CDCl}_3$ )  $\delta$  = 126.2, 123.8, 83.4, 24.9.

*Note: The peak belonging to the boron-bound carbon was not observed due to quadrupolar relaxation.*

**HRMS (EI)** for  $\text{C}_{18}\text{H}_{32}\text{B}_2\text{O}_4^+ [\text{M}]^+$ : calcd.: 334.2487, found: 334.2479.

**IR (ATR):**  $\tilde{\nu}$  = 3403 (w), 2978 (w), 2931 (w), 2166 (w), 1986 (w), 1596 (w), 1479 (w), 1467 (w), 1379 (m), 1369 (s), 1319 (s), 1271 (m), , 1213 (w), 1164 (m), 983 (w), 964 (m), 844 (m), 817 (w).

### ***Rac*-(4*S*,5*R*,*Z*)-7-phenyl-4-vinylhept-2-ene-1,5-diol (**279**)**



Allylpinacolboronate **268** (167 mg, 500  $\mu\text{mol}$ , 1.00 eq., dried by azeotropic evaporation from benzene) was dissolved in toluene (3 mL) and 3-phenylpropionaldehyde (79  $\mu\text{L}$ , 600  $\mu\text{mol}$ , 1.20 eq.) was added dropwise and the resulting clear solution was stirred for 3 days at room temperature. After cooling to 0  $^\circ\text{C}$ , THF (3 mL) was added, followed by aqueous NaOH (10% w/w, 600  $\mu\text{L}$ , 1.02 mmol 3.00 eq.) and aqueous  $\text{H}_2\text{O}_2$  (30% w/w, 610  $\mu\text{L}$ , 6.00 mmol 12.00 eq.). After warming to room temperature over the course of 2 h, saturated aqueous  $\text{NH}_4\text{Cl}$  (10 mL) was added, followed by EtOAc (20 mL). The layers were separated and the aqueous layer was extracted with EtOAc (2 x 20 mL). The combined organic layers were washed brine (30 mL), dried over  $\text{MgSO}_4$  and filtered. The solvent was removed in vacuo and the crude product was purified by flash column chromatography ( $\text{SiO}_2$ , hexanes/EtOAc = 7/3) to afford **278** as colorless oil and as a 9/1 mixture of diastereomers (78 mg, 336  $\mu\text{mol}$ , 67%).

*Note: 278 is copolar with pinacol and separation can only be achieved by careful chromatography (staining with PAA). Alternatively, pinacol can be removed by azeotropic removal using MeOH and  $\text{H}_2\text{O}$  according to Aggarwal and coworkers, or by submitting the crude reaction mixture to  $\text{NaIO}_4$ .<sup>[337]</sup>*

The diastereomers of **278** could also be separated by semipreparative HPLC (Dynamax Microsorb 60-8 C18, 250 x 21.4 mm;  $\text{H}_2\text{O}$ /Acetonitrile containing 0.1% formic acid; gradient: 5% to 50% acetonitrile over 55 minutes; flow rate 20 mL/min; detection at 210 nm;  $t_{\text{R}}$  major isomer = 38.7 min;  $t_{\text{R}}$  minor isomer = 40.0 min) Spectral data match the previously reported values.<sup>[316]</sup>

#### **Data for *syn*-279 (major isomer)**

$R_f$  = 0.23 (hexanes/EtOAc = 1/1, PAA).

$^1\text{H NMR}$  (600 MHz,  $\text{CHCl}_3$ )  $\delta$  = 7.32 – 7.16 (m, 5H), 5.89 – 5.68 (m, 2H), 5.50 (ddt,  $J$  = 11.1, 9.9, 1.3 Hz, 1H), 5.21 – 5.06 (m, 2H), 4.26 – 4.11 (m, 2H), 3.56 (ddd,  $J$  = 9.4, 6.3, 2.6 Hz, 1H), 3.22 (dddd,  $J$  = 10.0, 7.5, 6.3,

1.2 Hz, 1H), 2.85 (ddd,  $J = 13.7, 10.0, 5.1$  Hz, 1H), 2.65 (ddd,  $J = 13.7, 9.6, 6.8$  Hz, 1H), 1.86 (dddd,  $J = 13.9, 9.7, 6.8, 2.6$  Hz, 1H), 1.64 (dtd,  $J = 14.5, 9.7, 5.2$  Hz, 2H).

$^{13}\text{C}$  NMR (150 MHz,  $\text{CHCl}_3$ )  $\delta = 142.0, 137.5, 131.0, 130.9, 128.6, 128.6, 126.0, 117.4, 73.1, 58.6, 49.1, 35.6, 32.5$ .

HRMS (ESI) for  $\text{C}_{15}\text{H}_{21}\text{O}_2^+ [\text{M}+\text{H}]^+$ : calcd.: 233.1536, found: 233.1539.

IR (ATR):  $\tilde{\nu} = 3332$  (br), 3083 (w), 3024 (w), 2919 (w), 2861 (w), 2361 (w), 2340 (w), 1949 (w), 1635 (w), 1602 (w), 1495 (w), 1454 (m), 1417 (w), 1316 (w), 1154 (w), 1132 (w), 1029 (s), 823 (w), 747 (s), 699 (s), 668 (s).

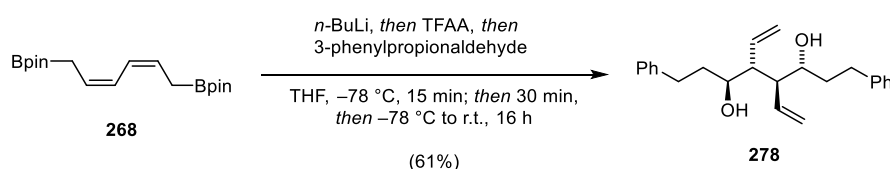
#### Data for *anti*-279 (minor isomer)

$R_f = 0.23$  (hexanes/EtOAc = 1/1, PAA).

$^1\text{H}$  NMR (600 MHz,  $\text{CHCl}_3$ )  $\delta = 7.47 - 7.07$  (m, 5H), 5.93 (dt,  $J = 10.6, 6.9$  Hz, 1H), 5.76 (ddd,  $J = 17.5, 9.9, 7.7$  Hz, 1H), 5.59 (td,  $J = 10.4, 9.8, 1.2$  Hz, 1H), 5.20 – 5.09 (m, 2H), 4.28 (ddd,  $J = 12.5, 7.4, 1.4$  Hz, 1H), 4.14 (ddd,  $J = 12.6, 6.4, 1.0$  Hz, 1H), 3.55 (ddd,  $J = 9.1, 7.3, 2.9$  Hz, 1H), 3.28 – 3.17 (m, 1H), 2.92 (ddd,  $J = 13.7, 10.0, 5.1$  Hz, 1H), 2.72 (ddd,  $J = 13.7, 9.7, 6.8$  Hz, 1H), 1.95 (dddd,  $J = 14.0, 9.9, 6.8, 2.9$  Hz, 1H), 1.75 (dtd,  $J = 14.3, 9.5, 5.1$  Hz, 1H).

$^{13}\text{C}$  NMR (150 MHz,  $\text{CHCl}_3$ )  $\delta = 142.1, 137.5, 131.8, 130.9, 128.6, 128.5, 126.0, 117.0, 72.5, 58.3, 49.4, 36.3, 32.1$ .

#### (3*R*,4*S*,5*R*,6*S*)-1,8-diphenyl-4,5-divinyloctane-3,6-diol (278)



Allylpinacolboronate **268** (170 mg, 509  $\mu\text{mol}$ , 1.00 eq., dried by azeotropic evaporation from benzene) was dissolved in THF (5 mL) and was cooled to  $-78\text{ }^\circ\text{C}$ . Then,  $n\text{-BuLi}$  (2.5 M in hexanes, 448  $\mu\text{L}$ , 1.12 mmol, 2.20 eq.) was added dropwise and the light red colored solution was stirred for 15 minutes at  $-78\text{ }^\circ\text{C}$ . Afterwards, TFAA (171  $\mu\text{L}$ , 1.23 mmol, 2.40 eq.) was added dropwise and the resulting white suspension was stirred for 30 min. Then, a solution of 3-phenylpropionaldehyde (201  $\mu\text{L}$ , 1.53 mmol, 3.00 eq.) was added dropwise and the resulting mixture was left to warm to room temperature over the course of 16 h. After cooling to  $0\text{ }^\circ\text{C}$ , aqueous NaOH (10% w/w, 407  $\mu\text{L}$ , 1.02 mmol 2.00 eq.) was added, followed by aqueous  $\text{H}_2\text{O}_2$  (30% w/w, 520  $\mu\text{L}$ , 5.09 mmol 10.00 eq.). After warming to room temperature over the course of 2 h, saturated aqueous  $\text{NH}_4\text{Cl}$  (20 mL) was added, followed by EtOAc (20 mL). The layers were separated and the aqueous layer was extracted with EtOAc (2 x 20 mL). The combined organic layers were washed brine (30 mL), dried over  $\text{MgSO}_4$

and filtered. The solvent was removed in vacuo and the crude product was purified by flash column chromatography (SiO<sub>2</sub>, hexanes/EtOAc = 9/1 to 8/2) to afford **278** as colorless oil that solidified upon standing (109 mg, 311 μmol, 61%).

Crystals suitable for X-ray analysis were obtained from hexane/*i*-Pr<sub>2</sub>O.

$R_f$  = 0.30 (hexanes/EtOAc = 8/2, PAA).

**Melting point** = 86.8 – 88.5 °C.

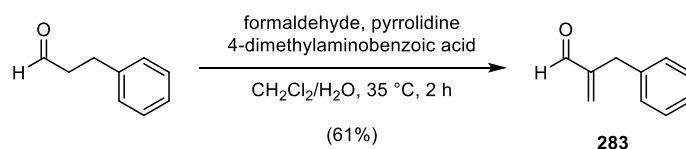
**<sup>1</sup>H NMR** (400 MHz, CHCl<sub>3</sub>) δ = 7.20 – 7.11 (m, 4H), 7.09 – 7.02 (m, 5H), 5.52 (dt,  $J$  = 17.1, 10.0 Hz, 2H), 5.05 – 4.89 (m, 4H), 3.54 (ddd,  $J$  = 10.0, 5.7, 2.4 Hz, 2H), 2.73 (ddd,  $J$  = 13.6, 10.2, 5.1 Hz, 2H), 2.47 (ddd,  $J$  = 13.7, 9.8, 6.6 Hz, 2H), 2.32 – 2.19 (m, 4H), 1.71 (dddd,  $J$  = 14.1, 10.1, 6.7, 2.4 Hz, 2H), 1.42 (dtd,  $J$  = 14.9, 9.8, 5.1 Hz, 2H).

**<sup>13</sup>C NMR** (100 MHz, CHCl<sub>3</sub>) δ = 142.3, 136.8, 128.6, 128.5, 125.9, 118.8, 71.5, 52.5, 35.6, 32.4.

**HRMS (ESI)** for C<sub>24</sub>H<sub>31</sub>O<sub>2</sub><sup>+</sup> [M+H]<sup>+</sup>: calcd.: 351.2319, found: 351.2327.

**IR (ATR):**  $\tilde{\nu}$  = 3344 (b, w), 3064 (w), 3002 (w), 2860 (w), 1944 (w), 1706 (m), 1637 (w), 1603 (w), 1584 (w), 1495 (m), 1453 (m), 1419 (m), 1220 (w), 1042 (m), 1030 (m), 999 (m), 916 (s), 844 (w), 819 (m), 746 (s), 697 (s).

## 2-benzylacrylaldehyde (**283**)



To a solution of 3-phenylpropionaldehyde (2.90 mL, 22.0 mmol, 1.00 eq.) in CH<sub>2</sub>Cl<sub>2</sub> (55 mL) were added formaldehyde (37% w/w in H<sub>2</sub>O, 1.98 ml, 26.4 mmol, 1.20 eq.), pyrrolidine (181 μL, 2.20 mmol, 0.10 eq) and 4-Dimethylaminobenzoic acid (363 mg, 2.20 mmol, 0.10 eq.). The mixture was heated to 35 °C for 2 h. Afterwards, the solution was cooled to room temperature and saturated aqueous NaHCO<sub>3</sub> (50 mL) was added. The organic layer was separated, and the aqueous layer was extracted with CH<sub>2</sub>Cl<sub>2</sub> (2 x 30 mL). The combined organic layers were washed with brine, dried over MgSO<sub>4</sub>, filtered and concentrated in vacuo. The resulting oil was purified by flash column chromatography (SiO<sub>2</sub>, hexane/Et<sub>2</sub>O = 9/1) to afford **283** as a colorless oil (1.975 g, 13.5 mmol, 61%). Spectral data match the previously reported values.<sup>[319]</sup>

$R_f$  = 0.52 (hexanes/Et<sub>2</sub>O = 9/1, UV 254 nm, CAM).

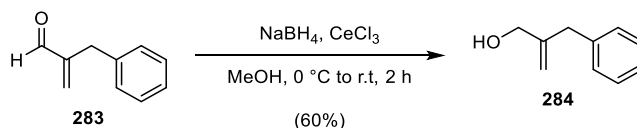
**<sup>1</sup>H NMR** (400 MHz, CDCl<sub>3</sub>) δ = 9.57 (s, 1H), 7.29 – 7.11 (m, 5H), 6.08 – 6.05 (m, 1H), 6.03 (d,  $J$  = 0.9, 1H), 3.53 (t,  $J$  = 1.1, 2H).

**<sup>13</sup>C NMR** (100 MHz, CDCl<sub>3</sub>) δ = 194.1, 149.8, 138.2, 135.4, 129.3, 128.7, 126.6, 34.3.

**HRMS (EI)** for  $C_{10}H_{10}O^+$ : calcd.: 146.0732  $[M]^+$ , found: 146.0708.

**IR (ATR):**  $\tilde{\nu}$  = 3361 (w), 3086 (w), 3029 (w), 2922 (w), 2700 (w), 1686 (s), 1602 (w), 1496 (m), 1453 (m), 1344 (w), 1313 (w), 1245 (w), 1075 (w), 950 (m), 737 (m), 698 (s).

### 2-benzylprop-2-en-1-ol (**284**)



Aldehyde **283** (2.70 g, 18.5 mmol, 1.00 eq.) was dissolved in MeOH (22 mL). CeCl<sub>3</sub>·H<sub>2</sub>O (8.95 g, 24.00 mmol, 1.30 eq.) was added and the solution was cooled to 0 °C. NaBH<sub>4</sub> (838 mg, 22.2 mmol, 1.20 eq.) was added slowly (gas evolution) and the mixture was allowed to warm to room temperature for 2 h. Saturated aqueous NaHCO<sub>3</sub> (20 mL) was added and the aqueous layer was extracted with EtOAc (3 x 20 mL). The combined organic layers were washed with brine (25 mL), dried over MgSO<sub>4</sub> and concentrated in vacuo. The crude product was purified by flash column chromatography (SiO<sub>2</sub>, hexanes/EtOAc = 8/2) to afford allylic alcohol **284** (1.65 g, 11.10 mmol, 60%) as colorless oil. Spectral data match the previously reported values.<sup>[338]</sup>

$R_f$  = 0.78 (hexanes/EtOAc = 7/3, UV 254 nm, CAM).

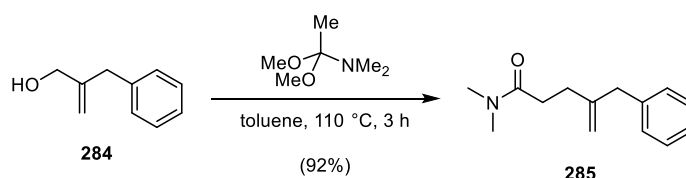
<sup>1</sup>H NMR (400 MHz, CDCl<sub>3</sub>)  $\delta$  = 7.34 – 7.28 (m, 2H), 7.25 – 7.20 (m, 3H), 5.13 (q,  $J$  = 1.6 Hz, 1H), 4.91 (p,  $J$  = 1.3 Hz, 1H), 4.04 (s, 2H), 3.42 (s, 2H).

<sup>13</sup>C NMR (100 MHz, CDCl<sub>3</sub>)  $\delta$  = 148.3, 139.1, 129.0, 128.5, 126.4, 111.5, 65.4, 40.0.

**HRMS (EI)** for  $C_{10}H_{12}O^+$   $[M]^+$ : calcd.: 148.0888, found: 148.0881.

**IR (ATR):**  $\tilde{\nu}$  = 3321 (br, w), 3027 (w), 2915 (w), 1882 (w), 1650 (w), 1494 (m), 1452 (m), 1432 (w), 1226 (w), 1154 (w), 1054 (m), 899 (m), 739 (m), 696 (s).

### 4-benzyl-N,N-dimethylpent-4-enamide (**285**)



Alcohol **284** (1.66 g, 11.2 mmol, 1.00 eq.) was dissolved in toluene (48 mL) and *N,N*-dimethylacetamide dimethyl acetal (2.46 mL, 16.8 mmol, 1.50 eq.) was added. The colorless solution was heated to 110 °C open to air and a gentle stream of N<sub>2</sub> was bubbled through the solvent via a thin glass capillary to remove liberated MeOH. After 3 h, the resulting yellow solution was cooled to room temperature and the volatiles were removed in vacuo. The crude product was purified

by flash column chromatography (SiO<sub>2</sub>, hexanes/EtOAc = 7/3) to give **285** (2.23 g, 10.3 mmol, 92%) as colorless oil.

$R_f$  = 0.18 (hexanes/EtOAc = 7/3, UV 254 nm, CAM).

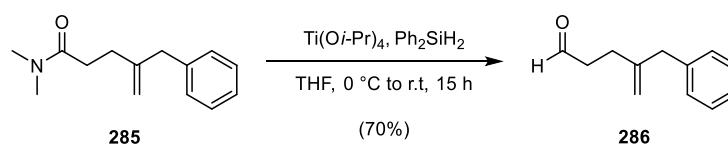
<sup>1</sup>H NMR (400 MHz, CDCl<sub>3</sub>)  $\delta$  = 7.37 – 7.27 (m, 2H), 7.25 – 7.20 (m, 3H), 4.86 (dd,  $J$  = 14.7, 1.9 Hz, 2H), 3.41 (s, 2H), 2.94 (d,  $J$  = 1.6 Hz, 6H), 2.53 – 2.29 (m, 4H).

<sup>13</sup>C NMR (100 MHz, CDCl<sub>3</sub>)  $\delta$  = 172.2, 148.0, 139.3, 128.8, 128.2, 126.0, 111.2, 43.3, 37.0, 35.2, 31.6, 30.5.

HRMS (ESI) for C<sub>14</sub>H<sub>20</sub>ON<sup>+</sup> [M+H]<sup>+</sup>: calcd.: 217.1467, found: 218.1537.

IR (ATR):  $\tilde{\nu}$  = 3062 (w), 2917 (w), 1946 (w), 1639 (s), 1493 (m), 1452 (m), 1432 (w), 1395 (m), 1265 (m), 1137 (m), 1029 (w), 981 (w), 891 (m), 828 (w), 735 (m), 699 (s).

#### 4-benzylpent-4-enal (**286**)



Amide **285** (1037 mg, 4.77 mmol, 1.00 eq.) was dissolved in THF (24 ml), cooled to 0 °C and Ti(O*i*-Pr)<sub>4</sub> (1.50 ml, 5.01 mmol, 1.05 eq.) was added. Then, diphenylsilane (1022  $\mu$ L, 5.49 mmol, 1.15 eq.) was added dropwise and the resulting solution was stirred for 15 h while warming to room temperature. Then, the solution was cooled to 0 °C and aqueous HCl (1 M, 10 mL) was added slowly (exotherm!) and a white precipitate was observed. Et<sub>2</sub>O (30 mL) was added, the phases were separated and the aqueous layer was extracted with Et<sub>2</sub>O (2 x 30 mL). The combined organic layers were washed with brine, dried over MgSO<sub>4</sub>, filtered, and concentrated in vacuo. The resulting crude product was purified by flash column chromatography (SiO<sub>2</sub>, hexanes/EtOAc = 9/1 to 7/3) to afford **286** as colorless oil (587 mg, 3.37 mmol, 70%). Spectral data match the previously reported values.<sup>[151]</sup>

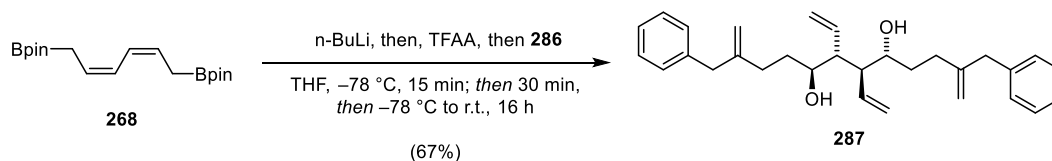
$R_f$  = 0.29 (hexanes/EtOAc = 7/3, UV 254 nm, CAM).

<sup>1</sup>H NMR (400 MHz, CDCl<sub>3</sub>)  $\delta$  = 9.72 (t,  $J$  = 1.7, 1H), 7.34 – 7.28 (m, 2H), 7.25 – 7.16 (m, 2H), 4.85 (dd,  $J$  = 8.6, 1.4, 2H), 3.38 (s, 2H), 2.56 (td,  $J$  = 7.5, 1.7, 2H), 2.35 – 2.29 (m, 2H).

<sup>13</sup>C NMR (100 MHz, CDCl<sub>3</sub>)  $\delta$  = 202.1, 147.0, 139.2, 129.0, 128.5, 126.4, 112.0, 43.5, 41.8, 27.5.

HRMS (EI) for C<sub>12</sub>H<sub>14</sub>O<sup>+</sup> [M]<sup>+</sup>: calcd.: 174.1045, found: 174.1042.

IR (ATR):  $\tilde{\nu}$  = 3431 (br, w), 3066 (w), 3026 (w), 2918 (w), 2724 (w), 2362 (w), 2138 (w), 1950 (w), 1722 (m), 1645 (w), 1601 (w), 1591 (w), 1494 (w), 1452 (w), 1429 (m), 1388 (w), 1335 (w), 1262 (w), 1182 (w), 1124 (m), 1074 (m), 1028 (m), 997 (w), 949 (w), 893 (m), 822 (w), 737 (m), 716 (m), 697 (s).

**(5*R*,6*S*,7*R*,8*S*)-2,11-dibenzyl-6,7-divinyldodeca-1,11-diene-5,8-diol (287)**

Allylpinacolboronate **268** (511 mg, 1.53 mmol, 1.00 eq., dried by azeotropic evaporation from benzene) was dissolved in THF (15 mL) and was cooled to  $-78$  °C. Then, *n*-BuLi (2.3 M in hexanes, 1.46 mL, 3.37 mmol, 2.20 eq.) was added dropwise and the light red colored solution was stirred for 15 minutes at  $-78$  °C. Afterwards, TFAA (515  $\mu$ L, 3.7 mmol, 2.40 eq.) was added dropwise and the resulting white suspension was stirred for 30 min. Then, a solution of aldehyde **286** (587 mg, 3.37 mmol, 2.20 eq.) in THF (1 mL) was added dropwise and the resulting mixture was left to warm to room temperature over the course of 16 h. After cooling to 0 °C, aqueous NaOH (10% w/w, 1.22 mL, 3.06 mmol, 2.00 eq.) was added, followed by aqueous H<sub>2</sub>O<sub>2</sub> (30% w/w, 1.56, 15.3 mmol, 10.00 eq.). After warming to room temperature over the course of 2 h, saturated aqueous NH<sub>4</sub>Cl (30 mL) was added, followed by EtOAc (50 mL). The layers were separated and the aqueous layer was extracted with EtOAc (2 x 50 mL). The combined organic layers were washed brine (50 mL), dried over MgSO<sub>4</sub> and filtered. The solvent was removed in vacuo and the crude product was purified by flash column chromatography (SiO<sub>2</sub>, hexanes/EtOAc = 9/1) to afford **287** as colorless oil (440 mg, 1.02  $\mu$ mol, 67%).

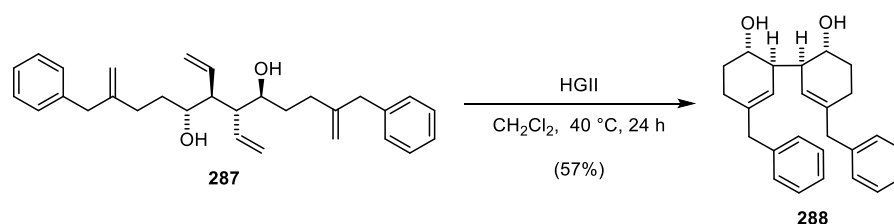
$R_f$  = 0.66 (hexanes/EtOAc = 8/2, PAA, violet).

<sup>1</sup>H NMR (400 MHz, CDCl<sub>3</sub>)  $\delta$  = 7.31 – 7.25 (m, 4H), 7.22 – 7.16 (m, 6H), 5.74 – 5.60 (m, 2H), 5.17 – 5.04 (m, 4H), 4.81 (dd,  $J$  = 30.5, 1.8 Hz, 4H), 3.59 (ddd,  $J$  = 9.3, 5.7, 2.4 Hz, 2H), 3.34 (s, 4H), 2.41 (s, 2H), 2.37 – 2.28 (m, 2H), 2.19 (ddd,  $J$  = 15.0, 10.0, 5.1 Hz, 2H), 1.98 (ddd,  $J$  = 15.3, 9.7, 6.5 Hz, 2H), 1.69 (dddd,  $J$  = 13.9, 10.0, 6.3, 2.6 Hz, 2H), 1.45 – 1.23 (m, 2H).

<sup>13</sup>C NMR (100 MHz, CDCl<sub>3</sub>)  $\delta$  = 149.0, 139.7, 137.1, 129.1, 128.4, 126.2, 118.4, 111.5, 71.6, 52.4, 43.2, 31.9, 31.8.

HRMS (ESI) for C<sub>30</sub>H<sub>39</sub>O<sub>2</sub><sup>+</sup> [M+H]<sup>+</sup>: calcd.: 431.2945, found: 431.2945.

IR (ATR):  $\tilde{\nu}$  = 3697 (w), 3663 (w), 3275 (w), 3072 (w), 1805 (w), 1642 (m), 1511 (w), 1494 (m), 1452 (m), 1332 (w), 1072 (m), 999 (w), 915 (m), 734 (s), 697 (s).

**(1R,1'S,2S,2'R)-5,5'-dibenzyl-[1,1'-bi(cyclohexane)]-5,5'-diene-2,2'-diol (288)**

A solution of **287** (113 mg, 262  $\mu\text{mol}$ , 1.00 eq) in  $\text{CH}_2\text{Cl}_2$  (10.8 mL) was deoxygenated by subsurface purging of  $\text{N}_2$  for 20 min. Then, HG2 (16.5 mg, 26.2  $\mu\text{mol}$ , 0.1 eq.) was added and the green solution was heated to 40  $^\circ\text{C}$ . After 24 h, the brown solution was cooled to room temperature and the solvent was removed in vacuo. The resulting crude product was purified by flash column chromatography ( $\text{SiO}_2$ , hexanes/ $\text{EtOAc}$  = 9/1 to 1/1) to afford **288** as a light grey solid (56 mg, 150  $\mu\text{mol}$ , 57%).

Crystals suitable for X-ray analysis were obtained from  $\text{CH}_2\text{Cl}_2$  by slow evaporation.

$R_f$  = 0.32 (hexanes/ $\text{EtOAc}$  = 2/1, CAM).

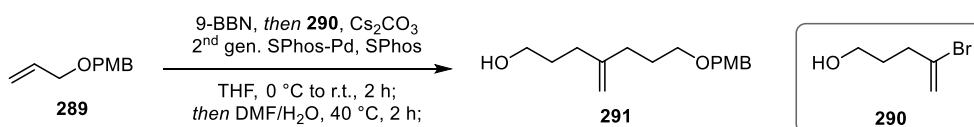
**Melting point** = 141.1 – 143.5  $^\circ\text{C}$ .

$^1\text{H}$  NMR (400 MHz,  $\text{CDCl}_3$ )  $\delta$  = 7.28 – 7.14 (m, 4H), 7.15 – 7.10 (m, 2H), 7.08 – 7.03 (m, 4H), 5.07 (q,  $J$  = 1.6, 2H), 3.73 (ddd,  $J$  = 11.2, 7.9, 3.6, 2H), 3.19 (s, 4H), 2.38 (dt,  $J$  = 8.0, 2.2, 2H), 2.27 (s, 2H), 1.96 – 1.87 (m, 4H), 1.80 (dq,  $J$  = 12.1, 4.0, 2H), 1.53 (tt,  $J$  = 11.9, 8.7, 2H).

$^{13}\text{C}$  NMR (100 MHz,  $\text{CDCl}_3$ )  $\delta$  = 139.9, 138.8, 128.8, 128.3, 126.1, 123.8, 69.6, 45.8, 44.0, 31.9, 27.4.

**HRMS (ESI)** for  $\text{C}_{26}\text{H}_{34}\text{NO}_2^+$  [ $\text{M}+\text{NH}_4$ ] $^+$ : calcd.: 392.2584, found: 392.2588.

**IR (ATR)**:  $\tilde{\nu}$  = 3300 (br, w), 2930 (w), 2828 (w), 1599 (w), 1349 (w), 1224 (w), 1157 (w), 1080 (m), 1038 (m), 785 (w), 746 (w), 699 (s), 597 (m).

**7-((4-methoxybenzyl)oxy)-4-methyleneheptan-1-ol (291)**

To a solution of **289** (891 mg, 5.00 mmol, 1.0 eq.) in THF (10 mL) at 0  $^\circ\text{C}$  was added 9-Borabicyclo[3.3.1]nonane (0.5 M in THF, 12.0 mL, 6.00 mmol, 1.2 eq.) and the reaction mixture was stirred for 2 h. In a separate flask, a solution of  $\text{Cs}_2\text{CO}_3$  (3.25 g 10.0 mmol, 2 eq.) in  $\text{H}_2\text{O}$  (5 mL) and DMF (10 mL) was deoxygenated by subsurface purging with  $\text{N}_2$  for 20 minutes. Then, the reaction mixture containing hydroborated **289** was added to the  $\text{Cs}_2\text{CO}_3$  solution via cannula. Thereafter, 2<sup>nd</sup> generation SPhos palladacycle (90.3 mg, 125  $\mu\text{mol}$ , 0.025 eq.), SPhos (51.3 mg, 125  $\mu\text{mol}$ , 0.025 eq.), and **290** (825 mg, 5.00 mmol, 1.0 eq., prepared according to Hoveyda and

Gao)<sup>[323]</sup> were added. The resulting orange mixture was heated to 40°C for 2 h. Then, it was cooled to room temperature and saturated aqueous NH<sub>4</sub>Cl (30 mL) was added, followed by EtOAc (30 mL). The layers were separated and the aqueous layer was extracted with EtOAc (2 x 50 mL). The combined organic layers were washed with LiCl (10% w/w, 3 x 30 mL), brine (30 mL), dried over MgSO<sub>4</sub>, filtered and concentrated in vacuo. The crude product was purified by flash column chromatography (SiO<sub>2</sub>, hexanes/EtOAc = 8/2 to 1/1) to afford **291** as colorless oil (810 mg, 3.06 mmol, 61%).

$R_f$  = 0.50 (hexanes/EtOAc = 1/1, UV 254 nm, CAM).

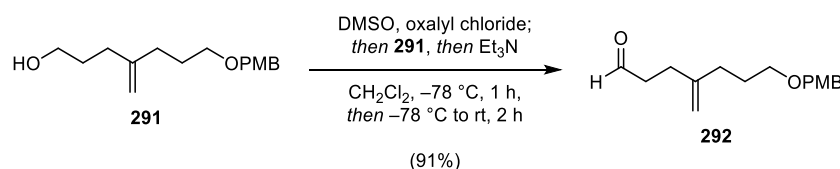
<sup>1</sup>H NMR (400 MHz, CDCl<sub>3</sub>)  $\delta$  = 7.29 – 7.23 (m, 2H), 6.92 – 6.84 (m, 2H), 4.77 – 4.72 (m, 2H), 4.43 (s, 2H), 3.81 (s, 3H), 3.69 – 3.60 (m, 2H), 3.45 (t,  $J$  = 6.5 Hz, 2H), 2.10 (t,  $J$  = 7.7 Hz, 4H), 1.78 – 1.65 (m, 4H).

<sup>13</sup>C NMR (100 MHz, CDCl<sub>3</sub>)  $\delta$  = 159.2, 148.9, 130.8, 129.4, 129.4, 113.9, 109.5, 72.7, 69.8, 62.9, 55.4, 32.6, 32.5, 30.8, 28.0.

HRMS (ESI): for C<sub>16</sub>H<sub>25</sub>O<sub>3</sub><sup>+</sup> [M+H]<sup>+</sup> calcd.: 265.1798, found: 265.1798.

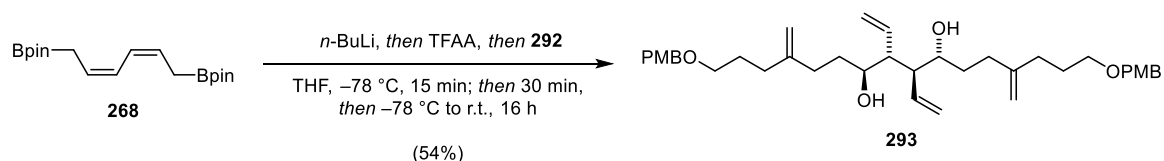
IR (ATR):  $\tilde{\nu}$  = 3379 (br, w), 2397 (m), 1612 (m), 1513 (m), 1548 (w), 1502 (w), 1462 (w), 1302 (m), 1247 (s), 1173 (m), 1099 (m), 1035 (w), 861 (w), 820 (m), 611 (w), 556 (w).

### 7-((4-methoxybenzyl)oxy)-4-methyleneheptanal (**292**)



To solution of DMSO (537  $\mu$ L, 7.57 mmol, 4.00 eq.) in CH<sub>2</sub>Cl<sub>2</sub> (9 mL) at –78°C was added oxalyl chloride (2.0 M in CH<sub>2</sub>Cl<sub>2</sub>, 1.89 mL, 3.78 mmol, 2.00 eq.) dropwise. After complete addition, the reaction mixture was stirred at –78 °C for 15 min. Then a solution of **291** (500 mg, 1.89 mmol, 1.00 eq.) in CH<sub>2</sub>Cl<sub>2</sub> (128 mL) was added dropwise. After complete addition the reaction mixture was stirred at –78°C for 45 min, followed by the dropwise addition of Et<sub>3</sub>N (1.57 mL, 11.3 mmol, 6.00 eq.) at the same temperature. The cooling bath was removed, and the reaction was stirred for 1 h. Water (100 mL) was added, and the aqueous phase was extracted with CH<sub>2</sub>Cl<sub>2</sub> (2 x 100 mL). The combined organic phases were washed successively with aqueous HCl (1 M, 100 mL) saturated aqueous NaHCO<sub>3</sub> (100 mL) and brine (100 mL), dried over MgSO<sub>4</sub>, filtered, and concentrated in vacuo. Purification by flash column chromatography (SiO<sub>2</sub>, hexanes/EtOAc = 8/2) afforded aldehyde **292** (450 mg, 1.72 mmol, 91%) as a clear oil. It was immediately used for the next step (synthesis of **293**) without further purification.

**(7R,8S,9R,10S)-1,17-bis((4-methoxybenzyl)oxy)-4,14-dimethylene-8,9-divinylheptadecane-7,10-diol (293)**



Allylpinacolboronate **268** (287 mg, 858  $\mu\text{mol}$ , 1.00 eq., dried by azeotropic evaporation from benzene) was dissolved in THF (6 mL) and was cooled to  $-78\text{ }^\circ\text{C}$ . Then, *n*-BuLi (2.14 M in hexanes, 882  $\mu\text{L}$ , 1.89 mmol, 2.20 eq.) was added dropwise and the light red colored solution was stirred for 15 minutes at  $-78\text{ }^\circ\text{C}$ . Afterwards, TFAA (289  $\mu\text{L}$ , 2.08 mmol, 2.40 eq.) was added dropwise and the resulting white suspension was stirred for 30 min. Then, a solution of aldehyde **292** (450 mg, 1.72 mmol, 2.00 eq.) in THF (3 mL) was added dropwise and the resulting mixture was left to warm to room temperature over the course of 16 h. After cooling to  $0\text{ }^\circ\text{C}$ , aqueous NaOH (10% w/w, 1.02 mL, 2.57 mmol 3.00 eq.) was added, followed by aqueous  $\text{H}_2\text{O}_2$  (30% w/w, 964  $\mu\text{L}$ , 9.43 mmol 11.00 eq.). After warming to room temperature over the course of 2 h, saturated aqueous  $\text{NH}_4\text{Cl}$  (20 mL) was added, followed by EtOAc (20 mL). The layers were separated and the aqueous layer was extracted with EtOAc (2 x 20 mL). The combined organic layers were washed brine (30 mL), dried over  $\text{MgSO}_4$  and filtered. The solvent was removed in vacuo and the crude product was purified by flash column chromatography ( $\text{SiO}_2$ , hexanes/EtOAc = 9/1 to 3/7) to afford **293** as colorless oil (208 mg, 461  $\mu\text{mol}$ , 54%).

$R_f = 0.45$  (hexanes/EtOAc = 1/1, UV 254 nm, PAA).

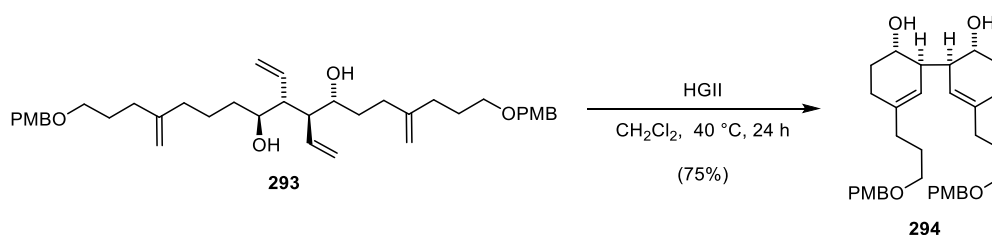
$^1\text{H NMR}$  (400 MHz,  $\text{CDCl}_3$ )  $\delta = 7.31 - 7.21$  (m, 4H), 6.92 – 6.83 (m, 4H), 5.68 (ddd,  $J = 17.1, 11.2, 8.5$  Hz, 2H), 5.24 – 5.00 (m, 4H), 4.73 (s, 4H), 4.42 (s, 4H), 3.80 (s, 6H), 3.69 – 3.58 (m, 2H), 3.44 (t,  $J = 6.5$  Hz, 4H), 2.41 – 2.32 (m, 3H), 2.23 (ddd,  $J = 14.9, 9.9, 5.1$  Hz, 3H), 2.14 – 1.92 (m, 6H), 1.85 – 1.54 (m, 6H), 1.34 (dtd,  $J = 14.6, 9.7, 5.2$  Hz, 2H).

$^{13}\text{C NMR}$  (100 MHz,  $\text{CDCl}_3$ )  $\delta = 159.1, 149.2, 137.0, 130.7, 129.3, 118.4, 113.8, 109.3, 72.6, 71.7, 69.7, 55.3, 52.4, 32.5, 32.4, 31.8, 27.8$ .

**HRMS (ESI)** for  $\text{C}_{38}\text{H}_{58}\text{NO}_6^+$   $[\text{M}+\text{H}]^+$ : calcd.: 624.4259, found: 624.4279.

**IR (ATR)**:  $\tilde{\nu} = 3374$  (br, w), 3073 (w), 2936 (w), 2857 (w), 1612 (m), 1512 (m), 1463 (w), 1245 (s), 1172 (m), 1097 (m), 1034 (m), 912 (m), 819 (m), 731 (s), 574 (m).

**(1*R*,1'*S*,2*S*,2'*R*)-5,5'-bis(3-((4-methoxybenzyl)oxy)propyl)-[1,1'-bi(cyclohexane)]-5,5'-diene-2,2'-diol (294)**



A solution of **293** (22 mg, 36.3  $\mu\text{mol}$ , 1.00 eq) in toluene (1.45 mL) was deoxygenated by subsurface purging of  $\text{N}_2$  for 20 min. Then, HG2 (2.27 mg, 3.63  $\mu\text{mol}$ , 0.1 eq.) was added and the green solution was heated to 90  $^\circ\text{C}$ . After 4 h, the brown solution was cooled to room temperature and the solvent was removed in vacuo. The resulting crude product was purified by flash column chromatography ( $\text{SiO}_2$ , hexanes/EtOAc = 1/1 to EtOAc) to afford **294** as a colorless oil (15 mg, 27.2  $\mu\text{mol}$ , 75%).

$R_f$  = 0.58 (EtOAc, UV 254 nm, CAM).

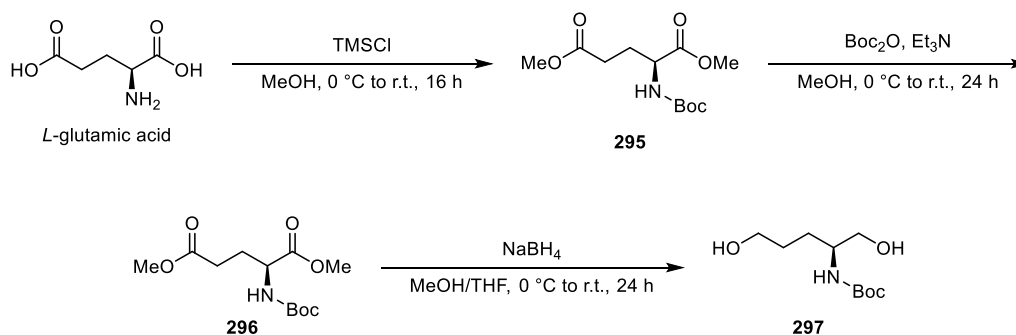
$^1\text{H NMR}$  (400 MHz,  $\text{CDCl}_3$ )  $\delta$  = 7.18 (dd,  $J$  = 8.3, 1.8 Hz, 4H), 6.86 – 6.74 (m, 4H), 4.97 (s, 2H), 4.34 (s, 4H), 3.72 (s, 8H), 3.34 (t,  $J$  = 6.6 Hz, 2H), 2.36 – 2.18 (m, 2H), 2.04 – 1.89 (m, 4H), 1.88 – 1.79 (m, 1H), 1.70 – 1.48 (m, 8H).

$^{13}\text{C NMR}$  (100 MHz,  $\text{CDCl}_3$ )  $\delta$  = 159.1, 138.7, 130.7, 129.3, 121.9, 113.8, 72.6, 69.7, 69.7, 55.3, 45.8, 33.8, 31.9, 27.9, 27.6.

**HRMS (ESI)** for  $\text{C}_{34}\text{H}_{50}\text{NO}_6^+$  [ $\text{M}+\text{NH}_4$ ] $^+$ : calcd.: 568.3638, found 568.3647.

**IR (ATR)**:  $\tilde{\nu}$  = 3377 (br, w), 2926 (m), 2855 (m), 1725 (w), 1691 (w), 1658 (w), 1513 (w), 1462 (w), 1365 (w), 1302 (w), 1247 (m), 1173 (m), 1097 (m), 1035 (m), 819 (w), 612 (w).

***tert*-butyl (*S*)-(1,5-dihydroxypentan-2-yl)carbamate (297)**



L-glutamic acid (20.0 g, 135.9 mmol, 1.00 eq.) was dissolved in MeOH (220 mL) and the solution was cooled to 0  $^\circ\text{C}$ . TMSCl (64.9 g, 598.1 mmol, 4.40 eq.) was added dropwise and the reaction mixture was stirred at room temperature for 16 hours.

The resulting solution containing L-glutamic acid dimethyl ester (**295**) was cooled to 0 °C and Et<sub>3</sub>N (146 mL, 1052 mmol, 6.50 eq.) was added dropwise. Then, a solution of Boc<sub>2</sub>O (38.9 g, 178.1 mmol, 1.10 eq.) in MeOH (80 mL) was added slowly and the reaction mixture was stirred at room temperature for 24 h. The solvent was removed in vacuo and the residue was dissolved in water (100 mL). The aqueous layer was extracted with EtOAc (3 x 100 mL), the combined organic layers were washed with water (150 mL) and brine (150 mL), dried over MgSO<sub>4</sub> and concentrated in vacuo.

The crude product (**296**) was dissolved in THF (250 mL) and MeOH (50 mL) and the solution was cooled to 0 °C. NaBH<sub>4</sub> (16.6 g, 438 mmol, 4.00 eq.) was added slowly (gas evolution!). The mixture was stirred for 24 h and allowed to warm to room temperature. The solvent was removed under reduced pressure and the residue was diluted in water (200 mL). Citric acid was added until pH = 6. The aqueous solution was extracted with EtOAc (3 x 150 mL) and the combined organic layers were dried over MgSO<sub>4</sub> and concentrated in vacuo. The resulting crude product **297** was used in the next step without purification. An aliquot was purified by flash column chromatography (SiO<sub>2</sub>, hexanes/EtOAc = 7/3) for analysis. Spectral data match the previously reported values.<sup>[325]</sup>

**R<sub>f</sub>** = 0.10 (hexanes/EtOAc = 8/2, CAM).

*Note: NMR spectra are complex due to the presence of rotamers.*

**<sup>1</sup>H NMR** (400 MHz, CDCl<sub>3</sub>) δ = 4.86 (br s, 1H), 3.84–3.50 (m, 5H), 2.84 (br s, 1H), 2.29 (br s, 1H), 1.85–1.55 (m, 3H), 1.52–1.28 (m, 10H).

**<sup>13</sup>C NMR** (100 MHz, CDCl<sub>3</sub>) δ = 156.7, 79.8, 79.4, 65.6, 62.5, 62.0, 52.5, 50.3, 28.9, 28.5, 28.1.

**HRMS (ESI):** for C<sub>10</sub>H<sub>22</sub>O<sub>4</sub>N<sup>+</sup> [M+H]<sup>+</sup>: calcd.: 220.1549, found: 220.1543.

**IR (ATR):**  $\tilde{\nu}$  = 3338 (m), 2938 (m), 1688 (s), 1530 (m), 1392 (m), 1366 (m), 1170 (s), 1052 (m).

**[ $\alpha$ ]<sub>D</sub><sup>25</sup>** = -15.7 (c = 1.00, CH<sub>2</sub>Cl<sub>2</sub>).

### **tert-butyl (S)-4-(3-hydroxypropyl)-2,2-dimethyloxazolidine-3-carboxylate (**298**)**



Crude product **297** (24.0 g, 109.5 mmol, 1 eq., 100% yield assumed from the previous step) was dissolved in acetone (200 mL) and 2,2-Dimethoxypropane (60 mL) was added. The solution was cooled to 0 °C and boron trifluoride diethyl etherate (0.31 g, 2.17 mmol, 0.02 eq.) was added. After 24 h the solvent was removed under reduced pressure and the residue was diluted with water (100 mL) and the pH adjusted to 7 using saturated aqueous NaHCO<sub>3</sub>. The aqueous layer was extracted with EtOAc (3 x 100 mL) and the combined organic layers were washed with water (100 mL) and brine

(100 mL). The solution was dried over  $\text{MgSO}_4$  and concentrated in vacuo. An aliquot of the crude product was separated for the analytical data and purified by flash column chromatography ( $\text{SiO}_2$ , hexanes/EtOAc = 4/6). Protecting product **298** was obtained as colorless oil. The residual crude product (27.1 g, 104.4 mmol, 95 %) was used in the next step without purification. Spectral data match the previously reported values.<sup>[325]</sup>

$R_f = 0.14$  (hexanes/EtOAc = 3/7, CAM).

*Note: NMR spectra are complex due to the presence of rotamers.*

$^1\text{H NMR}$  (400 MHz,  $\text{CDCl}_3$ )  $\delta = 3.98\text{--}3.66$  (m, 5H), 2.24 (br, 1H), 1.86–1.71 (m, 1H), 1.66–1.31 (m, 18H).

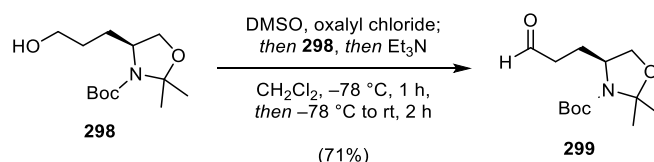
$^{13}\text{C NMR}$  (100 MHz,  $\text{CDCl}_3$ )  $\delta = 152.6, 151.9, 93.9, 93.4, 80.4, 79.7, 67.2, 62.8, 62.6, 57.2, 30.1, 29.9, 29.5, 29.1, 28.6, 27.7, 26.9, 24.6, 23.4$ .

**HRMS (ESI)** for  $\text{C}_{13}\text{H}_{26}\text{O}_4\text{N}^+$   $[\text{M}+\text{H}]^+$ : calcd.: 260.1856, found: 260.1858.

**IR (ATR)**:  $\tilde{\nu} = 3442$  (w), 2936 (w), 2870 (w), 1692 (s), 1364 (s), 1256 (m), 1171 (m), 1083 (s), 844 (m), 768 (m).

$[\alpha]_{\text{D}}^{25} = +21.9$  ( $c = 0.98, \text{CH}_2\text{Cl}_2$ ).

### *tert*-butyl (*S*)-2,2-dimethyl-4-(3-oxopropyl)oxazolidine-3-carboxylate (**299**)



To solution of DMSO (4.69 mL, 66.0 mmol, 3.30 eq.) in  $\text{CH}_2\text{Cl}_2$  (15 mL) at  $-78^\circ\text{C}$  was added oxalyl chloride (2.0 M in  $\text{CH}_2\text{Cl}_2$ , 12.00 mL, 24.00 mmol, 1.20 eq.) dropwise. After complete addition, the reaction mixture was stirred at  $-78^\circ\text{C}$  for 15 min. Then a solution of **298** (5.19 g, 20.0 mmol, 1.00 eq.) in  $\text{CH}_2\text{Cl}_2$  (128 mL) was added dropwise. After complete addition the reaction mixture was stirred at  $-78^\circ\text{C}$  for 45 min, followed by the dropwise addition of  $\text{Et}_3\text{N}$  (18.3 mL, 132.0 mmol, 6.60 eq.) at the same temperature. The cooling bath was removed, and the reaction was stirred for 1 h. Water (100 mL) was added, and the aqueous phase was extracted with  $\text{CH}_2\text{Cl}_2$  (2 x 100 mL). The combined organic phases were washed successively with aqueous HCl (1 M, 100 mL) saturated aqueous  $\text{NaHCO}_3$  (100 mL) and brine (100 mL), dried over  $\text{MgSO}_4$ , filtered, and concentrated in vacuo. Purification by flash column chromatography ( $\text{SiO}_2$ , hexanes/EtOAc = 8/2) afforded aldehyde **299** (3.66 g, 14.2 mmol, 71%) as a clear oil. Spectral data match the previously reported values.<sup>[325]</sup>

$R_f = 0.42$  (hexanes/EtOAc = 7/3, CAM)

*Note: NMR spectra are complex due to the presence of rotamers.*

**<sup>1</sup>H NMR** (400 MHz, CDCl<sub>3</sub>) δ = 9.77 (br, 1H), 4.02–3.80 (m, 2H), 3.73–3.68 (m, 1H), 2.55–2.33 (m, 2H), 2.05–1.84 (m, 2H), 1.56–1.52 (m, 3H), 1.47 (s, 12H).

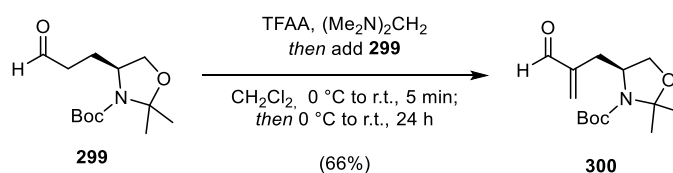
**<sup>13</sup>C NMR** (100 MHz, CDCl<sub>3</sub>) δ = 201.7, 201.4, 152.6, 151.9, 94.1, 93.6, 80.4, 80.0, 67.1, 56.7, 56.3, 40.6, 40.4, 28.7, 28.6, 28.5, 28.5, 28.4, 27.7, 26.9, 26.1, 26.0, 24.6, 24.4, 23.1.

**HRMS (ESI)** for C<sub>13</sub>H<sub>24</sub>O<sub>4</sub>N<sup>+</sup> [M+H]<sup>+</sup>: calcd.: 258.1700, found: 258.1700.

**IR (ATR):**  $\tilde{\nu}$  = 2979 (w), 1695 (s), 1390 (s), 1367 (s), 1257 (m), 1171 (m), 1084 (m), 855 (w), 767 (w).

$[\alpha]_D^{25} = +3.8$  (c = 1.05, CH<sub>2</sub>Cl<sub>2</sub>).

### ***tert*-butyl (S)-4-(2-formylallyl)-2,2-dimethyloxazolidine-3-carboxylate (300)**



*N,N,N',N'*-Tetramethyldiaminomethane (2.00 mL, 14.7 mmol, 1.10 eq.) was dissolved in CH<sub>2</sub>Cl<sub>2</sub> (25 mL) and the solution was cooled to 0 °C. TFAA (2.10 mL, 14.7 mmol, 1.10 eq.) was added slowly dropwise. The cooling bath was removed and the reaction mixture was stirred at room temperature for 5 min and cooled to 0 °C. A solution of aldehyde **299** (3.45 g, 13.4 mmol, 1 eq.) in CH<sub>2</sub>Cl<sub>2</sub> (20 mL) was prepared in a second flask, cooled to 0 ° and transferred to the other flask via cannula. After stirring at room temperature for 18 h, it saturated aqueous NaHCO<sub>3</sub> (40 mL) was added and the organic layer was and extracted with EtOAc (3 x 50 mL). The combined organic layers were washed with brine (75 mL), dried over MgSO<sub>4</sub> and concentrated in vacuo. The crude product was purified by flash column chromatography (SiO<sub>2</sub>, hexanes/EtOAc = 7/3) to afford **300** (2.37 g, 8.80 mmol, 66%) as colorless oil. Spectral data match the previously reported values.<sup>[329]</sup>

**R<sub>f</sub>** = 0.46 (hexanes/EtOAc = 7/3, CAM)

*Note: NMR spectra are complex due to the presence of rotamers.*

**<sup>1</sup>H NMR** (400 MHz, CDCl<sub>3</sub>) δ = 9.53 (d, *J* = 8.5 Hz, 1H), 6.27 (d, *J* = 18.0 Hz, 1H), 6.05 (d, *J* = 24.0 Hz, 1H), 4.18 – 3.95 (m, 1H), 3.86 (ddd, *J* = 14.1, 8.9, 5.6 Hz, 1H), 3.69 (d, *J* = 9.0 Hz, 1H), 2.69 – 2.39 (m, 2H), 1.59 (d, *J* = 22.8 Hz, 3H), 1.49 – 1.42 (m, 12H).

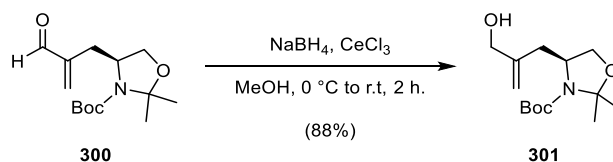
**<sup>13</sup>C NMR** (100 MHz, CDCl<sub>3</sub>) δ = 194.3, 194.2, 152.4, 151.9, 147.2, 146.9, 136.6, 135.3, 94.1, 93.6, 80.3, 80.1, 67.0, 66.7, 56.5, 55.9, 32.8, 31.9, 28.6, 28.5, 27.8, 27.2, 24.5, 23.3.

**HRMS (ESI)** for C<sub>14</sub>H<sub>24</sub>O<sub>4</sub>N<sup>+</sup> [M+H]<sup>+</sup>: calcd.: 270.1700, found: 270.1701.

**IR (ATR):**  $\tilde{\nu}$  = 2980 (w), 1688 (s), 1456 (w), 1385 (s), 1364 (s), 1255 (m), 1172 (m), 1059 (m), 949 (w), 856 (m), 769 (m).

$[\alpha]_{\text{D}}^{25} = -4.0$  (c = 1.09, CH<sub>2</sub>Cl<sub>2</sub>).

**tert-butyl (S)-4-(2-(hydroxymethyl)allyl)-2,2-dimethyloxazolidine-3-carboxylate (301)**



Enal **300** (0.25 g, 0.91 mmol, 1.00 eq.) was dissolved in MeOH (4.4 mL). CeCl<sub>3</sub>·H<sub>2</sub>O (0.41 g, 1.09 mmol, 1.20 eq.) was added and the solution was cooled to 0 °C. NaBH<sub>4</sub> (0.04 g, 1.09 mmol, 1.20 eq.) was added slowly (gas evolution!). The mixture was allowed to warm to room temperature over the course of 2 h, and saturated aqueous NaHCO<sub>3</sub> (10 mL) was added. The mixture was extracted with EtOAc (3 x 15 mL) and the combined organic layers were washed with brine (25 mL), dried over MgSO<sub>4</sub> and concentrated in vacuo. The crude product was purified by flash column chromatography (SiO<sub>2</sub>, hexanes/EtOAc = 6/4). Allylic alcohol **301** (0.22 g, 0.81 mmol, 88%) was obtained as colorless oil.

$R_f = 0.36$  (hexanes/EtOAc = 6/4, CAM)

*Note: NMR spectra are complex due to the presence of rotamers.*

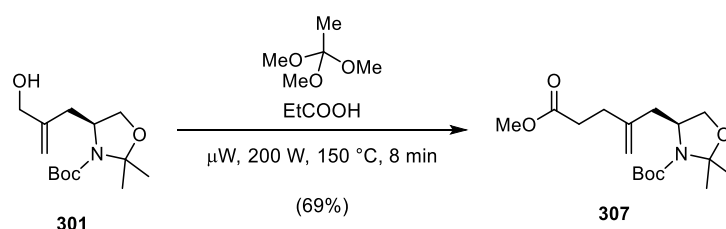
**<sup>1</sup>H NMR** (400 MHz, CDCl<sub>3</sub>)  $\delta$  = 5.21 – 4.78 (m, 2H), 4.21 (q,  $J$  = 6.6 Hz, 1H), 4.16 – 4.05 (m, 2H), 3.98 – 3.67 (m, 2H), 3.61 – 3.53 (m, 1H), 2.58 – 2.18 (m, 2H), 1.59 (s, 3H), 1.46 (s, 12H).

**<sup>13</sup>C NMR** (100 MHz, CDCl<sub>3</sub>)  $\delta$  = 152.9, 151.7, 146.0, 145.8, 113.4, 112.6, 94.0, 93.7, 80.7, 79.9, 67.5, 67.0, 66.5, 65.7, 56.6, 56.1, 39.0, 37.5, 28.6, 28.5, 27.9, 27.1, 24.5, 23.3.

**HRMS (ESI)** for C<sub>14</sub>H<sub>26</sub>O<sub>4</sub>N<sup>+</sup> [M+H]<sup>+</sup>: calcd.: 272.1856, found: 272.185.

**IR (ATR):**  $\tilde{\nu}$  = 3436 (w), 2979 (w), 2874 (w), 1694 (m), 1386 (s), 1365 (s), 1246 (m), 1171 (m), 1096 (m), 900 (w), 852 (m), 769 (w).

$[\alpha]_{\text{D}}^{25} = +10.8$  (c = 1.03, CH<sub>2</sub>Cl<sub>2</sub>).

**tert-butyl (S)-4-(5-methoxy-2-methylene-5-oxopentyl)-2,2-dimethyloxazolidine-3-carboxylate (307)**

Alcohol **301** (150.0 mg, 550  $\mu\text{mol}$ , 1.00 eq.), propionic acid (2  $\mu\text{L}$ , 30.0  $\mu\text{mol}$ , 0.05 eq.) and 1,1,1-trimethoxyethane (1.06 mL, 8.29 mmol, 15.0 eq.) were added in a 10 mL glass microwave tube. The reaction mixture was irradiated in a CEM Discover microwave apparatus (200 watt, 150  $^\circ\text{C}$ ) for 8 min. After cooling to room temperature, the solvent was removed under reduced pressure. The crude product was purified by flash column chromatography ( $\text{SiO}_2$ , hexanes/EtOAc = 9/1 to 8/2) to afford rearrangement product **307** (130 mg, 380  $\mu\text{mol}$ , 69%) as colorless oil.

$R_f = 0.18$  (hexanes/EtOAc = 9/1, CAM)

*Note: NMR spectra are complex due to the presence of rotamers.*

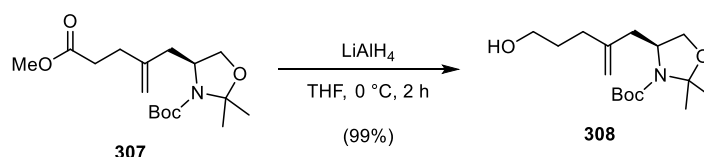
$^1\text{H NMR}$  (400 MHz,  $\text{CDCl}_3$ )  $\delta = 4.81\text{--}4.78$  (m, 2H), 4.09–3.76 (m, 3H), 3.66 (s, 3H), 2.60–2.04 (m, 6H), 1.58 (app d,  $J = 20.0$  Hz, 1H), 1.48 (s, 12H).

$^{13}\text{C NMR}$  (100 MHz,  $\text{CDCl}_3$ )  $\delta = 173.5, 173.4, 152.0, 151.6, 145.1, 144.7, 112.7, 112.1, 93.8, 93.3, 80.0, 79.7, 66.1, 66.0, 55.8, 55.7, 51.6, 51.6, 40.3, 39.3, 32.4, 32.3, 30.8, 30.5, 28.5, 28.5, 28.4, 27.8, 26.9, 24.5, 23.2$ .

**HRMS (ESI)** for  $\text{C}_{17}\text{H}_{30}\text{O}_5\text{N}^+$   $[\text{M}+\text{H}]^+$ : calcd.: 328.2124, found: 328.2119.

**IR (ATR)**:  $\tilde{\nu} = 2980$  (w), 1740 (m), 1693 (s), 1438 (w), 1385 (s), 1364 (s), 1244 (m), 1170 (s), 1078 (m), 898 (w), 852 (m), 769 (m).

$[\alpha]_{\text{D}}^{25} = +11.8$  ( $c = 1.11$ ,  $\text{CH}_2\text{Cl}_2$ ).

**tert-butyl (S)-4-(5-hydroxy-2-methylenepentyl)-2,2-dimethyloxazolidine-3-carboxylate (308)**

Methyl ester **307** (650 mg, 1.99 mmol, 1.00 eq.) was dissolved in THF (16.1 mL) and the solution was cooled to 0  $^\circ\text{C}$ .  $\text{LiAlH}_4$  (2 M in THF, 1.09 mL, 2.18 mmol, 1.10 eq.) was added dropwise and the

reaction mixture was stirred at 0 °C for 2 h. The reaction was quenched by the slow addition of EtOAc (20 mL). Water (20 mL) was added, the layers were separated and the aqueous layer was extracted with EtOAc (3 x 25 mL). The combined organic layers were washed with brine (50 mL), dried over MgSO<sub>4</sub> and concentrated in vacuo. The crude product was purified by flash column chromatography (SiO<sub>2</sub>, hexanes/EtOAc = 6/4) to afford **308** as colorless oil (587 mg, 1.98 mmol, 99%).

$R_f$  = 0.23 (hexanes/EtOAc = 7/3, CAM).

*Note: NMR spectra are complex due to the presence of rotamers.*

<sup>1</sup>H NMR (400 MHz, CDCl<sub>3</sub>) δ = 4.80 (app dd,  $J$  = 22.3, 10.4 Hz, 2H), 4.15 – 3.56 (m, 6H), 2.63 – 2.42 (m, 1H), 2.25 – 1.99 (m, 3H), 1.80 – 1.66 (m, 2H), 1.58 (app d,  $J$  = 18.8 Hz, 3H), 1.47 (s, 12H).

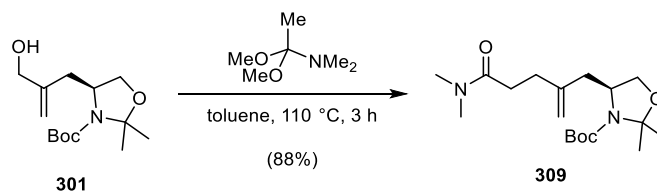
<sup>13</sup>C NMR (100 MHz, CDCl<sub>3</sub>) δ = 152.3, 151.7, 146.3, 146.1, 113.5, 112.7, 112.2, 93.9, 93.5, 80.3, 79.8, 66.3, 62.5, 62.3, 55.9, 40.0, 39.7, 32.2, 31.7, 30.8, 28.7, 28.6, 28.5, 27.9, 27.1, 24.6, 23.3.

HRMS (ESI) for C<sub>16</sub>H<sub>30</sub>O<sub>4</sub>N<sup>+</sup> [M+H]<sup>+</sup>: calcd.: 300.2169, found: 300.2172.

IR (ATR):  $\tilde{\nu}$  = 3441 (w), 2979 (w), 2873 (w), 1694 (s), 1386 (s), 1365 (s), 1254 (m), 1171 (m), 1061 (s), 897 (w), 850 (m), 768 (m).

$[\alpha]_D^{25}$  = +16.8 (c = 1.01, CH<sub>2</sub>Cl<sub>2</sub>).

### ***tert*-butyl(*S*)-4-(5-(dimethylamino)-2-methylene-5-oxopentyl)-2,2-dimethyloxazolidine-3-carboxylate (**309**)**



Alcohol **301** (4.81 g, 17.7 mmol, 1.00 eq.) was dissolved in toluene (150 mL) and *N,N*-dimethylacetamide dimethyl acetal (3.89 mL, 26.6 mmol, 1.50 eq.) was added. The colorless solution heated to 100 °C open to air and a gentle stream of N<sub>2</sub> was bubbled through the solvent via a thin glass capillary to remove liberated MeOH. After 3 h, the resulting yellow solution was cooled to room temperature and the volatiles were removed in vacuo. The crude product was purified by flash column chromatography (SiO<sub>2</sub>, hexanes/EtOAc = 1/1) to afford **309** as light yellow oil (5.30 g, 15.6 mmol, 88%).

$R_f$  = 0.21 (hexanes/EtOAc = 1/1, KMnO<sub>4</sub>).

*Note: NMR spectra are complex due to the presence of rotamers.*

$^1\text{H NMR}$  (400 MHz,  $\text{CDCl}_3$ )  $\delta$  =  $^1\text{H NMR}$  (400 MHz,  $\text{CDCl}_3$ )  $\delta$  4.78 – 4.67 (m, 2H), 4.06 – 3.86 (m, 1H), 3.83 – 3.76 (m, 1H), 3.76 – 3.67 (m, 1H), 2.96 (d,  $J$  = 3.6 Hz, 3H), 2.88 (d,  $J$  = 2.8 Hz, 3H), 2.61 – 2.19 (m, 5H), 2.10 (ddd,  $J$  = 23.4, 13.7, 11.0 Hz, 1H), 1.52 (app d,  $J$  = 20.9 Hz, 3H), 1.41 (s, 12H).

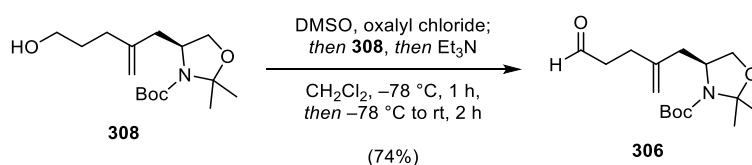
$^{13}\text{C NMR}$  (100 MHz,  $\text{CDCl}_3$ )  $\delta$  = 172.6, 172.2, 152.2, 151.8, 145.9, 112.2, 93.9, 93.4, 80.1, 79.8, 66.3, 66.3, 56.0, 56.0, 40.6, 39.3, 37.4, 37.3, 35.6, 31.7, 31.6, 31.4, 30.8, 28.7, 28.6, 27.9, 27.1, 24.6, 23.3.

**HRMS (ESI):** for  $\text{C}_{18}\text{H}_{33}\text{N}_2\text{O}_4^+$   $[\text{M}+\text{H}]^+$ : calcd.: 341.2435, found: 341.2437.

**IR (ATR):**  $\tilde{\nu}$  = 2978 (m), 2935 (w), 3029 (w), 1692 (s), 1643 (m), 1686 (s), 1547 (w), 1480 (w), 1446 (m), 1365 (s), 1256 (m), 1173 (m), 1096 (m), 1061 (m), 894 (w), 848 (w).

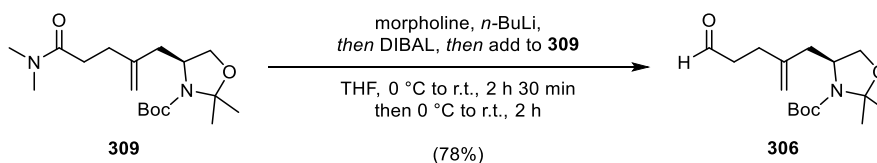
$[\alpha]_{\text{D}}^{25}$  = +16.0 ( $c$  = 2.00,  $\text{CH}_2\text{Cl}_2$ ).

### *tert*-butyl(*S*)-2,2-dimethyl-4-(2-methylene-5-oxopentyl)oxazolidine-3-carboxylate (**306**)



DMSO (90  $\mu\text{L}$ , 1.27 mmol, 4.00 eq.) was diluted with  $\text{CH}_2\text{Cl}_2$  (2 mL) and the solution was cooled to  $-78\text{ }^\circ\text{C}$ . Oxalyl chloride (2 M in  $\text{CH}_2\text{Cl}_2$ , 270  $\mu\text{L}$ , 540  $\mu\text{mol}$ , 1.70 eq.) was added dropwise and the reaction mixture was stirred at  $-78\text{ }^\circ\text{C}$  for 15 min. Alcohol **308** (100 mg, 320  $\mu\text{mol}$ , 1.00 eq.) was dissolved in  $\text{CH}_2\text{Cl}_2$  (1 mL) and the solution was added dropwise to the reaction mixture. After further stirring at  $-78\text{ }^\circ\text{C}$  for 45 min,  $\text{Et}_3\text{N}$  (350  $\mu\text{L}$ , 2.54 mmol, 8.00 eq.) was slowly added. The cooling bath was removed and the mixture was allowed to reach room temperature for 2 h. The reaction was quenched with water (5 mL) and extracted with  $\text{CH}_2\text{Cl}_2$  (3 x 10 mL). The combined organic layers were washed with aqueous HCl (1 M, 20 mL), saturated aqueous  $\text{NaHCO}_3$  (20 mL), brine (20 mL), dried over  $\text{MgSO}_4$  and concentrated in vacuo. The crude product was purified by flash column chromatography ( $\text{SiO}_2$ , hexanes/ $\text{EtOAc}$  = 8/2) to afford aldehyde **306** as colorless oil (70 mg, 240  $\mu\text{mol}$ , 74%).

### Alternative Procedure for the Synthesis of **306** by reduction of **309**:



Morpholine (227  $\mu\text{L}$ , 2.29 mmol, 1.70 eq.) was dissolved in THF (4.4 mL) and cooled to 0  $^{\circ}\text{C}$  and *n*-BuLi (2.4 M in hexane, 900  $\mu\text{L}$ , 2.17 mmol, 1.60 eq.). After 30 minutes, DIBALH (1.0 M in THF, 1.00 mL, 2.03 mmol, 1.50 eq.) was added. The resulting aluminate reagent solution was allowed to warm to room temperature over 2 h and added dropwise to a precooled solution (0  $^{\circ}\text{C}$ ) of amide **309** (460 mg, 1.35 mmol, 1.00 eq.) in THF (8 mL). After 2 hours, the reaction was quenched with saturated aqueous  $\text{NH}_4\text{Cl}$  (20 mL). After the addition of EtOAc (20 mL) the layers were separated and the aqueous phase was extracted with EtOAc (2 x 20 mL). The combined organic layers were dried over  $\text{MgSO}_4$ , filtered and concentrated under reduced pressure. The crude product was purified by flash column chromatography ( $\text{SiO}_2$ , hexanes/EtOAc = 8/2) to afford aldehyde **306** as colorless oil (312 mg, 1.05 mmol, 78%).

$R_f$  = 0.43 (hexanes/EtOAc = 8/2, CAM)

*Note: NMR spectra are complex due to the presence of rotamers.*

$^1\text{H NMR}$  (400 MHz,  $\text{CDCl}_3$ ):  $\delta$  = 9.77 (s, 1H), 4.82 – 4.78 (m, 2H), 4.07 – 3.67 (m, 3H), 2.69 – 2.25 (m, 5H), 2.21 – 2.10 (m, 1H), 1.58 (d,  $J$  = 19.6 Hz, 1H), 1.46 (s, 12H).

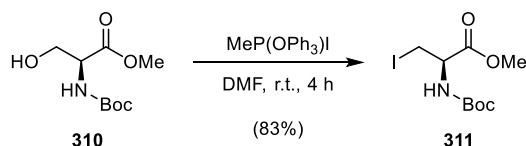
$^{13}\text{C NMR}$  (100 MHz,  $\text{CDCl}_3$ ):  $\delta$  = 202.2, 201.6, 152.2, 151.6, 144.8, 144.6, 113.0, 112.7, 94.0, 93.5, 80.2, 79.8, 66.2, 66.2, 55.8, 55.8, 41.9, 41.8, 40.5, 39.5, 28.7, 28.6, 28.5, 28.5, 28.2, 27.9, 27.8, 27.0, 24.5, 23.3.

**IR (ATR):**  $\tilde{\nu}$  = 2979 (w), 1726 (w), 1692 (s), 1454 (w), 1386 (s), 1365 (s), 1256 (m), 1172 (m), 1097 (m), 852 (w), 769 (w).

**HRMS (ESI)** for  $\text{C}_{16}\text{H}_{28}\text{O}_4\text{N}^+$   $[\text{M}+\text{H}]^+$ : calcd. 298.2013, found: 298.2014.

$[\alpha]_D^{25}$  = +15.2 (c = 1.08,  $\text{CH}_2\text{Cl}_2$ ).

### methyl (*R*)-2-((tert-butoxycarbonyl)amino)-3-iodopropanoate (**311**)



Methyl (tert-butoxycarbonyl)-L-serinate (**310**, 3.00 g, 13.7 mmol, 1.00 eq.) was dissolved in DMF (30 mL) and methyltriphenoxyphosphonium iodide (6.50 g, 14.4 mmol, 1.05 equiv.) was added portionwise. After 4 h, the reaction mixture was cooled to 0  $^{\circ}\text{C}$  and solid  $\text{NaHCO}_3$  (3.45 g, 41.1 mmol, 3.00 eq.) was added. The mixture was stirred vigorously for 15 min, and  $\text{Et}_2\text{O}$  (50 mL) and  $\text{H}_2\text{O}$  (50 mL) were added. The organic phase was separated and the aqueous layer was extracted with  $\text{Et}_2\text{O}$  (2 x 50 mL). The combined organic extracts were washed with aqueous  $\text{NaOH}$  (0.2 M, 4 x 20 mL), brine (50 mL), dried over  $\text{MgSO}_4$ , filtered and concentrated in vacuo. The crude product was purified by flash column chromatography ( $\text{SiO}_2$ , hexanes/EtOAc = 9/1 to 7/3) to afford **311** as a light orange

oil that solidified upon storage at  $-24\text{ }^{\circ}\text{C}$  (3.74 g, 11.4 mmol, 83%). Spectral data match the previously reported values.<sup>[339]</sup>

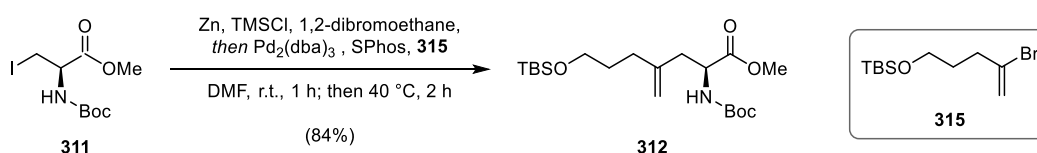
*Note: 311 degrades upon prolonged exposure to silica gel; rapid chromatography is recommended.*

$R_f = 0.55$  (hexanes/EtOAc = 8/2,  $\text{KMnO}_4$ ).

**HRMS** (ESI) for  $\text{C}_9\text{H}_{16}\text{INO}_4\text{Na}^+$   $[\text{M}+\text{Na}]^+$ : calcd.: 352.0016, found: 352.0021.

$[\alpha]_D^{25} = -3.7$  ( $c = 2.78$ , MeOH).

### methyl (S)-2-((tert-butoxycarbonyl)amino)-7-((tert-butyldimethylsilyl)oxy)-4-methyleneheptanoate (312)



Zn dust (2.05 g, 31.4 mmol, 4.0 eq.) was added to DMF (31.6 mL). 1,2-dibromoethane (295 mg, 1.57 mmol, 0.2 eq.) was added and the suspension was brought to ebullition by heating with a heat gun. After cooling to room temperature, TMSCl (201  $\mu\text{L}$ , 1.57 mmol, 0.2 eq.) was added and the reaction mixture was stirred for 15 min. Then, a solution of **311** (2.58 g, 7.85 mmol, 1.0 eq., prepared according to Hoveyda and Gao)<sup>[323]</sup> in DMF (2 mL) was added and the reaction mixture is stirred until complete disappearance of the starting material (1 h, monitored by TLC of reaction aliquots quenched with  $\text{NH}_4\text{Cl}$ ). Then, stirring was discontinued and after 5 min. To remove excess Zn dust the supernatant solution was transferred via syringe to a separate flask (washing with DMF 2 x 2 mL). To the solution was added  $\text{Pd}_2(\text{dba})_3$  (144 mg, 0.157 mmol, 0.02 eq.), SPhos (129 mg, 0.314 mmol, 0.02 eq.), and vinyl bromide **316** (1.75 g, 6.28 mmol, 0.8 eq.). The resulting red solution was heated to  $40\text{ }^{\circ}\text{C}$  for 2 h. Then, it is cooled to room temperature and saturated aqueous  $\text{NH}_4\text{Cl}$  (50 mL) was added, followed by EtOAc (50 mL). The mixture was filtered over cotton, the aqueous layer was separated and extracted with EtOAc (2 x 50 mL). The combined organic layers are washed with brine, dried over  $\text{MgSO}_4$ , filtered and evaporated in vacuo. The crude product was purified by flash column chromatography ( $\text{SiO}_2$ , hexanes/EtOAc = 1/0 to 9/1) to afford **312** as an orange oil (2.11 g, 5.26 mmol, 84%).

$R_f = 0.72$  (hexanes/EtOAc = 8/2,  $\text{KMnO}_4$ ).

**$^1\text{H}$  NMR** (400 MHz,  $\text{CDCl}_3$ )  $\delta = 4.92$  (d,  $J = 8.0$  Hz, 1H), 4.88 – 4.75 (m, 2H), 4.38 (td,  $J = 8.2$ , 5.5 Hz, 1H), 3.71 (s, 3H), 3.59 (t,  $J = 6.4$  Hz, 2H), 2.53 (dd,  $J = 14.2$ , 5.6 Hz, 1H), 2.35 (dd,  $J = 14.2$ , 8.3 Hz, 1H), 2.05 (dd,  $J = 8.7$ , 6.7 Hz, 2H), 1.69 – 1.57 (m, 2H), 1.42 (s, 9H), 0.88 (s, 9H), 0.03 (s, 6H).

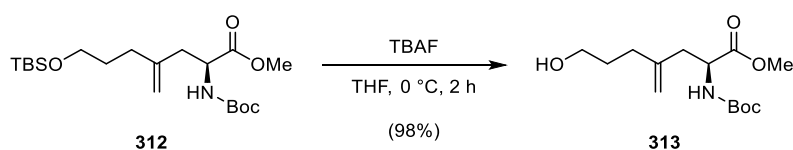
**$^{13}\text{C}$  NMR** (100 MHz,  $\text{CDCl}_3$ )  $\delta = 173.2$ , 155.3, 144.2, 113.5, 80.0, 62.7, 52.3, 52.1, 39.2, 31.5, 30.8, 28.4, 26.1, 18.5, -5.2.

**HRMS** (ESI) for  $C_{20}H_{40}O_5NSi^+ [M+H]^+$ : calcd.: 402.2676, found: 402.2676.

**IR (ATR)**:  $\tilde{\nu}$  = 3444 (w), 3378 (br, w), 3076 (w), 2953 (m), 2857 (m), 1746 (m), 1719 (s), 1501 (m), 1439 (m), 1390 (m), 1366 (m), 1213 (w), 1168 (s), 1053 (m), 1023 (s), 939 (w).

$[\alpha]_D^{20}$  = +3.7 (c = 2.78,  $CH_2Cl_2$ ).

**methyl (S)-2-((tert-butoxycarbonyl)amino)-7-hydroxy-4-methyleneheptanoate (313)**



A solution of alcohol **312** (2.11 g, 5.26 mmol, 1.00 eq.) in THF (28 mL) was cooled to 0 °C and a solution of TBAF (1 M in THF, 7.89 mL, 1.50 eq.) was added dropwise over 15 minutes. The reaction was stirred for 2 h 0 °C, quenched with saturated aqueous  $NH_4Cl$  (20 mL) and diluted with EtOAc (30 mL). The layers were separated and the aqueous phase was extracted with EtOAc (3 x 30 mL). The combined organic layers were washed with brine, dried over  $MgSO_4$  and concentrated under reduced pressure. Purification by flash column chromatography ( $SiO_2$ , hexanes/EtOAc = 7/3 to 1/1) gave **313** as a yellow oil (1.80 g, 6.28 mmol, 98%).

$R_f$  = 0.31 (hexanes/EtOAc = 1/1,  $KMnO_4$ ).

$^1H$  NMR (400 MHz,  $CDCl_3$ )  $\delta$  = 5.05 (d,  $J$  = 8.3 Hz, 1H), 4.87 – 4.75 (m, 2H), 4.37 (td,  $J$  = 8.4, 5.4 Hz, 1H), 3.68 (s, 3H), 3.59 (t,  $J$  = 6.4 Hz, 2H), 2.55 – 2.25 (m, 3H), 2.16 – 2.01 (m, 2H), 1.73 – 1.63 (m, 2H), 1.38 (s, 9H).

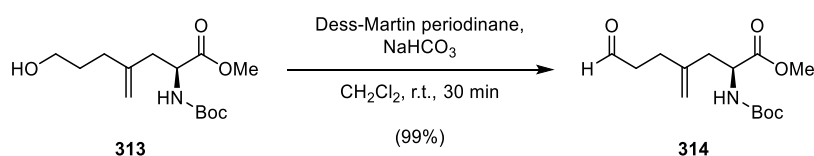
$^{13}C$  NMR (100 MHz,  $CDCl_3$ )  $\delta$  = 173.1, 155.4, 143.8, 113.4, 80.0, 61.9, 52.3, 52.0, 39.6, 31.0, 30.3, 28.3.

**HRMS** (ESI) for  $C_{14}H_{26}NO_5^+ [M+H]^+$ : calcd.: 288.1805, found: 288.1808.

**IR** (ATR):  $\tilde{\nu}$  = 3361 (br, w), 3077 (w), 2977 (m), 2875 (w), 1740 (m), 1692 (s), 1648 (m), 1612 (m), 1562 (m), 1513 (m), 1248 (w), 1163 (s), 1053 (m), 1023 (s), 901 (m).

$[\alpha]_D^{20}$  = +6.9 (c = 2.86,  $CH_2Cl_2$ ).

**methyl (S)-2-((tert-butoxycarbonyl)amino)-4-methylene-7-oxoheptanoate (314)**



A solution of **313** (110 mg, 383  $\mu\text{mol}$ , 1.00 eq.) in  $\text{CH}_2\text{Cl}_2$  (3.93 mL) was cooled to 0 °C and powdered  $\text{NaHCO}_3$  (276 mg, 2.29 mmol, 6.00 eq.) was added, followed by Dess-Martin periodinane (276 mg, 651  $\mu\text{mol}$ , 1.70 eq.). After 1 h, a half-saturated solution of  $\text{Na}_2\text{SO}_3$  (10 mL) was added and the reaction mixture was vigorously stirred for 30 minutes. The reaction was diluted with water (10 mL) and  $\text{CH}_2\text{Cl}_2$  (20 mL). The layers were separated and the aqueous layer was extracted with  $\text{CH}_2\text{Cl}_2$  (2 x 20 mL). The combined organic layers brine (20 mL), dried over  $\text{MgSO}_4$ , filtered and concentrated under reduced pressure. Purification of the crude product by flash column chromatography ( $\text{SiO}_2$ , hexanes/EtOAc = 8/2) gave **314** as a yellow oil (108 mg, 383  $\mu\text{mol}$ , 99%).

*Note: 314 decomposes within a week if stored neat at room temperature.*

$R_f$  = 0.67 (hexanes/EtOAc = 1/1,  $\text{KMnO}_4$ ).

$^1\text{H NMR}$  (400 MHz,  $\text{CDCl}_3$ )  $\delta$  = 9.75 (t,  $J$  = 1.6 Hz, 1H), 4.99 (d,  $J$  = 8.4 Hz, 1H), 4.85 (d,  $J$  = 7.8 Hz, 2H), 4.43 (td,  $J$  = 8.3, 5.6 Hz, 1H), 3.72 (s, 3H), 2.65 – 2.46 (m, 3H), 2.43 – 2.28 (m, 3H), 1.42 (s, 9H).

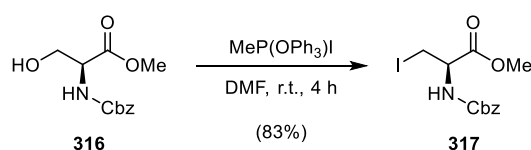
$^{13}\text{C NMR}$  (100 MHz,  $\text{CDCl}_3$ )  $\delta$  = 201.9, 173.0, 155.3, 142.7, 114.1, 80.1, 52.4, 52.1, 41.7, 39.8, 28.4, 28.3, 27.4.

**HRMS (ESI)** for  $\text{C}_{14}\text{H}_{24}\text{NO}_5^+$   $[\text{M}+\text{H}]^+$ : calcd.: 286.1654, found: 286.1650.

**IR (ATR)**:  $\tilde{\nu}$  = 3790 (w), 3363 (br, w), 3082 (w), 2932 (w), 2728 (w), 1742 (m), 1711 (s), 1512 (m), 1438 (m), 1391 (m), 1366 (m), 1277 (m), 1249 (m), 1164 (s), 1052 (m), 904 (m).

$[\alpha]_{\text{D}}^{20}$  = +10.2 ( $c$  = 1.26,  $\text{CH}_2\text{Cl}_2$ ).

### methyl (*R*)-2-(((benzyloxy)carbonyl)amino)-3-iodopropanoate (**317**)



methyl ((benzyloxy)carbonyl)-L-serinate (**316**, 1.00 g, 3.957 mmol, 1.00 eq.) was dissolved in DMF (10 mL) and methyltriphenoxyphosphonium iodide (1.87 g, 4.15 mmol, 1.05 equiv.) was added portionwise. After 4 h, the reaction mixture was cooled to 0 °C and solid  $\text{NaHCO}_3$  (995 mg, 11.8 mmol, 3.00 eq.) was added. The mixture was stirred vigorously for 15 min, and  $\text{Et}_2\text{O}$  (20 mL) and  $\text{H}_2\text{O}$  (20 mL) were added. The organic phase was separated and the aqueous layer was extracted with  $\text{Et}_2\text{O}$  (2 x 20 mL). The combined organic extracts were washed with aqueous  $\text{NaOH}$  (0.2 M, 4 x 20 mL), brine (20 mL), dried over  $\text{MgSO}_4$ , filtered and concentrated in vacuo. The crude product was purified by flash column chromatography ( $\text{SiO}_2$ , hexanes/EtOAc = 9/1 to 7/3) to afford **317** as a light yellow oil (1.21 g, 3.3 mmol, 84%). Spectral data match the previously reported values.<sup>[340]</sup>

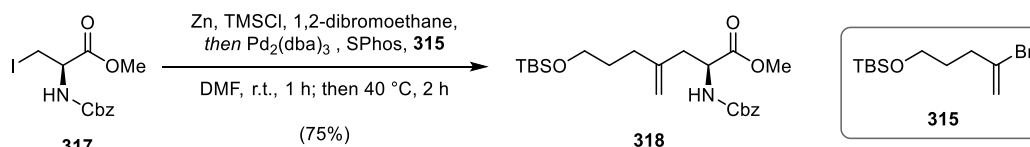
*Note: 317 degrades upon prolonged exposure to silica gel; rapid chromatography is recommended.*

$R_f = 0.50$  (hexanes/EtOAc = 8/2,  $\text{KMnO}_4$ ).

**HRMS** (ESI) for  $\text{C}_{12}\text{H}_{14}\text{INO}_4\text{Na}^+$  [ $\text{M}+\text{Na}$ ] $^+$ : calcd.: 385.9860, found: 385.9862.

$[\alpha]_{\text{D}}^{22} = -6.3$  ( $c = 1.01$ ,  $\text{CHCl}_3$ ).

**methyl (S)-2-(((benzyloxy)carbonyl)amino)-7-((tert-butyldimethylsilyl)oxy)-4-methyleneheptanoate (318)**



Zn dust (1.37 g, 21.0 mmol, 4.00 eq.) was added to DMF (24.0 mL). 1,2-dibromoethane (91  $\mu\text{L}$ , 1.05 mmol, 0.20 eq.) was added and the suspension was brought to ebullition by heating with a heat gun. After cooling to room temperature, TMSCl (134  $\mu\text{L}$ , 1.05 mmol, 0.20 eq.) was added and the reaction mixture was stirred for 15 min. Then, a solution of **317** (1.91 g, 5.25 mmol, 1.0 eq.) in DMF (2 mL) was added and the reaction mixture is stirred until complete disappearance of the starting material (1 h, monitored by TLC of reaction aliquots quenched with  $\text{NH}_4\text{Cl}$ ). Then, stirring was discontinued and after 5 min. To remove excess Zn dust the supernatant solution is transferred via syringe to a separate flask (washing with DMF 2 x 2 mL). To the solution was added  $\text{Pd}_2(\text{dba})_3$  (48.1 mg, 52.5  $\mu\text{mol}$ , 0.01 eq.), SPhos (43.1 mg, 105  $\mu\text{mol}$ , 0.02 eq.), and vinyl bromide **315** (1.3 g, 4.68 mmol, 0.89 eq.). The resulting red solution was heated to 40  $^\circ\text{C}$  for 2 h. Then, it is cooled to room temperature and saturated aqueous  $\text{NH}_4\text{Cl}$  (50 mL) was added, followed by EtOAc (50 mL). The mixture was filtered over cotton, the aqueous layer was separated and extracted with EtOAc (2 x 50 mL). The combined organic layers are washed with brine, dried over  $\text{MgSO}_4$ , filtered and evaporated in vacuo. The crude product was purified by flash column chromatography ( $\text{SiO}_2$ , hexanes/EtOAc = 95/5 to 8/2) to afford **318** as a slightly red oil (1.71 g, 3.92 mmol, 75%).

$R_f = 0.62$  (hexanes/EtOAc = 8/2, CAM).

$^1\text{H NMR}$  (400 MHz,  $\text{CDCl}_3$ )  $\delta = 7.32 - 7.21$  (m, 4H), 5.23 (d,  $J = 8.1$  Hz, 1H), 5.03 (s, 1H), 4.88 - 4.68 (m, 2H), 4.41 (td,  $J = 8.2, 5.5$  Hz, 1H), 3.66 (s, 3H), 3.54 (t,  $J = 6.4$  Hz, 2H), 2.51 (dd,  $J = 14.2, 5.5$  Hz, 1H), 2.33 (dd,  $J = 14.2, 8.4$  Hz, 1H), 2.00 (t,  $J = 7.7$  Hz, 2H), 1.69 - 1.39 (m, 2H), 0.84 (s, 9H), -0.01 (s, 6H).

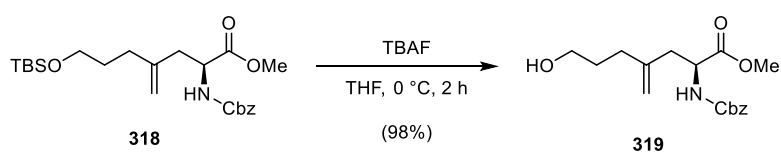
$^{13}\text{C NMR}$  (100 MHz,  $\text{CDCl}_3$ )  $\delta = 172.8, 155.8, 143.9, 136.3, 128.5, 128.2, 128.1, 113.6, 67.0, 62.6, 52.4, 52.3, 39.0, 31.4, 30.7, 26.0, 18.4, -5.2$ .

**HRMS** (ESI) for  $\text{C}_{23}\text{H}_{41}\text{N}_2\text{O}_5\text{Si}^+$  [ $\text{M}+\text{NH}_4$ ] $^+$ : calcd.: 453.2779, found: 453.2786

**IR** (ATR):  $\tilde{\nu} = 3344$  (br, w), 2952 (m), 2929 (m), 2857 (m), 1724 (s), 1647 (w), 1521 (m), 1472 (m), 1347 (s), 1254 (s), 1212 (s), 1100 (s), 1053 (m), 1028 (m), 899 (m).

$[\alpha]_{\text{D}}^{20} = +5.3$  ( $c = 1.90$ ,  $\text{CH}_2\text{Cl}_2$ ).

**methyl (S)-2-(((benzyloxy)carbonyl)amino)-7-hydroxy-4-methyleneheptanoate (319)**



A solution of alcohol **318** (1.50 g, 3.44 mmol, 1.00 eq.) in THF (17.2 mL) was cooled to 0 °C and a solution of TBAF (1 M in THF, 5.16 mL, 1.50 eq.) was added dropwise over 15 minutes. The reaction was stirred for 2 h 0 °C, quenched with saturated aqueous  $\text{NH}_4\text{Cl}$  (20 mL) and diluted with EtOAc (30 mL). The layers were separated and the aqueous phase was extracted with EtOAc (3 x 30 mL). The combined organic layers were washed with brine, dried over  $\text{MgSO}_4$  and concentrated under reduced pressure. Purification by flash column chromatography ( $\text{SiO}_2$ , hexanes/EtOAc = 9/1 to 1/9) gave **319** as a yellow oil (930 mg, 2.89 mmol, 84%).

$R_f = 0.32$  (hexanes/EtOAc = 1/1, CAM).

$^1\text{H NMR}$  (400 MHz,  $\text{CDCl}_3$ )  $\delta = 7.29 - 7.22$  (m, 5H), 5.16 (t,  $J = 6.9$  Hz, 1H), 5.00 (d,  $J = 2.2$  Hz, 2H), 4.86 - 4.67 (m, 2H), 4.40 (td,  $J = 8.4, 5.3$  Hz, 1H), 3.64 (s, 3H), 3.52 (t,  $J = 6.5$  Hz, 2H), 2.48 (dd,  $J = 14.1, 5.4$  Hz, 1H), 2.29 (dd,  $J = 14.1, 8.5$  Hz, 1H), 2.02 (q,  $J = 7.6$  Hz, 2H), 1.84 - 1.41 (m, 3H).

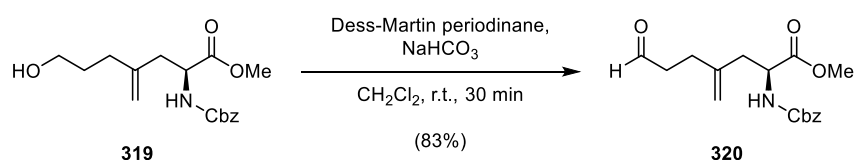
$^{13}\text{C NMR}$  (100 MHz,  $\text{CDCl}_3$ )  $\delta = 172.8, 156.0, 143.6, 136.3, 128.7, 128.3, 128.2, 113.9, 67.2, 62.2, 52.5, 52.5, 52.4, 39.6, 31.1, 30.3$ .

**HRMS (ESI)** for  $\text{C}_{17}\text{H}_{24}\text{NO}_5^+$   $[\text{M}+\text{H}]^+$ : calcd.: 322.1649, found: 322.1650.

**IR (ATR)**:  $\tilde{\nu} = 3349$  (br, m), 3068 (w), 2950 (m), 1703 (s), 1647 (w), 1530 (m), 1438 (m), 1345 (m), 1265 (m), 1215 (s), 1180 (m), 1054 (m), 1028 (m), 904 (m).

$[\alpha]_D^{20} = +2.2$  ( $c = 1.20, \text{CH}_2\text{Cl}_2$ ).

**methyl (S)-2-(((benzyloxy)carbonyl)amino)-4-methylene-7-oxoheptanoate (320)**



A solution of **319** (122 mg, 380  $\mu\text{mol}$ , 1.00 eq.) in  $\text{CH}_2\text{Cl}_2$  (3.65 mL) was cooled to 0 °C and powdered  $\text{NaHCO}_3$  (159 mg, 1.90 mmol, 5.00 eq.) was added, followed by Dess-Martin periodinane (242 mg, 569  $\mu\text{mol}$ , 1.50 eq.). After 1 h, a half-saturated solution of  $\text{Na}_2\text{SO}_3$  (10 mL) was added and the reaction mixture was vigorously stirred for 30 minutes. The reaction was diluted with water (10 mL) and  $\text{CH}_2\text{Cl}_2$  (20 mL). The layers were separated and the aqueous layer was extracted with  $\text{CH}_2\text{Cl}_2$  (2 x 20

mL). The combined organic layers brine (20 mL), dried over  $\text{MgSO}_4$ , filtered and concentrated under reduced pressure. Purification of the crude product by flash column chromatography ( $\text{SiO}_2$ , hexanes/EtOAc = 9/1 to 1/1) gave **320** as a yellow oil (100 mg, 313  $\mu\text{mol}$ , 83%).

$R_f$  = 0.62 (hexanes/EtOAc = 1/1, CAM).

$^1\text{H NMR}$  (400 MHz,  $\text{CDCl}_3$ )  $\delta$  = 9.72 (d,  $J$  = 1.7 Hz, 1H), 7.37 – 7.27 (m, 5H), 5.34 (d,  $J$  = 8.3 Hz, 1H), 5.08 (d,  $J$  = 2.6 Hz, 2H), 4.88 – 4.77 (m, 2H), 4.50 (td,  $J$  = 8.3, 5.6 Hz, 1H), 3.72 (s, 3H), 2.63 – 2.49 (m, 3H), 2.46 – 2.28 (m, 3H).

$^{13}\text{C NMR}$  (100 MHz,  $\text{CDCl}_3$ )  $\delta$  = 201.7, 172.6, 155.8, 142.4, 136.3, 128.6, 128.3, 128.2, 114.2, 67.1, 52.5, 52.4, 41.6, 39.6, 27.3.

**HRMS (ESI)** for  $\text{C}_{17}\text{H}_{22}\text{NO}_5^+$   $[\text{M}+\text{H}]^+$ : calcd.: 320,1492, found: 320,1494.

**IR (ATR)**:  $\tilde{\nu}$  = 3338 (br, w), 3066 (w), 3034 (w), 2953 (w), 2846 (w), 1715 (s), 1648 (w), 1524 (m), 1454 (m), 1437 (m), 1345 (m), 1261 (m), 1213 (s), 1050 (m), 1027 (m), 905 (w), 741 (w), 698 (m).

$[\alpha]_{\text{D}}^{20}$  = +3.1 ( $c$  = 1.86,  $\text{CH}_2\text{Cl}_2$ ).

## 4.3. X-Ray Crystallographic Data

## Data for piperazine 201 (hydrochloride salt).

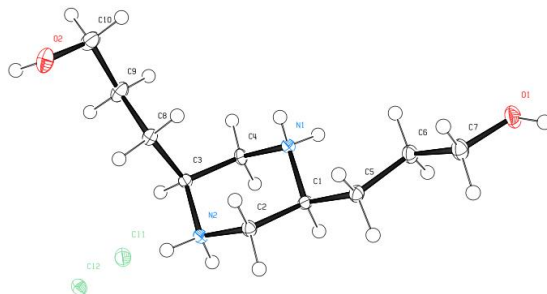


Figure 18. ORTEP plot of the molecular structure of 201.

net formula	$C_{10}H_{24}Cl_2N_2O_2$
$M_r/g\ mol^{-1}$	275.21
crystal size/mm	$0.100 \times 0.080 \times 0.040$
$T/K$	100(2)
radiation	MoK $\alpha$
diffractometer	'Bruker D8Venture'
crystal system	orthorhombic
space group	'P 21 21 21'
$a/\text{\AA}$	5.9400(2)
$b/\text{\AA}$	12.7285(4)
$c/\text{\AA}$	18.5201(6)
$\alpha/^\circ$	90
$\beta/^\circ$	90
$\gamma/^\circ$	90
$V/\text{\AA}^3$	1400.25(8)
$Z$	4
calc. density/ $g\ cm^{-3}$	1.305
$\mu/mm^{-1}$	0.454
absorption correction	Multi-Scan
transmission factor range	0.9211–0.9590
refls. measured	69977
$R_{int}$	0.0392
mean $\sigma(I)/I$	0.0163
$\theta$ range	2.720–27.52
observed refls.	3166
$x, y$ (weighting scheme)	0.0225, 0.3030
hydrogen refinement	mixed
Flack parameter	–0.011(13)
refls in refinement	3214
parameters	169
restraints	0
$R(F_{obs})$	0.0177
$R_w(F^2)$	0.0484
$S$	1.115
shift/error $_{max}$	0.001
max electron density/ $e\ \text{\AA}^{-3}$	0.252
min electron density/ $e\ \text{\AA}^{-3}$	–0.154

C-H: constr, N-H and O-H: refall.

## Data for Boc-piperazine 202.

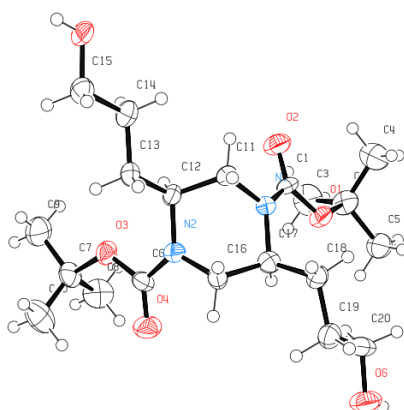


Figure 19. ORTEP plot of the molecular structure of piperazine 202

net formula	$C_{20}H_{38}N_2O_6$
$M_r/g\ mol^{-1}$	402.526
crystal size/mm	$0.16 \times 0.12 \times 0.09$
$T/K$	173(2)
radiation	MoK $\alpha$
diffractometer	'KappaCCD'
crystal system	orthorhombic
space group	$P2_12_12_1$
$a/\text{\AA}$	9.4705(6)
$b/\text{\AA}$	10.3778(6)
$c/\text{\AA}$	23.7593(14)
$\alpha/^\circ$	90
$\beta/^\circ$	90
$\gamma/^\circ$	90
$V/\text{\AA}^3$	2335.1(2)
$Z$	4
calc. density/ $g\ cm^{-3}$	1.14499(10)
$\mu/mm^{-1}$	0.084
absorption correction	none
refls. measured	9417
$R_{int}$	0.1936
mean $\sigma(I)/I$	0.1095
$\theta$ range	3.24–23.07
observed refls.	1498
$x, y$ (weighting scheme)	0.0637, 2.5081
hydrogen refinement	constr
Flack parameter	5(4)
refls in refinement	1872
parameters	259
restraints	0
$R(F_{obs})$	0.0829
$R_w(F^2)$	0.1736
$S$	1.099
shift/error <sub>max</sub>	0.001
max electron density/ $e\ \text{\AA}^{-3}$	0.232
min electron density/ $e\ \text{\AA}^{-3}$	-0.291

The absolute configuration could not be determined due to a meaningless Flack-parameter (caused by missing heavy atoms und the use of MoK $\alpha$  radiation)

## Data for piperazine 235 (hydrobromide salt).

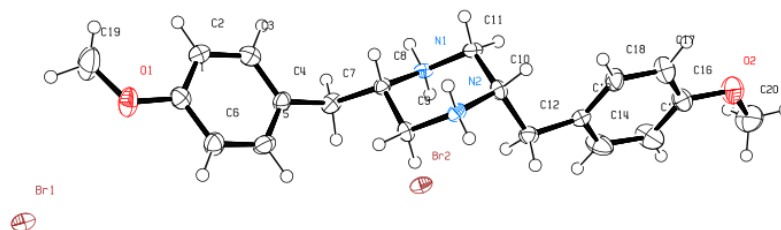


Figure 20. ORTEP plot of the molecular structure of piperazine 235.

net formula	$C_{20}H_{28}Br_2N_2O_2$
Mr/g mol <sup>-1</sup>	488.257
crystal size/mm	0.132 × 0.107 × 0.034
T/K	173(2)
radiation	Mo K $\alpha$
diffractometer	'Bruker D8Venture'
crystal system	monoclinic
space group	P21
a/Å	13.0595(6)
b/Å	6.0367(3)
c/Å	27.1867(14)
$\alpha$ /°	90
$\beta$ /°	101.8222(15)
$\gamma$ /°	90
V/Å <sup>3</sup>	2097.83(18)
Z	4
calc. density/g cm <sup>-3</sup>	1.54594(13)
$\mu$ /mm <sup>-1</sup>	3.881
absorption correction	multi-scan
transmission factor range	0.8118–0.9585
refls. measured	23315
Rint	0.0437
mean $\sigma(I)/I$	0.0630
$\theta$ range	2.30–26.45
observed refls.	6964
x, y (weighting scheme)	0.0292, 0.4909
hydrogen refinement	mixed
Flack parameter	–0.005(10)
refls in refinement	8497
parameters	490
restraints	1
R(Fobs)	0.0395
Rw(F2)	0.0823
S	1.037
shift/errormax	0.001
max electron density/e Å <sup>-3</sup>	1.020

C-bound H: constr, N-bound H: refxyz. Disorder in phenyl ring and methyl moiety handled by split models. The figure shows only one (the better one) of the two symmetrically independent formula units.

## Data for allylic boronate 268.

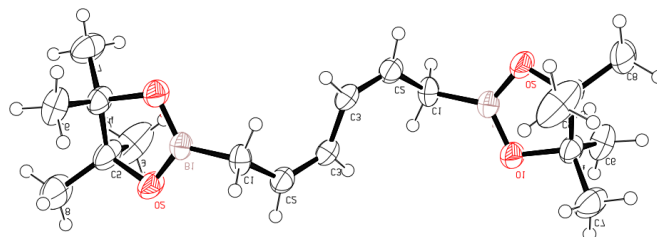


Figure 21. ORTEP plot of the molecular structure of 268.

net formula	$C_{18}H_{32}B_2O_4$
$M_r/g\ mol^{-1}$	334.05
crystal size/mm	$0.574 \times 0.435 \times 0.366$
$T/K$	173(2)
radiation	MoK $\alpha$
diffractometer	'Oxford XCalibur'
crystal system	monoclinic
space group	'C 2/c'
$a/\text{\AA}$	12.4424(5)
$b/\text{\AA}$	11.3140(6)
$c/\text{\AA}$	14.7187(7)
$\alpha/^\circ$	90
$\beta/^\circ$	99.507(4)
$\gamma/^\circ$	90
$V/\text{\AA}^3$	2043.55(17)
$Z$	4
calc. density/ $g\ cm^{-3}$	1.086
$\mu/mm^{-1}$	0.072
absorption correction	'multi-scan'
transmission factor range	0.94622–1.00000
refls. measured	5891
$R_{int}$	0.0206
mean $\sigma(I)/I$	0.0232
$\theta$ range	4.568–26.367
observed refls.	1697
$x, y$ (weighting scheme)	0.0573, 1.3019
hydrogen refinement	constr
refls in refinement	2083
parameters	113
restraints	0
$R(F_{obs})$	0.0491
$R_w(F^2)$	0.1328
$S$	1.055
shift/error $_{max}$	0.001
max electron density/ $e\ \text{\AA}^{-3}$	0.299
min electron density/ $e\ \text{\AA}^{-3}$	-0.172

## Data for 1,4-diol 278.

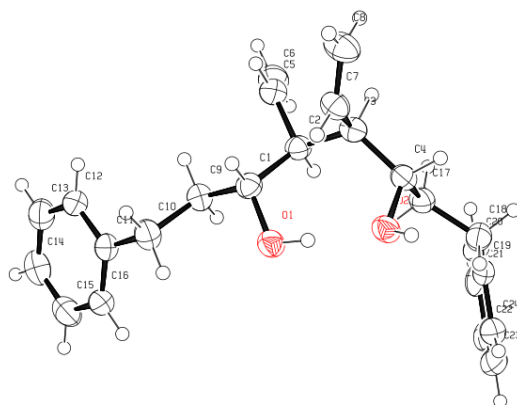


Figure 22. ORTEP plot of the molecular structure of 1,4-diol 278.

net formula	$C_{78}H_{104}O_7$
$M_r/g\ mol^{-1}$	1153.61
crystal size/mm	$0.447 \times 0.283 \times 0.130$
$T/K$	123(2)
radiation	MoK $\alpha$
diffractometer	'Oxford XCalibur'
crystal system	monoclinic
space group	'P 21/n'
$a/\text{\AA}$	17.4355(13)
$b/\text{\AA}$	12.1380(7)
$c/\text{\AA}$	32.989(2)
$\alpha/^\circ$	90
$\beta/^\circ$	101.288(7)
$\gamma/^\circ$	90
$V/\text{\AA}^3$	6846.6(8)
$Z$	4
calc. density/ $g\ cm^{-3}$	1.119
$\mu/mm^{-1}$	0.069
absorption correction	'multi-scan'
transmission factor range	0.95282–1.00000
refls. measured	35251
$R_{int}$	0.0743
mean $\sigma(I)/I$	0.1065
$\theta$ range	4.227–25.024
observed refls.	6026
$x, y$ (weighting scheme)	0.0640, 0.6413
hydrogen refinement	mixed
refls in refinement	12035
parameters	791
restraints	9
$R(F_{obs})$	0.0742
$R_w(F^2)$	0.1907
$S$	1.020
shift/error $_{max}$	0.001
max electron density/ $e\ \text{\AA}^{-3}$	0.434
min electron density/ $e\ \text{\AA}^{-3}$	-0.243

Only one molecule shown (solvent omitted); C-H: constr; O-H: located from difference map, then fixed,  $U(\text{H})=1.5U(\text{O})$ . Each hydroxyl function has two hydrogen positions, each with sof 0.5.  
Disorder described by split models.

### Data for cyclohexene 288.

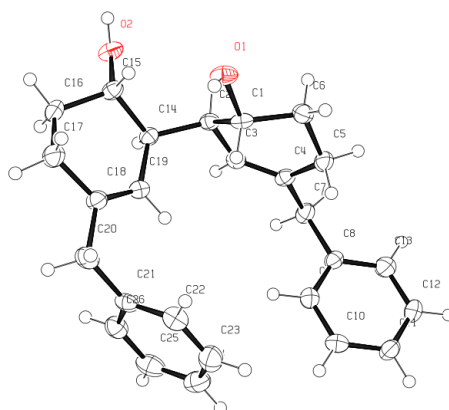


Figure 23. ORTEP plot of the molecular structure of cyclohexene 288.

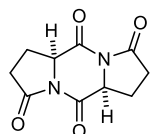
net formula	$\text{C}_{26}\text{H}_{30}\text{O}_2$
$M_r/\text{g mol}^{-1}$	374.50
crystal size/mm	$0.434 \times 0.066 \times 0.054$
$T/\text{K}$	123(2)
radiation	MoK $\alpha$
diffractometer	'Oxford XCalibur'
crystal system	monoclinic
space group	'C 2'
$a/\text{\AA}$	18.945(2)
$b/\text{\AA}$	5.3576(6)
$c/\text{\AA}$	20.611(2)
$\alpha/^\circ$	90
$\beta/^\circ$	90.200(9)
$\gamma/^\circ$	90
$V/\text{\AA}^3$	2092.0(4)
$Z$	4
calc. density/ $\text{g cm}^{-3}$	1.189
$\mu/\text{mm}^{-1}$	0.073
absorption correction	'multi-scan'
transmission factor range	0.83264–1.00000
refls. measured	5427
$R_{\text{int}}$	0.0355
mean $\sigma(I)/I$	0.0793
$\theta$ range	4.303–25.342
observed refls.	2651
$x, y$ (weighting scheme)	0.0262, 0.0000
hydrogen refinement	mixed
Flack parameter	0.5
refls in refinement	3470
parameters	261
restraints	1
$R(F_{\text{obs}})$	0.0511
$R_w(F^2)$	0.0917

*Part II: Experimental Part*

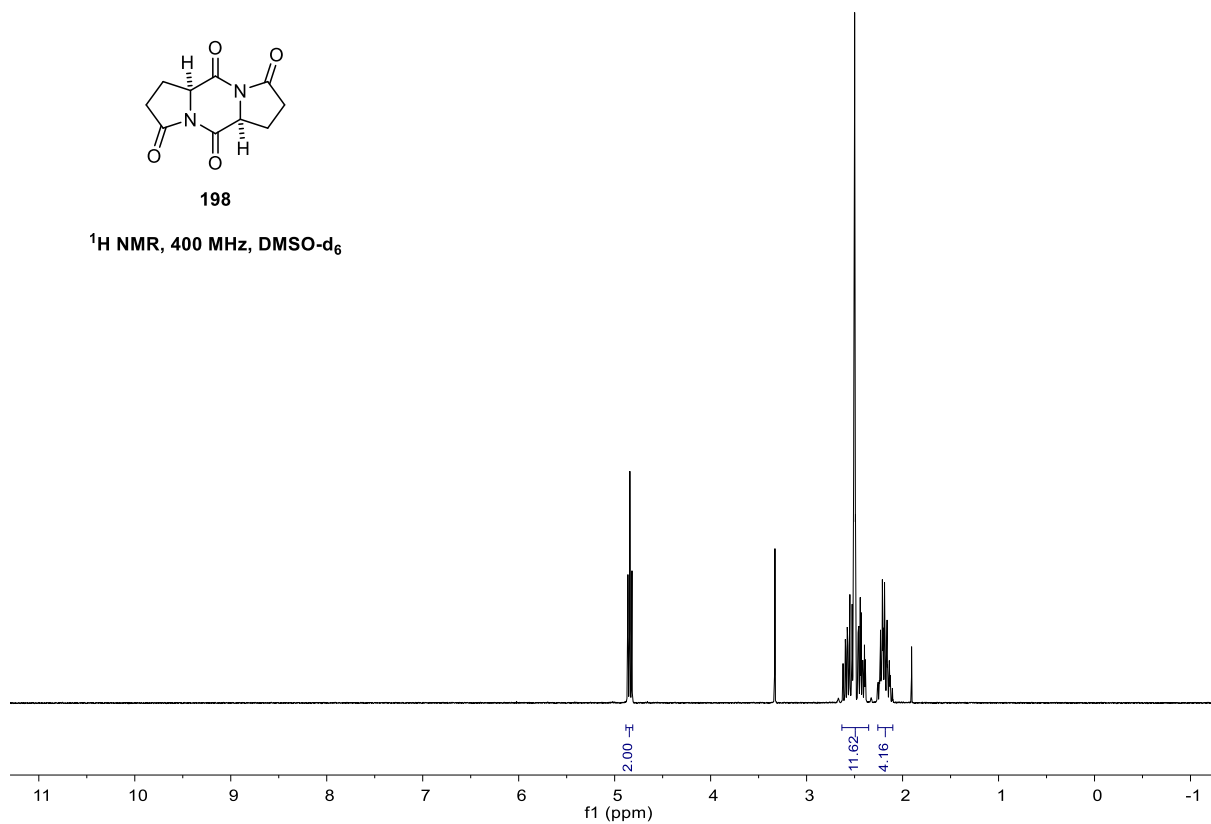
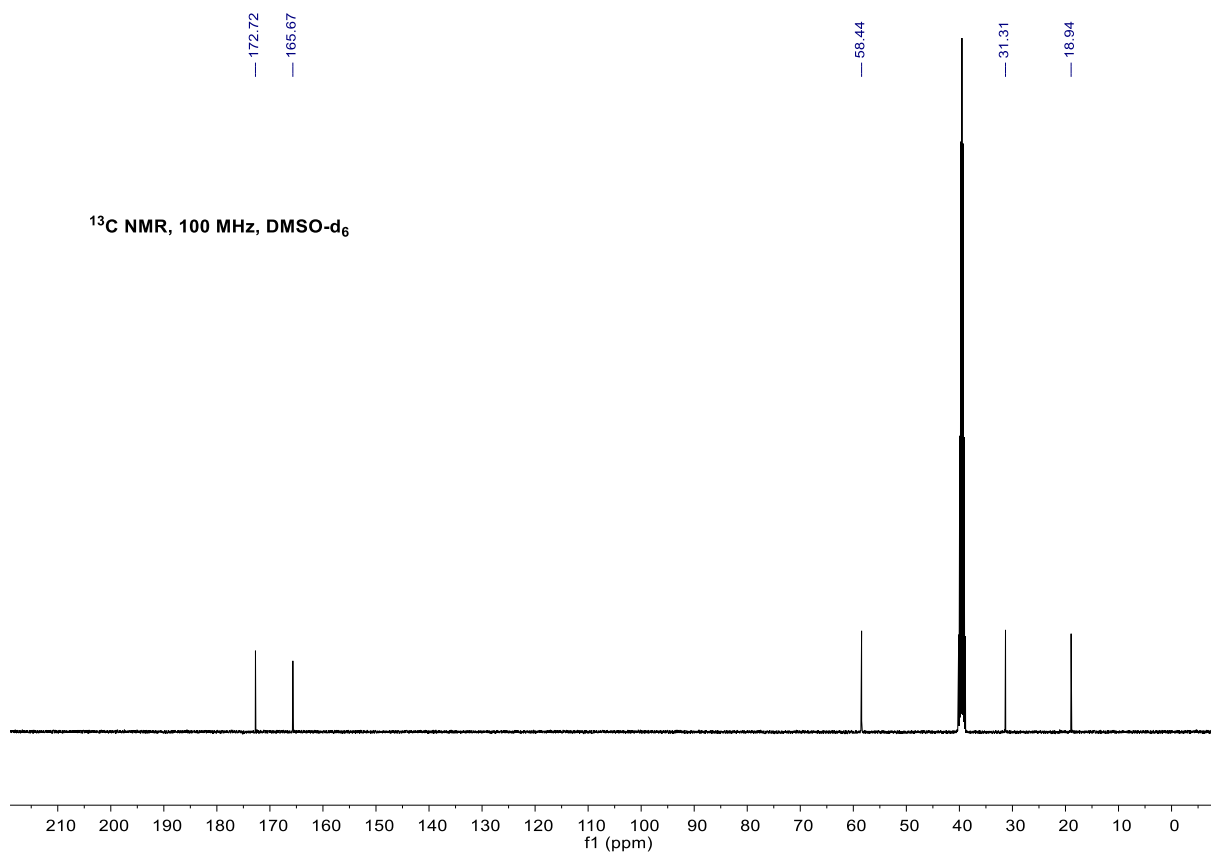
$S$	0.996
shift/error <sub>max</sub>	0.001
max electron density/e $\text{\AA}^{-3}$	0.161

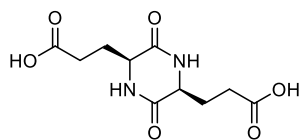
Refined as perfect racemic twin. C-H: constr, O-H: refall.

## 4.4. NMR Spectra



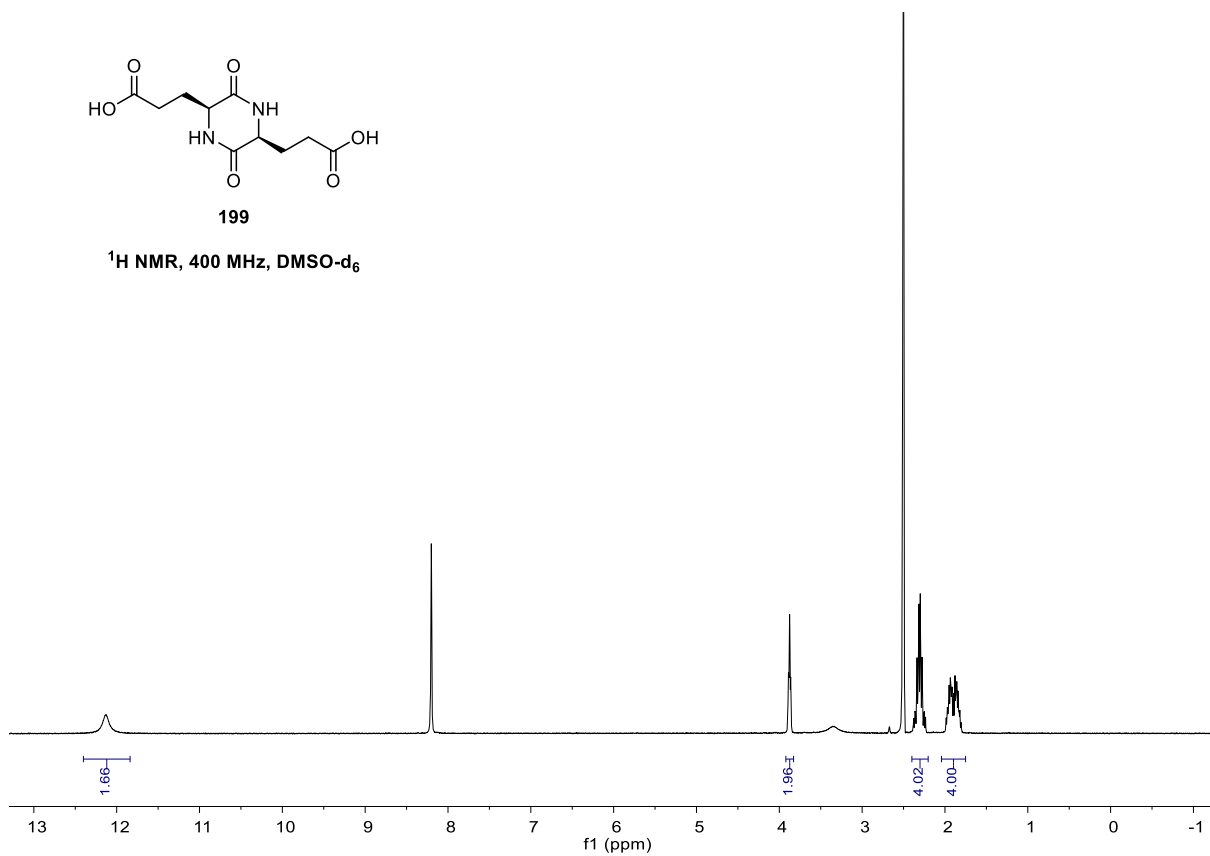
198

 $^1\text{H}$  NMR, 400 MHz, DMSO- $d_6$  $^{13}\text{C}$  NMR, 100 MHz, DMSO- $d_6$ 

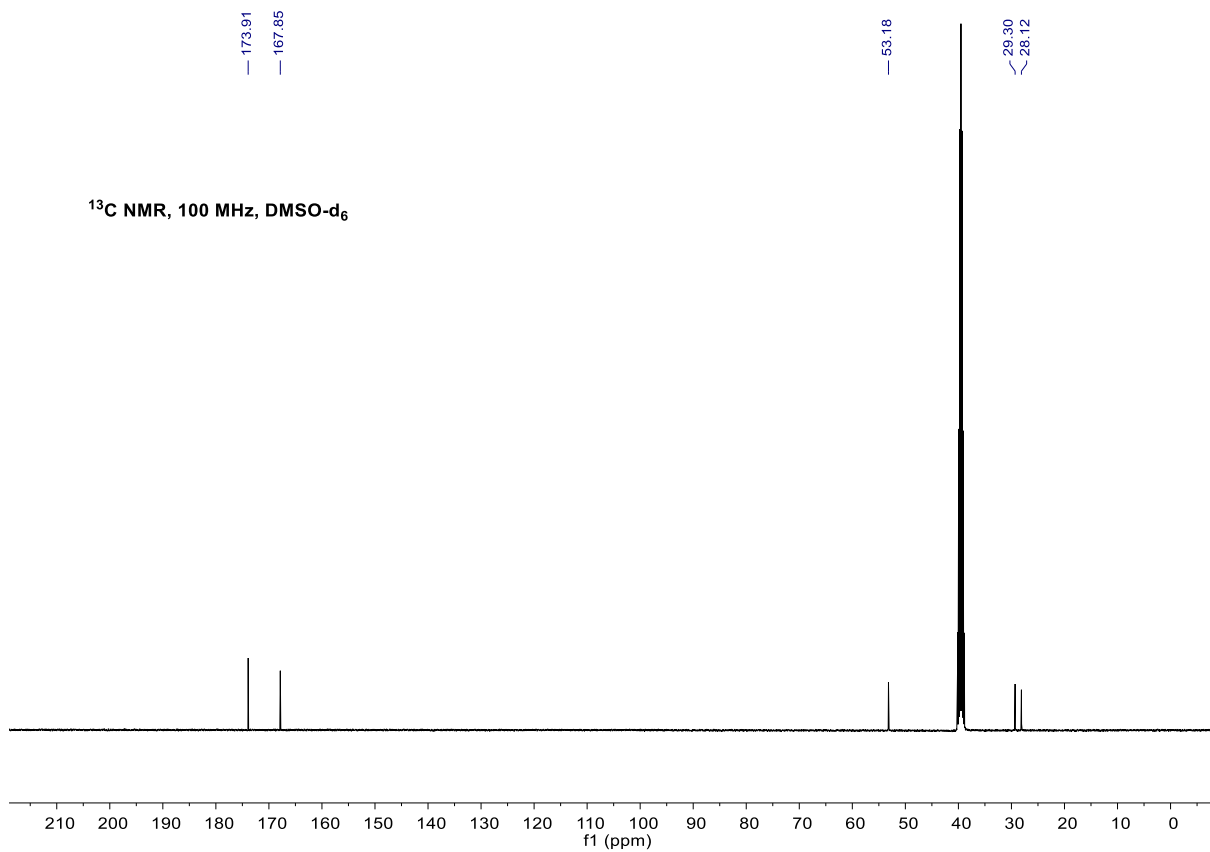


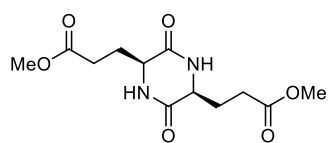
199

$^1\text{H}$  NMR, 400 MHz,  $\text{DMSO-d}_6$

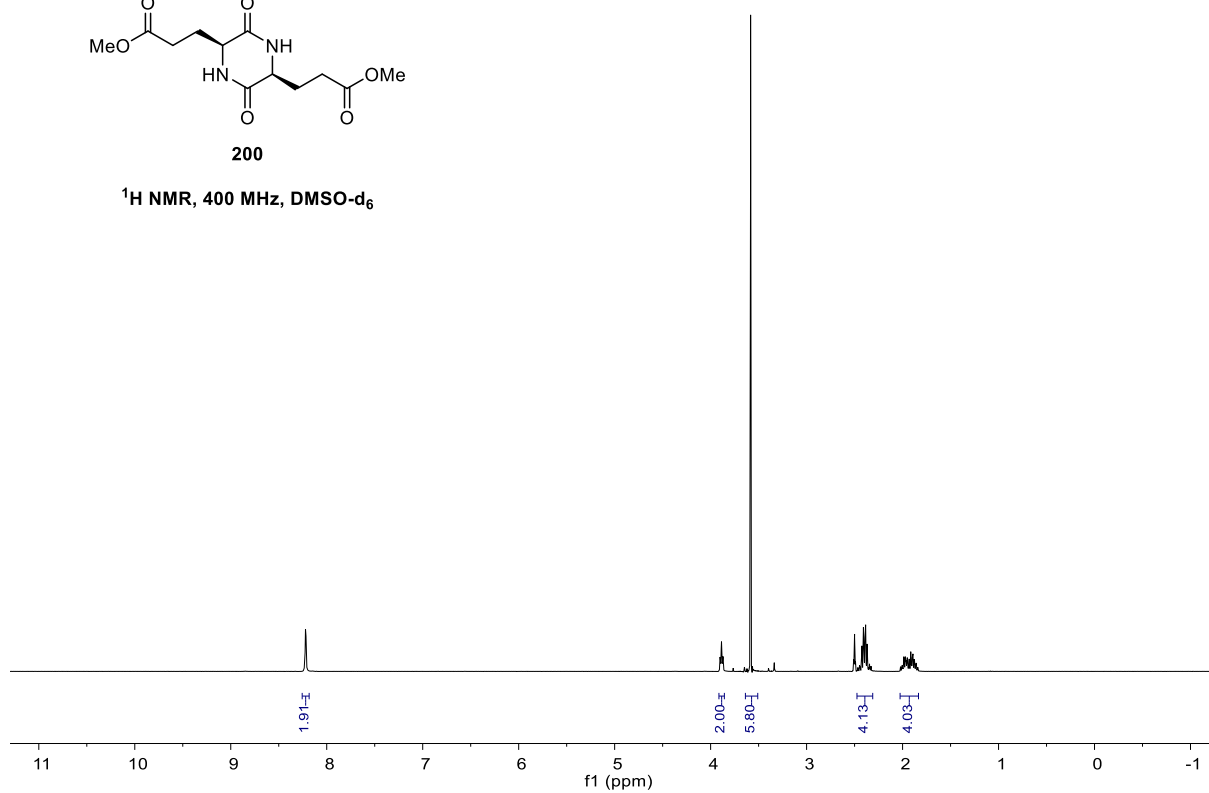
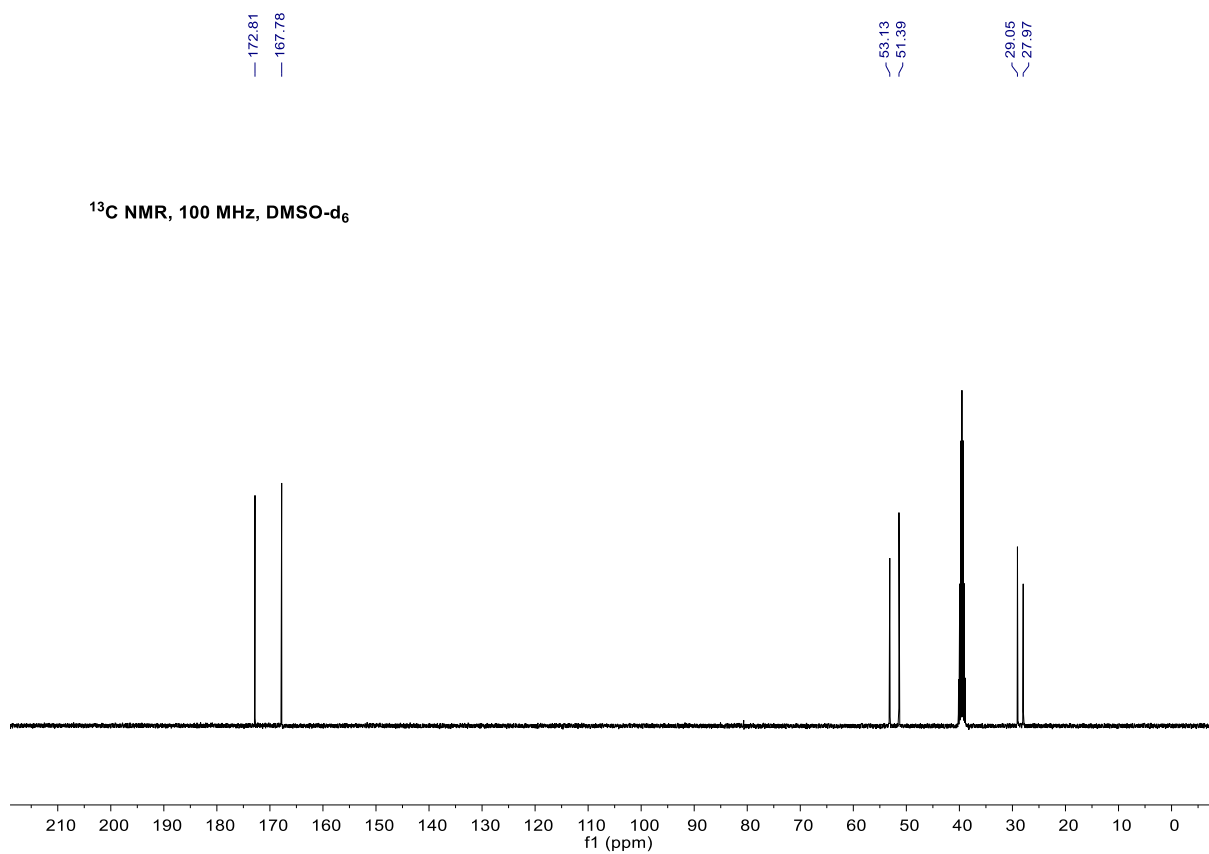


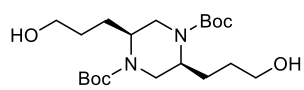
$^{13}\text{C}$  NMR, 100 MHz,  $\text{DMSO-d}_6$





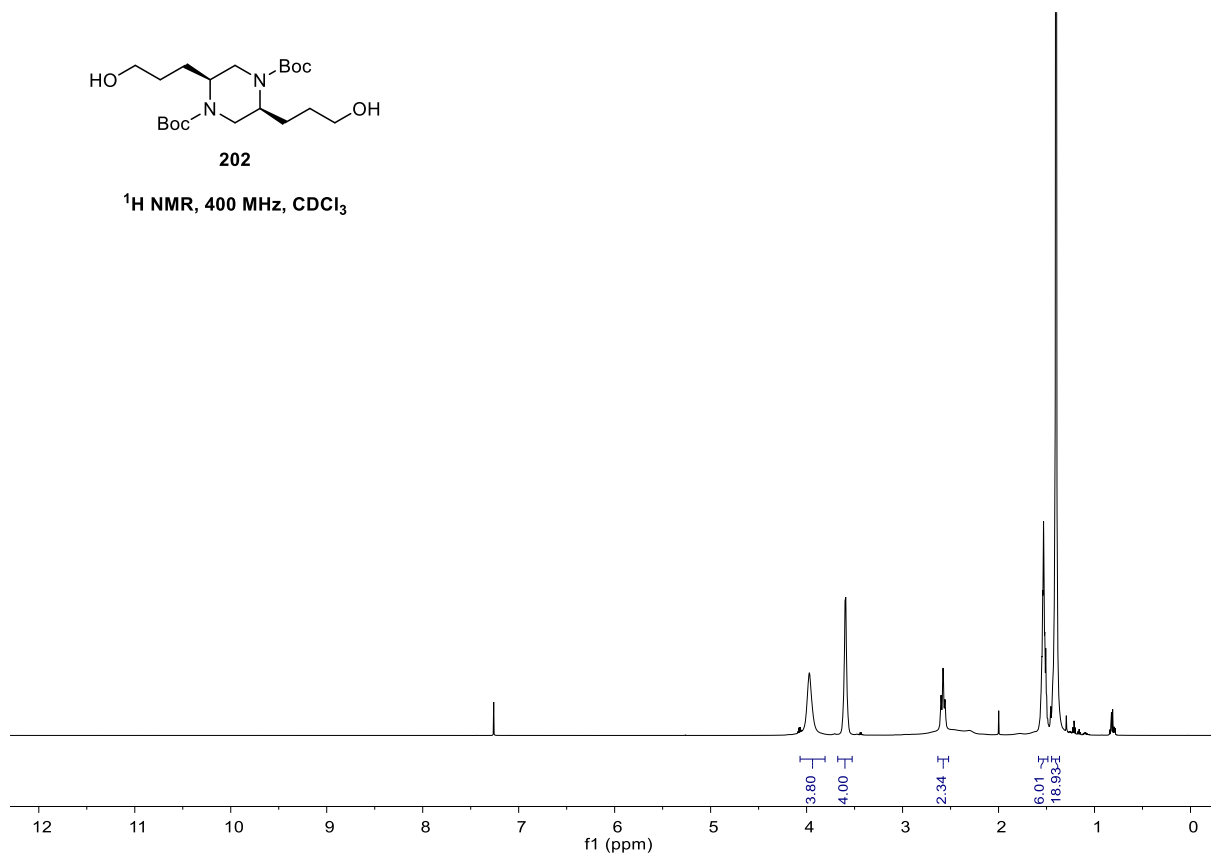
200

<sup>1</sup>H NMR, 400 MHz, DMSO-d<sub>6</sub><sup>13</sup>C NMR, 100 MHz, DMSO-d<sub>6</sub>

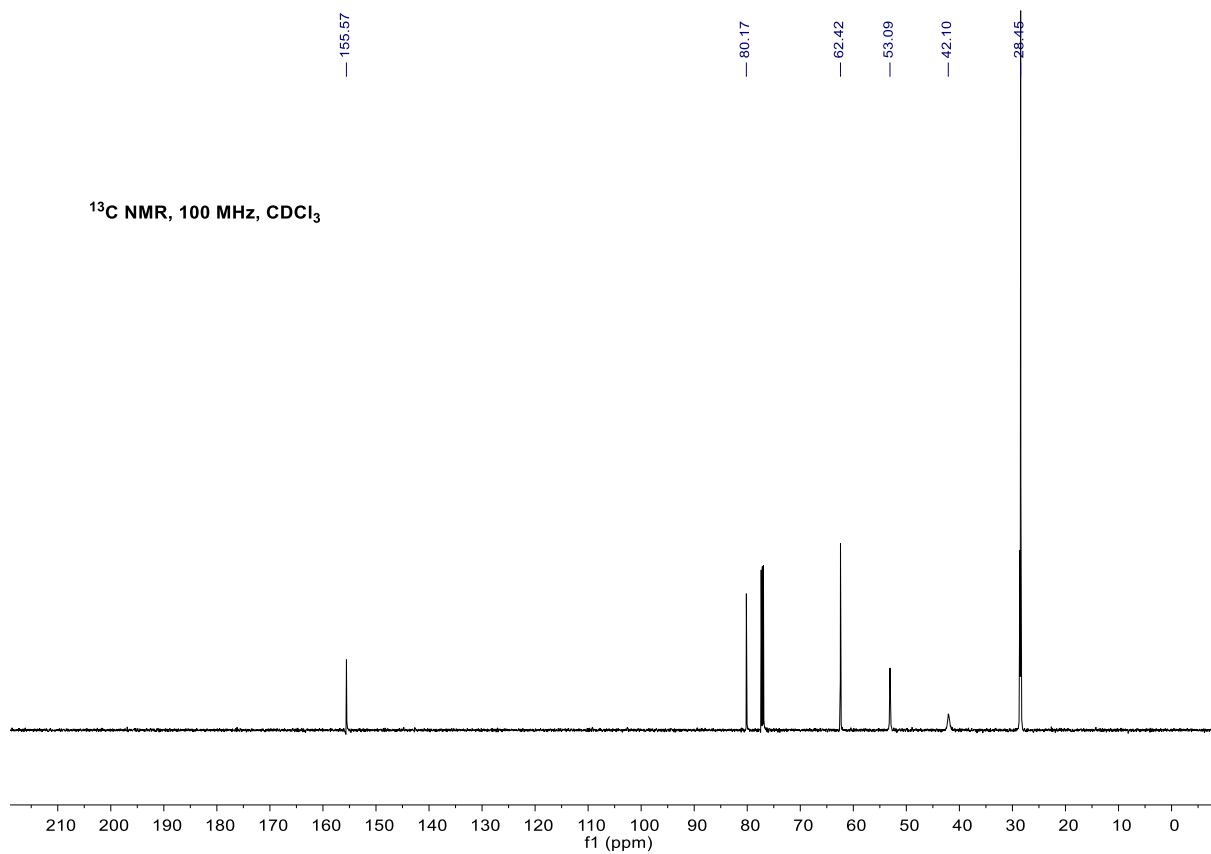


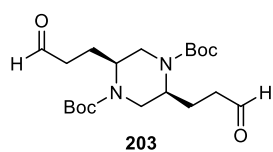
202

<sup>1</sup>H NMR, 400 MHz, CDCl<sub>3</sub>

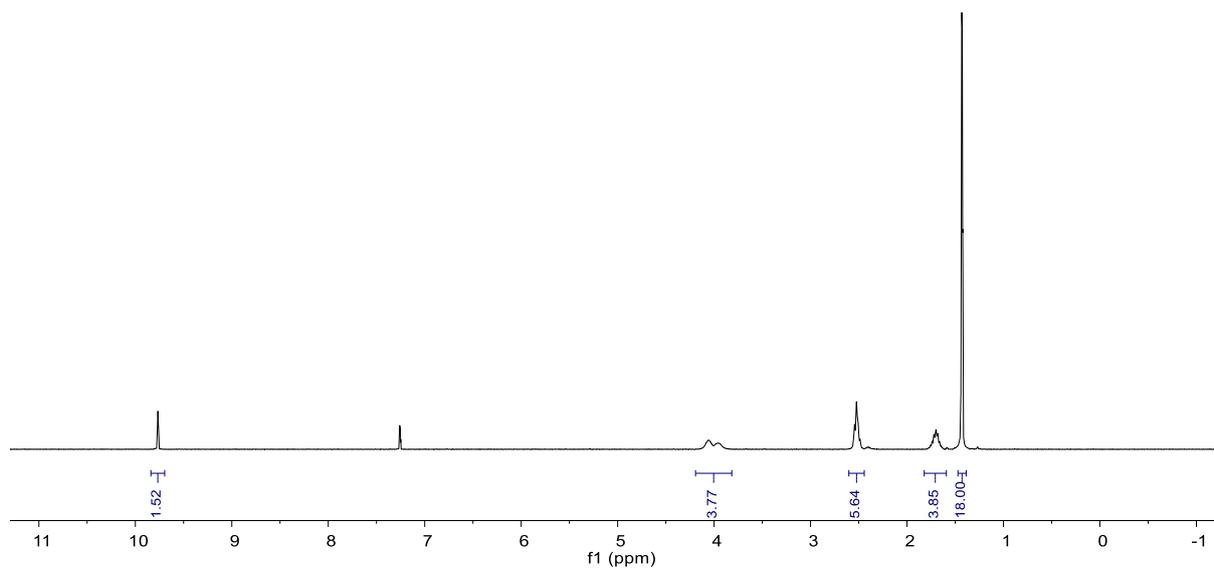


<sup>13</sup>C NMR, 100 MHz, CDCl<sub>3</sub>





$^1\text{H}$  NMR, 400 MHz,  $\text{CDCl}_3$



— 201.46

— 155.70

— 80.61

— 52.65

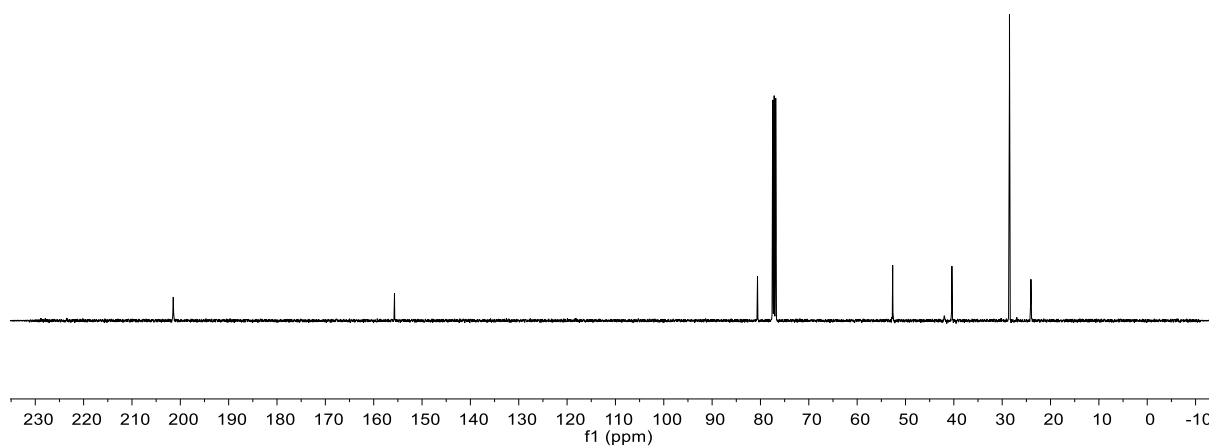
— 41.98

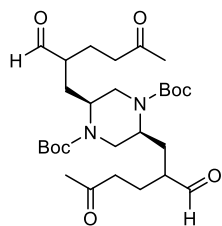
— 40.41

— 28.49

— 24.05

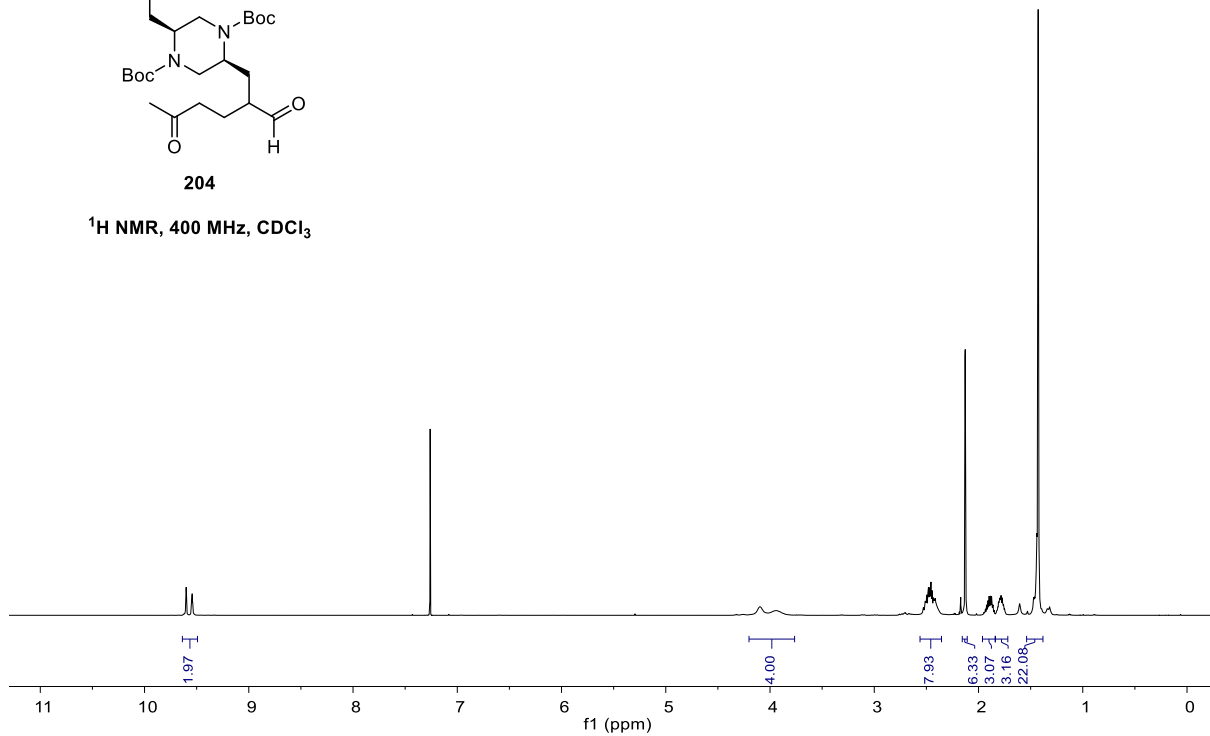
$^{13}\text{C}$  NMR, 100 MHz,  $\text{CDCl}_3$





204

$^1\text{H}$  NMR, 400 MHz,  $\text{CDCl}_3$



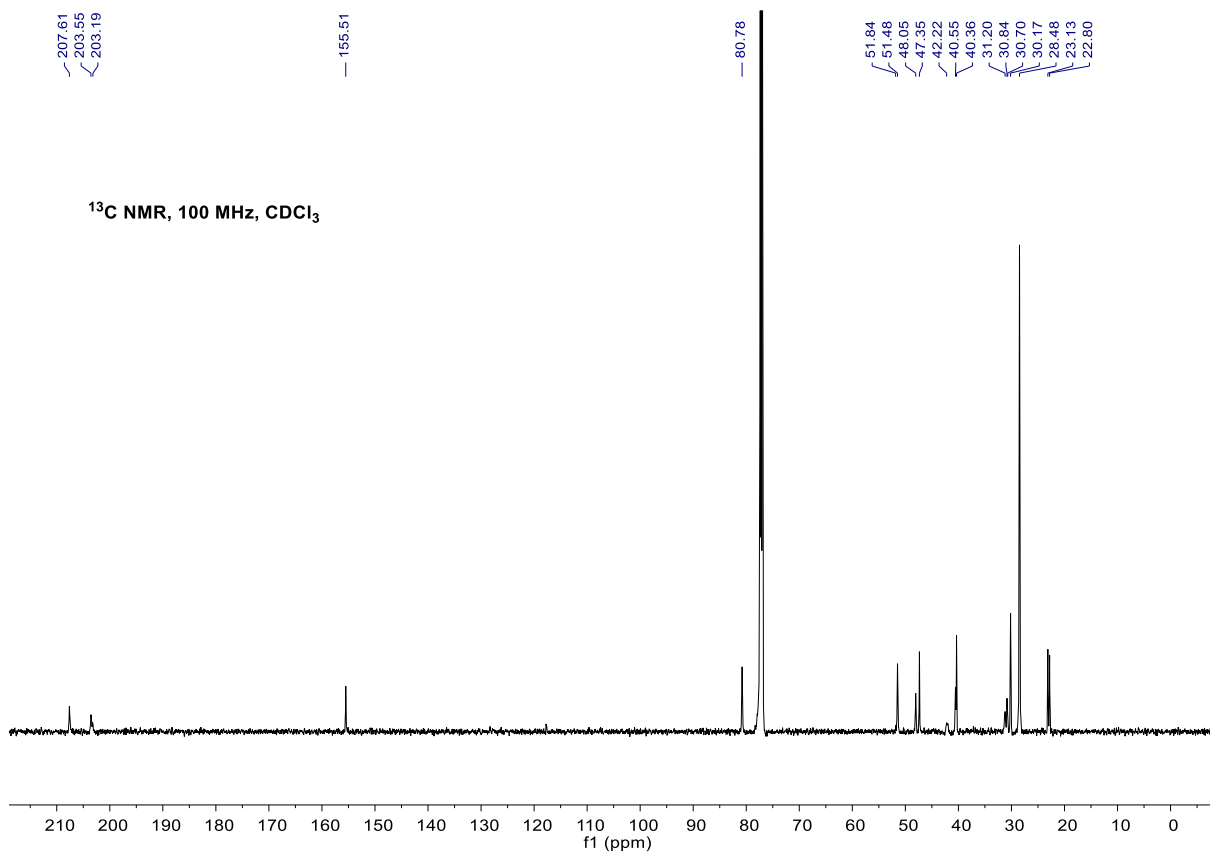
207.61  
203.55  
203.19

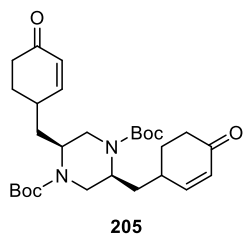
155.51

80.78

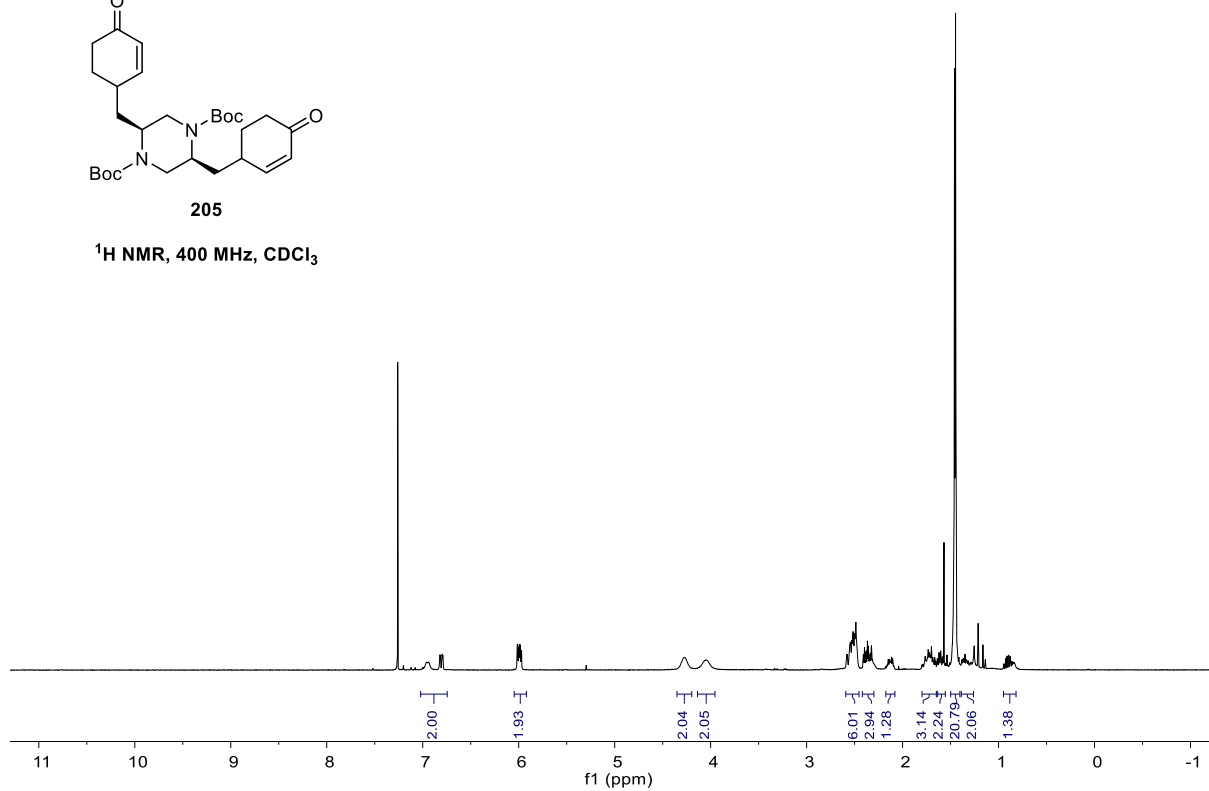
51.84  
51.48  
48.05  
47.35  
42.22  
40.55  
40.36  
31.20  
30.84  
30.70  
30.17  
28.48  
23.13  
22.80

$^{13}\text{C}$  NMR, 100 MHz,  $\text{CDCl}_3$

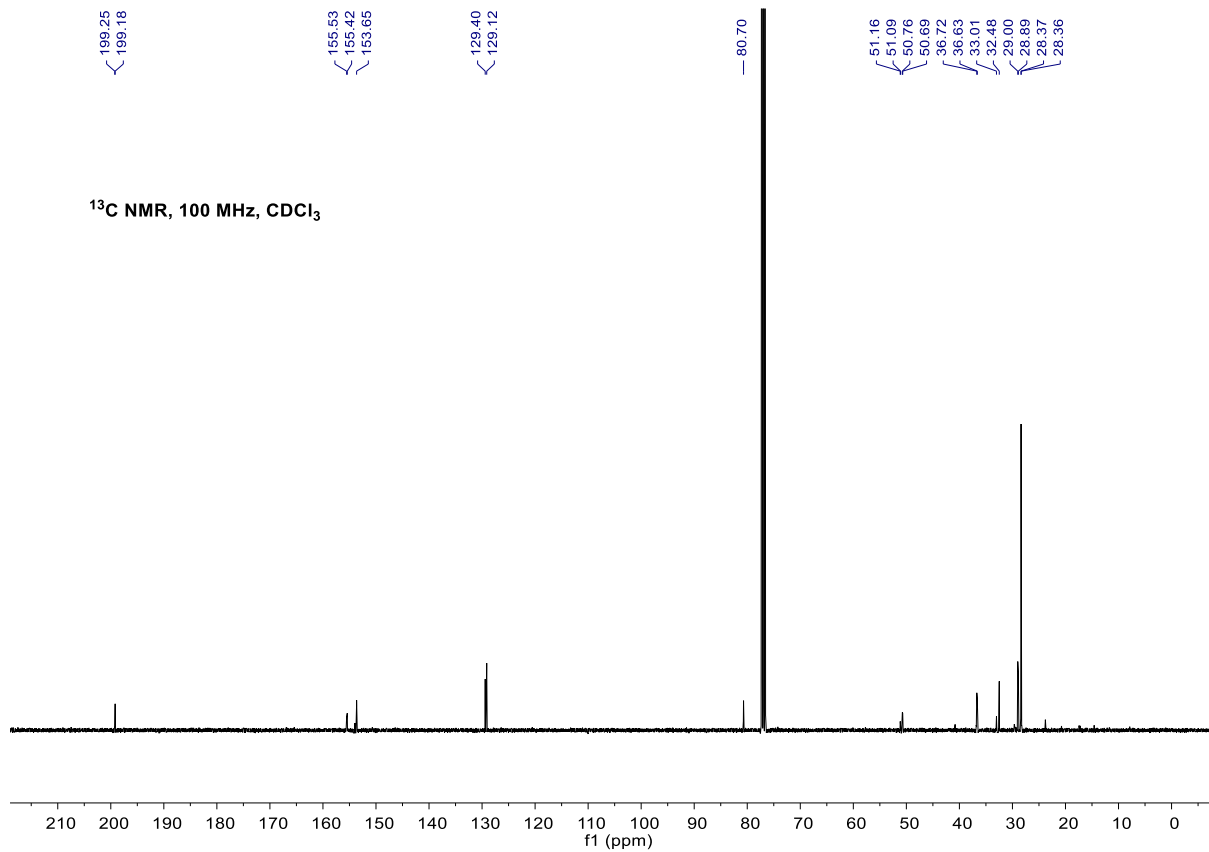


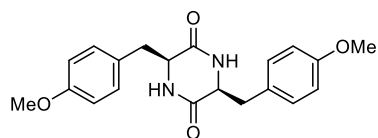


205

 $^1\text{H}$  NMR, 400 MHz,  $\text{CDCl}_3$ 199.25  
199.18155.53  
155.42  
153.65129.40  
129.12

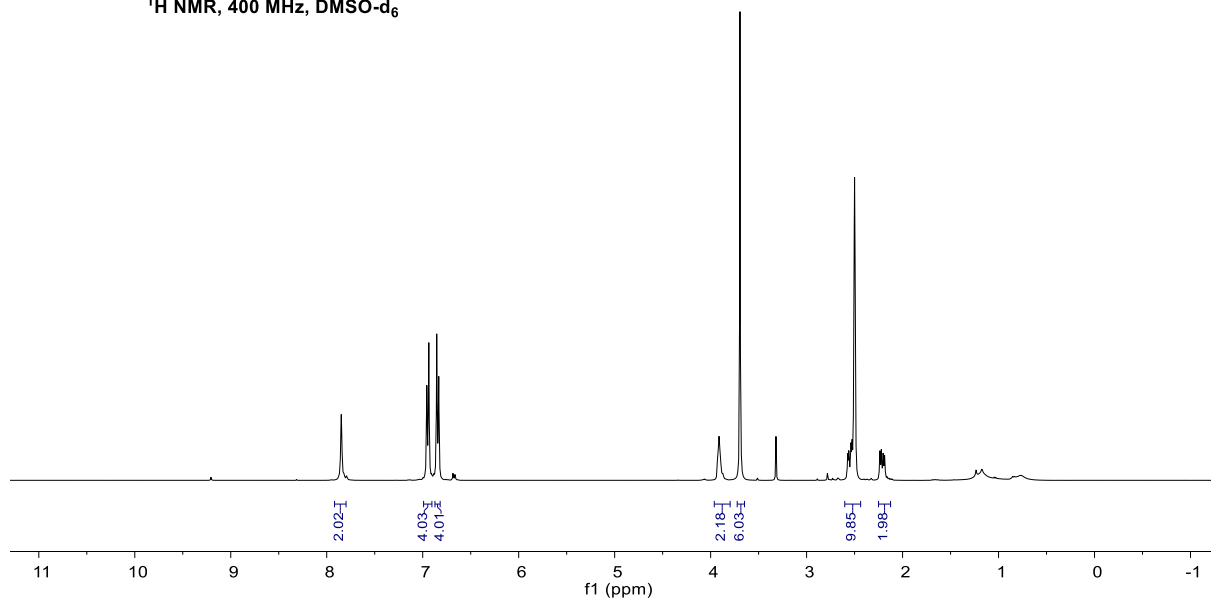
80.70

51.16  
51.09  
50.76  
50.69  
36.72  
36.63  
33.01  
32.48  
29.00  
28.69  
28.37  
28.36 $^{13}\text{C}$  NMR, 100 MHz,  $\text{CDCl}_3$ 

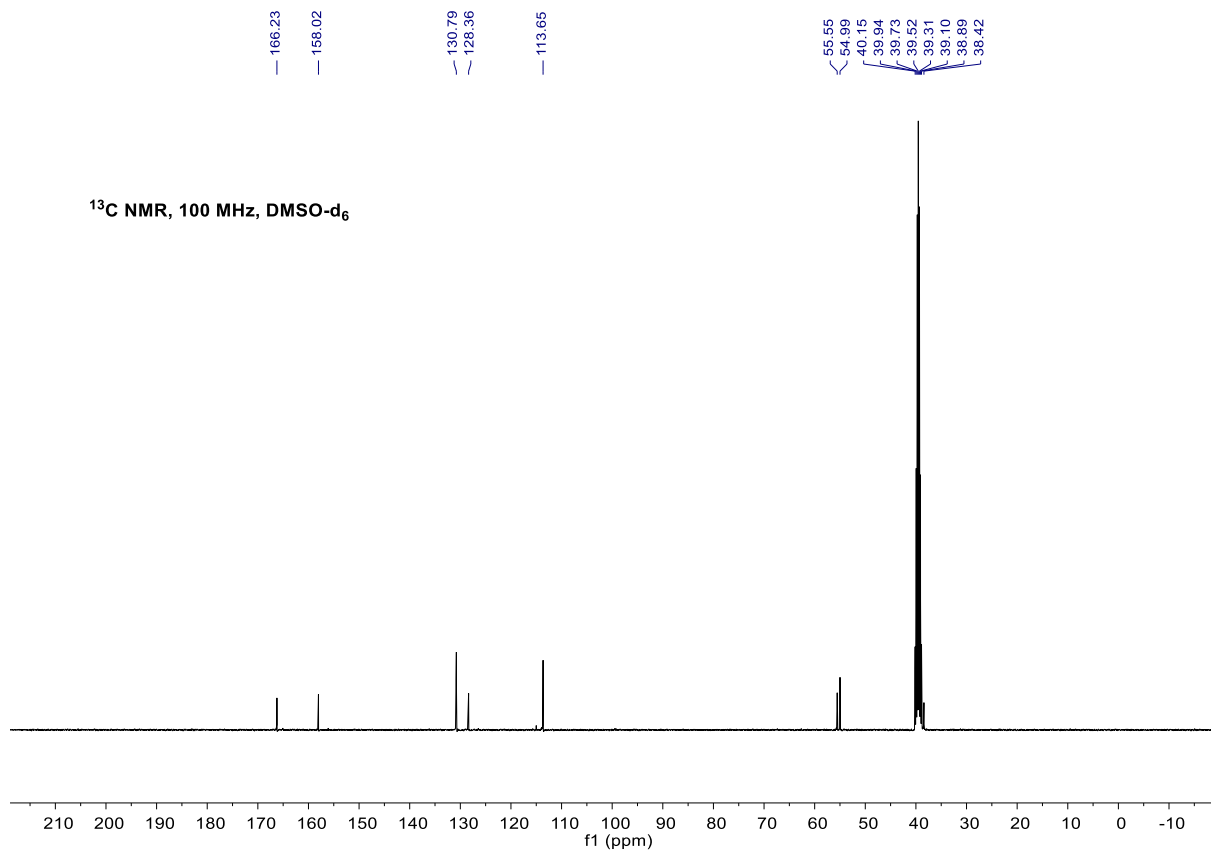


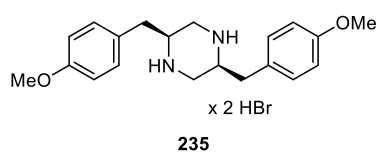
234

<sup>1</sup>H NMR, 400 MHz, DMSO-d<sub>6</sub>

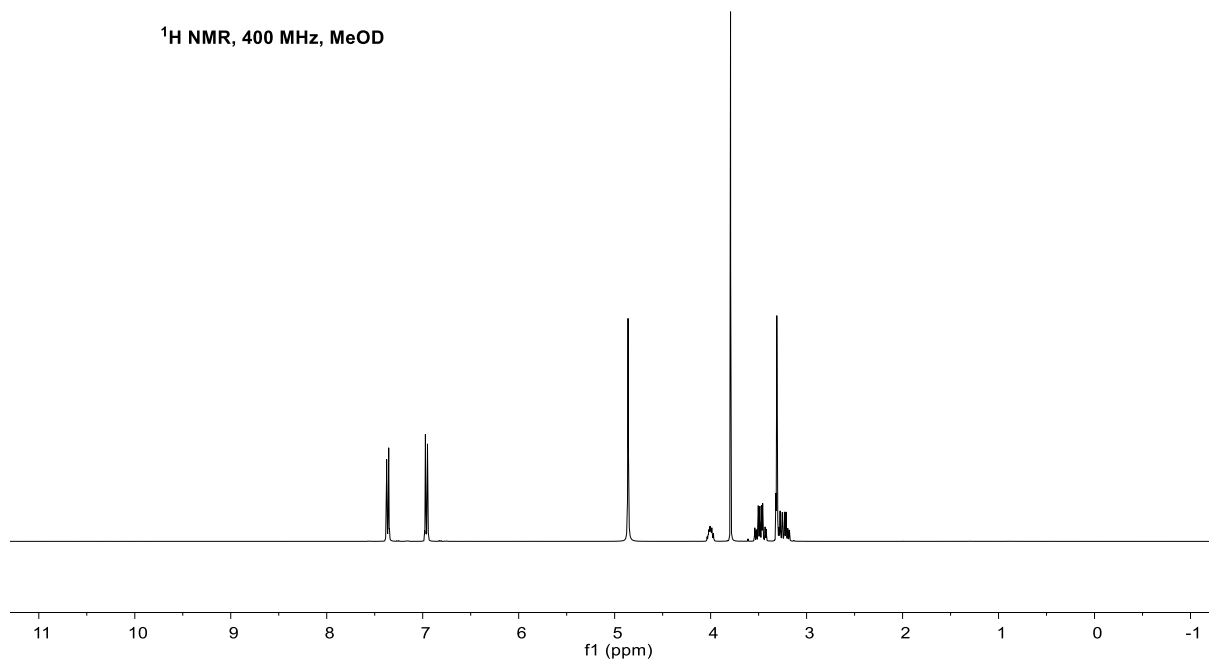


<sup>13</sup>C NMR, 100 MHz, DMSO-d<sub>6</sub>

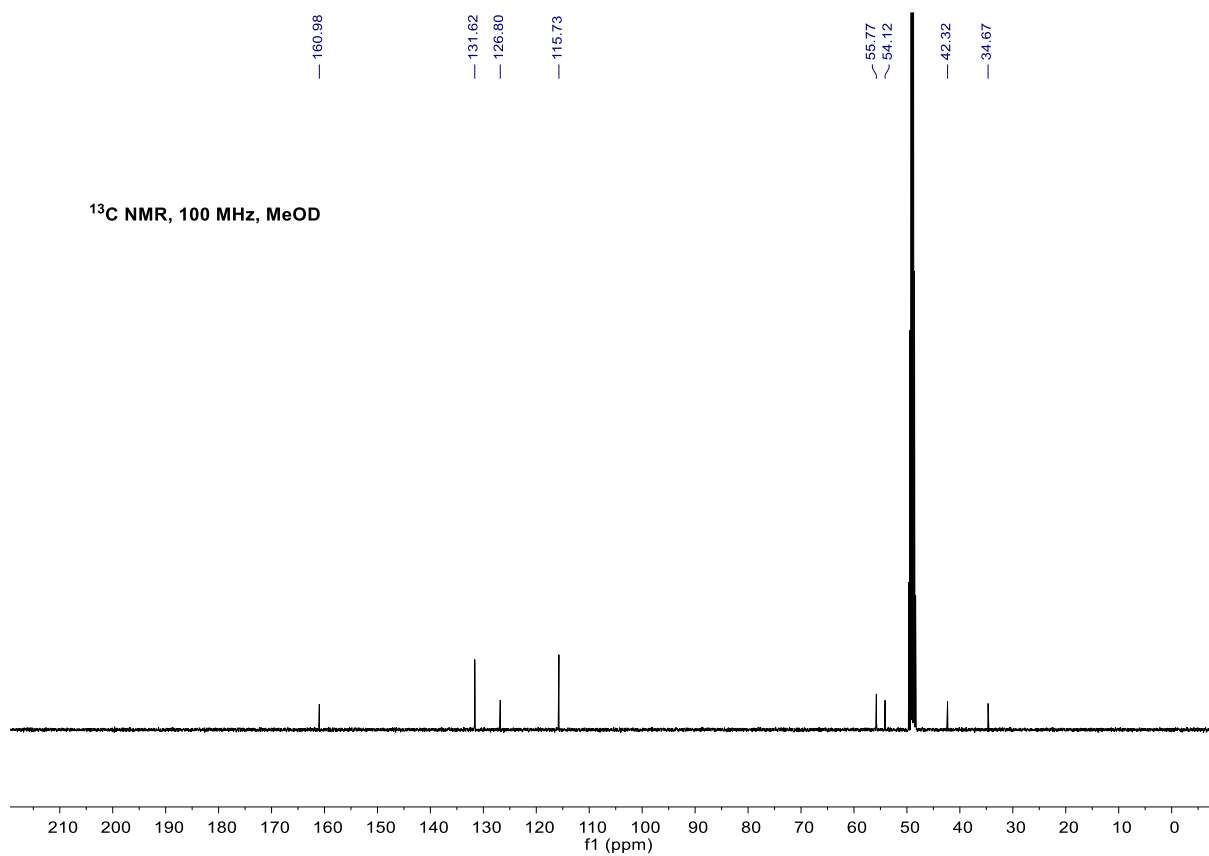


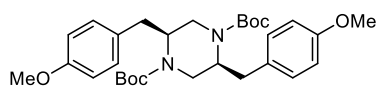


$^1\text{H}$  NMR, 400 MHz, MeOD



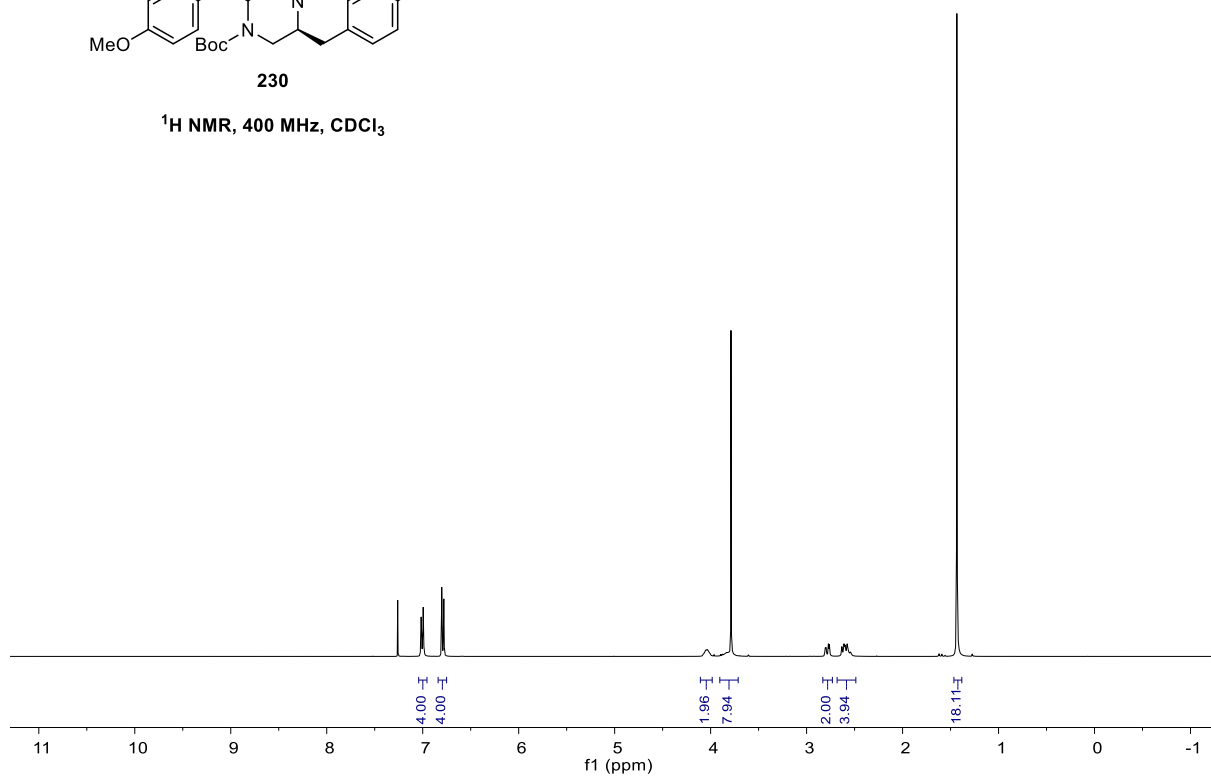
$^{13}\text{C}$  NMR, 100 MHz, MeOD





230

$^1\text{H}$  NMR, 400 MHz,  $\text{CDCl}_3$



158.27  
155.11

130.26  
129.14

113.89

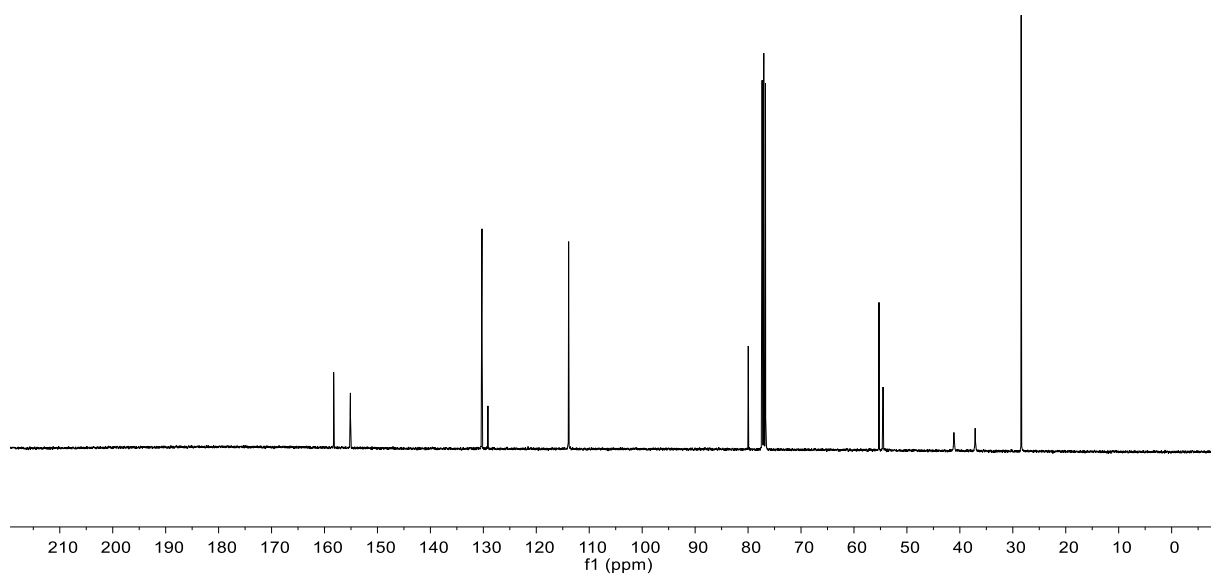
79.97

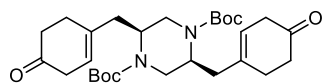
55.27  
54.51

41.12  
37.10

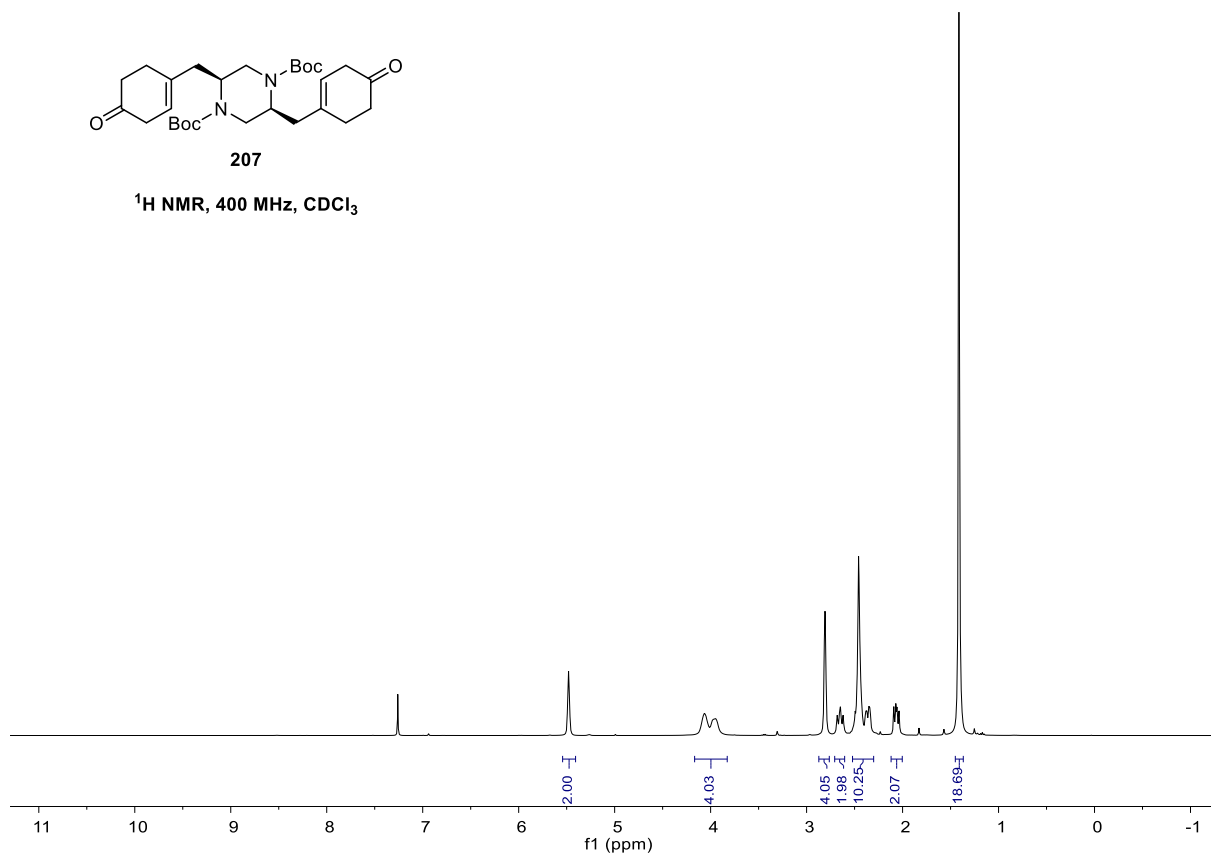
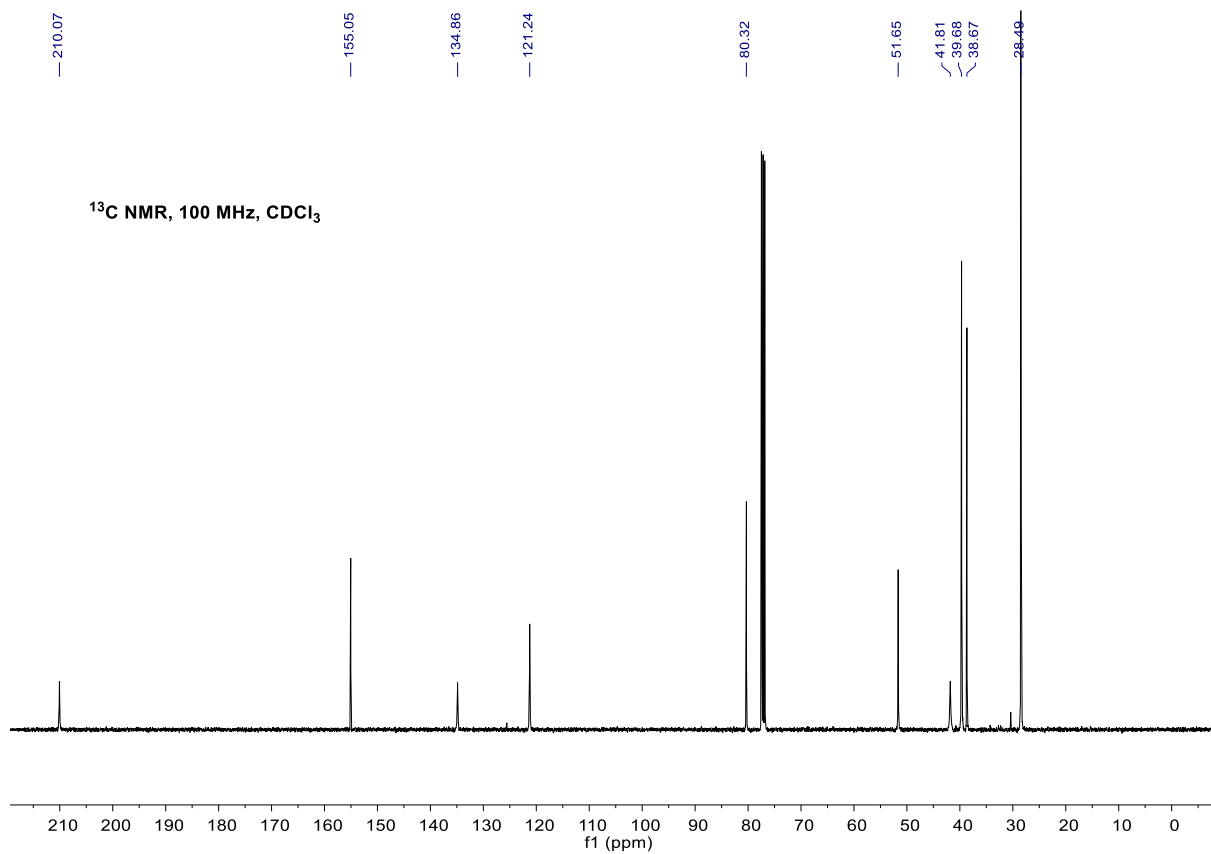
28.42

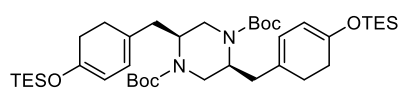
$^{13}\text{C}$  NMR, 100 MHz,  $\text{CDCl}_3$





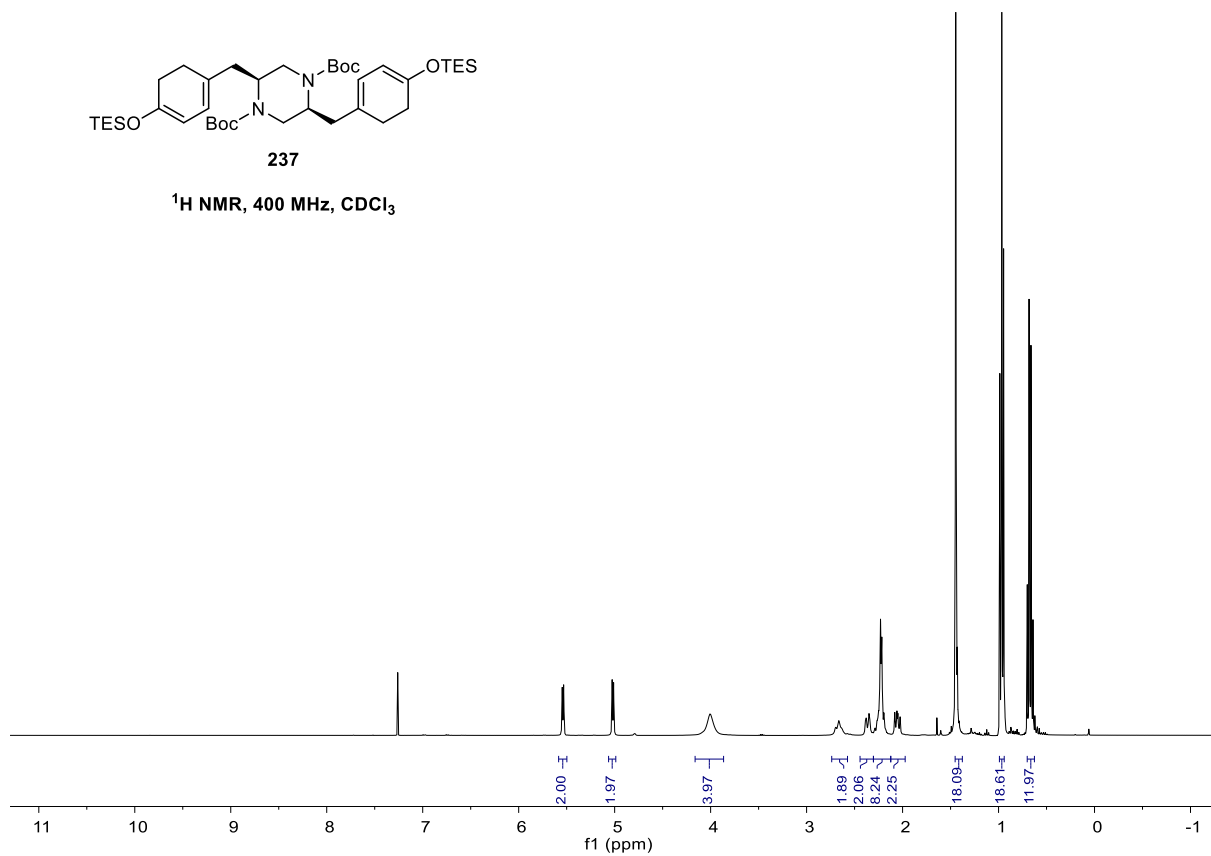
207

 $^1\text{H}$  NMR, 400 MHz,  $\text{CDCl}_3$  $^{13}\text{C}$  NMR, 100 MHz,  $\text{CDCl}_3$ 

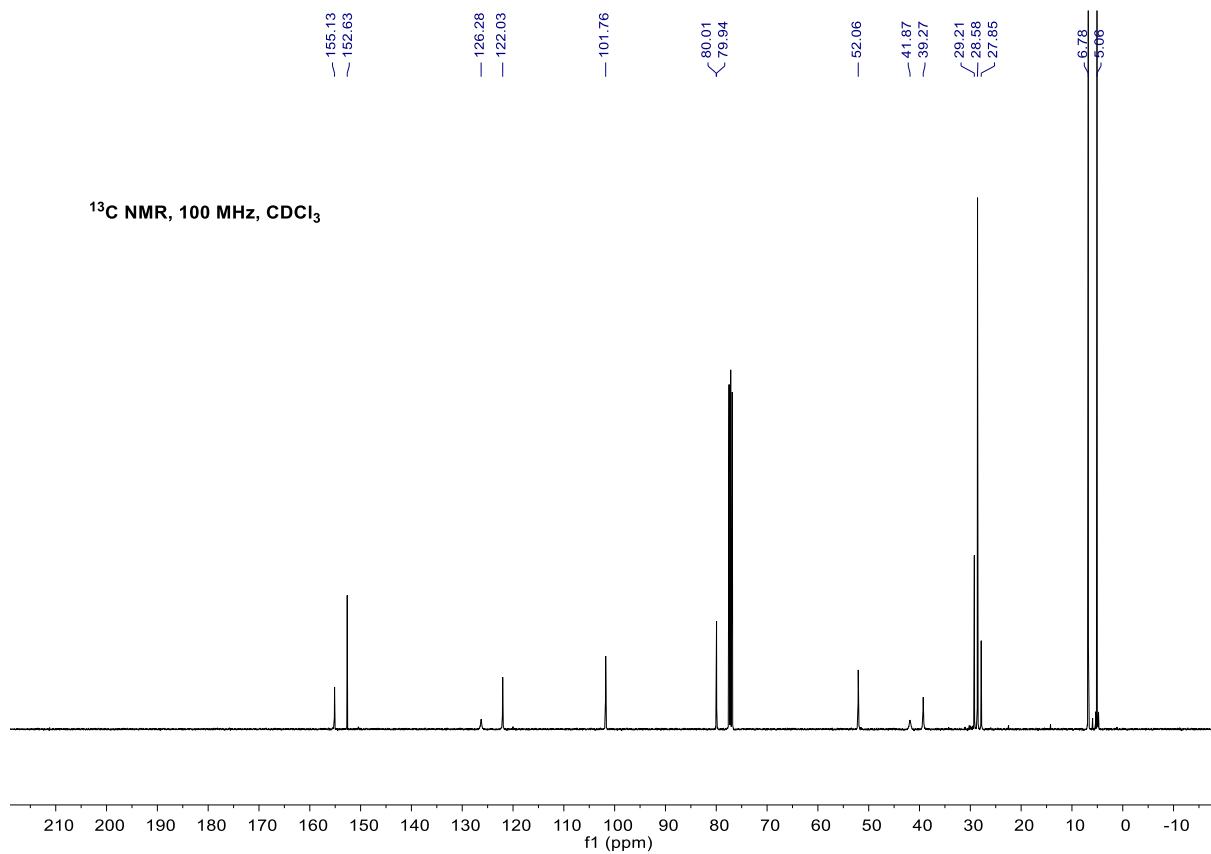


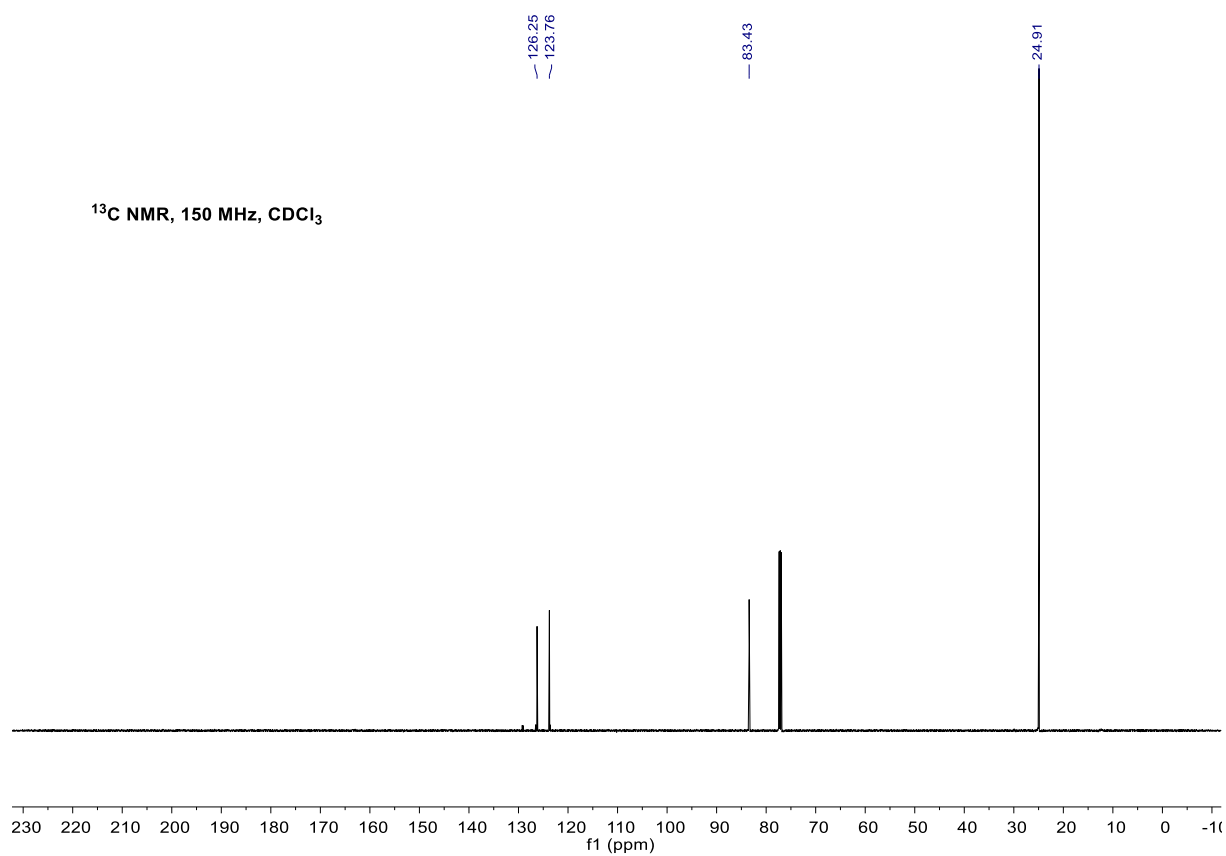
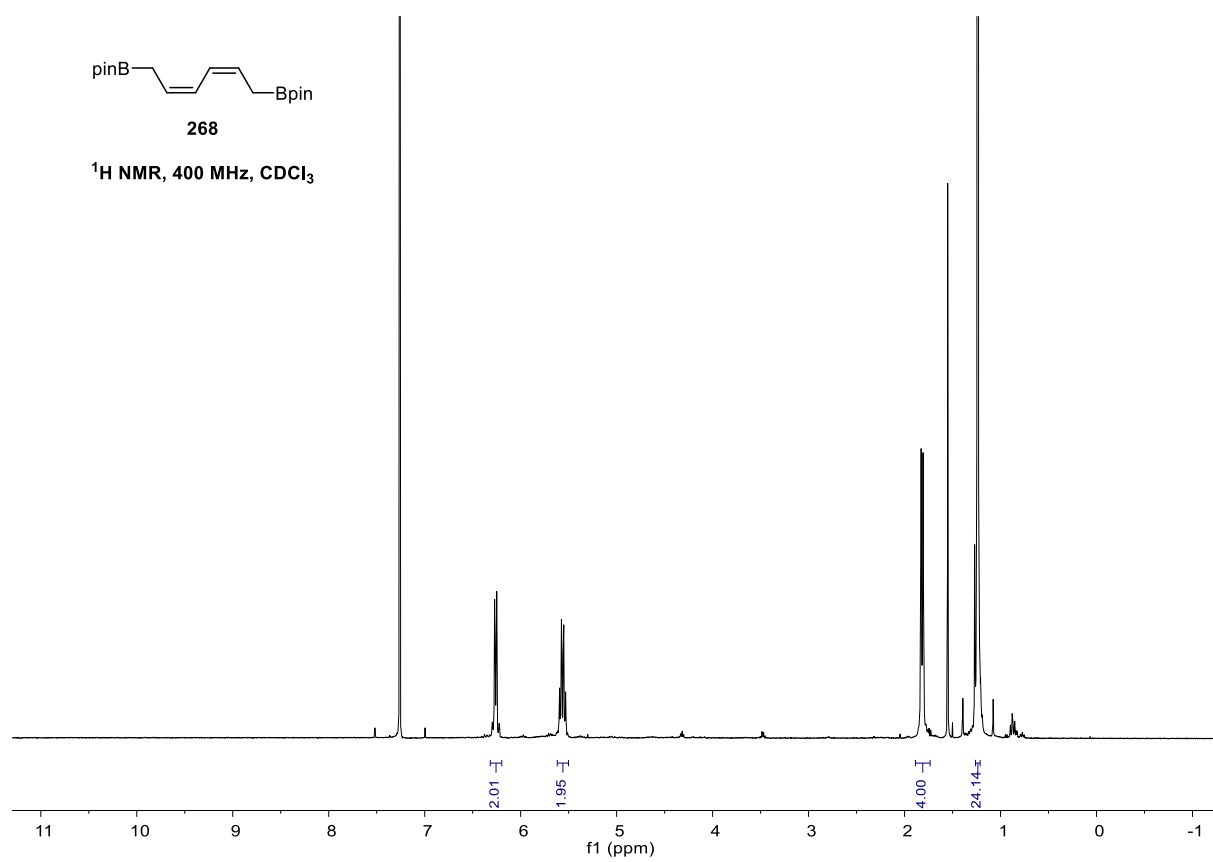
237

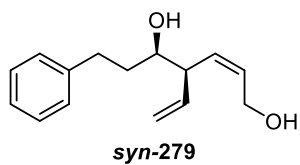
<sup>1</sup>H NMR, 400 MHz, CDCl<sub>3</sub>



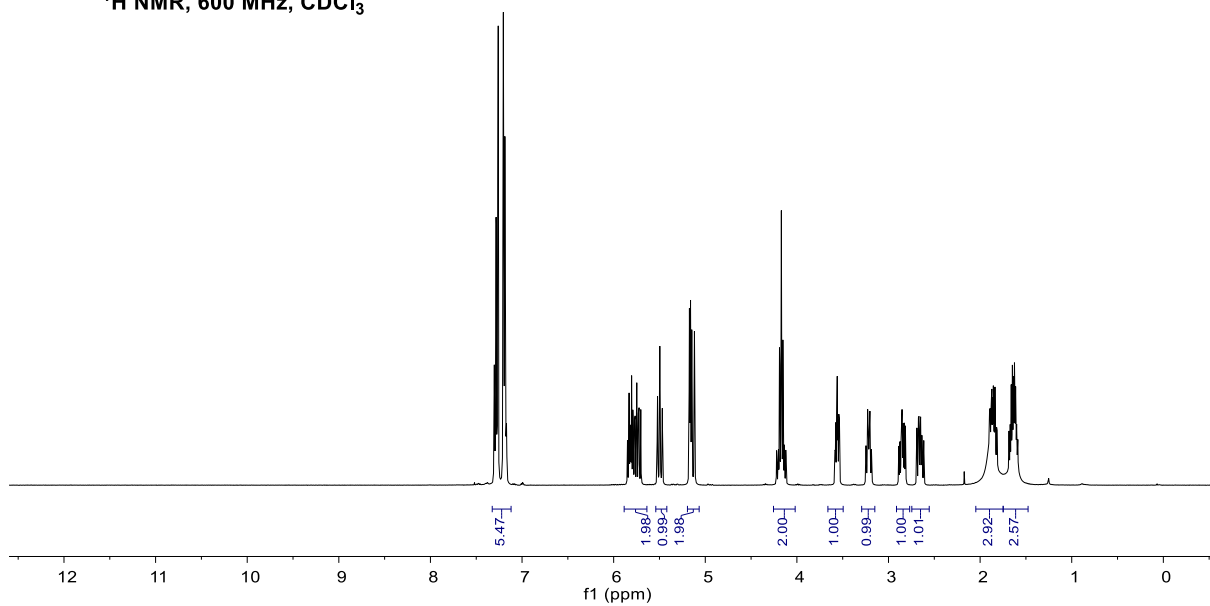
<sup>13</sup>C NMR, 100 MHz, CDCl<sub>3</sub>



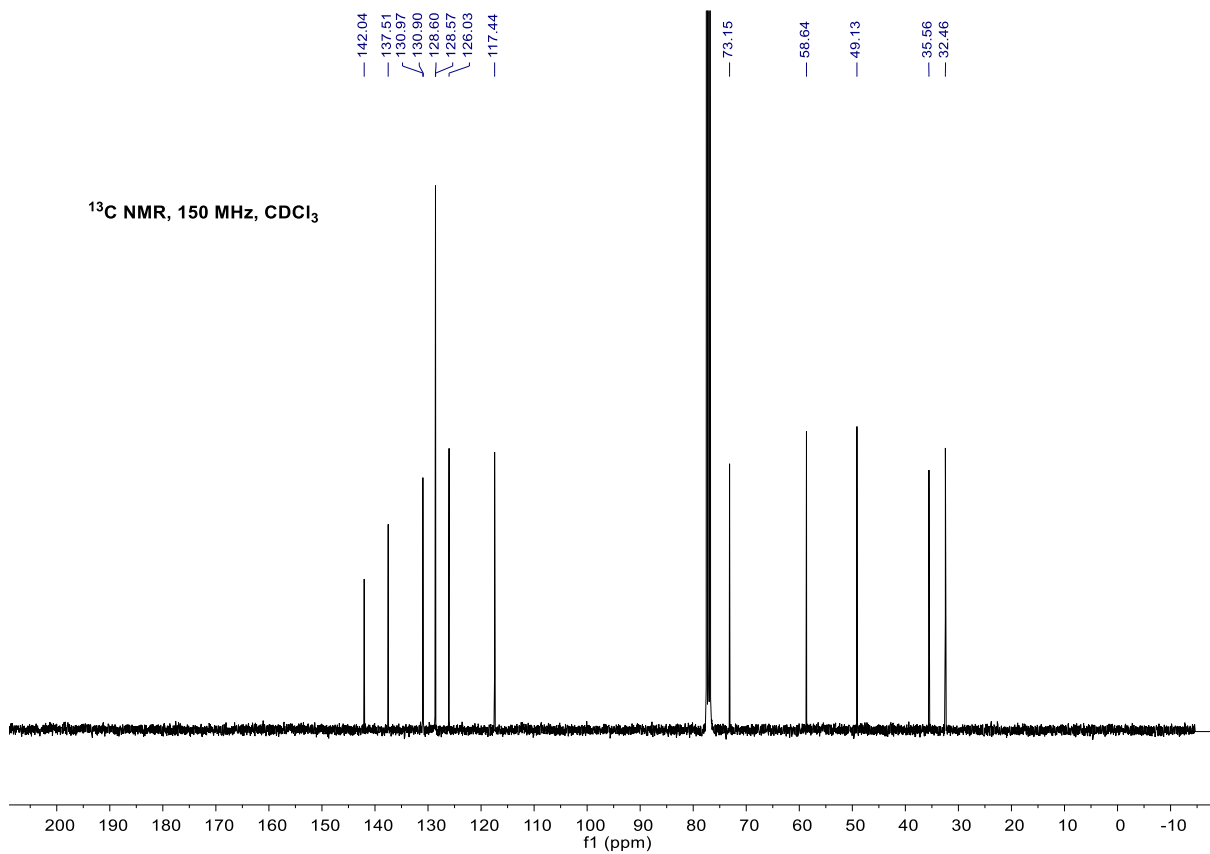


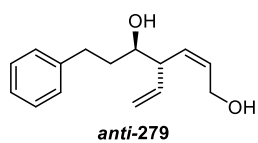


<sup>1</sup>H NMR, 600 MHz, CDCl<sub>3</sub>

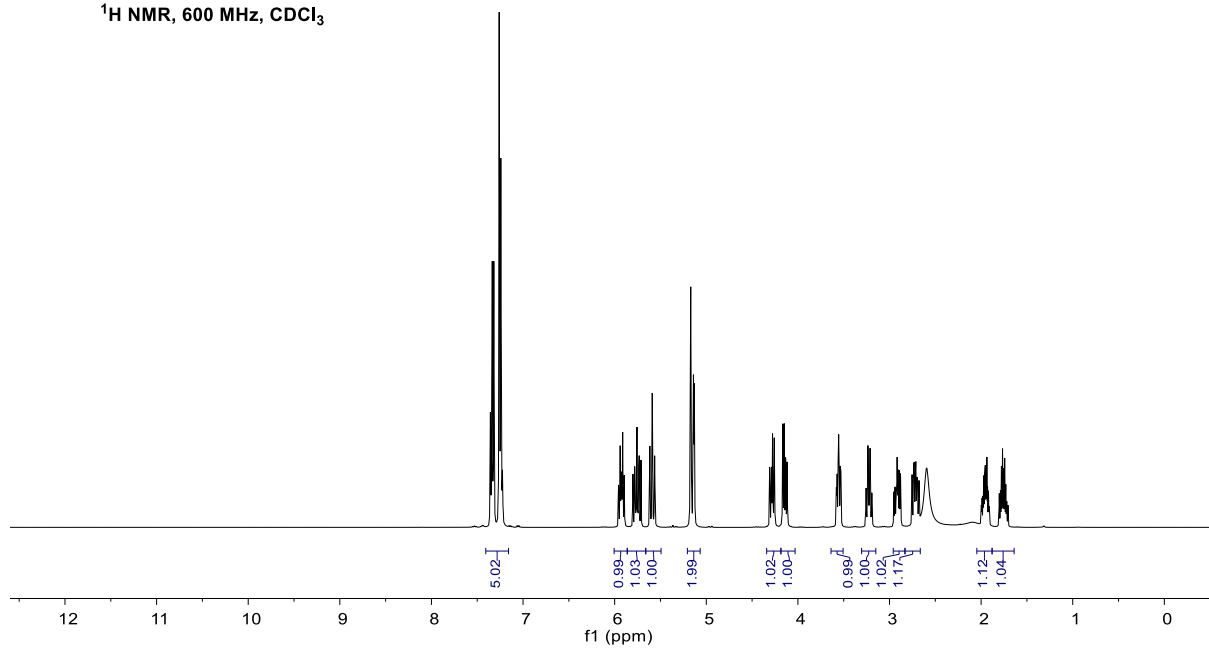


<sup>13</sup>C NMR, 150 MHz, CDCl<sub>3</sub>

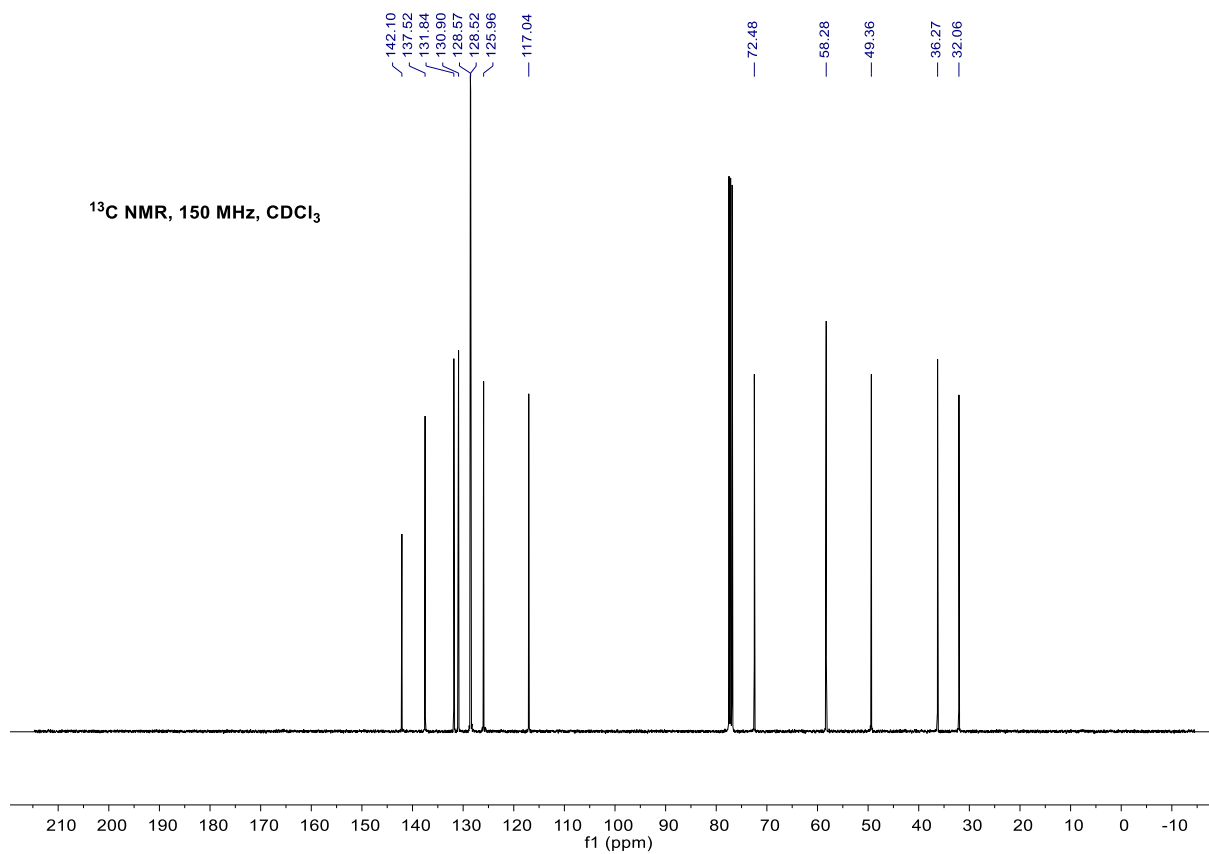


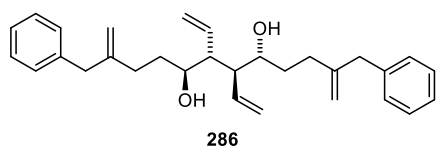


<sup>1</sup>H NMR, 600 MHz, CDCl<sub>3</sub>

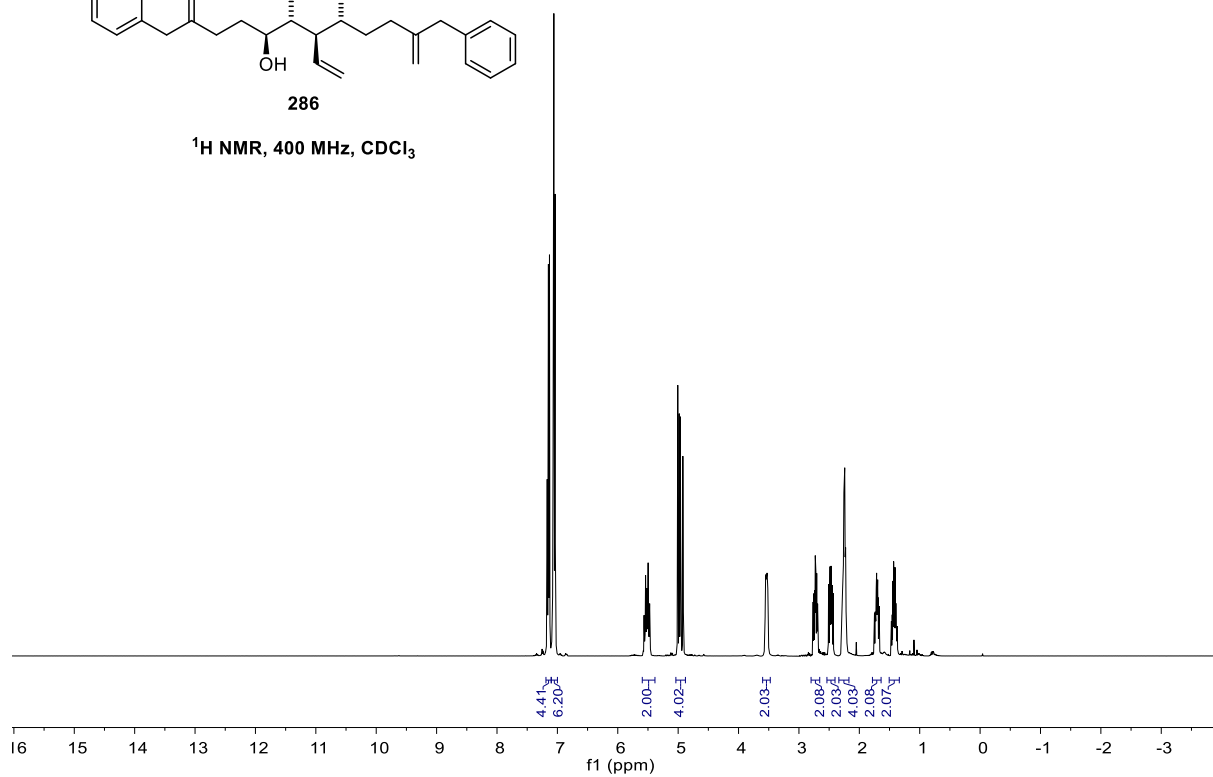


<sup>13</sup>C NMR, 150 MHz, CDCl<sub>3</sub>

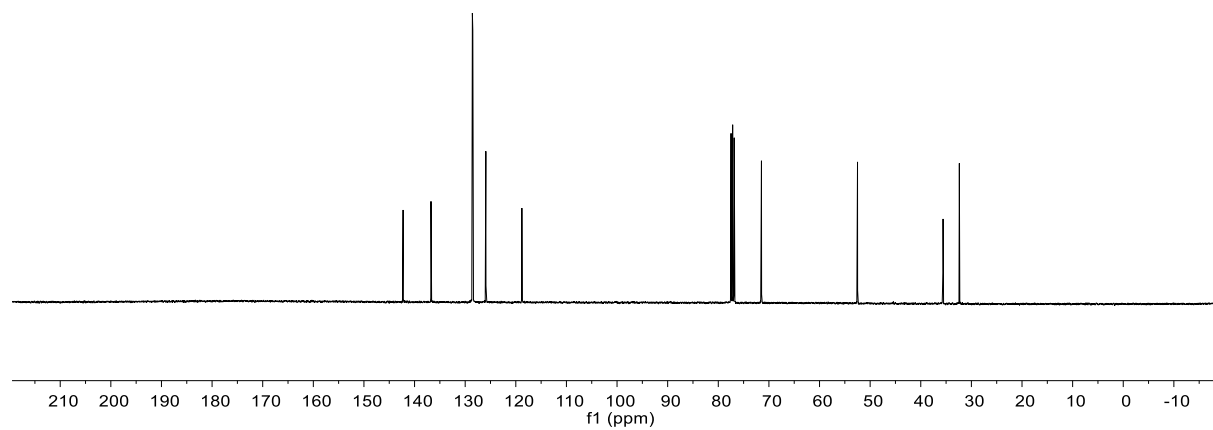


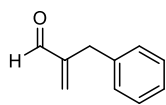


<sup>1</sup>H NMR, 400 MHz, CDCl<sub>3</sub>

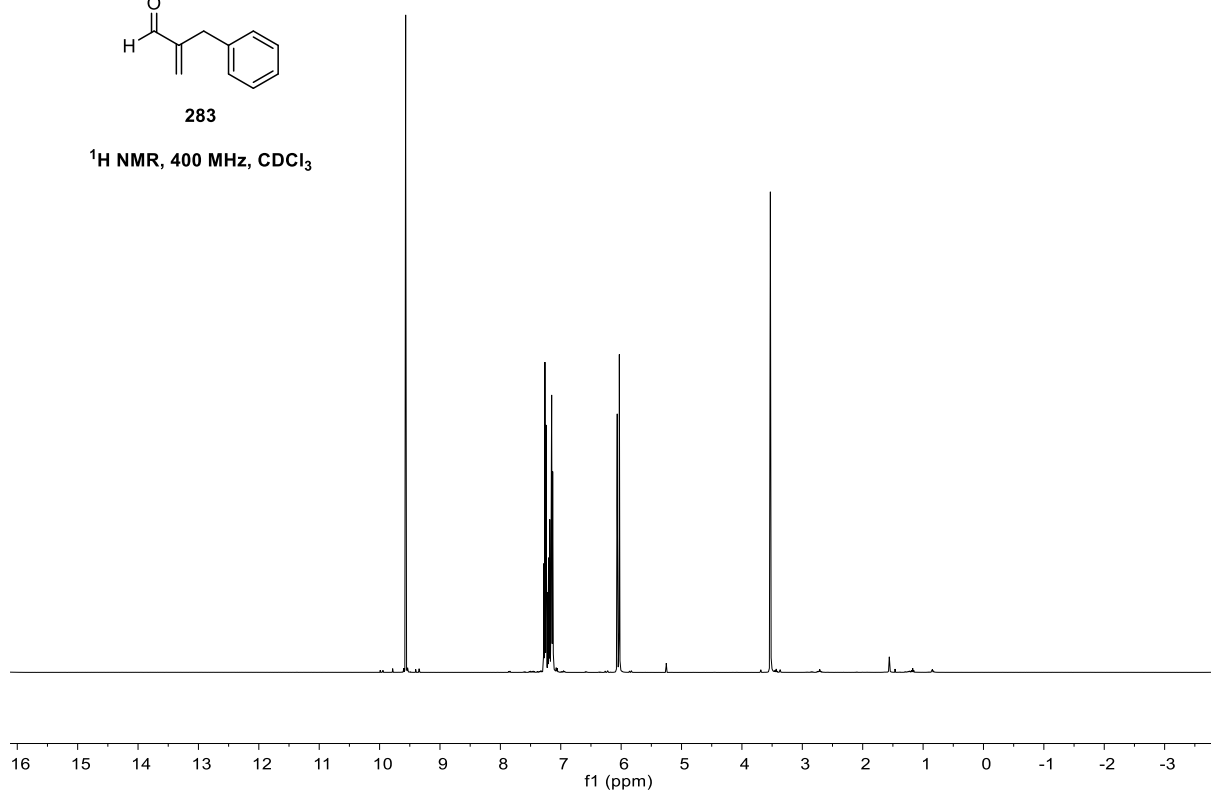


<sup>13</sup>C NMR, 100 MHz, CDCl<sub>3</sub>





283

 $^1\text{H}$  NMR, 400 MHz,  $\text{CDCl}_3$ 

— 194.14

— 149.85

— 138.23

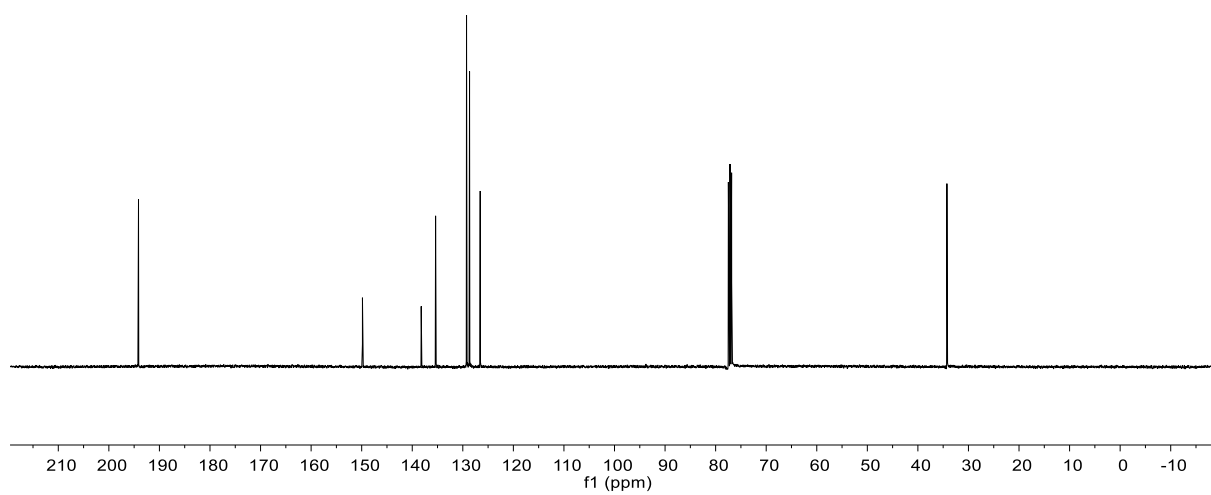
— 135.38

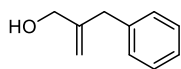
— 129.26

— 128.67

— 128.56

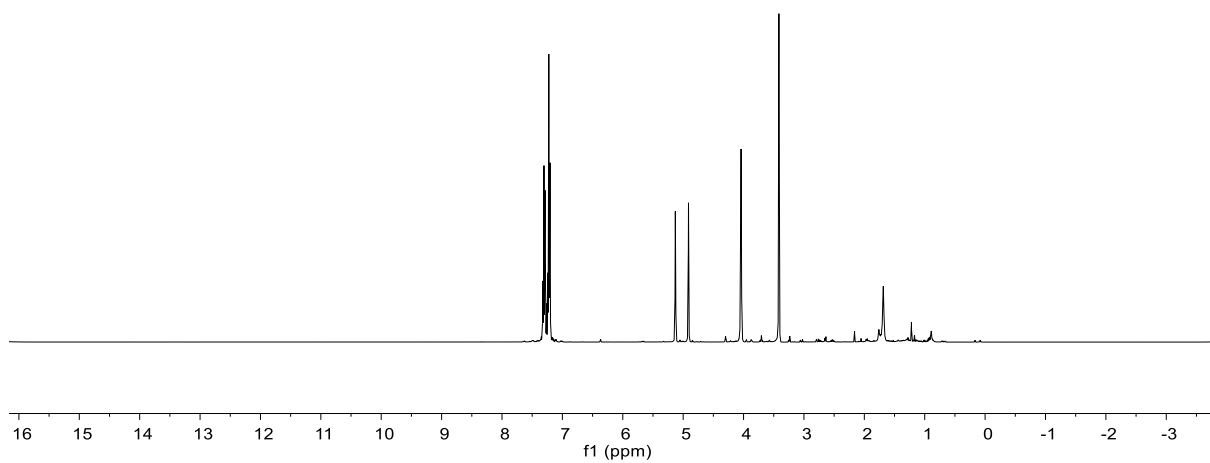
— 34.26

 $^{13}\text{C}$  NMR, 100 MHz,  $\text{CDCl}_3$ 



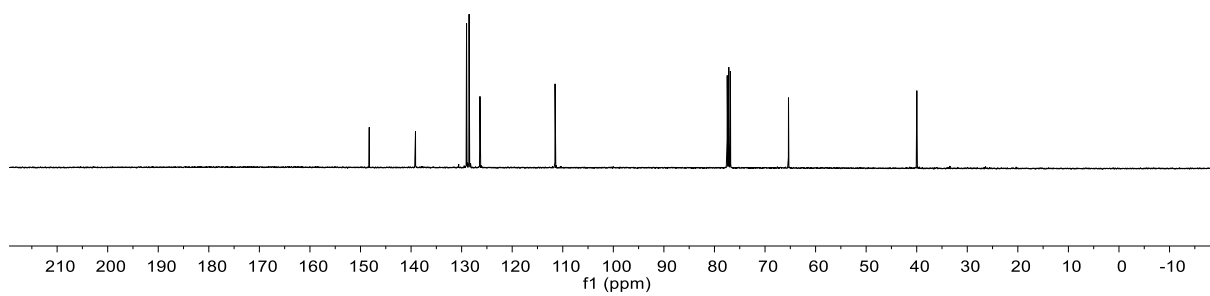
284

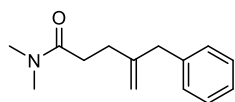
<sup>1</sup>H NMR, 400 MHz, CDCl<sub>3</sub>



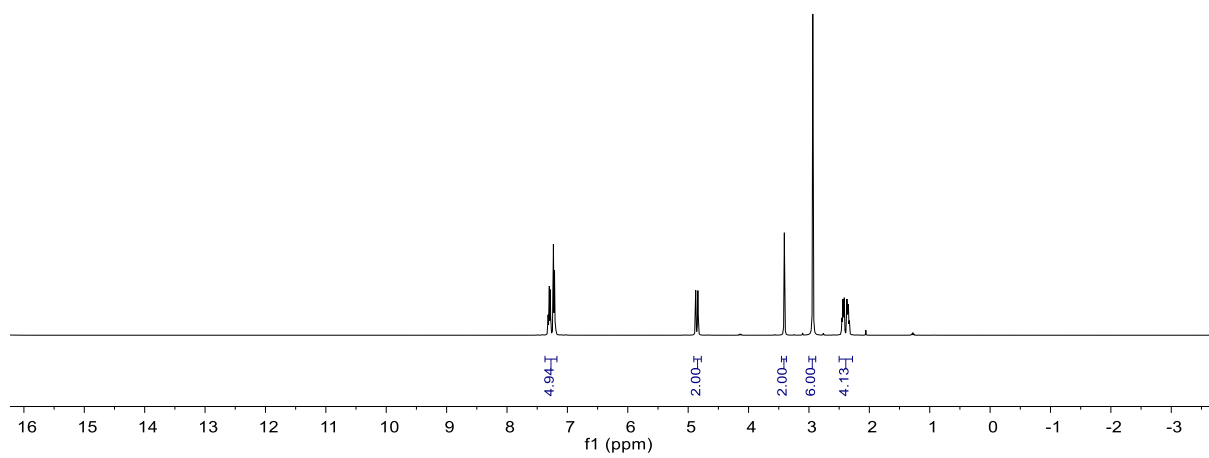
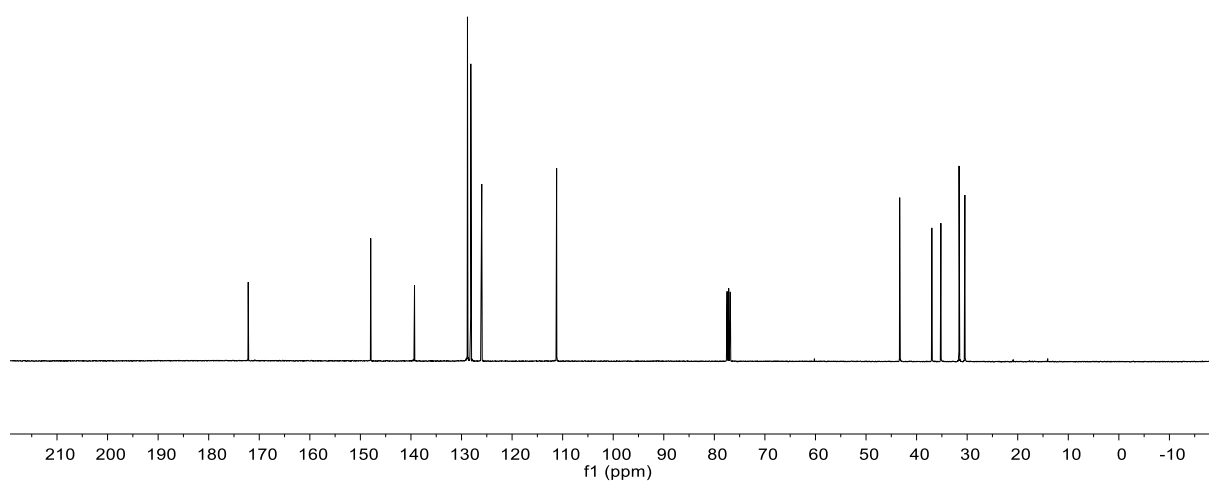
148.27  
139.12  
129.03  
128.52  
126.37  
111.52  
65.36  
39.98

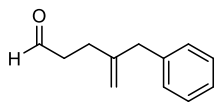
<sup>13</sup>C NMR, 100 MHz, CDCl<sub>3</sub>





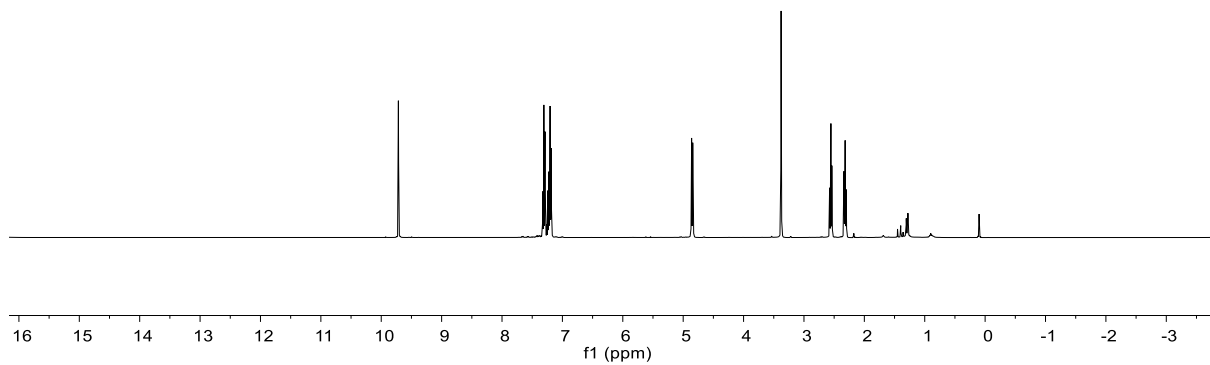
285

 $^1\text{H}$  NMR, 400 MHz,  $\text{CDCl}_3$  $^{13}\text{C}$  NMR, 100 MHz,  $\text{CDCl}_3$ 

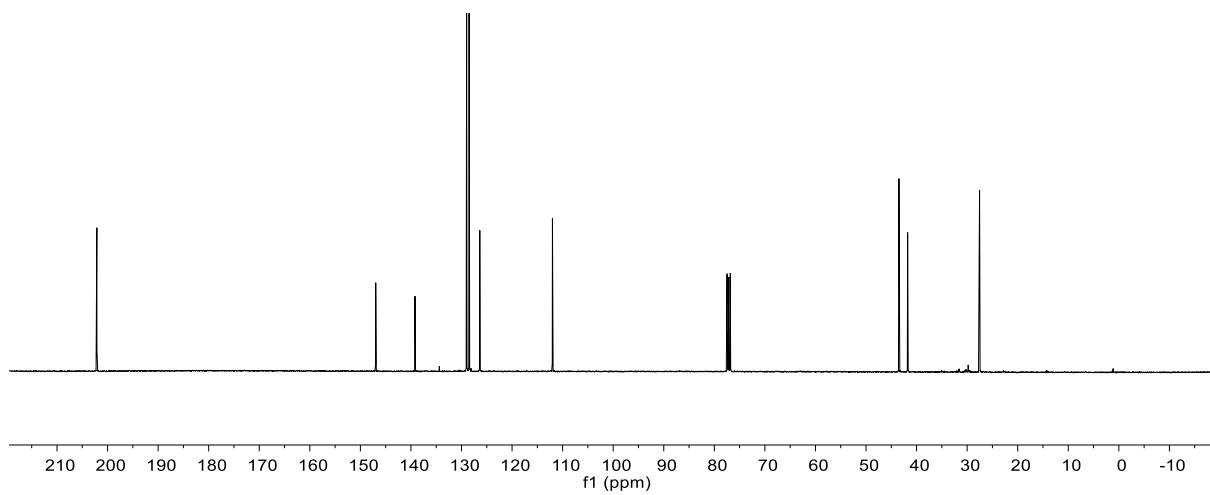


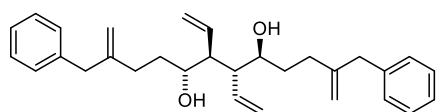
286

<sup>1</sup>H NMR, 400 MHz, CDCl<sub>3</sub>

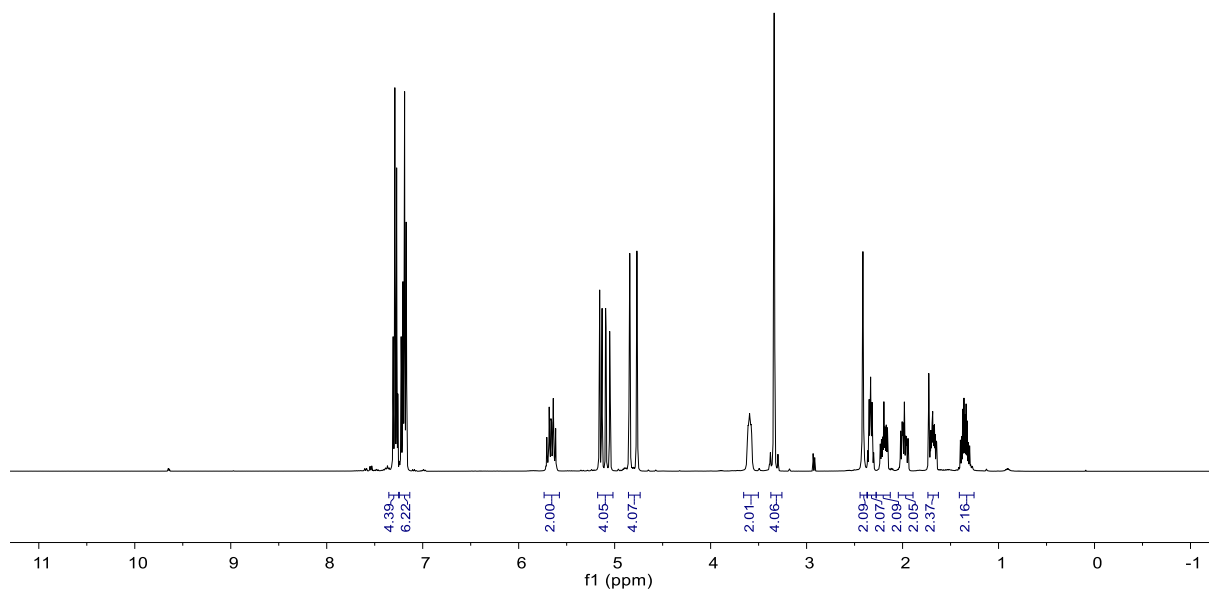


<sup>13</sup>C NMR, 100 MHz, CDCl<sub>3</sub>



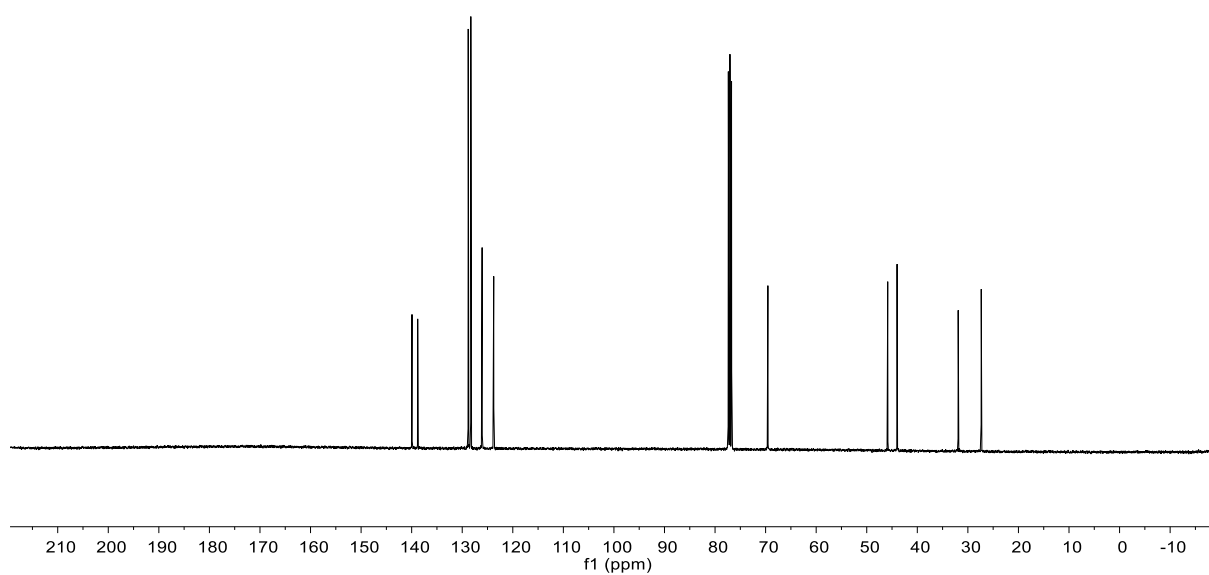


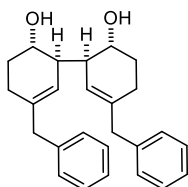
287

 $^1\text{H}$  NMR, 400 MHz,  $\text{CDCl}_3$ 

$^{13}\text{C}$  NMR chemical shifts (ppm):

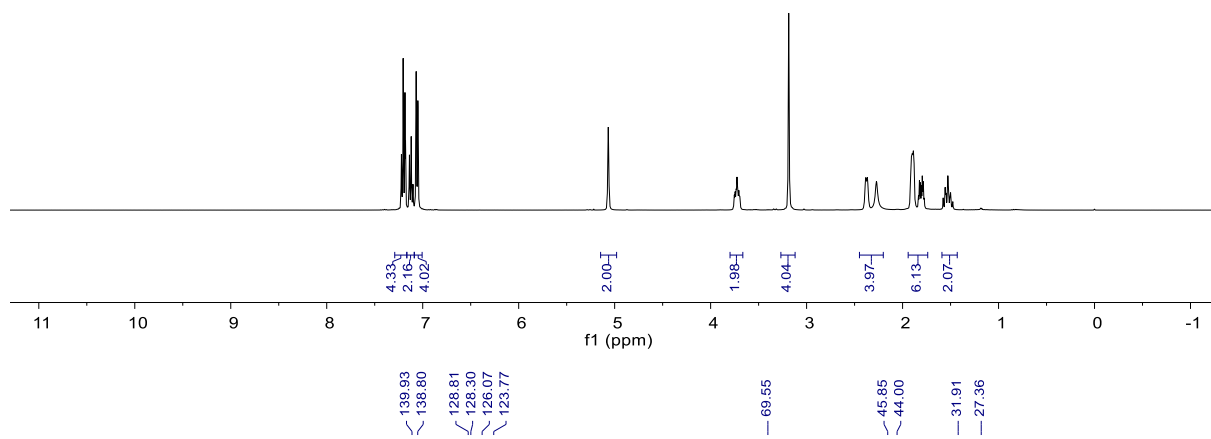
- 139.93
- 138.80
- 128.81
- 128.30
- 126.07
- 123.77
- 69.55
- 45.85
- 44.00
- 31.91
- 27.36

 $^{13}\text{C}$  NMR, 100 MHz,  $\text{CDCl}_3$ 

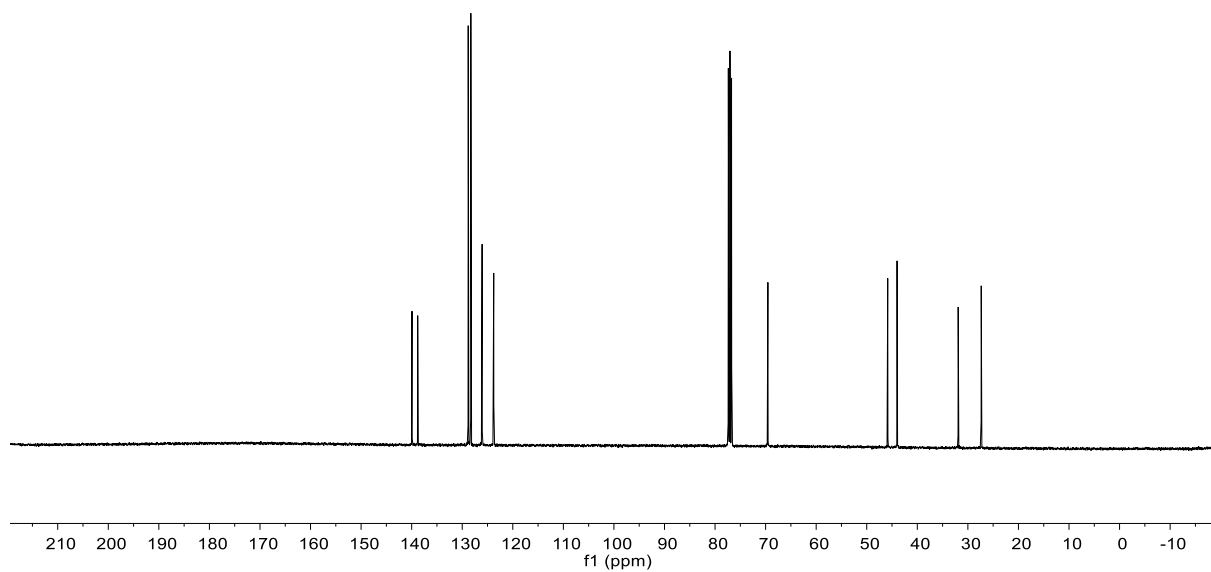


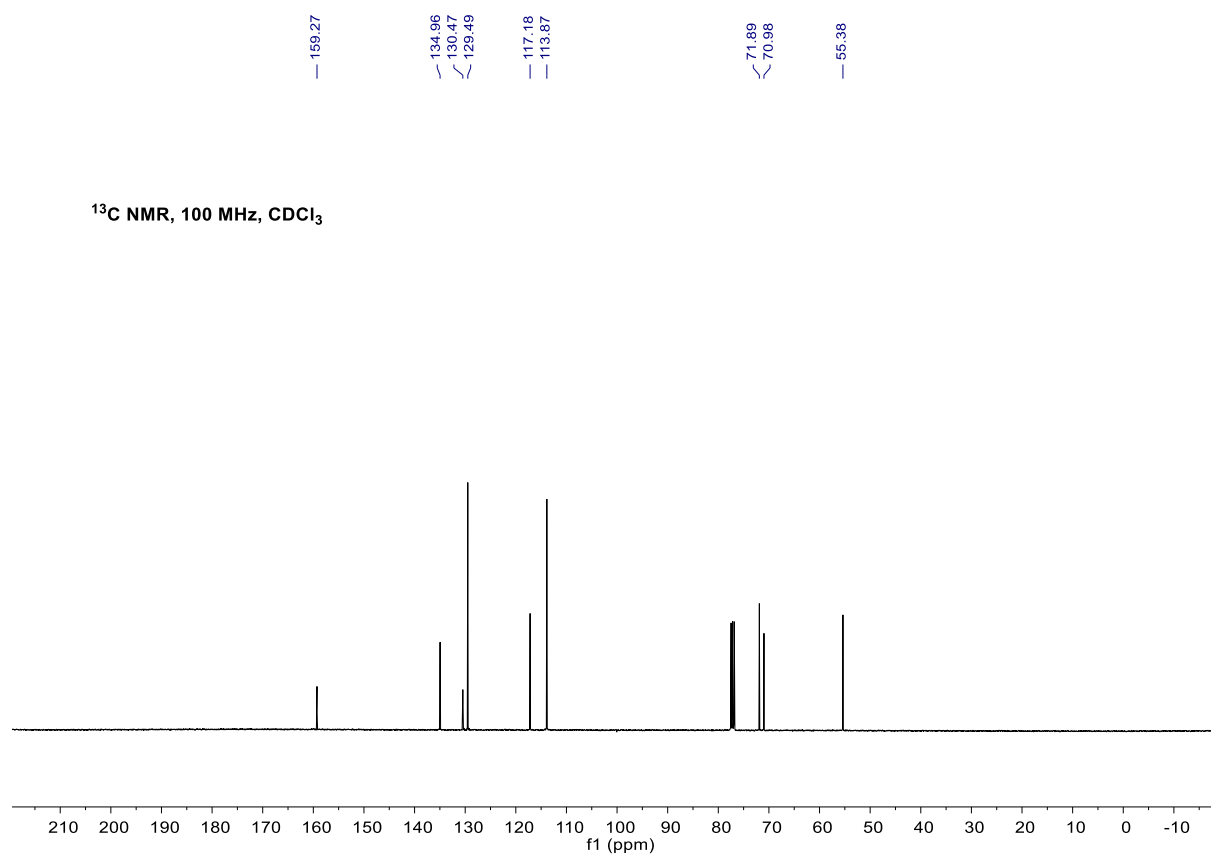
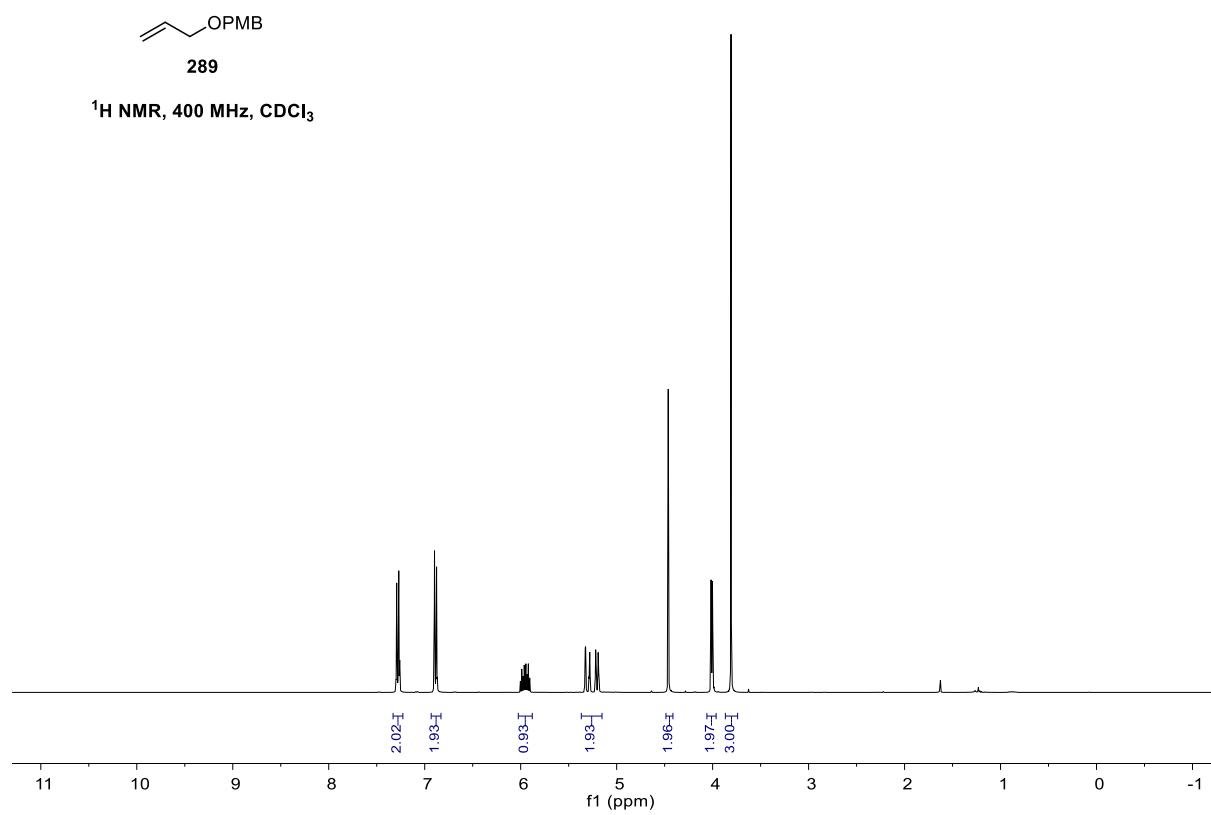
288

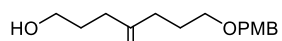
$^1\text{H}$  NMR, 400 MHz,  $\text{CDCl}_3$



$^{13}\text{C}$  NMR, 100 MHz,  $\text{CDCl}_3$

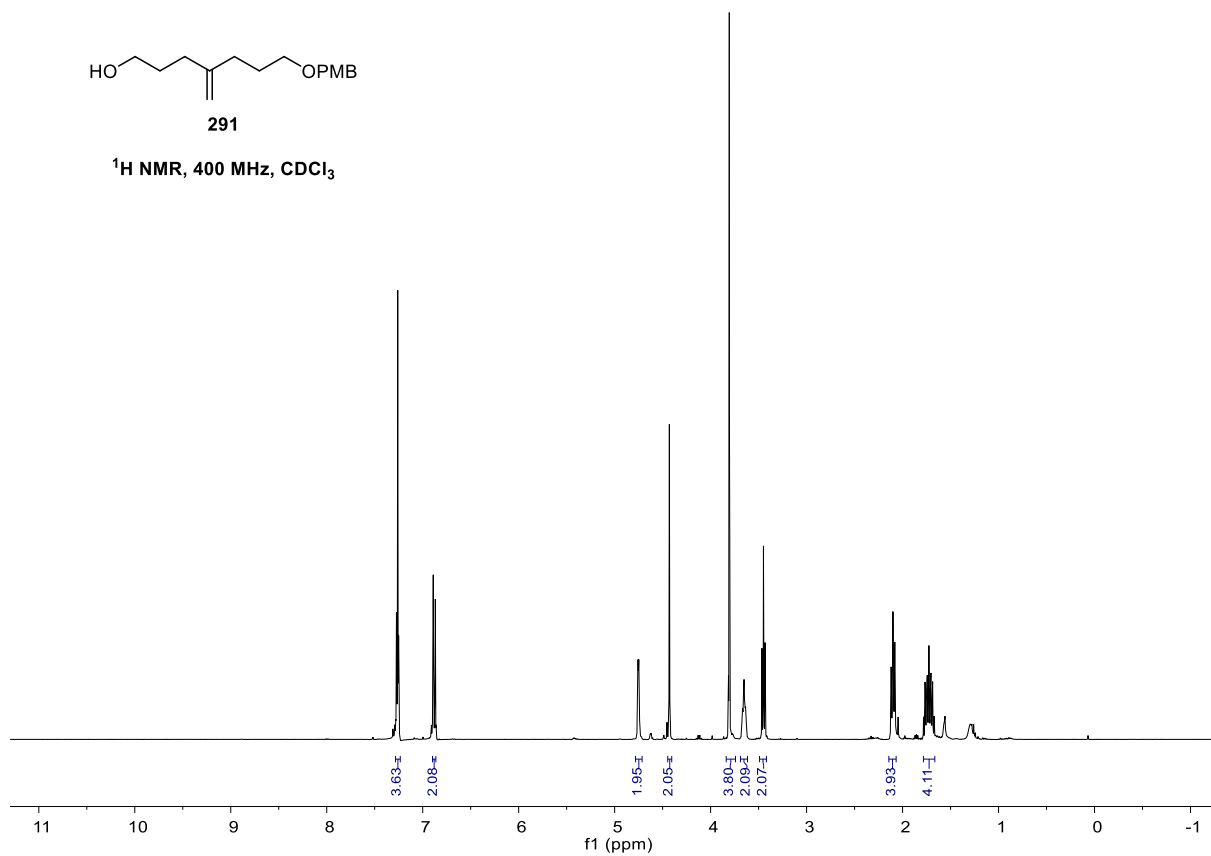




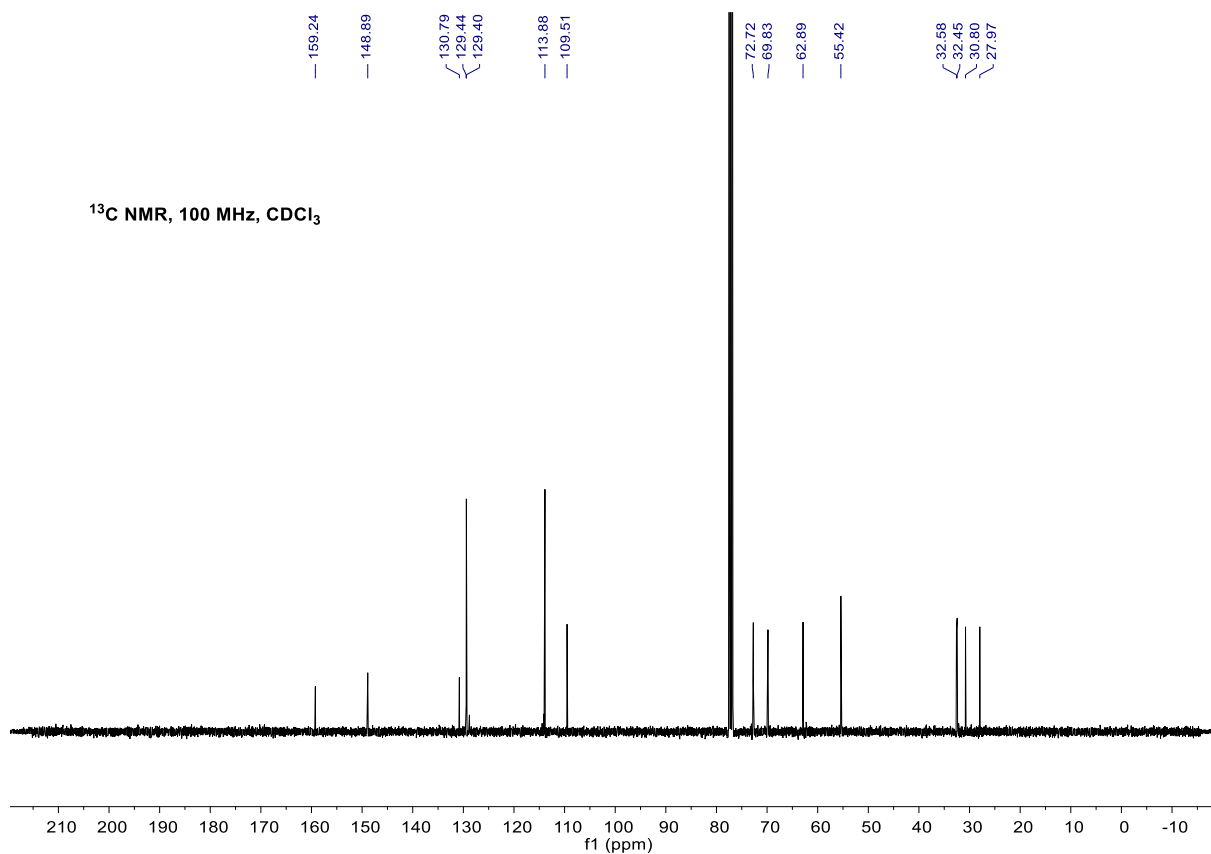


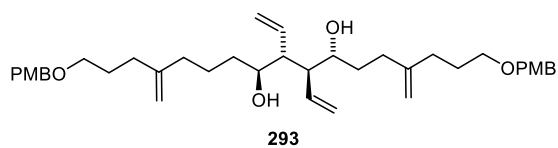
291

<sup>1</sup>H NMR, 400 MHz, CDCl<sub>3</sub>

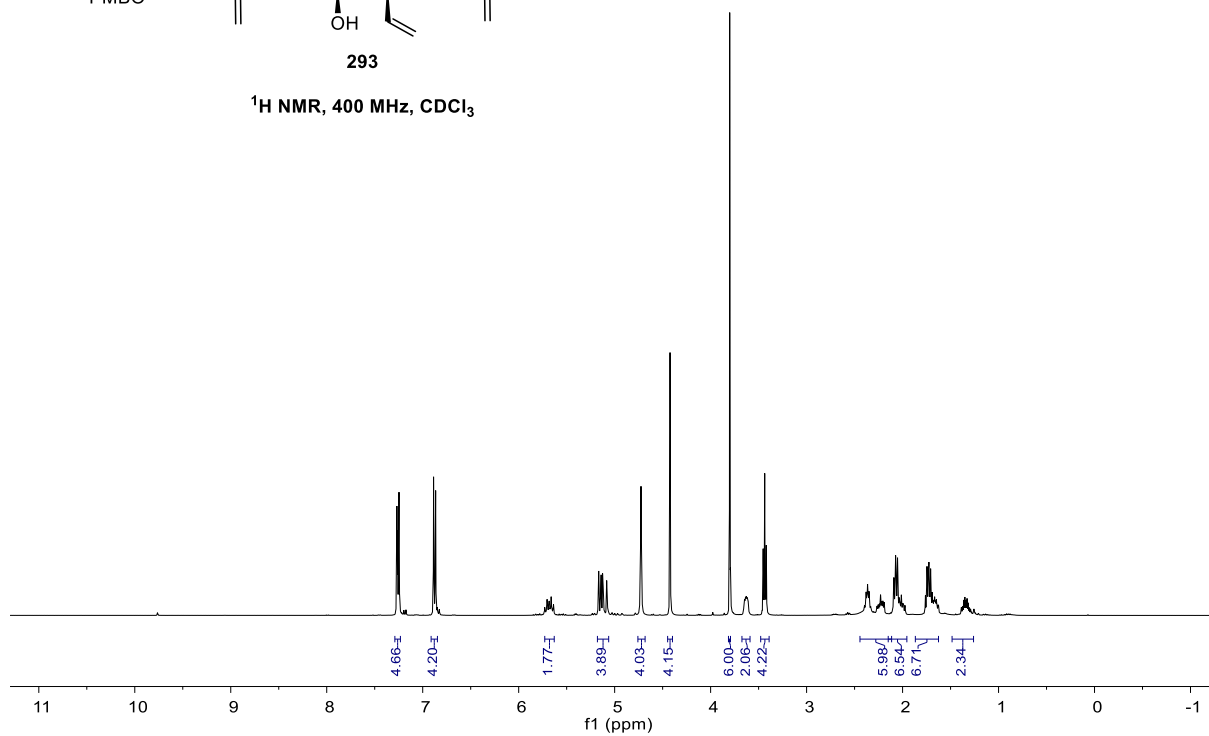


<sup>13</sup>C NMR, 100 MHz, CDCl<sub>3</sub>





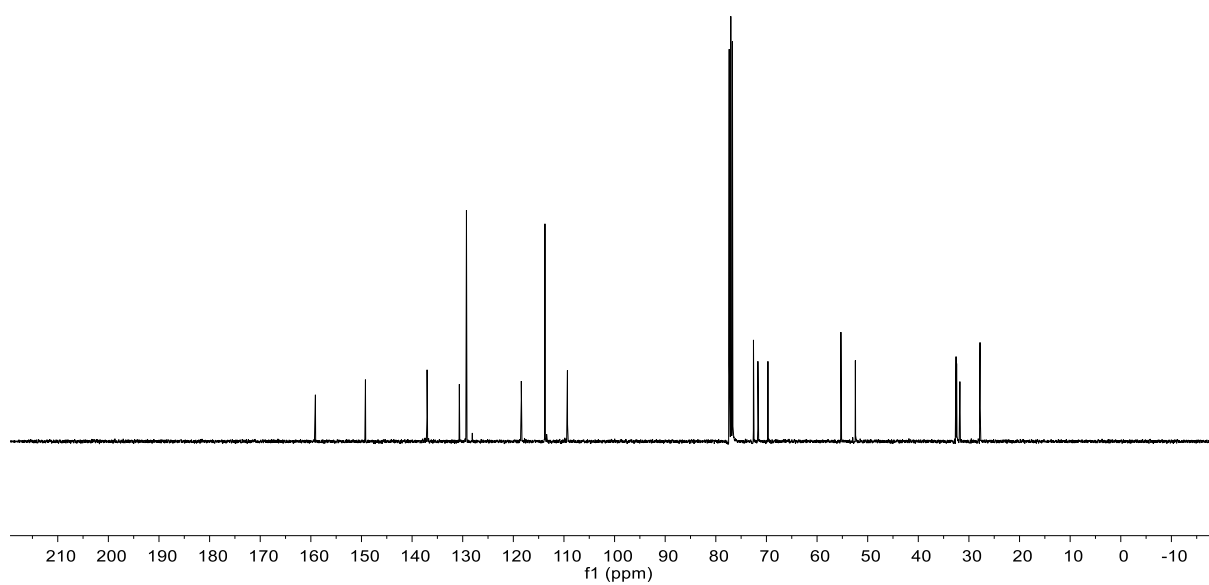
$^1\text{H NMR}$ , 400 MHz,  $\text{CDCl}_3$

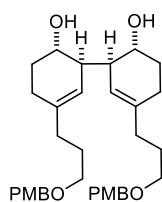


$^{13}\text{C NMR}$  chemical shifts (ppm):

- 159.10
- 149.22
- 137.04
- 130.67
- 129.26
- 118.42
- 113.75
- 109.31
- 72.56
- 71.69
- 69.71
- 55.29
- 52.43
- 32.54
- 32.43
- 31.78
- 27.80

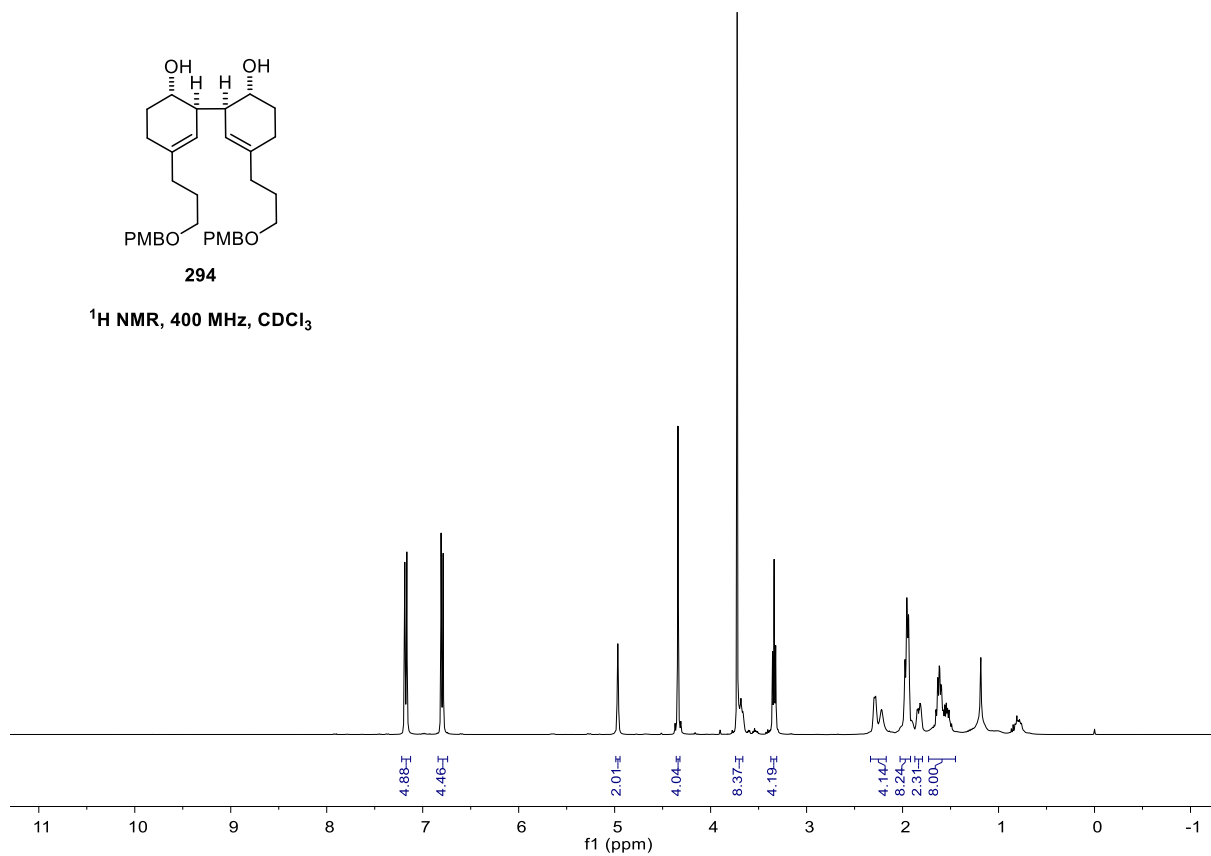
$^{13}\text{C NMR}$ , 100 MHz,  $\text{CDCl}_3$



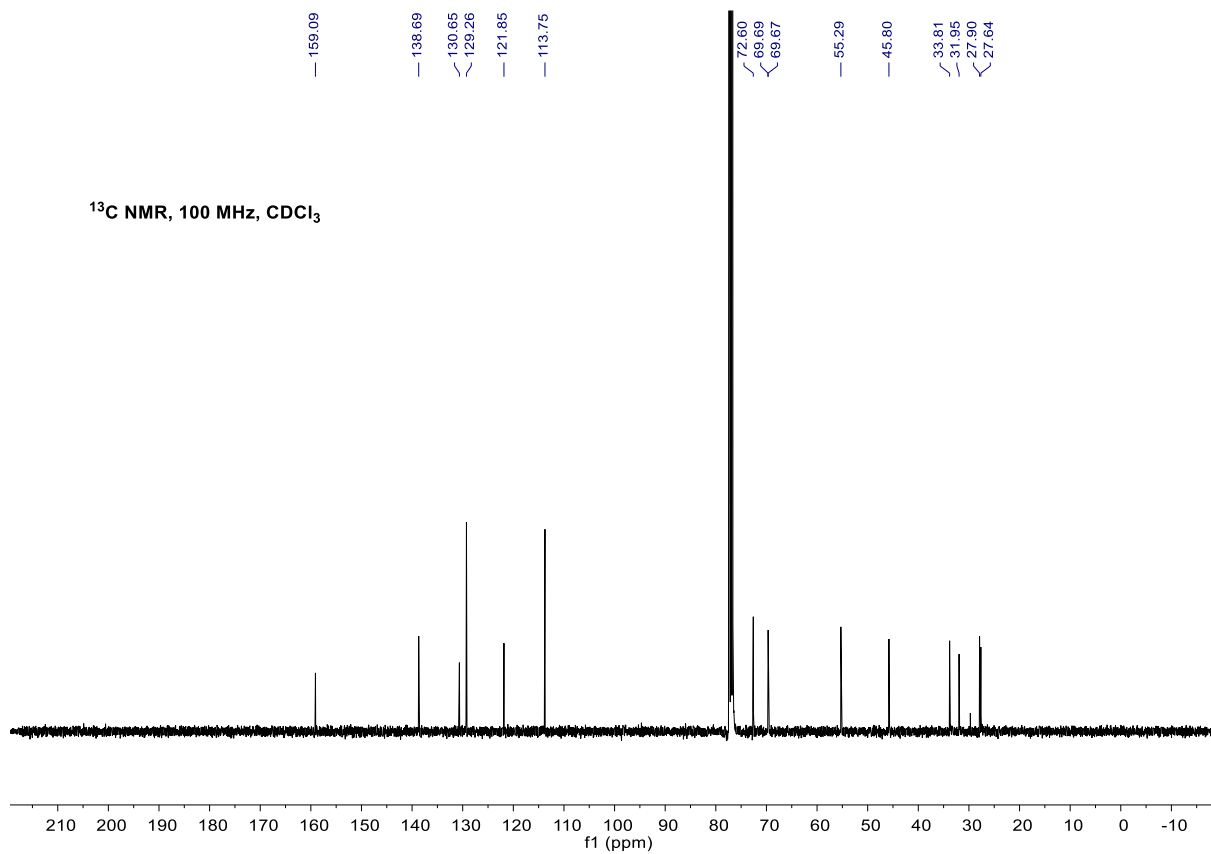


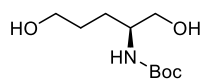
294

$^1\text{H}$  NMR, 400 MHz,  $\text{CDCl}_3$

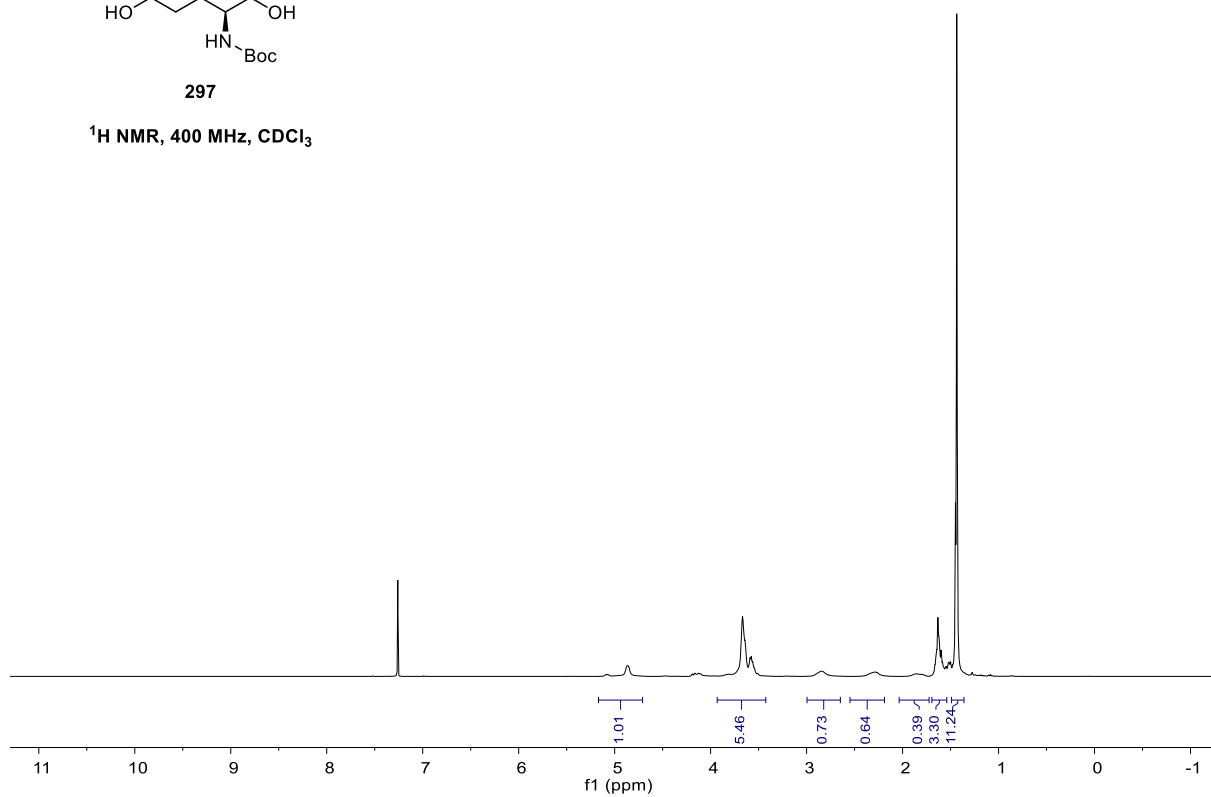
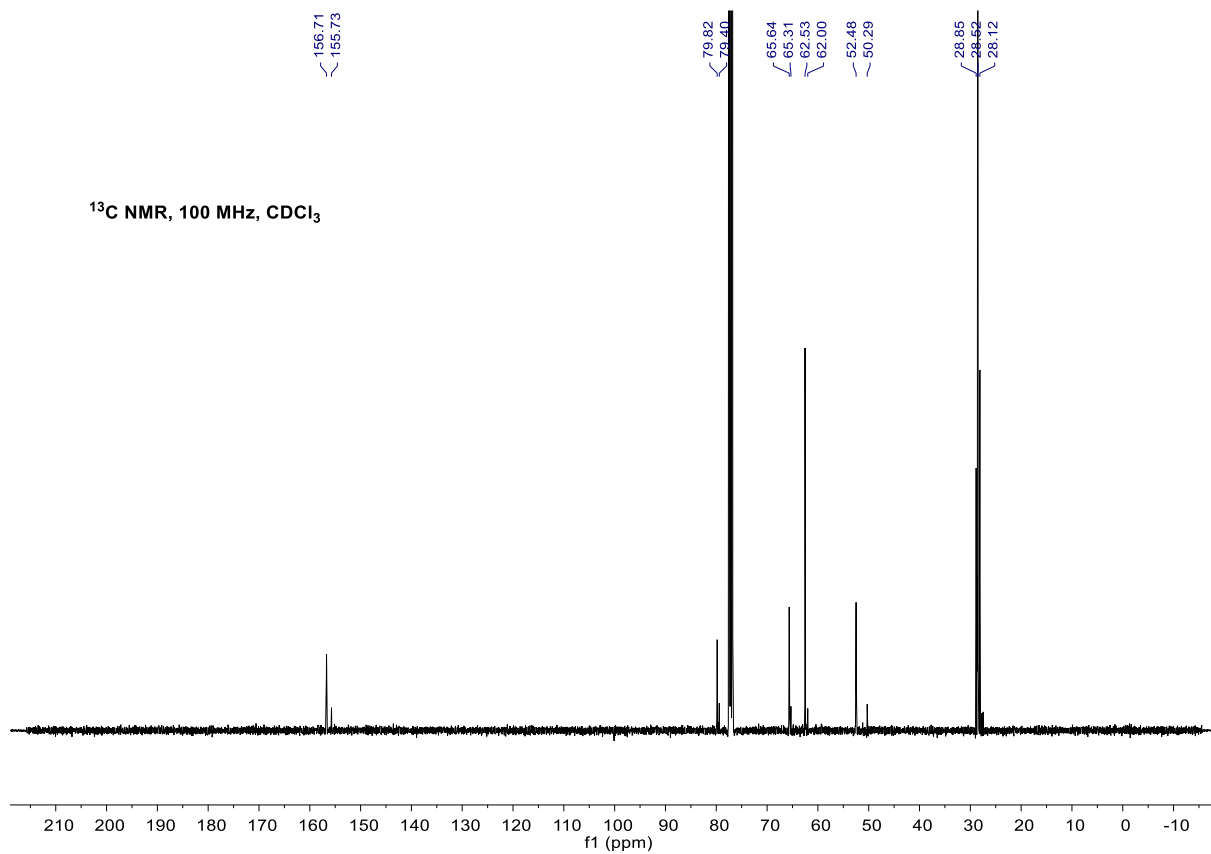


$^{13}\text{C}$  NMR, 100 MHz,  $\text{CDCl}_3$

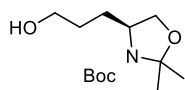




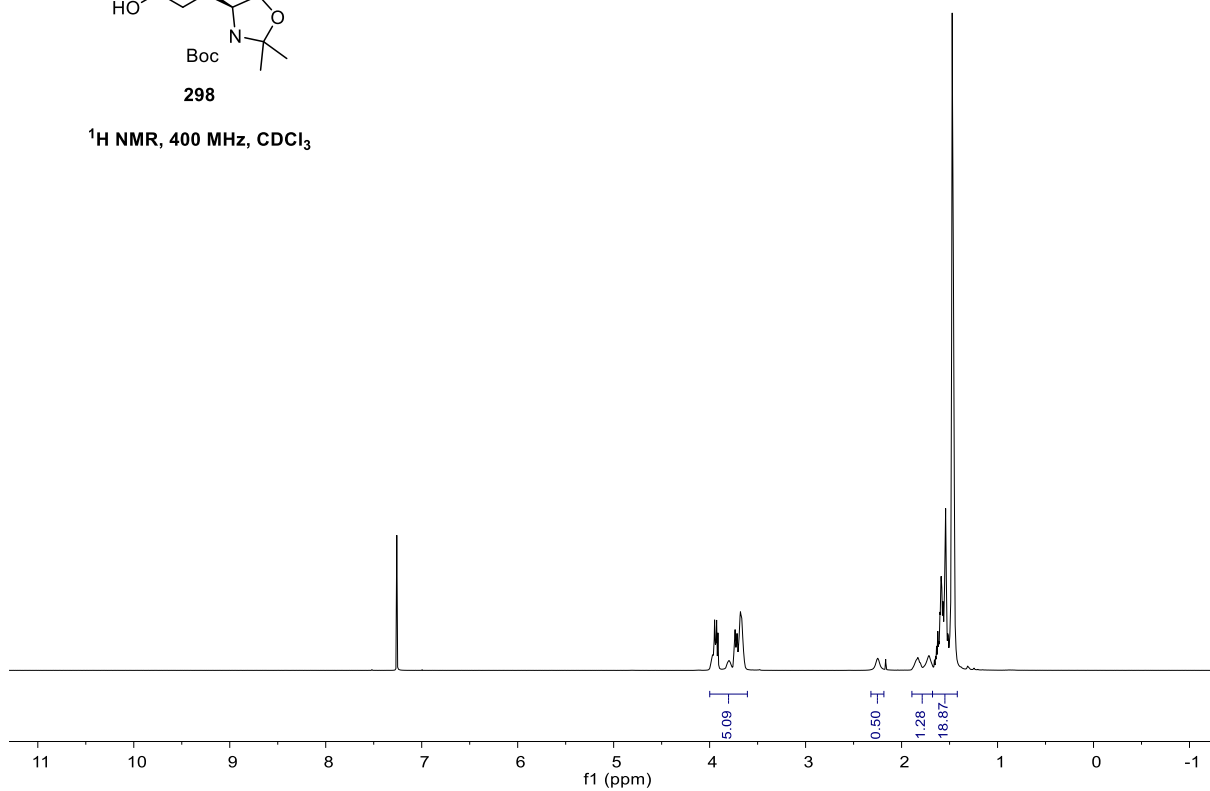
297

 $^1\text{H}$  NMR, 400 MHz,  $\text{CDCl}_3$  $^{13}\text{C}$  NMR, 100 MHz,  $\text{CDCl}_3$ 

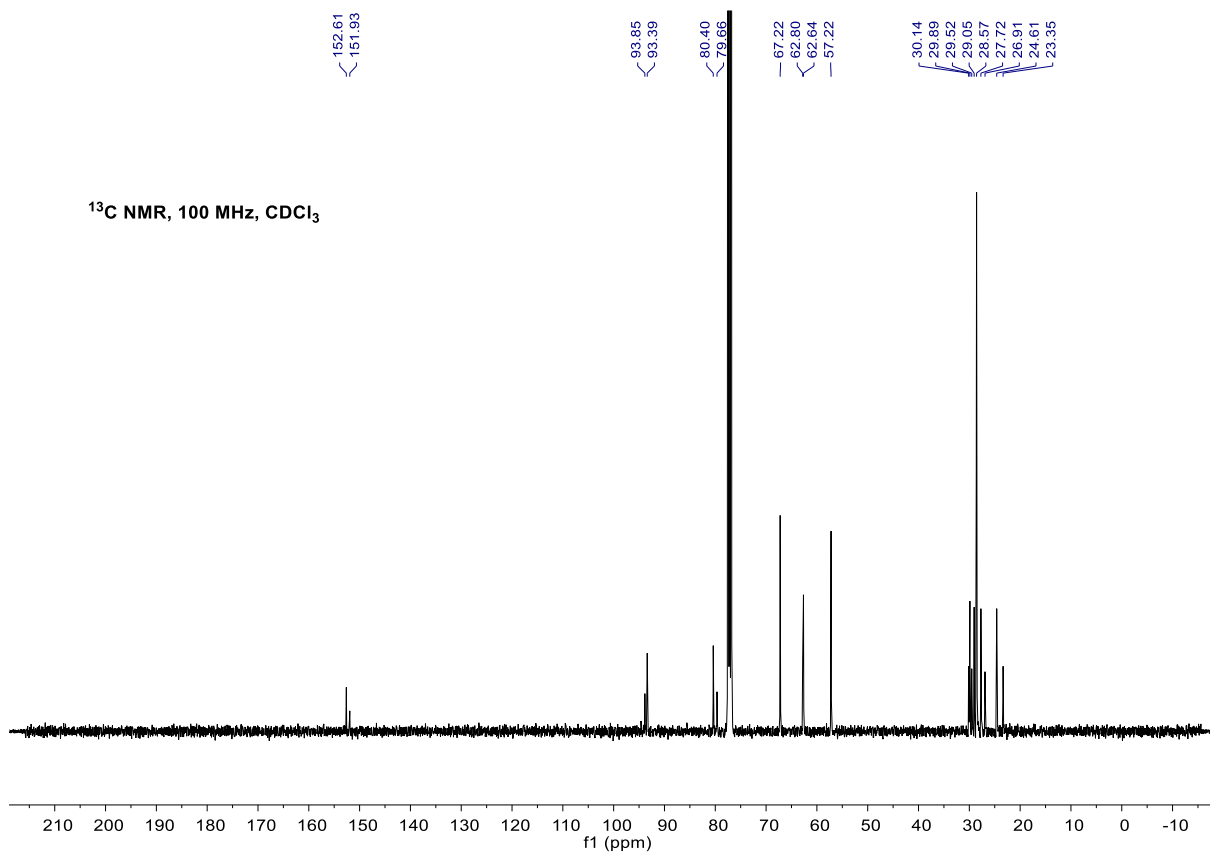
Part II: NMR Spectra

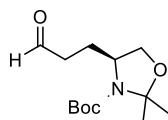


<sup>1</sup>H NMR, 400 MHz, CDCl<sub>3</sub>

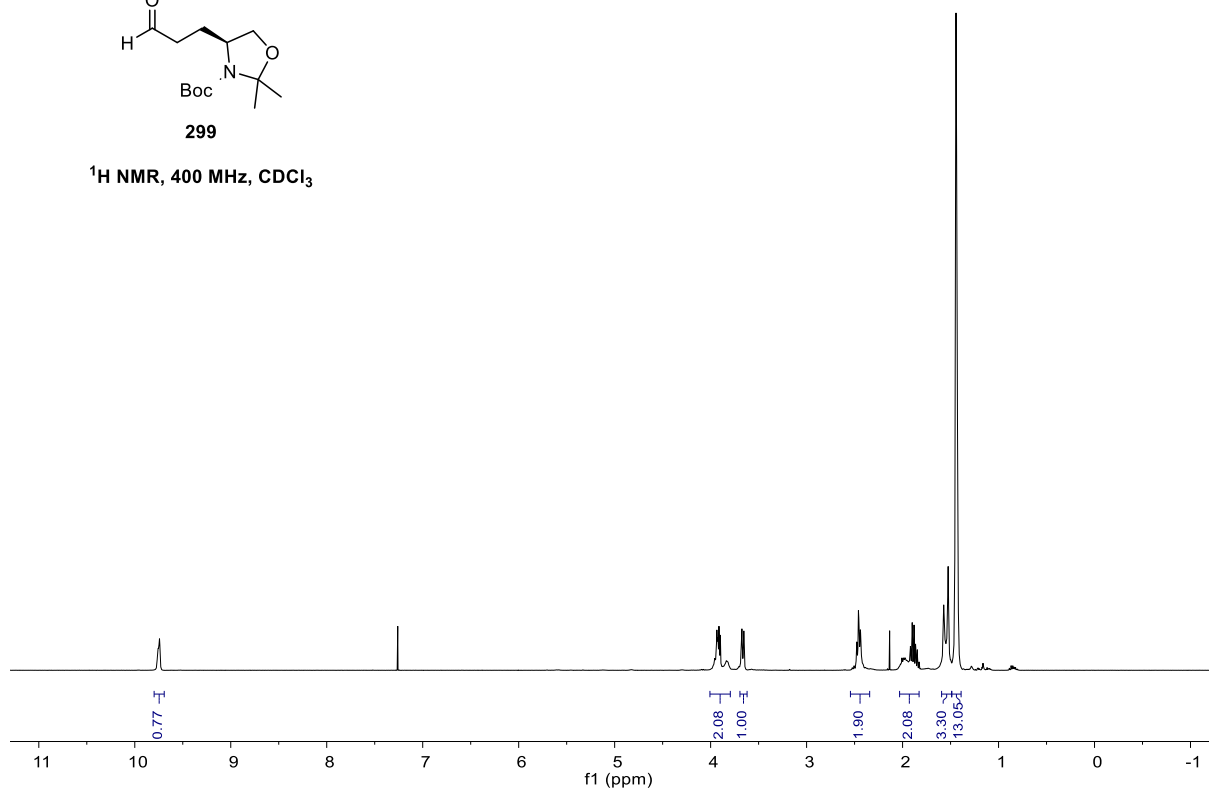


<sup>13</sup>C NMR, 100 MHz, CDCl<sub>3</sub>



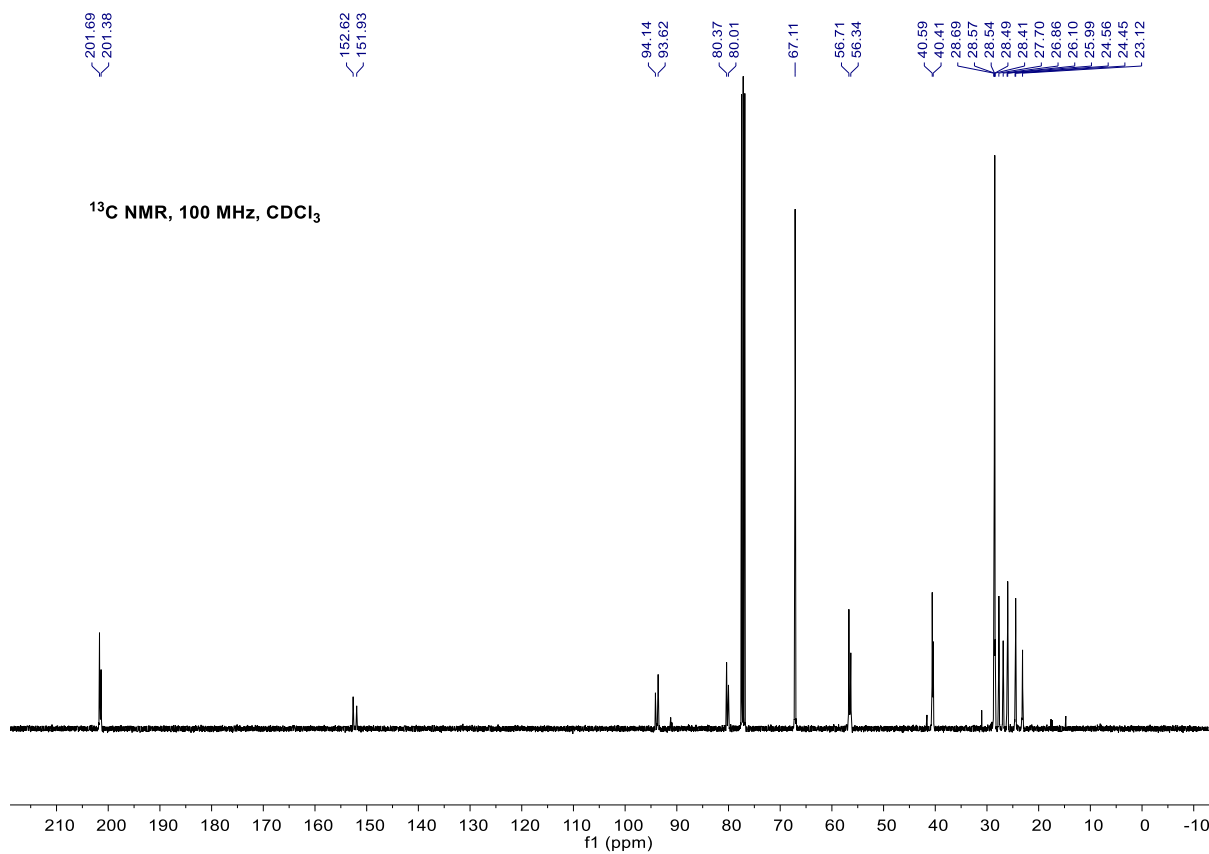


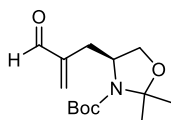
299

 $^1\text{H}$  NMR, 400 MHz,  $\text{CDCl}_3$ 

$^{13}\text{C}$  NMR, 100 MHz,  $\text{CDCl}_3$

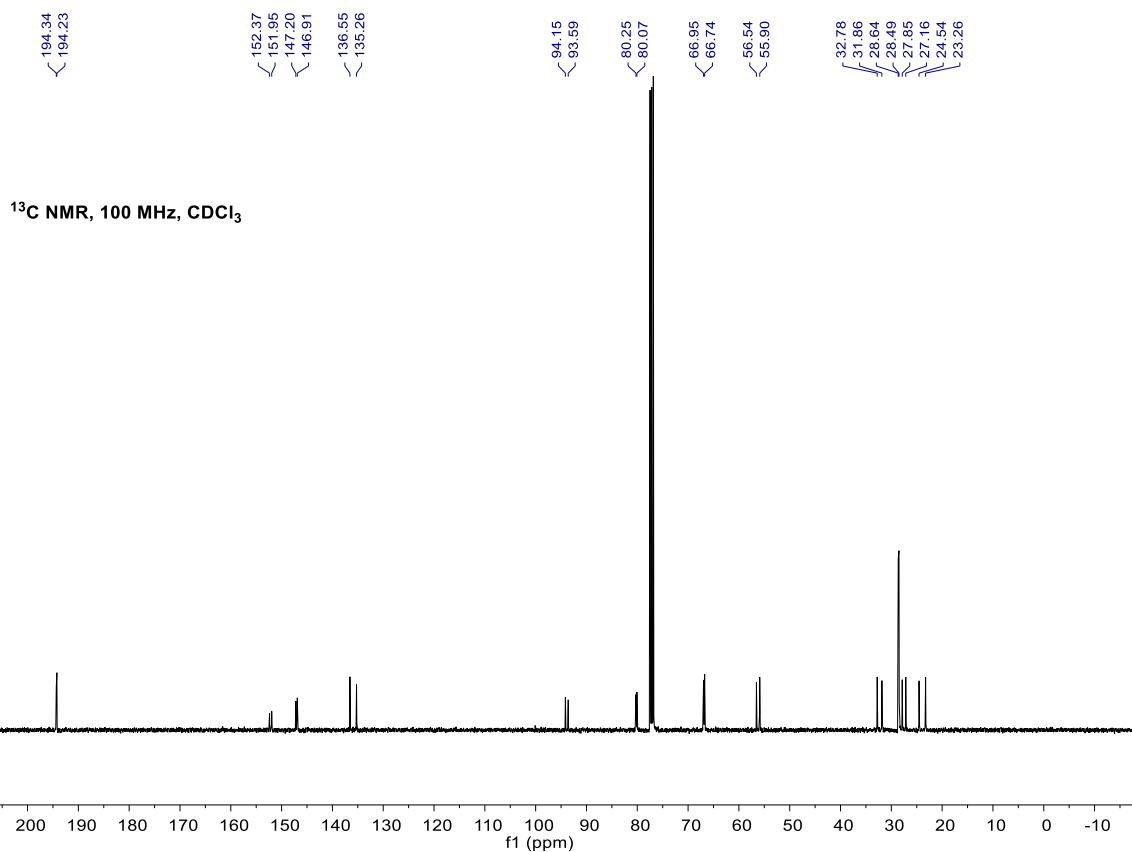
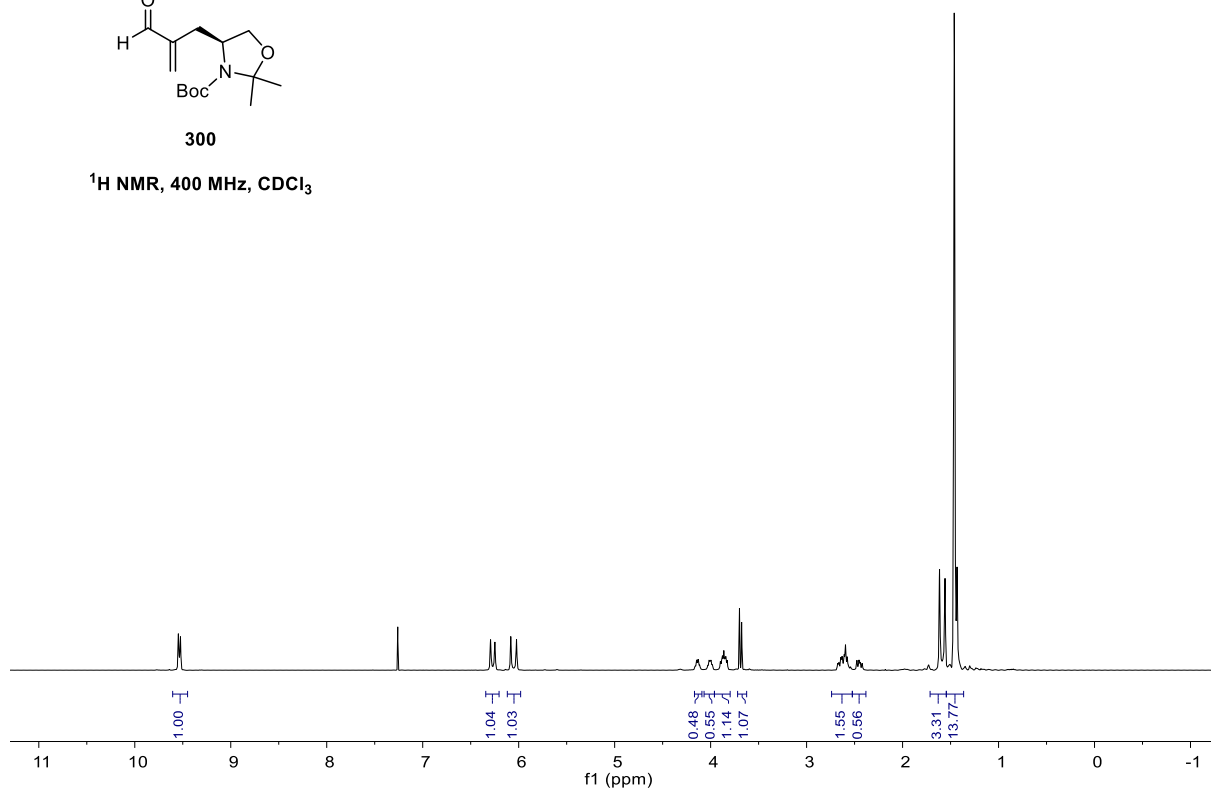
Chemical Shift (ppm)
201.69
201.38
152.62
151.93
94.14
93.62
80.37
80.01
67.11
56.71
56.34
40.59
40.41
28.69
28.57
28.54
28.49
28.41
27.70
26.86
26.10
25.99
24.56
24.45
23.12

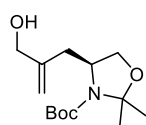




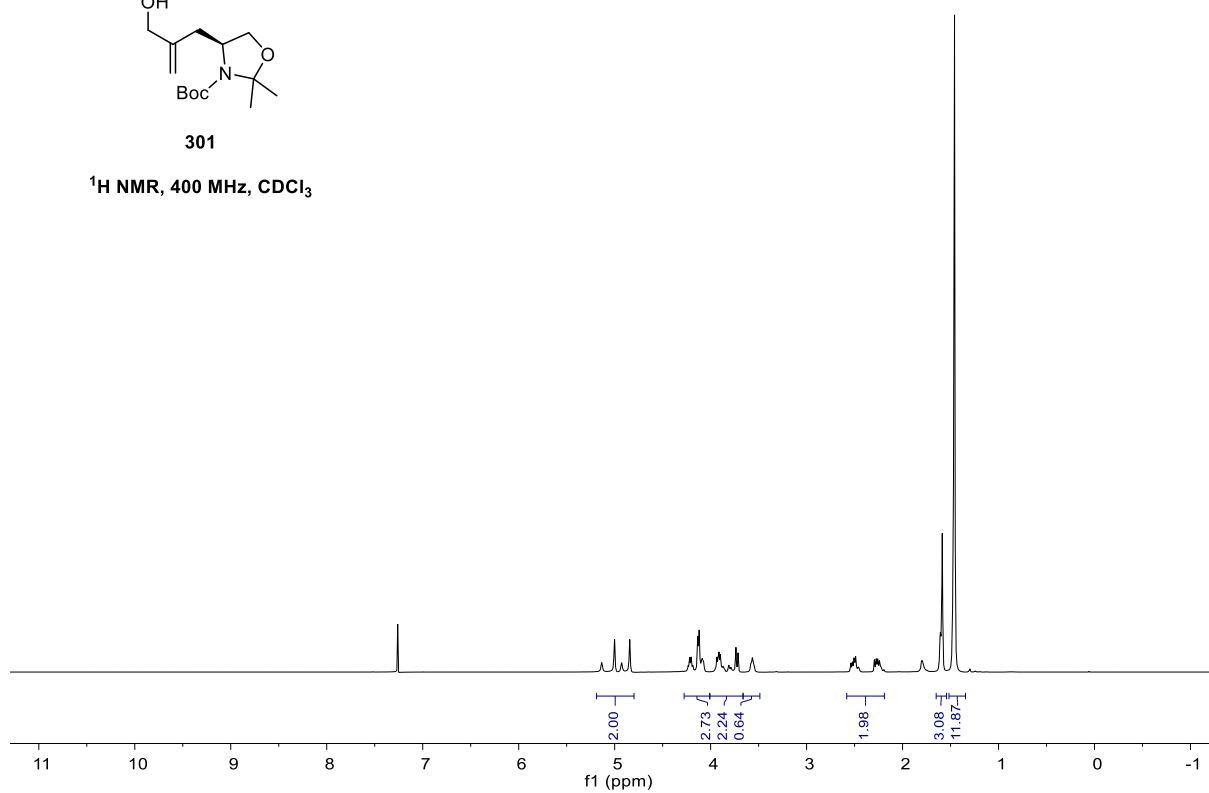
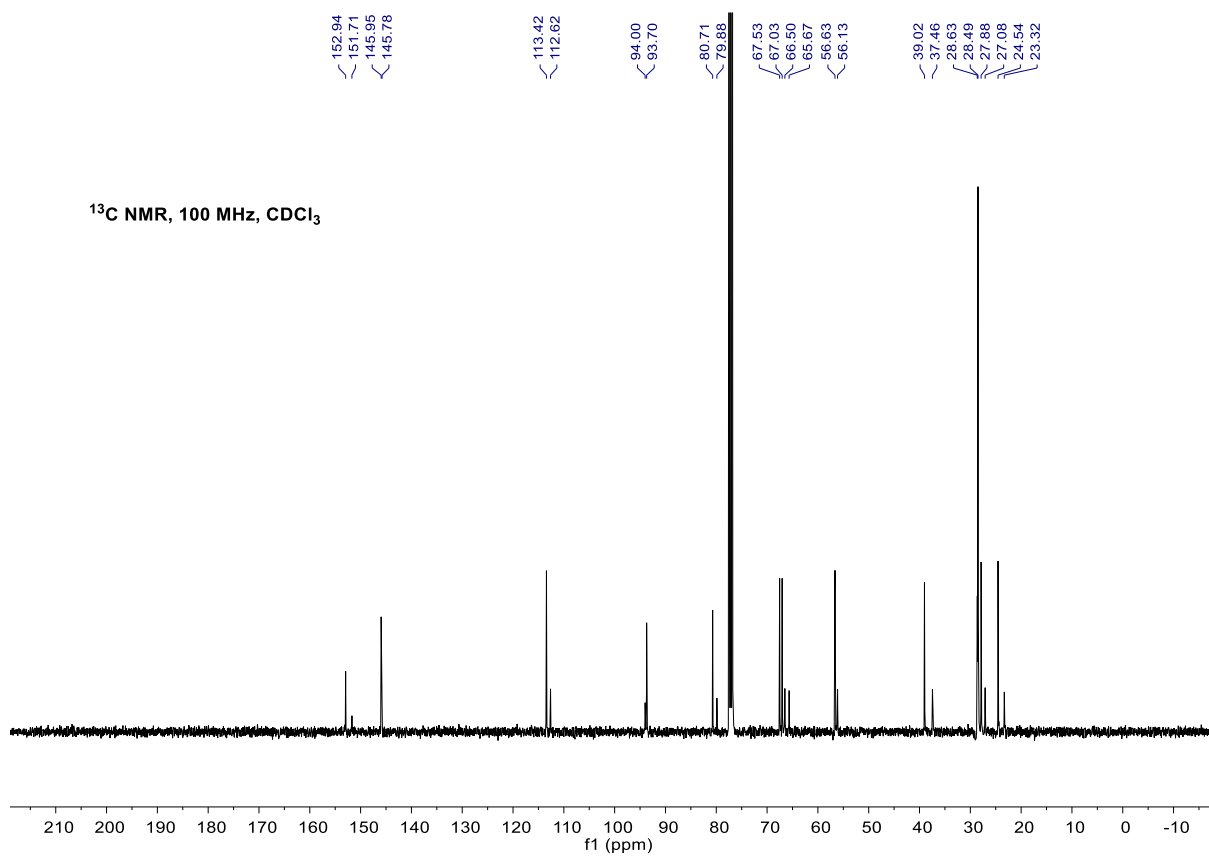
300

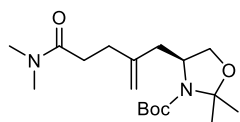
<sup>1</sup>H NMR, 400 MHz, CDCl<sub>3</sub>





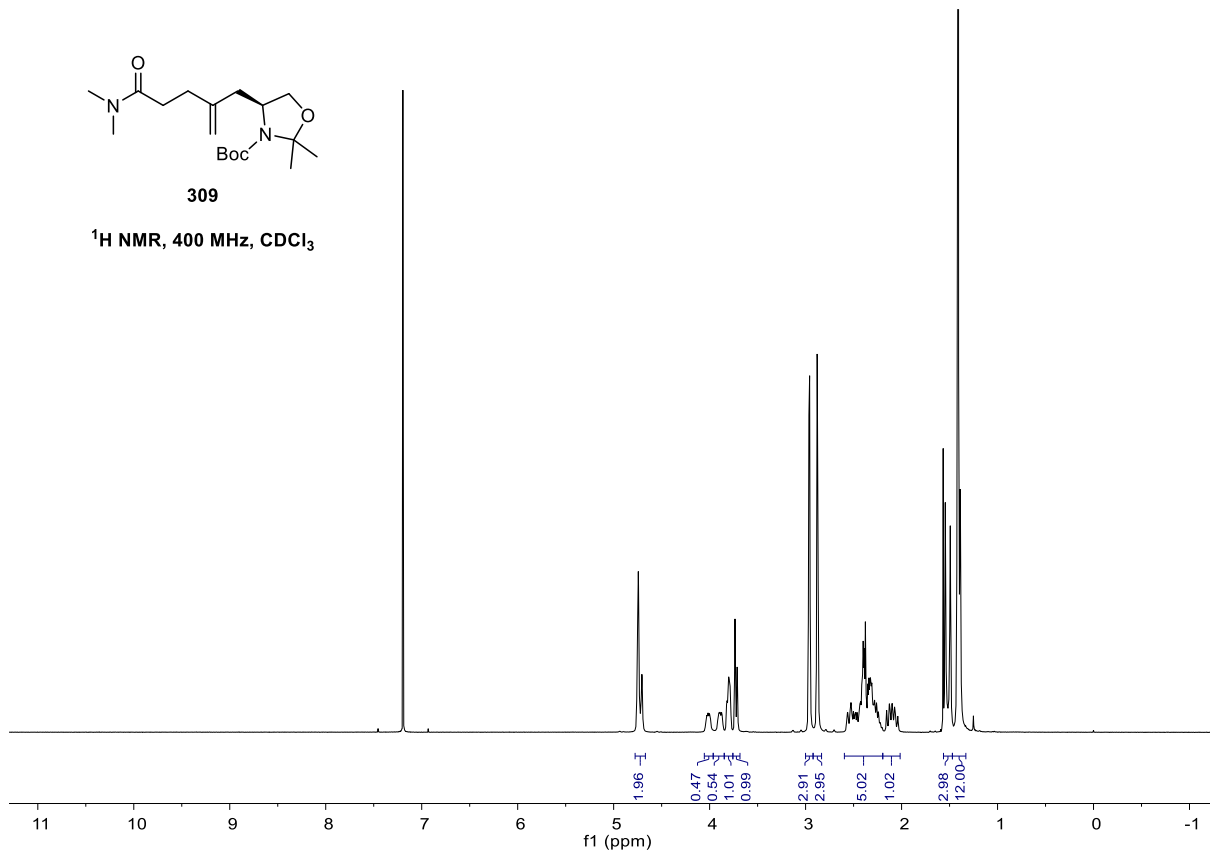
301

 $^1\text{H}$  NMR, 400 MHz,  $\text{CDCl}_3$  $^{13}\text{C}$  NMR, 100 MHz,  $\text{CDCl}_3$ 

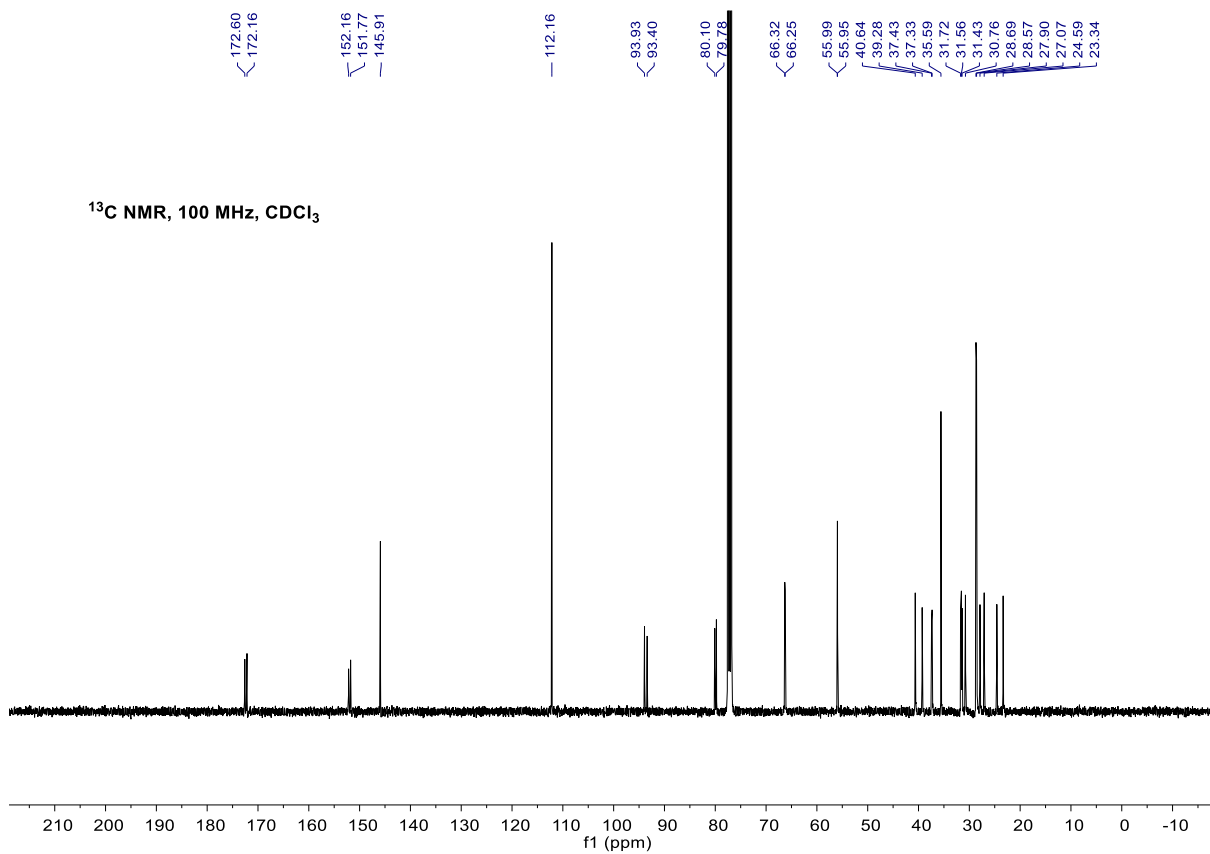


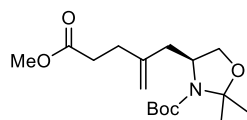
309

<sup>1</sup>H NMR, 400 MHz, CDCl<sub>3</sub>

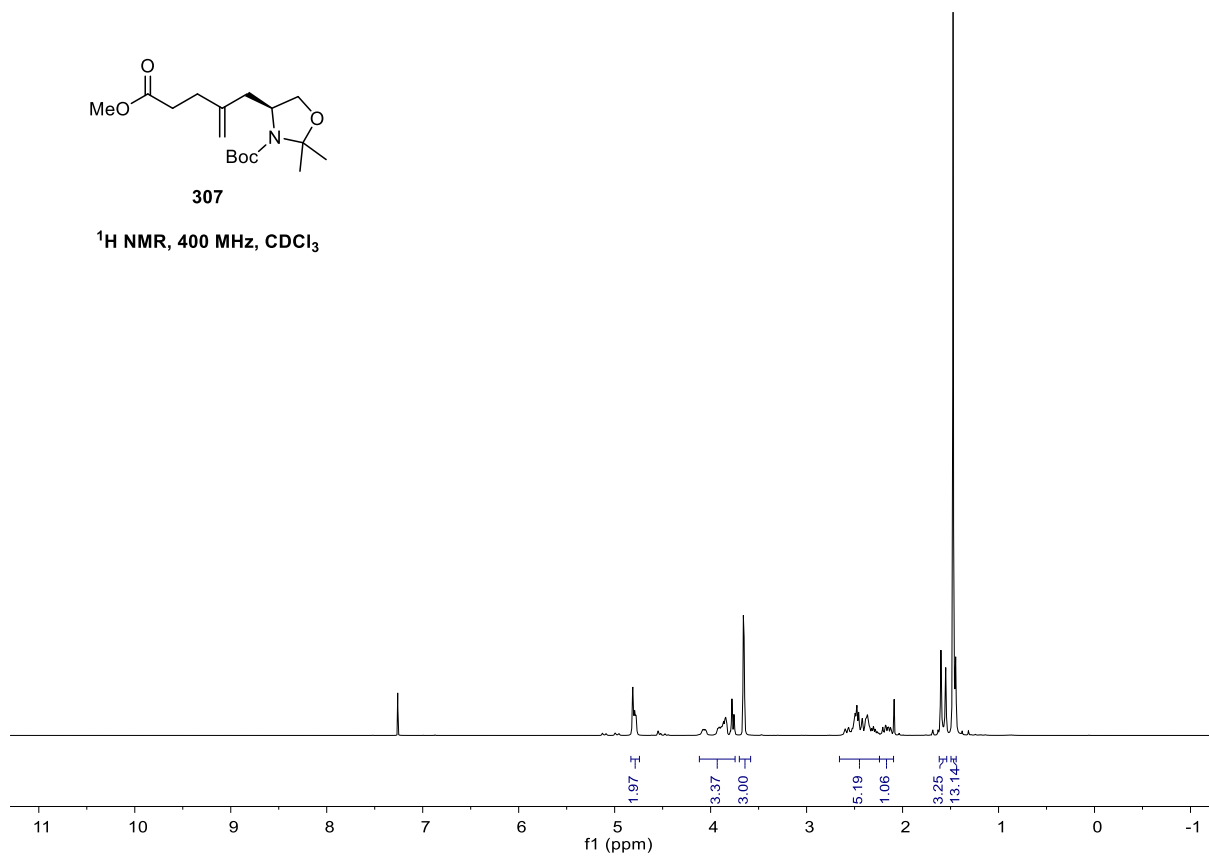
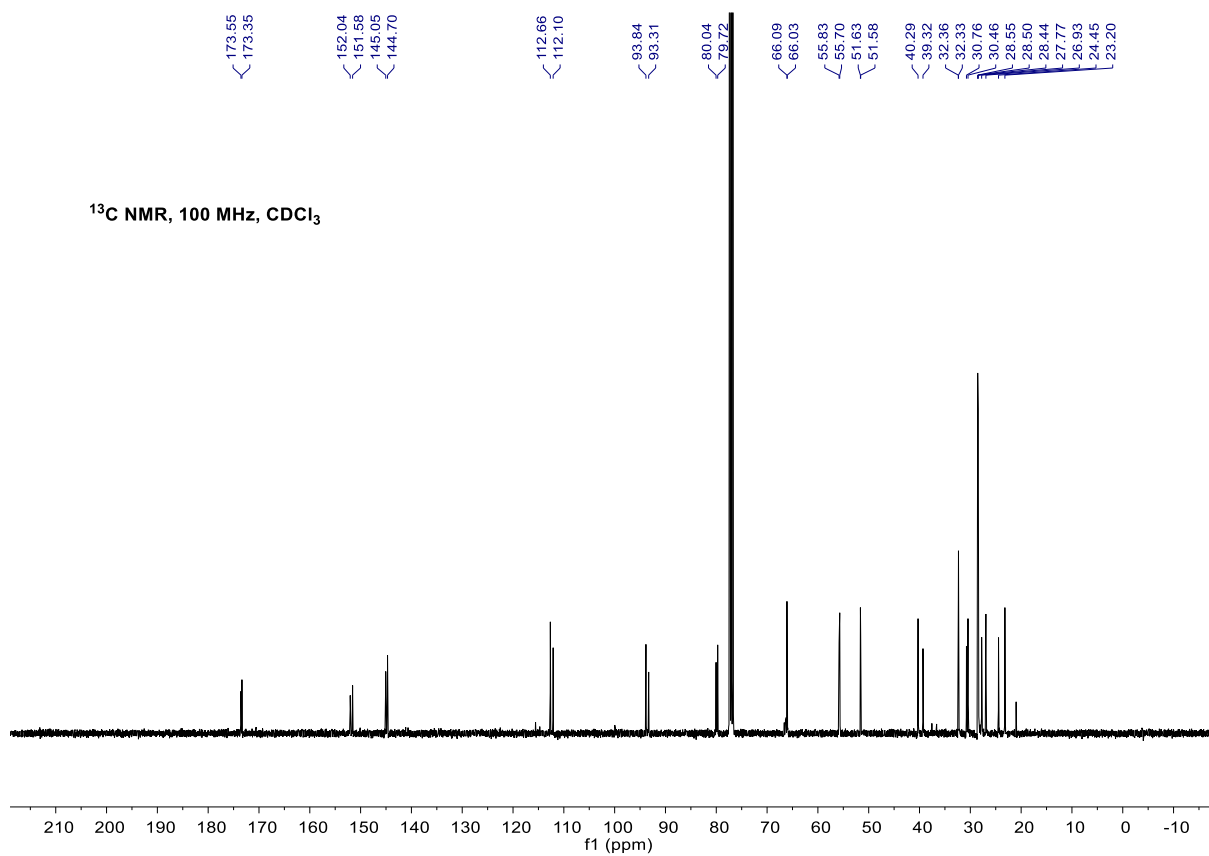


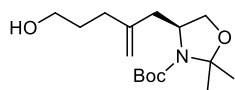
<sup>13</sup>C NMR, 100 MHz, CDCl<sub>3</sub>





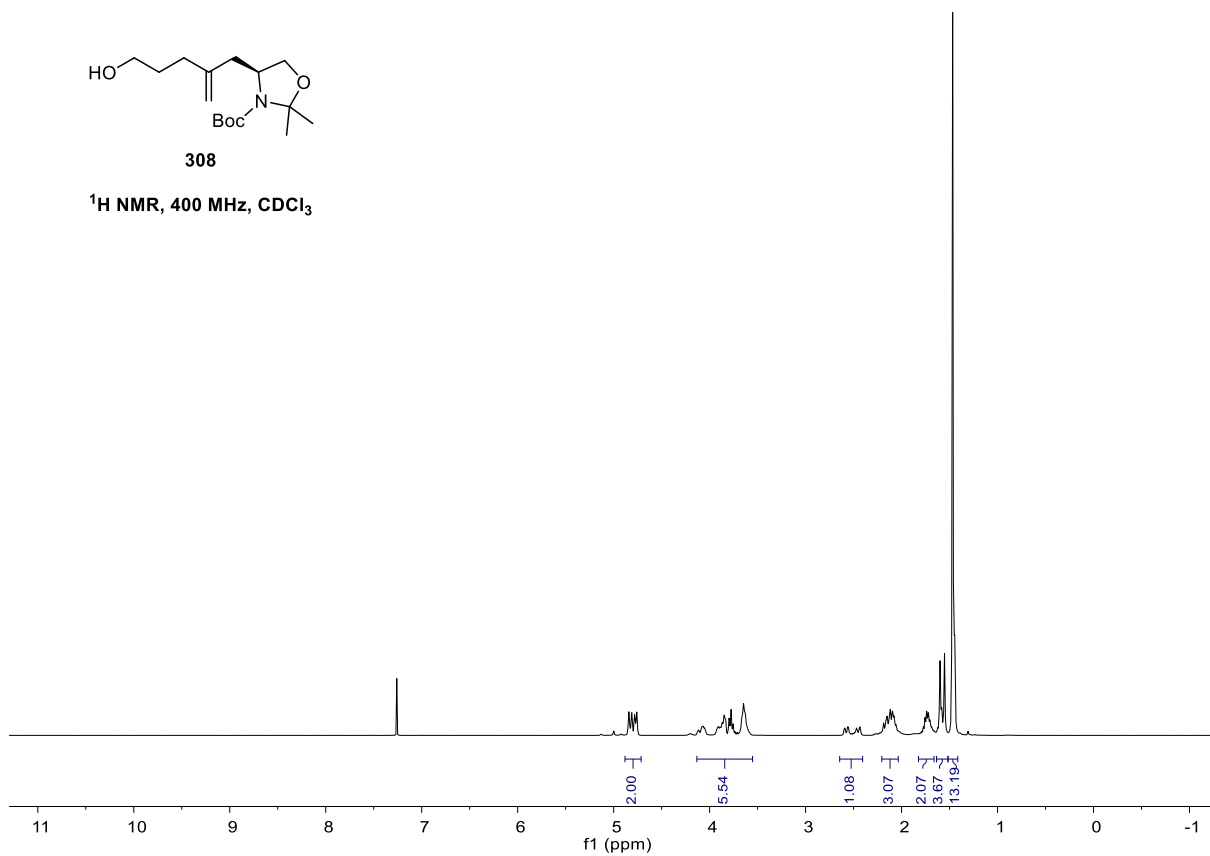
307

 $^1\text{H}$  NMR, 400 MHz,  $\text{CDCl}_3$  $^{13}\text{C}$  NMR, 100 MHz,  $\text{CDCl}_3$ 

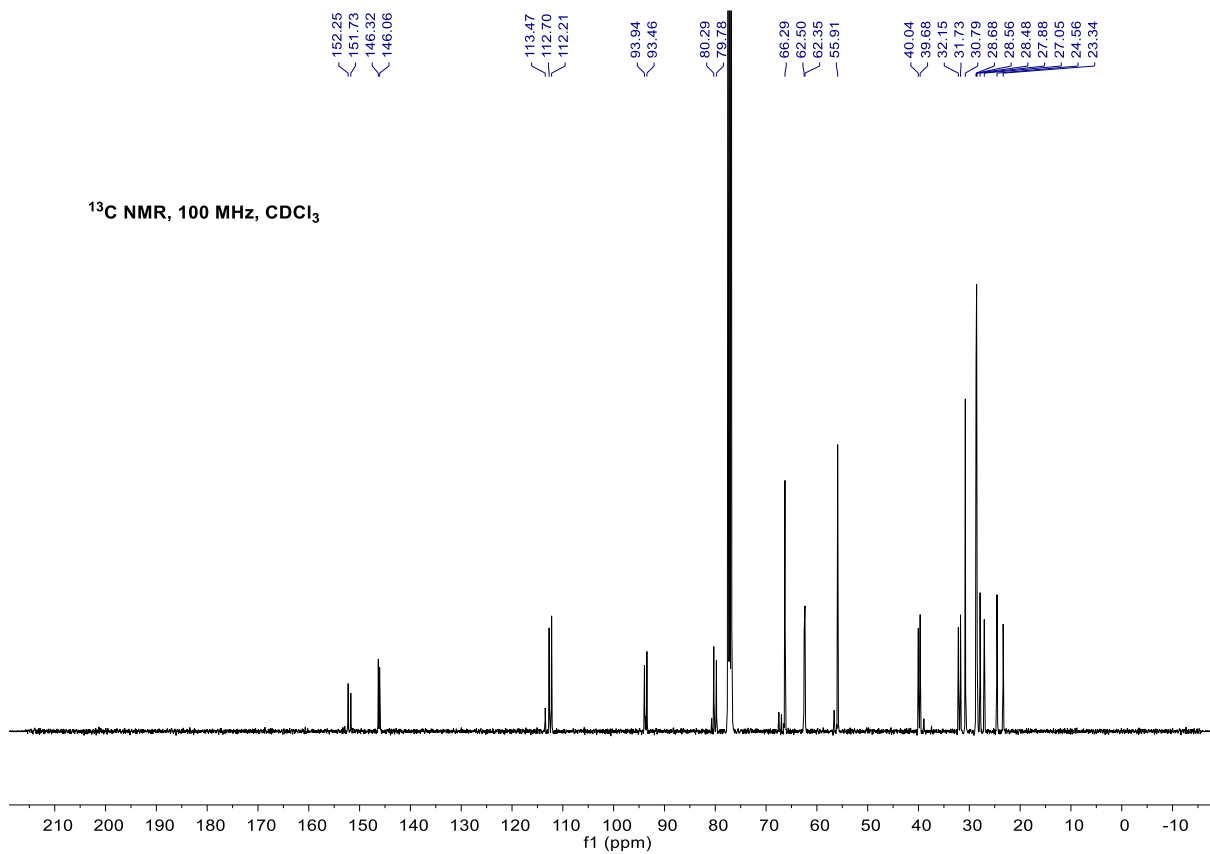


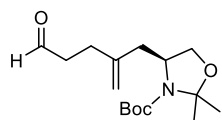
308

$^1\text{H}$  NMR, 400 MHz,  $\text{CDCl}_3$

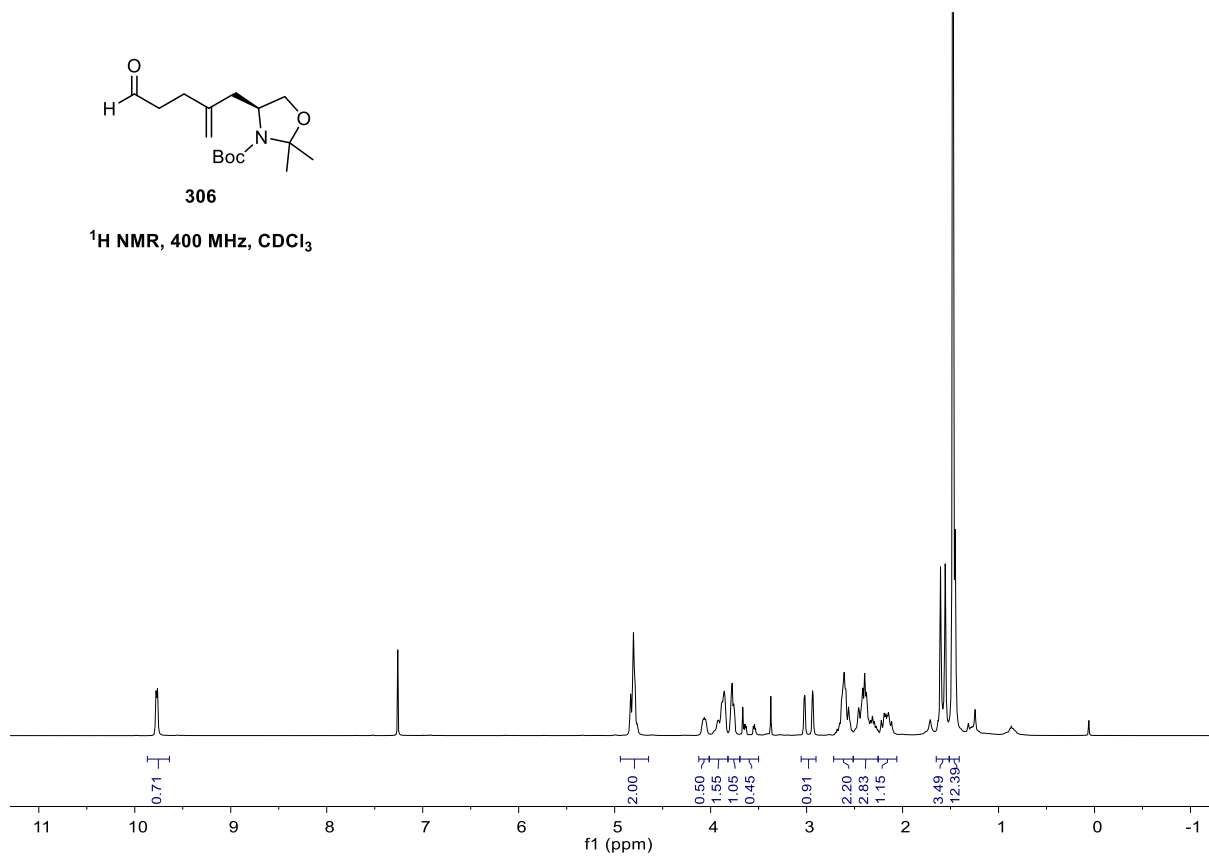
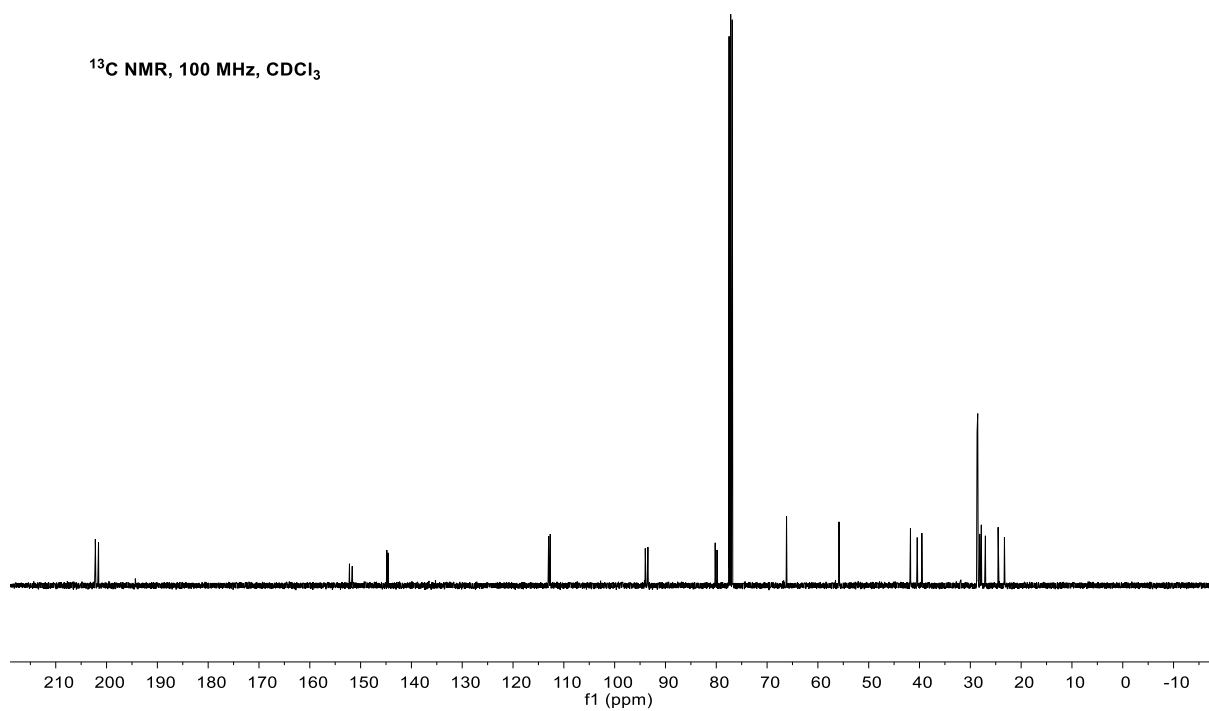


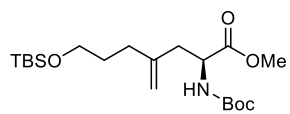
$^{13}\text{C}$  NMR, 100 MHz,  $\text{CDCl}_3$





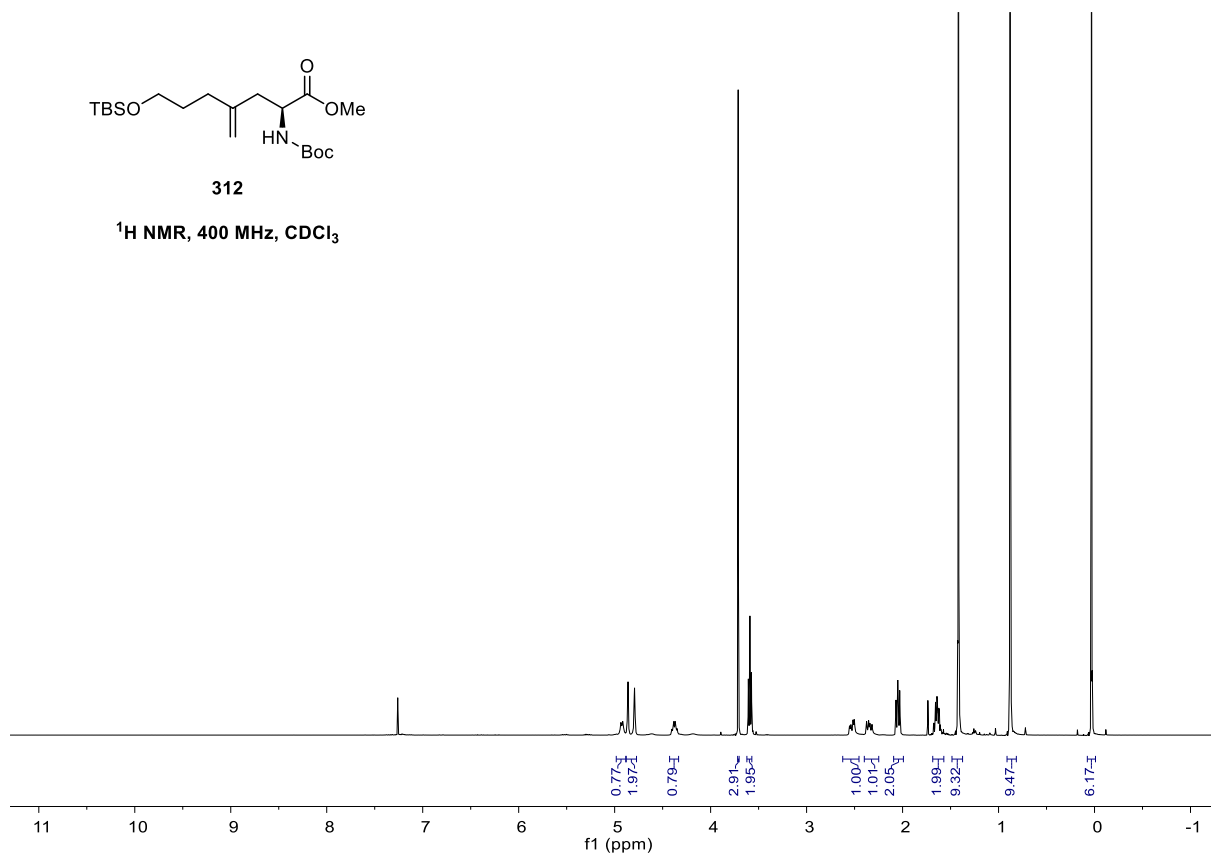
306

 $^1\text{H}$  NMR, 400 MHz,  $\text{CDCl}_3$ 202.21  
201.58152.19  
151.65  
144.83  
144.57113.00  
112.6893.97  
93.4580.21  
79.8566.20  
66.1755.85  
55.8041.86  
41.78  
40.45  
39.5428.68  
28.63  
28.54  
28.48  
28.15  
27.88  
27.84  
27.04  
24.53  
23.29 $^{13}\text{C}$  NMR, 100 MHz,  $\text{CDCl}_3$ 

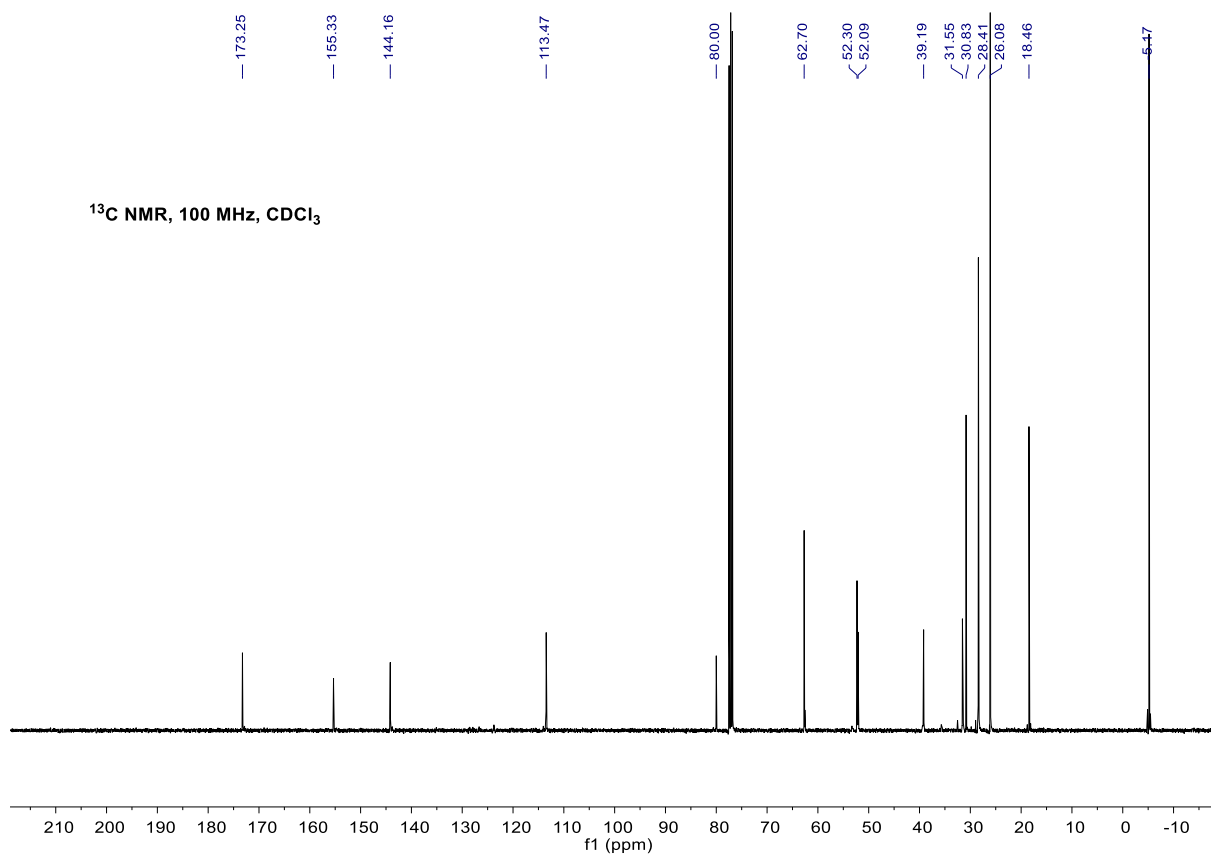


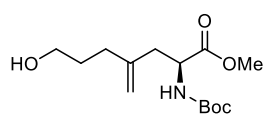
312

<sup>1</sup>H NMR, 400 MHz, CDCl<sub>3</sub>

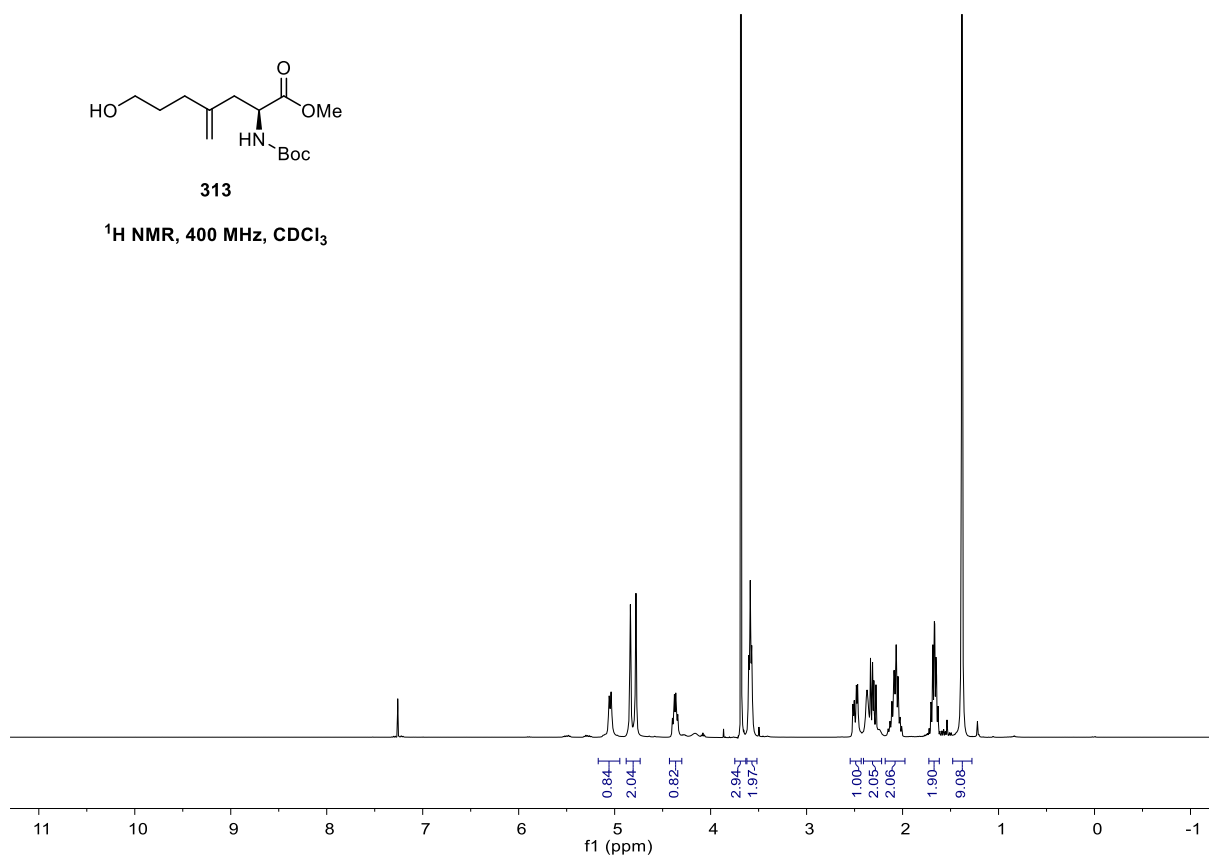
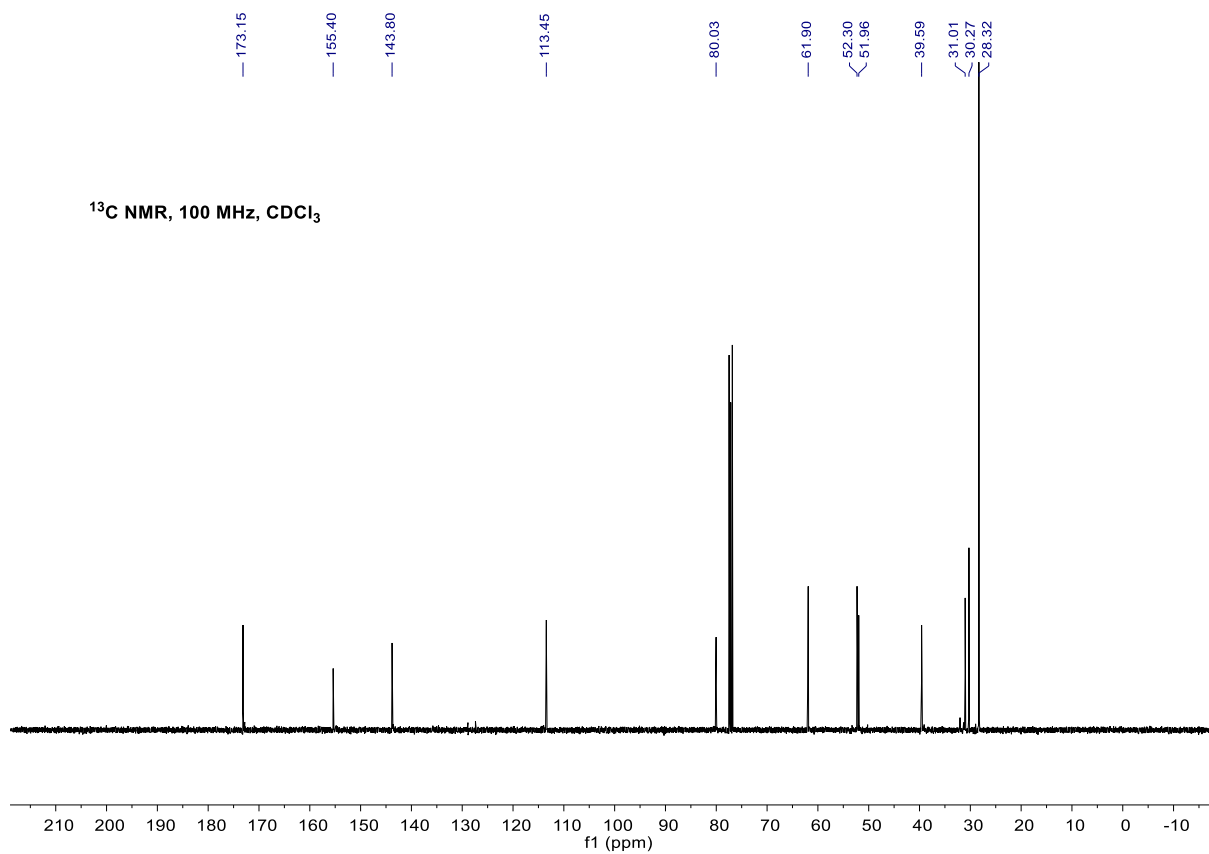


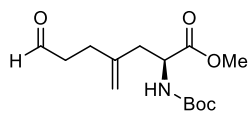
<sup>13</sup>C NMR, 100 MHz, CDCl<sub>3</sub>





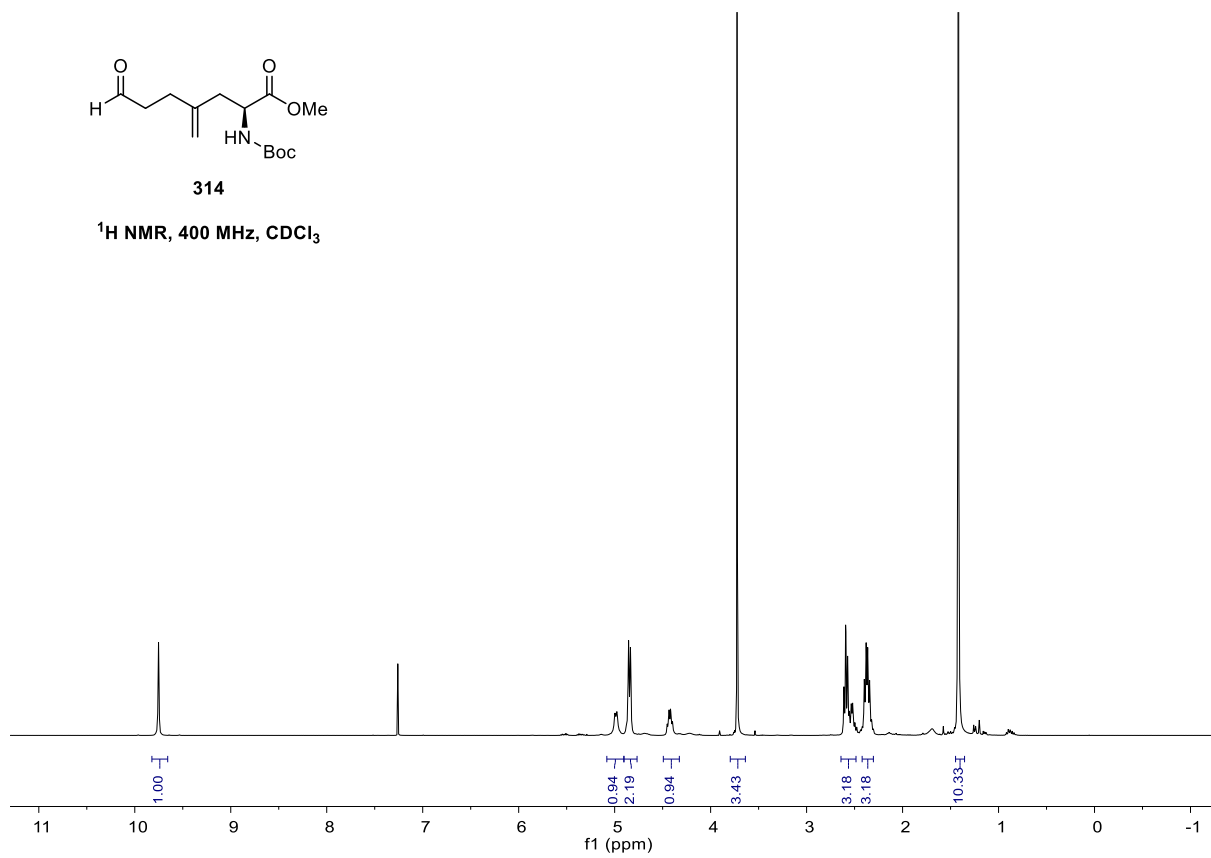
313

 $^1\text{H}$  NMR, 400 MHz,  $\text{CDCl}_3$  $^{13}\text{C}$  NMR, 100 MHz,  $\text{CDCl}_3$ 

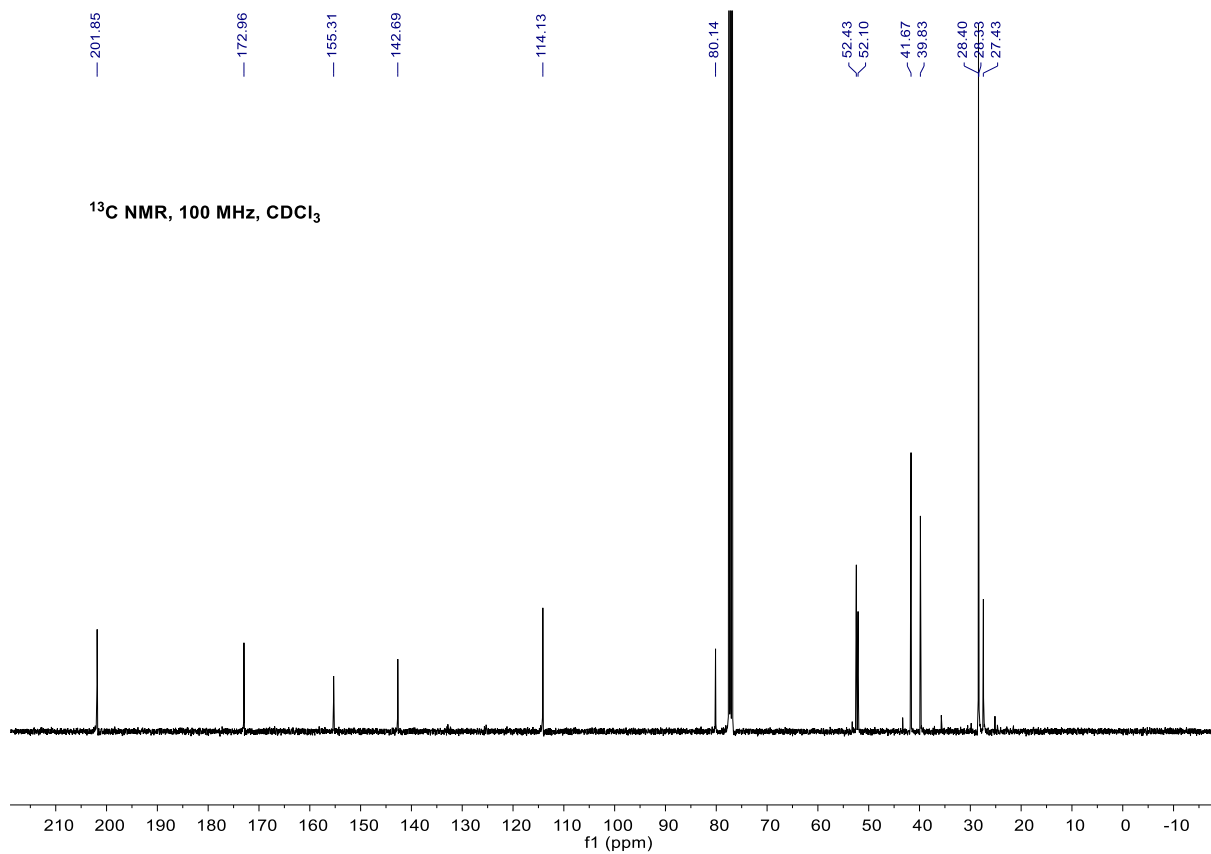


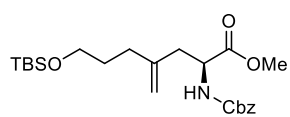
314

$^1\text{H}$  NMR, 400 MHz,  $\text{CDCl}_3$

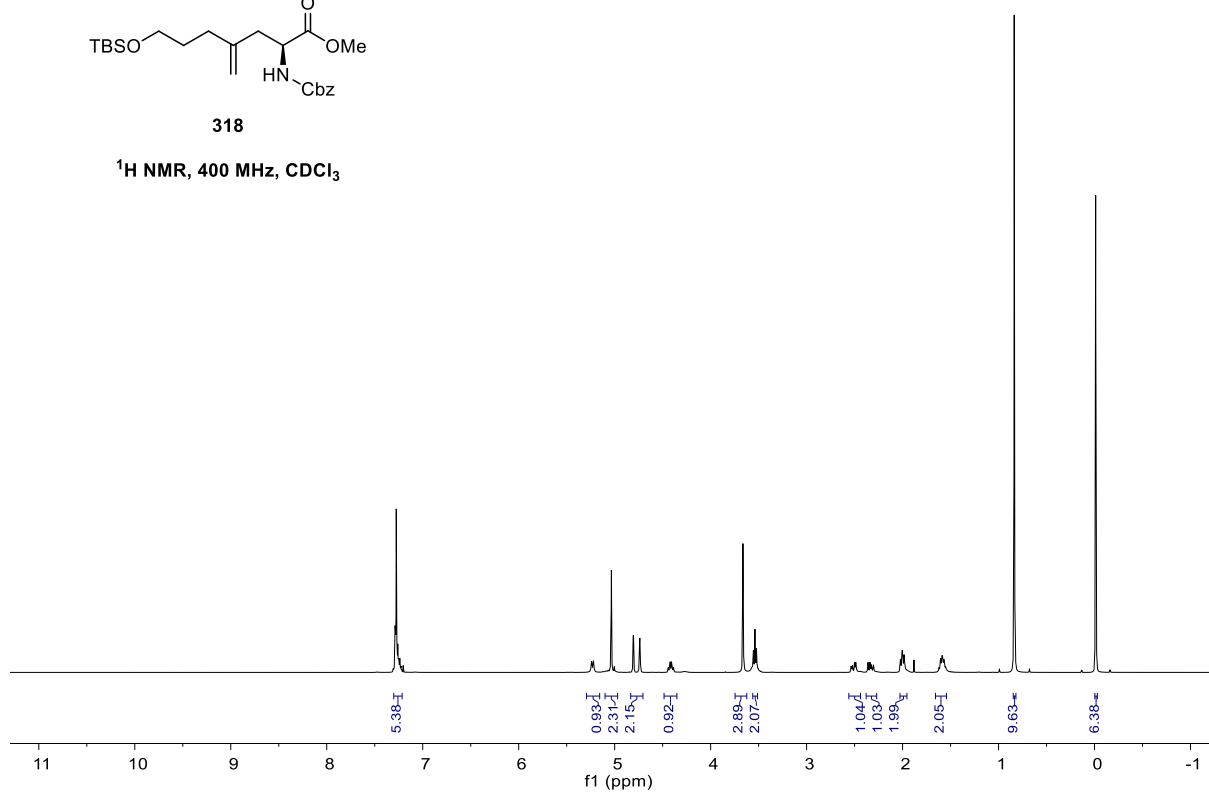
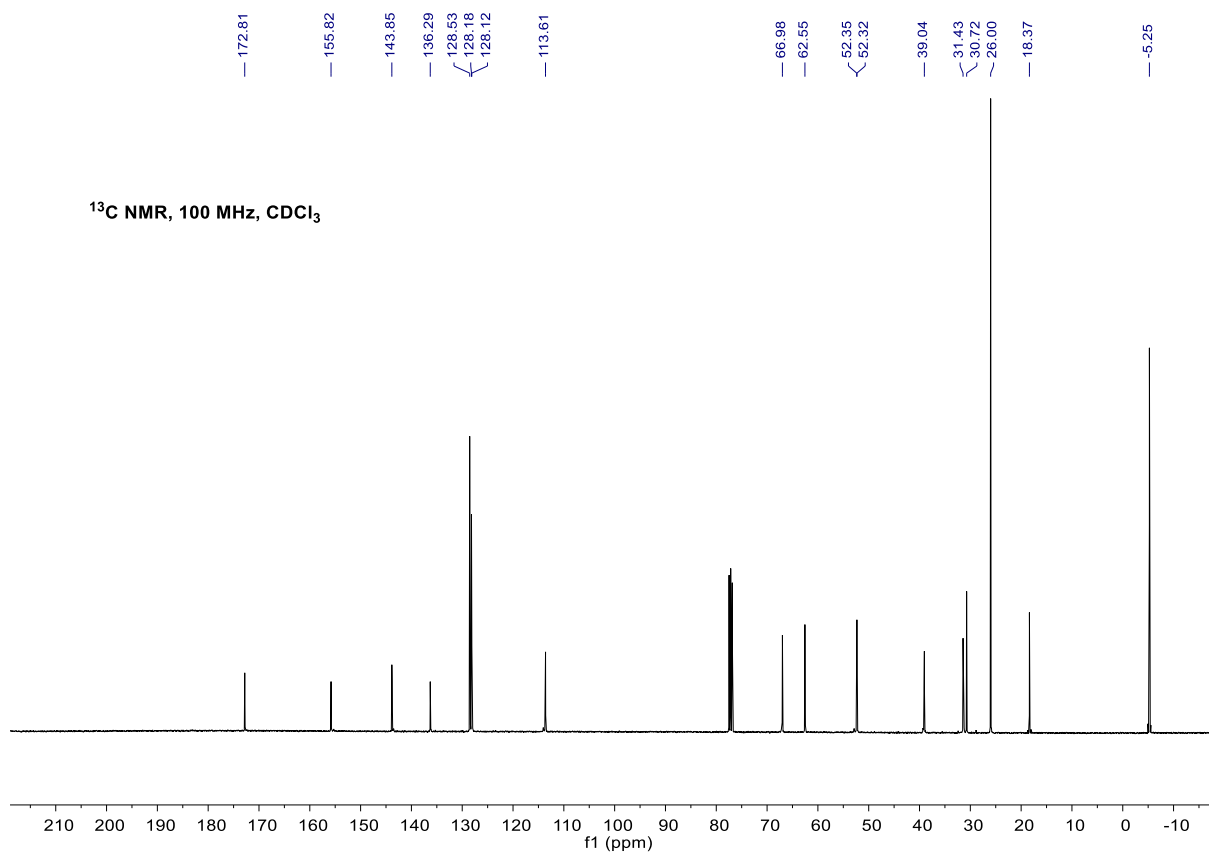


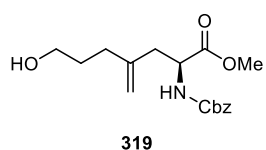
$^{13}\text{C}$  NMR, 100 MHz,  $\text{CDCl}_3$



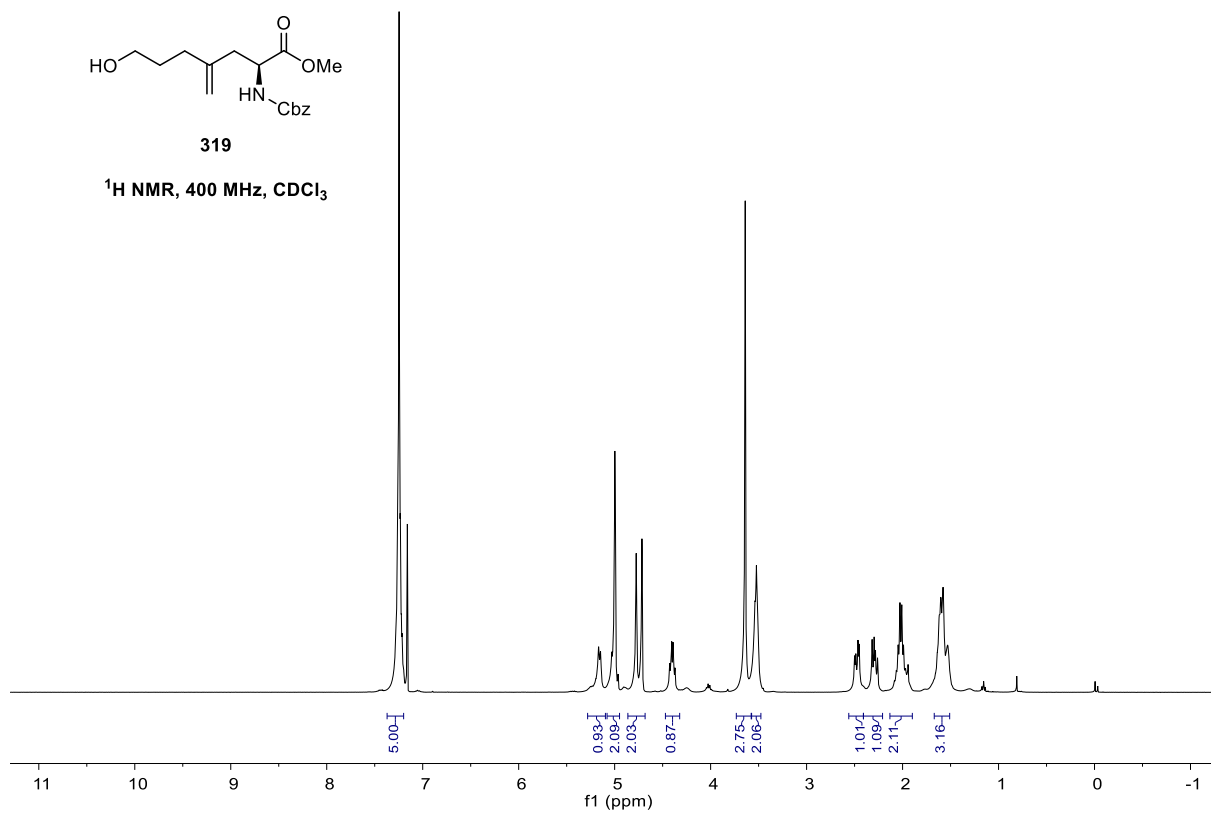


318

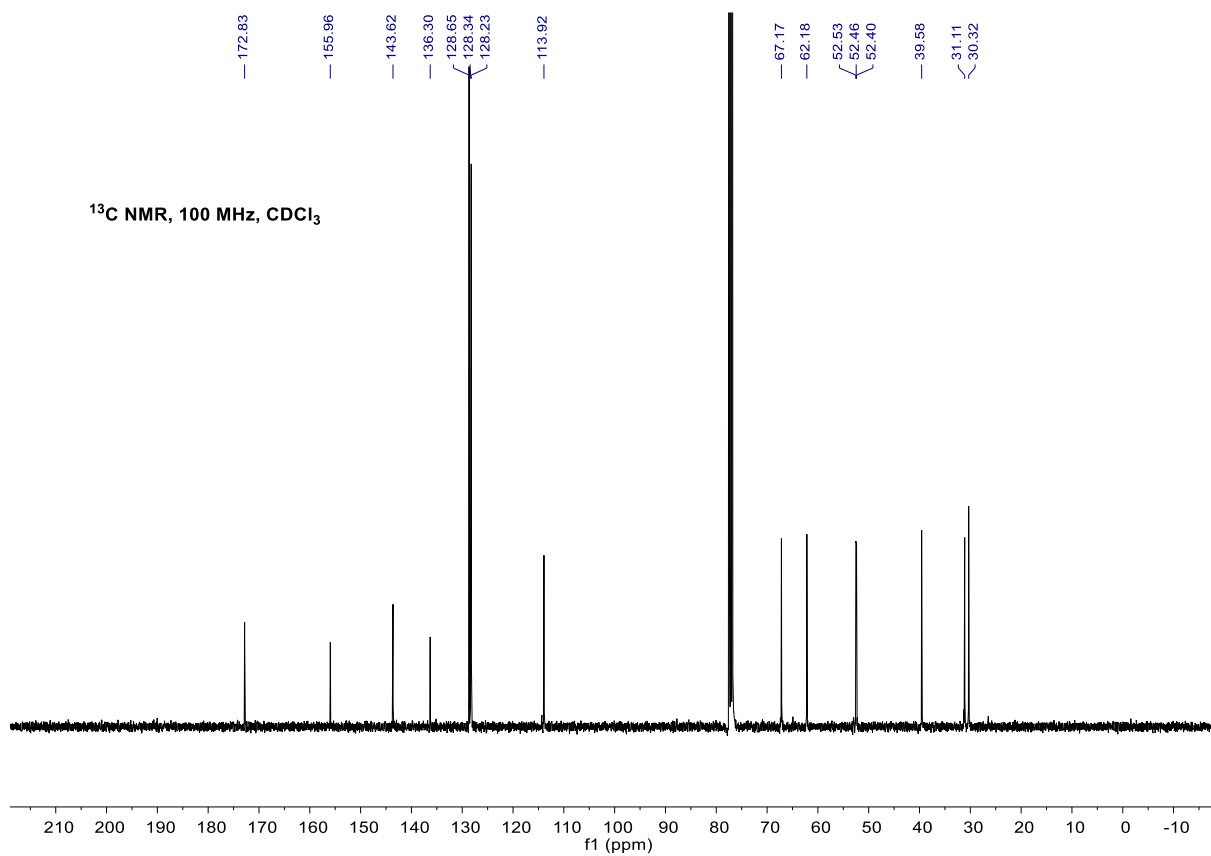
 $^1\text{H NMR}$ , 400 MHz,  $\text{CDCl}_3$  $^{13}\text{C NMR}$ , 100 MHz,  $\text{CDCl}_3$ 

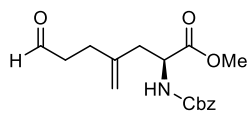


$^1\text{H}$  NMR, 400 MHz,  $\text{CDCl}_3$

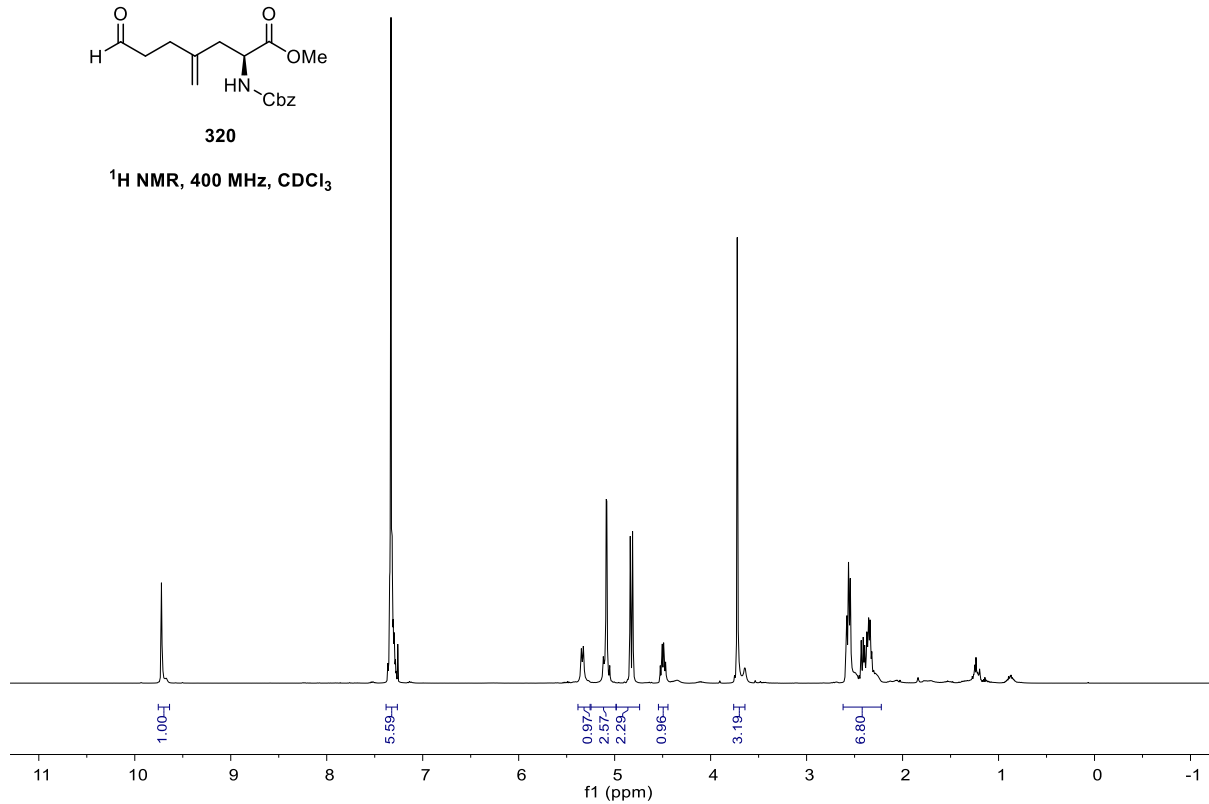


$^{13}\text{C}$  NMR, 100 MHz,  $\text{CDCl}_3$

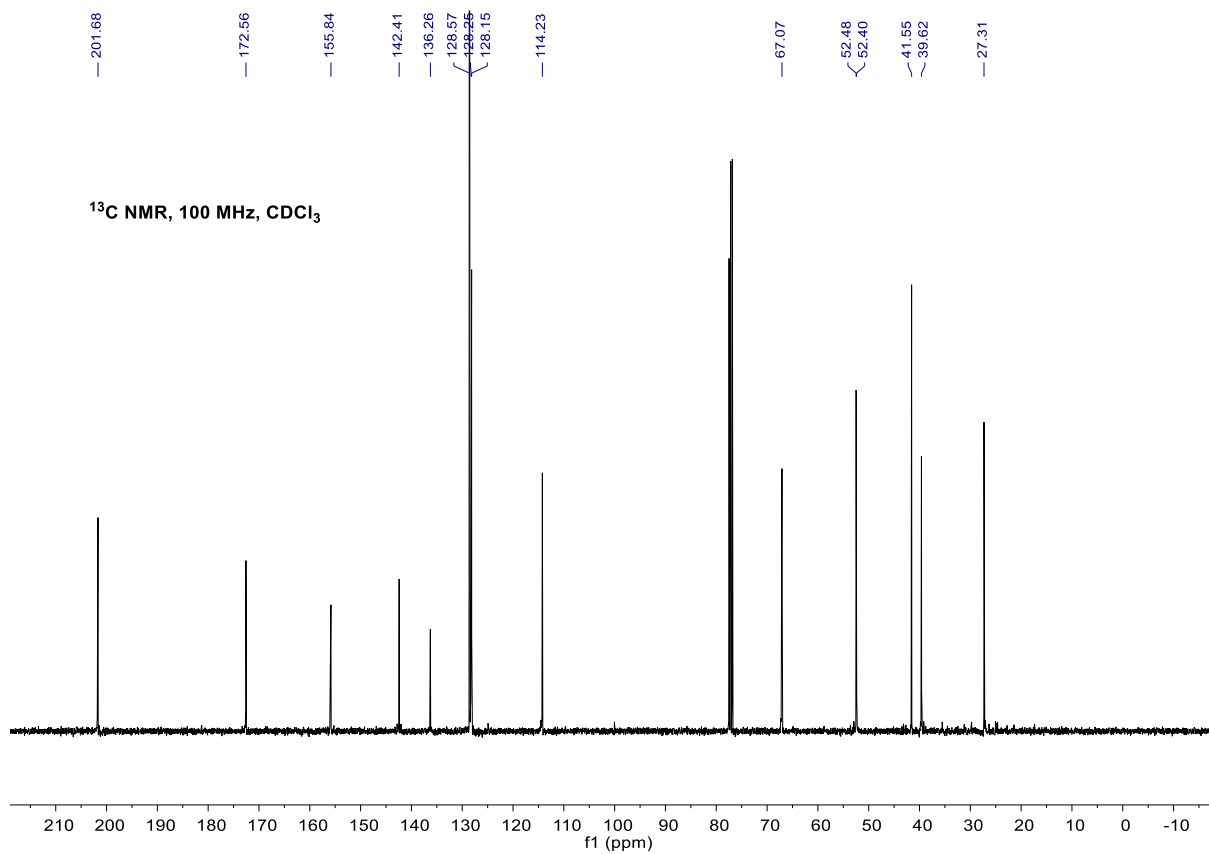




320

 $^1\text{H}$  NMR, 400 MHz,  $\text{CDCl}_3$ 

— 201.68 — 172.56 — 155.84 — 142.41 — 136.26 — 128.57 — 128.25 — 128.15 — 114.23 — 67.07 — 52.48 — 52.40 — 41.55 — 39.62 — 27.31

 $^{13}\text{C}$  NMR, 100 MHz,  $\text{CDCl}_3$ 

## References

- [1] B. B. Petrovska, *Pharmacogn. Rev.* **2012**, *6*, 1–5.
- [2] J. P. Hou, *Comp. Med. East West* **1977**, *5*, 117–122.
- [3] A. G. Atanasov, B. Waltenberger, E.-M. Pferschy-Wenzig, T. Linder, C. Wawrosch, P. Uhrin, V. Temml, L. Wang, S. Schwaiger, E. H. Heiss, et al., *Biotechnol. Adv.* **2015**, *33*, 1582–1614.
- [4] G. Bagetta, M. Cosentino, M. T. Corasaniti, S. Sakurada, *Herbal Medicines: Development and Validation of Plant-Derived Medicines for Human Health*, CRC Press, **2016**.
- [5] J. F. Borzelleca, *Toxicol. Sci.* **2000**, *53*, 2–4.
- [6] J.-P. Llored, *The Philosophy of Chemistry: Practices, Methodologies, and Concepts*, Cambridge Scholars Publishing, **2014**.
- [7] W. Pagel, *Paracelsus: An Introduction to Philosophical Medicine in the Era of the Renaissance*, Karger Medical And Scientific Publishers, **1982**.
- [8] C. Cobb, H. Goldwhite, *Creations of Fire: Chemistry's Lively History from Alchemy to the Atomic Age*, Springer Science & Business Media, **2013**.
- [9] W.-D. Müller-Jahncke, *J. Pharm. Belg.* **2005**, *60*, 35–40.
- [10] R. L. Myers, *The 100 Most Important Chemical Compounds: A Reference Guide*, ABC-CLIO, **2007**.
- [11] C. Krishnamurti, S. C. Rao, *Indian J. Anaesth.* **2016**, *60*, 861–862.
- [12] J. Giere, *Friedrich Wilhelm Adam Sertuerner*, **1830**.
- [13] E. Fenderson, *Raw Opium*, **2005**.
- [14] F. Dodds, *Opium Poppy (Papaver Somniferum)*, **2010**.
- [15] B. Zebroski, *A Brief History of Pharmacy: Humanity's Search for Wellness*, Routledge, Abingdon, **2015**.
- [16] F. W. Sertuerner, *Ann. Phys.* **1817**, *57*, 183–202.
- [17] J. E. Lesch, *Hist. Stud. Phys. Sci.* **1981**, *11*, 305–328.
- [18] T. Thomson, R. Philips, E. W. Brayley, *The Annals of Philosophy*, Baldwin, **1818**.
- [19] A. Cohen, *Br. J. Clin. Pharmacol.* **2007**, *64*, 249–252.
- [20] R. J. Huxtable, S. K. W. Schwarz, *Mol. Interv.* **2001**, *1*, 189.
- [21] W. Sneader, in *Drug Discov.*, John Wiley & Sons, Ltd, Hoboken, **2005**, pp. 88–105.
- [22] M. Hesse, *Alkaloids*, Wiley-VCH, Weinheim, **2002**.
- [23] D. Dalozze, J.-C. Braekman, J. M. Pasteels, *Chemoecology* **1994**, *5–6*, 173–183.
- [24] J. W. Daly, B. Witkop, P. Bommer, K. Biemann, *J. Am. Chem. Soc.* **1965**, *87*, 124–126.
- [25] S. Kohmoto, Y. Kashman, O. J. McConnell, K. L. Rinehart, A. Wright, F. Koehn, *J. Org. Chem.* **1988**, *53*, 3116–3118.
- [26] K. Biemann, G. Büchi, B. H. Walker, *J. Am. Chem. Soc.* **1957**, *79*, 5558–5564.
- [27] P. Ryan, *Dendrobates Azureus, Blue Poison Dart Frog, Captive*, **2016**.

- [28] H. Braxmeier, *Ladybug*, **2016**.
- [29] Khaled bin Sultan Living Oceans Foundation, *Dragmacidon Reticulatum*, **2016**.
- [30] N. Usik, *Taiga Musk Deer, Siberian Musk Deer*, **2011**.
- [31] N. L. Sass, M. Rounsavill, H. Combs, *J. Agric. Food Chem.* **1977**, *25*, 1419–1420.
- [32] A. A. Abdellatif, N. Elkhali, *Am. J. Ther.* **2014**, *21*, 523–534.
- [33] A. A. Abdelgadir, E. M. Ahmed, M. S. Eltohami, *Environ. Health Insights* **2011**, *5*, 1–8.
- [34] S. M. Colegate, D. R. Gardner, T. Z. Davis, S. L. Welsh, J. M. Betz, K. E. Panter, *Biochem. Syst. Ecol.* **2013**, *48*, 132–135.
- [35] R. Chau, J. A. Kalaitzis, B. A. Neilan, *Aquat. Toxicol.* **2011**, *104*, 61–72.
- [36] S. Funayama, G. A. Cordell, *Alkaloids: A Treasury of Poisons and Medicines*, Elsevier, Amsterdam, **2014**.
- [37] D. J. Newman, G. M. Cragg, *J. Nat. Prod.* **2016**, *79*, 629–661.
- [38] K. Kenan, K. Mack, L. Paulozzi, *Open Med.* **2012**, *6*, e41–e47.
- [39] T. H. Stanley, *J. Pain Symptom Manage.* **1992**, *7*, S3–7.
- [40] C. J. E. Niemegeers, F. C. Colpaert, F. H. L. Awouters, *Drug Dev. Res.* **1981**, *1*, 1–20.
- [41] G. M. Cragg, D. J. Newman, *Biochim. Biophys. Acta BBA - Gen. Subj.* **2013**, *1830*, 3670–3695.
- [42] K. Speck, T. Magauer, *Beilstein J. Org. Chem.* **2013**, *9*, 2048–2078.
- [43] E. O. Wilson, F. M. Peter, *Screening Plants for New Medicines*, National Academies Press, Washington, D.C., **1988**.
- [44] G. A. Cordell, M. L. Quinn-Beattie, N. R. Farnsworth, *Phytother. Res.* **2001**, *15*, 183–205.
- [45] J. M. Hagel, P. J. Facchini, *Plant Cell Physiol.* **2013**, *54*, 647–672.
- [46] G. A. W. Beaudoin, P. J. Facchini, *Planta* **2014**, *240*, 19–32.
- [47] K. Hirata, C. Poeaknapo, J. Schmidt, M. H. Zenk, *Phytochemistry* **2004**, *65*, 1039–1046.
- [48] W. De-Eknamkul, M. H. Zenk, *Phytochemistry* **1992**, *31*, 813–821.
- [49] A. Hager, N. Vrieling, D. Hager, J. Lefranc, D. Trauner, *Nat. Prod. Rep.* **2016**, *33*, 491–522.
- [50] Y. Watanabe, M. Matsui, M. Uchida, *Phytochemistry* **1975**, *14*, 2695–2698.
- [51] L. He, Y.-H. Zhang, H.-Y. Guan, J.-X. Zhang, Q.-Y. Sun, X.-J. Hao, *J. Nat. Prod.* **2011**, *74*, 181–184.
- [52] P. Magnus, C. Seipp, *Org. Lett.* **2013**, *15*, 4870–4871.
- [53] K. V. Chuang, R. Navarro, S. E. Reisman, *Angew. Chem. Int. Ed.* **2011**, *50*, 9447–9451.
- [54] T. Furumoto, Y. Sugimoto, *Planta Med.* **2001**, *67*, 194–195.
- [55] N. A. Calandra, S. M. King, S. B. Herzon, *J. Org. Chem.* **2013**, *78*, 10031–10057.
- [56] F. Li, S. S. Tartakoff, S. L. Castle, *J. Am. Chem. Soc.* **2009**, *131*, 6674–6675.
- [57] M. Carraz, A. Jossang, P. Rasoanaivo, D. Mazier, F. Frappier, *Bioorg. Med. Chem.* **2008**, *16*, 6186–6192.

- [58] G.-H. Bao, X.-L. Wang, X.-C. Tang, P. Chiu, G.-W. Qin, *Tetrahedron Lett.* **2009**, *50*, 4375–4377.
- [59] L. He, Z. Yuanhu, T. Lijia, S. Shaohui, S. Qianyun, *China J. Chin. Mater. Medica* **2010**, *35*, 1272–1275.
- [60] B.-R. Liu, X.-L. Wang, J.-R. Wang, *Z. Für Krist. - New Cryst. Struct.* **2014**, *225*, 733–734.
- [61] L. He, L.-L. Deng, S.-Z. Mu, Q.-Y. Sun, X.-J. Hao, Y.-H. Zhang, *Helv. Chim. Acta* **2012**, *95*, 1198–1201.
- [62] X.-X. Zhao, C. Peng, H. Zhang, L.-P. Qin, *Pharm. Biol.* **2012**, *50*, 1053–1061.
- [63] K. Apel, H. Hirt, *Annu. Rev. Plant Biol.* **2004**, *55*, 373–399.
- [64] X. Chen, C. Guo, J. Kong, *Neural Regen. Res.* **2012**, *7*, 376–385.
- [65] G. Yang, Y. Wang, J. Tian, J.-P. Liu, *PLOS ONE* **2013**, *8*, e74916.
- [66] B.-F. Qi, F.-W. Wu, Y.-Y. Han, Y.-Z. Zhou, C.-M. Yu, Y.-L. Zhu, J.-S. Liu, *Can. J. Chem.* **1986**, *64*, 837–839.
- [67] F. Inagaki, M. Kinebuchi, N. Miyakoshi, C. Mukai, *Org. Lett.* **2010**, *12*, 1800–1803.
- [68] Y. Hayashi, F. Inagaki, C. Mukai, *Org. Lett.* **2011**, *13*, 1778–1780.
- [69] P. Magnus, M. R. Fielding, C. Wells, V. Lynch, *Tetrahedron Lett.* **2002**, *43*, 947–950.
- [70] T. Sugihara, M. Yamada, M. Yamaguchi, M. Nishizawa, *Synlett* **1999**, *1999*, 771–773.
- [71] S. K. Woo, L. M. Geary, M. J. Krische, *Angew. Chem. Int. Ed.* **2012**, *51*, 7830–7834.
- [72] D. R. Fandrick, K. R. Fandrick, J. T. Reeves, Z. Tan, W. Tang, A. G. Capacci, S. Rodriguez, J. Song, H. Lee, N. K. Yee, et al., *J. Am. Chem. Soc.* **2010**, *132*, 7600–7601.
- [73] L. C. Hirayama, K. K. Dunham, B. Singaram, *Tetrahedron Lett.* **2006**, *47*, 5173–5176.
- [74] P. Jain, H. Wang, K. N. Houk, J. C. Antilla, *Angew. Chem. Int. Ed.* **2012**, *51*, 1391–1394.
- [75] S. Konishi, H. Hanawa, K. Maruoka, *Tetrahedron Asymmetry* **2003**, *14*, 1603–1605.
- [76] J. Wang, X. Jia, T. Meng, L. Xin, *Synthesis* **2005**, *2005*, 2838–2844.
- [77] J. Choi, H. Kim, S. Park, J. Tae, *Synlett* **2013**, *24*, 379–382.
- [78] K. L. Billingsley, S. L. Buchwald, *J. Org. Chem.* **2008**, *73*, 5589–91.
- [79] K. Uchida, S. Yokoshima, T. Kan, T. Fukuyama, *Org. Lett.* **2006**, *8*, 5311–5313.
- [80] Y. Jurong, V. Truc, P. Riebel, E. Hierl, B. Mudryk, *Org. Synth.* **2008**, *85*, 64–71.
- [81] A. Padwa, P. Rashatasakhon, A. D. Ozdemir, J. Willis, *J. Org. Chem.* **2005**, *70*, 519–528.
- [82] A. H. Clark, J. D. McCorvy, J. M. Conley, W. K. Williams, M. Bekkam, V. J. Watts, D. E. Nichols, *Bioorg. Med. Chem.* **2012**, *20*, 6366–6374.
- [83] N. O. Silva, A. S. Abreu, P. M. T. Ferreira, L. S. Monteiro, M.-J. R. P. Queiroz, *Eur. J. Org. Chem.* **2002**, *2002*, 2524–2528.
- [84] A. Larivée, A. B. Charette, *Org. Lett.* **2006**, *8*, 3955–3957.
- [85] P. M. T. Ferreira, L. S. Monteiro, G. Pereira, *Amino Acids* **2010**, *39*, 499–513.
- [86] P. M. T. Ferreira, L. S. Monteiro, G. Pereira, *Eur. J. Org. Chem.* **2008**, *2008*, 4676–4683.
- [87] H. Zhang, D. P. Curran, *J. Am. Chem. Soc.* **2011**, *133*, 10376–10378.

- [88] K. Kiewel, Z. Luo, G. A. Sulikowski, *Org. Lett.* **2005**, *7*, 5163–5165.
- [89] H. Zhang, K. O. Jeon, E. B. Hay, S. J. Geib, D. P. Curran, M. G. LaPorte, *Org. Lett.* **2014**, *16*, 94–97.
- [90] Q. Wu, J. Hu, X. Ren, J. Zhou, *Chem. Weinh. Bergstr. Ger.* **2011**, *17*, 11553–11558.
- [91] M. H. Becker, P. Chua, R. Downham, C. J. Douglas, N. K. Garg, S. Hiebert, S. Jaroch, R. T. Matsuoka, J. A. Middleton, F. W. Ng, et al., *J. Am. Chem. Soc.* **2007**, *129*, 11987–12002.
- [92] P. A. Vadola, D. Sames, *J. Org. Chem.* **2012**, *77*, 7804–7814.
- [93] H. Zhang, K. O. Jeon, E. Ben Hay, S. J. Geib, D. P. Curran, M. G. LaPorte, *Org. Lett.* **2014**, *16*, 94–7.
- [94] Y. Xia, P. Qu, Z. Liu, R. Ge, Q. Xiao, Y. Zhang, J. Wang, *Angew. Chem. Int. Ed.* **2013**, *52*, 2543–2546.
- [95] T. Ishiyama, M. Murata, N. Miyaura, *J. Org. Chem.* **1995**, *60*, 7508–7510.
- [96] L. Zhu, J. Duquette, M. Zhang, *J. Org. Chem.* **2003**, *68*, 3729–3732.
- [97] P. Zhao, C. M. Beaudry, *Org. Lett.* **2013**, *15*, 402–405.
- [98] A. K. L. Yuen, C. A. Hutton, *Tetrahedron Lett.* **2005**, *46*, 7899–7903.
- [99] V. Bagutski, A. Ros, V. K. Aggarwal, *Tetrahedron* **2009**, *65*, 9956–9960.
- [100] P. Teo, Z. K. Wickens, G. Dong, R. H. Grubbs, *Org. Lett.* **2012**, *14*, 3237–3239.
- [101] Z. K. Wickens, B. Morandi, R. H. Grubbs, *Angew. Chem. Int. Ed.* **2013**, *52*, 11257–11260.
- [102] B. M. Trost, A. H. Weiss, *Adv. Synth. Catal.* **2009**, *351*, 963–983.
- [103] E. R. Ashley, E. G. Cruz, B. M. Stoltz, *J. Am. Chem. Soc.* **2003**, *125*, 15000–15001.
- [104] A. Speicher, M. Groh, M. Hennrich, A.-M. Huynh, *Eur. J. Org. Chem.* **2010**, *2010*, 6760–6778.
- [105] S. B. Jones, L. He, S. L. Castle, *Org. Lett.* **2006**, *8*, 3757–3760.
- [106] A. J. J. Lennox, G. C. Lloyd-Jones, *Chem. Soc. Rev.* **2014**, *43*, 412–443.
- [107] C. M. So, F. Y. Kwong, *Chem. Soc. Rev.* **2011**, *40*, 4963–4972.
- [108] R. M. Gay, F. Manarin, R. Brandão, G. Zeni, *J. Braz. Chem. Soc.* **2010**, *21*, 1635–1641.
- [109] N. Y. Adonin, D. E. Babushkin, V. N. Parmon, V. V. Bardin, G. A. Kostin, V. I. Mashukov, H.-J. Frohn, *Tetrahedron* **2008**, *64*, 5920–5924.
- [110] B. Schmidt, S. Krehl, A. Kelling, U. Schilde, *J. Org. Chem.* **2012**, *77*, 2360–2367.
- [111] J. Liu, Y. Deng, H. Wang, H. Zhang, G. Yu, B. Wu, H. Zhang, Q. Li, T. B. Marder, Z. Yang, et al., *Org. Lett.* **2008**, *10*, 2661–2664.
- [112] J. E. Milne, S. L. Buchwald, *J. Am. Chem. Soc.* **2004**, *126*, 13028–32.
- [113] Y. Yang, N. J. Oldenhuis, S. L. Buchwald, *Angew. Chem. Int. Ed.* **2013**, *52*, 615–619.
- [114] C. Valente, M. E. Belowich, N. Hadei, M. G. Organ, *Eur. J. Org. Chem.* **2010**, *2010*, 4343–4354.
- [115] N. Miyaura, A. Suzuki, *Chem. Rev.* **1995**, *95*, 2457–2483.

- [116] J. Carreras, G. Gopakumar, L. Gu, A. Gimeno, P. Linowski, J. Petušková, W. Thiel, M. Alcarazo, *J. Am. Chem. Soc.* **2013**, *135*, 18815–18823.
- [117] R. Singha, S. Dhara, M. Ghosh, J. K. Ray, *RSC Adv.* **2015**, *5*, 8801–8805.
- [118] O. Baudoin, D. Guénard, F. Guéritte, *J. Org. Chem.* **2000**, *65*, 9268–71.
- [119] M. Heffernan, L. Hardy, F. Wu, L. Saraswat, K. Spear, *WO2012/170845A2*, **2012**.
- [120] A. B. Northrup, M. H. Katcher, M. D. Altman, M. Chenard, M. H. Daniels, S. V. Deshmukh, D. Falcone, D. J. Guerin, H. Hatch, C. Li, et al., *J. Med. Chem.* **2013**, *56*, 2294–2310.
- [121] L. Zhu, J. Duquette, M. Zhang, *J. Org. Chem.* **2003**, *68*, 3729–3732.
- [122] P. Harrisson, J. Morris, T. Marder, P. Steel, *Org. Lett.* **2009**, *11*, 3586–3589.
- [123] B. Cheng, S. Zhang, L. Zhu, J. Zhang, Q. Li, A. Shan, L. He, *Synthesis* **2009**, *2009*, 2501–2504.
- [124] P. Magnus, N. Sane, B. P. Fauber, V. Lynch, *J. Am. Chem. Soc.* **2009**, *131*, 16045–16047.
- [125] L. McMurray, E. M. Beck, M. J. Gaunt, *Angew. Chem. Int. Ed.* **2012**, *51*, 9288–9291.
- [126] P. Harrisson, J. Morris, T. B. Marder, P. G. Steel, *Org. Lett.* **2009**, *11*, 3586–3589.
- [127] A. Bellan, Master's Thesis, LMU München, **2014**.
- [128] P. Rabe, K. Kindler, *Berichte Dtsch. Chem. Ges.* **1918**, *51*, 466–467.
- [129] J. I. Seeman, *Angew. Chem. Int. Ed.* **2007**, *46*, 1378–1413.
- [130] A. S. Lee, B. B. Liau, M. D. Shair, *J. Am. Chem. Soc.* **2014**, *136*, 13442–13452.
- [131] L. M. Kreis, E. M. Carreira, *Angew. Chem. Int. Ed.* **2012**, *51*, 3436–3439.
- [132] J. S. Clark, C. Xu, *Angew. Chem. Int. Ed.* **2016**, *55*, 4332–4335.
- [133] K. Ogasawara, M. Kawamura, *Heterocycles* **1997**, *44*, 129.
- [134] C. Martínez, K. Muñiz, *Angew. Chem. Int. Ed.* **2015**, *54*, 8287–8291.
- [135] E. Rodríguez, M. N. Grayson, A. Asensio, P. Barrio, K. N. Houk, S. Fustero, *ACS Catal.* **2016**, *6*, 2506–2514.
- [136] C. Y. Hong, N. Kado, L. E. Overman, *J. Am. Chem. Soc.* **1993**, *115*, 11028–11029.
- [137] J. Fischer, G. P. Savage, M. J. Coster, *Org. Lett.* **2011**, *13*, 3376–3379.
- [138] Y. Tang, L. Deng, Y. Zhang, G. Dong, J. Chen, Z. Yang, *Org. Lett.* **2005**, *7*, 593–595.
- [139] L. Pérez-Serrano, L. Casarrubios, G. Domínguez, J. Pérez-Castells, *Org. Lett.* **1999**, *1*, 1187–1188.
- [140] D. Lesage, A. Milet, A. Memboeuf, J. Blu, A. E. Greene, J.-C. Tabet, Y. Gimbert, *Angew. Chem. Int. Ed.* **2014**, *53*, 1939–1942.
- [141] J. Mulzer, G. Dürner, D. Trauner, *Angew. Chem. Int. Ed. Engl.* **1996**, *35*, 2830–2832.
- [142] M. A. Grundl, A. Kaster, E. D. Beaulieu, D. Trauner, *Org. Lett.* **2006**, *8*, 5429–5432.
- [143] T. Reinhardt, Bachelor's Thesis, LMU München, **2015**.
- [144] A. García Martínez, E. Teso Vilar, A. García Fraile, S. de la Moya Cerero, P. Martínez Ruiz, L. R. Subramanian, *Tetrahedron Asymmetry* **1996**, *7*, 2177–2180.

- [145] S. N. Chavre, H. Choo, J. K. Lee, A. N. Pae, Y. Kim, Y. S. Cho, *J. Org. Chem.* **2008**, *73*, 7467–7471.
- [146] D. A. Evans, A. M. Golob, *J. Am. Chem. Soc.* **1975**, *97*, 4765–4766.
- [147] L. A. Paquette, *Tetrahedron* **1997**, *53*, 13971–14020.
- [148] A. E. Wick, D. Felix, K. Steen, A. Eschenmoser, *Helv. Chim. Acta* **1964**, *47*, 2425–2429.
- [149] M. Ichiki, H. Tanimoto, S. Miwa, R. Saito, T. Sato, N. Chida, *Chem. – Eur. J.* **2013**, *19*, 264–269.
- [150] S. Handerson, M. Schlaf, *Org. Lett.* **2002**, *4*, 407–409.
- [151] X. Wei, J. C. Lorenz, S. Kapadia, A. Saha, N. Haddad, C. A. Busacca, C. H. Senanayake, *J. Org. Chem.* **2007**, *72*, 4250–4253.
- [152] W. H. Watanabe, L. E. Conlon, *J. Am. Chem. Soc.* **1957**, *79*, 2828–2833.
- [153] P. A. Grieco, E. B. Brandes, S. McCann, J. D. Clark, *J. Org. Chem.* **1989**, *54*, 5849–5851.
- [154] T. Mandai, M. Ueda, S. Hasegawa, M. Kawada, J. Tsuji, S. Saito, *Tetrahedron Lett.* **1990**, *31*, 4041–4044.
- [155] A. Nakayama, N. Kogure, M. Kitajima, H. Takayama, *Angew. Chem.* **2011**, *123*, 8175–8178.
- [156] N. Vepřek, Master's Thesis, LMU München, **2016**.
- [157] S. E. Denmark, J. H.-C. Liu, J. M. Muhuhi, *J. Org. Chem.* **2011**, *76*, 201–215.
- [158] N. M. Benjamin, S. F. Martin, *Org. Lett.* **2011**, *13*, 450–453.
- [159] Q.-Y. Hu, P. D. Rege, E. J. Corey, *J. Am. Chem. Soc.* **2004**, *126*, 5984–5986.
- [160] C. S. Schindler, C. R. J. Stephenson, E. M. Carreira, *Angew. Chem. Int. Ed.* **2008**, *47*, 8852–8855.
- [161] C. Grandclaoudon, V. Michelet, P. Y. Toullec, *Org. Lett.* **2016**, *18*, 676–679.
- [162] D. Dolenc, *Synth. Commun.* **2003**, *33*, 2917–2924.
- [163] B. Ganem, R. K. Boeckman, *Tetrahedron Lett.* **1974**, *15*, 917–920.
- [164] H. Nace, J. Monagle, *J. Org. Chem.* **1959**, *24*, 1792–1793.
- [165] T. Mukaiyama, J. Matsuo, H. Kitagawa, *Chem. Lett.* **2000**, *29*, 1250–1251.
- [166] P. S. Baran, N. Z. Burns, *J. Am. Chem. Soc.* **2006**, *128*, 3908–3909.
- [167] M. Matveenko, G. Liang, E. M. W. Lauterwasser, E. Zubía, D. Trauner, *J. Am. Chem. Soc.* **2012**, *134*, 9291–9295.
- [168] K. Okano, H. Tokuyama, T. Fukuyama, *Chem. – Asian J.* **2008**, *3*, 296–309.
- [169] K. Okano, K. Okuyama, T. Fukuyama, H. Tokuyama, *Synlett* **2008**, *13*, 1977–1980.
- [170] H. Yoshino, M. Tsuji, M. Kodama, K. Komeda, N. Niikawa, T. Tanase, N. Asakawa, K. Nose, K. Yamatsu, *Chem. Pharm. Bull. (Tokyo)* **1990**, *38*, 1735–1737.
- [171] H. Yoshino, Y. Tsuchiya, I. Saito, M. Tsujii, *Chem. Pharm. Bull. (Tokyo)* **1987**, *35*, 3438–3441.
- [172] F. Hessler, R. Betík, A. Kadlčíková, R. Belle, M. Kotora, *Eur. J. Org. Chem.* **2014**, *2014*, 7245–7252.

- [173] K. Kubota, J. L. Leighton, *Angew. Chem. Int. Ed.* **2003**, *42*, 946–948.
- [174] H. Kim, S. Ho, J. L. Leighton, *J. Am. Chem. Soc.* **2011**, *133*, 6517–6520.
- [175] Y. Huang, L. Yang, P. Shao, Y. Zhao, *Chem. Sci.* **2013**, *4*, 3275–3281.
- [176] H. C. Brown, P. K. Jadhav, *J. Am. Chem. Soc.* **1983**, *105*, 2092–2093.
- [177] P. V. Ramachandran, G.-M. Chen, H. C. Brown, *Tetrahedron Lett.* **1997**, *38*, 2417–2420.
- [178] U. S. Racherla, H. C. Brown, *J. Org. Chem.* **1991**, *56*, 401–404.
- [179] H. C. Brown, R. S. Randad, K. S. Bhat, M. Zaidlewicz, U. S. Racherla, *J. Am. Chem. Soc.* **1990**, *112*, 2389–2392.
- [180] E. J. Corey, C. J. Helal, *Angew. Chem. Int. Ed.* **1998**, *37*, 1986–2012.
- [181] M. A. Brimble, C. J. Bryant, *Chem. Commun.* **2006**, 4506.
- [182] H. C. Brown, J. Chandrasekharan, P. V. Ramachandran, *J. Am. Chem. Soc.* **1988**, *110*, 1539–1546.
- [183] F.-X. Felpin, G. Vo-Thanh, J. Villiéras, J. Lebreton, *Tetrahedron Asymmetry* **2001**, *12*, 1121–1124.
- [184] F.-X. Felpin, M.-J. Bertrand, J. Lebreton, *Tetrahedron* **2002**, *58*, 7381–7389.
- [185] W. C. Still, M. Kahn, A. Mitra, *J. Org. Chem.* **1978**, *43*, 2923–2925.
- [186] A. F. Burchat, J. M. Chong, N. Nielsen, *J. Organomet. Chem.* **1997**, *542*, 281–283.
- [187] L. J. Farrugia, *J. Appl. Crystallogr.* **2012**, *45*, 849–854.
- [188] J. Yu, V. Truc, P. Riebel, E. Hierl, B. Mudryk, *Tetrahedron Lett.* **2005**, *46*, 4011–4013.
- [189] M. Spittler, K. Lutsenko, C. Czekelius, *J. Org. Chem.* **2016**, *81*, 6100–6105.
- [190] J. F. Teichert, S. Zhang, A. W. van Zijl, J. W. Slaa, A. J. Minnaard, B. L. Feringa, *Org. Lett.* **2010**, *12*, 4658–4660.
- [191] P. A. Vadola, D. Sames, *J. Org. Chem.* **2012**, *77*, 7804–7814.
- [192] H. Zhang, K. O. Jeon, E. Ben Hay, S. J. Geib, D. P. Curran, M. G. LaPorte, *Org. Lett.* **2014**, *16*, 94–97.
- [193] P. Zhao, C. M. Beaudry, *Org. Lett.* **2013**, *15*, 402–405.
- [194] N. Kardos, A. L. Demain, *Appl. Microbiol. Biotechnol.* **2011**, *92*, 677.
- [195] S. A. Sieber, M. A. Marahiel, *J. Bacteriol.* **2003**, *185*, 7036–7043.
- [196] S. A. Sieber, M. A. Marahiel, *Chem. Rev.* **2005**, *105*, 715–738.
- [197] S. Ōmura, *Tetrahedron* **2011**, *67*, 6420–6459.
- [198] C. J. Schofield, J. E. Baldwin, M. F. Byford, I. Clifton, J. Hajdu, C. Hensgens, P. Roach, *Curr. Opin. Struct. Biol.* **1997**, *7*, 857–864.
- [199] C. T. Walsh, H. Chen, T. A. Keating, B. K. Hubbard, H. C. Losey, L. Luo, C. G. Marshall, D. A. Miller, H. M. Patel, *Curr. Opin. Chem. Biol.* **2001**, *5*, 525–534.
- [200] T. Hamada, S. Matsunaga, M. Fujiwara, K. Fujita, H. Hirota, R. Schmucki, P. Güntert, N. Fusetani, *J. Am. Chem. Soc.* **2010**, *132*, 12941–12945.
- [201] D. L. Boger, *Med. Res. Rev.* **2001**, *21*, 356–381.

- [202] D. A. Evans, M. R. Wood, B. W. Trotter, T. I. Richardson, J. C. Barrow, J. L. Katz, *Angew. Chem.-Int. Ed.* **1998**, *37*, 2700–2704.
- [203] E. Black, T. T. Y. Lau, M. H. H. Ensom, *Ann. Pharmacother.* **2011**, *45*, 629–638.
- [204] M. Lachia, C. J. Moody, *Nat. Prod. Rep.* **2008**, *25*, 227–253.
- [205] K. C. Nicolaou, J. L. Hao, M. V. Reddy, P. B. Rao, G. Rassias, S. A. Snyder, X. H. Huang, D. Y. K. Chen, W. E. Brenzovich, N. Giuseppone, et al., *J. Am. Chem. Soc.* **2004**, *126*, 12897–12906.
- [206] R. R. Knowles, J. Carpenter, S. B. Blakey, A. Kayano, I. K. Mangion, C. J. Sinz, D. W. C. MacMillan, *Chem. Sci.* **2011**, *2*, 308–311.
- [207] B. Shen, L. Du, C. Sanchez, D. J. Edwards, M. Chen, J. M. Murrell, *J. Nat. Prod.* **2002**, *65*, 422–431.
- [208] H. Umezawa, K. Maeda, T. Takeuchi, Y. Okami, *J. Antibiot. (Tokyo)* **1966**, *19*, 200–209.
- [209] J.-C. Zhao, S.-M. Yu, Y. Liu, Z.-J. Yao, *Org. Lett.* **2013**, *15*, 4300–4303.
- [210] J.-C. Zhao, S.-M. Yu, H.-B. Qiu, Z.-J. Yao, *Tetrahedron* **2014**, *70*, 3197–3210.
- [211] J. R. Cochrane, J. M. White, U. Wille, C. A. Hutton, *Org. Lett.* **2012**, *14*, 2402–2405.
- [212] D. Boger, J. Zhou, *J. Am. Chem. Soc.* **1993**, *115*, 11426–11433.
- [213] S. Ghosh, A. S. Kumar, G. N. Mehta, R. Soundararajan, S. Sen, *Arkivoc* **2009**, 72–78.
- [214] R. Beugelmans, A. Bigot, M. BoisChoussy, J. P. Zhu, *J. Org. Chem.* **1996**, *61*, 771–774.
- [215] M. Kaneda, S. Tamai, S. Nakamura, T. Hirata, Y. Kushi, T. Suga, *J. Antibiot. (Tokyo)* **1982**, *35*, 1137–1140.
- [216] S. Omura, A. Hirano, Y. Iwai, R. Masuma, *J. Antibiot. (Tokyo)* **1979**, *32*, 786–790.
- [217] A. Furusaki, T. Matsumoto, H. Ogura, H. Takayanagi, A. Hirano, S. Omura, *J. Chem. Soc. Chem. Commun.* **1980**, 698–698.
- [218] Y. Enomoto, K. Shiomi, M. Hayashi, R. Masuma, T. Kawakubo, K. Tomosawa, Y. Iwai, S. Omura, *J. Antibiot. (Tokyo)* **1996**, *49*, 50–53.
- [219] M. Boll, *J. Mol. Microbiol. Biotechnol.* **2006**, *10*, 132–142.
- [220] S. P. Roche, J. A. Porco, *Angew. Chem. Int. Ed.* **2011**, *50*, 4068–4093.
- [221] X. Yu, F. Liu, Y. Zou, M.-C. Tang, L. Hang, K. N. Houk, Y. Tang, *J. Am. Chem. Soc.* **2016**, *138*, 13529–13532.
- [222] J. F. Viles-Gonzalez, V. Fuster, J. J. Badimon, *Eur. Heart J.* **2004**, *25*, 1197–1207.
- [223] D. Capodanno, J. L. Ferreira, D. J. Angiolillo, *J. Thromb. Haemost.* **2013**, *11*, 316–329.
- [224] C. Geeganage, R. Wilcox, P. M. Bath, *BMC Med.* **2010**, *8*, 36.
- [225] D. J. Angiolillo, J. Luis Ferreira, *Rev. Esp. Cardiol. Engl. Ed.* **2010**, *63*, 60–76.
- [226] T. Chiba, Y. Asami, T. Suga, Y. Watanabe, T. Nagai, F. Momose, K. Nonaka, M. Iwatsuki, H. Yamada, S. Ōmura, et al., *Biosci. Biotechnol. Biochem.* **2016**, *0*, 1–4.
- [227] E. D. Kilbourne, *Emerg. Infect. Dis.* **2006**, *12*, 9–14.
- [228] M. R. Hilleman, *Vaccine* **2002**, *20*, 3068–3087.

- [229] G. Stiver, *CMAJ Can. Med. Assoc. J.* **2003**, *168*, 49–57.
- [230] H. Suzuki, R. Saito, H. Masuda, H. Oshitani, M. Sato, I. Sato, *J. Infect. Chemother. Off. J. Jpn. Soc. Chemother.* **2003**, *9*, 195–200.
- [231] K. M. Chan-Tack, J. S. Murray, D. B. Birnkrant, *N. Engl. J. Med.* **2009**, *361*, 1713–1714.
- [232] G. T. Kim, PhD Thesis, Korea Advanced Institute of Science and Technology, **1997**.
- [233] P. Wipf, Y. Kim, D. M. Goldstein, *J. Am. Chem. Soc.* **1995**, *117*, 11106–11112.
- [234] G. Lin, R. Hong, *J. Org. Chem.* **2001**, *66*, 2877–2880.
- [235] J. M. Hart, PhD Thesis, University of Leeds, **2004**.
- [236] D. A. Evans, C. J. Dinsmore, D. A. Evrard, K. M. DeVries, *J. Am. Chem. Soc.* **1993**, *115*, 6426–6427.
- [237] P. Stawski, PhD Thesis, LMU München, **2012**.
- [238] H. Yang, PhD Thesis, University of Birmingham, **2015**.
- [239] J. H. Lee, L. Deng, *J. Am. Chem. Soc.* **2012**, *134*, 18209–18212.
- [240] D. Seebach, *Angew. Chem. Int. Ed. Engl.* **1979**, *18*, 239–258.
- [241] Y. Zhang, B. O'Connor, E. Negishi, *J. Org. Chem.* **1988**, *53*, 5588–5590.
- [242] F. Guo, M. D. Clift, R. J. Thomson, *Eur. J. Org. Chem.* **2012**, *2012*, 4881–4896.
- [243] Y. Ito, T. Konoike, T. Harada, T. Saegusa, *J. Am. Chem. Soc.* **1977**, *99*, 1487–1493.
- [244] R. H. Frazier, R. L. Harlow, *J. Org. Chem.* **1980**, *45*, 5408–5411.
- [245] C. T. Avetta, L. C. Konkol, C. N. Taylor, K. C. Dugan, C. L. Stern, R. J. Thomson, *Org. Lett.* **2008**, *10*, 5621–5624.
- [246] R. M. Moriarty, R. Penmasta, I. Prakash, *Tetrahedron Lett.* **1987**, *28*, 873–876.
- [247] L. C. Konkol, F. Guo, A. A. Sarjeant, R. J. Thomson, *Angew. Chem. Int. Ed.* **2011**, *50*, 9931–9934.
- [248] B. T. Jones, C. T. Avetta, R. J. Thomson, *Chem. Sci.* **2014**, *5*, 1794–1798.
- [249] C. L. Martin, L. E. Overman, J. M. Rohde, *J. Am. Chem. Soc.* **2010**, *132*, 4894–4906.
- [250] D. A. Parrish, L. J. Mathias, *J. Org. Chem.* **2002**, *67*, 1820–1826.
- [251] M.-Y. Chen, A. S.-Y. Lee, *J. Chin. Chem. Soc.* **2003**, *50*, 103–108.
- [252] H. C. Brown, P. V. Ramachandran, in *Reduct. Org. Synth.*, American Chemical Society, **1996**, pp. 1–30.
- [253] M. E. Jung, J. C. Rohloff, *J. Org. Chem.* **1985**, *50*, 4909–4913.
- [254] H. Hagiwara, N. Komatsubara, H. Ono, T. Okabe, T. Hoshi, T. Suzuki, M. Ando, M. Kato, *J. Chem. Soc. [Perkin 1]* **2001**, 316–322.
- [255] K. Chen, Y. Ishihara, M. M. Galán, P. S. Baran, *Tetrahedron* **2010**, *66*, 4738–4744.
- [256] K. C. Nicolaou, S. Sanchini, T. R. Wu, D. Sarlah, *Chem. – Eur. J.* **2010**, *16*, 7678–7682.
- [257] P. A. Grieco, M. Nishizawa, N. Marinovic, W. J. Ehmann, *J. Am. Chem. Soc.* **1976**, *98*, 7102–7104.
- [258] P. A. Grieco, R. P. Nargund, D. T. Parker, *J. Am. Chem. Soc.* **1989**, *111*, 6287–6294.

- [259] R. Ding, J.-G. Fu, G.-Q. Xu, B.-F. Sun, G.-Q. Lin, *J. Org. Chem.* **2014**, *79*, 240–250.
- [260] T. Hamura, S. Tsuji, T. Matsumoto, K. Suzuki, *Chem. Lett.* **2002**, *31*, 280–281.
- [261] M. E. Krafft, R. A. Holton, *J. Am. Chem. Soc.* **1984**, *106*, 7619–7621.
- [262] A. Fürstner, H. Krause, C. W. Lehmann, *Angew. Chem. Int. Ed.* **2006**, *45*, 440–444.
- [263] O. Z. Pereira, T. H. Chan, *Tetrahedron Lett.* **1995**, *36*, 8749–8752.
- [264] M. Ogasawara, Y. Ge, K. Uetake, T. Takahashi, *Org. Lett.* **2005**, *7*, 5697–5700.
- [265] S.-P. Luo, L.-D. Guo, L.-H. Gao, S. Li, P.-Q. Huang, *Chem. – Eur. J.* **2013**, *19*, 87–91.
- [266] T.-L. Ho, R.-J. Chein, *Helv. Chim. Acta* **2006**, *89*, 231–239.
- [267] I. S. Marcos, F. A. Hernández, M. J. Sexmero, D. Díez, P. Basabe, A. B. Pedrero, N. García, J. G. Urones, *Tetrahedron* **2003**, *59*, 685–694.
- [268] B. V. S. Reddy, B. Someswarao, N. Prudhviraju, B. J. M. Reddy, B. Sridhar, S. K. Kumar, *Org. Biomol. Chem.* **2015**, *13*, 6737–6741.
- [269] T. Ibuka, G. N. Chu, *Chem. Pharm. Bull. (Tokyo)* **1986**, *34*, 2380–2390.
- [270] Y. Hitotsuyanagi, S. Motegi, T. Hasuda, K. Takeya, *Org. Lett.* **2004**, *6*, 1111–1114.
- [271] M. Couturier, J. L. Tucker, B. M. Andresen, P. Dubé, J. T. Negri, *Org. Lett.* **2001**, *3*, 465–467.
- [272] Z. Shao, J. Chen, R. Huang, C. Wang, L. Li, H. Zhang, *Synlett* **2003**, *2003*, 2228–2230.
- [273] E. Dinca, P. Hartmann, J. Smrček, I. Dix, P. G. Jones, U. Jahn, *Eur. J. Org. Chem.* **2012**, *2012*, 4461–4482.
- [274] J. McNulty, M. J. Millar, G. Bernardinelli, C. W. Jefford, *J. Org. Chem.* **1999**, *64*, 5312–5314.
- [275] C. Kitamura, C. Matsumoto, N. Kawatsuki, A. Yoneda, K. Asada, T. Kobayashi, H. Naito, *Bull. Chem. Soc. Jpn.* **2008**, *81*, 754–756.
- [276] S. Mao, Y.-R. Gao, S.-L. Zhang, D.-D. Guo, Y.-Q. Wang, *Eur. J. Org. Chem.* **2015**, *2015*, 876–885.
- [277] N. Kise, T. Ueda, K. Kumada, Y. Terao, N. Ueda, *J. Org. Chem.* **2000**, *65*, 464–468.
- [278] R. M. Moriarty, O. Prakash, M. P. Duncan, *J. Chem. Soc. Chem. Commun.* **1985**, *0*, 420–420.
- [279] M. Schmittel, A. Burghart, W. Malisch, J. Reising, R. Söllner, *J. Org. Chem.* **1998**, *63*, 396–400.
- [280] T. Fujii, T. Hirao, Y. Ohshiro, *Tetrahedron Lett.* **1992**, *33*, 5823–5826.
- [281] E. S. Krygowski, K. Murphy-Benenato, M. D. Shair, *Angew. Chem. Int. Ed.* **2008**, *47*, 1680–1684.
- [282] P. Mizar, T. Wirth, *Angew. Chem. Int. Ed.* **2014**, *53*, 5993–5997.
- [283] J. Burés, M. Martín, F. Urpí, J. Vilarrasa, *J. Org. Chem.* **2009**, *74*, 2203–2206.
- [284] C. J. White, A. K. Yudin, *Nat. Chem.* **2011**, *3*, 509–524.
- [285] S. Yokoshima, T. Ueda, S. Kobayashi, A. Sato, T. Kuboyama, H. Tokuyama, T. Fukuyama, *J. Am. Chem. Soc.* **2002**, *124*, 2137–2139.
- [286] A. Fujiwara, T. Kan, T. Fukuyama, *Synlett* **2000**, *2000*, 1667–1669.
- [287] W. Kurosawa, T. Kan, T. Fukuyama, *J. Am. Chem. Soc.* **2003**, *125*, 8112–8113.

- [288] A. de Meijere, B. Stecker, A. Kourdioukov, C. M. Williams, *Synthesis* **2000**, 2000, 929–934.
- [289] T. Hirashita, S. Kambe, H. Tsuji, H. Omori, S. Araki, *J. Org. Chem.* **2004**, 69, 5054–5059.
- [290] C. Brouard, J. Pornet, L. Miginiac, *Tetrahedron* **1992**, 48, 2385–2400.
- [291] J. P. Foulon, M. Bourgain-Commerçon, J. F. Normant, *Tetrahedron* **1986**, 42, 1389–1397.
- [292] A. N. Anfimov, S. Y. Erdyakov, M. E. Gurskii, A. V. Ignatenko, K. A. Lyssenko, Y. N. Bubnov, *Mendeleev Commun.* **2011**, 21, 1–3.
- [293] M. E. Gursky, A. V. Geiderikh, A. V. Ignatenko, Y. N. Bubnov, *Russ. Chem. Bull.* **1993**, 42, 144–148.
- [294] R. Köster, H. Bellut, G. Benedikt, E. Ziegler, *Justus Liebigs Ann. Chem.* **1969**, 724, 34–55.
- [295] K. M. Cergol, M. J. Coster, *Nat. Protoc.* **2007**, 2, 2568–2573.
- [296] M. D. Clay, D. Riber, A. G. Fallis, *Can. J. Chem.* **2005**, 83, 559–568.
- [297] A. Melekhov, A. G. Fallis, *Tetrahedron Lett.* **1999**, 40, 7867–7870.
- [298] O. Kwon, S. B. Park, S. L. Schreiber, *J. Am. Chem. Soc.* **2002**, 124, 13402–13404.
- [299] T. Hiyama, K. Kimura, H. Nozaki, *Tetrahedron Lett.* **1981**, 22, 1037–1040.
- [300] N. Selander, K. J. Szabó, *J. Org. Chem.* **2009**, 74, 5695–5698.
- [301] C. Diner, K. J. Szabo, *J. Am. Chem. Soc.* **2016**, 137, 11262–11265.
- [302] H. Lachance, D. G. Hall, in *Org. React.*, John Wiley & Sons, Inc., Hoboken, **2004**.
- [303] R. W. Hoffmann, H.-J. Zeiss, *Angew. Chem. Int. Ed. Engl.* **1979**, 18, 306–307.
- [304] F. W. van der Mei, H. Miyamoto, D. L. Silverio, A. H. Hoveyda, *Angew. Chem. Int. Ed.* **2016**, 55, 4701–4706.
- [305] W. R. Roush, A. E. Walts, L. K. Hoong, *J. Am. Chem. Soc.* **1985**, 107, 8186–8190.
- [306] J. Pietruszka, N. Schöne, W. Frey, L. Grundl, *Chem. – Eur. J.* **2008**, 14, 5178–5197.
- [307] H. Lachance, X. Lu, M. Gravel, D. G. Hall, *J. Am. Chem. Soc.* **2003**, 125, 10160–10161.
- [308] J. W. J. Kennedy, D. G. Hall, *J. Am. Chem. Soc.* **2002**, 124, 11586–11587.
- [309] T. Ishiyama, T. Ahiko, N. Miyaura, *J. Am. Chem. Soc.* **2002**, 124, 12414–12415.
- [310] V. Rauniyar, H. Zhai, D. G. Hall, *J. Am. Chem. Soc.* **2008**, 130, 8481–8490.
- [311] M. Chen, W. R. Roush, *J. Am. Chem. Soc.* **2012**, 134, 10947–10952.
- [312] M. Chen, W. R. Roush, *J. Am. Chem. Soc.* **2013**, 135, 9512–9517.
- [313] M. Schlosser, *Pure Appl. Chem.* **2009**, 60, 1627–1634.
- [314] S. Hitosugi, D. Tanimoto, W. Nakanishi, H. Isobe, *Chem. Lett.* **2012**, 41, 972–973.
- [315] M. Schmicker, Bachelor's Thesis, LMU München, **2016**.
- [316] B. Hetzler, Master's Thesis, **2016**.
- [317] J. L.-Y. Chen, V. K. Aggarwal, *Angew. Chem. Int. Ed.* **2014**, 53, 10992–10996.
- [318] J. L.-Y. Chen, H. K. Scott, M. J. Hesse, C. L. Willis, V. K. Aggarwal, *J. Am. Chem. Soc.* **2013**, 135, 5316–5319.
- [319] A. Erkkilä, P. M. Pihko, *Eur. J. Org. Chem.* **2007**, 2007, 4205–4216.
- [320] S. Bower, K. A. Kreutzer, S. L. Buchwald, *Angew. Chem. Int. Ed. Engl.* **1996**, 35, 1515–1516.

- [321] S. B. Garber, J. S. Kingsbury, B. L. Gray, A. H. Hoveyda, *J. Am. Chem. Soc.* **2000**, *122*, 8168–8179.
- [322] S. R. Chemler, D. Trauner, S. J. Danishefsky, *Angew. Chem. Int. Ed.* **2001**, *40*, 4544–4568.
- [323] F. Gao, A. H. Hoveyda, *J. Am. Chem. Soc.* **2010**, *132*, 10961–10963.
- [324] M. S. Sanford, J. A. Love, R. H. Grubbs, *J. Am. Chem. Soc.* **2001**, *123*, 6543–6554.
- [325] Z. Xu, F. Zhang, L. Zhang, Y. Jia, *Org. Biomol. Chem.* **2011**, *9*, 2512–2517.
- [326] H. Böhme, E. Mundlos, O.-E. Herboth, *Chem. Ber.* **1957**, *90*, 2003–2008.
- [327] C. Nsanzumuhire, J.-L. Clément, O. Ouari, H. Karoui, J.-P. Finet, P. Tordo, *Tetrahedron Lett.* **2004**, *45*, 6385–6389.
- [328] N. M. Barl, E. Sansiaume-Dagousset, G. Monzón, A. J. Wagner, P. Knochel, *Org. Lett.* **2014**, *16*, 2422–2425.
- [329] G. Raju, J. P. Rao, B. V. Rao, *Helv. Chim. Acta* **2014**, *97*, 861–867.
- [330] H. Tokuyama, T. Makido, T. Ueda, T. Fukuyama, *Synth. Commun.* **2002**, *32*, 869–873.
- [331] A. Hirschvogel, Bachelor's Thesis, LMU München, **2015**.
- [332] Y. R. Kim, D. K. An, *Bull Korean Chem Soc* **2012**, *33*, 4194–4196.
- [333] J.-C. Hannachi, J. Vidal, J.-C. Mulatier, A. Collet, *J. Org. Chem.* **2004**, *69*, 2367–2373.
- [334] A. J. Ross, H. L. Lang, R. F. W. Jackson, *J. Org. Chem.* **2010**, *75*, 245–248.
- [335] T. Okitsu, S. Yumitate, K. Sato, Y. In, A. Wada, *Chem. – Eur. J.* **2013**, *19*, 4992–4996.
- [336] L. Nolasco, M. Perez Gonzalez, L. Caggiano, R. F. W. Jackson, *J. Org. Chem.* **2009**, *74*, 8280–8289.
- [337] V. Bagutski, A. Ros, V. K. Aggarwal, *Tetrahedron* **2009**, *65*, 9956–9960.
- [338] L. Nielsen, T. Skrydstrup, *J. Am. Chem. Soc.* **2008**, *130*, 13145–13151.
- [339] R. F. W. Jackson, M. Perez-Gonzalez, in *Org. Synth.*, John Wiley & Sons, Inc., Hoboken, **2003**.
- [340] Y. Hattori, T. Asano, M. Kiriata, Y. Yamaguchi, T. Wakamiya, *Tetrahedron Lett.* **2008**, *49*, 4977–4980.